The calculation of fluid flow using vortex singularities.

Weakley, G. M D.

Award date:
1976

Awarding institution:
University of Bath

THE CALCULATION OF FLUID FLOW USING VORTEX SINGULARITIES

Submitted by: G.M.D. WEAKLEY

For the degree of Ph.D.

of the University of Bath

1976

G.M.D. Weakley

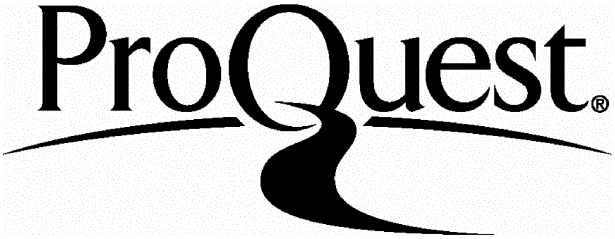

ACKNOWLEDGEMENTS

The number of people who have helped the author during the investigation and the writing of this thesis are too numerous to mention individually. The author is grateful to them all for their help, and would especially like to thank the following:

Mr. H. Hardisty, my University supervisor, for his continuous help and guidance.

Mr. P. Hubble, my Industrial supervisor, for providing the project.

Rolls-Royce(1971)Ltd., Aero Division- Bristol, for the computer facilities, the time and the majority of the financial support.

The S.R.C, also for financial support.

Mr. J. Sims, for the first critical reading of the thesis, and his many helpful suggestions.

Mr. K. Blackmore, School of Mathematics, University of Bath, for his help in deriving the finite-difference equations.

Mrs. J. Hill for always being willing to do the typing.

Miss J. Wilshire for her care in preparing the figures.

Finally, but by no means least, my parents and my wife, Lynne, who gave unstinting support throughout, and for their encouragement to finish this thesis.

CONTENTS

		Page No
Notation		vii
List of figures.		x
1. SUMMARY		1
2. INTRODUCTION		2
2.1.	General Design Considerations for Jet Engine Combustion Chambers	2
2.2.	Aerodynamic Processes	4
2.3.	The Historical Development of the Computer Method	5
2.4.	The Development of the Flow Model to be Described in this Thesis	6
3. INTRODUCTION TO POTENTIAL THEORY		11
3.1.	Basic Theory	11
3.11.	Laplaces Equation	11
3.12.	Superposition principle	12
3.2	Problems specified by Boundary Conditions	13
3.3	Solution of Potential Problems by means of Integral Equations	14
4. 3-D JET IN A CROSSWIND		16
4.1	Introduction	16
4.11	Literature Survey	18
4.2	Theory	20
4.21	Super position of 3 Potentials	20
4.211	Uniform Flow	21
4.212	Axial vorticity vector vortex sheet (AVS)	21
4.213	Circumferential vorticity vector vortex sheet (CVS)	22
4.22	Calculation of the singularity strengths	24
4.221	Axial vorticity vector vortex sheet	24
4.222	Circumferential vorticity vector vortex sheet	28

CONTENTS(Contd) Page No

4.23 Velocities induced by the singularities 29

4.231 Axial vorticity vector vortex sheet 29

4.232 Circumferential vorticity vector vortex sheet 32

4.24 The analytical calculation of velocities induced by the singularities 33

4.241 Infinite vortex filament 33

4.242 Semi-infinite cylindrical vortex sheet 34

4.243 Vortex ring 37

4.244 Finite length cylindrical section of vortex sheet 38

4.25 Comparison between analytic velocities and singularity approximations 41

4.26 Conclusions from tests 44

4.3 Program tests 45

4.4. Discussion 46

4.5 Conclusions 50

4.6 Further work 50

5. TESTS OF ORIGINAL METHOD 71

5.1 Conclusions 78

6. ROTATIONAL FLOWS-VISCOUS INTERNAL FLOWS 79

6.1 Introduction 79

6.11 The computer model 79

6.12 Literature survey 80

6.2 Theory 82

6.21 Calculation of potential flow 82

6.22 Calculation of vorticity 85

6.23 Calculation of velocity components 92

6.24 Effect of the field vorticity at the surface 97

6.241 Recalculation of the surface singularities 99

6.3 Test runs 100

6.4 Results 101

6.5 Discussion 102

CONTENTS (Contd) Page No

6.51 Parallel duct 102

6.52 Stepped duct 107

6.53 Computer time and finite-difference equations 110

6.6. Conclusions 112

6.7 Further work 113

7. GENERAL DISCUSSION 154

7.1 Three-dimensional jet 154

7.2 The solution of two-dimensional viscous flows by Vorticity/Integral Methods 156

7.3 Relevance to prediction of combustion chamber flows 160

8. CONCLUSIONS 161

8.1 Three-dimensional jet 161

8.2 Two-dimensional viscous flow 161

8.3 Relevance to combustion chamber flows 162

REFERENCES 163

APPENDIX 1 Verification that the potential for a source satisfies Laplaces equation 168

APPENDIX 2 Derivation and method of solution of second kind Fredholm integral equations 169

APPENDIX 3 To calculate the velocity induced by a vortex sheet strip 173

APPENDIX 4 Description of 3-D jet computer program 179

A4.1. Selection of interrogation points 179

A4.2. Program logic 181

APPENDIX 5 Flow diagram, input, output and program coding for 3-D jet 194

APPENDIX 6 Solution of the diffusion equation for two characteristic cases 228

A6.1. Diffusion of vorticity from a solid boundary 228

A6.2 Diffusion of vorticity already present in the flowfield 234

CONTENTS(Contd) Page No

APPENDIX 7	Order of magnitudes Argument on the vorticity transport equation	237
APPENDIX 8	Stability criteria	240
APPENDIX 9	Derivation of finite-difference equations	242
A9.1	Second order advective scheme	243
A9.2	Fourth order advective scheme	245
A9.3	Second order conservative scheme	249
A9.4	Fourth order conservative scheme	250
APPENDIX 10	Description of the computer program to predict viscous flows	253
A10.1	Introduction	253
A10.2	Data input and mesh creation	254
A10.3	Mesh markers and matrix of coefficients	256
A10.4	Solution of singularity strengths	259
A10.5	Calculation of the velocity	260
A10.6	Calculation of vorticity	262
A10.7	Effect of vorticity at surface	265
A10.8	Control program	267
A10.9	Plotting coordinates and instructions	267
APPENDIX 11	Flow diagram, input, output and coding for two-dimensional viscous flow program.	271

NOTATION

Symbol	Meaning
A	Area under velocity profile or matrix of coefficients
a	Mesh interval
AVS	Axial vorticity vector vortex sheet
B	Column matrix of sheet boundary conditions
CVS	Circumferential vorticity vector vortex sheet
D(k)	Elliptic integral with independent variable k
$\underline{dS}$	Element of surface
E(k)	Elliptic integral with independent variable k
H	Height of a vortex sheet cylindrical section
k(k)	Elliptic integral with independent variable k
ℓ	Length of surface element
N	Number of vortices representing a vortex sheet or number of segments representing a vortex filament.
n	A particular vortex
P	Static pressure
q	The direct contribution to the velocity from the adjacent source singularity
R	Vortex cylinder radius
Re	Reynolds Number or Real part of
Ro	Source disc radius or Vortex cylinder/ring radius
$\lvert r \rvert$	Distance between vortex and interrogation point
S	Length around surface from origin
ΔS	Length of surface element
$\hat{\underline{t}}$	Tangential unit vector
Δt	Timestep
u	Velocity component in the x-direction
$\underline{V}$	Velocity Vector
v	Velocity component in the y - direction
δv	Velocity increment
$\underline{w}$	Vorticity vector
$\omega(y,\epsilon)$	New vorticity distribution
$\omega(\zeta,\epsilon)$	Previous vorticity distribution
(x,y)	Position of interrogation points
(x',y')	Position of vortex filament

NOTATION (Contd)

Symbol	Meaning
α	Non-dimensional u velocity component
β	Non-dimensional v velocity component
δ	Non-dimensional boundary layer thickness
σ	Source/vortex sheet strength
	or Column matrix of source/vortex sheet strengths
ϕ	Potential
ψ	Streamfunction
∇	Vector differential operator
Γ	Circulation
ν	Kinematic viscosity
ρ	Density
λ	Convergence criteria for vorticity prediction
ζ	Value of γ for previous vorticity distribution

Subscripts

DIFF	Difference
EXIT	At the duct exit section
I,j	Duct exit mesh point location
IN	Into the duct
INLET	At the duct inlet section
i,j	Mesh point location
JET	Jet component
OUT	Out of the duct
o	Non-dimensional quantity
r	Radial Component
s	Surface component
X	Component in x direction
Y	Component in y direction
Z	Component in z direction
θ	Component at angle θ
∞	Component at infinity

Superscript

n Iteration marker

Greek characters $\theta, \delta, \alpha, \beta, \gamma$ were used to indicate angles in the figures. Also, lower case letters were used as distances in the figures and in the text.

COLLOCATION POINT

A point in the flowfield, usually on the solid surface, where the solution of an equation e.g. a Fredholm Integral equation, is exact.

INTERROGATION POINT

A point in the flowfield at which certain quantities, e.g. velocity, are to be calculated.

N.B.

Where appropriate, the figures have been drawn within the text. Those figures occupying a complete page have been placed together at the end of their relevant chapter. For easier reference to these figures, their page number is given as a superscript to the figure number wherever it occurs in the text.

LIST OF FIGURES

CHAPTER 2

2.1. Typical combustion chamber

2.2. Introduction of vortex rings

2.3. Diffusion of vorticity to allow for turbulent mixing

CHAPTER 4

4.1(a) Typical combustor flow pattern

4.1(b) Distortion of a jet in a crosswind

4.1(c) Vortex sheets used for 3-D jet in a crosswind

4.1(d) Original method for 3-D jet

4.1(e) Pictorial view of 3-D jet

4.2(a) Distribution of sinks and doublets along jet path

4.2(b) Skifstad's model for the 3-D jet

4.2(c) Pictorial representation of the 3 potentials

4.3(a) Approximations for AVS

4.3(b) Approximations for CVS

4.3(c) Strip approximations for the semi-infinite vortex sheets

4.4(a) Axial vorticity vector vortex sheet

4.4(b) Calculation of velocity distribution around cylinder

4.5 Axial vortices circulation calculation

4.6(a) Circumferential vorticity vector vortex sheet

4.6(b) Vortex ring representation of a portion of a vortex sheet

4.7 Velocity field of a vortex filament in 2D

4.8 Velocity field of a vortex filament in 3D

4.9 Approximation of a semi-infinite cylindrical vortex sheet

4.10 Source disc with interrogation point

4.11 Comparison of velocity induced at interrogation points of the semi-infinite vortex sheet

4.12 Position of interrogation point with respect to a vortex ring

4.13 Comparison between velocities induced at points by approximations to a vortex ring

4.14 Position of interrogation point with respect to a cylindrical section

4.15 Comparison of velocities induced at an interrogation point by the vortex strips and vortex segments

4.16 Interrogation point on a cylindrical section

4.17 Working section at X-flow 1500

4.18 Plan view of working section x-flow 2000

4.19 Plan view of working section x-flow 2500

4.20 Working section at x-flow 3000 (4th iteration)

4.21 Working section at x-flow 3000 (12th iteration)

4.22 Better representations of the cylindrical section sheet strips

CHAPTER 5

5.1 Integration interval on column

CHAPTER 6

6.1 Definition of duct walls

6.2(a) Flow around curve c

6.2(b) Possible streamlines within c

6.3 Calculation of surface vorticity

6.4 Calculation of vorticity at concave corners

6.5 Calculation of vorticity at convex corners

6.6 Calculation of velocity components

6.7 Velocity components on mesh rows and columns

6.8(a) Source sheet

6.8(b) Vortex sheet

6.9 Replacing vorticity by a vortex

6.10 Exit velocity profile

6.11 Parallel duct

6.12 Stepped duct

(Figures 6.13 to 6.27 refer to the parallel duct)

6.13 Velocity profile at 30%, t = 0, Re = 40

6.14 Velocity profile at 30%, t =.01,Re = 40

6.15 Velocity profile at 30%, t =.02,Re = 40

6.16 Velocity profile at 30%, t =.03,Re = 40

6.17 Velocity profile at 30%, t =.035 Re = 40

6.18 Velocity profile at 30%, t =.04,Re = 40

6.19 Velocity profile at 30%, t = .04,Re = 40

6.20 Velocity profile at 30%, t = 0, Re = 300
6.21 Velocity profile at 30%, t = .004, Re = 300
6.22 Velocity profile at 30%, t = .014, Re = 300
6.23 Velocity profile at 30%, t = .03, Re = 300
6.24 Velocity profile at 30%, t = .078, Re = 300
6.25 Comparison of velocity profiles at 30%
6.26 Comparison of velocity profiles at 100%
6.27 Corrected velocity profile at 30%

(Figures 6.28 to 6.51 refer to the stepped duct)

6.28 Velocity profile at 29%, t = 0, Re = 16
6.29 Velocity profile at 29%, t = .02, Re = 16
6.30 Velocity profile at 29%, t = .04, Re = 16
6.31 Velocity profile at 29%, t = .06, Re = 16
6.32 Velocity profile at 29%, t = .1, Re = 16
6.33 Velocity profile at 76%, t = 0, Re = 16
6.34 Velocity profile at 76%, t = .02, Re = 16
6.35 Velocity profile at 76%, t = .04, Re = 16
6.36 Velocity profile at 76%, t = .06. Re = 16
6.37 Velocity profile at 76%, t = .1, Re = 16
6.38 Calculation of reattachment point
6.39 Variation of reattachment point with time
6.40 Variation of standing vortex length with Reynolds Number
6.41 Correlation of numerical and experimental results for eddy length
6.42 Profiles for Re = 4, t = 0
6.43 Streakline profiles Re = 4
6.44 Profiles for Re = 4, t = .135
6.45 Streaklines for Re = 8, t =0
6.46 Profiles for Re = 8, t = 0
6.47 Streaklines for Re = 8
6.48 Streaklines for Re = 8
6.49 Profiles for Re = 8, t = .28
6.50 Streaklines for Re = 16
6.51 Streaklines for Re = 16, t = .66

LIST OF FIGURES (Contd)

APPENDIX 2

A2.F1 Source distribution over surface S

A2.F2 Boundary vortex sheets

APPENDIX 3

A3.F1 Velocity field of a 3-D vortex sheet strip

APPENDIX 4

A4.F1 Superposition of infinite cylindrical vortex sheets (+ approximations)

A4.F2 Position of interrogation points and cylindrical vortex sheet boundaries on developed cylinders

A4.F3 Developed view of working section

A4.F4 Position of vortex strip edges on points and vortex rings

A4.F5 Position of vortex ring segment and cylindrical section strip in relation to field point

A4.F6 Vortex segments used in FILRIN

A4.F7 Vortex strip section for use in SHEET

A4.F8(a) Field point on cylindrical strip

A4.F8(b) Field point on semi-infinite strip

APPENDIX 5

A5.F1 Flow diagram for 3-D jet in crosswind

A5.F2 Subroutine flow diagrams

APPENDIX 6

A6.F1 Vortex sheet

APPENDIX 10

A10.F1 Storage of data in entities

A10.F2 Mesh point markers

A10.F3 Velocity component markers

A10.F4 Mesh point location for storing surface sheet strength

A10.F5 Mesh point selection

A10.F6 Mesh point orientation

A10.F7 Calculation of average velocities

A10.F8 Fourth-order mesh positions

A10.F9 Second-order mesh positions

A10.F10 Calculation of streakline components

APPENDIX 11

A11.F1 Program suite flow diagram

(Figures A11.F2 to A11.F10 are the individual program flow diagrams)

A11.F2 Program 55: Data input and mesh creation

A11.F3 Program 10002: Mesh markers and matrix of coefficients

A11.F4 Program 10003: Gauss-Seidal routine

A11.F5 Program 10004: Calculation of velocity components

A11.F6 Program 10005: Calculation of vorticity

A11.F7 Program 10006: Calculation of effect of field vorticity around surface

A11.F8 Program 10007: Control program

A11.F9 Program 10008: Assembly of the plotting coordinates

A11.F10 Program 10009: Assembly of the plotting instructions

A11.F11 Data type 50

A11.F12 Data type 55

A11.F13 Part of data type 52

1. SUMMARY

The work described in this thesis concerns the development of a vortex singularity flow model for the prediction of jet engine combustion chamber flows. In an attempt to understand the operation of the chamber dilution zone, a program was written which successfully predicted an irrotational three-dimensional jet in a crosswind.

A novel approach for the inclusion of viscous effects was successfully tested by predicting flows in both a parallel and a stepped duct. The approach consists of a finite-difference solution of the Vorticity transport equation and an Integral Equation solution of the Poisson equation for stream function. The results obtained with this approach have shown general agreement with those of other investigators.

Suggestions are made as to how the computer methods for the irrotational and rotational predictions could be improved.

It was concluded that the Vorticity/Integral method was a sound theoretical approach to predicting viscous flows, and could eventually be used to predict combustion chamber flows.

2. INTRODUCTION

The work described in this thesis has its origins in an attempt at Rolls-Royce (1971) Ltd., Bristol Engine Group, to put the design of jet engine combustion chambers on a more rational basis. Combustion chambers are extremely difficult to analyse theoretically because the flow is three-dimensional, viscous, turbulent, separated etc. Also, the combustion process itself entails that chemical reactions require consideration, with possible dissociation and association. The practical design of chambers is a mixture of empirical and theoretical approaches with computer programs (such as that by Close (1970) which gives the airflow distribution, and that by Gosman et al (1969) which gives the flow field including combustion effects) being used, together with practical tests on water analogy and combustion rigs. In the latter, the performance of an ignited chamber can be measured in representative conditions.

The work described here is concerned with a theoretical flow model which, ultimately, will be applicable to the flows within a chamber; this model would contain the minimum of empirical data. Nevertheless, in order to place the work in context, basic design criteria will be briefly reviewed, together with their relevance to the chamber aerodynamics. A more detailed description of these criteria can be found in Whittaker (1965).

2.1. General Design Considerations for Jet Engine Combustion Chambers.

One of the more obvious requirements for a long engine life is that the chamber metal temperatures be kept as low as possible. By this means the effect of metal stress is alleviated and the necessity for special materials is reduced. Film cooling is generally employed, fig. 2.1,[9] for wall temperature control and this method uses a large percentage (20 to 30%) of the total air flow.

Film cooling flows are difficult to predict, especially in those regions where gas layers having different origins and temperatures mix together. For example, the flow in the slot is of the boundary layer type and 2 - dimensional, while the flow in the chamber is swirling and three-dimensional. The equations are therefore of different types, being parabolic for the slot flow, and elliptic for the chamber flow. In practice it is found that film cooling flows are not as effective for mixing purposes as a penetrating jet; also film flows tend to quench combustion near the wall leading to a loss in combustion efficiency.

Another overall design criterion is that a good outlet temperature distribution should be obtained. Should the temperature be high at one position, this could result in a "hot spot" on the turbine stator blades, which could reduce their life. Similarly an uneven pressure distribution over the turbine rotor blades might reduce their fatigue life. In order to obtain an even outlet temperature distribution, as much of the total airflow as possible must be used for mixing purposes, by means of penetrating jets, fig. 2.1.[9] This conflicts with the film cooling requirement, previously mentioned.

In order to predict the temperature distribution in the combustion chamber, the effect of penetrating jets and film cooling flows on the main flow of combustion air must be estimated. The aerodynamics of the mixing can be calculated from the Navier-Stokes equations with suitable turbulence models, and the chemical reactions from rate equations.

As previously mentioned, the work reported here describes the development of a basic flow model which was inspired by a desire to calculate these complex flows. Further development work will be necessary before this model becomes capable of calculating flows in a practical situation.

2.2. Aerodynamic Processes

As background material, a number of practical flows will be briefly described.

(i) Diffuser Flow

The diffuser will be defined here as those components lying between planes 1 and 2 in fig. 2.1.[9] Here the pressure rise should be brought about as efficiently as possible. To do so, either separation should be avoided entirely or it should be controlled. For the prediction of unseparated flow in a diffuser, the parabolic equations of boundary layer theory can be used. In diffusers with controlled separation, the full elliptic Navier-Stokes equations are necessary.

(ii) Annulus Flow

The flow in the chamber annulus controls the flow inside the flame tube to a very marked extent, and also affects the flame tube temperatures which occur. In any computer prediction, therefore, this flow must be calculated accurately. One practical consideration is that film cooling slots should receive adequate airflow under all conditions. This implies that for a sound design, the velocity and pressure variations in the annulus must be known for all operating conditions.

It is also desirable to prevent separation near the inlet to the film cooling slots because of its effect on the cooling flow. Hence the computer method should be capable of predicting those operating conditions which would result in flow separation.

(iii) Central Core

The primary combustion zone is dominated by a quasi-stable recirculating flow which forms a toroidal vortex, fig. 2.1[9] Downstream of the primary zone is the mixing region where the hot combustion gas is diluted by the air from the penetrating jets. This is in itself a very complex region considering the turbulence of the flow and the variety of chemical species present.

2.3 The Historial Development of the Computer Method

A computer program to design and optimise a combustion chamber, taking into account all the above relevant factors, as well as the overall size dictated by the engine designer, does not, to the authors knowledge, exist at the present moment. Even a numerical model of the flow field (diffuser, annulus and central core, see above) is a problem of considerable complexity. It was against this background, and the desire to predict these complex flows, that Hubble(1967) proposed a method of predicting viscous flows which he believed would eventually form the aerodynamic core of such an optimising program.

Flow visualisation tests on a flame tube have shown that the upstream flow is small enough to be neglected, and that the penetrating jets may be treated as if all the flow from them passed downstream. From this result, it was felt that a possible insight into the operation of a dilution zone could be obtained by studying the interaction of jets exhausting into a crossflow.

Hubble's (1964,1967) intention was to predict the behaviour of a three-dimensional irrotational jet in a crosswind, and develope techniques for incorporating viscous and turbulent effects from there.

The prediction method for the three-dimensional irrotational jet was based on the two-dimensional method of Chang (1942), where the jet boundary is represented by a number of infinite line vortices perpendicular to the plane of the crossflow. In order to extend this to three-dimensions, ring vortices were placed around the jet circumference to represent flow within the jet, fig. 2.2.[10] Hubble further suggested that if the vorticity bound within the infinitesimally thin vortex sheets on the jet circumference were allowed to diffuse into the flowfield, then the entrainment into the jet due to turbulent mixing could be estimated, fig. 2.3.[10]

These ideas formed the basis of a general method for solving fluid dynamic problems based on the concept of vorticity. The method combined an Integral equation solution of the Poisson equation, with an approximate solution of the Vorticity transport equation. The former enabled the strengths of the surface vortex sheets to be calculated, whilst the latter gave the distribution of vorticity in the flowfield. This approach was considered capable of predicting separated flows, and a computer program to predict the two-dimensional viscous flow over a cylinder was initiated within Rolls-Royce (1971) Ltd., Bristol.

2.4 The Development of the Flow Model to be described in this Thesis.

The order in which the work is described reflects the historical order in which it was performed. Although the broad outlines of the work were known at the beginning, the final structure was dependent on the results of intermediate investigations.

The overall objectives were:-

a) To write a computer program for the three-dimensional inviscid jet in a crosswind.

b) To use the general approach for viscous flows to predict two-dimensional flow, with if possible, its application to the three-dimensional jet.

Certain assumptions which had been built into the original program for predicting the three-dimensional jet caused the results to be unstable. Following a suggestion by Hubble these faults were remedied by the author, and the resulting program was then capable of predicting a stable jet, which exhibited the well-known kidney shaped deformation, Chapter 4. For the viscous flow investigation, Hubble proposed to solve the Vorticity transport equation by an approximate method. A detailed

examination of this method, however, cast doubt on its validity, chapter 5. The use of finite-difference methods would remove the necessity for any approximation of the fundamental equations, give a much more straightforward approach and probably not involve a significant amount of extra work. In view of these considerations, work was then concentrated on solving the complete Vorticity transport equation by finite-difference methods.

At this point, a brief literature survey was carried out, section 6.12, and the various numerical methods most appropriate to a particular flow situation were examined. Based on this survey and an assessment of the various finite-difference equations, a decision was taken to use Fromms(1969) form of the Vorticity transport equation.

It was also decided to limit the investigation contained in this thesis to low Reynolds number flows. The reason for this was as follows:- The program for predicting the two-dimensional viscous flow over a cylinder had been started some three years prior to the work described here, but was of such complexity that further work on it was discontinued. Because of this situation, the proposed method of linking Integral equations with the solution of the Vorticity transport equation had never been properly tested. Since the work of this thesis was a completely new start on an, as yet, untried but complex method, it was decided to prove the method on non-turbulent flows.

The work to be described for the viscous flow investigation concerned the calculation of two characteristic flow situations,(i) a parallel duct, and (ii) a duct with a backward facing step. The main effort has gone into writing and finally testing a rather complex program capable of solving these two cases numerically. Results have been obtained which generally

agree with those of other investigators. In order to accommodate fluid boundaries of complex shape, the initial program was rewritten to incorporate a general mesh-filling program which was already in existence within Rolls-Royce.

Much more detail concerning the flow model development will be found in the relevant chapters. A brief introduction to the potential theory used throughout this investigation is given in chapter 3, forming a basis for the theory which follows in the subsequent chapters.

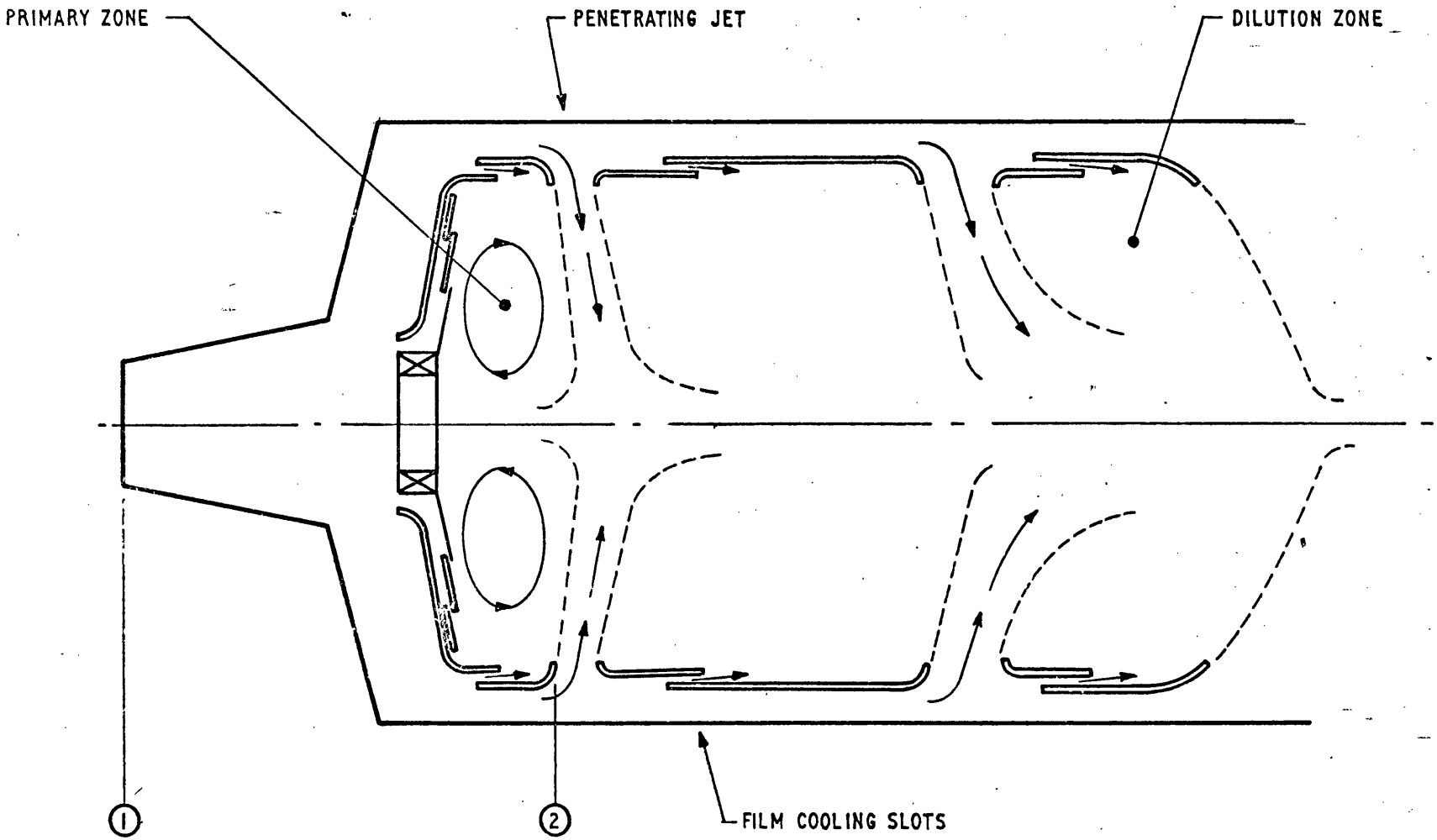

FIG. 2.1 TYPICAL COMBUSTION CHAMBER

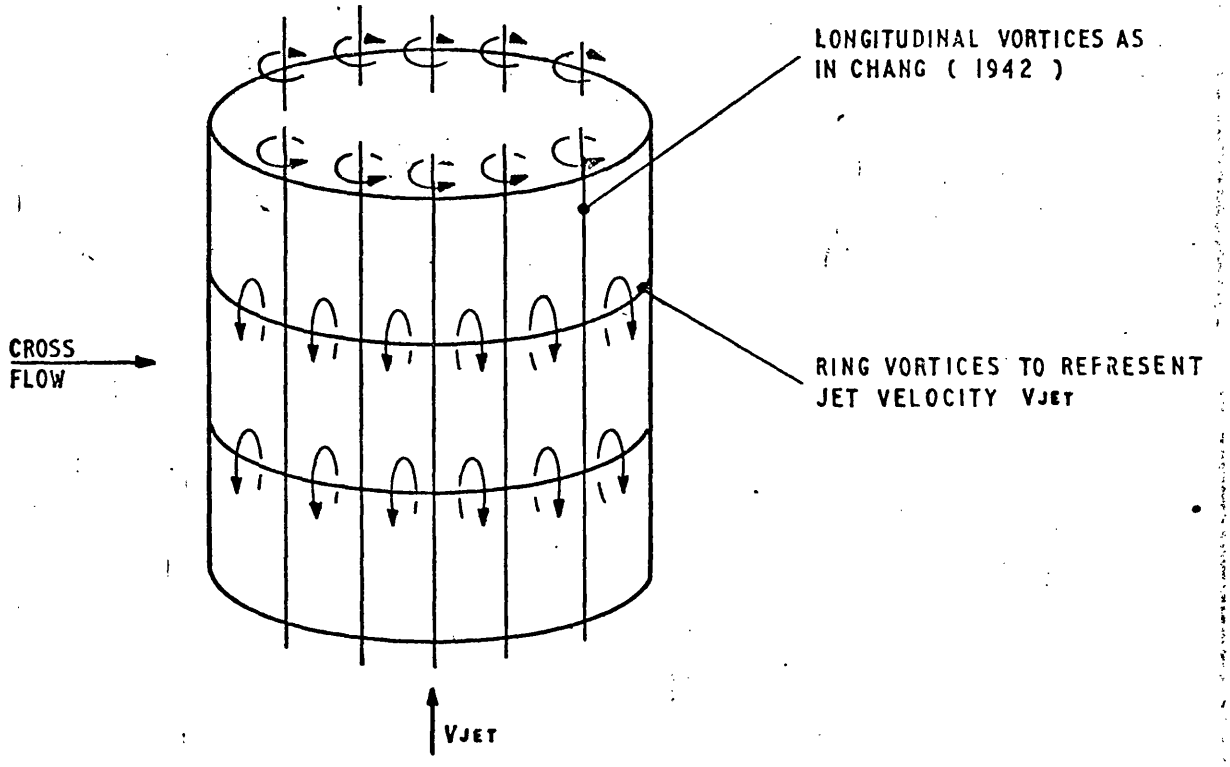

FIG. 2.2 INTRODUCTION OF VORTEX RINGS

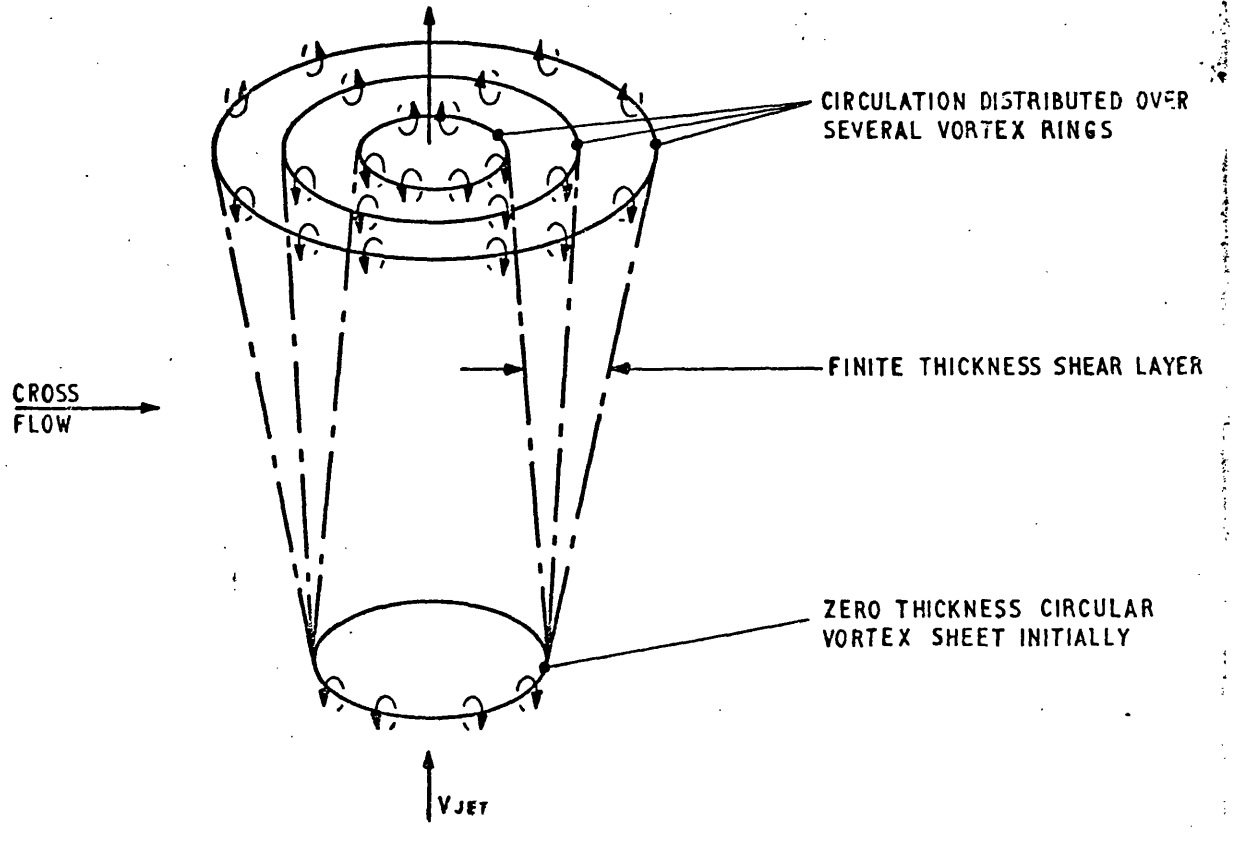

FIG. 2.3 DIFFUSION OF VORTICITY TO ALLOW FOR TURBULENT MIXING

DISTORTION OF VORTEX RINGS BY CROSS FLOW NOT SHOWN FOR CLARITY

3.0. INTRODUCTION TO POTENTIAL THEORY

The theory is well set out in a number of standard texts, Robertson (1965), Lamb (1932), and only the salient points necessary for understanding the computer model will be repeated here.

3.1. Basic Theory.

3.11. Laplace's Equation

The motion of an inviscid, incompressible fluid can be conveniently expressed in terms of a scalar field function whose gradient is the velocity. This function is termed the velocity potential or just the potential.

For such a potential to exist, the fluid motion must be irrotational, hence

$$\underline{\omega} = \nabla \wedge \underline{V} = 0 \qquad 3.1$$

Where $\underline{\omega}$ is the vorticity vector

∇ is the vector differential operator, defined as

$$\nabla = \underline{i}\frac{\partial}{\partial x} + \underline{j}\frac{\partial}{\partial y} + \underline{k}\frac{\partial}{\partial z}$$

and $\underline{V}$ is the velocity vector.

Consider an irrotational, 2-D plane motion, then

$$\underline{V} = \nabla \phi$$

$$\left(u = \frac{\partial \phi}{\partial x}\ ,\ v = \frac{\partial \phi}{\partial y}\right) \qquad 3.2$$

Where u, v are the x and y components of $\underline{V}$ and ϕ is the potential

In 2-D, irrotationality becomes (from 3.1)

$$\omega_z = \frac{\partial v}{\partial x} - \frac{\partial u}{\partial y} = 0 \qquad 3.3$$

Hence substituting from 3.2 into 3.3

$$\frac{\partial}{\partial x}\left(\frac{\partial \phi}{\partial y}\right) - \frac{\partial}{\partial y}\left(\frac{\partial \phi}{\partial x}\right) = 0 \qquad 3.4$$

Since ϕ is a scalar, the order of differentiating is unimportant, so 3.4 shows that irrotationality and velocity potential are inseparably connected. Changing the order of differentiating gives 3.3 again.

However, the fluid motion under consideration is incompressible, which implies

$$\nabla . \underline{V} = 0 \qquad 3.5$$

If 3.2 is substituted into 3.5

$$\nabla . \nabla \phi = 0 \qquad 3.6$$

or in rectangular cartesian coordinates

$$\frac{\partial^2 \phi}{\partial x^2} + \frac{\partial^2 \phi}{\partial y^2} = 0 \qquad 3.6$$

(Laplace's equation)

Thus the potential for all possible irrotational motions of an incompressible fluid must satisfy the Laplace equation.

For the solution of irrotational flows, the solution of 3.6 is required.

Laplace's equation may also be derived in terms of stream function. For a plane 2-D motion of an incompressible fluid, the streamfunction is defined by

$$u = \frac{\partial \psi}{\partial y} \qquad v = -\frac{\partial \psi}{\partial x} \qquad 3.7$$

substituting 3.7 into the irrotationality condition 3.1,

$$\frac{\partial^2 \psi}{\partial x^2} + \frac{\partial^2 \psi}{\partial y^2} = 0 \qquad 3.8$$

3.12 Superposition Principle.

This principle is based on the assumption that potentials may be superimposed, and may be applied if the differential equations characterising the particular case are linear. The equations expressing continuity and irrotationality are proved to be linear in Robertson. Using similiar techniques, it may be shown that Laplace's equation is also linear.

Therefore, superposition can be applied to either stream function or to potentials. Thus

$$\phi_{1+2} = \phi_1 + \phi_2 \qquad 3.9$$

The potential for a source singularity ϕ_s in a parallel stream ϕ_p is

$$\phi_{s+p} = \phi_s + \phi_p \qquad 3.10$$

It can be shown that the potential of a source and that of a parallel stream individually satisfy Laplace's equation, Appendix 1. Hence from 3.10, the combined potential also satisfies Laplace's equation, giving the potential of a uniform flow passing a source. Thus the source etc. may be used as a 'building block' to construct other flows. The potentials for other singularities for both plane and axisymmetric cases have been tabulated in Robertson (1965).

Summarising the above, it can be seen that many potential solutions can be found by combining simpler known solutions. This technique is usually known as the Method of Singularities since the simple potential solutions all involve mathematically singular functions. At the location of one of these functions the velocity is infinite, hence the term singular. The Laplace equation is not satisfied at the singularities although it is satisfied in the flow about them.

3.2 Problems Specified by Boundary Conditions.

Flow problems which can be represented in the form of potentials are uniquely specified by the boundary conditions of the problem. The manner in which these boundary conditions are specified is usually limited to 3 principal types:

1) If the potential is defined over the region boundary, this is termed a Dirichlet boundary-value problem.
2) If the normal derivative of the potential is defined over the region boundary, this is known as a Neumann boundary-value problem.
3) Where both the potential and its normal derivative are defined over the region boundary, then the problem is known as a Cauchy boundary-value problem.

Cauchy is normally an overspecification of the problem, but solutions are sometimes possible.

As well as these 3 specifications, it is sometimes possible to have mixed boundary-value problems, where Dirichlet conditions apply over part of the boundary and Neumann conditions over the rest.

3.3. Solution of Potential Problems by means of Integral Equations.

The solutions of some potential problems, specified in terms of their boundary-values, can be written in integral form as implicit equations for ϕ . In fluid dynamics, these integral equations are usually in a form known as Fredholm Integral equations.

The significance of considering these integral equations is given in the equivalence theorem, which may be stated

- the solution of an integral equation is a solution of the corresponding boundary-value problem and vice versa -

Using this theorem, a problem of determining the potential for a particular fluid flow may be transformed into a boundary-value problem. The latter type of problem entails finding the solution of Laplace's equation $(\nabla^2 \phi = 0)$ for certain boundary conditions. Hence if the solution to the boundary-value problem can be obtained from solving a corresponding integral equation, then the solution for the potential will have been achieved.

The viscous flow investigation, described later, was concerned with Fredholm Integral equations of the second kind. Such equations usually result from a formalized solution of the Dirichlet or Neumann boundary-value problems. For a general derivation of such an integral equation, see Appendix 2.

There are several advantages in using an Integral Equation technique, rather than other field methods, to obtain a solution of Laplace's equation. These are listed below:-

1. Laplace's equation is formally solved, it is the solution which is approximated.

2. In contrast, the solution of a field problem by the use of finite - difference techniques involves making an approximation of Laplace's equation. The number of equations to be solved is directly related to the number of points in the field. With integral equations, only the conditions on the flow field boundary are involved, thus the order of the matrix is specified by the number of boundary points. These are usually considerably less than the number of field points.

3. The boundary conditions at infinity are already contained within the formulation of the integral equation. This is not so with other field techniques, where the infinity conditions are usually prescribed at the mesh points relatively a long way from the inner boundary.

Details of some of the solutions available of Fredholm Integral equations are given by Robertson. Further details of the particular solution technique adopted by the author for the viscous flow investigation, are in Appendix. 2.

4. 3-D JET IN A CROSSWIND

4.1 Introduction

The starting point for this work was the development of a theoretical model which would predict combustion chamber performance. Hubble (1967) suggested that the theoretical behaviour of a 3-D jet in a crosswind was a basis for the attempt to calculate such a flow, from the similarity between dilution hole jet flows and 3-D jets. An artists impression of flow in a combustor, fig 4.1(a)[51], shows the dilution hole flows being bent downstream due to the complex flow present. The 3-D jet in a crosswind will also bend downstream, and distort into the traditional kidney shape.

If the prediction of the 3-D jet proved successful, then a routine to calculate the diffusion and convection of vorticity could be included within the program, thus enabling single 3-D viscous jets to be calculated. The methods could be extended to include other jets, cylindrical boundaries etc, thus building up a computer prediction method for combustion chamber flows.

The method used for calculating the 3-D jet was based on the work of Chang (1942) who concentrated on the 2-D jet in a crosswind. One of her methods was to superimposed a uniform flow with an infinite cylindrical vortex sheet, which she represented by a series of infinite vortex filaments spaced around the sheet boundary. The distortion of the jet was calculated from the mutual influence of the singularities on each other, with the uniform flow moving the distorted section downstream. A typical result is shown in fig 4.1 (b)[52].

To extend her method to three dimensions, another infinite cylindrical vortex sheet is superimposed onto the system, this representing the fluid flow up the jet. Half of the resulting cylinder, fig. 4.1(c)[52], would be kept fixed, whilst the other half would be free to move under the influence of the singularitie

The movement is calculated at specific points on the jet boundary within the working section, known as interrogation points.

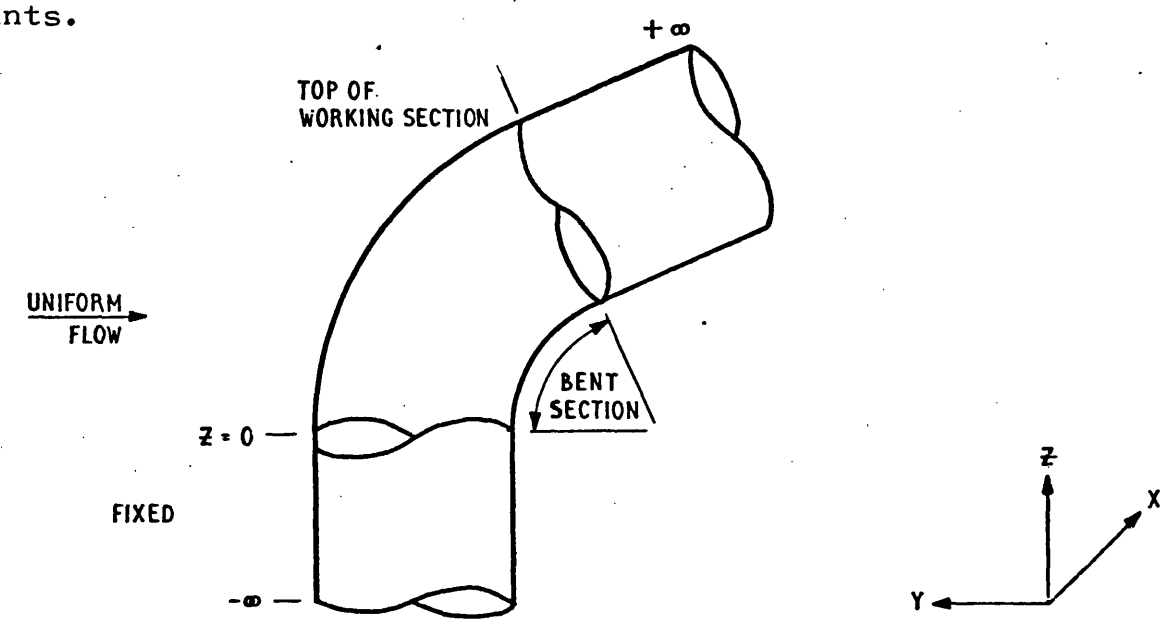

FIG 4.1(d) ORIGINAL METHOD FOR 3-D JET.

The first method Hubble used, was to move the jet at $+\infty$ until it was in line with the normal to the top of the working section, fig. 4.1(d). This meant that the end of the jet at $+\infty$ would have to move with infinite velocity, instead of a rate consistent with the free stream. Consequently the jet was unstable.

From intuition it was felt that the general stage of the jet trajectory was likely to be as shown in 4.1(e). The jet, from the top of the working section to $+\infty$, merely translating and distorting under the influence of the free stream

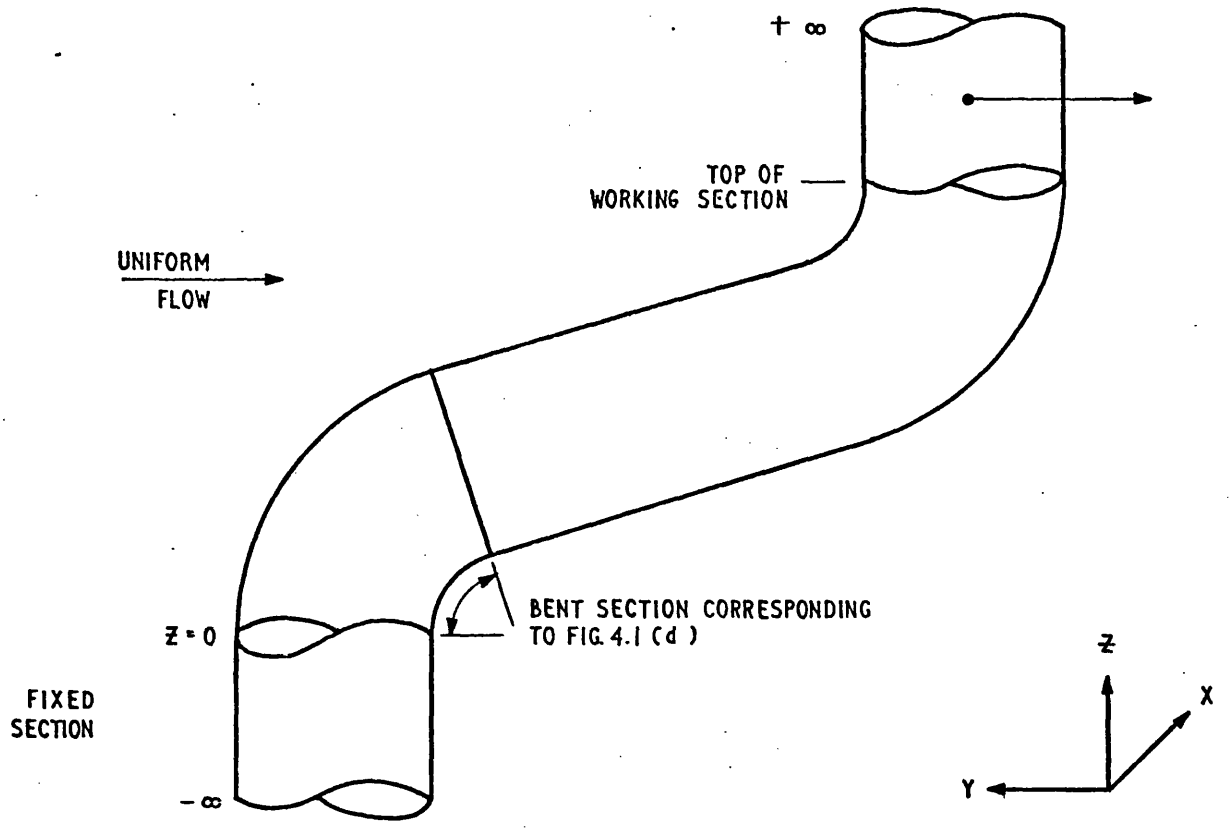

FIG 4.1(e) PICTORIAL VIEW OF 3-D JET.

This was the basis for jet development in the model used by the author. At each timestep, a portion of the fixed jet was incorporated into the working section. This increased the flexibility of the jet, and thus the distortion of the working section could be more accurately calculated.

4.11. LITERATURE SURVEY.

At this point opportunity was taken to survey the methods used by other investigators in this field. In a number of instances, experimental data for the jet path was curve-fitted, and line singularities placed along the path. Wooler (1969), for example, uses a 2-D doublet along the jet path with a line of 2-D sinks on the major axes of the jet section, fig. 4.2(a)[53].

Some 3-D methods, NASA SP-218(1969), have used appropriately spaced 3-D singularities. The simplest of these, Skifstad (1969), uses 2 vortex lines with a line sink halfway between them. The 3 singularities have a common tangent plane at each point, fig. 4.2(b[53]

In order to take account of the interaction of the jet on adjacent bodies, 3-D distribution of sources and doublets over the 3-D bodies have been developed, Rubbert (1969). The jet geometry is predetermined, and is placed on an empirical jet path and is usually not allowed to move.

Few methods allow the jet to deform into the characteristic kidney shape. One attempt to do this, Margason (1969), was to have a stack of 2-D vortex rings, each deforming under its own influence as time progresses. Those farthestfrom the jet exit will have been deforming longer, but no account is taken of the mutual influence of the rings on one another.

In NASA SP-218(1969), many researchers have included 3-D vortex lattices in their models. The lattices have been kept in a predetermined configuration rather than be free to calculate their own configuration. Thus these lattices cannot represent the true 3-D jet, and serve only as a tool to calculate some influence on associated bodies.

Hackett (1969) uses a 3-D lattice of short unconnected vortex segments which move under their mutual influence. Thompson (1971) notes that this method violates Kelvin's Theorem, which states that the circulation remains constant when the following three conditions are satisfied :-

a) the fluid is inviscid.

b) the fluid is barotropic, i.e. the density is constant or a function of the pressure alone during the motion

c) the body forces, if any, are desirable from a single-valued potential.

Thompson's method is the closest to the present method, where a lattice of vortex filaments and rings is used to describe the jet surface. The lattice is allowed to move under its own influence.

4.2 THEORY

Some of the other methods listed used singularities to model the experimentally known jet behaviour e.g. the degeneration into two contra-rotating vortices was simulated by two contra-rotating Vortex filaments. Thompson's method is the only other method, to the authors knowledge, which set up the problem as one of superpositioning singularities, and allowing them to affect one another. Thus the degeneration would come as a result of the mutual influence of the singularities on each other.

4.21 SUPERPOSITION OF 3 POTENTIALS

In this study, three singularities were superpositioned:

1) a uniform stream
2) an infinite cylindrical vortex sheet with an axial vorticity vector (AVS), fig 4.2(c)[54] This sheet can be simulated by infinite vortex filaments parallel to the vorticity vector.
3) an infinite cylindrical vortex sheet with a circumferential vorticity vector (CVS), fig 4.2(c)[54] This sheet can be simulated by vortex rings, also parallel to the vorticity vector.

Since the flow is irrotational, Laplace's equation must be satisfied over the whole of the flow field. As already established in chapter 3, singularities may be used together to give complex flows, provided that their potentials individually satisfy Laplace's equation. The three singularities chosen do satisfy that criteria.

The model does not incorporate a mechanism for mixing between the stream and the jet, so the strength of the AVS is such that the combined potentials of the uniform flow and the AVS gives the irrotational flow around the jet.

The strength of the CVS is directly proportional to the jet velocity. Thus, combining the potential of the CVS to the other singularities, gives the flow around and through the jet.

4.211. UNIFORM FLOW

The strength of the uniform flow, or crossflow, is equal to the velocity at infinity. This flow moves the distorted jet downstream a distance proportional to the time step and flow strength, at the end of each iteration.

4.212 AXIAL VORTICITY VECTOR VORTEX SHEET (AVS)

This sheet is approximated by a series of infinite vortex filaments spaced evenly around the vortex sheet, fig. 4.3(a). This makes easier the calculation of the velocity induced by the AVS. Provided that the strength of the vortices accurately represents the local strength of the AVS, then the velocity will also be accurate.

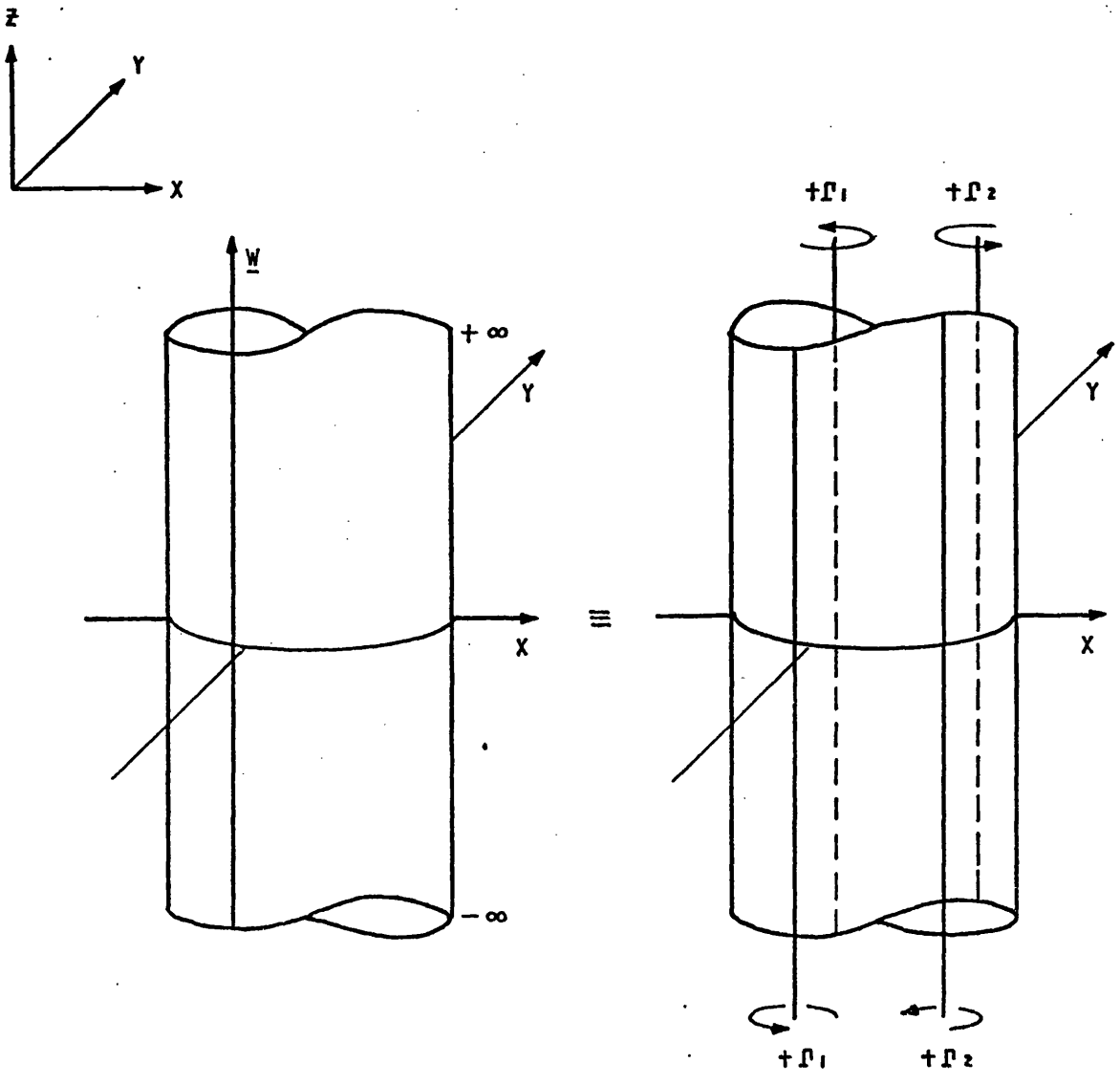

FIG.4.3(a) APPROXIMATIONS FOR AVS

4.213 CIRCUMFERENTIAL VORTICITY VECTOR VORTEX SHEET (CVS)

This sheet is divided into the following regions:

1) 2 semi-infinite cylindrical vortex sheets from $Z = -\infty$ to $Z = 0$ and from Z = top of working section to $Z = +\infty$

2) The working section is divided into cylindrical sections, fig 4.3(b).

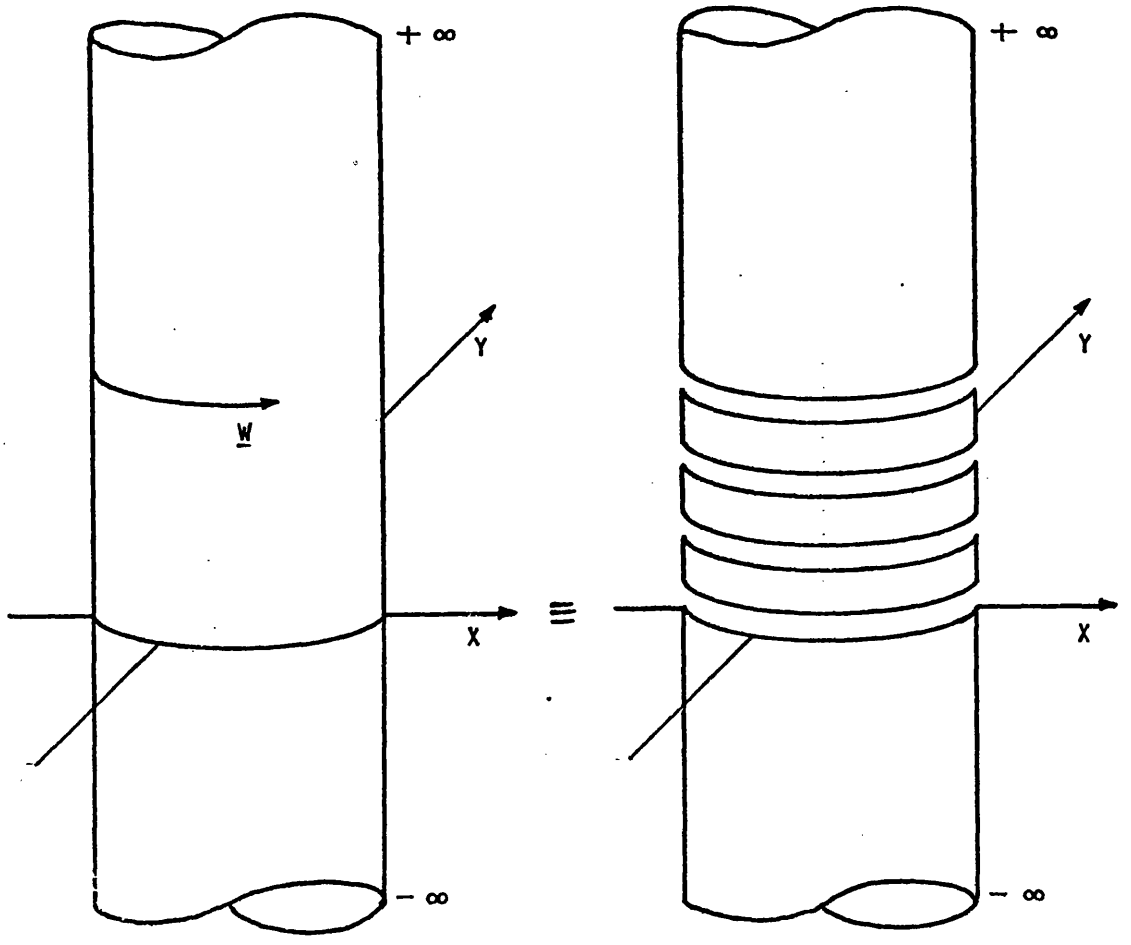

FIG. 4.3(b) APPROXIMATIONS FOR CVS

This arrangement allows the working section to be flexible.

The regions are approximated as follows:

1) The semi-infinite cylinders are represented by a series of plane semi-infinite strips on the sheet boundary fig 4.3 (c).

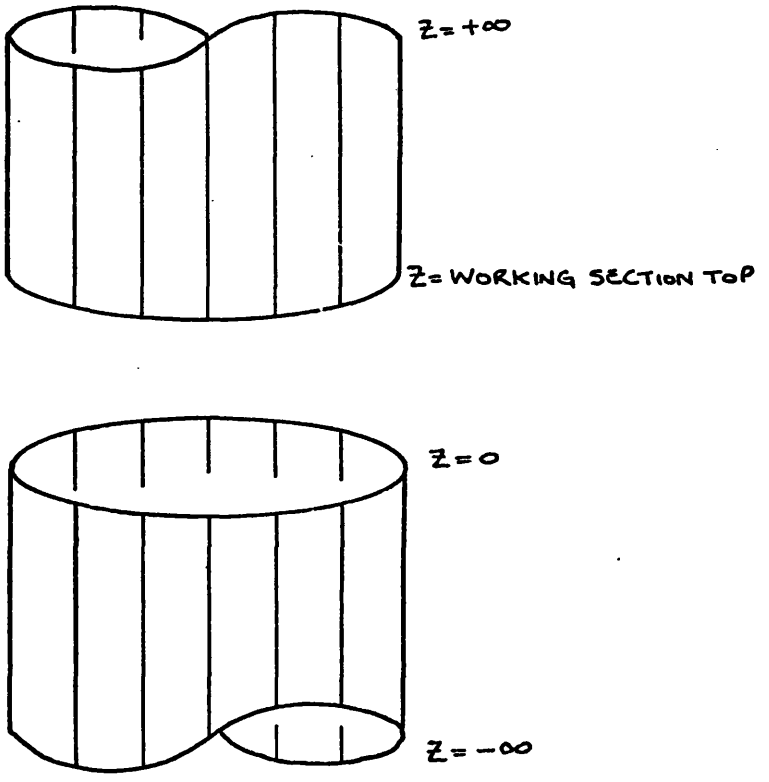

FIG.4.3(c) STRIP APPROXIMATIONS FOR SEMI-INFINITE VORTEX SHEETS

2) Each cylindrical section can be represented in 2 ways:
   a) similiar to a semi-infinite cylinder i.e. plane strips around the sheet boundary or,
   b) by a vortex ring at the mid-height of the cylindrical section.

4.22 CALCULATION OF THE SINGULARITY STRENGTHS

4.221 AXIAL VORTICITY VECTOR VORTEX SHEET

The irrotational flow around the jet can be calculated from the interaction of this sheet and the uniform flow. If the flow around the jet is already known, then the strength of the AVS may be calculated from it. The AVS is approximated by a series of vortex filaments around the sheet surface, their strengths depending on the local strength of the vortex sheet.

There are two methods of calculating the local sheet strength, depending upon whether or not the velocity distribution is known.

1. USING THE KNOWN VELOCITY DISTRIBUTION

Considering only the uniform flow and the AVS, then the velocity inside the sheet is zero everywhere, Von Mises(1953). The effect of the CVS may be neglected at this stage.

The irrotational flow is everywhere tangential to the AVS fig. 4.4(a)[55]

The strength of the sheet is equal to the velocity distribution around the cylinder, Chang (1942).

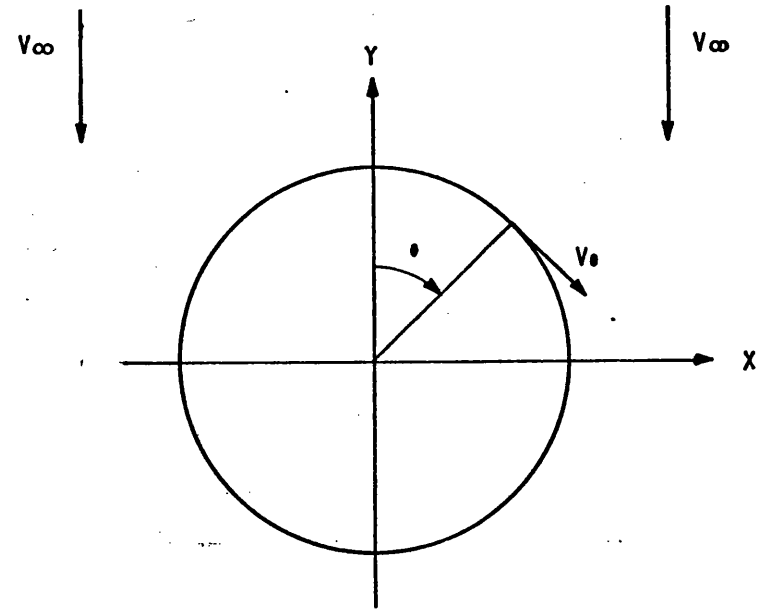

FIG.4.4 (b). CALCULATION OF VELOCITY DISTRIBUTION AROUND CYLINDER

The velocity distribution is given by, see fig 4.4(b)

$$V_\theta = 2V_\infty \sin\theta \qquad 4.1$$

Hence the strength of the AVS is given by

$$\sigma = 2V_\infty \sin\theta \qquad 4.2$$

The sheet is approximated by vortex filaments on the sheet surface. Consider fig. 4.5, where the surface is divided into N segments of which 3 are shown. Vortices are at position A,B and C.

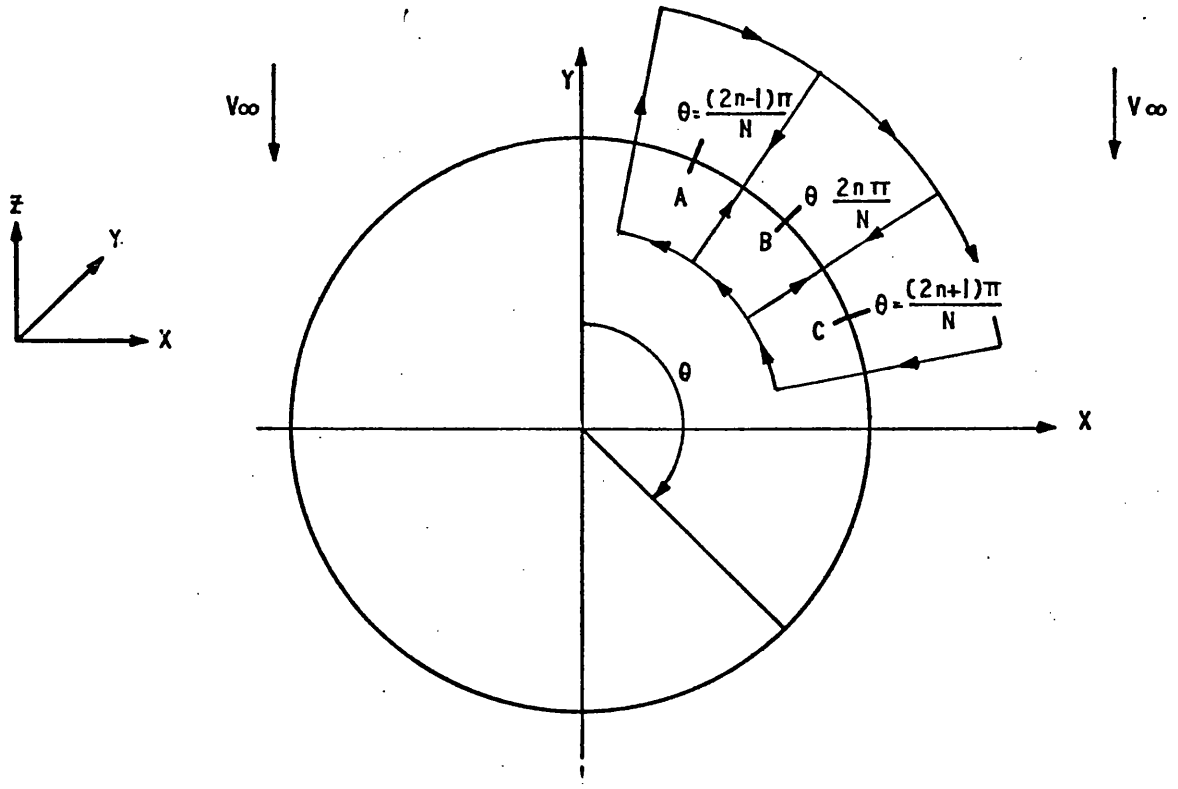

FIG.4.5 AXIAL VORTICES CIRCULATION CALCULATION

The strength of these vortices can be calculated from 4.2, see Chang (1942), as follows:

$$\Gamma = \oint \underline{V} . \underline{ds} \qquad 4.3$$

Where Γ = circulation

$\underline{V}$ = velocity vector

$\underline{ds}$ = element of surface.

Substituting 4.2 in 4.3

$$\Gamma = 2V_\infty \oint \sin\theta \, d\theta$$

$$\Gamma = 2V_\infty \int_{\theta_1}^{\theta_2} \sin\theta \, R \, d\theta$$

$$\Gamma_n = 2V_\infty R \int_{\frac{2n-1}{N}\pi}^{\frac{2n+1}{N}\pi} \sin\theta \, d\theta$$

$$\Gamma_n = -2V_\infty R \left[\cos\left(\frac{2n+1}{N}\right)\pi - \cos\left(\frac{2n-1}{N}\right)\pi\right]$$

$$\Gamma_n = -4V_\infty R \sin\frac{2n}{N}\pi \sin\frac{\pi}{N} \qquad 4.4$$

This was the method used in the model to calculate Γ_n

2. IF THE VELOCITY DISTRIBUTION IS NOT KNOWN

In the general case of a non circular jet the velocity distribution around the jet would be unknown and must first be calculated. Exactly the same technique as described in Chapter 3, Appendix 2, would be used to calculate the vortex sheet strengths.

In this method, the strengths of vortex sheets placed around the non-porous surface are calculated so that the tangential velocity boundary condition at the surface is satisfied. Thus a Fredholm Integral equation of the second kind is to be solved for this Neumann problem.

For the jet case, only Boundary Condition 1 (Appendix 2) is relevant since there are no source sheet strengths to calculate. In order to satisfy that boundary condition at each of the sheet collocation points, the induced effect of all the vortex sheets must be equal and opposite to the free stream velocity component at those points.

On solving the matrix equation A2.8 for the vortex sheet strengths, the velocity distribution is found directly, Duncan et al (1960). The vortex filament strength can be calculated either by method (1) or directly from the collocation point velocity.

4.222 CIRCUMFERENTIAL VORTICITY VECTOR VORTEX SHEET

The velocity field associated with CVS is divided into two. Everywhere inside the sheet, the velocity equals the specified jet velocity whereas the velocity is zero everywhere outside the sheet, Fig. 4.6(a)[56]. From Von Mises (1953), Duncan et al(1960), the strength of the CVS is equal to the jet velocity.

The strengths of the semi-infinite vortex sheets and the sheet cylindrical sections are also equal to the jet velocity. If any cylindrical section is represented by a vortex ring, then the circulation of the ring is given by

$$\Gamma_{RING} = V_{JET} * H \qquad 4.5$$

Where H is the height of the sheet cylindrical section, fig 4.6 (b)[56].

4.23. VELOCITIES INDUCED BY THE SINGULARITIES

In order to calculate the distortion and trajectory of the jet, the velocity induced by the singularities is calculated at various interrogation points. These are the intersection points between the vortex filaments, AVS, and the vortex rings, CVS. If a cylindrical section is used to represent a part of the CVS, then the interrogation points are at the intersection of the vortex filaments and the midheight of the cylindrical section.

4.231 AXIAL VORTICITY VECTOR VORTEX SHEET

The induced effect of the AVS at the interrogation points is calculated from the vortices representing it.

A vortex filament at $A'(x', y')$ fig 4.7, induces a velocity at $A(x,y)$ given by

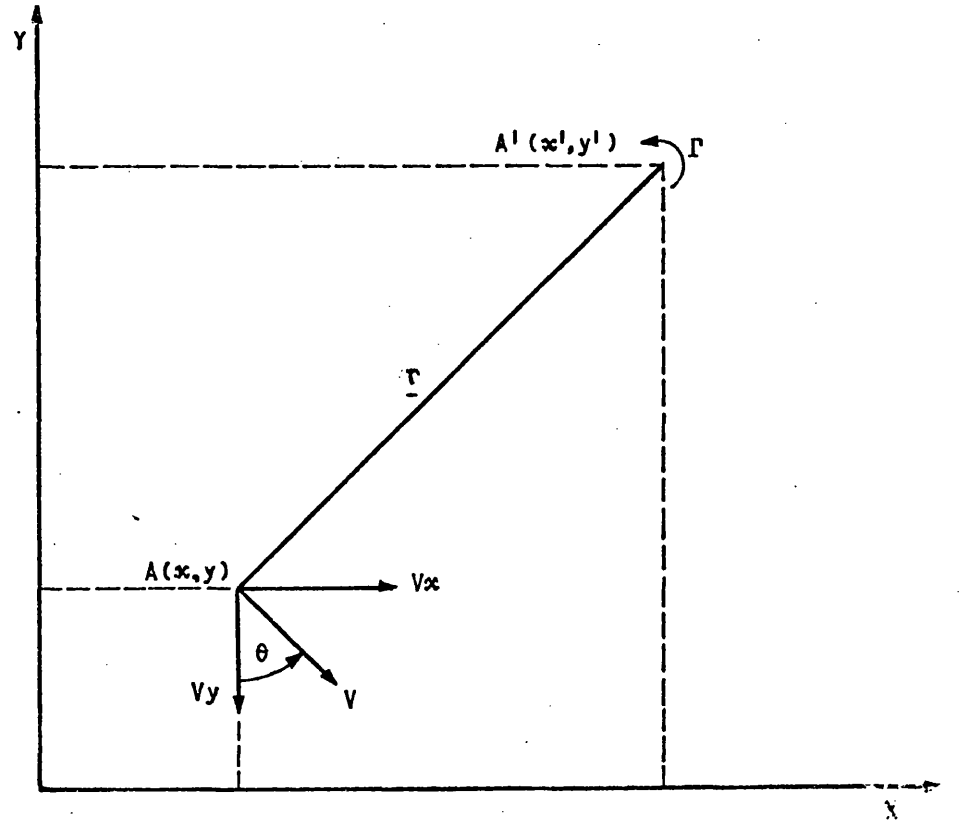

FIG.4.7 VELOCITY FIELD OF A VORTEX FILAMENT IN 2D

$$V_A = \Gamma / 2\pi |\underline{r}| \qquad 4.6$$

Where $|\underline{r}|$ is the distance from the vortex to the interrogation point A. Resolving 4.6 into components.

$$V_{x_A} = \frac{\Gamma (y' - y)}{2\pi \left[(y'-y)^2 + (x'-x)^2 \right]} \quad , \quad V_{y_A} = \frac{\Gamma (x - x')}{2\pi \left[(y'-y)^2 + (x'-x)^2 \right]} \qquad 4.7$$

Combining equations 4.4 and 4.7

$$V_{x_A} = -\frac{2}{\pi} V_\infty R \, \text{SIN} \left(\frac{\pi}{N} \right) \sum_{n=1}^{n=N} \frac{(y_n - y_A) \, \text{SIN} \left(\frac{2n}{N} \right) \pi}{\left[(y_n - y_A)^2 + (x_n - x_A)^2 \right]}$$

$$V_{y_A} = -\frac{2}{\pi} V_\infty R \, \text{SIN} \left(\frac{\pi}{N} \right) \sum_{n=1}^{n=N} \frac{(x_A - x_n) \, \text{SIN} \left(\frac{2n}{N} \right) \pi}{\left[(y_n - y_A)^2 + (x_n - x_A)^2 \right]} \qquad 4.8$$

Where N = total number of vortices representing the sheet.

When $n = A$, then $V_{x_A} = V_{y_A} = 0$, since a vortex cannot induce a velocity on itself.

These equations are for the velocity induced by a vortex in 2-D. When the jet is bent, such equations will not be valid.

Fig 4.8 shows a typical vortex filament which is approximated by a series of straight lines. The velocity induced by each of these straight line segments is summed to give the velocity induced by the vortex.

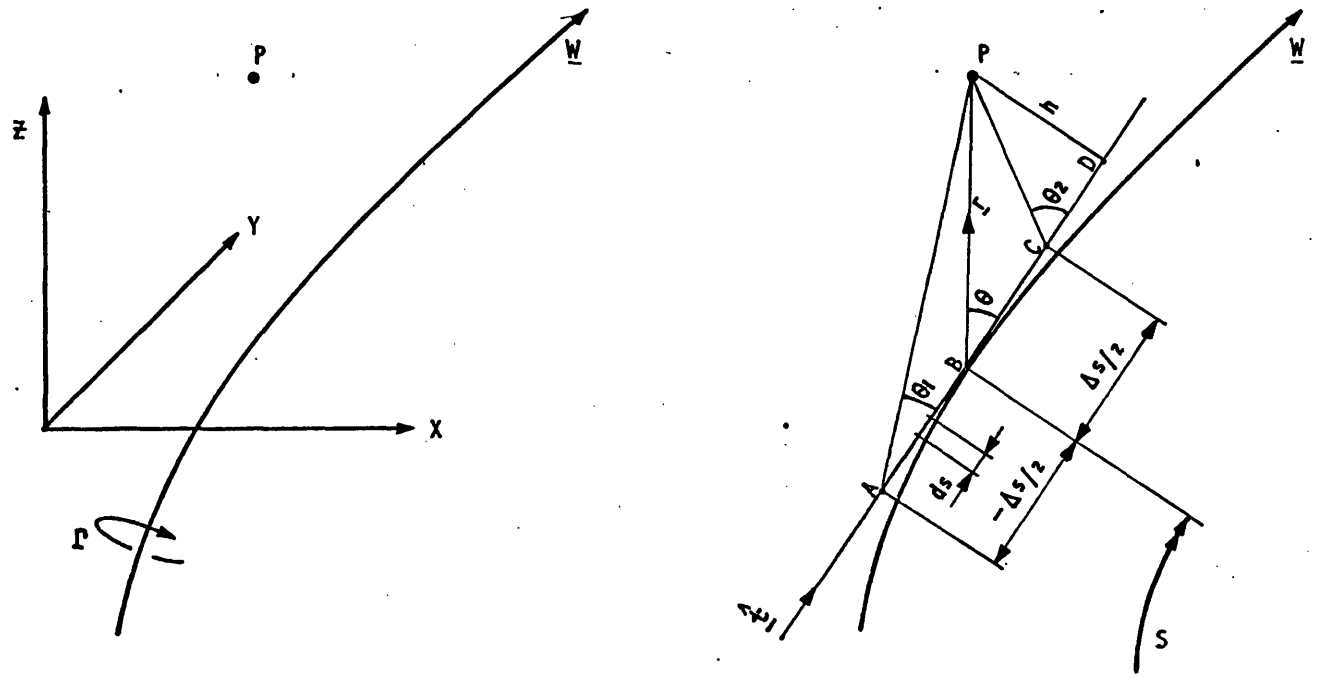

FIG.4.8 VELOCITY FIELD OF A VORTEX FILAMENT IN 3D

Following Skifstad (1969), the following equation for the velocity induced by one such segment can be derived.

$$\Delta V_p \left[= \frac{\Gamma}{4\pi} \int_{s-\Delta s/2}^{s+\Delta s/2} \frac{d\underline{s} \wedge \underline{r}}{|\underline{r}|^3} \right] = \frac{\Gamma}{4\pi} \frac{\hat{\underline{t}} \wedge \underline{r}}{h^2} I_1 \qquad 4.9$$

Where $\hat{\underline{t}}$ is a unit vector tangential to the vortex filament,

$h = |\hat{\underline{t}} \wedge \underline{r}|$ and

$$I_1 = \frac{\hat{\underline{t}} \cdot \underline{r} + \Delta s/2}{\left[h^2 + \left(\hat{\underline{t}} \cdot \underline{r} + \Delta s/2\right)^2\right]^{1/2}} - \frac{\hat{\underline{t}} \cdot \underline{r} - \Delta s/2}{\left[h^2 + \left(\hat{\underline{t}} \cdot \underline{r} - \Delta s/2\right)^2\right]^{1/2}}$$

The total velocity V_p induced at point P fig 4.8, is given by

$$V_p = \sum_{n=1}^{N} (\Delta V_p)$$

Where N = number of segments.

Hence

$$V_p = \frac{\Gamma}{4\pi} \sum_{n=1}^{N} \left[\frac{\hat{\underline{\epsilon}} \wedge \underline{r}}{h^2} \underline{I}_1 \right]_n \qquad 4.10$$

4.232 CIRCUMFERENTIAL VORTICITY VECTOR VORTEX SHEET

This sheet is approximated by 2 singularities:-

1) a semi-infinite cylindrical vortex sheet and
2) a cylindrical section vortex sheet (see section 4.213)

The induced effect of the CVS at the interrogation points is calculated using those approximations.

1) Semi-infinite cylindrical vortex sheet.

This sheet is represented by a series of plane rectangular semi-infinite vortex sheet strips spread around the sheet fig 4.9.[57] It is necessary to calculate the velocity induced by each of these vortex strips.

Fig A3.F1[178] shows asegment of one of these strips. The velocity components induced by this segment at the interrogation point P, are given by

$$V_{p_x} = \frac{\sigma}{4\pi} \left\{ \left[\sin^{-1}(\cos\beta_2 \cos\delta_1) - \sin^{-1}(\cos\beta_2 \cos\delta_2) \right] \right.$$

$$\left. - \left[\sin^{-1}(\cos\beta_1 \cos\delta_1) - \sin^{-1}(\cos\beta_1 \cos\delta_2) \right] \right\}$$

$$V_{p_y} = \frac{\sigma}{4\pi} \left\{ \left[\sinh^{-1}\left(\frac{\sin\beta_2}{\tan\delta_1}\right) - \sinh^{-1}\left(\frac{\sin\beta_2}{\tan\delta_2}\right) \right] \right.$$

$$\left. - \left[\sinh^{-1}\left(\frac{\sin\beta_1}{\tan\delta_1}\right) - \sinh^{-1}\left(\frac{\sin\beta_1}{\tan\delta_2}\right) \right] \right\} \qquad 4.11$$

Where σ is the sheet strength.
The derivation of these components is given in Appendix 3.

2) Cylindrical Section Vortex Sheet

This may be approximated in 2 ways (section 4.213). If plane strips are used, as above, the velocity components are calculated using equations 4.11.

If a vortex ring is used to represent the cylindrical section, the velocity induced by it is calculated using equation 4.10. Thus a vortex ring is approximated in the same manner as a 3-D vortex.

4.24 THE ANALYTICAL CALCULATION OF VELOCITIES INDUCED BY THE SINGULARITIES

To predict the distortion of the jet, it is necessary to calculate the influence of the various singularities on each other. This is made easier by approximating the singularities as already shown (section 4.21). For the jet to be modelled correctly, however, these approximations must accurately represent their parent singularities.

The analytic equations for the induced effect of the various singularities are given in this section. Details of the tests performed to establish the accuracy of the singularity approximations, are also given.

4.241 INFINITE VORTEX FILAMENT

The velocity induced by an infinite 2-D vortex filament is given by equation 4.6, and for an infinite 3-D vortex filament by equation 4.10. For the test, the velocity induced at an interrogation point was calculated, using first 8, then 16, vortices spaced evenly around the AVS boundary. The interrogation point was on the $Z = 0$ plane, and +ve and −ve infinity were taken at $Z = 1 \times 10^6$ and $Z = -1 \times 10^6$ units respectively.

The 2-D velocity components at the interrogation point were calculated using equations 4.8. To test the 3-D equation, 4.10, each vortex consists of 1 straight line, 2×10^6 units long. The corresponding velocity components were then calculated, and the results shown below.

	V_x	V_y	V_z	ERROR %
8 FILAMENTS ANALYTIC SOLUTION	-.730814	0	0	-
" " USING FILRIN	-.730872	0	0	.007936
16 " ANALYTIC SOLUTION	-.869378	0	0	-
" " USING FILRIN	- 869388	0	0	.000575

TABLE 4.1 VELOCITY INDUCED BY INFINITE FILAMENTS AND SIMULATED INFINITE FILAMENTS.

4.242. SEMI-INFINITE CYLINDRICAL VORTEX SHEET

In order to calculate the velocities induced by the CVS, the following equivalence was used:

- a surface covered uniformly with sources is equivalent to a vortex cylinder of semi-infinite length, whose generators pass through the boundary of the surface and are normal to it - Kuchemann (1953).

Two tests were performed:- calculating the velocity components at points both on and off the sheet.

1) INTERROGATION POINTS OFF THE SHEET

The velocity components induced by a disc uniformly covered with sources are tabulated in Kuchemann. They were obtained from graphical integration of the results for a single source ring. Fig 4.10 shows the disc & interrogation point.

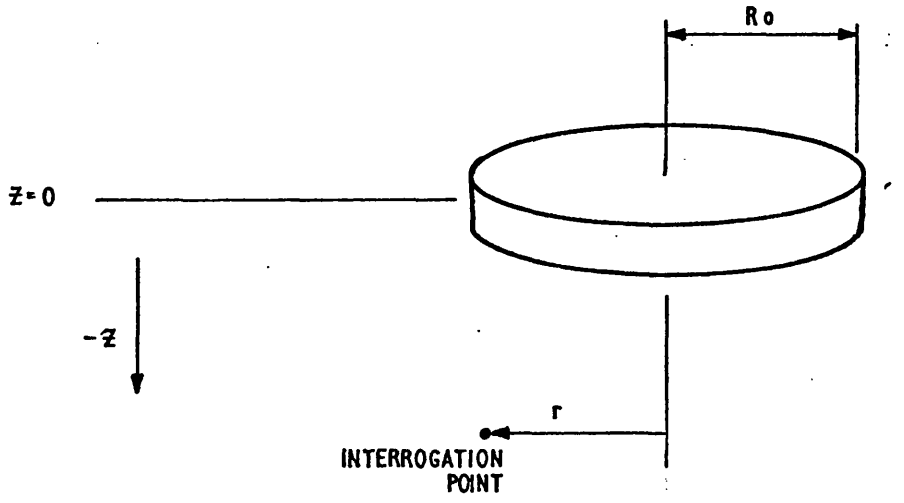

FIG.4.10 SOURCE DISC WITH INTERROGATION POINT

The velocity components induced by the plane rectangular strips approximating the CVS, are given by equations 4.11.

Using +ve infinity at $Z = 1 \times 10^6$, the velocity components at several points were calculated, and the results shown in table 4.2[58] and fig 4.11.[59]

2) INTERROGATION POINT ON THE SHEET

The velocity components induced by the CVS at a point on itself, Kuchemann (1953), are

$$\frac{\sigma}{2\pi}\frac{2}{\sqrt{(z/R_o)^2+4}}\left\{K\left(\frac{2}{\sqrt{(z/R_o)^2+4}}\right)-2D\left(\frac{2}{\sqrt{(z/R_o)^2+4}}\right)\right\}=V_r(z,R_o)$$

$$\frac{\sigma}{2\pi}\left\{\frac{\pi}{2}+\frac{z/R_o}{\sqrt{(z/R_o)^2+4}}K\left(\frac{2}{\sqrt{(z/R_o)^2+4}}\right)\right\}=V_z(z,R_o)$$

4.12

Where σ = sheet strength

$$k(k)=\int_0^{\pi/2}\frac{1}{\sqrt{1-k^2\sin^2\alpha}}\,d\alpha$$

$$E(k) = \int_0^{\pi/2} \sqrt{1 - k^2 \sin^2 \alpha}\, d\alpha$$

$$D(k) = \left(k(k) - E(k)\right) / k^2$$

The elliptic integrals were evaluated using a polynomial approximation, Abramowitz (1965), of order of accuracy 2×10^{-8}. The use of this approximation means that the velocities are no longer calculated analytically, but the the results will still be used to judge the accuracy of the velocities calculated from equation 4.11. The results are at least as accurate as Kuchemann, with whom they will be compared.

Numerical difficulties were experienced with equations 4.11, if the interrogation points were chosen on the strip edges.

Using +ve infinity at $Z = 1 \times 10^6$ and $Z = 1 \times 10^{12}$, the effect of lengthening the strips could be established. No difference was noticed, as the results below show

COMPUTATIONAL INFINITY	CASE	V_{RADIAL}	V_{AXIAL}	ERROR IN V_R %	ERROR IN V_Z %
	ANALYTIC SOLUTION	3.803189	7.151456		
1×10^6	8 segment sheet	3.375127	6.006623	-11.255	-16.008
1×10^6	16 segment sheet	3.757698	7.102613	-1.196	- .683
1×10^{12}	8 segment sheet	3.375127	6.606623	-11.255	-16.008
1×10^{12}	16 segment sheet	3.757698	7.102613	- 1.196	- .683

TABLE 4.3. VELOCITY INDUCED BY A SEMI-INFINITE CYLINDRICAL VORTEX SHEET AT A POINT ON ITSELF.

4.243 VORTEX RING

The velocity components induced analytically by a vortex ring are:

$$V_z(z,r) = \frac{\Gamma}{2\pi R_0} \frac{1}{\sqrt{z^2+(r+1)^2}} \left\{ K(k) - \left[1 + \frac{2(r-1)}{z^2+(r-1)^2} \right] E(k) \right\}$$

$$V_r(z,r) = \frac{\Gamma}{2\pi R_0} \frac{-z}{r\sqrt{z^2+(r+1)^2}} \left\{ K(k) - \left[1 + \frac{2r}{z^2+(r-1)^2} \right] E(k) \right\}$$

4.13

(Kuchemann)

Where Γ = circulation of vortex ring

R_0 = radius of vortex ring, $z = z/R_0$, $r = r/R_0$

$$k^2 = 4r/\left(z^2+(r+1)^2\right)$$

and elliptic integrals are as defined above.

The same polynomical approximation was used as above to evaluate the elliptic integrals.

Equation 4.10 is used to calculate the velocity components, using first 8 then 16, straight line segments defining the vortex ring. The position of the interrogation point relative to the ring is shown in fig. 4.12.

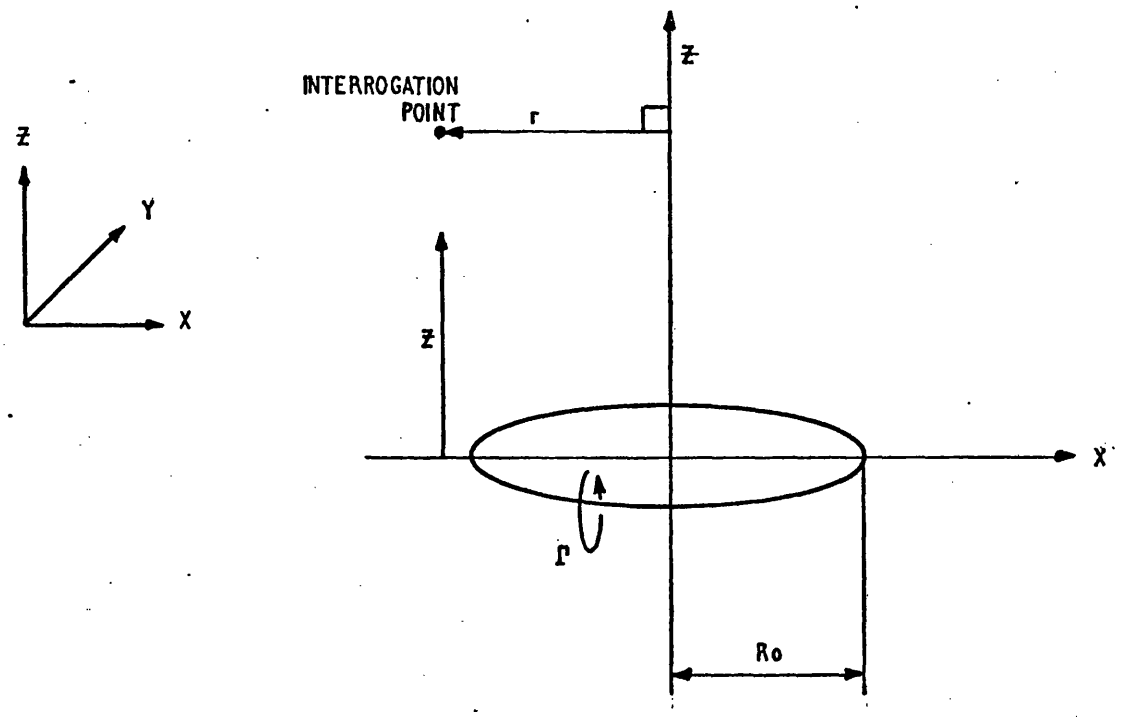

FIG 4.12. POSITION OF INTERROGATION POINT WITH RESPECT TO A VORTEX RING.

The results are shown in table 4.4[60] and fig. 4.13.[61] Very large errors were found in the calculated velocities when the interrogation points were near the vortex ring.

4.244. FINITE LENGTH CYLINDRICAL SECTION OF VORTEX SHEET

Section 4.213 described two ways of representing the cylindrical section. If the interrogation point was on the sheet, the vortex ring approximation breaks down by predicting infinite velocities. For this case, the plane strips approximation has to be used.

If the interrogation point is off the sheet, then either approximation could be used. Tests were performed to establish which gave the most accurate result.

1) INTERROGATION POINT OFF THE SHEET

Equation 4.10 was used to calculate the velocity induced by the vortex ring, using first 8, then 16, straight line segments. The use of the vortex ring implies using a double approximation i.e. the ring approximates the cylindrical section, and equation 4.10 uses straight line elements to approximate the ring.

The induced velocity using the plane strips approximation was obtained using equations 4.11. Fig. 4.14 shows the position of the interrogation point relative to the cylindrical section and vortex ring.

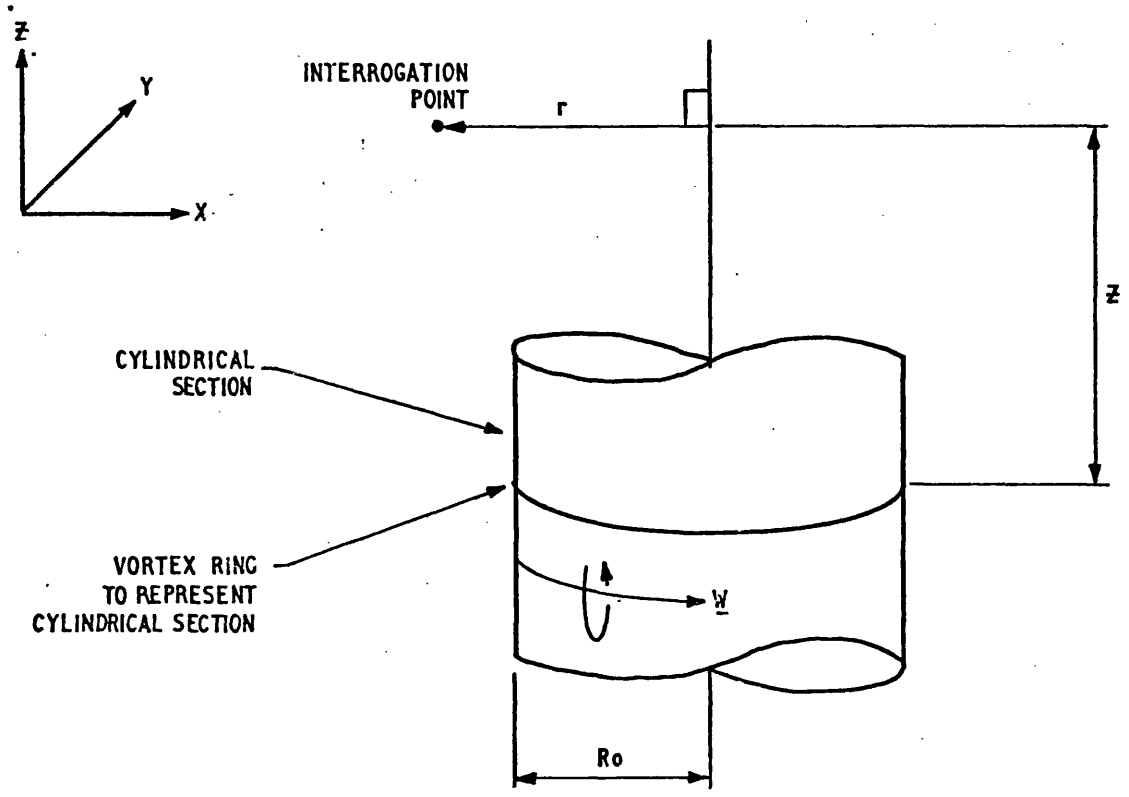

FIG 4.14. POSITION OF INTERROGATION POINT WITH RESPECT TO A CYLINDRICAL SECTION.

Kuchemann does not give the interrogation point velocities explicitly, but the values may be inferred from the velocities quoted for the source disc.

The results are shown in table 4.5 and in fig . 4.15.

2) INTERROGATION POINT ON THE SHEET

The analytic velocity components induced by the cylindrical section at a point on itself, are:

$$V_z(z,R_o) = -\frac{\sigma}{2\pi}\left\{\left[\sqrt{1-k_2^2}\,k(k_2)\right] - \left[\sqrt{1-k_1^2}\,k(k_1)\right]\right\}$$

$$V_r(z,R_o) = -\frac{\sigma}{2\pi}\left\{\left[k_2\left(k(k_2) - 2D(k_2)\right)\right] - \left[k_1\left(k(k_1) - 2D(k_1)\right)\right]\right\}$$

4.14

Where σ = sheet strength

$$k_1 = 2/\sqrt{(z/R_o)^2 + 4}$$

$$k_2 = 2/\sqrt{\left(\frac{z}{R_o} - \frac{L}{R_o}\right)^2 + 4}$$

and elliptic integrals are as defined above. The polynomial approximation was used as before to solve these integrals. Fig. 4.16 shows the interrogation point on the cylindrical section.

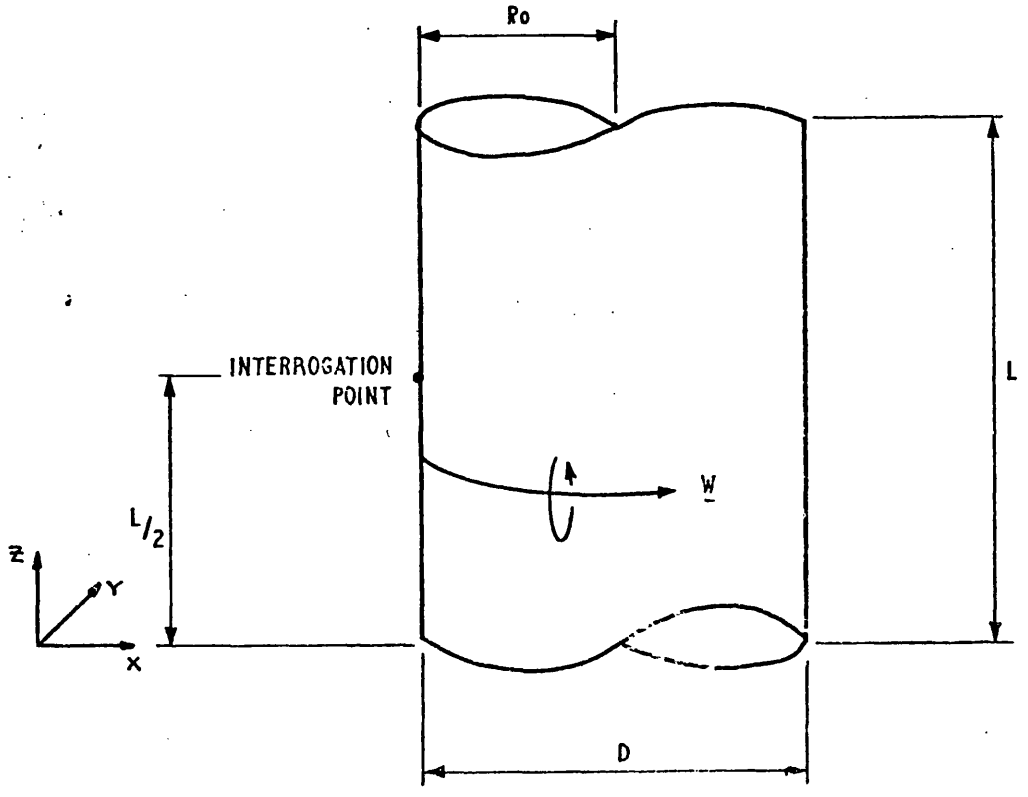

FIG 4.16. INTERROGATION POINT ON A CYLINDRICAL SECTION.

Equation 4.11 was used to calculate the velocity components using the strip approximation. The interrogation point was never chosen to be at any of the strip edges.

The results, shown in table 4.6, indicate large errors if 8 strips are used to represent the section.

Z/L	L/D	CASE	$V_{AXIAL(Z)}$	ERROR IN V_Z %
0.5	0.1	ANALYTIC SOLN.	5.697189	-
"	"	8 Segment Sheet	3.26297	-42.727
"	"	16 " "	4.830	-15.219

TABLE 4.6 VELOCITY INDUCED BY A CYLINDRICAL VORTEX SHEET OF FINITE LENGTH AT A POINT ON THE SHEET.

4.25 COMPARISON BETWEEN ANALYTIC VELOCITIES AND SINGULARITY APPROXIMATIONS.

[34]

Table 4.1 shows the velocities calculated both analytically and using equation 4.10, for a series of filaments. It can be seen that very little error is associated with dividing straight vortices into discrete elements, and summing the effect of the elements. This would be expected since no geometrical approximation to the original vortices is used.

When the 3-D Vortex filament is bent, however, then the straight line approximation, inherent in using equation 4.10, will not prove so accurate. A Vortex ring is a bent 3-D Vortex filament, and provides a means of testing the accuracy of the straight line approximation.

[61]

Fig. 4.13 shows the percentage error variation between the analytic velocities and those calculated using equation 4.10 for a vortex ring. There are two trends noticeable:

1) The errors are lower for a ring defined by 16 elements rather than 8. This would be expected since 16 straight line segment are a better approximation to the ring.

2) The errors decrease as the distance between the ring and the interrogation point increases. This again would be expected, since the farther the point is from the ring the smaller the difference between the segments and the ring becomes.

Also, the errors in V_Z are higher than those for V_R This may be due to the axial components at the interrogation point not being resolved in the axial direction. Thus all the individual errors accumulate. Each radial component at the interrogation point has to be resolved into the local radial direction, and so the errors tend to be self-cancelling.

The straight-line approximation for a vortex ring gives reasonable results provided there are a lot of segments , and the interrogation point is far away from the ring. These comments apply directly to a bent 3-D Vortex filament.

There were two tests performed on the approximation to the CVS:

1) For points off the sheet
2) For points on the sheet.

For interrogation points off the sheet, Fig 4.11[59] shows the error between the analytic velocities and those obtained using equation 4.11. It can be seen that 16 strips gives better results than 8 strips, which is the same trend as for the vortex ring approximation.

Also, as the distance of the interrogation point from the semiinfinite cylindrical vortex sheet increases, so the errors for the 16 strips first increase, then decrease. For the 8 strips, the errors generally increase. The fact that the errors decrease for the 16 strips is consistent, since the farther away the interrogation point is, then the effects

of any potential perturbation must diminish. Eventually, the errors for the 8 strips must decrease with increasing distance.

For points actually on the sheet, the results are given in table 4.3.[36] Again, the most accurate results are those with the higher definition sheet. The results of changing the position of the numerical infinity from $Z = 10^6$ to $Z = 10^{12}$ are included, and no increase in accuracy was achieved. Thus if greater accuracy were required then the number of strips should be increased.

The analytic velocities were calculated from a polynominal approximation to the elliptic integrals from Abramowitz. This approximation was at least as accurate as the results from Kuchemann, and was of the order of 2×10^{-8}

Tests were performed for the cylindrical section sheet as follows:-

1) To show whether it was the strip or vortex ring approximation which gave the most accurate representation of the cylindrical section at off-sheet interrogation points.
2) To establish how accurate the strip approximation was for points on the cylindrical section.

For the off-sheet interrogation points, the results are shown in table 4.5[62] and fig. 4.15.[64] Considering the 16 strip cylindrical section compared with the 16 segment ring, it can be seen that the strips gave the most accurate results for the points nearest the singularity, and the ring for points furthest away.

It can also be seen that the 8 strip approximation behaves quite contrary to expectation. Not only is it more accurate than the 8 segment ring for all distances tried, it is consistently more accurate than the 16 strip sheet. The reasons for this are unknown without further testing.

For interrogation points on the cylindrical section, the results are shown in table 4.6.[41] Again, a more accurate answer is obtained with the higher number of strips. Even with 16 strips, the answers are not sufficiently accurate, but the use of more strips would involve more computer time.

4.26 CONCLUSIONS FROM TESTS.

1) Subdividing the vortex sheets into vortex filaments, rings etc, is a sufficiently good approximation for calculating the induced velocities of the vortex sheets.
2) Using more singularities to approximate the vortex sheet increases the accuracy of the induced velocity.

To summarise, the two cylindrical vortex sheets, the AVS and CVS, are approximated as follows:-

a) By semi-infinite cylindrical vortex sheets, which are represented by semi-infinite plane strips around the sheet circumference.

b) By infinite filament and vortex rings, which are represented by straight line elements, along the filaments and around the rings.

c) By vortex sheet cylindrical sections which are represented by plane strips for points on the section and on the ring adjacent to the section.

For all other interrogation points, the cylindrical section can be represented by a vortex ring.

A computer program, described in Appendix 4, was written to predict the behaviour of the 3-D jet in a crossflow. The approximations listed above were used to calculate the velocities induced at the interrogation points by the CVS and AVS. The points were then allowed to move at those velocities for a certain time, before the jet was frozen and the velocity field recalculated.

4.3. PROGRAM TESTS.

The following runs were performed maintaining the jet speed at 100, and varying the crossflow velocity as follows:

CROSSFLOW VELOCITY	
40	
100	
500	
1000	
1500	
2000	
2500	
3000	4 iterations
3000	8 iterations
3000	12 iterations.

Table 4.7

The end elevation, plan & isometric views of the working section were obtained for the fourth iteration of each of the runs. The same views were obtained for the eight and twelth iterations of the 3000 crossflow velocity case.

Fig. 4.17[65] shows the working section at X - flow 1500

Fig. 4.18[66] shows the plan of the working section at X-flow 2000

Fig. 4.19[67] shows the plan of the working section at X-flow 2500

Fig. 4.20[68] shows the working section at X-flow 3000 4th iteration

Fig. 4.21[69] shows the working section at X-flow 3000 12th iteration

4.4. DISCUSSION

The general shape of the working section was known from Thompson (1971), Wooler (1969), Hackett (1969) etc. To achieve this shape, the jet speed was maintained constant whilst the wind speed was altered, see table 4.7. Altering the jet speed would not have radically altered the working section shape.

At dimensionless wind speeds of 40 and 100, no movement was detected away from the cylindrical shape. Between wind speeds of 500 and 1000, there was a very slight movement progressing to a more definite movement downstream of the working section top.

Fig. 4.17[65] shows anisometric view of the working section at wind speed of 1500. Although there was a smooth transition between the bottom and top of the working section, at this stage of the calculation there was no tendency to develop into a kidney shape.

The vortex filament strength can be seen from equation 4.4 to be proportional to the wind speed. Thus increasing the wind speed will make the induced effect of the vortices on each other greater, since their circulation will have increased. This results in the jet cross-section distorting into a kidney shape in fewer iterations. Figs. 4.18[66] and 4.19[67] show this effect for wind speeds of 2000 and 2500 respectively.

The solution for the wind speed of 3000 was built up by a sequence of 12 iterations. Figs. 4.20[68] and 4.21[69] show the isometric views of the working section after the 4th and 12th iterations respectively. The working section has developed further as a result.

Fig. 4.21[69] shows that the transition between the bottom and top of the working sections is disjointed. This could be caused by:

1) errors in the approximations.

2) Disregarding several Vortex rings. This was necessary because the total number of interrogation points was too great for the plotting programme.

Actual running showed that a timestep of 0.0001 usually led to stable results. If the timestep was incorrect for a particular combination of jet and wind speeds, then instability, characterised by the vortex sheets crossing one another, set in.

Thompson (1971), also calculated the 3-D jet using a vortex lattice method, but his method differed in the treatment of the semi-infinite cylindrical vortex sheets. Instead of the bottom semi-infinite sheet,he used a source covered disc, and approximated this with triangular patches. Thompson did not include any correlation of the accuracy of this approximation. It is not known whether Thompson's method leads either to quicker computation or yields greater accuracy than the strip method.

Other techniques used by Thompson were:-

1. Spiralling effect.

At an interrogation point near a vortex filament, Thompson introduced a correction for the spiralling effect in the velocity induced by the vortex. However, considering the degree of approximation already used in describing the filaments, it is doubtful whether such a correction would increase the overall accuracy of the method.

2. Jet rolling up.

He found that the jet rolled up soon after the calculation had started. He overcame this by displacing the interrogation points a distance proportional to a weighted velocity. This was an average between the velocity induced at the interrogation point, and a corresponding point above the plane boundary. As the calculation progressed, this initial stabilization process gradually became inoperative.

The rolling up was probably due to the jet coming out from an infinite flat plate. The present writer had no such problems, provided the timestep was carefully chosen.

3. Jet exit procedure.

Since the jet was exhausting from a plane boundary, Thompson had to take into account the image vortices, both filaments and rings. This was a major difference between the two methods, and meant that Thompsons approach did represent more accurately a combustion chamber dilution hole jet.

Using the image vortices is a means of satisfying the boundary conditions on the infinite plane. In order to extend either method to predict a 3-D jet inside a combustion can, the boundary conditions on the can surface could be satisfied using an Integral equation approach. This would have meant superimposing source sheets over the surface, and calculating their strengths each time the jet moved i.e. at each iteration.

Thompson also introduced a new vortex ring at the exit of the hole, representing the section just exhausted. In order to keep the number of rings constant, he removed one from the top of the jet. The author also introduced a new ring into the working section, but this represented unfreezing the jet and allowing the working section to have more flexibility. No rings were removed from the authors method, as this would have meant the CVS was not being properly approximated.

If the current method were to be made more accurate, the following improvements should be incorporated:-

1) Circulation of filaments and rings.

The circulation of the filaments and rings is calculated from the strengths of the AVS and CVS. As the jet bends and distorts, so the shape of the two sheets will alter. Since the filaments and rings approximate a local section of those sheets, so their circulation ought to be calculated from the shape of the local sections. This could be done at each iteration, and would incorporate the effect of shape change on circulation. This is not done at present.

2) Cylindrical Section Sheet Strips.

When the jet was bent and distorted, the shape of the cylindrical section was assumed to be the same as when the jet was unaltered. The strip edges were assumed to be perpendicular to the ring and the same length i.e. equal to $A_1 A_2$ or $A_2 A_3$ fig A4.F2,[191] as at the start of the calculation.

This is in error since the strips no longer follow accurately the CVS, fig. 4.22.[70] Some mechanism to allow the strips to follow the CVS would have to be incorporated.

3) Infinite filament or infinite strip.

In the program at present, where a filament passes through an interrogation point, that filament is ignored when calculating the interrogation point velocity. This is not accurate when the filament is bent. In this case, an infinite strip of the AVS should have been used in place of the filament in exactly the same way as a cylindrical section strip is used in place of a vortex ring.

This would also have to be incorporated in any future program.

Thompson also calculated the surface pressure distribution behind the deformed jet. He found that this was not greatly different from that of an undeformed jet, because of the dominant influence of the lower portion of the lattice. He further concluded that the full Navier-Stokes equations need to be solved in order to predict the true development of the 3-D jet flow.

Predicting the 3-D jet flow was meant as a preliminary to calculating the combustion chamber flow. Considering that some mechanism for predicting the vorticity has to be added to the 3-D method, and that a cannular combustor would have typically 6-7 dilution holes, the final program would be computationally slow.

4.5 CONCLUSIONS

1. Using the techniques shown, it is possible to predict the behaviour of an irrotational 3-D jet in a crosswind.
2. Methods of improving the program have been highlighted.
3. The surface pressure distribution is not accurately predicted.
4. This method is not readily extendable to predicting viscous flows.
5. For viscous flows, a solution of the full Navier-Stokes equation should be attempted.

4.6 FURTHER WORK

1. Instead of using strip approximations to the semi-infinite sheets, the source covered discs technique of Thompson should be used.
2. The methods of improving the programme described in section 4.4 should be incorporated.
4. For calculating an irrotational 3-D jet in a combustion chamber, this method coupled with an Integral equation approach for satisfying the boundary conditions should be attempted.

ROLLS ROYCE

TYPICAL COMBUSTOR FLOW PATTERN

Date

FIG. 4-1 (a)

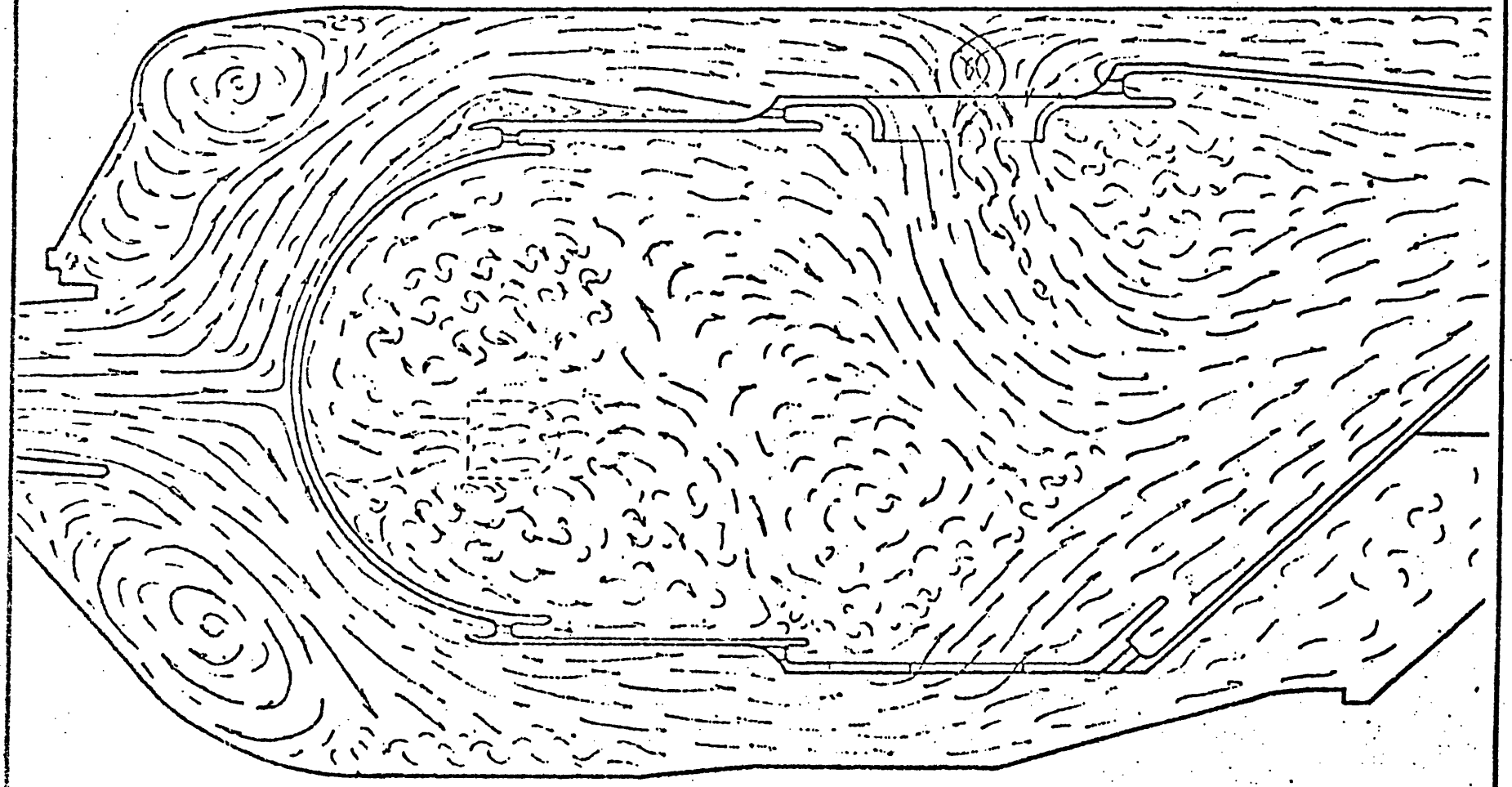

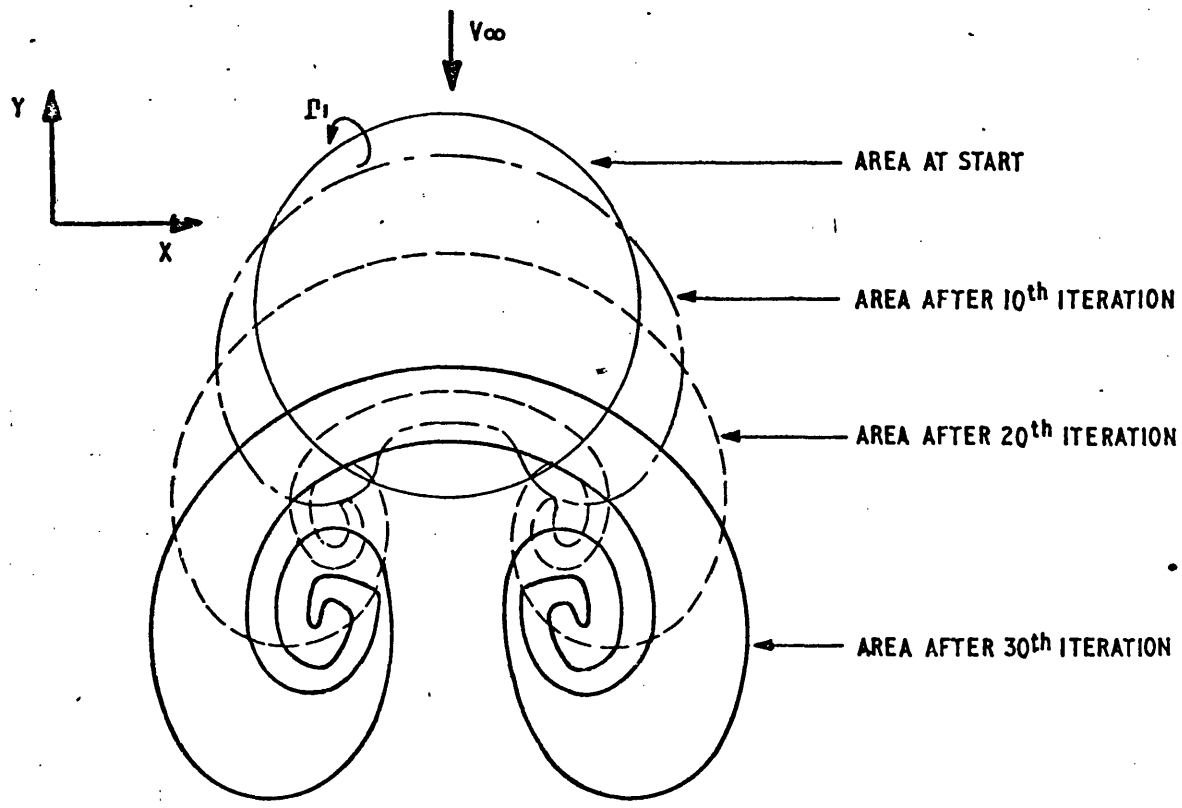

FIG.4.1(b). DISTORTION OF A 2-D JET IN A CROSSFLOW

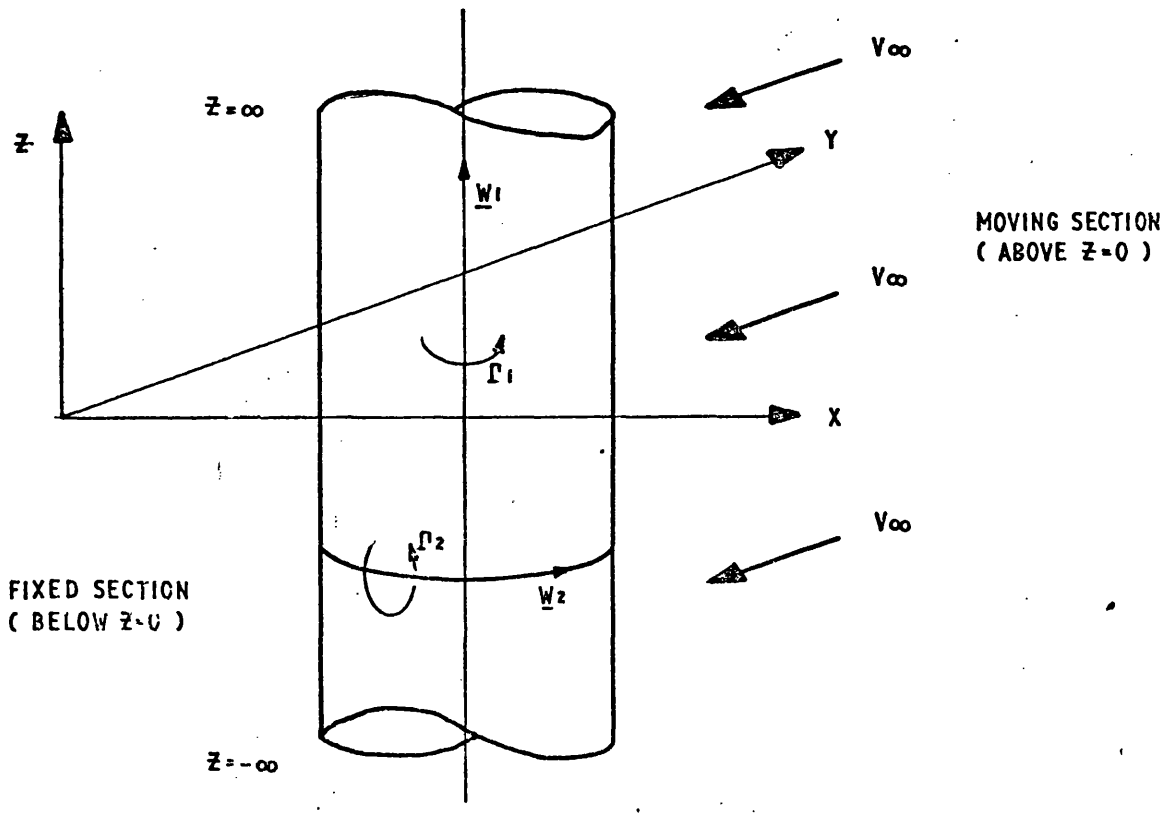

FIG.4.1(c). VORTEX SHEETS USED FOR A 3-D JET IN A CROSSFLOW

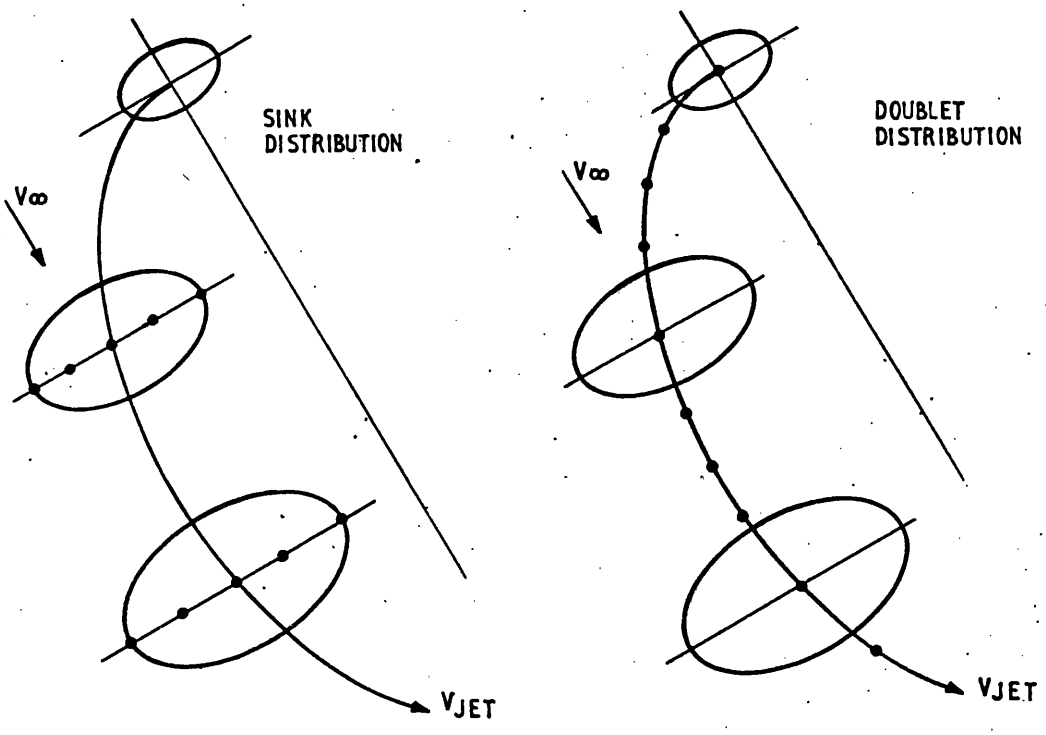

FIG 4.2(a) DISTRIBUTION OF SINKS AND DOUBLETS ALONG JET PATH

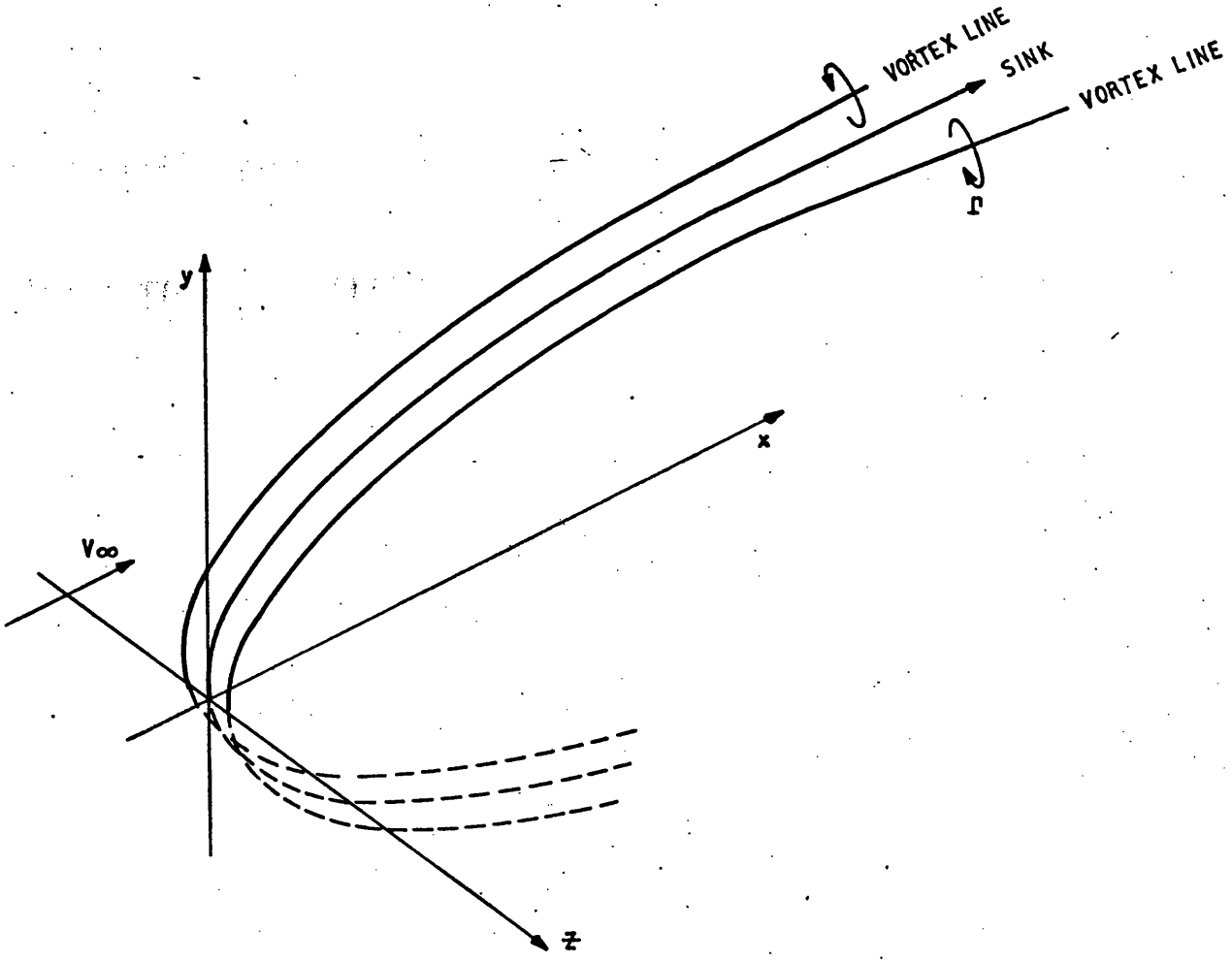

FIG 4.2(b) SKIFSTAD'S MODEL FOR THE 3-D JET.

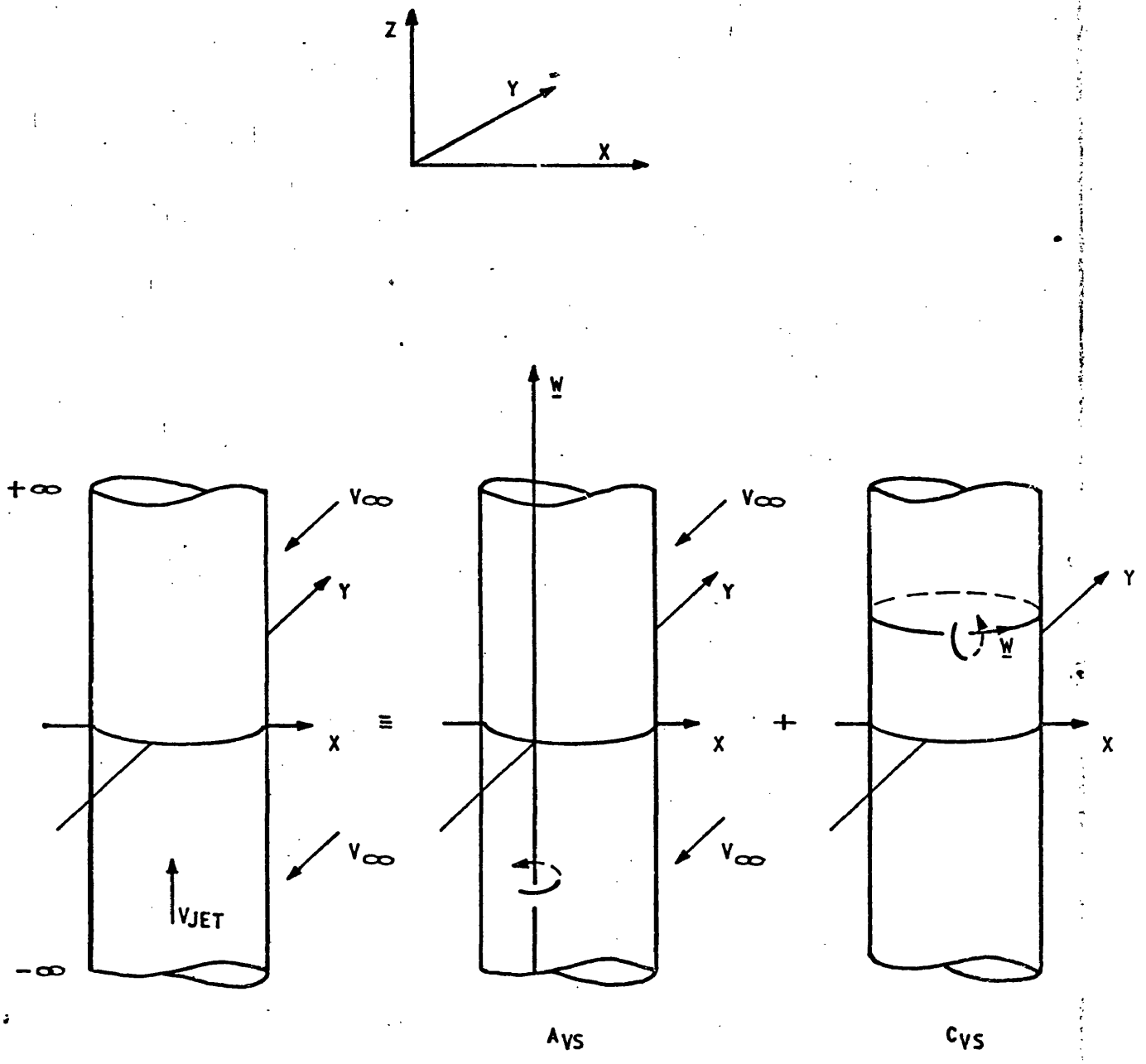

FIG.4.2c. PICTORIAL REPRESENTATION OF THE THREE POTENTIALS SUPERPOSITIONED TO GIVE IRROTATIONAL FLOW OF 3-D JET IN SUBSONIC CROSSWIND

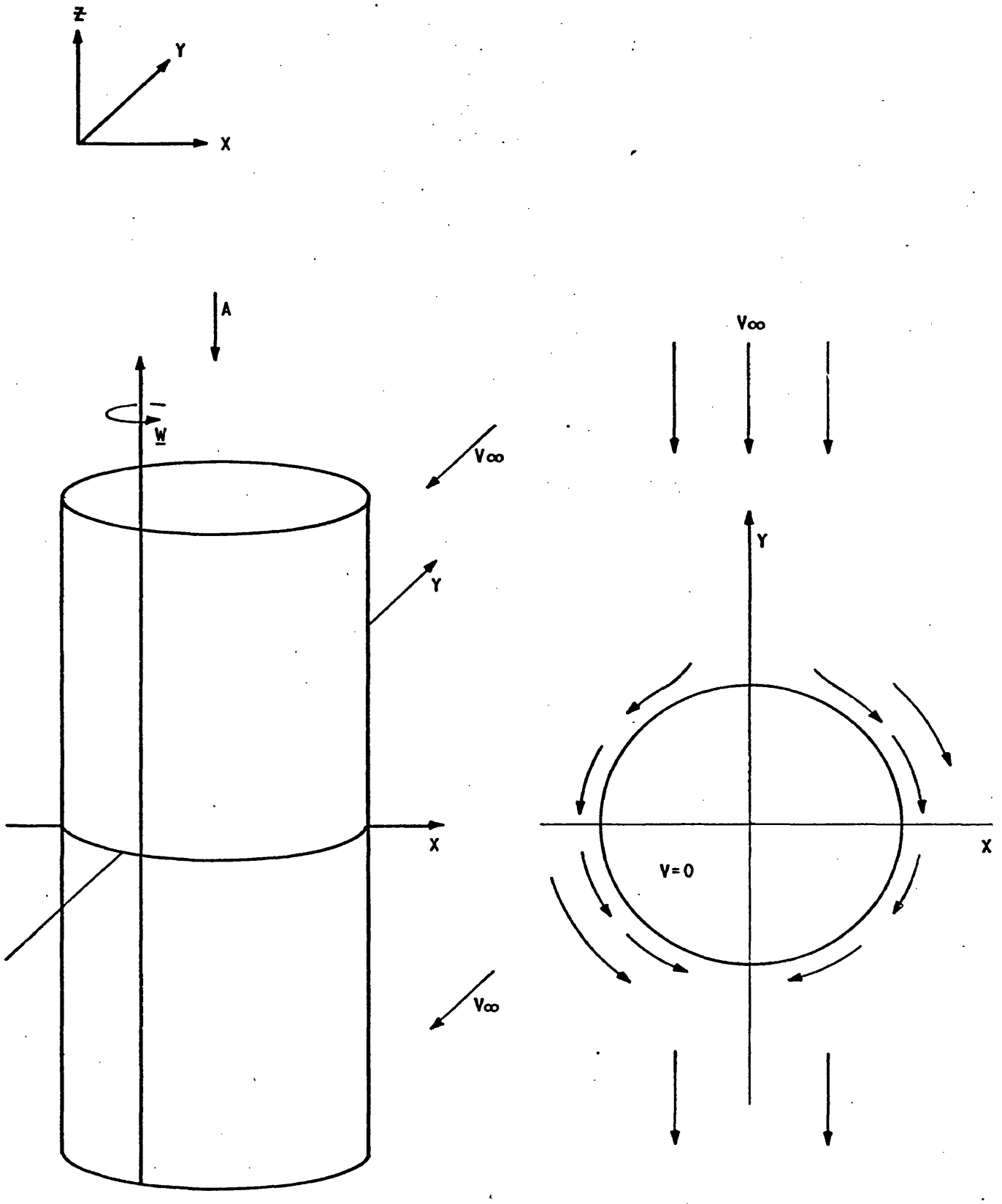

GENERAL VIEW OF AXIAL VORTICITY VECTOR VORTEX SHEET

VIEW OF SHEET IN DIRECTION 'A'

FIG.4.4 (a). AXIAL VORTICITY VECTOR VORTEX SHEET SHOWING FLOW AROUND VORTEX SHEET

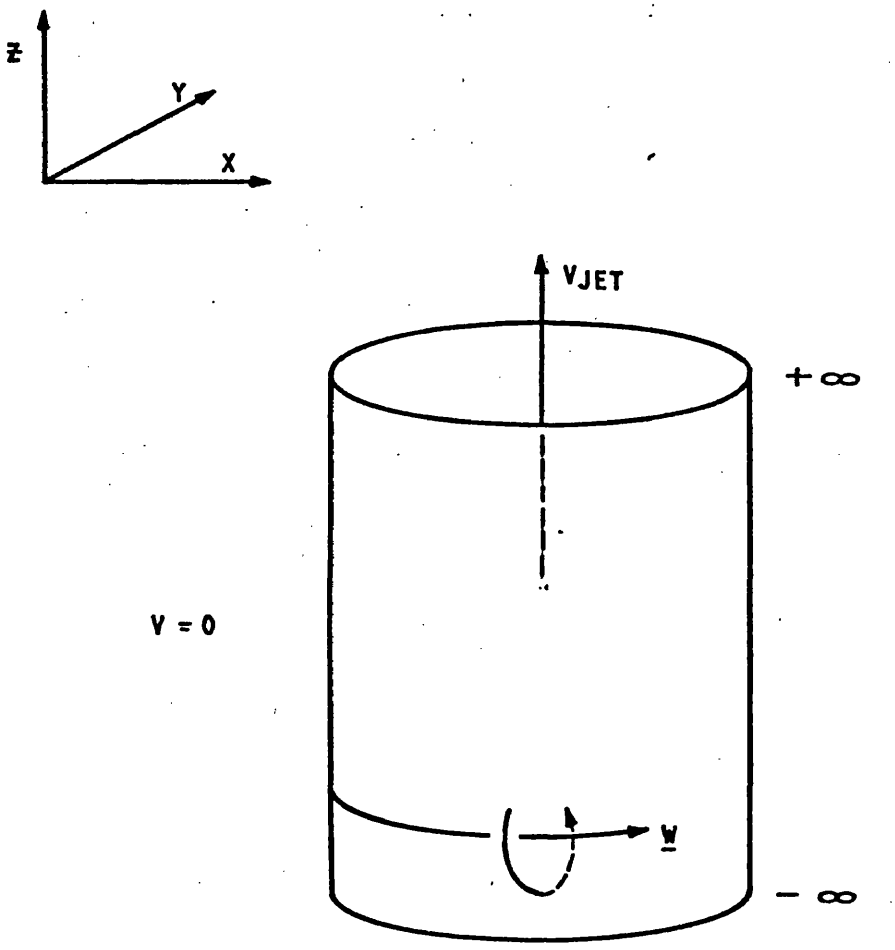

FIG.4.6(a) CIRCUMFERENTIAL VORTICITY VECTOR VORTEX SHEET
(SHOWING JET VELOCITY)

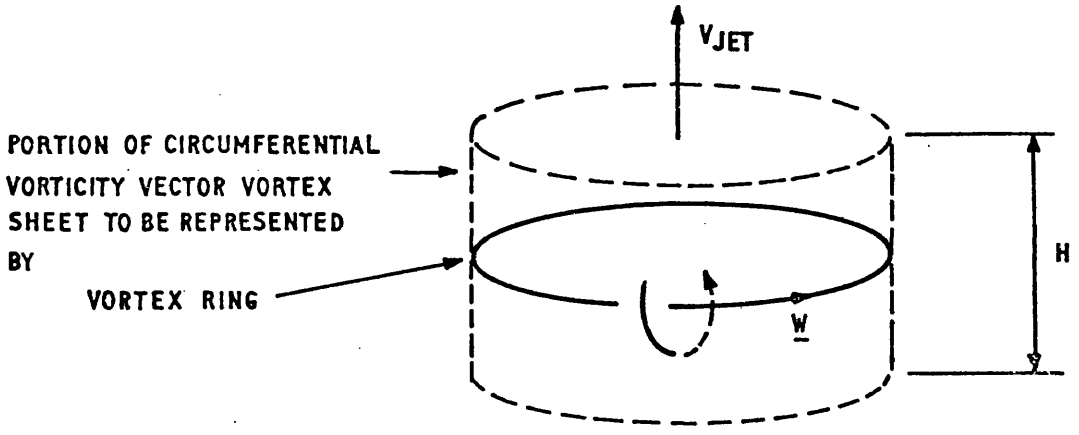

FIG. 4.6(b). VORTEX RING REPRESENTATION OF A PORTION OF VORTEX SHEET

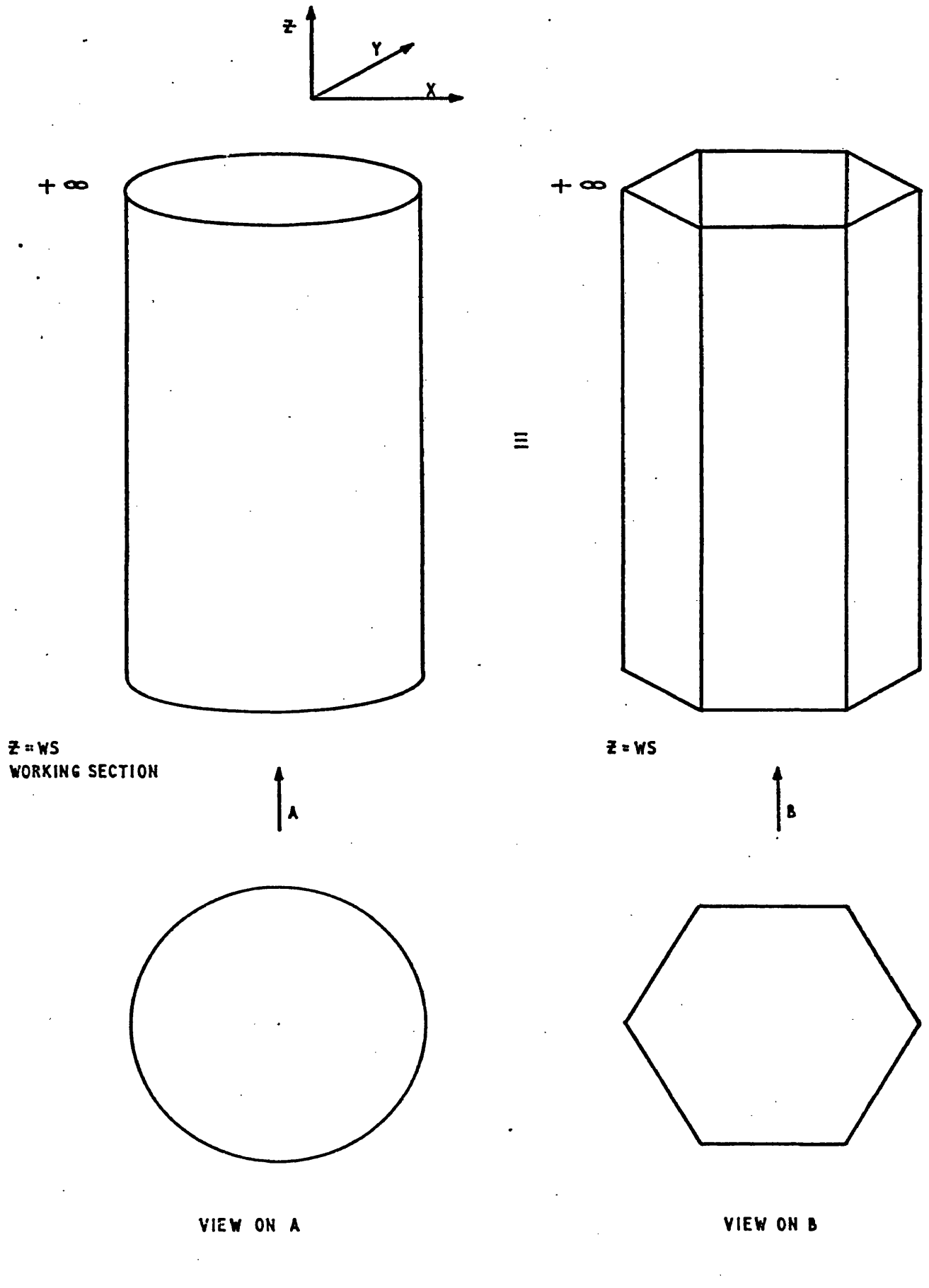

FIG. 4.9. APPROXIMATION OF A SEMI-INFINITE CYLINDRICAL VORTEX SHEET

z/Ro	r/Ro	CASE	V_{RADIAL}	$V_{AXIAL(z)}$	ERROR IN Vr %	ERROR IN V_Z %
1	1	Ref Kuchemann	- .629	.891	-	-
		8 segmentsheet	- .566	.853	-10.016	-4.26
		16 " "	- .616	.878	- 2.067	-1.46
		Ref	- .852	1.066	-	-
.8	1	8 segment sheet	- .788	1.027	- 7.51	-3.66
		16 " "	- .804	1.047	- 5.63	-1.78
		Ref	-1.178	1.273	-	-
.6	1	8 segment sheet	-1.109	1.255	- 5.86	-1.41
		16 " "	-1.154	1.26	- 2.04	-1.02
		Ref	-1.711	1.544	-	-
.4	1	8 segment sheet	-1.618	1.574	- 5.44	1.94
		16 " "	-1.720	1.535	+ 0.526	-.58
		Ref	-2.730	1.910	-	-
.2	1	8 segment sheet	-2.566	2.129	- 6.01	11.47
		16 " "	-2.710	1.93	- 6.733	1.047
		Ref	00	2.499	-	-
0	1	8 segment sheet	-4.162	4.375		75. 07
		16 " "	-6.4	4.688		87.60

TABLE 4.2. VELOCITY INDUCED BY A SEMI-INFINITE CYLINDRICAL VORTEX SHEET (EQUIVALENT TO A UNIFORM DISTRIBUTION OF SOURCES OVER A CIRCULAR DISC).

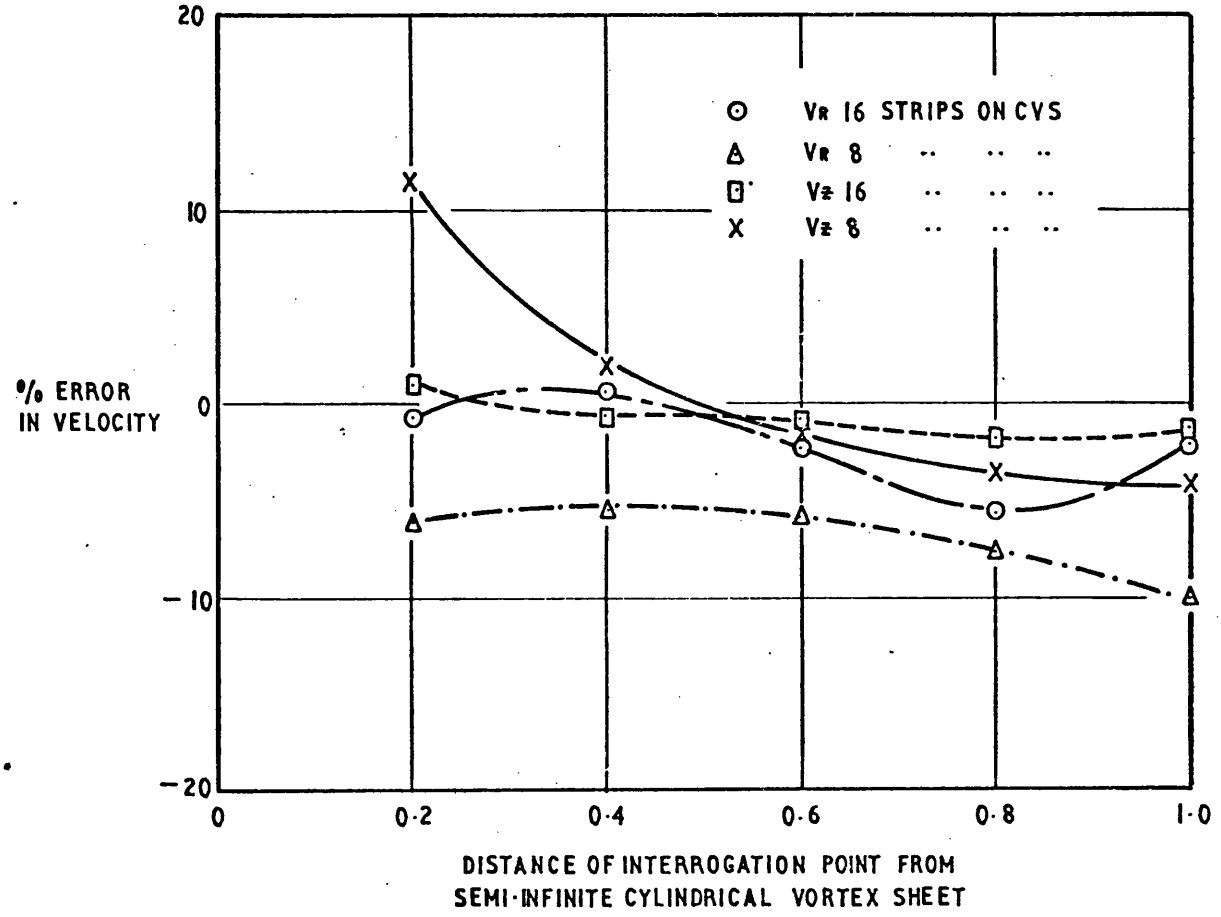

FIG.4.11. COMPARISON OF VELOCITY INDUCED AT INTERROGATION POINTS OFF THE SEMI INFINITE VORTEX SHEET

z/Ro	r/Ro	CASE	V_{RADIAL}	V_{AXIAL}	ERROR IN V_R %	ERROR IN V_Z %
		ANALYTIC SOLN.	-3.140797	.537859	-	-
.1	1	8 POINT RING	-2.919076	.269526	-7.059	-49.842
		16 " "	-3.092856	.372704	-1.526	-30.642
		ANALYTIC SOLN.	-1.523734	.425162	-	-
.2	1	8 POINT RING	-1.4285	.261338	-6.25	-38.532
		16 " "	-1.506072	.348126	-1.159	-18.119
		ANALYTIC SOLN.	-.974254	.358286	-	-
.3	1	8 POINT	-.919904	.248790	-5.582	-30.561
		16 POINT	-.964308	.316974	-1.0239	-11.53
		ANALYTIC SOLN.	-.694505	.309974	-	-
.4	1	8 POINT	-.659022	.233442	-5.109	-24.69
		16 POINT	-.688044	.285313	-.9303	-7.956
		ANALYTIC SOLN.	-.524179	.271958	-	-
.5	1	8 POINT	-.498756	.216482	-4.85	-20.399
		16 POINT	-.519270	.255830	-.936	-5.9303
		ANALYTIC SOLN.	-.409585	.240616	-	-
.6	1	8 POINT	-.390184	.199128	-4.737	-17.242
		16 POINT	-.405612	.22927	-.97	-4.715
		ANALYTIC SOLN.	-.327506	.214046	-	-
.7	1	8 POINT	-.311936	.182010	-4.754	-14.967
		16 POINT	-.324172	.205595	-1.018	-3.947
		ANALYTIC SOLN.	-.266198	.191126	-	-
.8	1	8 POINT	-.253326	.16573	-4.836	-13.288
		16 POINT	-.26298	.184554	-1.209	- 3.439
		ANALYTIC SOLN.	-.219034	.171130	-	-
.9	1	8 POINT	-.208116	.150442	-4.985	-12.089
		16 POINT	-.216552	.165846	-1.133	-3.0877

TABLE 4.4 VELOCITY INDUCED BY VORTEX RING; ANALYTIC & APPROXIMATE RESULTS.

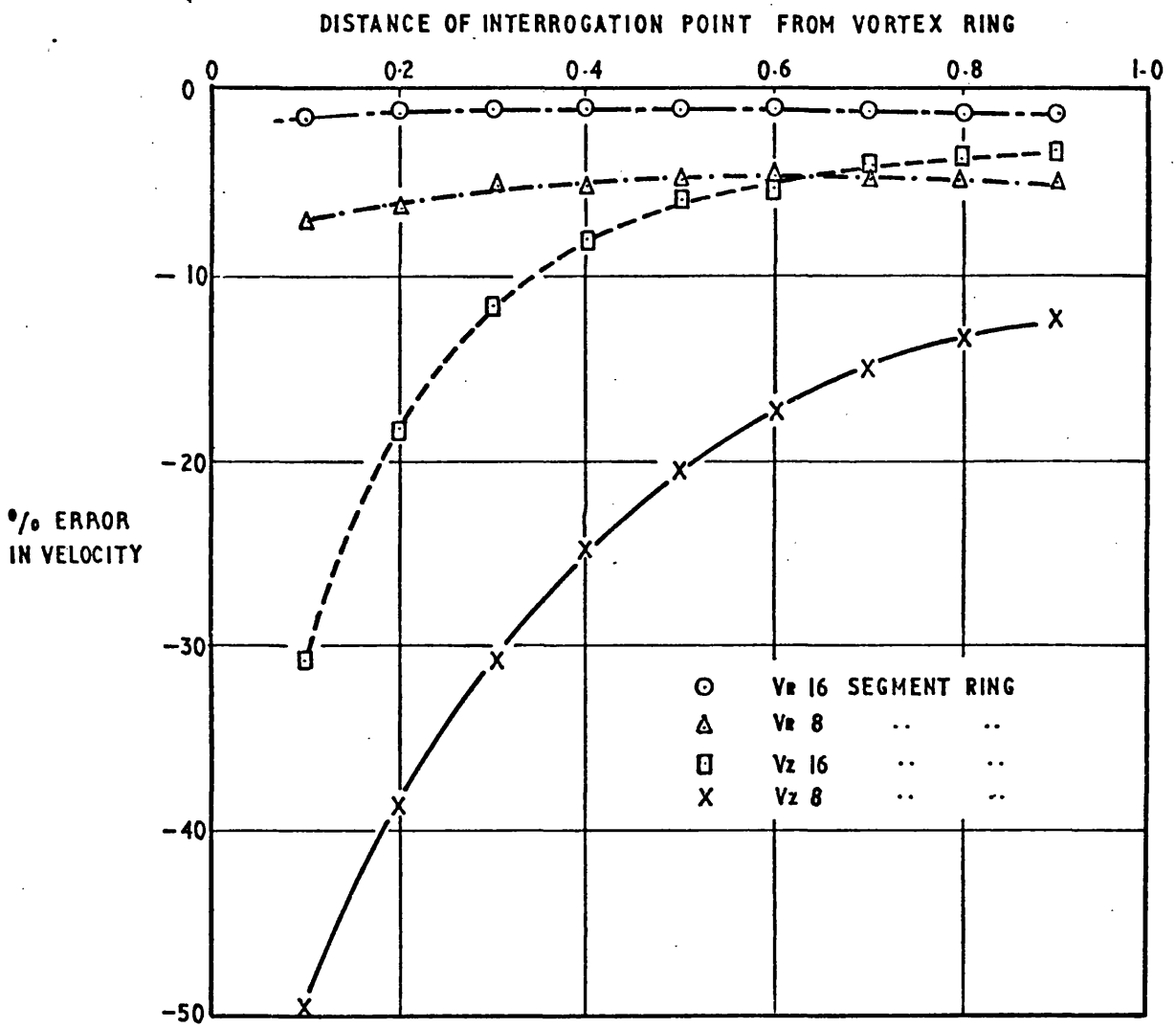

FIG.4.13. COMPARISON BETWEEN VELOCITIES INDUCED AT POINTS BY APPROXIMATIONS TO A VORTEX RING

Z/R_o	r/R_o	CASE	V_{RADIAL}	V_{AXIAL}	ERROR IN V_R %	ERROR IN V_Z %
MEAN		Ref Kuchemann Page 328	-1.0186	.3661	-	-
.3	1	8 segment Sheet	-.9486	.5546	-6.873	51.519
		16 " "	-.9866	.3936	-3.141	7.512
.3	1	8 segment Ring	-.9199	.2488	-9.688	-32.035
		16 " "	-.9643	.3170	-5.329	-13.408
MEAN		Ref Kuchemann Page 328	-.5332	.2706	-	-
.5	1	8 segment Sheet	-.5088	.3195	-4.569	18.097
		16 " "	-.5737	.2751	7.600	1.667
.5	1	8 segment Ring	-.4988	.2165	-6.454	-19.99
		16 " "	-.5193	.2558	-2.607	-5.445
MEAN		Ref Kuchemann Page 328	-.3263	.2069	-	-
.7	1	8 segment Sheet	-.3213	.2276	-1.535	10.017
		16 " "	-.3492	.2130	7.045	2.936
.7	1	8 segment Ring	-.3119	.1820	-4.392	-12.03
		16 " "	-.3242	.2056	-.6421	-.6297
MEAN		Ref Kuchemann Page 328	-.2228	.1751	-	-
.9	1	8 segment sheet	-.2273	.1739	2.0227	-.6837
		16 " "	-.1925	.1695	-13.611	-3.206
.9	1	8 segment Ring	-.2081	.1504	-6.597	-14.068
		16 " "	-.2166	.1658	-2.811	-5.269

P.T.O.

TABLE 4.5 VELOCITY INDUCED AT A POINT BY A CYLINDRICAL SECTION OF VORTEX SHEET WHICH IS REPRESENTED BY SHEET SEGMENTS/RING SEGMENTS/DISTRIBUTION OF SOURCES OVER DISC.

Z/R_o	r/R_o	CASE	TOTAL VELOCITY	% ERROR.
Mean		Kuchemann et al	1.0824	-
.3	1	8 segment Sheet	1.0988	1.5215
		16 " "	1.0622	-1.8641
.3	1	8 segment Ring	0.9530	-11.9568
		16 " "	1.0151	-6.2180
Mean		Kuchemann et al	0.5979	-
.5	1	8 segment Sheet	0.6008	0.4898
		16 " "	0.6362	6.4121
.5	1	8 segment Ring	0.5437	-9.0616
		16 " "	0.5789	-3.1812
Mean		Kuchemann et al	0.3863	-
.7	1	8 segment Sheet	0.3937	1.9121
		16 " "	0.4091	5.8828
.7	1	8 segment Ring	0.3612	-6.5192
		16 " "	0.3839	-.6386
Mean		Kuchemann et al	0.2834	-
.9	1	8 segment Sheet	0.2862	.9982
		16 " "	0.2564	-9.4981
.9	1	8 segment Ring	0.2568	-9.3760
		16 " "	0.2728	-3.7419

TABLE. 4.5 CON'T ABSOLUTE TOTAL VELOCITY INDUCED AT A POINT BY A CYLINDRICAL SECTION OF VORTEX SHEET REPRESENTED BY SHEET SEGMENTS/RING SEGMENTS/DISTRIBUTION OF SOURCES OVER DISC.

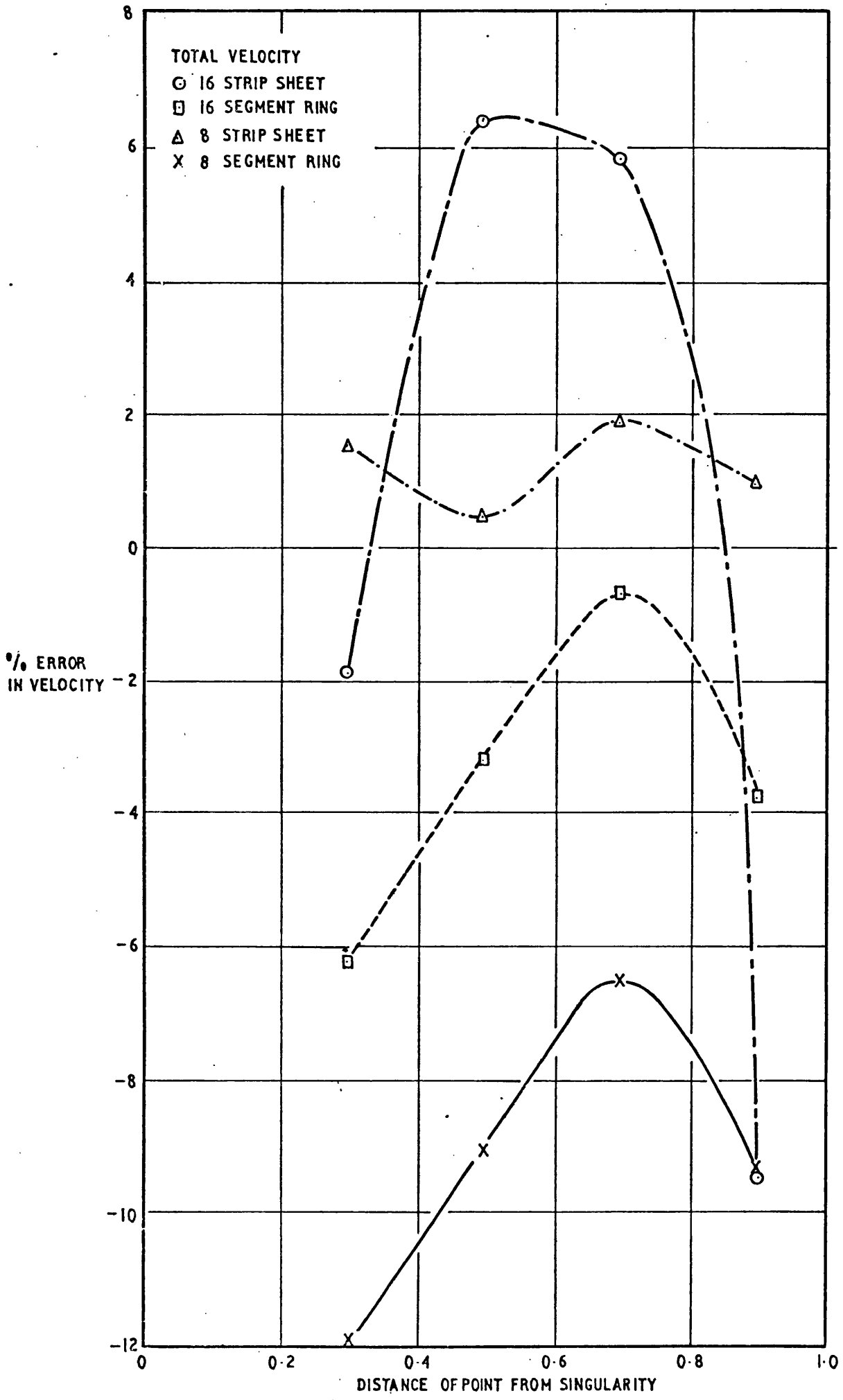

FIG 4.15. COMPARISON OF VELOCITIES INDUCED AT AN INTERROGATION POINT BY THE VORTEX STRIPS AND VORTEX SEGMENTS

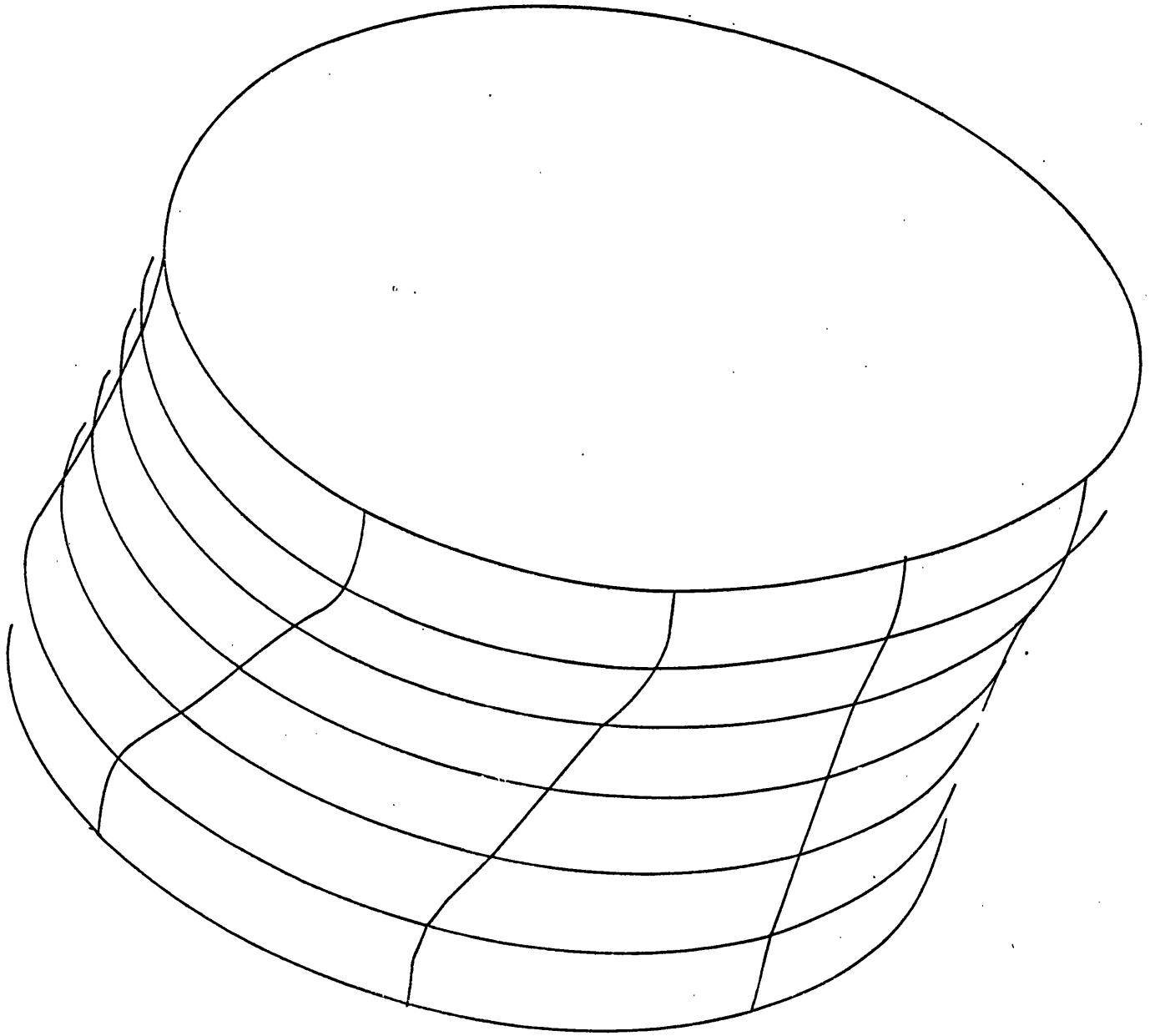

FIG. 4.17 WORKING SECTION AT X-FLOW 1500

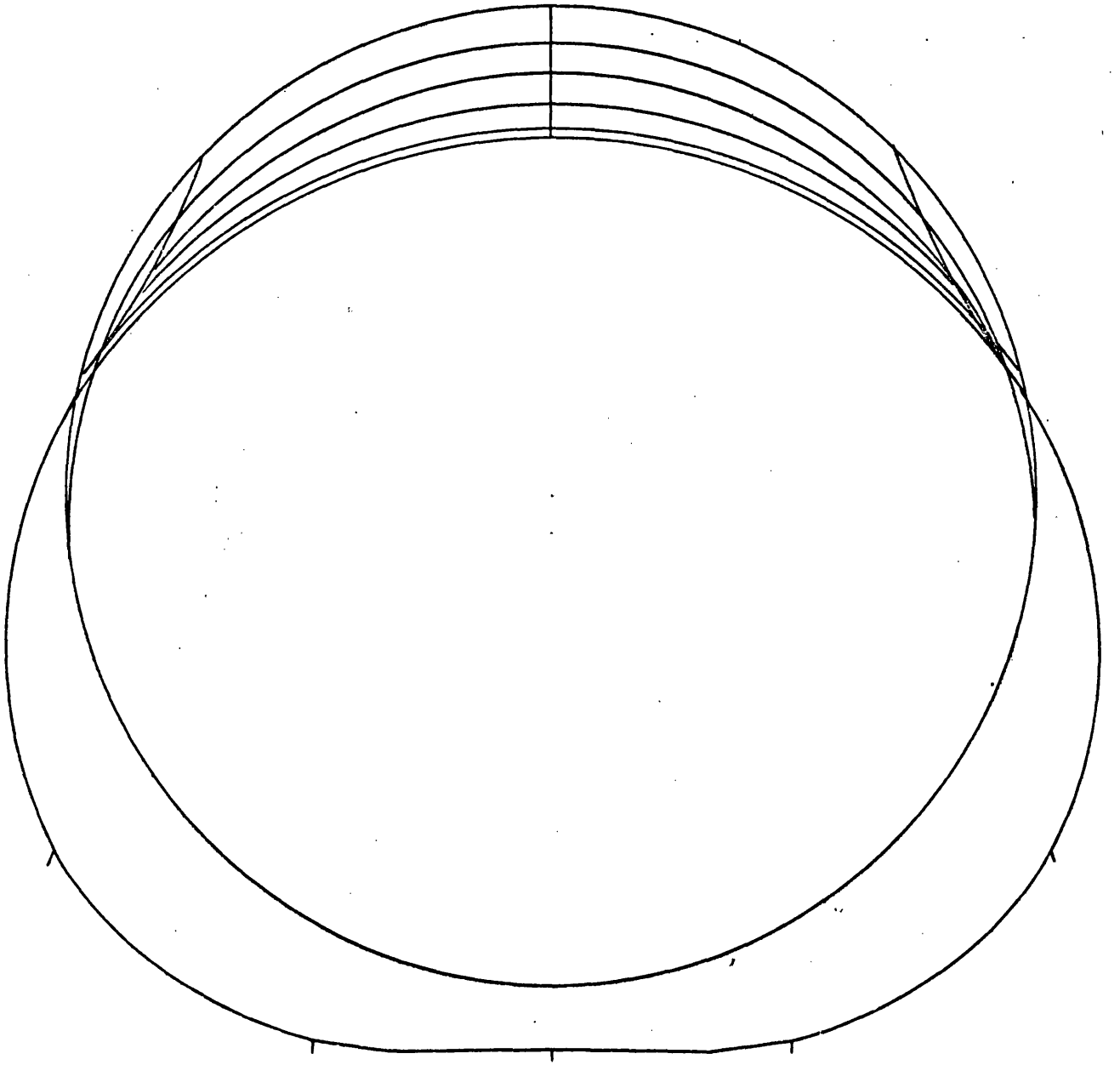

FIG.4.18 PLAN VIEW OF WORKING SECTION X-FLOW 2000

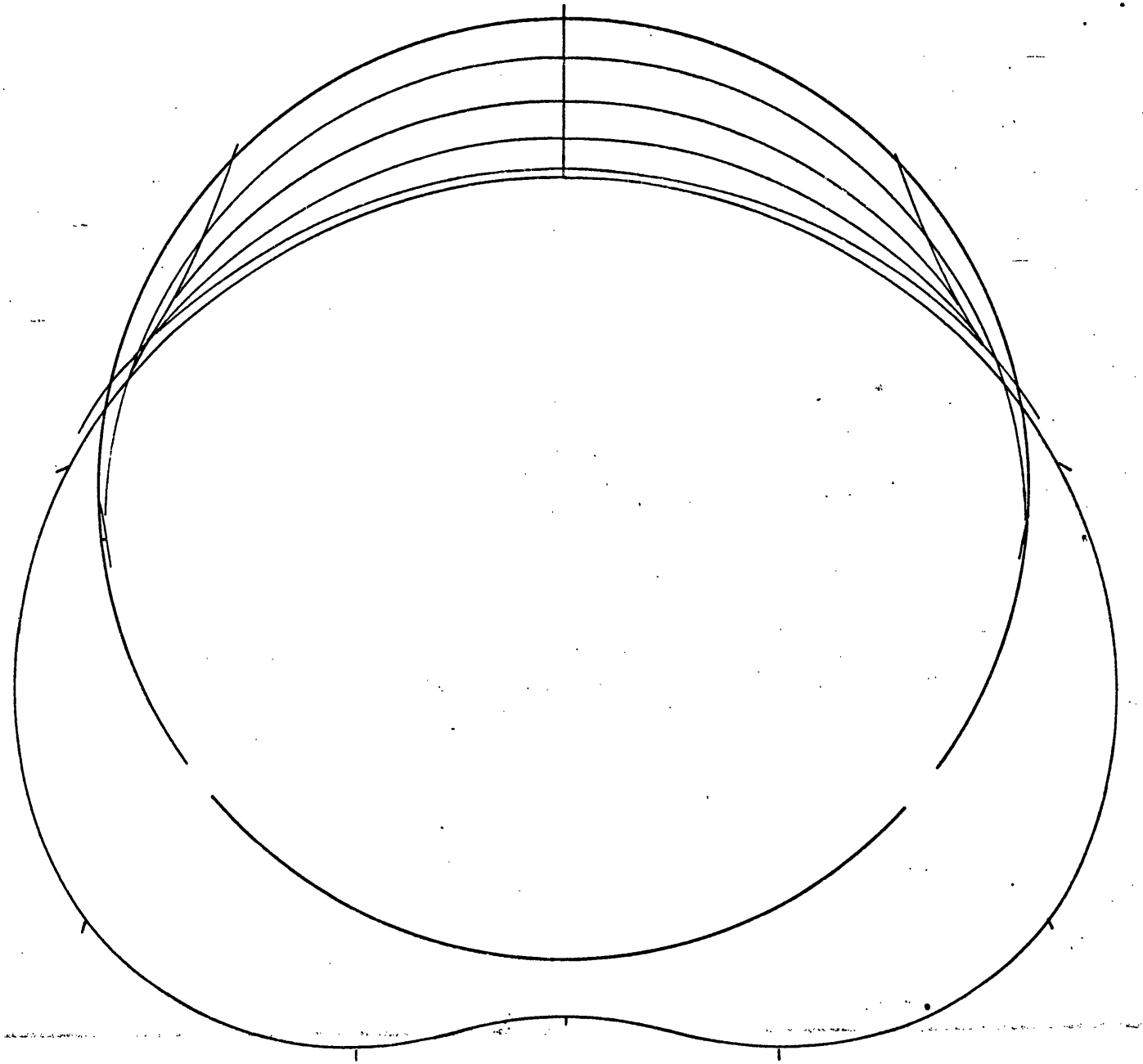

FIG.4.19 PLAN VIEW OF WORKING SECTION X-FLOW 2500

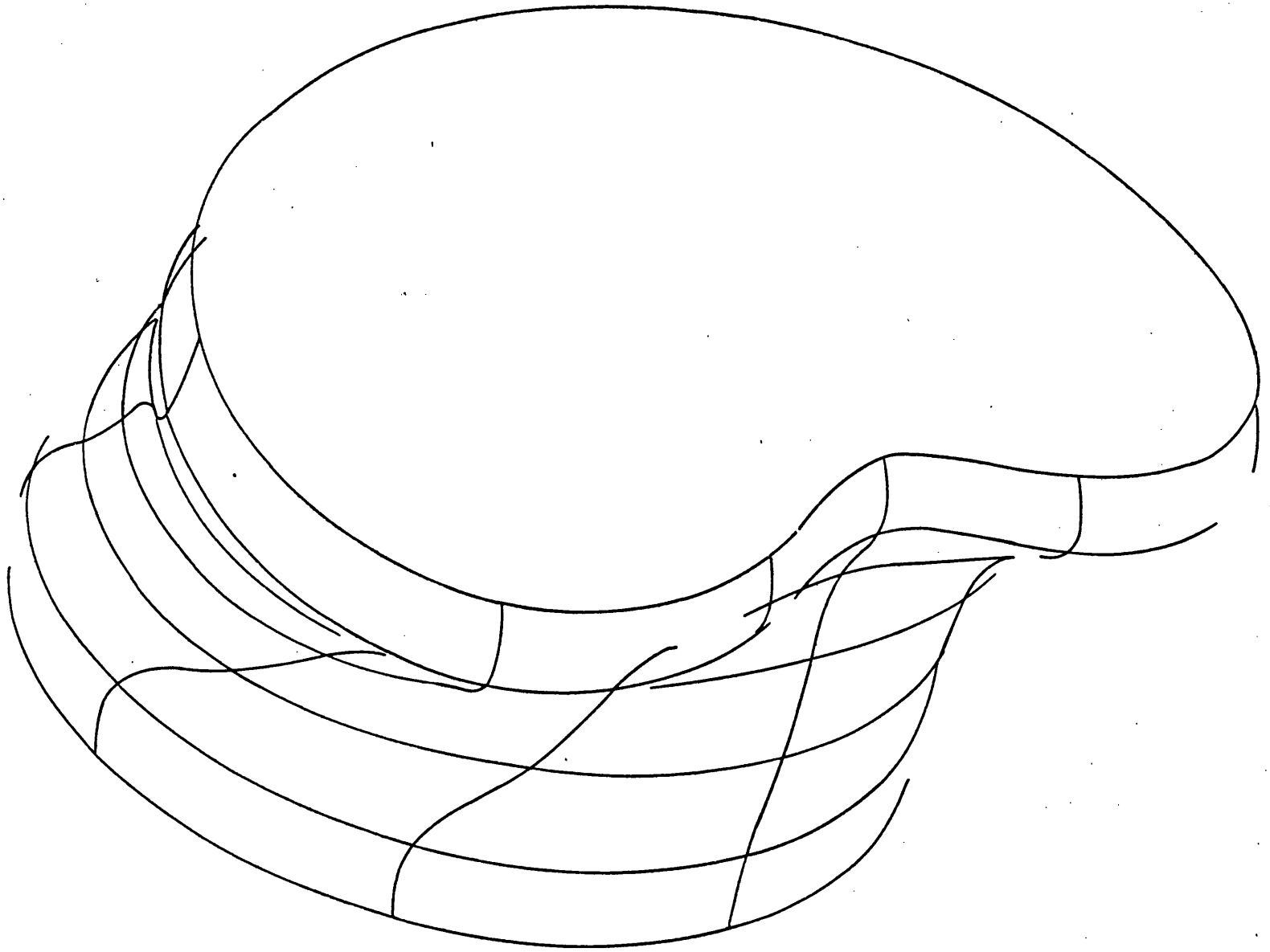

FIG.4.20 WORKING SECTION AT X-FLOW 3000 (4th ITERATION)

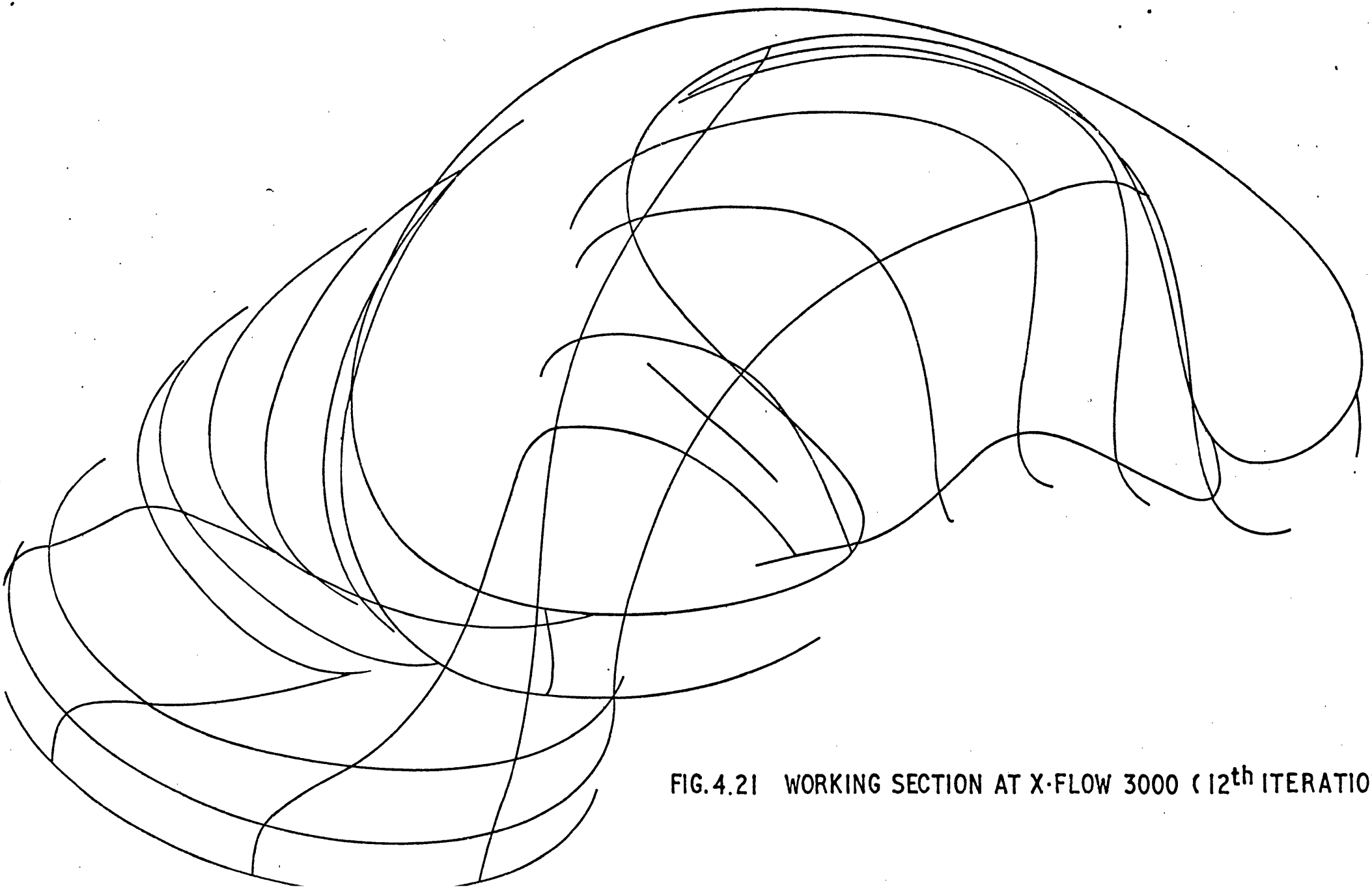

FIG. 4.21 WORKING SECTION AT X-FLOW 3000 (12th ITERATION)

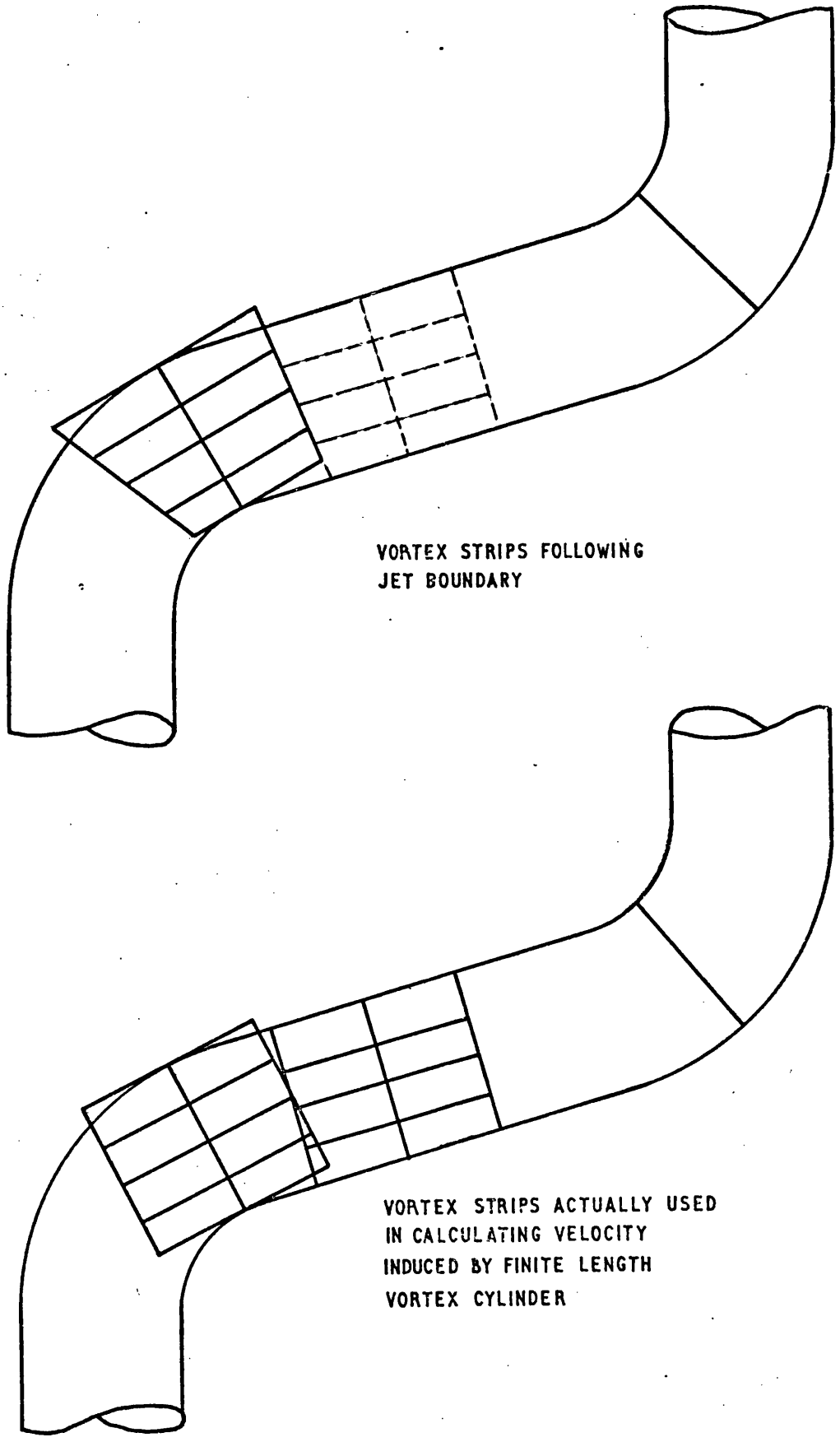

FIG.4.22. BETTER REPRESENTATIONS OF THE CYLINDRICAL SECTION SHEET STRIPS

5.0. TESTS OF ORIGINAL METHOD

To make the previous work on the inviscid jet relevant to real jets in gas turbine combustion chambers, it was necessary to incorporate a model of the viscous mixing process. This would allow the effect of entrainment on the shape and trajectory of the jet to be studied.

In addition, the viscous mixing model should be capable of predicting accurately the behaviour of as many different flows as possible, in order to predict a combustion chamber flow. Hubble (1967) proposed such a model consisting of 3 essential parts:-

1) The solution of a Fredholm integral equation of the second kind for the irrotational flow which exists before viscosity has caused the vorticity to diffuse and convect away from the solid surface.

2) The vorticity diffusion and convection processes are calculated separately as follows:-

a) The diffusion of the vorticity follows a Gaussian probability distribution, obtained from a solution of the differential equation

$$\frac{\partial \omega}{\partial t} = \nu \frac{\partial^2 \omega}{\partial y^2} \qquad 5.1$$

b) The convection of the vorticity with the flow, described by the equation

$$u \frac{\partial \omega}{\partial x} + v \frac{\partial \omega}{\partial y} = 0 \qquad 5.2$$

ASIDE. Adding equation 5.1 to 5.2 gives the simplified vorticity transport equation

$$\frac{\partial \omega}{\partial t} + u \frac{\partial \omega}{\partial x} + v \frac{\partial \omega}{\partial y} = \nu \frac{\partial^2 \omega}{\partial y^2}$$

Hubble further simplified equation 5.2 by omitting the second term $v\,\partial w/\partial y$ maintaining that it was of second order.

3) The resolution of the Fredholm integral equation to eliminate the effects of the field vorticity at the boundaries, thus ensuring the boundary conditions were always satisfied.

2a Diffusion

For the model described above, the solution of equation 5.1 was required for 2 characteristic cases:-

i) diffusion of vorticity from a solid boundary

ii) diffusion of the vorticity already present in the flowfield.

The relevant solutions of 5.1 are:-

i)
$$\omega(y,t) = \frac{u_s}{\sqrt{\pi \nu t}}\, e^{n} \qquad 5.3$$

Where $n = -y^2/4\nu t$

See Appendix 6.

ii)
$$\omega(y,t) = \frac{1}{2\sqrt{\pi \nu t}} \int_0^{\infty} \omega(z,t) \left[e^{\frac{-(z+y)^2}{4\nu t}} + e^{\frac{-(z-y)^2}{4\nu t}} \right] dz \qquad 5.4$$

Where u_s = Velocity of fluid at surface i.e. the increment by which the no-slip condition is violated

t = time

ν = kinematic viscosity

y = distance from surface

$\omega(y,t)$ = new vorticity distribution (at next time)

$\omega(\eta,t)$ = old vorticity distribution (at this time)

η = value of 'y' for old distribution.

See also Appendix 6.

2b Convection

This was calculated following Hubble (1968):-

a) Calculate the velocity at each point along a mesh column using the integral

$$v_x(y) = \int_0^y \omega_i \, dy \qquad 5.5$$

where y = position of point up the column

ω_i = vorticity at point i.

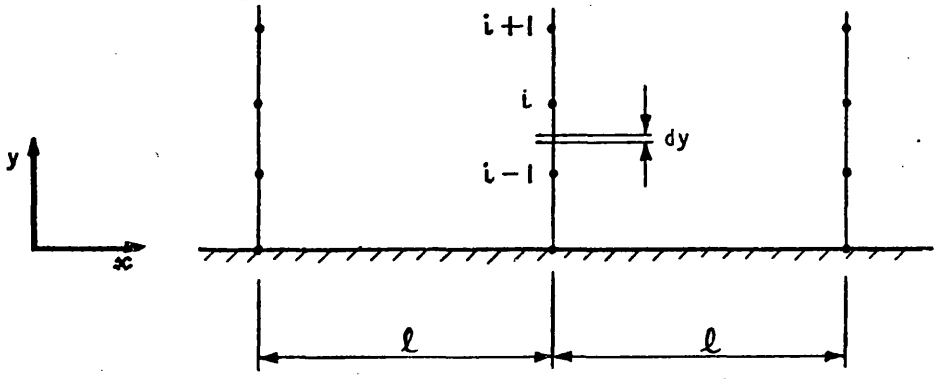

FIG.5.1 INTEGRATION INTERVAL ON COLUMN

b) Calculate the distance the vorticity moves in a timestep Δt using the finite difference formula:-

$$X(y) = \Delta t * v_x(y) \qquad 5.6.$$

c) Reallocate the vorticity between the surrounding mesh points on a linear basis:-

(i) Vorticity allocated to the ajacent downstream mesh point is

$$\omega_i(y)\,X(y)/l \qquad 5.7$$

(ii) Vorticity allocated back to the adjacent upstream mesh point is

$$\omega_i(y)\left[1-\frac{X(y)}{l}\right] \qquad 5.8$$

Although the diffusion and convection processes are calculated separately, Hubble maintained that a linear summation of these two effects served to represent the equation.

$$\frac{\partial \omega}{\partial t} + u\frac{\partial \omega}{\partial x} = \nu\frac{\partial^2 \omega}{\partial y^2} \qquad 5.9$$

In order to test this method, it was used to predict the boundary layer development on a flat plate in a uniform stream. Since the body geometry was simple, the Integral equation technique was not used. Image vortices were used, Payne (1956), to ensure that the normal velocity at the plate surface was zero.

Unfortunately, no sensible results were obtained with this method, even though 2 methods of calculating the vorticity generated at the plate surface were tried. The vorticity field calculated from equations 5.3 and 5.4 was represented by vortex filaments, section 6.23. The first method used these and their images to obtain the surface tangential velocity. This was substituted directly into equation 5.2 to give part of the vorticity distribution for the next iteration.

The second method used a velocity deficit , which was calculated from

$$V_\infty - \sum_{i=1}^{N} \omega_i\,dy \qquad 5.10$$

Where N = number of rows.

The new surface vorticity would then be equal to

$$\frac{V_{DEFICIT}}{\sqrt{\pi \nu t}} + \omega_{SURFACE(FROM\ PREVIOUS\ ITERATION)} \qquad 5.11$$

and its diffusion would be calculated from equation 5.3.

The reason why this method never gave realistic results is tied up with Hubbles' method of solution for equation 5.9, which is equivalent to assuming that the equation is linear. The velocity component u is a function of both dependant and independant variables which makes equation 5.9 non-linear. Hence it cannot be solved by the superposition type technique described above.

To demonstrate the non-linearity of equation 5.9, additional numerical calculations were carried through using the techniques described above. In these later calculations the order of the diffusion and convection calculations was interchanged, the results being shown below

DISTANCE FROM SURFACE	COLUMN 1	COLUMN 2
.0044167 (5)	.17116	54.8248
.0035334 (4)	5.25139	287.725
.00265 (3)	80.5431	1044.67
.0017667 (2)	627.517	2624.08
.000883 (1)	2537.46	4560.13
0 (S)	5482.48	5482.48

ORIGINAL VORTICITY DISTRIBUTION

DISTANCE FROM SURFACE	DIFFUSE, CONVECT REALLOCATE	CONVECT, REALLOCATE DIFFUSE.
5	65.434	103.143
4	265.165	451.205
3	827.633	1470.378
2	2019.744	3471.61
1	4269.943	5843.705
S	6657.64	6219.745

VORTICITY DISTRIBUTION COLUMN 1

TABLE 5.1 RESULTS OF CHANGING THE ORDER OF THE DIFFUSION AND CONVECTION CALCULATIONS.

Table 5.1 Contd/...

TABLE 5.1(Contd).

DISTANCE FROM SURFACE	DIFFUSE, CONVECT REALLOCATE	CONVECT, REALLOCATE DIFFUSE.
5	74.9766	174.892
4	320.411	674.926
3	1144.464	2016.461
2	3380.278	4511.694
1	7412.047	7380.415
S	8031.48	7095.526

COLUMN 2

It is evident that interchanging the order of the diffusion and convection calculations does not give the same vorticity distribution, which was to be expected since equation 5.9 is non-linear.

An order of magnitudes investigation was performed on the vorticity transport equation 5.12.

$$\frac{\partial w}{\partial t} + u\frac{\partial w}{\partial x} + v\frac{\partial w}{\partial y} = \nu\left[\frac{\partial^2 w}{\partial x^2} + \frac{\partial^2 w}{\partial y^2}\right] \qquad 5.12$$

Batchelor (1967).

The analysis is given in Appendix 7, and shows that the term $v\,\partial w/\partial y$ is as important as the term $u\partial w/\partial x$, and thus cannot be ignored. This is contrary to Hubble (1967). Equation 5.9 becomes.

$$\frac{\partial w}{\partial t} + u\frac{\partial w}{\partial x} + v\frac{\partial w}{\partial y} = \nu\left[\frac{\partial^2 w}{\partial y^2}\right] \qquad 5.13$$

The conclusions that can now be made concerning the method proposed by Hubble (1967) are:-

1) the term $v\,\partial w/\partial y$ must be included in the vorticity equation
2) because it is non-linear, the equation cannot be solved using the superposition technique.

Since a great deal of experience has been accumulated solving the vorticity transport equation by finite-difference methods, these are an obvious choice for solving equation 5.13. If recirculating flow problems are to be solved, then the term $\nu \partial^2\omega/\partial x^2$ must be included in 5.13, giving the complete vorticity transport equation 5.14.

$$\frac{\partial \omega}{\partial t} + u\frac{\partial \omega}{\partial x} + v\frac{\partial \omega}{\partial y} = \nu\left[\frac{\partial^2 \omega}{\partial x^2} + \frac{\partial^2 \omega}{\partial y^2}\right] \qquad 5.14$$

The inclusion of the extra term does not increase the complexity of the finite-difference solution, since it only increases the number of finite-difference terms used. However, it does alter the equation type from Parabolic, equation 5.13, to Elliptic, equation 5.14.

If the flows to be predicted were of the boundary layer type, with no recirculating flow regions, then equation 5.13 would be used. The finite-difference version of this equation can be formulated so that no information is required from the downstream direction, if backward differences are used for the term $u\partial\omega/\partial x$. Thus the downstream boundary conditions do not have to be specified in order to obtain a solution. At any fixed time, the solution propagates downstream in a step by step fashion, and is often said to march downstream.

For recirculating flows, the finite-difference version of 5.14 does require that information from the downstream direction is available. Thus the boundary conditions have to be specified everywhere, including downstream, before a solution can be obtained. For solving general flows, equation 5.14 would be used so that any recirculating flow regions would be predicted.

In the method proposed by Hubble, the solution of equation 5.14 by finite-differences replaces the solution of 5.9 by the superposition techniques. The other elements of his method remain intact.

5.1. CONCLUSIONS

Brief details of the proposed method for solving viscous flows are given below, much greater detail being given in Chapter 6.

1) Calculate the potential flow.

- This is done by an Integral equation solution to Laplaces equation, as before.

2) Calculate the diffusion and convection of vorticity in the flow.

- This is to be done from a finite-difference solution of the vorticity transport equation, 5.14.

3) Calculate the perturbation effects from the vorticity in the flowfield at the solid boundaries, using potential flow techniques.

- These effects are then removed by resolving the Integral equation.

6.0. ROTATIONAL FLOWS - VISCOUS INTERNAL FLOWS

6.1. INTRODUCTION

Details were given in chapter 5 of the alterations necessary to the calculation method proposed by Hubble(1967). This chapter describes the tests performed using the new method outlined at the end of that chapter, and described in greater detail below.

For the initial testing of this new method, it was decided to concentrate on the prediction of simple flows with a sufficiently low Reynold's number to ensure the flow was non-turbulent. If the model was successful in predicting a simple laminar case, then extension to cover turbulent flows could be formulated. Such an extension is vital if combustion chamber flows are to be predicted.

Two simple flows were chosen:-

a) 2-D parallel duct

b) 2-D parallel duct with a backward facing step in the lower wall.

These cases were selected since analytical, computational and experimental results exist in the literature for one or both of these flows.

6.11 The Computer Model

A brief outline of the model has already been given at the end of Chapter 5. In this section, each element of the model is explained in greater detail. Briefly, the model consists of:-

1) Calculation of the potential flow
2) Calculation of the diffusion and convection of vorticity
3) Calculation of the perturbation effects of the flowfield vorticity at the solid boundaries.

It is apparent from Lighthill(1963), that the computer model simulates the physical development of a viscous flowfield.

1. Calculation of the potential flow

A Fredholm integral equation of the second kind is solved for the potential flow (Chapter 3). Using this approach the flow through or around any shape of boundary can be calculated, provided the boundary shape is known.

This technique has already been demonstrated to give good results for aircraft and jet engine installation flows, Hess(1966), Mason (1968) respectively.

2. Calculation of the vorticity.

As described in Chapter 5,the vorticity development is to be calculated from a finite-difference form of the vorticity transport equation,eqn.5.14. The form chosen was that of Fromm(1969)(Sec.6.22).

3. Calculation of perturbation effects.

The development of the vorticity field over any one timestep will generally violate the condition specifying zero normal velocity at the solid surfaces. The effect of the flowfield vorticity is calculated at the surface,and the Integral equation re-solved. This gives a new source/vortex distribution around the duct boundary, from which the flowfield velocity may be calculated(Section 6.24).

Thus the flow prediction begins by calculating the potential flow. The iterative cycle then consists of repeating steps 2 and 3 above, until the solution has converged. This procedure numerically represents the actual flow development and is that described by Lighthill (1963).

6.12. Literature survey.

This can be divided into 2 sections:

1) Methods of Solution
2) Computational Methods

1. Method of Solution

The usual technique adopted for solving low Reynold's Number flows was the streamfunction-vorticity method. One of the first solutions available was by Thom(1933) who performed the calculation by hand. The methods developed by Thom were to make hand calculations quicker. Apelt (1961) used some features of Thom's method in his calculation.

Many other workers have used the same streamfunction - vorticity method.Fromm(1964)for calculating the wake flow behind obstacles etc, Fromm (1969a),for flow in diffusers.In the latter paper,Fromm used a more accurate representation of the vorticity transport equation than in his other paper.

Pearson(1965),Mills(1968),Son & Hanratty(1969), Mueller & O'leary(1970) and Fanning & Mueller(1973),all use a similar approach; however they differ from one another in their finite-difference representation of the vorticity equation, 5.14, and

the Poisson equation for streamfunction, 6.1

$$\frac{\partial^2 \psi}{\partial x^2} + \frac{\partial^2 \psi}{\partial y^2} = -\omega \qquad 6.1$$

Where ψ = Streamfunction.

ω = vorticity.

Payne (1956, 1958), solved the vorticity equation but did not solve the streamfunction equation. He used vortices, and their images, to ensure that the boundary condition of zero flux of mass at the solid boundaries was satisfied. By this means, he was able to calculate the flow field velocity.

Chorin (1973) solved neither the vorticity equation or the stream-function equation, but used computer generated pseudo-random numbers to simulate the generation and dispersal of vorticity from the body. Rather than use vortices and their images as Payne did, Chorin solved an Integral equation for the source strengths to be placed on the body circumference. The combined effects of the sources and vortices satisfies the zero flux condition and gives the flow field velocity.

2. Computational Methods.

Both Thom and Apelt mapped the physical region into a computational plane, and solved the transformed vorticity and streamfunction equation in this plane. Thus they eliminated any mesh-boundary intersection problems.

As already stated, the major difference between the various solutions was in their treatment of the vorticity equation. Pearson used an implicit finite-difference form of this equation if the non-linear terms were small, and the Alternating-Direction Implicit(ADI) method of Peaceman and Rachford (1955), if they were large. Fromm(1964) used central differences for the deviative terms at all times. The method of applying the two boundary conditions i.e. zero flux of mass and no-slip of the fluid at the solid boundary, can also vary between the methods listed above.

Payne avoided solving the streamfunction equation by integrating the effects of the vortices representing the vorticity field. By using a body of simple shape he ensured that calculations of the image position would also be simple.

The model proposed in 6.11 is a combination of the techniques of Payne and Chorin. The Integral equation method is used to satisfy the zero normal velocity condition and to give the flow field velocity. A finite-difference solution of the vorticity equation is obtained at specific mesh points, and vortices used to represent the vorticity at these points.

A consequence of using the Integral equation method is that it is unnecessary to find the image vortex position. Thus any boundary geometry may be used.

6.2. THEORY

6.2.1. Calculation of Potential Flow.

The potential flow through the stepped and parallel ducts is calculated by solving a Fredholm Integral equation of the second kind (chapter 3). The technique used follows that by Hess et al (1966) who calculated mainly external flows. Source sheets distributed over the solid surfaces were used to satisfy the Neumann boundary condition of zero normal velocity.

In calculating internal flows, they noted that the only difference between these and external flows, is the sign of the body outward normal vector. However, specifying a source distribution over the body surface for interior flow problems results in the Integral equation becoming indeterminative.

Even so, solutions of the Integral equations are sometimes possible because of errors in the approximations. It is generally dangerous to accept such numerical solutions because they have arisen from the presence of errors. If a sufficiently good approximation to the equation were used, then the matrix would be singular, and no answer would be obtained.

For this investigation, a source distribution was not used because of the indeterminate nature of the matrix outlined above. Rather, the duct walls would be parts of two infinite vortex sheets, fig. 6.1

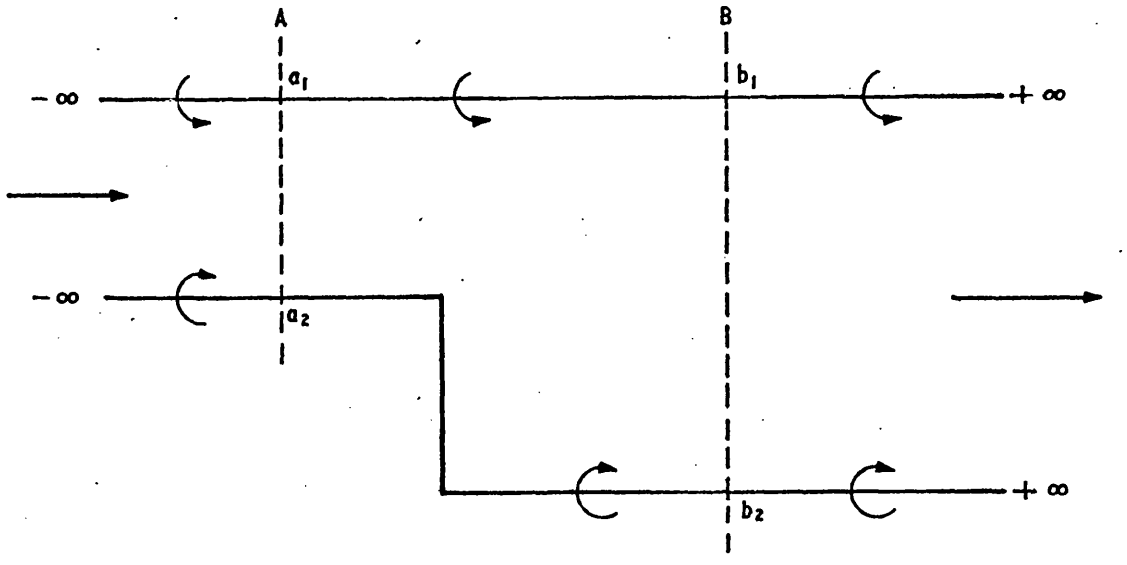

FIG 6.1 DEFINITION OF DUCT WALLS

The inlet and exit section of the duct are at A and B respectively. The equivalence of vortex and source distributions, given by Kuchemann et al (1953), is given in section 4.242. It follows that the portion of the vortex lines between $-\infty$ and A above, can be replaced by a distribution of sources between a_1 and a_2. Similarly, a distribution of sinks between b_1 and b_2 replaces the vortex lines between B and $+\infty$.

The solution of the Integral equation for the potential flow throughthe duct is described in Appendix 2.

Hess used the boundary condition that the normal velocity at the collocation point, usually the mid-point of the sheet, is zero. In this investigation, the boundary conditions are:

1) The normal velocity for the inlet source sheets is equal to the fluid velocity there, calculated from the Reynold's Number, the duct width and the kinematic viscosity.

2) The normal velocity for the exit source sheets is equal to the fluid velocity at exit, calculated from continuity.

3) Along the duct walls, represented by vortex sheets, the tangential velocity on the outside of the duct is zero. This can be explained by considering the opposite problem i.e. the external flow around a body.

Fig 6.2a shows a profile bounded by the contour C.

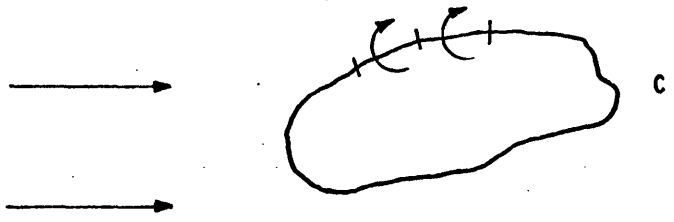

Fig. 6.2a FLOW AROUND CURVE C

The flow around this body can be found by subdividing C into a finite number of segments, and calculating the circulation of each segment from the zero normal velocity boundary condition, Von Mises (1953).

Since there is no flow normal to the boundary, then the streamlines of the flow resulting from the superposition of the uniform field and the vortex sheet around C, must not cross C. Each streamline must remain either inside or outside C.

The curve C itself is a closed streamline, and the neighbouring inner streamlines must also be closed curves, fig 6.2b.

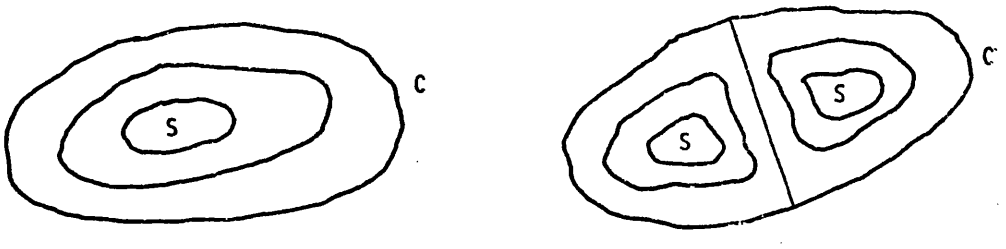

FIG 6.2b POSSIBLE STREAMLINES WITHIN C

If the streamlines are plotted over the interior of C, then some are bound to contract more and more around certain points S. At these points, the direction of the velocity is undefined. The velocity cannot be zero there, for the condition for an irrotational flow $dV/dn - V/R = 0$ (Von Mises), shows that the magnitude V of the velocity increases toward the concave side of the streamlines.

The existence of a finite velocity of undefined direction is inconsistent with the fact that the field of flow induced by a vortex sheet is regular and continuous everywhere but on the sheet. It follows that the field obtained by the superposition of the uniform flow and the vortex sheet on C must have the velocity zero throughout the interior of C.

So for the flow through the interior of the duct, the velocity is zero everywhere outside the duct.

6.22 CALCULATION OF VORTICITY.

This is to be performed by a finite-difference solution of the vorticity transport equation. Such solutions have been available for a number of years, and present any prospective user with many different formulations from which to choose. The author had been unable to find another method equivalent to the one proposed for this investigation, and as a result, decided to keep all components of his method as straightforward as possible.

This ruled out Implicit methods, whether Alternating Direction or not, in favour of an Explicit method. With an Implicit approach, a matrix has to be solved for each row and/or column at each iteration, before the new solution is known along that row or column. With an Explicit finite-difference equation, the new mesh point value is calculated as the point is selected, and the complete solution at each iteration can be obtained with one scan of the mesh. The major difference between the methods is that the stability of Explicit methods is not assumed without a stability analysis, whereas the Implicit methods are automatically stable.

The advantage in using an Explicit method from the literature is that the stability criteria are known, and the method will have been tested. Fromm published at least two papers in 1969, one on predicting diffuser flow (1969a) and the other on reducing dispersion in finite-difference schemes (1969b). A fourth-order accurate scheme was used for mesh points in the diffuser flowfield, whilst a second-order accurate scheme was used for mesh points adjacent to the

boundaries. The stability criteria for the schemes are given in Fromm (1964, 1969b).

A diffuser is not very much different to the cases selected by the author for investigation. Also, Fromm's scheme was one of the most accurate available at the start of this particular phase of the project, so it was decided to use the finite-difference formulation of the vorticity transport equation given in Fromm (1969a). The stability criteria are reproduced in Appendix 8.

As Fromm's scheme is limited to flows with a Reynolds number of less than 4000, if the investigation proves that the method of predicting viscous flows is viable, a new finite-difference scheme will have to be chosen before combustion chamber flows can be predicted.

For this investigation, the vorticity calculation in the duct is performed in 2 stages:-

1) The vorticity generated at the solid surface of the duct is calculated as a result of the no-slip boundary condition.

2) The vorticity diffused and convected in the flow field through the action of viscosity, is calculated from Fromm's (1969a) finite-difference scheme for the vorticity transport equation. The derivation of the finite-difference scheme is given in Appendix 9.

1. Calculation of Vorticity on the solid boundaries.

The vorticity generated at the solid, non-porous surfaces, is calculated from the velocity components adjacent to the surface. Fig. 6.3 shows 2 mesh points, e and f.

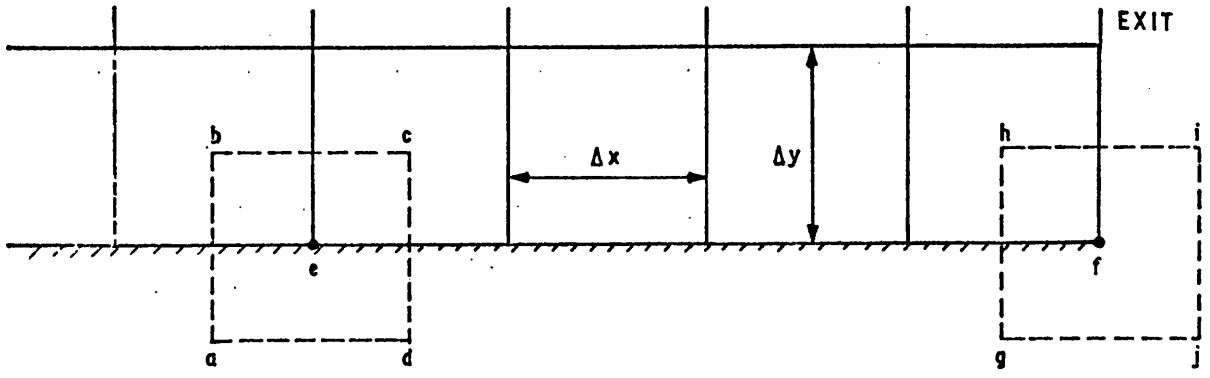

FIG 6.3 CALCULATION OF SURFACE VORTICITY

The circulation around the control volume abcd is given by

$$\Gamma_{abcd} = ab\,V_{ab} + bc\,V_{bc} + cd\,V_{cd} + da\,V_{da}$$

$$\therefore \quad \Gamma_{abcd} = bc\,V_{bc}$$

but $bc = \Delta x$, hence

$$\Gamma_{abcd} = \Delta x\,V_{bc} \quad \text{and}$$

$$\Gamma_{ghij} = \Delta x\,V_{hi} \qquad 6.2$$

Vorticity and circulation are related by equation 6.18.

$$\Gamma = \omega\,\Delta x\,\Delta y$$

hence

$$\omega_e = \frac{V_{bc}}{\Delta y} \quad , \quad \omega_f = \frac{V_{hi}}{\Delta y} \qquad 6.3$$

Once the velocity components half a mesh height from the surface are known, the vorticity on the surface can be calculated.

For concave corners, fig. 6.4, the procedure is similar.

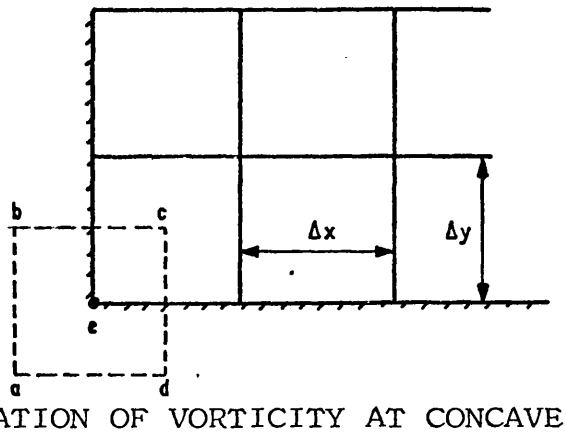

FIG 6.4 CALCULATION OF VORTICITY AT CONCAVE CORNERS.

In this case, the velocity components along the arms are zero, and hence the vorticity is also zero.

For convex corners, fig 6.5

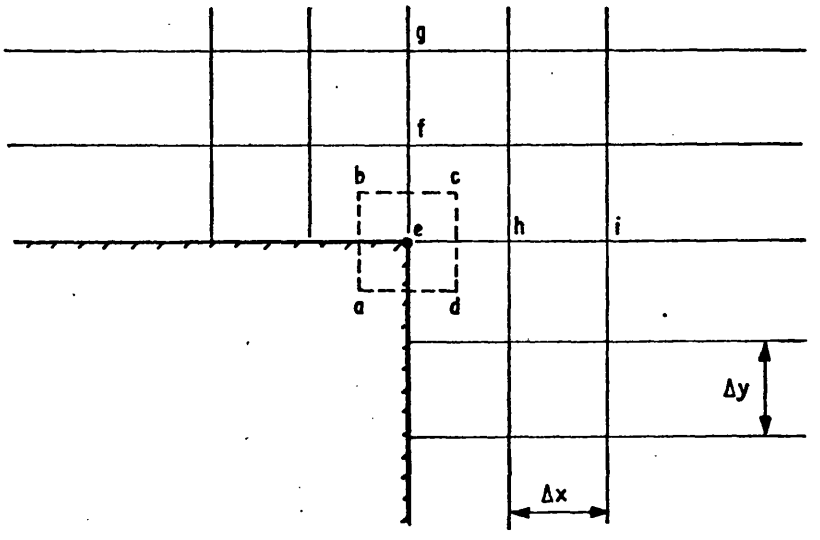

FIG 6.5 CALCULATION OF VORTICITY AT CONVEX CORNERS.

$$\omega_e = \frac{V_{bc}}{\Delta y} + \frac{V_{cd}}{\Delta x} \qquad 6.4$$

2. Calculation of the Vorticity in the flow field

The convection and diffusion of vorticity can be calculated by solving the vorticity transport equation. The derivation of this equation is given in Lighthill(1963) and Batchelor (1967),and the equation is given below in vector form

$$\frac{D\underline{\omega}}{Dt} = (\underline{\omega}.\nabla)\underline{V} + \nu\nabla^2\underline{\omega} \qquad 6.5$$

The term $(\underline{\omega}.\nabla)\underline{V}$ represents the stretching of the vortex lines giving an increase in vorticity. However, this term is zero for the current investigation since the flowfield is two-dimensional, and $\underline{\omega}$ is everywhere normal to it. Therefore equation 6.5 reduces to the scalar equation

$$\frac{D\omega}{Dt} = \nu \nabla^2 \omega \qquad 6.6$$

Where $$\frac{D}{Dt} = \frac{\partial}{\partial t} + u\frac{\partial}{\partial x} + v\frac{\partial}{\partial y}$$

The left hand side represents the variation of vorticity with time and its convection with the flow. The right hand side represents the rate of change of vorticity due to molecular diffusion, Batchelor (1967).

The calculation of the flow field vorticity using 6.6. is divided into four sections, as follows:-

a) general field point

b) field point adjacent to a solid boundary

c) a duct inlet boundary point

d) a duct exit boundary point.

a) <u>The discretized form for a general field point</u>

Equation 6.6. can be written.

$$\frac{\partial \omega}{\partial t} + u\frac{\partial \omega}{\partial x} + v\frac{\partial \omega}{\partial y} = \nu\left[\frac{\partial^2 \omega}{\partial x^2} + \frac{\partial^2 \omega}{\partial y^2}\right] \qquad 6.7$$

The fourth-order finite difference equation is

$$\omega^{*}_{i,j} + \nu\Delta t\left\{\left[\left(\omega^{n}_{i-1,j} - 2\omega^{n}_{i,j} + \omega^{n}_{i+1,j}\right)/\Delta x^2\right] + \left[\left(\omega^{n}_{i,j-1} - 2\omega^{n}_{i,j} + \omega^{n}_{i,j+1}\right)/\Delta y^2\right]\right\} = \omega^{n+1}_{i,j} \qquad 6.8$$

Where

$$\omega^{n}_{i,j} + (\Delta t/\Delta x)\left[F^{n}_{i-1/2,j} - F^{n}_{i+1/2,j}\right] + (\Delta t/\Delta y)\left[F^{n}_{i,j-1/2} - F^{n}_{i,j+1/2}\right] = \omega^{*}_{i,j} \qquad 6.9$$

Where

$$\begin{aligned}(\Delta t/\Delta x)F^{n}_{i-1/2,j} = {} & \frac{7}{12}\alpha^{n}_{i-1/2,j}\left(\omega^{n}_{i-1,j} + \omega^{n}_{i,j}\right) - \frac{1}{12}\alpha^{n}_{i-1/2,j}\left(\omega^{n}_{i-2,j} + \omega^{n}_{i-1,j}\right) \\ & + \frac{15}{24}\left(\alpha^{n}_{i-1/2,j}\right)^2\left(\omega^{n}_{i-1,j} - \omega^{n}_{i,j}\right) - \frac{1}{24}\left(\alpha^{n}_{i-1/2,j}\right)^2\left(\omega^{n}_{i-2,j} - \omega^{n}_{i-1,j}\right) \\ & - \frac{1}{12}\left(\alpha^{n}_{i-1/2,j}\right)^3\left(\omega^{n}_{i-1,j} + \omega^{n}_{i,j}\right) + \frac{1}{12}\left(\alpha^{n}_{i-1/2,j}\right)^3\left(\omega^{n}_{i-2,j} + \omega^{n}_{i-1,j}\right) \\ & - \frac{3}{24}\left(\alpha^{n}_{i-1/2,j}\right)^4\left(\omega^{n}_{i-1,j} - \omega^{n}_{i,j}\right) + \frac{1}{24}\left(\alpha^{n}_{i-1/2,j}\right)^4\left(\omega^{n}_{i-2,j} - \omega^{n}_{i-1,j}\right)\end{aligned} \qquad 6.10$$

Where $\alpha^{n}_{i-1/2,j} = (\Delta t/\Delta x)\, u^{n}_{i-1/2,j}$

The other terms in 6.9 are obtained by permutation of the suffices in equation 6.10.

The scheme is of the upwind differencing type, as can be seen from the terms $\omega^{n}_{i-2,j}$, and $\omega^{n}_{i,j-2}$ (obtained from suffice permutation). This means that more information is used from the upstream rather than downstream direction. As a result, due account must be taken of the signs of the local u and v components, to ensure that the necessary information is taken from the local upstream direction.

Equation 6.10 above is equation 7 in FROMM (1969a). The latter was subsequently found to be incorrect due to a printing error. The correct form of the equation, together with its derivation, is given in Appendix 9, page 242.

b) A field point adjacent to a solid boundary

Rather than cater for i-2, j-2 mesh points adjacent to a solid boundary, Fromm resorted to a second-order finite-difference version of equation 6.7 for these points. Equations 6.8 and 6.9 apply as before, but 6.10 is replaced by

$$\frac{1}{2}\alpha^{n}_{i-1/2,j}\left(\omega^{n}_{i-1,j}+\omega^{n}_{i,j}\right)+\frac{1}{2}\left(\alpha^{n}_{i-1/2,j}\right)^{2}\left(\omega^{n}_{i-1,j}-\omega^{n}_{i,j}\right)=\left(\Delta t/\Delta x\right)F^{n}_{i-1/2,j} \qquad 6.11$$

Again, permutation of the suffices gives the other terms in 6.9 for these mesh points. The definition of $\alpha^{n}_{i-1/2,j}$ is as before.

The calculation of the velocity components $u^{n}_{i-1/2,j}$, $v^{n}_{i,j+1/2}$ for cases (a) and (b) is worth investigating. Fig. 6.6 shows an enlarged view of part of the mesh.

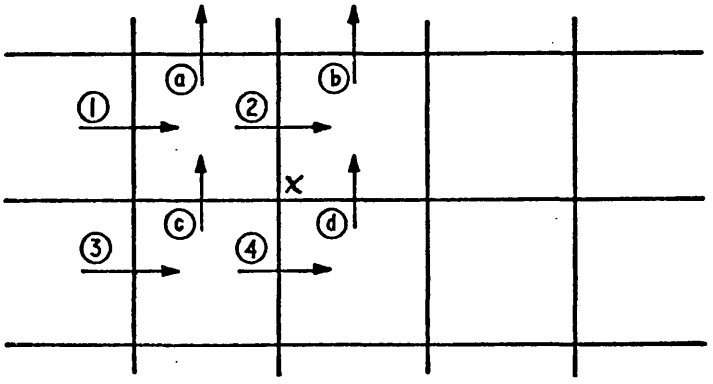

Fig. 6.6 CALCULATION OF VELOCITY COMPONENTS

For the calculation of $\omega_{i,j}$ at mesh point X

$$u^{n}_{i-1/2,j}=\left(u_1+u_2+u_3+u_4\right)/4$$

$$v^{n}_{i,j+1/2}=\left(u_a+u_b+u_c+u_d\right)/4 \qquad 6.12$$

c) An inlet boundary point

The vorticity along the inlet boundary is calculated from the velocity distribution prescribed at the boundary. Since this investigation is concerned with two-dimensional flow, vorticity is defined as

$$\omega=\frac{\partial v}{\partial x}-\frac{\partial u}{\partial y} \qquad 6.13$$

See Duncan et al (1960)

Since a uniform profile was prescribed on the inlet boundary, the vorticity is zero there. However, the vorticity is non-zero on the duct surfaces at the inlet boundary (section 6.22).

d) An exit boundary point

Fromm developed the following equation:-

$$\omega_{I,j}^{n+1} = \frac{1}{2}\left(\omega_{I,J+1}^{n} + \omega_{I,j-1}^{n}\right) + \frac{u_{I-\frac{1}{2},j}^{n}\,\Delta t}{\Delta x}\left[\omega_{I-1,j}^{n} - \frac{1}{2}\left(\omega_{I,j+1}^{n} + \omega_{I,j-1}^{n}\right)\right]$$

$$+ \frac{v_{I,j}^{n}\,\Delta t}{\Delta y}\left[\omega_{I,j-1}^{n} - \omega_{I,j+1}^{n}\right] \qquad 6.14$$

Where the subscript I refers to the duct exit points.

6.23 CALCULATION OF VELOCITY COMPONENTS.

The finite-difference scheme derived by Fromm (1969a) requires the velocity components to be known half-way between the mesh points. In general, the horizontal velocity components u, and the vertical velocity components

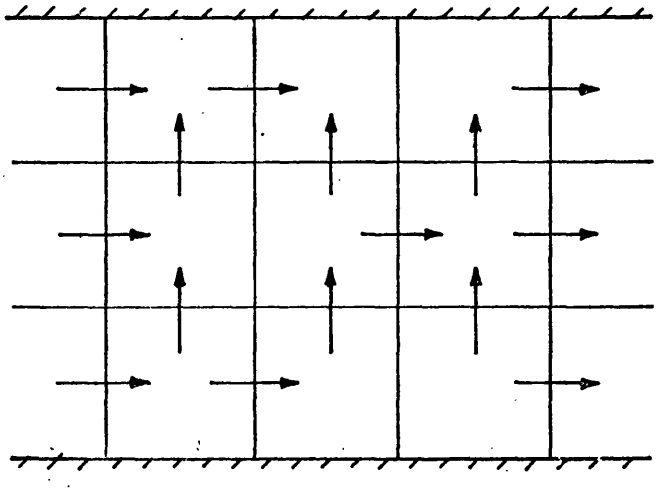

Fig. 6.7 VELOCITY COMPONENTS ON MESH ROWS & COLUMNS

v , are calculated on the intersections of the mesh columns and rows respectively. The velocity components halfway between the mesh points are found by linear interpolation, fig. 6.7. If any other components are required, they are calculated using the method outlined in section 6.22 (2b).

The calculation of the velocity components is divided into 2 sections:-

1) The first timestep - since the flow is potential i.e. irrotational
2) All subsequent timesteps - since there is now vorticity in the flowfield i.e. the flow is rotational.

1. Velocity components in potential flow.

At the instant the motion begins, the flow is everywhere potential, Lighthill (1963). This flow is calculated by using surface singularities to solve the Fredholm integral equation. These are:

a) Source sheets on the duct inlet and exit boundaries.

b) Vortex sheets on the solid walls of the duct.

Since the vorticity is zero throughout the flow at this stage, the velocity components were calculated halfway between the mesh intersection points directly.

a. Source Sheets

The velocity components induced at P, fig. 6.8a, by the source sheet lying between S_1 and S_2 are given by

$$V_x = 2\sigma \log_e (r_1/r_2)$$

$$V_y = 2\sigma (\varphi_2 - \varphi_1) \qquad 6.15$$

Where σ = source sheet strength/unit length.

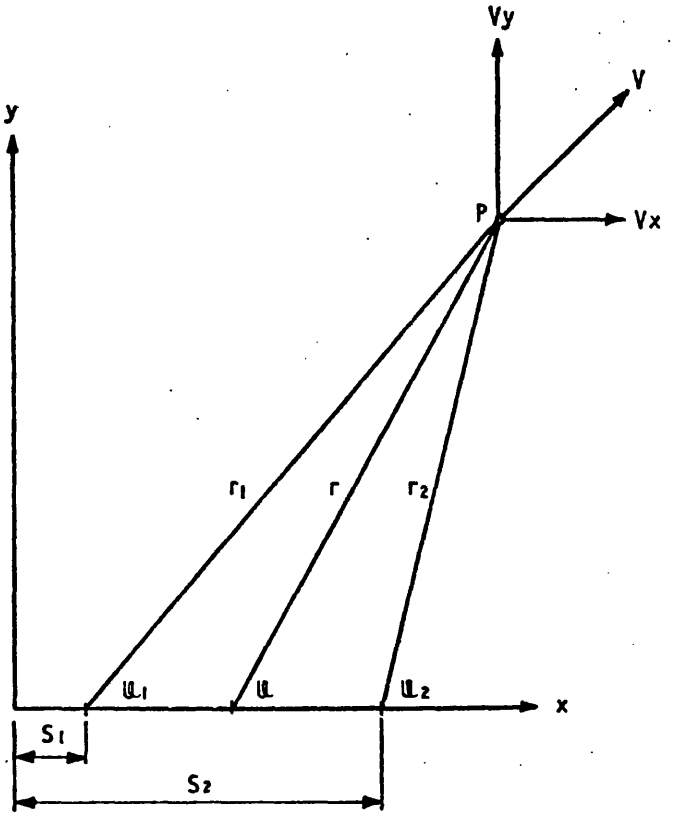

FIG. 6.8a SOURCE SHEET

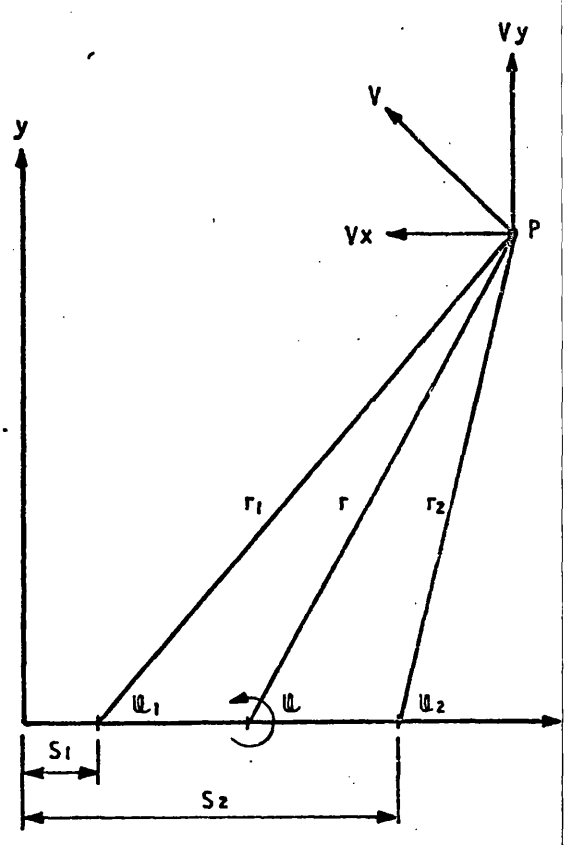

FIG.6.8b VORTEX SHEET

The components are derived in a similar manner to those for a vortex sheet.

b) Vortex Sheets

Consider a vortex sheet lying between S_1 and S_2 fig. 6.8b. The velocity components induced at P by the sheet are

$$V_x = 2\sigma(\varphi_1 - \varphi_2)$$

$$V_y = 2\sigma \text{Log}_e(r_1/r_2) \qquad 6.16$$

Where σ = Vortex sheet strength/unit length of sheet.

These components differ by a factor of 4π from those derived by Von Mises (1953), to maintain similarity with Hess et al (1966).

2. Velocity Components calculated when there is vorticity in the flowfield.

At all times after t = o, vorticity enters the flow field by diffusion and convection from the duct walls. The resulting Poisson type equation is solved by a Fredholm Integral equation, using surface singularities as before. The velocity components induced by these singularities are given by equation 6.15 and 6.16 above.

The velocity induced at a point by a distribution of vorticity is given by the Biot-Savart law, Lighthill (1963).

$$\underline{V} = \int \frac{\underline{\omega} \wedge \underline{r}}{4\pi r^3} \, dV \qquad 6.17$$

where $\underline{r}$ is the position vector relative to the volume element and the integration is over the whole vorticity field.

If the vorticity at a mesh point is assumed uniform over an area surrounding the point, fig. 6.9, then the strength of the Vortex can

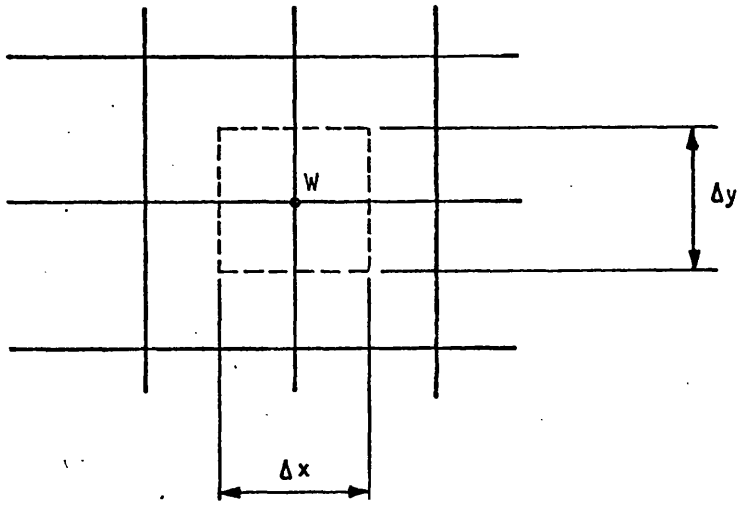

Fig. 6.9 REPLACING VORTICITY BY A VORTEX.

easily be calculated. The vortex circulation is given by Duncan et al (1960)

$$\Gamma = \iint \omega \, dx \, dy$$

which from Fig. 6.9 gives

$$\Gamma = \omega \Delta x \Delta y \qquad 6.18$$

Thus the calculation of the volume integral of 6.17 has been replaced by calculating the effect of all the mesh point vortices. The velocity components induced by a vortex are given by equation 4.7, except that for this investigation, they have been multiplied by 4π

Linear Interpolated Components.

Difficulties were found when using the vortex representation to calculate the velocity components at points halfway between the mesh points. Since these halfway points were too close to the adjacent vortex singularies, very high velocities were calculated from equation 4.7. The calculation procedure was modified so that the velocity components were calculated at the mesh points, and linear interpolation used to evaluate the components halfway between the mesh points.

On the duct inlet boundary, however, there is no vorticity because of the prescribed uniform velocity profile. The velocity components are calculated directly at the points halfway between the mesh points.

In order to calculate the velocity distribution across the duct exit boundary as accurately as possible, the following procedure was adopted:- The velocity induced at the exit mesh points by the exit vorticity is calculated. The velocity at the halfway mesh points is linearly interpolated from these values. The velocity induced at the halfway mesh points by the surface singularities and the remaining field vorticity is calculated directly, and added to the velocity from the linear interpolation.

The vertical velocity components at the halfway mesh points, immediately prior to the duct exit, are assumed equal to the components calculated at the penultimate mesh points. This is in line with Fromms (1969a) assumption that there is no change in $\partial\psi/\partial x$ at the duct exit.

6.24. EFFECT OF THE FIELD VORTICITY AT THE SURFACE

The boundary conditions which apply at all times are

1) zero tangential velocity immediately outside the duct.

2) uniform duct inlet velocity profile.

3) exit velocity profile which satisfies continuity.

4) no-slip of the fluid adjacent to the solid boundary.

The fourth condition is taken care of by the continual creation of vorticity at the solid surfaces. The amount of vorticity created depends on the velocity induced on the fluid side of the duct solid surfaces.

The remaining three conditions are affected by the diffusion and convection of vorticity away from the duct walls. At each iteration, the effects of the vorticity distribution in the duct are calculated at the surface collocation points where, in general, the boundary condition will have been violated by the vorticity. The strength of the surface sheets require alteration to counteract the effects of the vorticity at the collocation points.

The treatment for each collocation point varies as follows:-

1. Duct Solid Surface.

The tangential velocity immediately outside the duct surface collocation point is calculated from the field vorticity. In general this will be non-zero, violating the first boundary condition. The surface sheet singularities must induce a velocity at this point, equal and opposite to that induced by the field vorticity, in order to restore the boundary condition.

This velocity is inserted into B, eqn A2.8, for each particular sheet.

2. Duct Inlet Boundary.

Since source sheets are specified across the duct inlet, the normal velocity components, induced by the field vorticity, are calculated at the collocation points. The surface sheets, together with the field vorticity, must induce a velocity equal to the prescribed inlet velocity at these points. Thus knowing the total velocity and the contribution from the field vorticity enables the contribution from the surface sheets to be calculated.

This contribution is placed in B, eqn. A2.8, for each of the inlet sheets.

3. Duct Exit Boundary

Source sheets are also specified across the duct exit. The normal velocity components induced by the field vorticity at the sheet collocation points are calculated as before. The mass flow between the duct inlet and exit are compared using the prescribed inlet and calculated exit velocity profiles.

A typical exit velocity profile, obtained from the field vorticity, is shown in Fig. 6.10

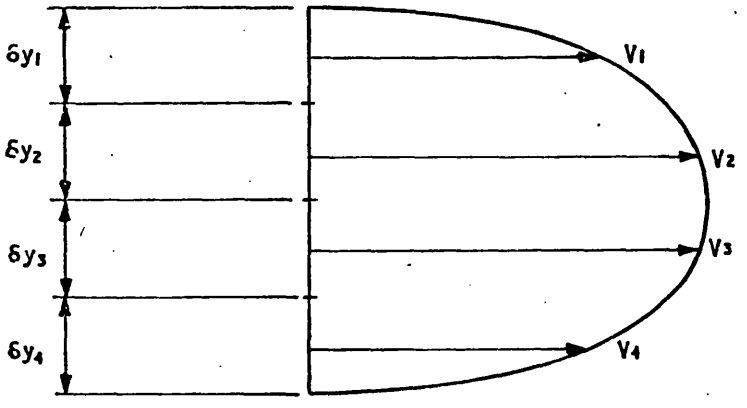

FIG 6.10 EXIT VELOCITY PROFILE

If each portion of the curve is approximated by straight lines, the area under the curve is

$$A_{EXIT} = V_1\left(\frac{\delta y_1}{2} + \frac{\delta y_2}{4}\right) + V_2\left(\frac{\delta y_1}{4} + \frac{\delta y_2}{2} + \frac{\delta y_3}{4}\right)$$

$$+ V_3\left(\frac{\delta y_2}{4} + \frac{\delta y_3}{2} + \frac{\delta y_4}{4}\right) + V_4\left(\frac{\delta y_3}{4} + \frac{\delta y_4}{2}\right) \qquad 6.19$$

For continuity.

$$A_{INLET} = A_{EXIT} \qquad 6.20$$

In general, the velocity distribution at the duct exit, obtained from the field vorticity, will not satisfy continuity. The difference in area, A_{DIFF} , is converted into a linear increment in velocity, eqn. 6.21, which when added to the duct exit velocity components, ensures continuity is satisfied.

$$A_{DIFF}\left(= A_{INLET} - A_{EXIT}\right) = \delta V\left(\frac{3\delta y_1}{4} + \delta y_2 + \delta y_3 + \frac{3\delta y_4}{4}\right)$$

Thus in general

$$\delta V = \frac{A_{DIFF}}{\left[\frac{3}{4}\left(\delta y_1 + \delta y_n\right) + \sum_{i=2}^{i=n-1} \delta y_i\right]} \qquad 6.21$$

Where n = number of velocity components.

Thus, the linear increment δV , is the contribution that all the surface singularities make at each exit collocation point, to ensure continuity of flow. Thus δv is inserted into B , eqn A2.8, for the exit sheets.

6.241 Recalculation of the Surface Singularities

The coefficients in the matrix B are recalculated to take account of the effect that the field vorticity has at the duct surface. Equation A2.8 is re-solved using the Gauss-Seidal solution routine, for the new strength of the surface sheet singularities. Thus the Poisson equation for ψ, 6.22, has been solved using the numerical solution of the second kind Fredholm Integral equation, A2.6, described in Appendix 2.

$$\frac{\partial^2 \psi}{\partial x^2} + \frac{\partial^2 \psi}{\partial y^2} = -\omega \qquad 6.22$$

The computer programs written for this method of calculating viscous flows are described in Appendix 10. The flow diagrams and the coding for the programs are shown in Appendix II.

6.3 TEST RUNS

The flow through a parallel duct, fig 6.11[114] was calculated for two Reynolds Numbers, 40 and 300. For Re = 40, the effect of varying the timestep was examined, whilst for Re = 300, the velocity profiles obtained were compared with those of Wang and Longwell (1964). The stability criteria established by Fromm (1964, 1969b) were used to decide the mesh size, viscosity and timestep. The criteria are reproduced in Appendix 8.

The run data for these flows is listed in the table below:

REYNOLDS NO.	INLET VELOCITY	ν	$\Delta x = \Delta y$	Δt
40	10	.1	.05	.005
40	10	.1	.05	.0025
40	10	.1	.05	.00125
300	20	.02667	.05	.001

Table 6.3 DATA FOR PARALLEL DUCT.

The flow through a duct with a backward facing step, fig. 6.12[114], was also calculated, at Reynold's numbers 4,8, 16. The length of the standing vortex formed behind the step was compared with that of Kawaguti (1965), Mueller (1974)

The run data is shown below.

REYNOLDS NO.	INLET VELOCITY	ν	Δx	Δy	Δt
4	5	.375	.1	.05	.001666667
8	5	.1875	.1	.05	.003333333
16	5	.09375	.1	.05	.006666667

Table 6.4 DATA FOR STEPPED DUCT

The details of how this data is supplied to the computer can be found in Appendix 11.

6.4 RESULTS

Figs 6.13[115] to 6.18[120] show the development of the velocity profiles in a parallel duct at the 30% station downstream of the duct inlet, using 3 timesteps and with Re = 40.

Fig 6.19[121] shows the various curve fitting routines applied to a velocity profile for the Re = 40 flow.

Figs 6.20[122] to 6.24[126] show the velocity profiles in a parallel duct with Re = 300.

Fig 6.25[127] shows the comparison between the velocity profiles for Wang and Longwell and for the present investigation at the 30% station.

Fig. 6.26[128] shows the comparison between Wang & Longwell and the profile obtained at the duct exit.

Fig. 6.27[129] shows the effect of the continuity correction on the profile at the 30% station.

Figs 6.28[130] to 6.37[139] show the development of the velocity profiles just downstream of the step (x = 2.1) and near the duct exit (x = 3.1) for Re = 16, with and without upstream differencing

Fig. 6.38[140] illustrates the method used to obtain the reattachment point coordinates.

Fig. 6.39[141] shows the variation of reattachment point with time for Re = 16.

Fig. 6.40[142] compares kawagutis results for the length of the standing vortex with those of this investigation.

Fig 6.41[143] compares the results of Mueller, kawaguti and the author for the prediction of the length of the standing vortex.

Fig. 6.42[144] to 6.51[153] show a selection of computer plots of the streaklines(instantaneous velocity vectors), velocity and vorticity profiles for flows at Re = 4,8 and 16 in the stepped duct.

6.5. DISCUSSION

It was decided to keep the first computer program as simple as possible, since this particular method of predicting viscous flows had not, to the authors belief, been tried previously. By doing this, some limited results could be obtained which would prove whether a more complex program was justified. For the first program, the geometry was limited to the parallel duct and the stepped duct, and the upwind differencing mechanism for the finite-difference equation was not included.

Some of the routines described in Appendix 10 were formulated as a result of testing this program. For example, when the velocity components were calculated at the $i + \frac{1}{2}$ and $j + \frac{1}{2}$ mesh positions directly, they were unacceptedly high as a result of the $1/r$ term in equation 4.7. By calculating the velocities at the mesh intersections, and linearly interpolating for the $i + \frac{1}{2}$ and $j + \frac{1}{2}$ velocity components, the results were more realistic.

The results from this first program being sufficiently promising, a second more general program, forming a part of the COMET data management system, was written. In this way programs which already existed, e.g. an automatic mesh fitting program, could be utilised. The upwind differencing mechanism was incorporated in the finite difference equations i.e. the complete scheme Fromm (1969a) was used. All the other routines were identical to those in the first program. This second program is described in Appendix 10 and its flow diagrams and coding are given in Appendix 11.

6.51 Parallel Duct

The first program was used to predict the flow at Reynolds number 40 using variable timesteps in the computation. The velocity profile development at the 30% station is shown in figs. 6.13[115] to 6.18[120], where it can be seen that the .005 sec timestep causes instability. The reason for the prediction

being unstable can be seen from examining the stability criteria, Appendix 8, where three criteria have been violated.

The data in Table 6.3[100] was calculated assuming $\beta = 0$ (for definition of β see Appendix 8) which will not be the case even for a parallel duct; therefore conditions A8,3 A8.4 and A8.5 will be violated as the calculation proceeds. It is not surprising that the velocity profiles show this instability. By halving the timestep to .0025 secs ensures that all criteria are satisfied, and as a result the velocity profiles show no sign of instability, figs. 6.16[118] to 6.18.[120]

The velocity profiles for the timesteps .0025 and .00125 secs have stabilised by t = .03 secs, fig. 6.16.[118] With the latter timestep, twice the number of iterations, and hence twice the computer time, were needed to achieve the same profile, which indicates that there is no real advantage in using smaller timesteps.

Although the profiles are stable, they do manifest a point of inflexion near the wall, This would appear to be erroneous since the expected profile is parabolic. It may be caused by:

a) the coarse grid chosen
b) the linear interpolation used in calculating the velocity profiles
c) the calculated velocity distribution.

To examine the possibility that the linear interpolation was the cause of the point of inflexion, a parametric cubic routine, Riley (1973), was used in its place. The resulting profile in fig. 6.19[121] shows that the point of inflexion remains although the portion in the middle of the duct is more parabolic. The original velocity profile at the mesh intersection points also exhibits this point of inflexion, due to the low velocity calculated at the mesh points adjacent to the walls. This could be due to the coarse mesh, and further testing is required to confirm this.

The flow at Re = 300 through the parallel duct, fig 6.11[114], was predicted using both first and second programs i.e. without and with upwind- differencing respectively. The flow data used for the prediction is given in Table 6.3,[100] and the velocity profiles for the 30% station are shown in Fig 6.20[122] to 6.24.[126] In the initial stages of flow development, no detectable difference can be seen between the velocity profiles, and in the final stages the difference is only slight, fig. 6.24.[126] Several points can be made regarding this figure:-

a) Although the points of inflexion near the wall are still present they are not so prominent.

The mesh spacing used was the same for both the Re = 40 and 300 prediction, yet the inflexion points appear to be disappearing. It is possible that this is a consequence of the higher inlet velocity used for the Re = 300 investigation, but no definite conclusion can be reached without further testing.

b) The velocity profiles without upstream differencing show an assymmetry between the velocities on opposite sides of the duct. This was also present at Re = 40.

The reason for this is that the mechanism for determining the local upstream direction was not included in the first program. Hence the values used in the finite-difference equations for one side of the duct would not be upstream, and would give different results to points on the other side of the duct. Once the mechanism was incorporated into the second program, the assymmetry disappeared.

c) The profile obtained is not parabolic.

This is not surprising as the profile was drawn for a station close to the duct inlet. Here the flow is not fully developed, resulting in a non-parabolic velocity profile. The profiles from Schlichting (1968) and Wang and Longwell (1964) confirm this, fig. 6.25.[127]

Schlichting integrated the boundary layer equations downstream from the duct inlet, joining this solution to one obtained by integrating the same equations upstream, from the asymptotic parabolic distribution. However, the accuracy of his results for the duct inlet region must be in question, since the boundary layer assumptions are not valid there. The derivative $\partial^2 u / \partial x^2$ is not negligible relative to $\partial^2 u / \partial y^2$, and the pressure gradients in the y direction are not necessarily small. These factors indicate that the momentum equation for v should also be solved for the inlet region.

Wang et al (1964) used the streamfunction-vorticity approach for predicting parallel duct flow, solving the equation by finite-difference methods. Their velocity profile, fig. 6.25[127], has a concave central portion which was judged by them to be a real effect, since it was also present when the mesh was coarser. The concavity was reduced by having a non-uniform inlet velocity profile as a consequence of the mesh being extended upstream of the duct inlet. Wang et al maintain that this was more realistic as the effect of the duct walls would be felt upstream, The author believes that the concavity is unlikely to be a real fluid effect, but to be due to inaccuracies present in the finite-difference equations they used. No concavity was present in either the authors results or those of Schlichting, fig. 6.25[127].

The error in the maximum velocity predicted at the 30% station is approximately 21% and 17%, when compared to the profiles of Schlichting and Wang et al respectively. Fig. 6.26[128] shows the comparison of the velocity profile at the duct exit section, with the equivalent profiles from Schlichting and Wang. Here, agreement is generally better with the error in maximum velocity decreasing to 20% and 9% compared to Schlichting and Wang. It was thought that adjusting the exit velocity profile (to satisfy continuity between duct inlet and exit) was the reason for the better agreement. However, when a similar

correction was applied to the 30% station, fig. 6.27[129], the errors increased to 27% and 22% from 21% and 17% obtained previously.

A parabolic velocity correction, based on the parabola used for the exit velocity boundary condition by Wang et al (1964) and Gosman (1969), was used to predict a velocity correction at the 30% station, fig. 6.27[129]. The error increased to 29% and 24% compared to 27% and 22% for the linear velocity correction. However, for flows other than those through a parallel duct, the exit velocity profile will not be parabolic, and the parabolic correction will not be relevant. As a result, the linear velocity correction was used at the duct exit, in predicting the flow in the stepped duct. It is not known, without further testing, why the application of these corrections at the 30% station should increase, rather than decrease, the maximum velocity error.

It is interesting to speculate why such corrections are necessary at all? One possible reason is that the higher-order terms missing from the finite-difference equation account for the mass imbalance through a vorticity imbalance. This implys that the correction should be applied at all mesh columns, not just at the duct exit, yet at the 30% station this led to an increased error. More sophisticated correction modelling on finer meshes could resolve the increasing error, but further testing is required.

It is believed that if an integral (or conservative) finite-difference method, Gosman(1969), were used, any errors arising from vorticity imbalances would be eliminated. Also, continuity should be checked at each mesh point to ensure that there are no mass imbalances. Fromm (1969a) does not state whether he uses a correction process similar to the one described here, but it is unlikely. The reason is given in Gosman (1969) i.e. if the vorticity terms are expressed in terms of streamfunction, then there is no need to make any explicit appeal to the mass-conservation principle.

6.52 Stepped Duct

Three flows were predicted using the stepped duct, at Reynolds numbers of 4,8 and 16. The flow data is given in Table 6.3[100], and was calculated using the stability criteria in Appendix 8.

As the development of the velocity profile in the duct upstream of the step will be very similar to that in the parallel duct, the distribution will not be shown. Figs. 6.28[130] to 6.37[139] show the velocity profile development at x = 2.1 and x = 3.1 i.e. just downstream of the step and near the exit respectively. Results, both with and without upstream differencing, are shown.

Just downstream of the step, the flow starts recirculating immediately, and there is very little difference between the results of the two programs. As time increases, negative velocities become greater as the recirculating region expands. The point of inflexion in the velocity profile adjacent to the wall is present again, probably due to the low inlet velocity used.

One interesting fact is shown in fig. 6.34[136]. It can be seen that the velocity adjacent to the wall and near the duct exit has become negative. This does not lead to an instability, as subsequent figures show that the velocity becomes positive there shortly afterwards. This could be a starting phenomena caused by the presence of more negative vorticity, from the lower wall, in the flow. As time progresses, and more positive vorticity is diffused and convected into the flow, this phenomena is removed.

It can be seen by comparing figs. 6.32[134] and 6.37[139], that the omission of upwind differencing has more effect near the step than further downstream. This will almost certainly be due to the rapidly changing conditions near the step compared with relatively calm exit conditions. The shape of the velocity profile near the exit is much more

rounded than the profile in fig. 6.24[126], and this could be due to there being more mesh points across the stepped duct than there were across the parallel duct,

The lengths of the standing vortex behind the step were to be compared with the results from Kawaguti's (1965) streamfunction - vorticity method. To measure this length, fig. 6.40[142], the reattachment point was required. The procedure used to obtain this measurement is illustrated in figs. 6.38[140] and 6.39[141]. Once the flow had begun to converge curves of velocity against x, distance down the duct, at several positions across the duct were plotted, fig. 6.38[140]. Where these curves crossed the $u = 0$ axis, gave the x value of the separation streamline for that y value across the duct. Hence the separation streamline could be plotted, fig. 6.38[140], and the reattachment point estimated.

It will be noted that the separation streamline for y = 2.4 was actually plotted at y = 2.425. The reason is that the U - velocity component stored at the mesh point along the row at y = 2.4, are calculated at y = 2.425 i.e. halfway between mesh rows at y = 2.4 and y = 2.45. The separation streamline at the other points are similarly plotted.

If the reattachment points are obtained at every timestep, or other timestep if convenient, then they can be plotted against flow elapsed time i.e. fluid time since prediction started, fig. 6.39[141]. Once estimates of these points stabilise, then the final position of the reattachment point can be obtained and hence the length of the standing vortex.

Lengths of the standing vortex are compared with those of Kawaguti (1965) in fig. 6.40[142]. The same trend is noticeable but the average difference between the predicted lengths is approximately 90%. Surprisingly, the results without upwind differencing are closer to those of Kawaguti than those with upwind differencing. Since the flow is most complex in the recirculation region, it would be expected that the upwind differencing model would produce the more accurate result. It could be that the

errors arising from the coarseness of the mesh are sufficiently large for them to mask the errors arising from not using the upwind differencing, and to account for the large discrepancy between predicted lengths.

Before writing the program with upwind differencing, the three flows in the stepped duct were predicted with the first program. The duct was much shorter for this investigation i.e. the duct exit was 2 mesh columns downstream of an estimated reattachment point. These results are not shown on fig. 6.40[142] because they bore no relation to either Kawagutis[1] results or to the more recent results from the two programs. The reason for this was that the effect of the linear correction process applied across the duct exit on adjacent mesh columns was much greater than anticipated.

With reference to the streakline pictures, fig. 6.42[144] onwards, it can be seen that for Re = 4, the effect of the linear correction is apparent at 2 or 3 adjacent mesh columns. For Re = 8, the effect is apparent at 3 or 4 columns and for Re = 16, at 5 or 6 adjacent mesh columns. With the duct exit only 2 mesh columns downstream of an estimated reattachment point, and the correction effect being transmitted upstream, it was to be expected that little agreement was obtained with the first trial runs. For the second series of predictions the duct was lengthened considerably so that the flow would reattach without hindrance from the downstream boundary.

Both Kawagutis[1] results and those from the present investigation were plotted with those from Mueller(1970), who predicted the length of the standing vortex obtained from the flow over a backward facing step in an open channel. Kawaguti's and the author's results were obtained for a ducted flow, so they are not directly comparable. Although the authors results agree fairly well with Muellers, it would be interesting to calculate the flow in an open channel, to see how the results were altered.

This could be done by using a duct with a roof 15 or 20 step heights away from the step, to ensure that the roof

caused as little disturbance as possible to the step flow. For reasons given below, this was not carried out.

Figs 6.42[144] onwards give a pictorial history of the three flows from the streakline, velocity and vorticity vector plots. Some of the plots were drawn on a kingmatic draughting machine, and the others were drawn on a drum plotter, which accounts for the squared paper on which some of the plots are drawn. The plots are produced completely automatically, the user requesting the particular plot required in the input data, Appendix II.

6.53 Computer Time and Finite-Difference Equations

Some comments must be made about the relatively long computer times required by the program. The number of iterations required to obtain convergence was about 80 on average, and with approximately 300 mesh points, each iteration took about 12 minutes CPU time and 40 minutes elapsed time i.e. physical time on the machine against 12 minutes actual numerical calculation time. All the computations were carried out on the Rolls-Royce (1971) limited, Bristol Group KDF9 computer, which is slow in comparison with machines currently available.

In line with other users of the computer, the run time was arbitrarily limited to between 20 to 30 minutes per day, which meant 3 iterations could be calculated each working day. Simple arithmetic then shows that 27 working days, or 5½ working weeks are required for each flow, excluding mishaps. After each run of 3 iterations, all mesh information was stored on disc by the ring processing package. A back up was kept of each days run, so that in the event of a mishap, it would be unnecessary to restart the calculation from the beginning.

During most weeks, it was quite usual to develop a minor computer fault which meant repeating a days run. As a result, only 4 working days were used in that week, and the converged solution could take anything from 6 to 8 weeks.

Occasionally a more serious fault might occur when even the back up was lost, which meant repeating the whole calculation. The complete solution could take 10 to 14 weeks depending on how far the solution was towards completion when the fault occurred.

The total time taken to obtain all the results presented here has been so long that any variation e.g. finer meshes, other inlet velocity profiles or other geometries, have not as yet been tried. Since this investigation is being carried out in conjunction with the authors company, some of these variations may be tried in the future.

The KDF 9 computers are shortly to be replaced by a CDC Cyber 74 computer which is approximately 30 times faster. A significant reduction in CPU time will be experienced when using this new machine.

Comments are also required concerning the derivation of Fromms finite-difference equations. Before the first program was written, the second-order form, as presented in Fromm (1969a), was derived from first principles and found to be correct. It was decided at that time that as the second-order form was correct, the derivation of the fourth-order form would be delayed and the programming completed. It was only as this thesis was being written that the fourth-order form was derived, and found to be incorrectly printed in Fromm (1969a). Thus the wrong equation had been used unknowingly throughout the viscous-flow investigation.

After the program was corrected, the Re = 8 and 16 cases were rerun to see if this vorticity equation error accounted for the discrepancy between the authors and Kawagutis results, fig 6.40[142]. However, the corrected equation caused no detectable difference in the standing Vortex length when plotted on that figure. Although this appears rather surprising, figs 6.42[144], 6.44[146], 6.49[151] all show that along any mesh row in the recirculating region, where the fourth order equation would be used, $\omega^n_{i-1,j} \simeq \omega^n_{i+1,j}$; $\omega^n_{i,j} \simeq \omega^n_{i+2,j}$.

It can be seen from Appendix 9 that the terms $\omega^{n}_{i+1,j}$ and $\omega^{n}_{i+2,j}$ should have been used instead of $\omega^{n}_{i-1,j}$ and $\omega^{n}_{i,j}$ respectively. The figures show that the vorticity is approximately the same at these corresponding points and hence correcting the equation will not have a significant effect on the standing vortex length.

The incorrect equation, as taken from Fromm (1969a), is given in section 6.22, and the correct version is given in Appendix 9.

6.6. Conclusions

1) The velocity profiles obtained in the parallel duct investigation agree reasonably well with those of Wang Longwell (1964)

2) The linear correction process used at the duct exit did not decrease the maximum velocity error at the 30% station. Further testing is required to establish the reasons for this, or why such corrections are required at all.

3) The points of inflexion in the velocity profile which are adjacent to the duct wall, could have been caused by the coarse mesh or the low inlet velocity used. Further investigations are needed to establish the correct cause.

4) A parabolic interpolation routine was used in place of the linear interpolation process for the velocities, resulting in an improved velocity profile for Re = 300.
For flows without a parabolic velocity profile, the parametric cubic routine, Riley (1973), is probably to be preferred since this is more general.

5) The same trend for the variation of the standing vortex length with Reynolds number was observed in the results of the author and Kawaguti. However, the magnitude of the difference between the predictions was rather high. Better agreement could probably be obtained by using a finer mesh in the recirculating region, and a coarser mesh elsewhere.

6) The prediction of these flows took an exceptionally long time in terms of CPU time and manhours. They were simple in nature compared with a combustion chamber flow, where both turbulence and chemical effects must also be considered. This would obviously lead to a further increase in computing time.

6.7 Further Work

1) In order to make the method usable outside the authors company, the COMET system and the ring processing package, and all the authors programs need to be in Fortran. The ring package has been translated, and work is in progress on translating the COMET system.

2) The strengths of the source and vortex sheets on the boundary could be described by a cubic spline distribution, rather than assuming the strengths are constant along the sheet. The use of the spline would give a continuous rather than the step distribution used at present.

3) Cubic splines could also be used to interpolate for the velocity components halfway between the mesh points, in place of the linear interpolation used at present.

4) The calculation of the vorticity at the convex corner could also be further investigated, since more complex models are used by other investigators.

5) Different flows should be predicted so that the results may be compared with other investigators., to see if the large difference found between the authors' and Kawagutis' results is repeated.

6) Methods for reducing the long computing times could be investigated in order to make this method competative with other methods available from the literature.

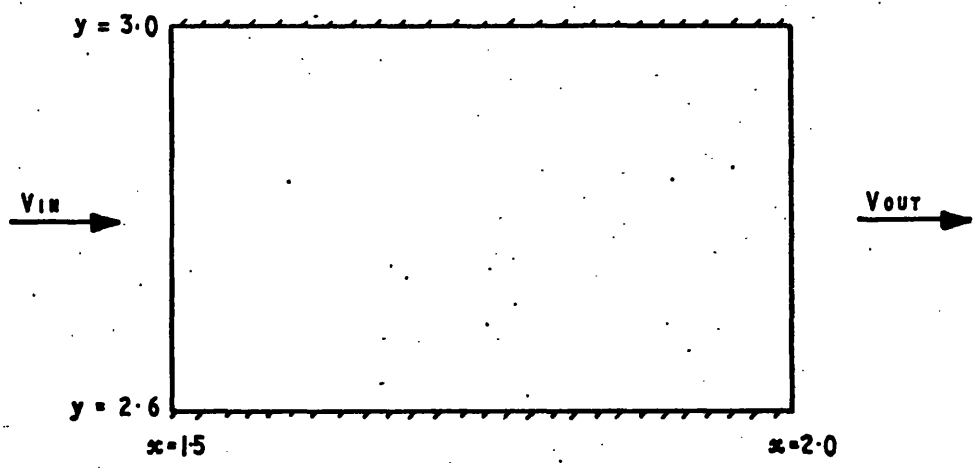

FIG.6.11 PARALLEL DUCT

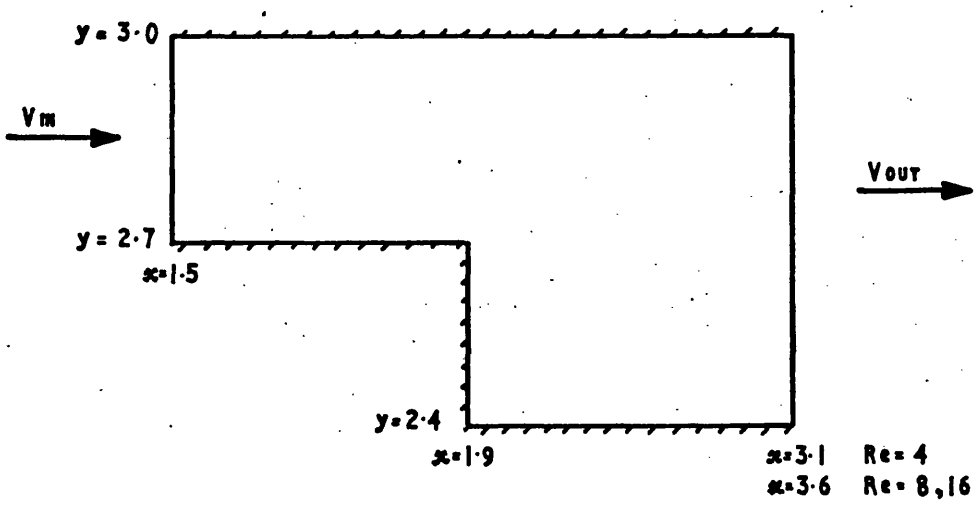

FIG.6.12. STEPPED DUCT

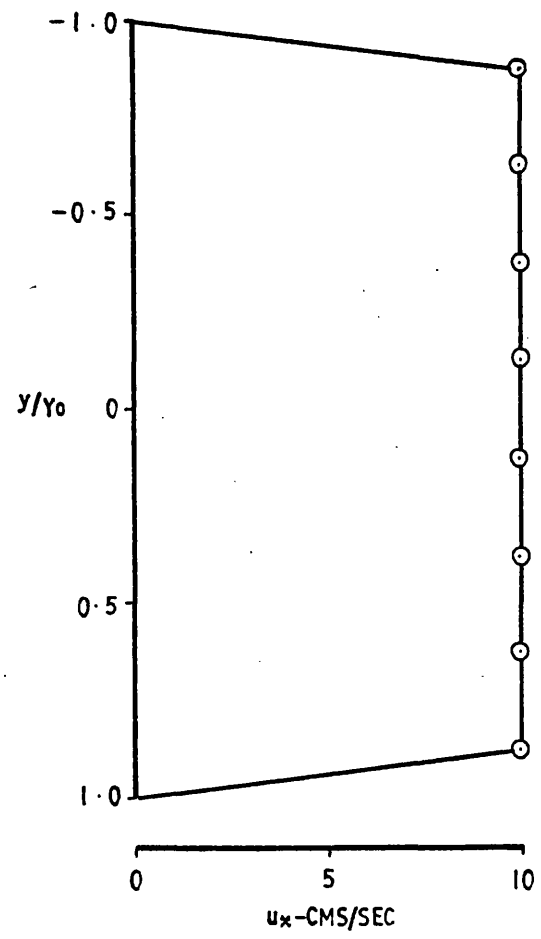

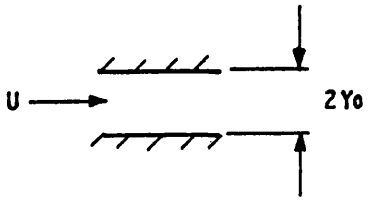

Δt
0·005
0·0025
0·00125

Re = 40
t = 0
x = 1·65

FIG. 6.13 VELOCITY PROFILE AT 30%

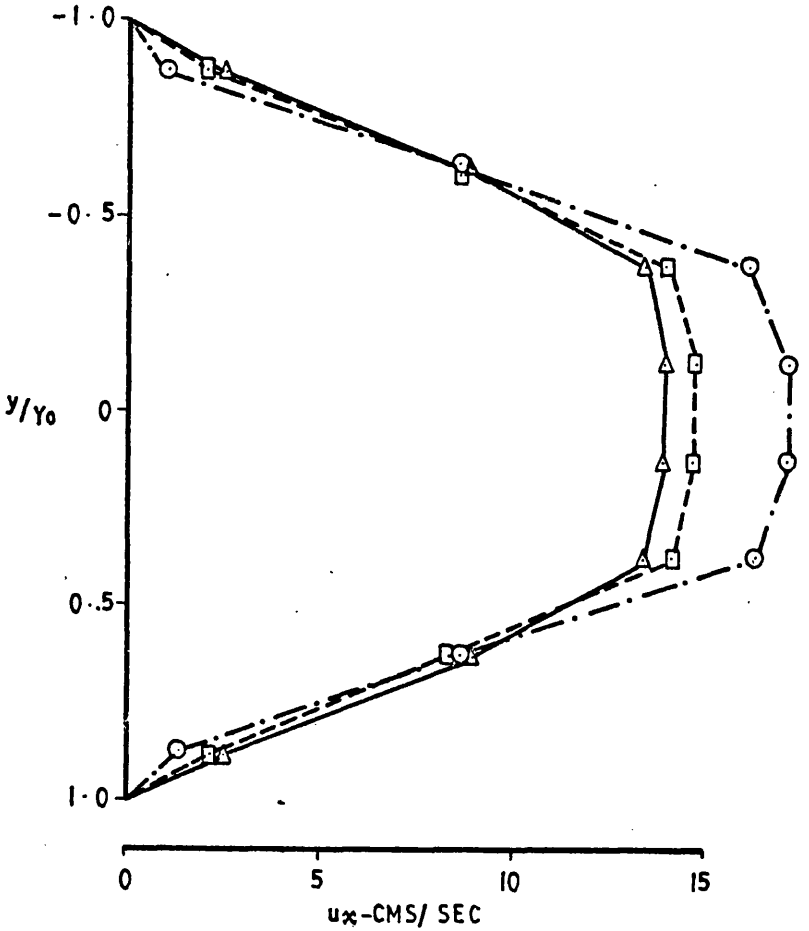

Δt
⊙ 0·005
⊡ 0·0025
Δ 0·00125

Re = 40
t = 0·01
x = 1·65

FIG. 6.14 VELOCITY PROFILE AT 30%

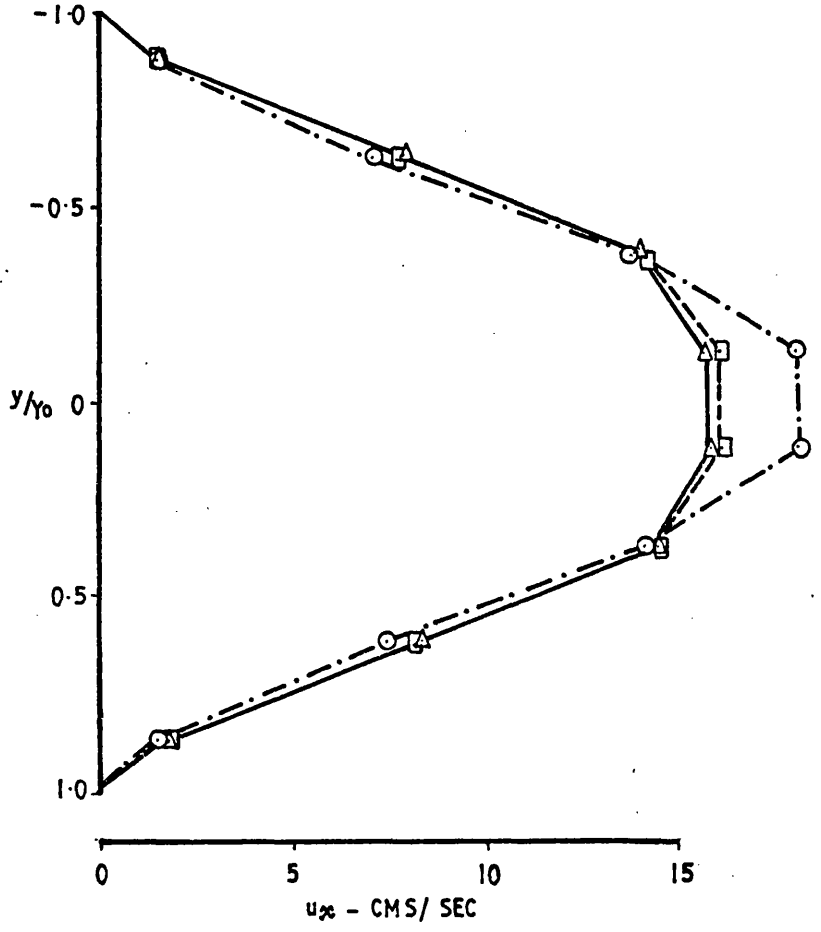

Δt
⊙ 0·005
⊡ 0·0025
△ 0·00125

Re = 40
t = 0·02
x = 1·65

FIG. 6. 15 VELOCITY PROFILE AT 30%

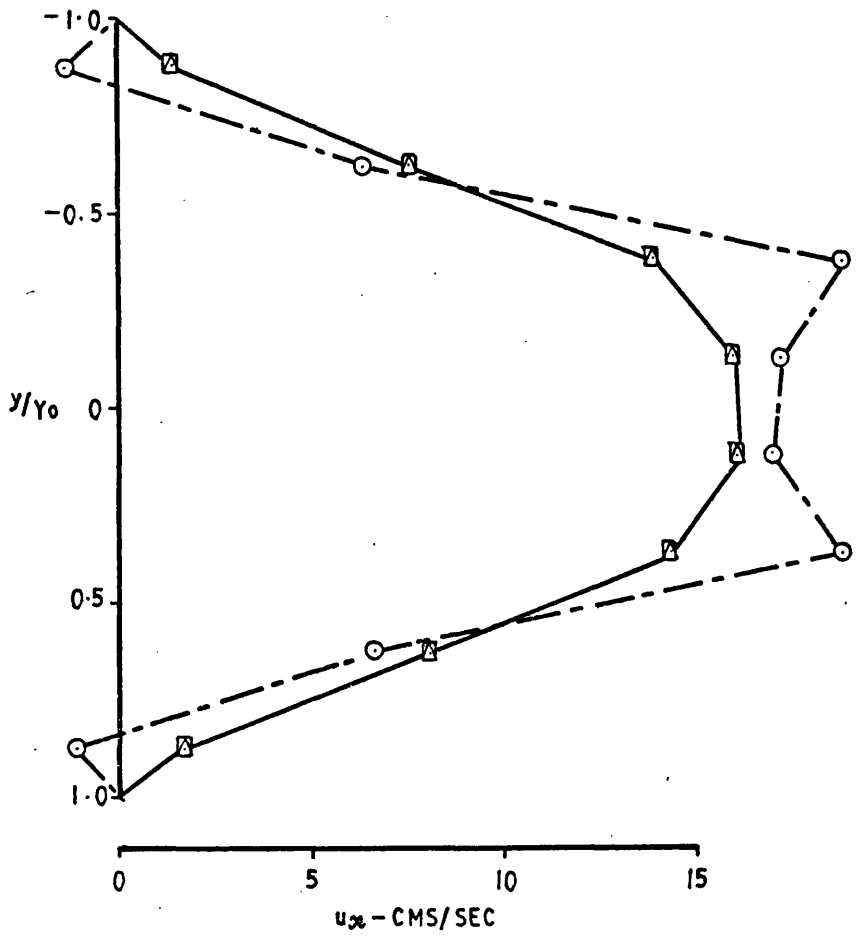

Δt
⊙ 0·005
⊡ 0·0025
△ 0·00125

Re = 40
t = 0·03
x = 1·65

FIG. 6.16 VELOCITY PROFILE AT 30%

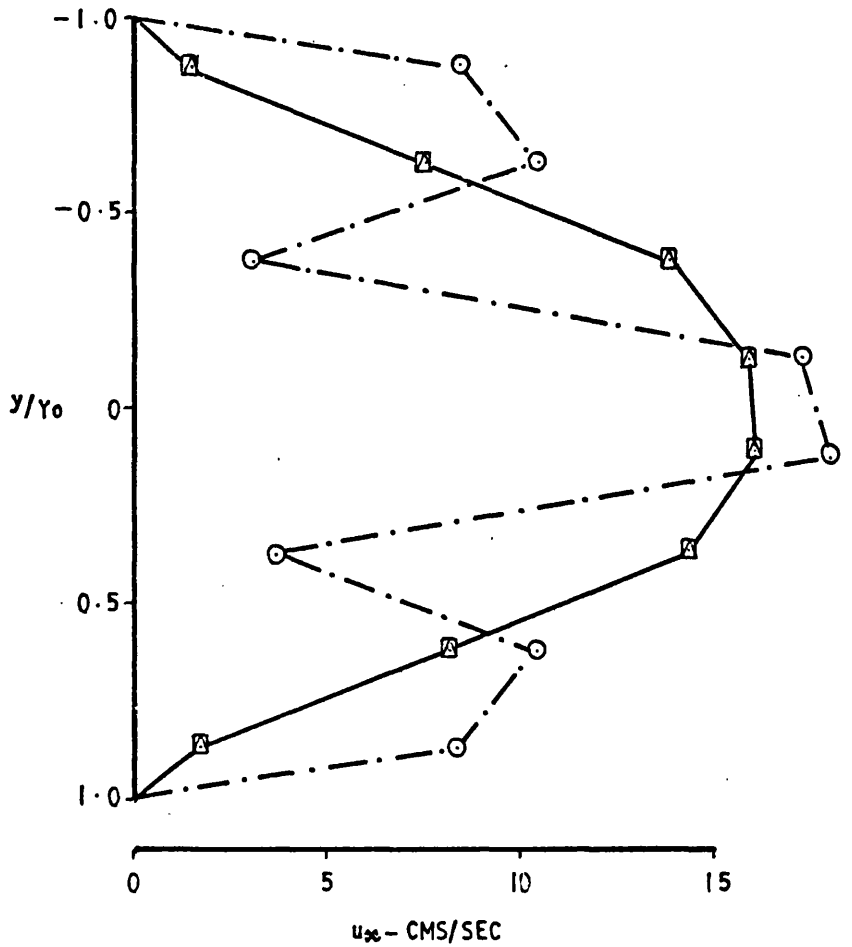

Δt
⊙ 0·005
⊡ 0·0025
△ 0·00125

Re = 40
t = 0·035
∞ = 1·65

FIG. 6.17 VELOCITY PROFILE AT 30%

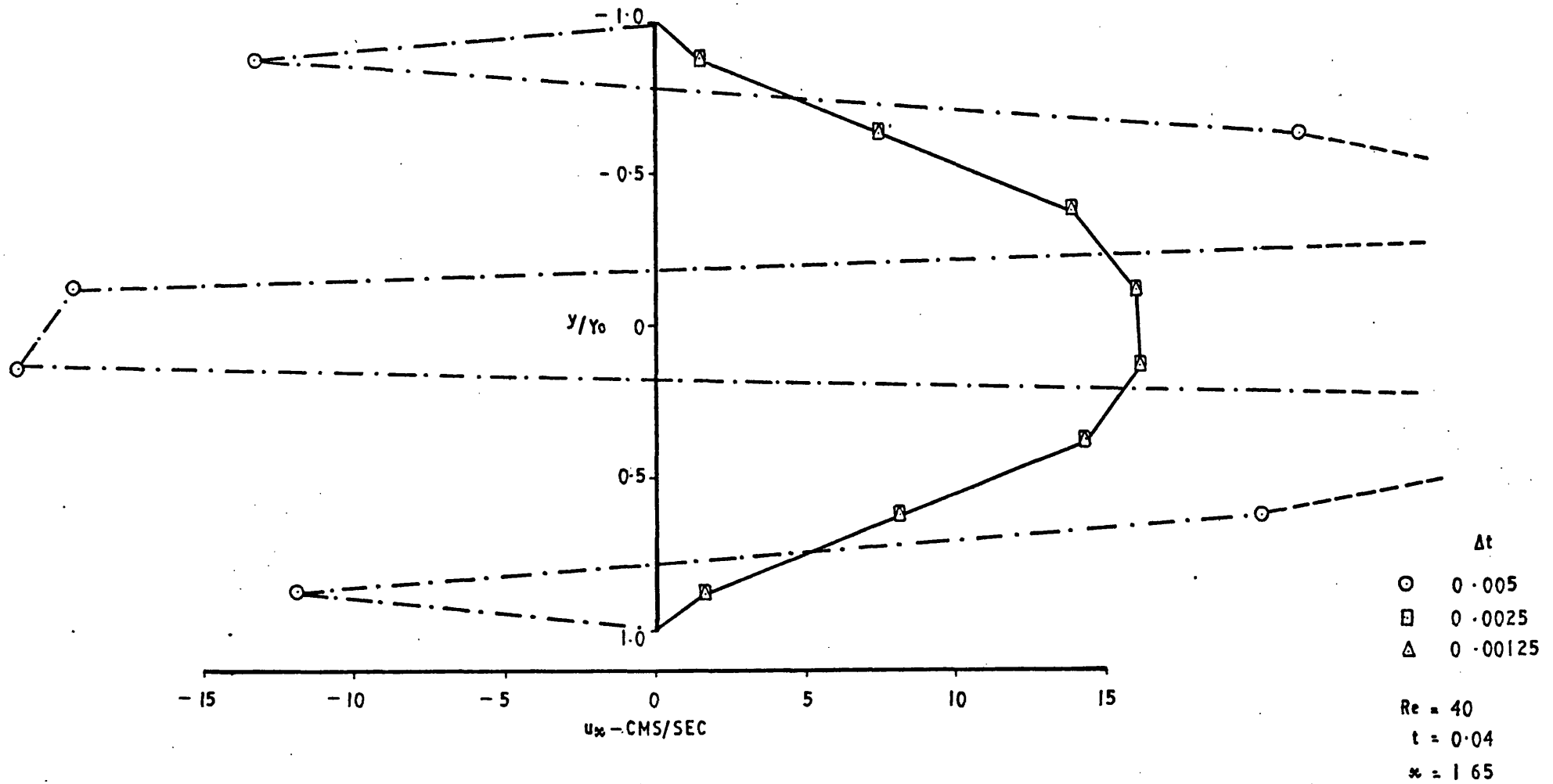

FIG. 6.18 VELOCITY PROFILE AT 30%

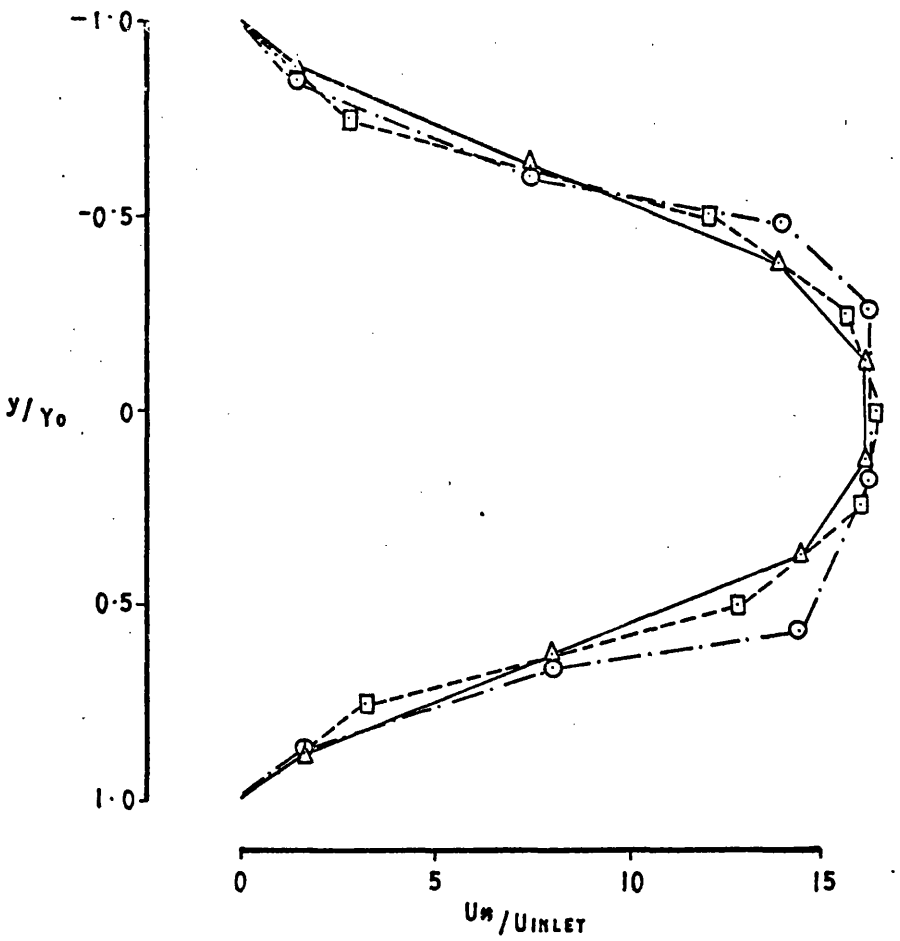

⊙ PARAMETRIC CUBIC INTERPOLATION
△ LINEAR INTERPOLATION
□ ORIGINAL PROFILE AT MESH POINTS

Re = 40
t = 0·04
α = 1·65

FIG 6.19 VELOCITY PROFILES AT 30%

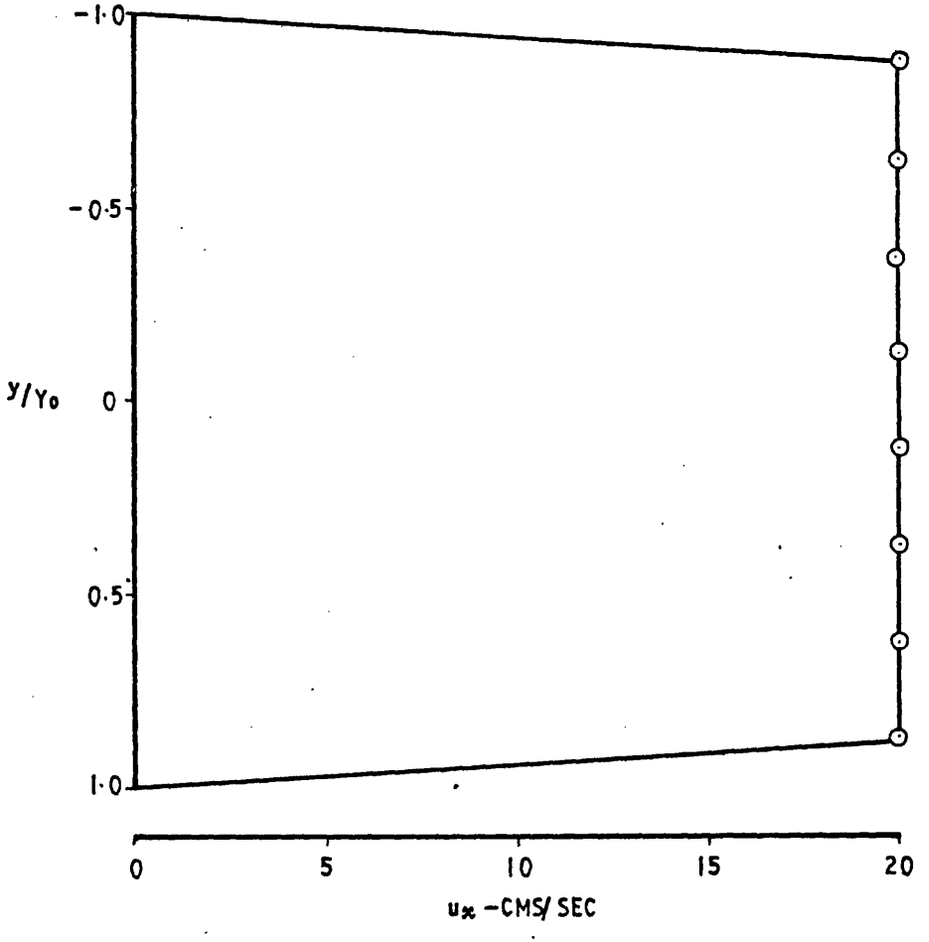

⊙ WITH AND WITHOUT UPSTREAM DIFFERENCING

Re = 300
t = 0
x = 1·65

FIG. 6.20 VELOCITY PROFILE AT 30%

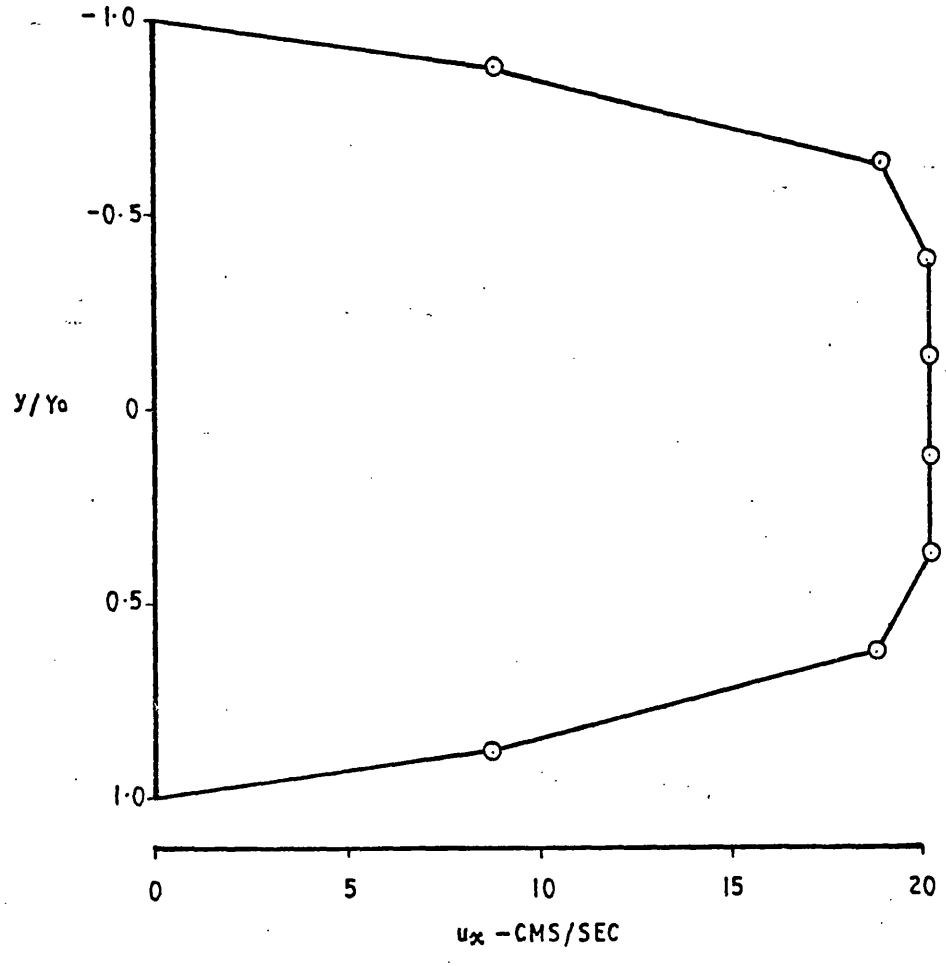

⊙ WITH AND WITHOUT UPSTREAM DIFFERENCING

Re = 300
t = 0·004
α = 1·65

FIG. 6.21 VELOCITY PROFILE AT 30%

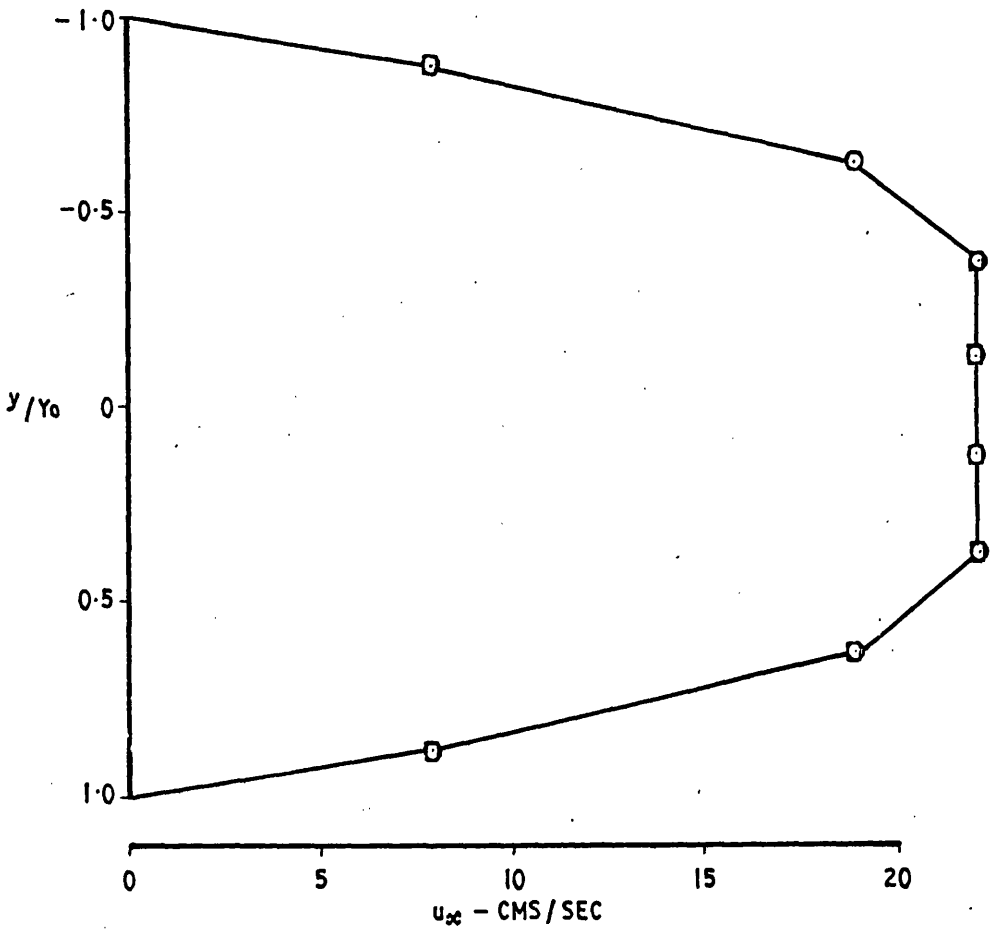

⊡ WITH UPSTREAM DIFFERENCING
⊙ WITHOUT UPSTREAM DIFFERENCING

Re = 300
t = 0·014
∝ = 1·65

FIG. 6.22 VELOCITY PROFILE AT 30%

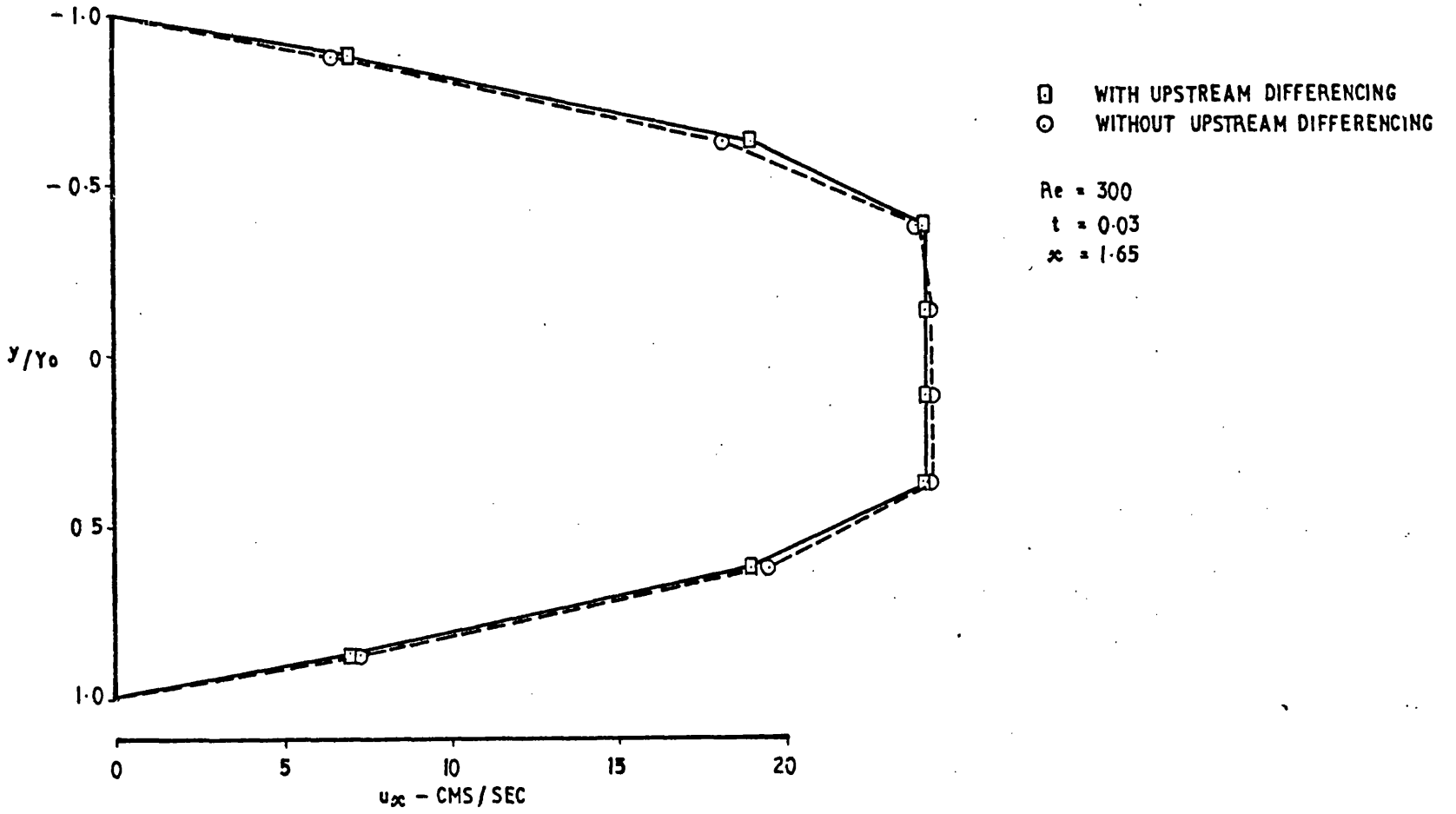

FIG. 6.23 VELOCITY PROFILE AT 30%

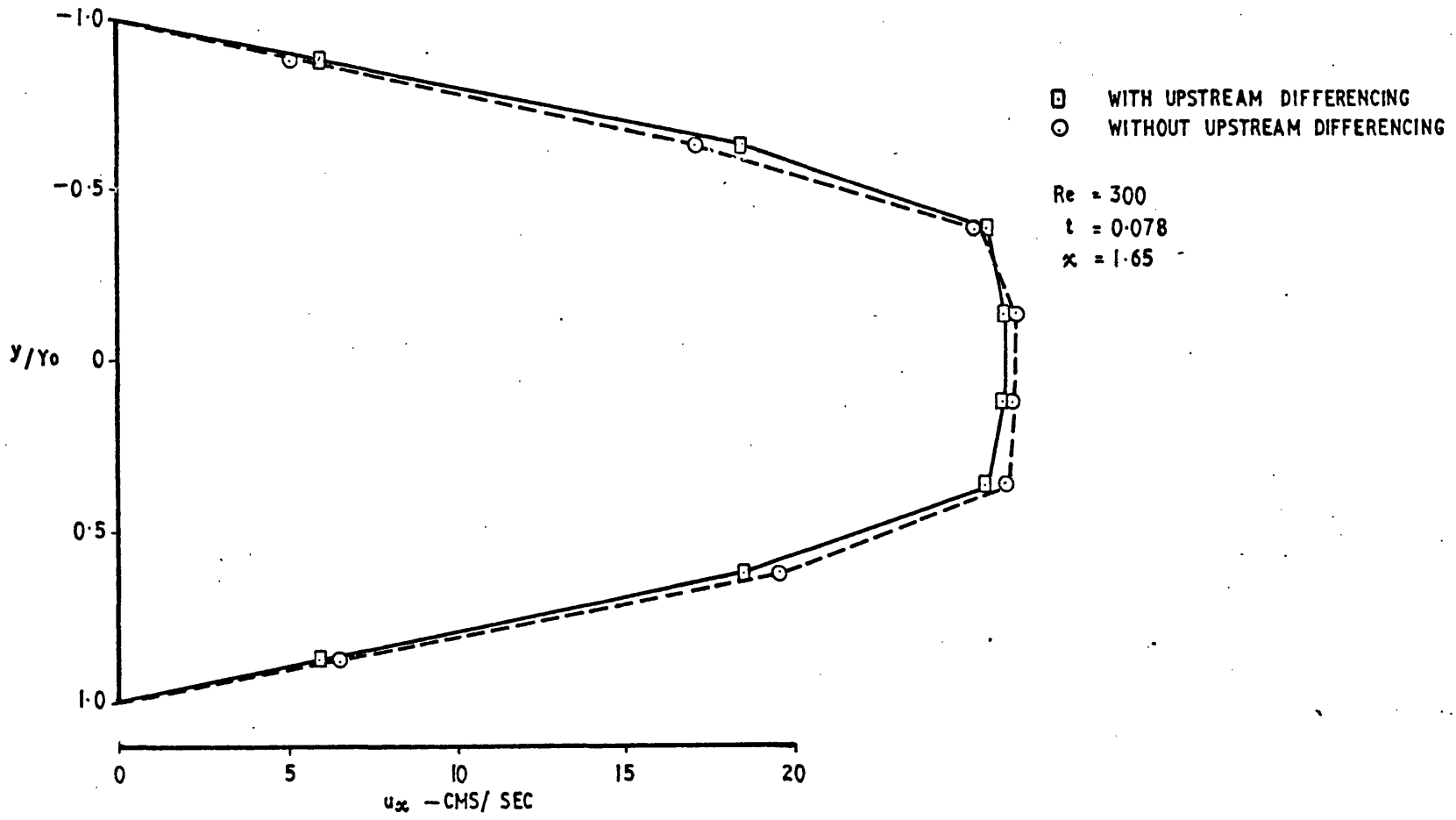

FIG. 6.24 VELOCITY PROFILE AT 30%

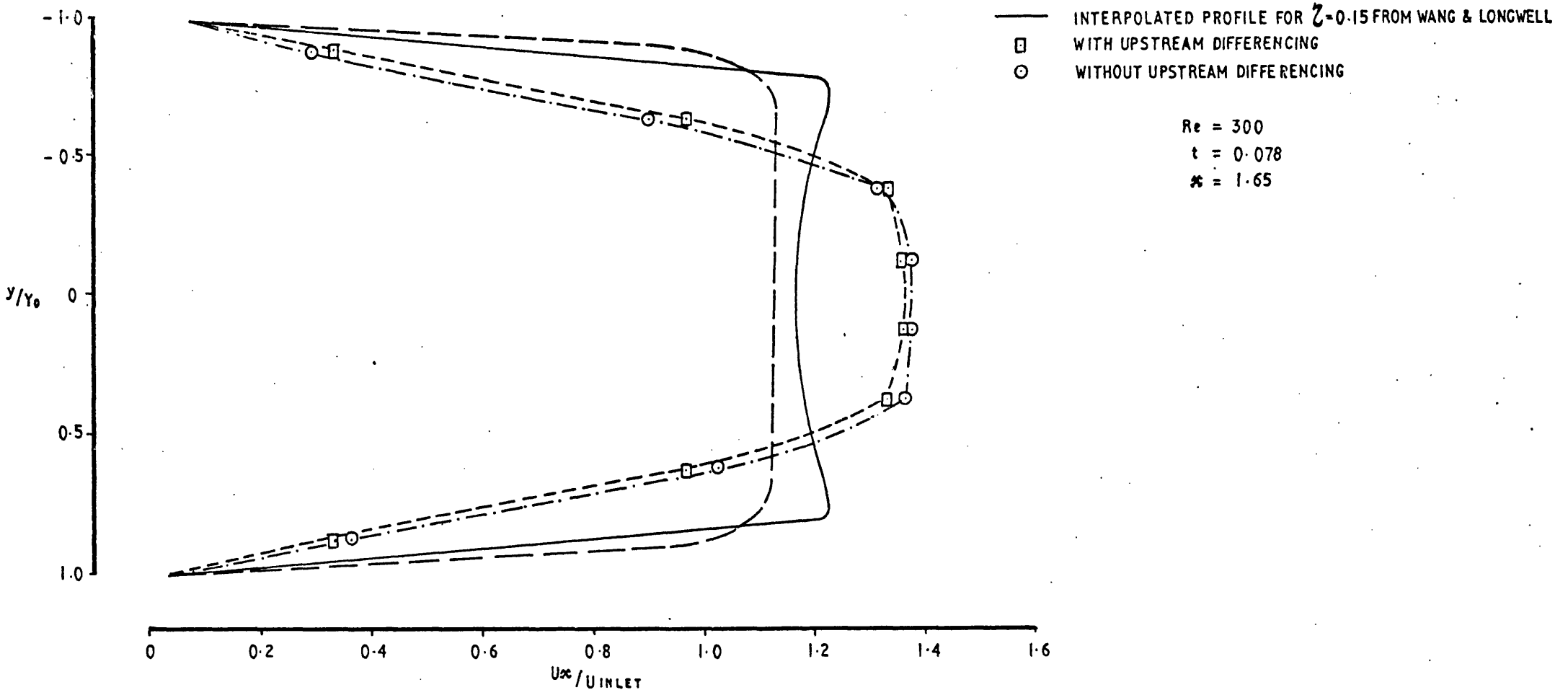

FIG.6.25 COMPARISON OF VELOCITY PROFILES AT 30%

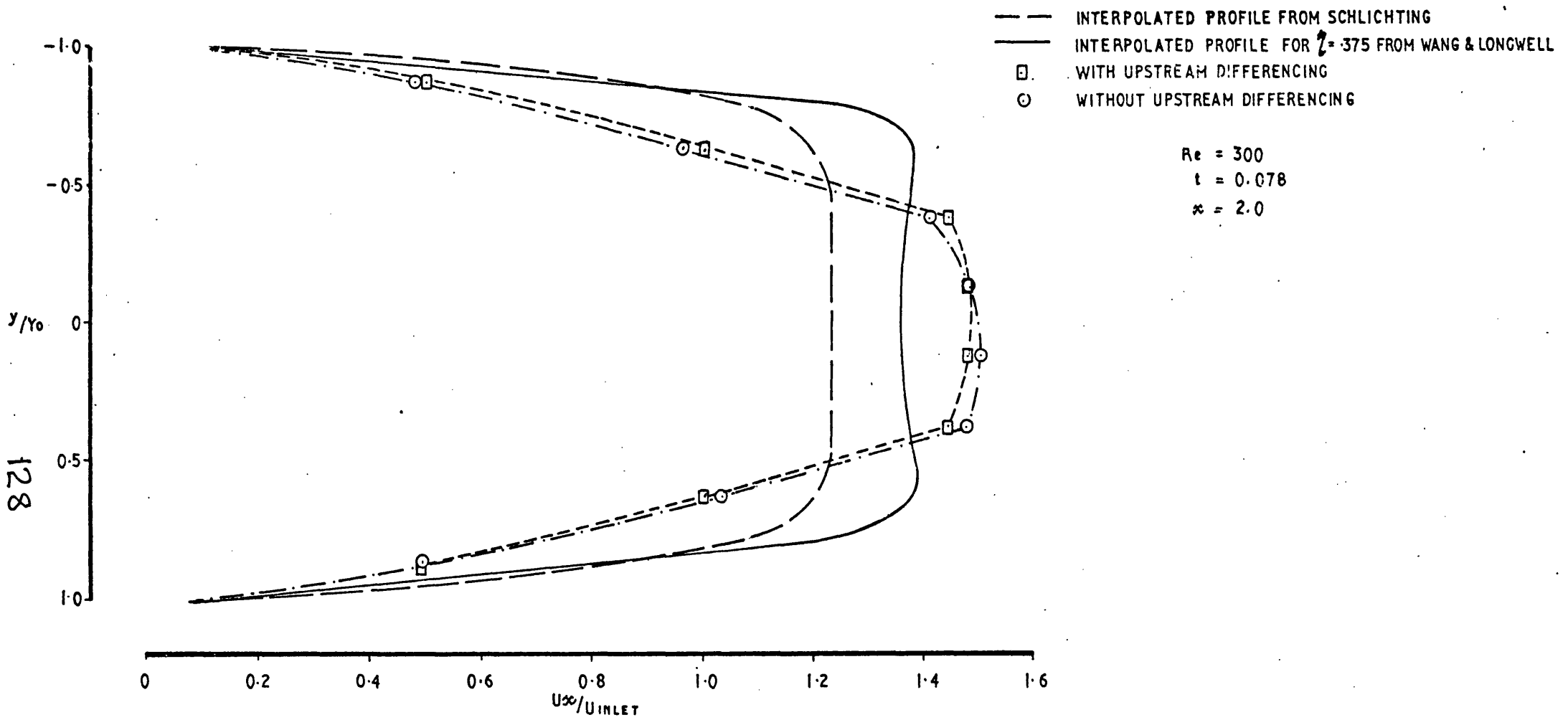

FIG. 6.26 COMPARISON OF VELOCITY PROFILES AT 100%

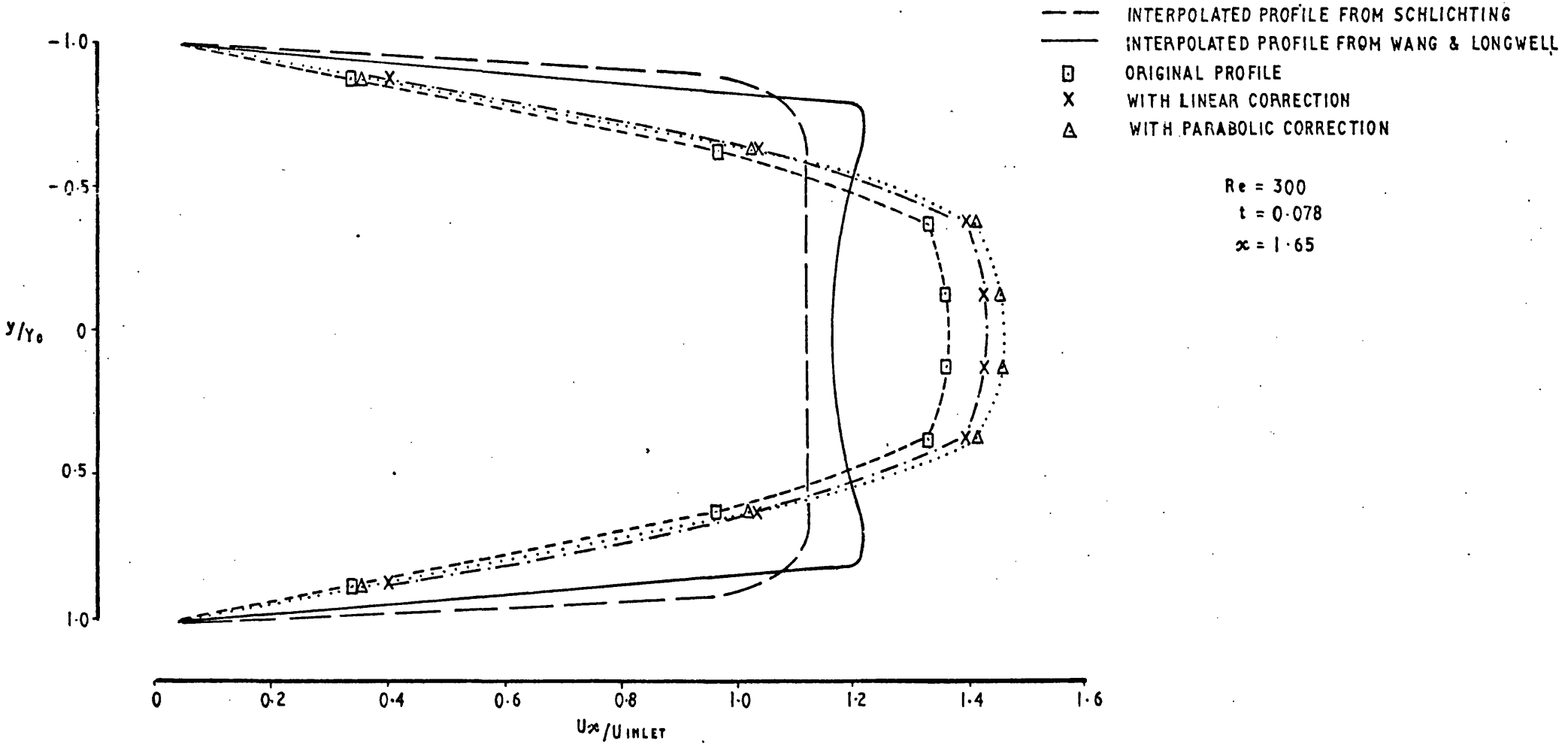

FIG. 6.27 CORRECTED VELOCITY PROFILE AT 30%

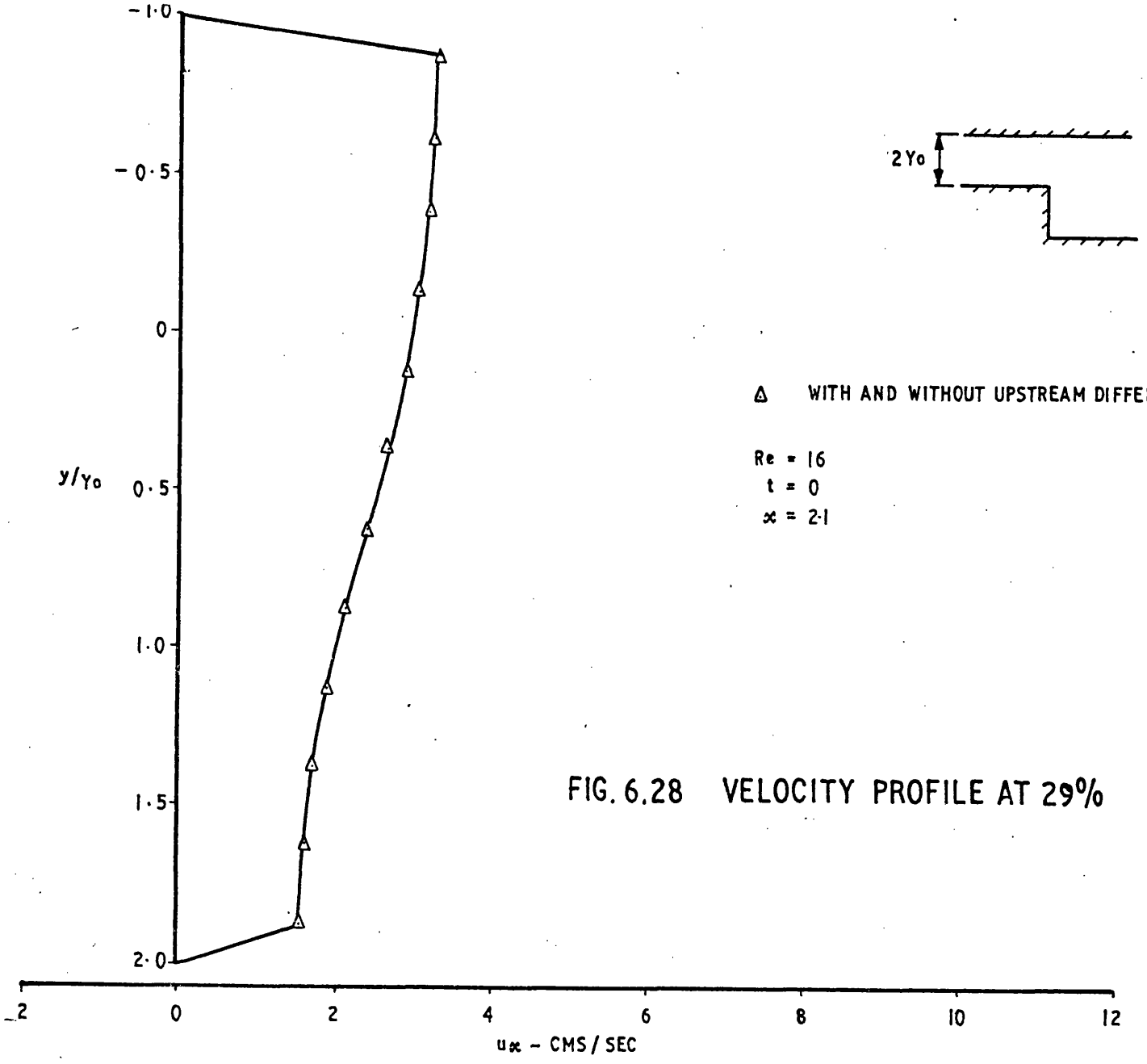

Δ WITH AND WITHOUT UPSTREAM DIFFERENCING

Re = 16
t = 0
∝ = 2·1

FIG. 6.28 VELOCITY PROFILE AT 29%

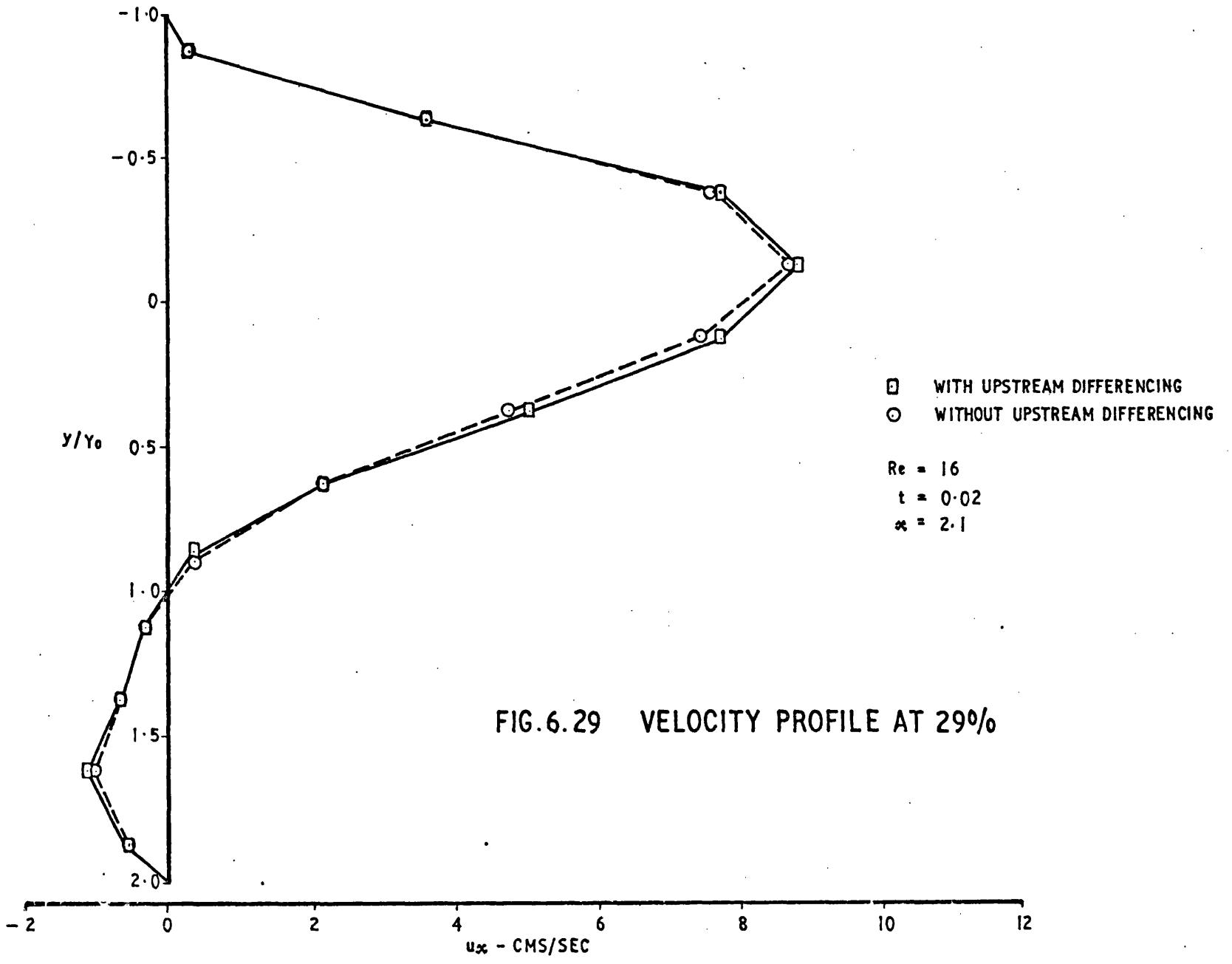

FIG.6.29 VELOCITY PROFILE AT 29%

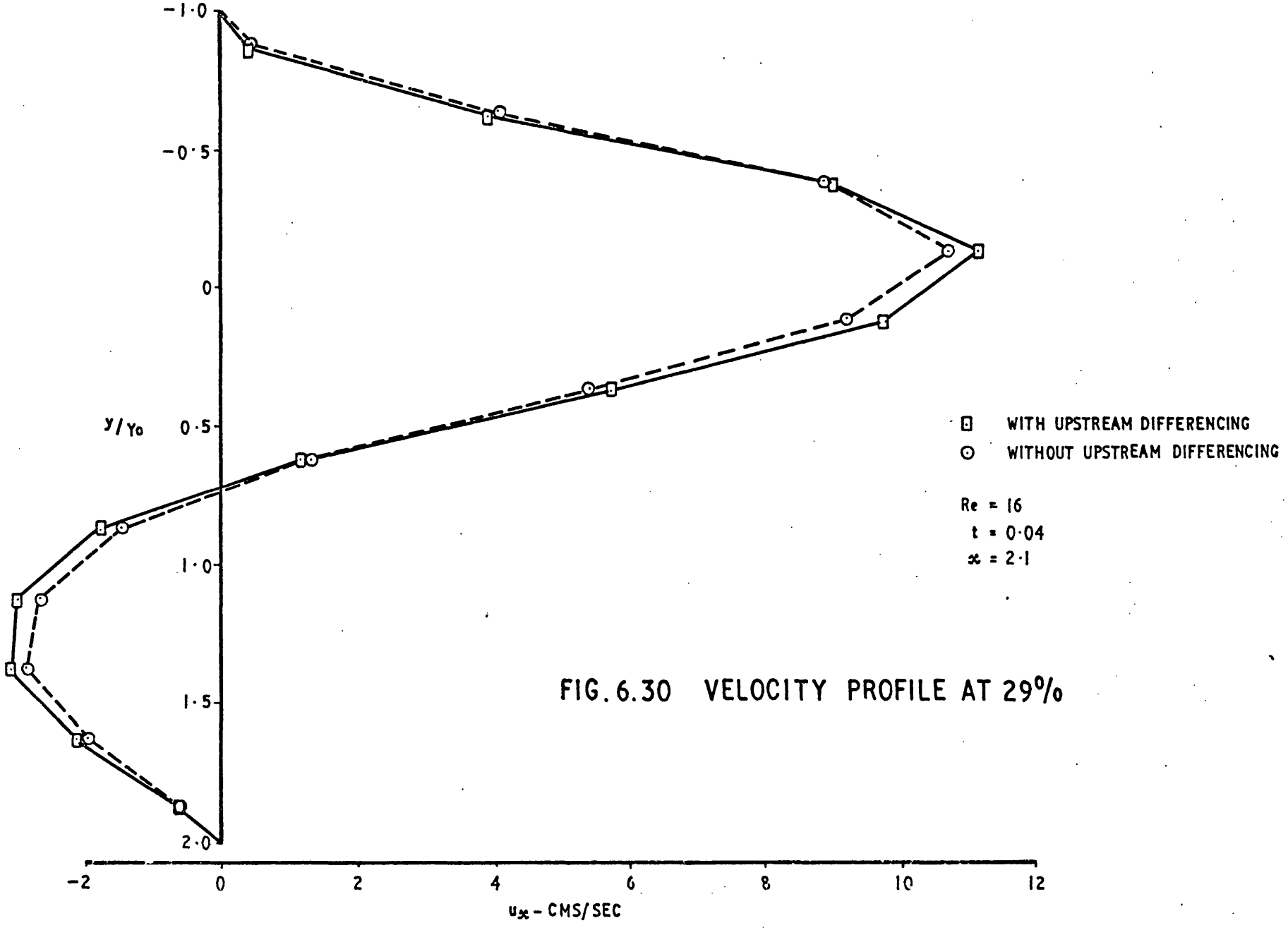

FIG. 6.30 VELOCITY PROFILE AT 29%

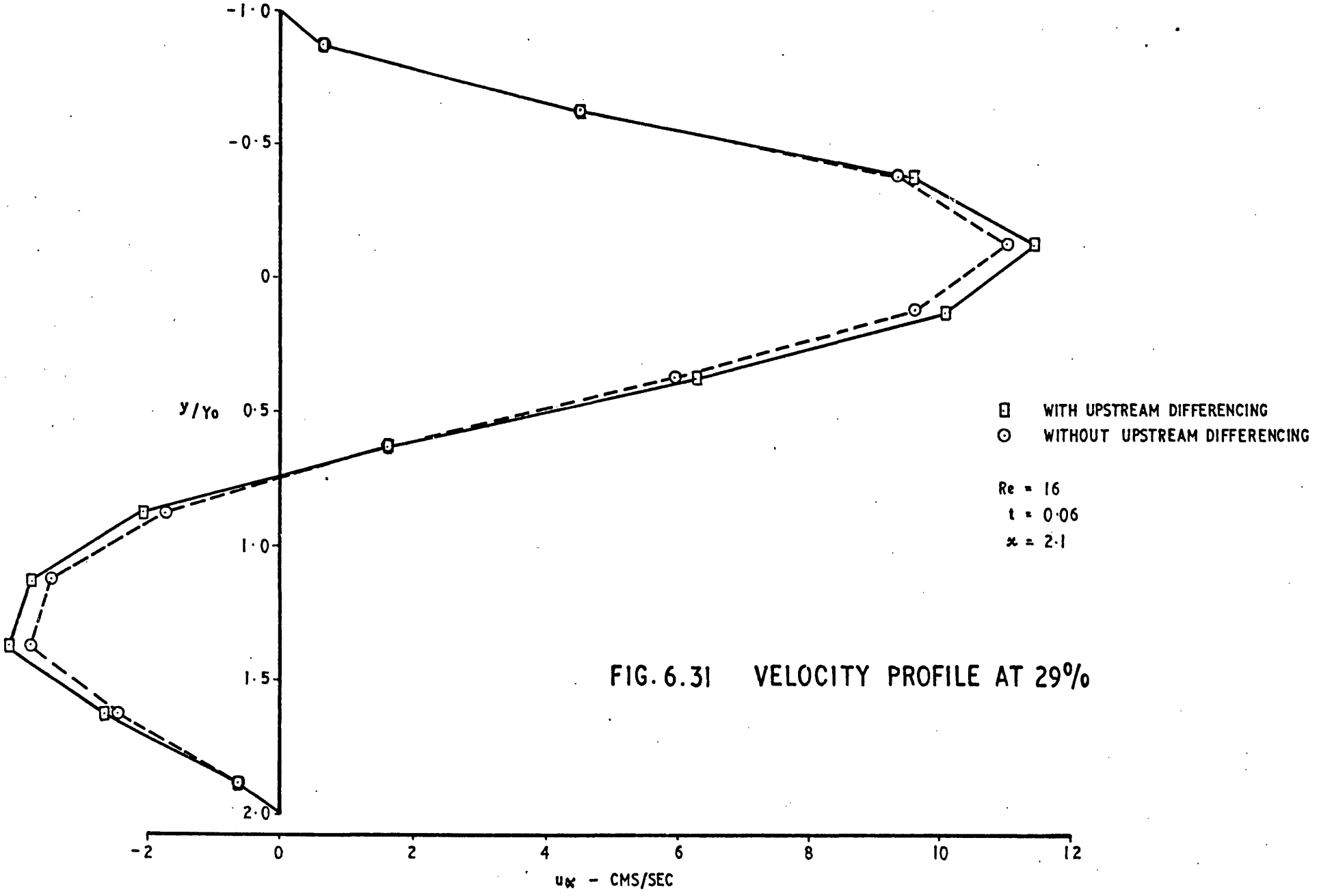

FIG. 6.31 VELOCITY PROFILE AT 29%

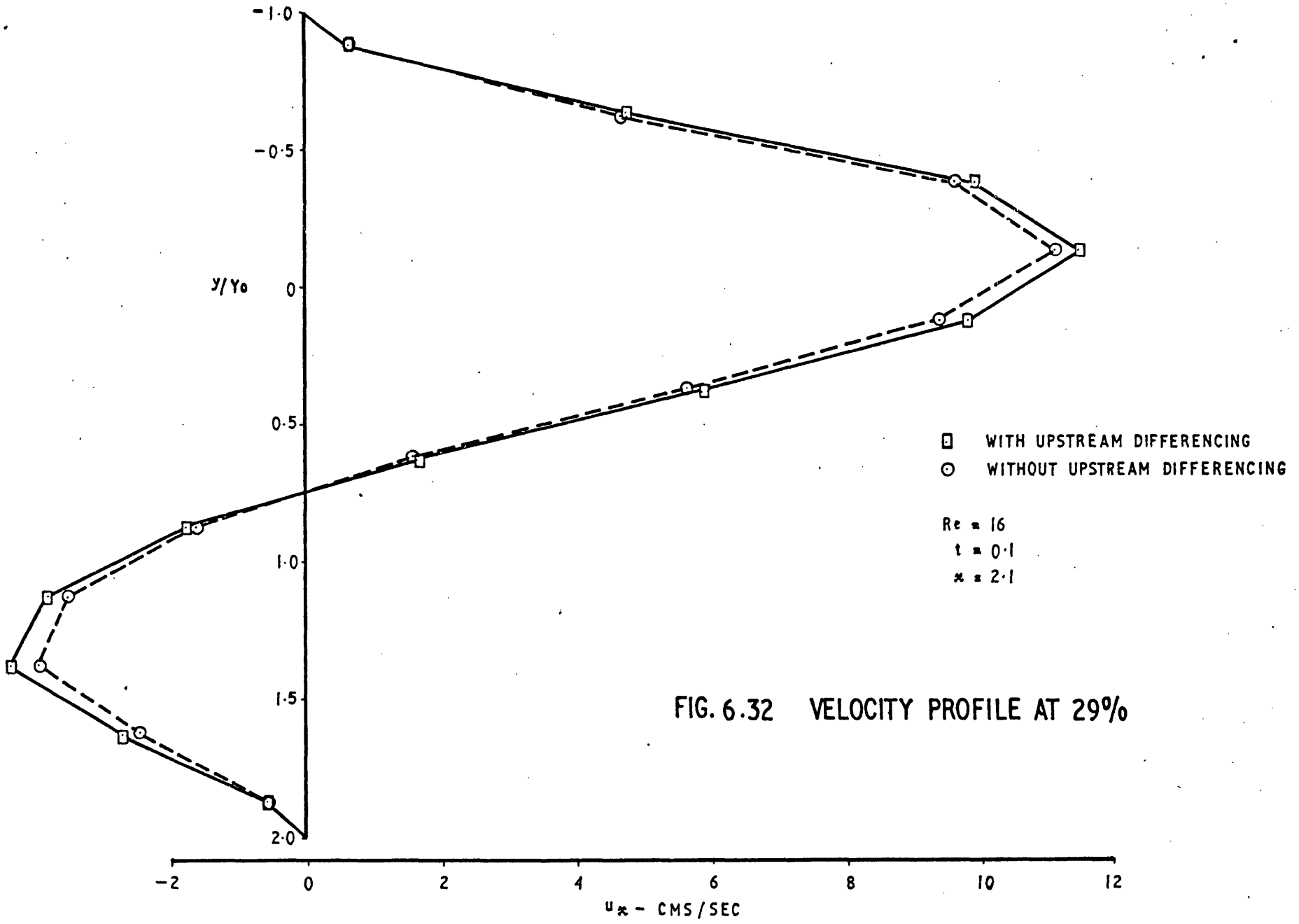

FIG. 6.32 VELOCITY PROFILE AT 29%

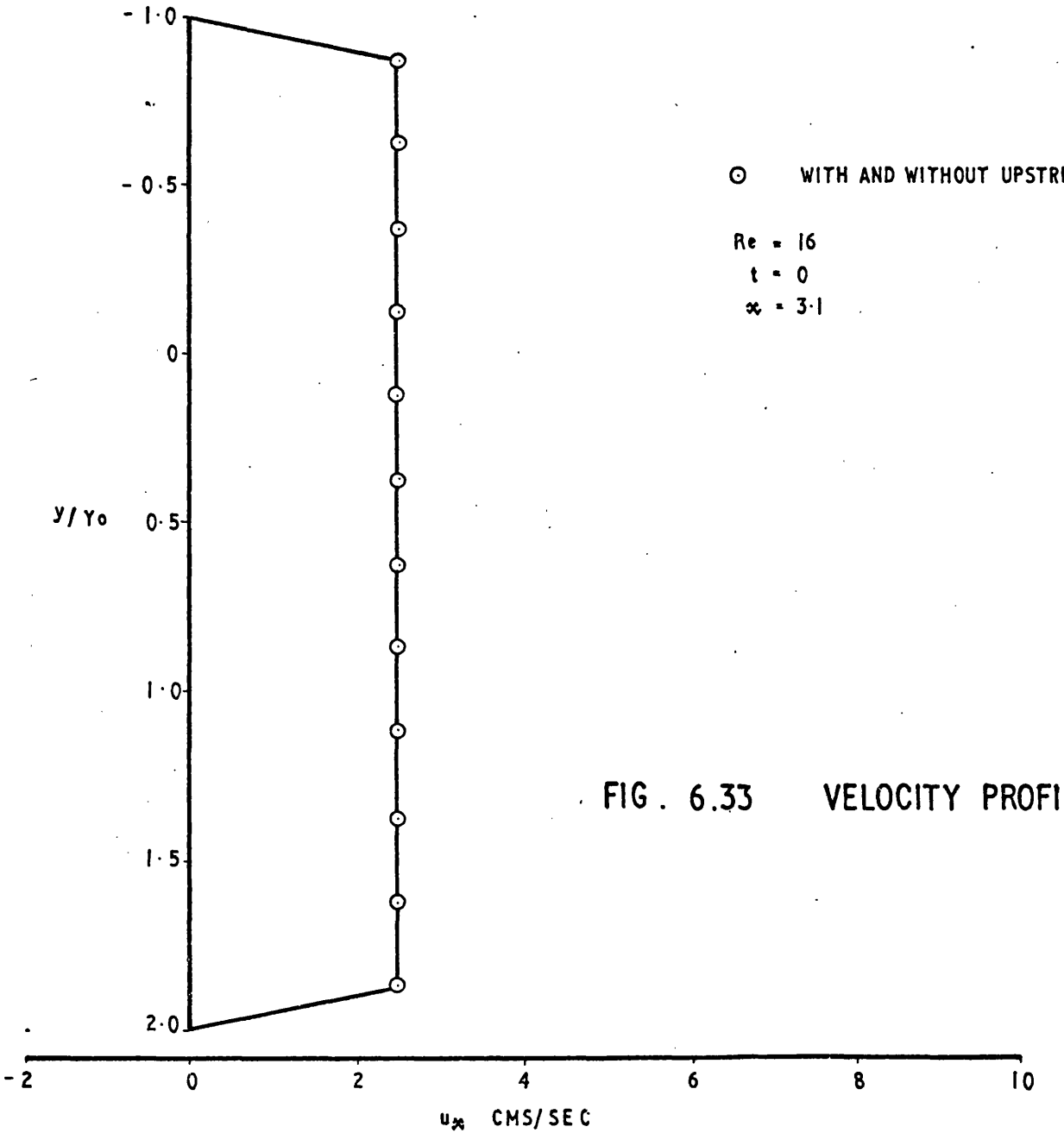

FIG. 6.33 VELOCITY PROFILE AT 76%

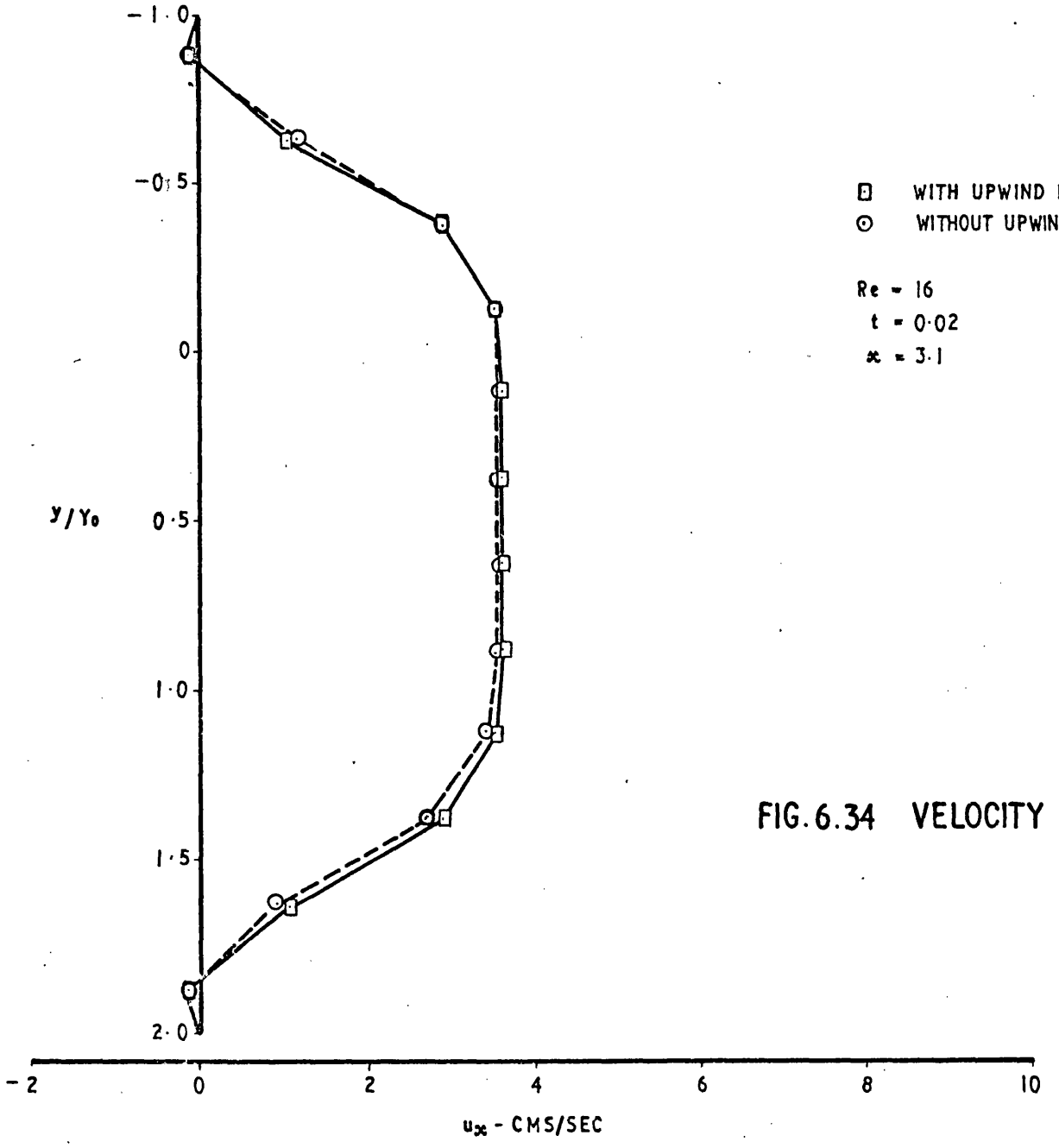

FIG. 6.34 VELOCITY PROFILE AT 76%

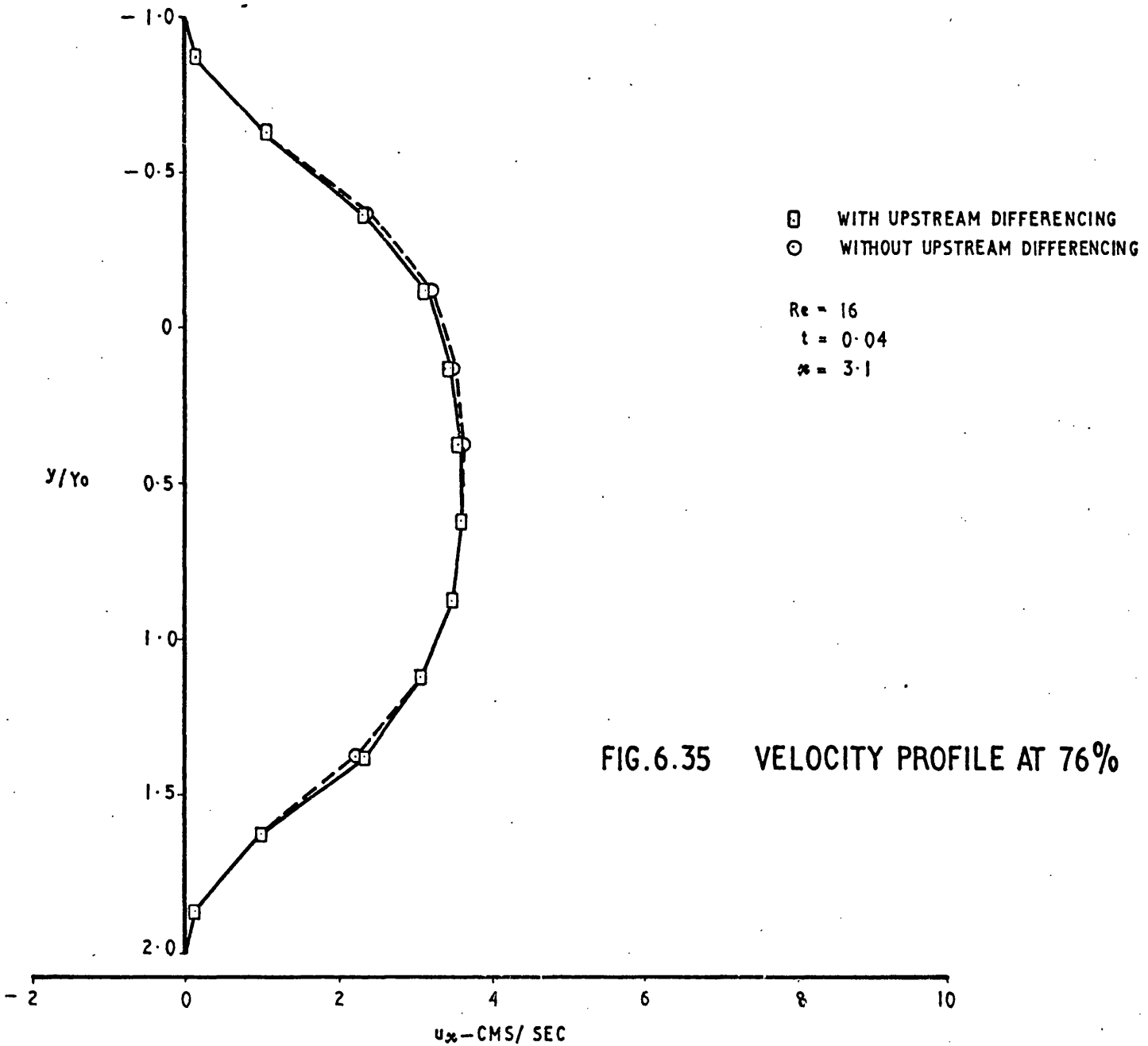

FIG.6.35 VELOCITY PROFILE AT 76%

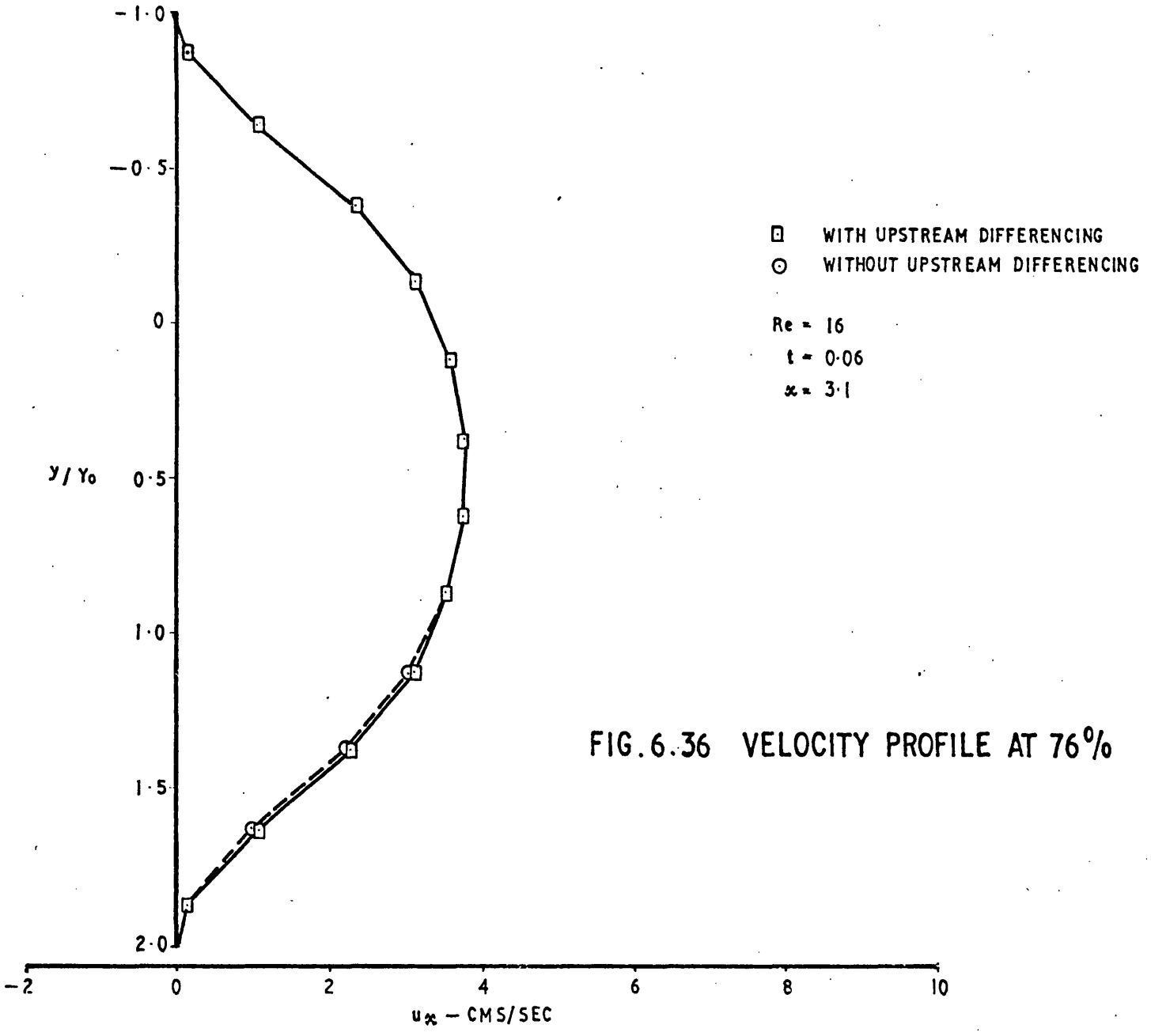

FIG. 6.36 VELOCITY PROFILE AT 76%

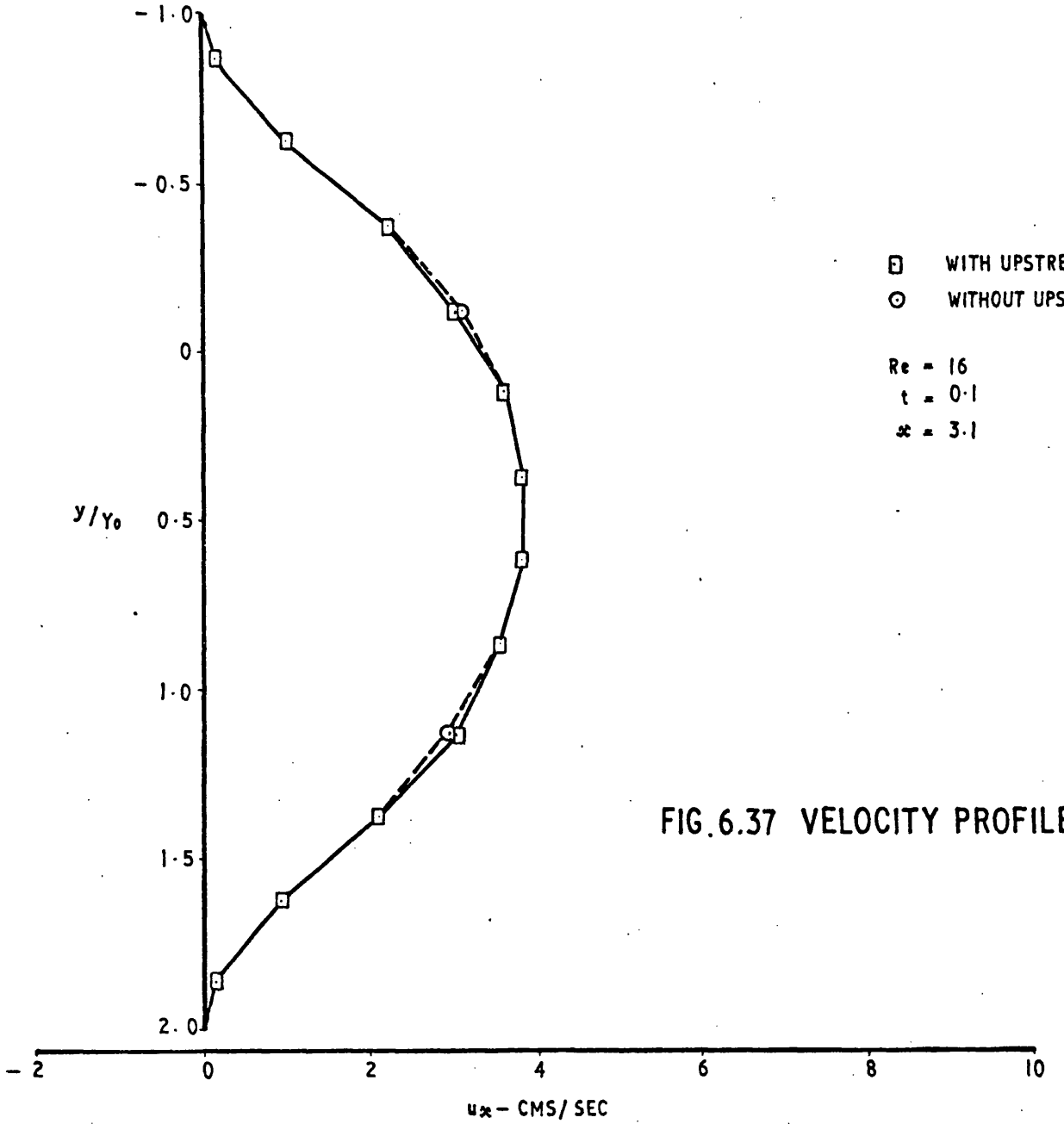

FIG. 6.37 VELOCITY PROFILE AT 76%

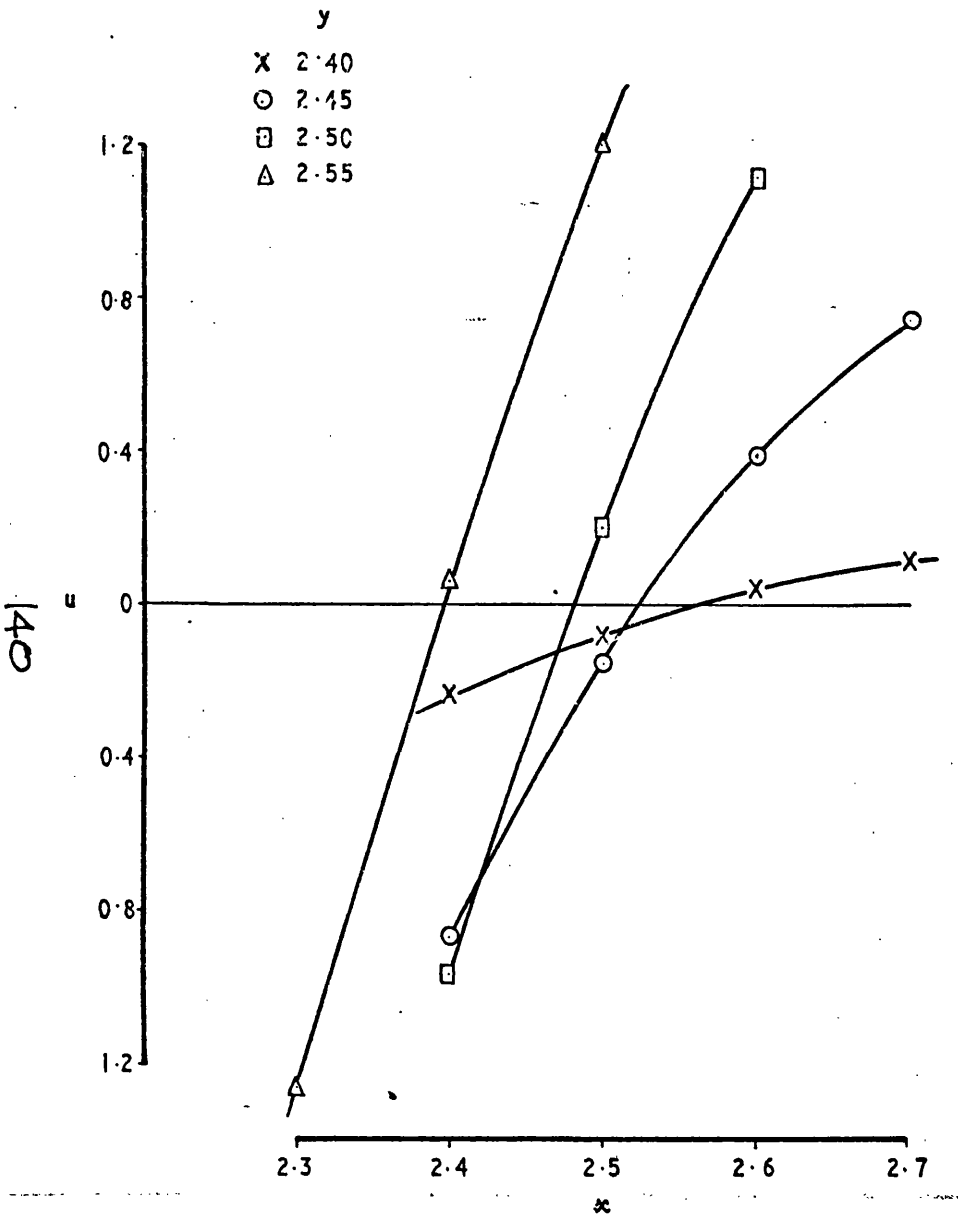

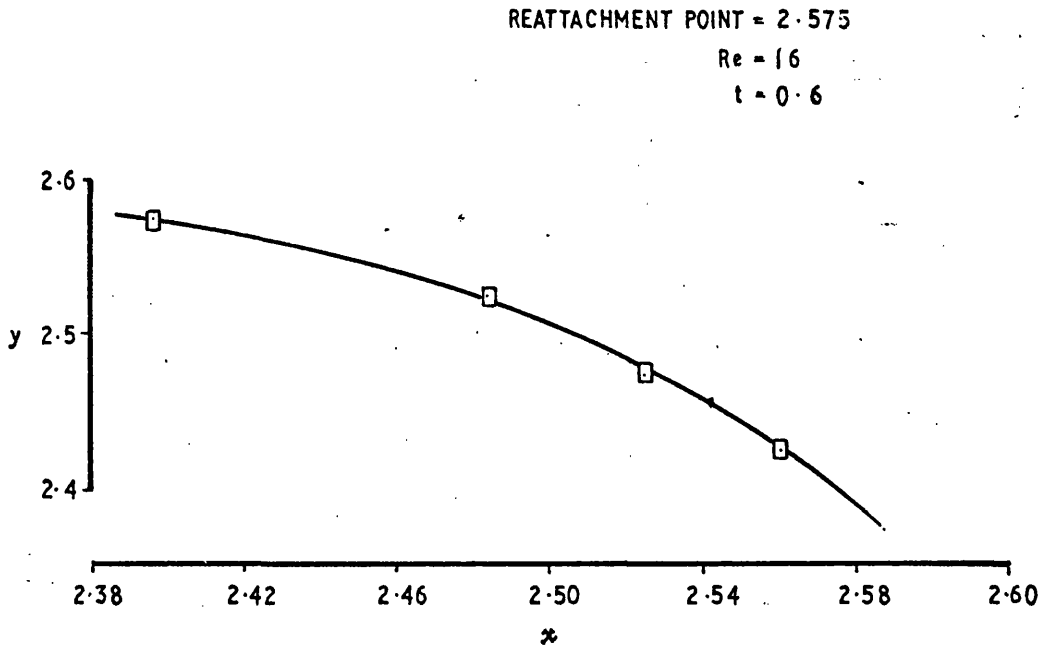

FIG. 6.38 CALCULATION OF REATTACHMENT POINT

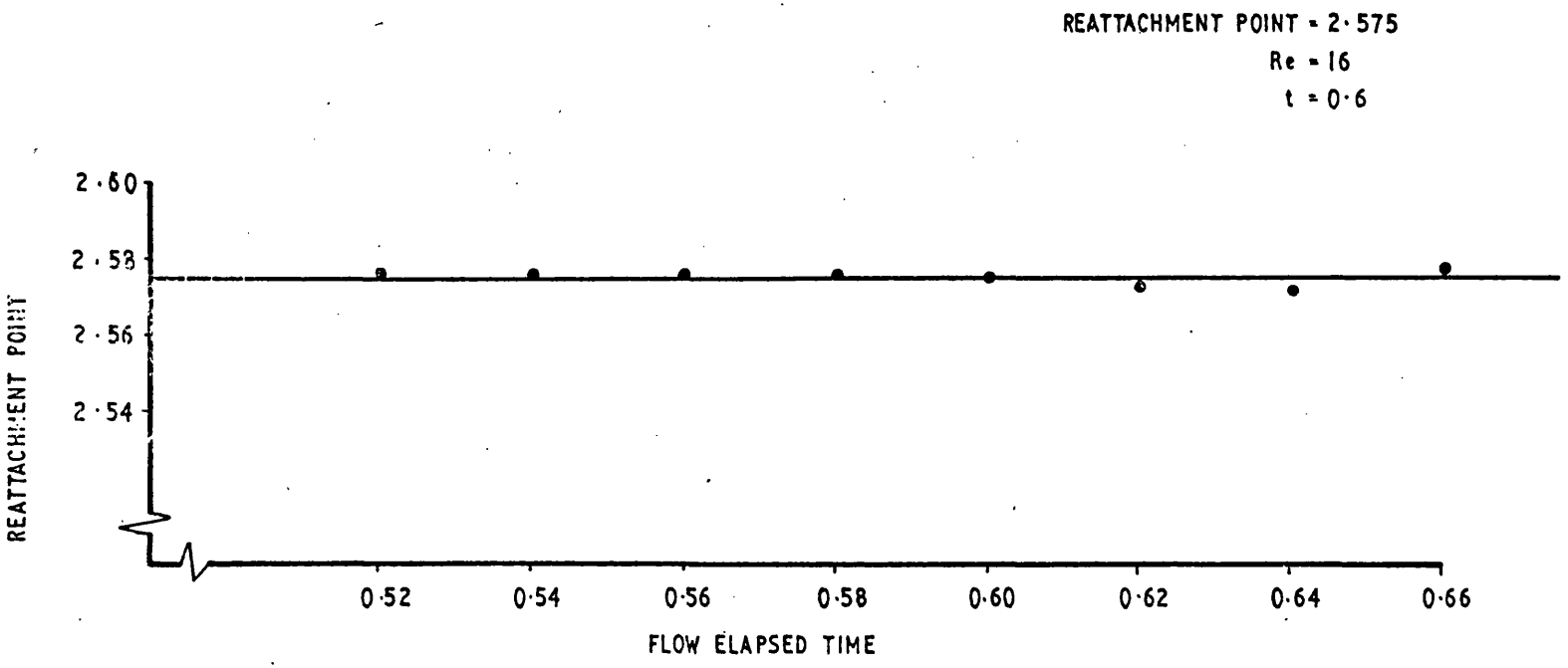

FIG. 6.39 VARIATION OF REATTACHMENT POINT WITH TIME

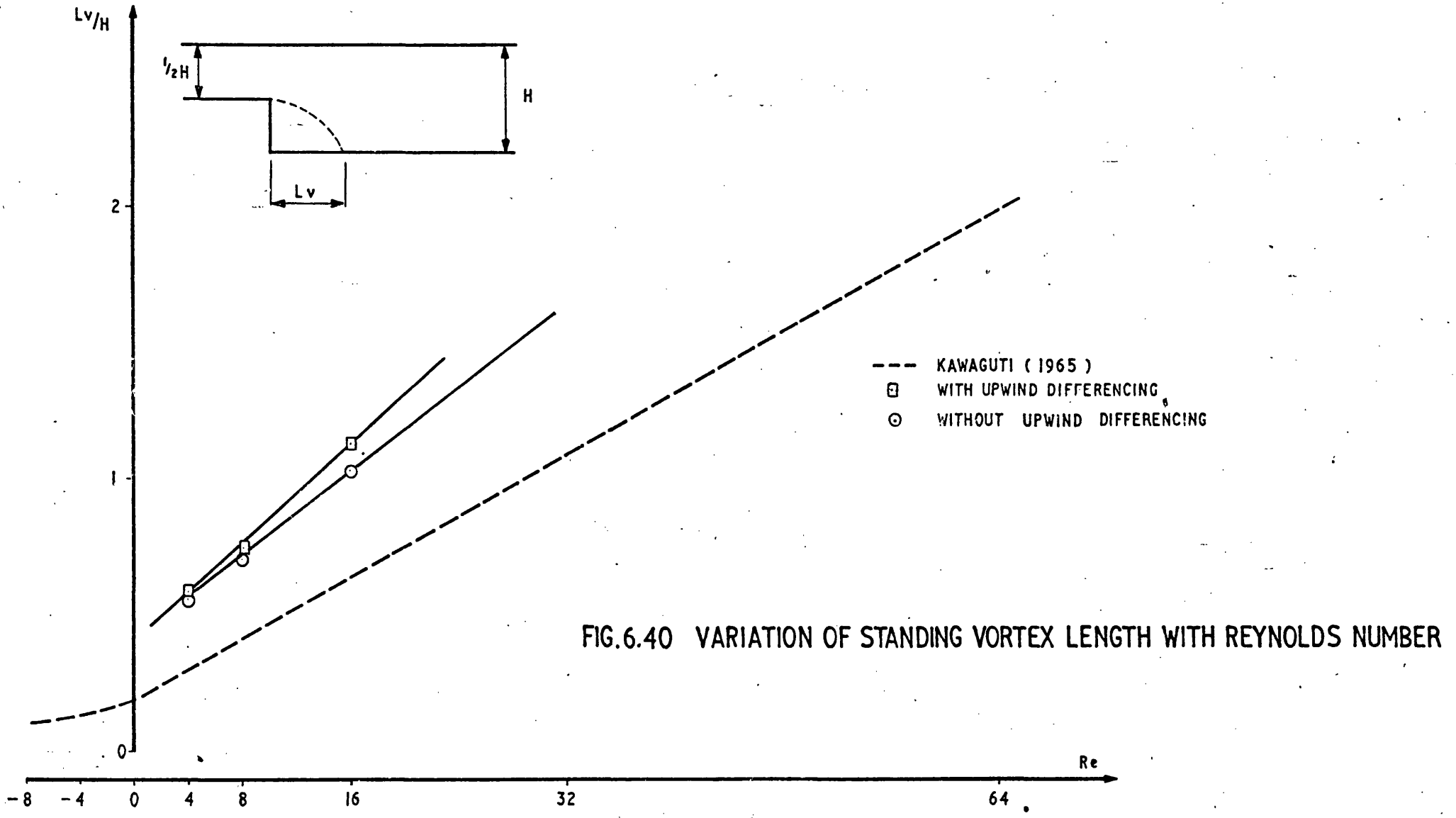

FIG.6.40 VARIATION OF STANDING VORTEX LENGTH WITH REYNOLDS NUMBER

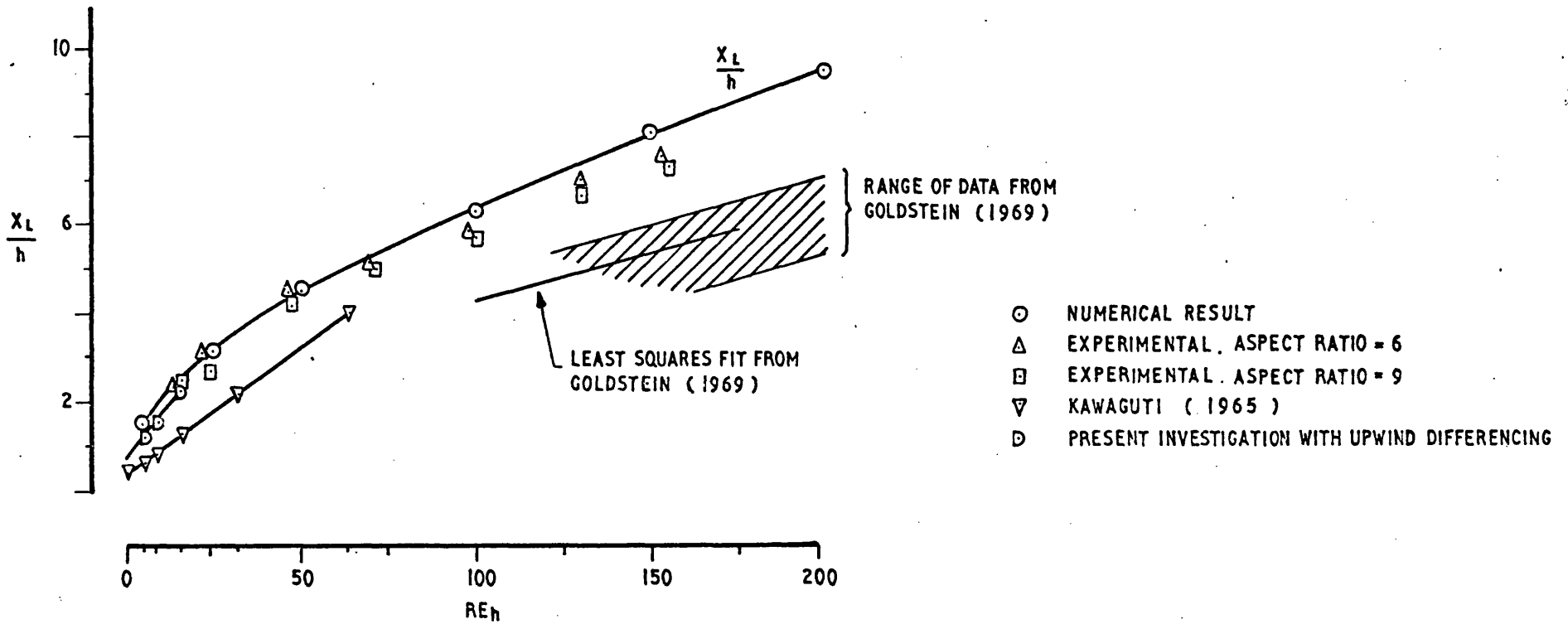

FIG.6.41 CORRELATION OF NUMERICAL AND EXPERIMENTAL RESULTS FOR EDDY LENGTH

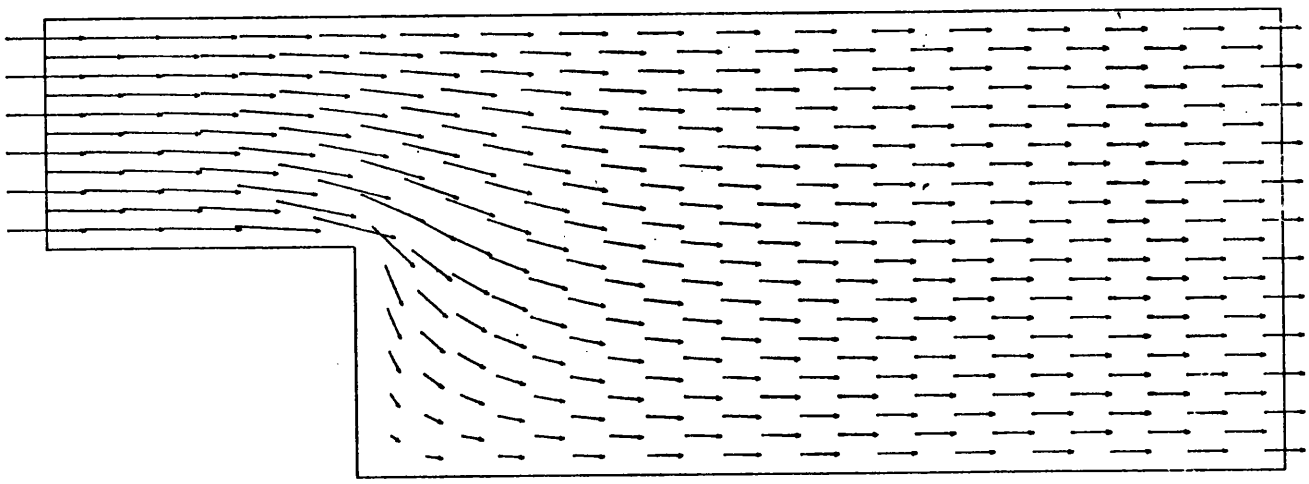

STREAKLINES

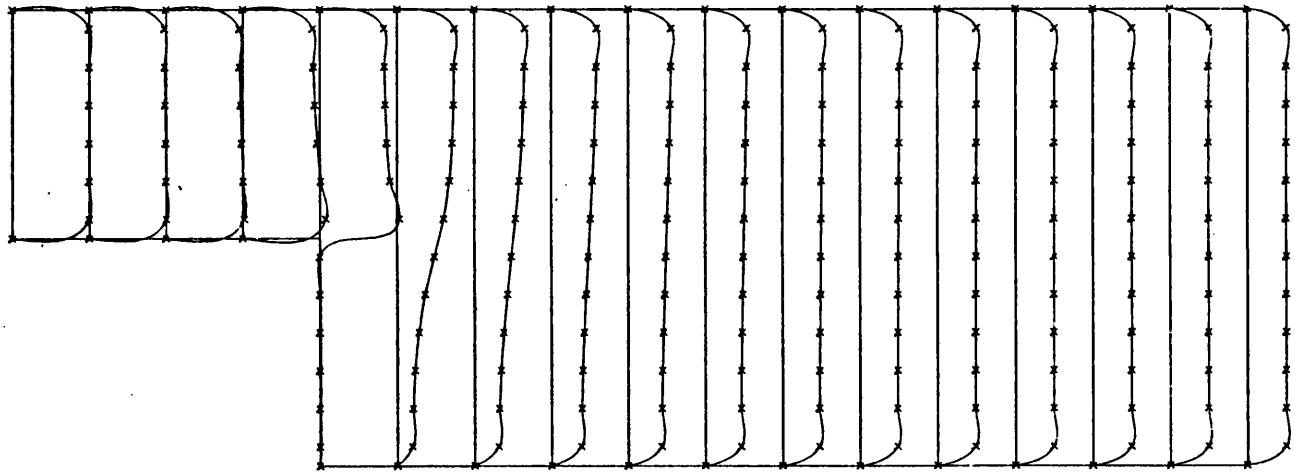

u - VELOCITY PROFILES

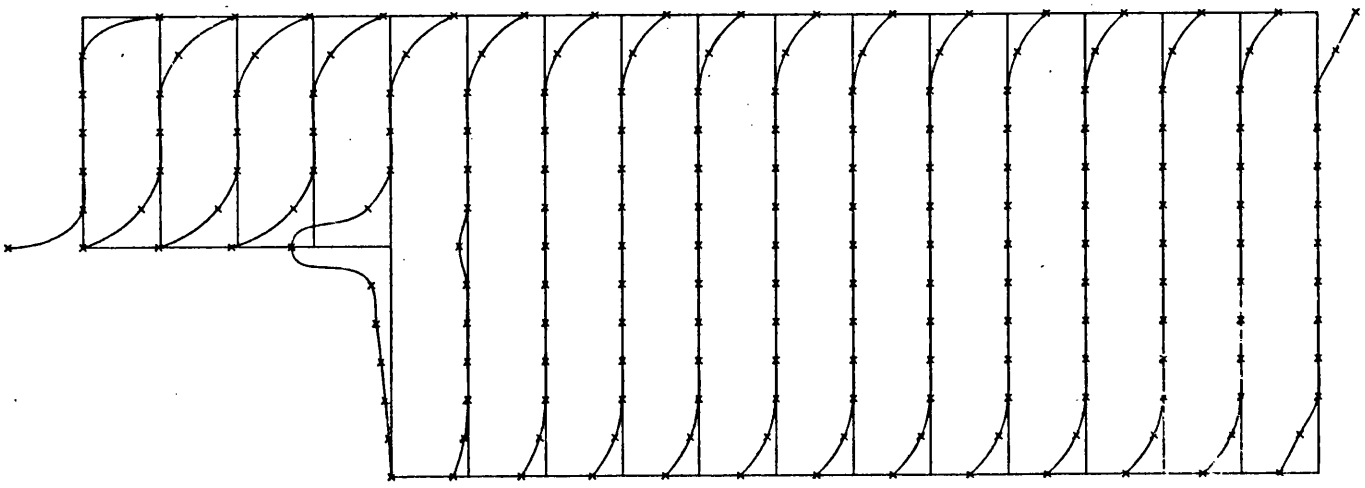

VORTICITY PROFILES

FIG.6.42. PROFILES FOR Re = 4 , t = 0

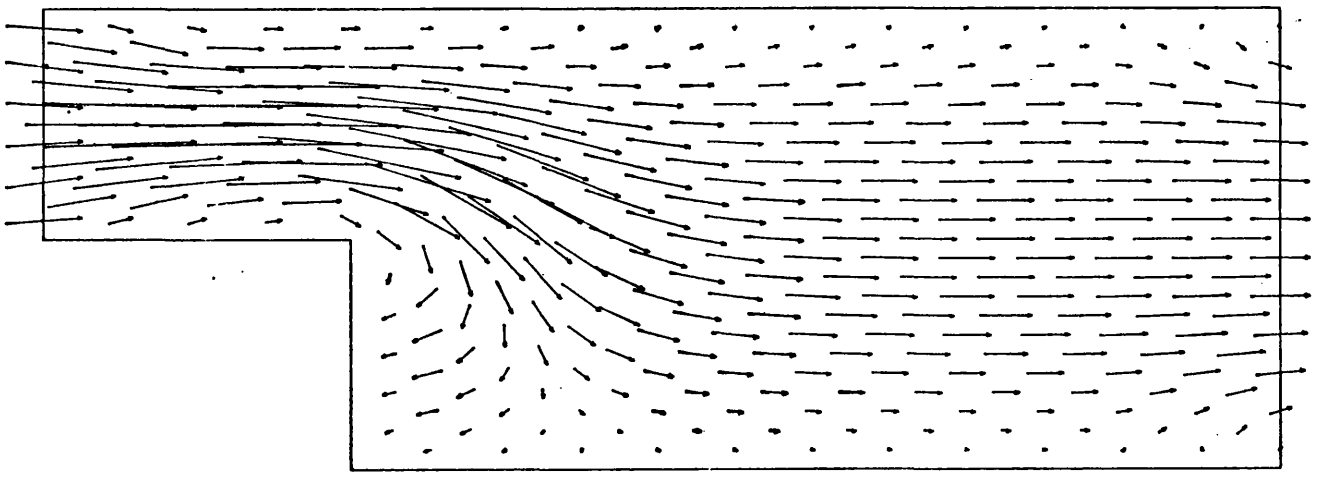

t = 0·01 SEC

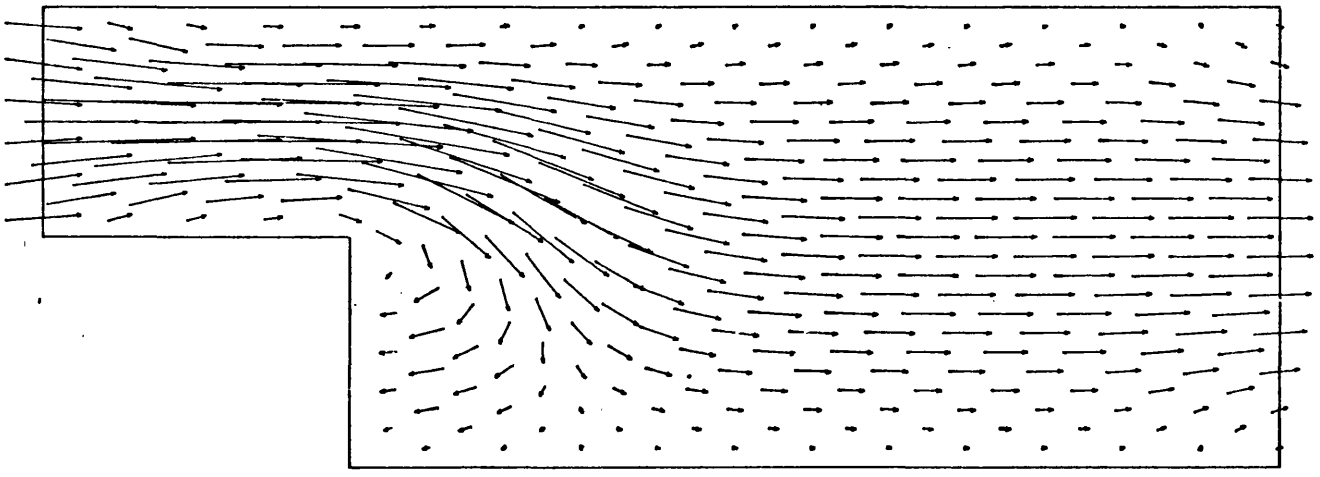

t = 0·02 SEC

FIG.6.43. STREAKLINE PROFILES Re=4

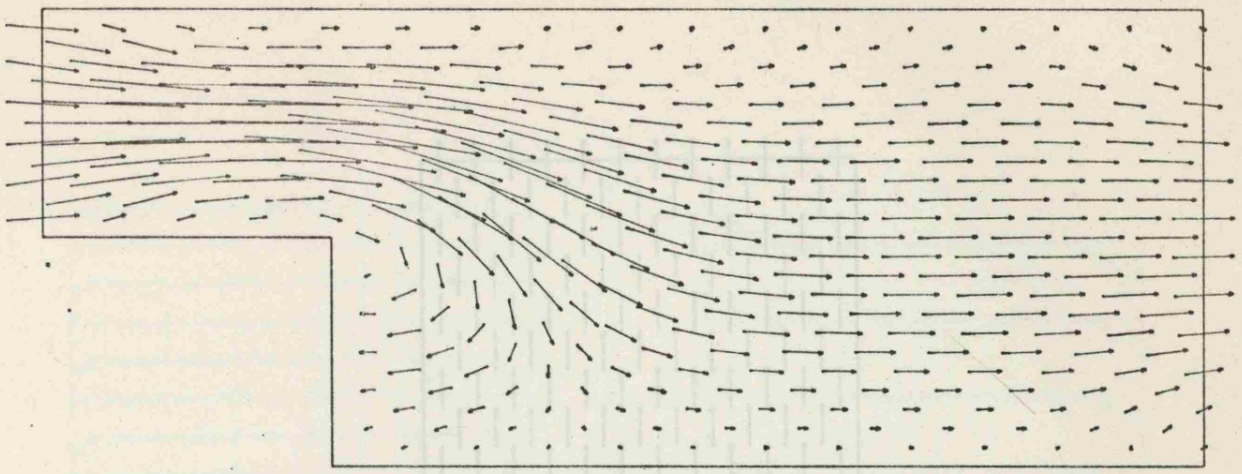

STREAKLINES

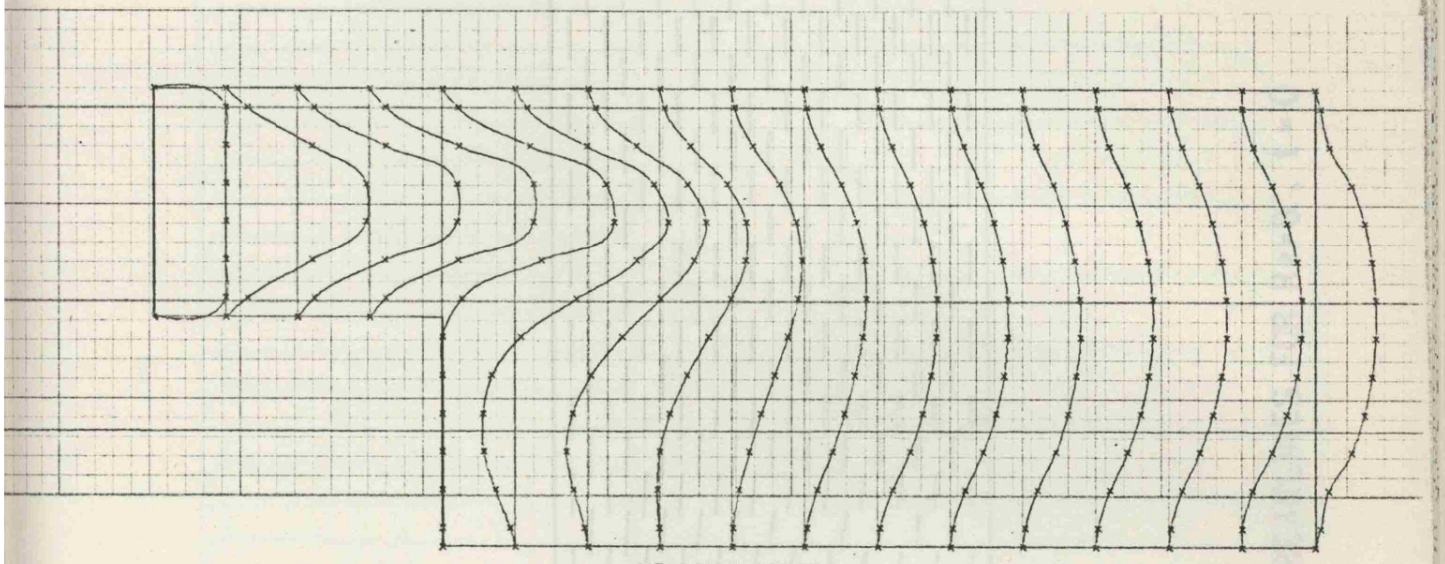

u-VELOCITY PROFILE

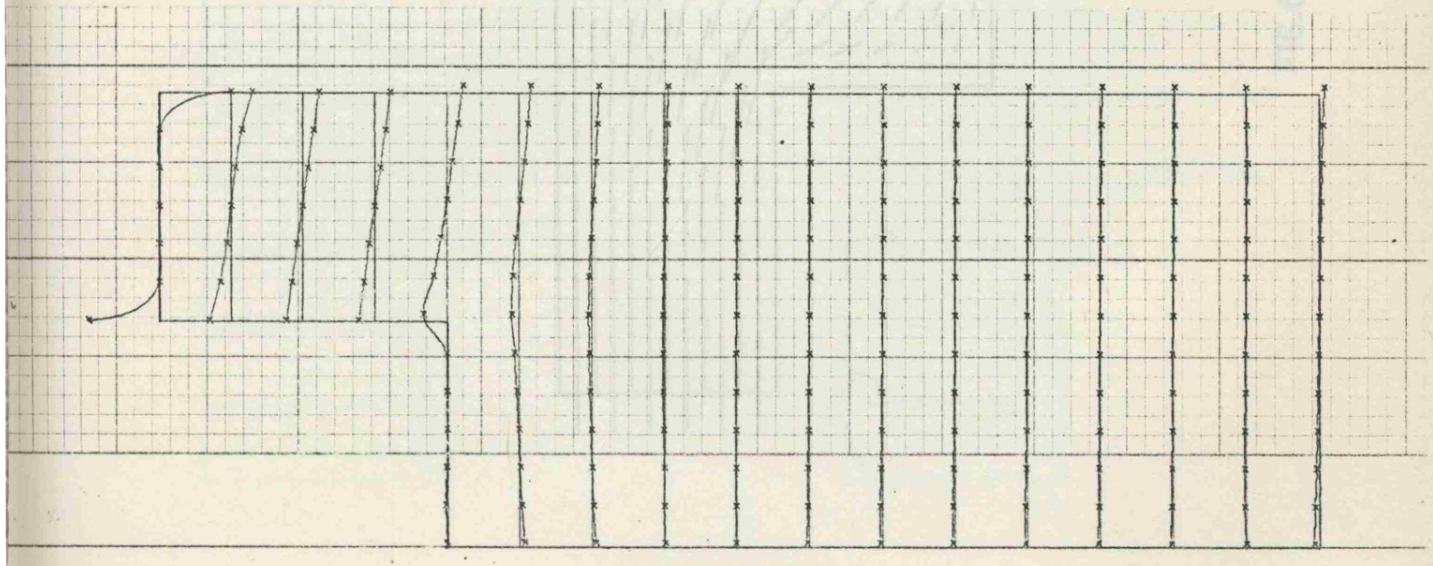

VORTICITY PROFILES

FIG.6.44. PROFILES FOR Re=4 , t=0·135 SEC

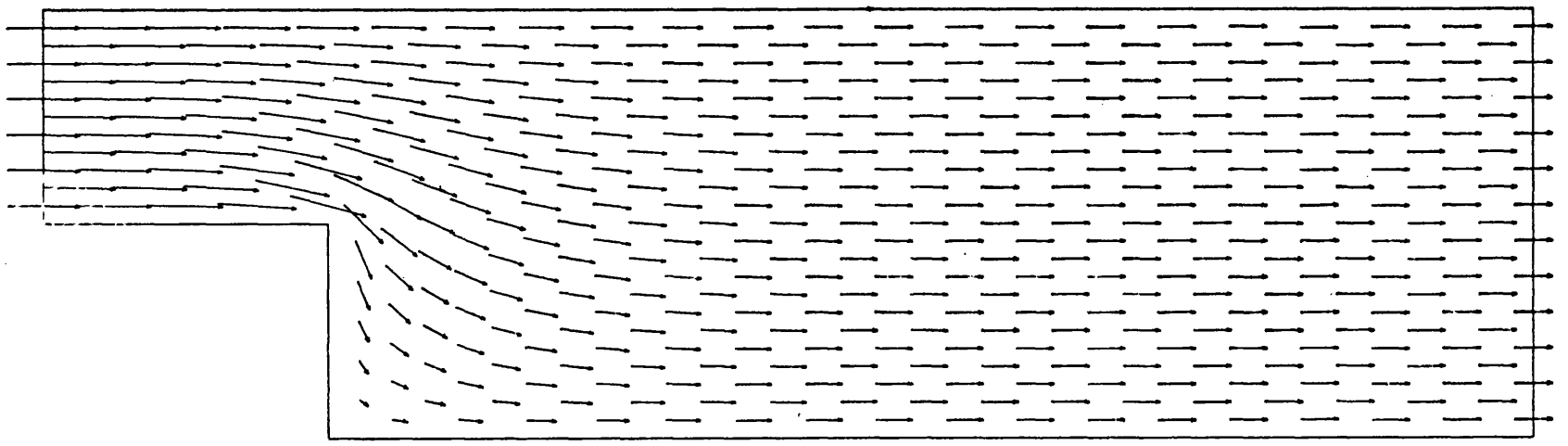

FIG.6.45. STREAKLINES FOR Re=8 , t = 0

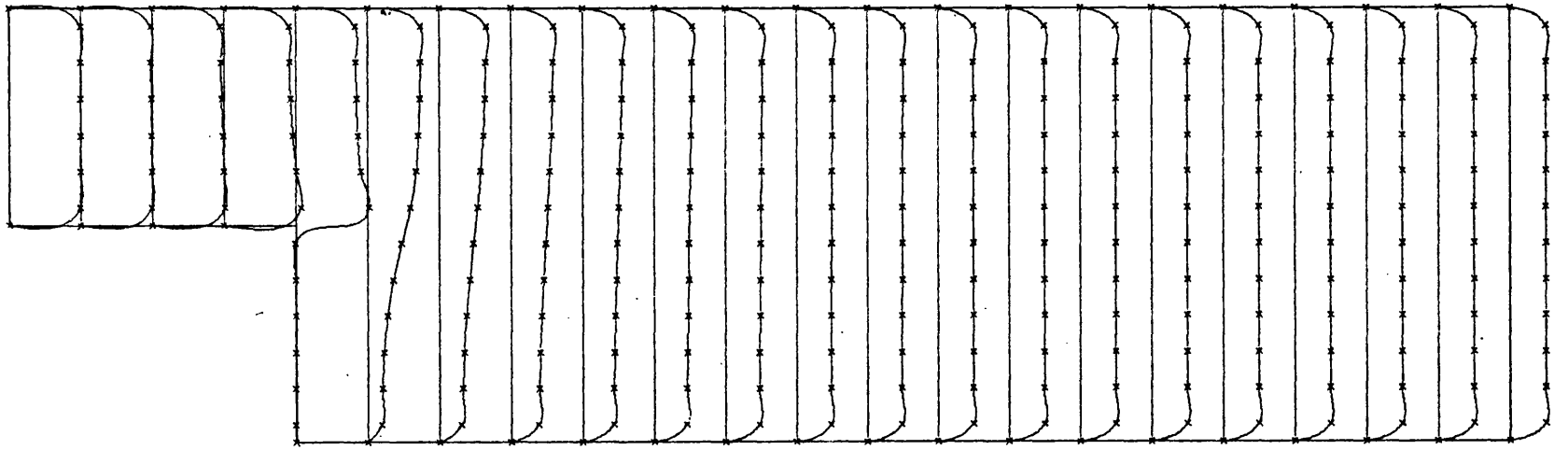

u – VELOCITY PROFILES

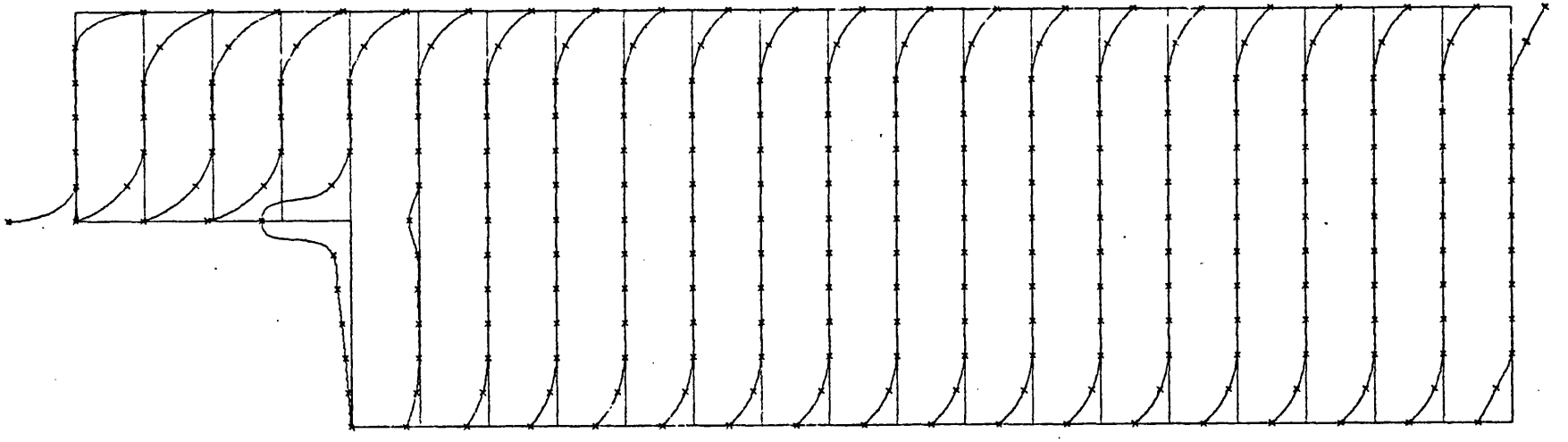

VORTICITY PROFILES

FIG 6.46 PROFILES FOR Re=8 , t =0

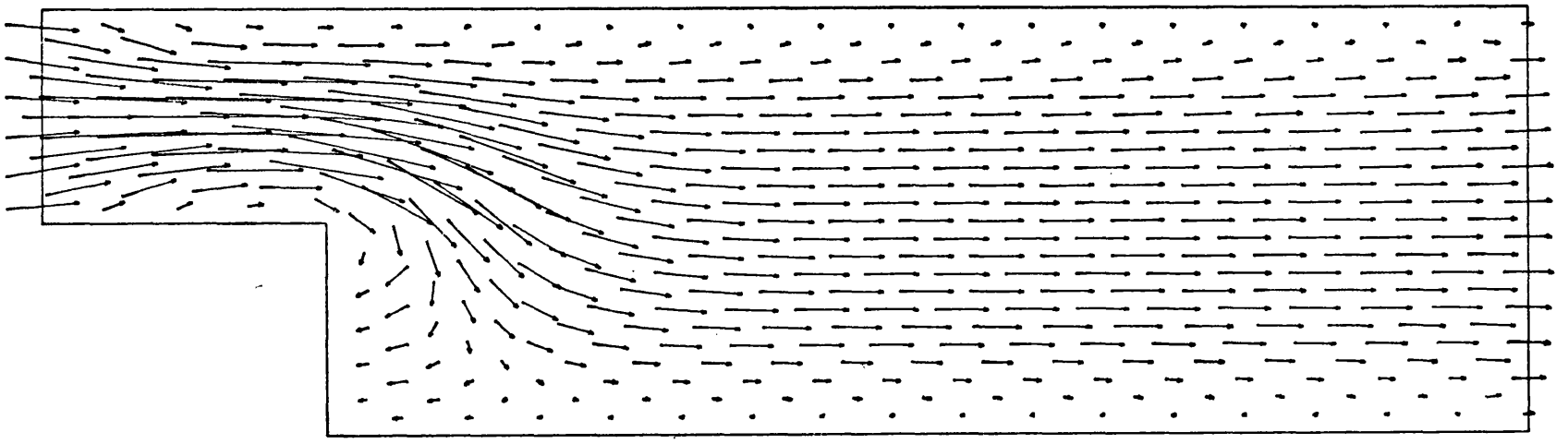

t = 0·01 SEC

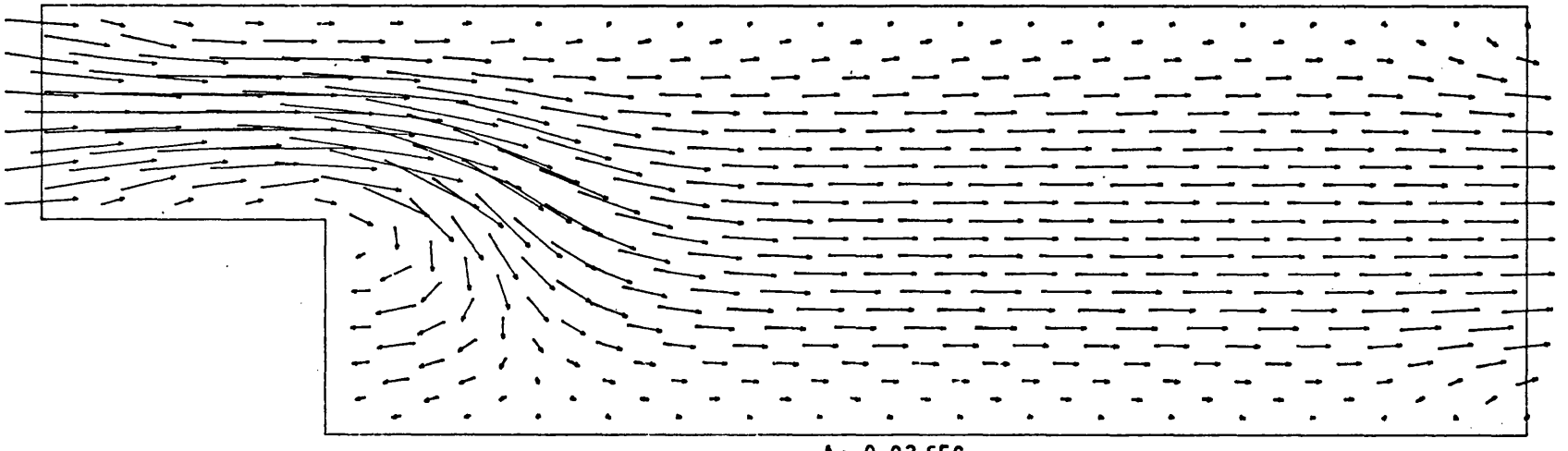

t = 0·02 SEC

FIG.6.47. STREAKLINES FOR Re=8

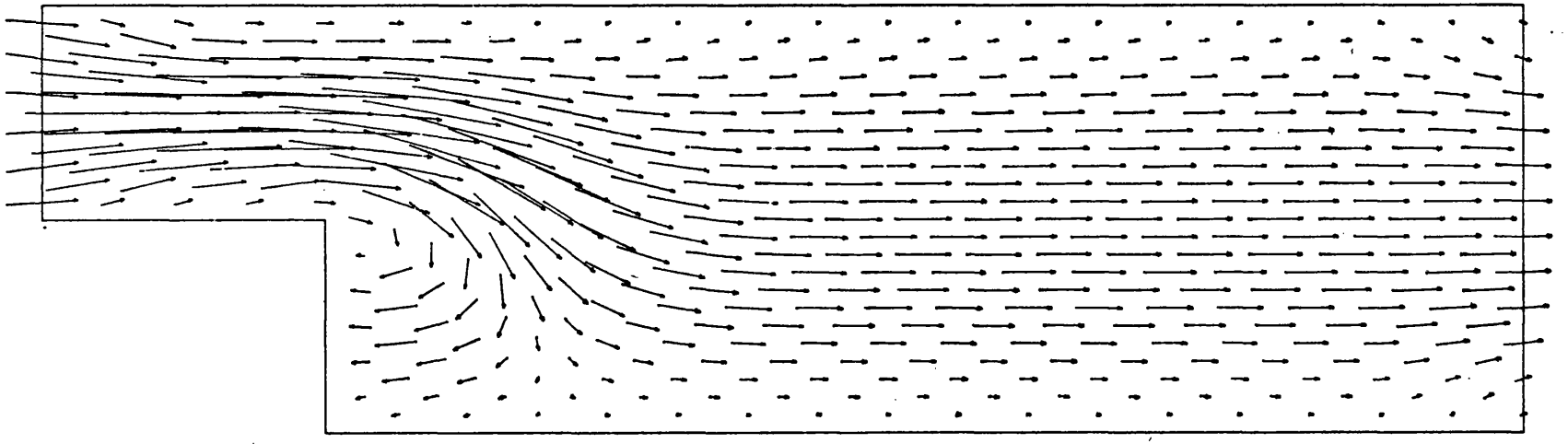

t = 0·03 SEC

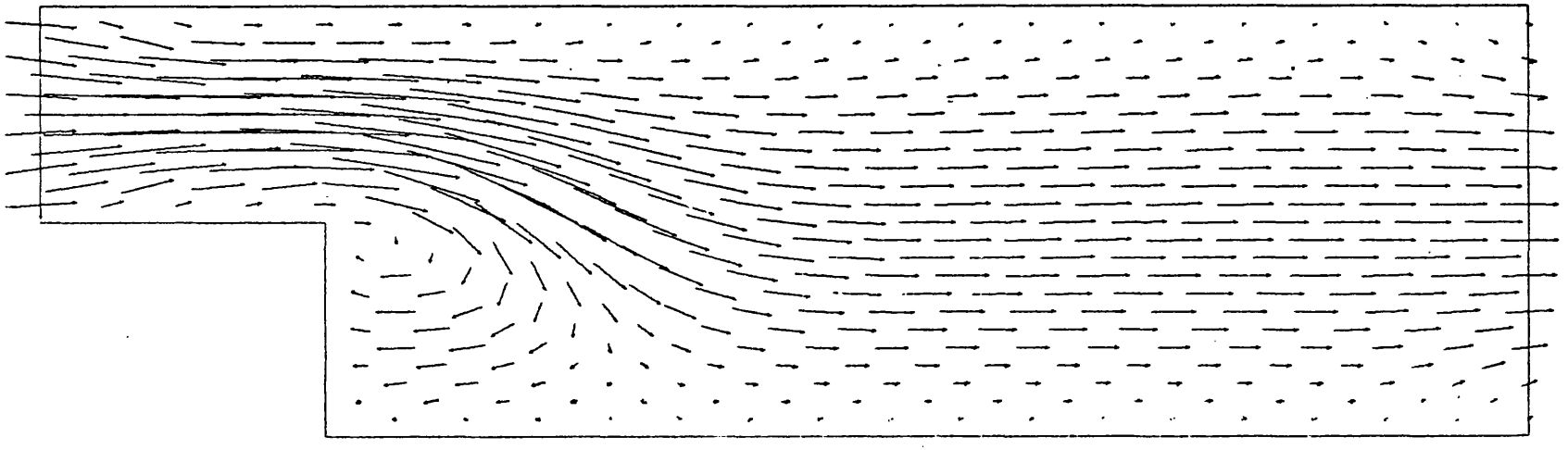

t = 0·28 SEC

FIG 6.48 STREAKLINES FOR Re=8

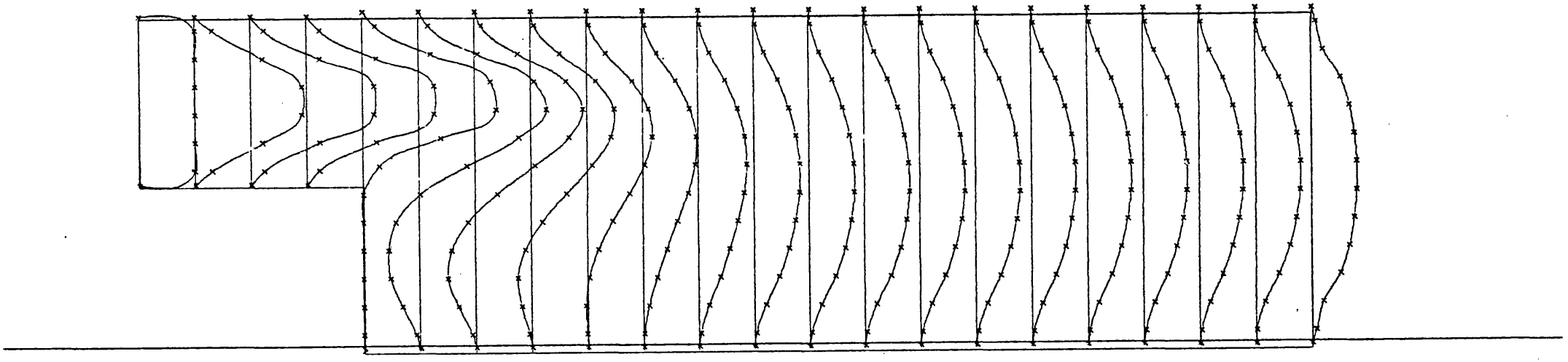

u-VELOCITY PROFILES

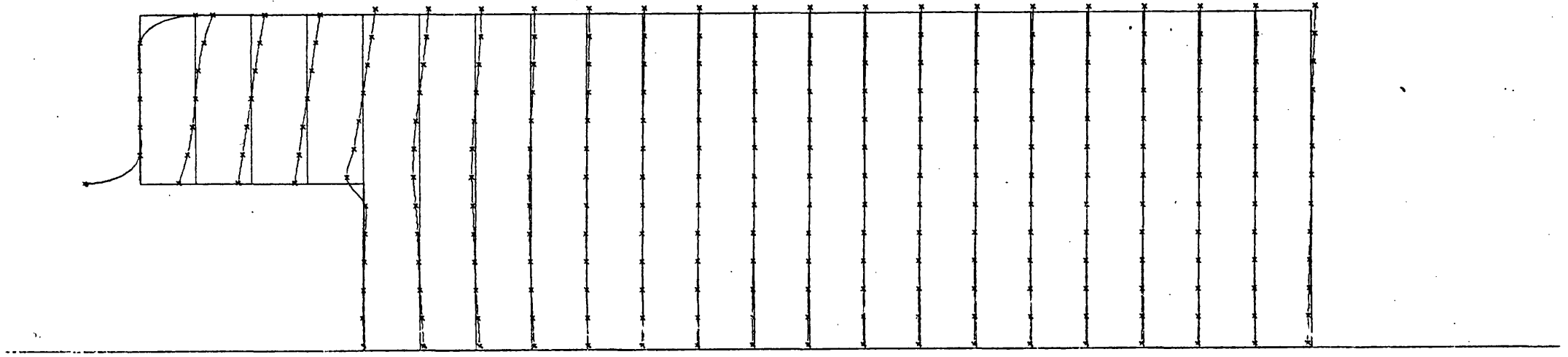

VORTICITY PROFILES

FIG 6.40 - PROFILES FOR Re = 8 t = 0.28 SEC

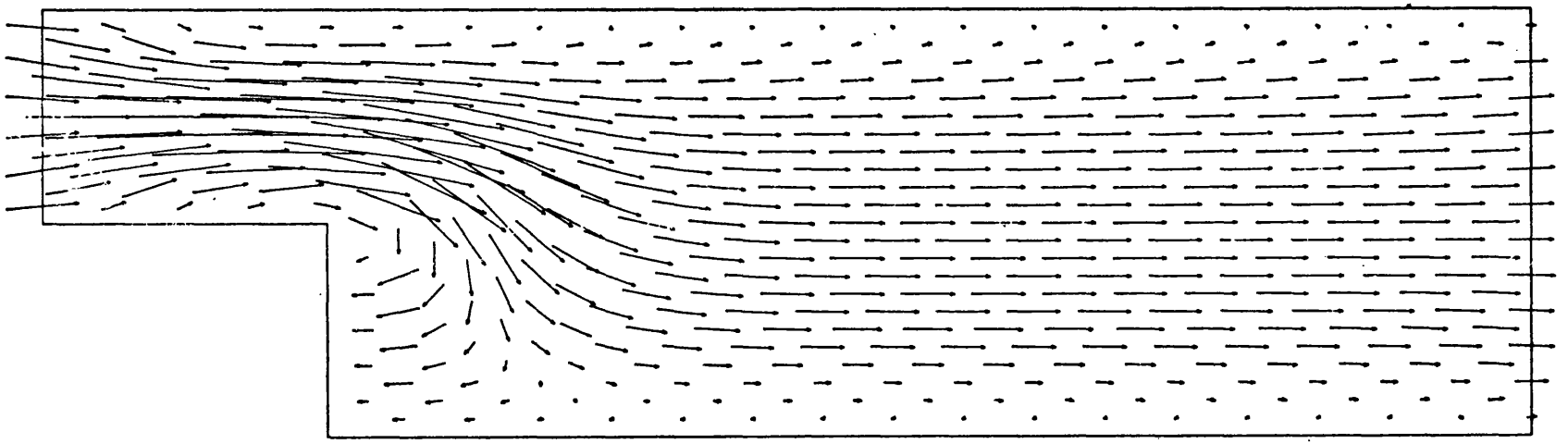

t = 0·02 SEC

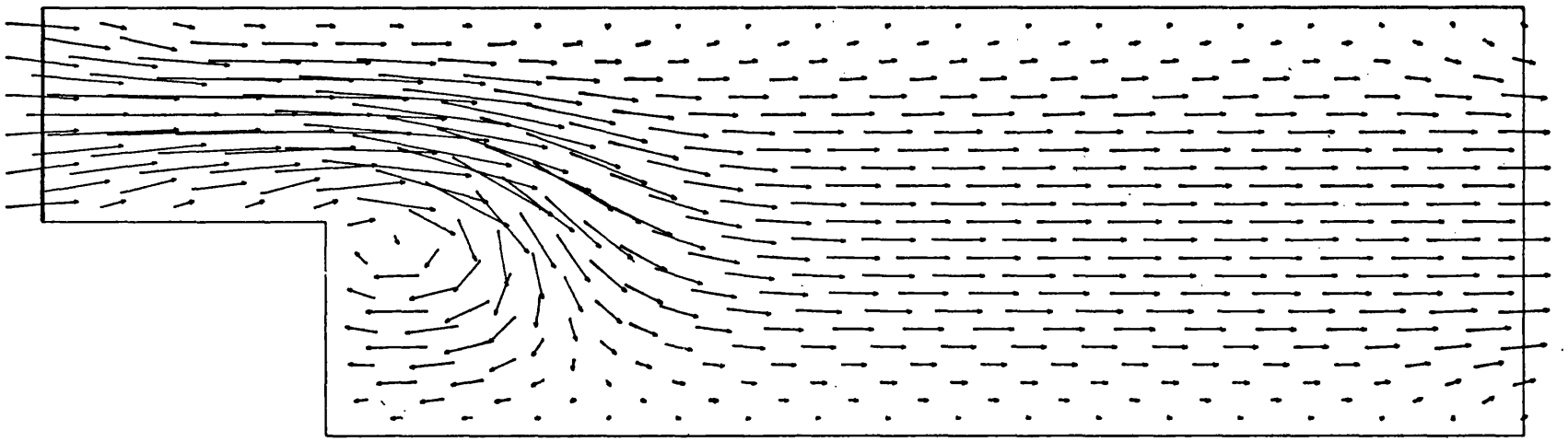

t = 0·04 SEC

FIG 6.50 STREAKLINES FOR Re 16

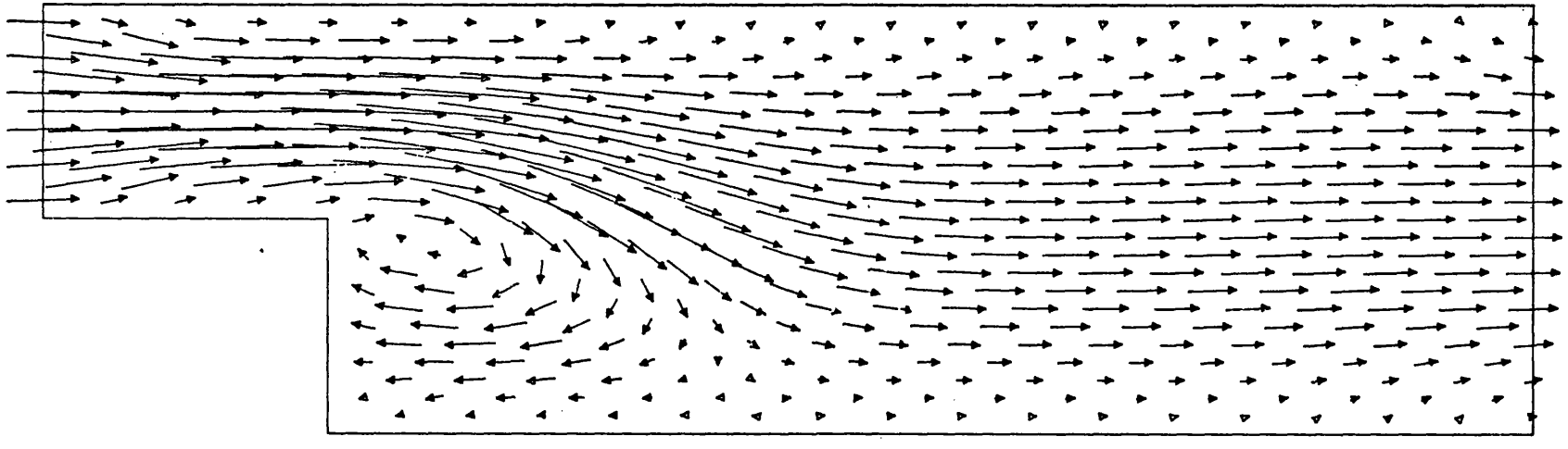

FIG. 6.51. STREAKLINES FOR Re=16, t=0·66 SEC

7. GENERAL DISCUSSION

This chapter will deal with the overall implications of the project, rather than confine itself to one particular topic. The subject matter will be dealt with in three sections; the three-dimensional jet, the two-dimensional viscous flow and their relevance to the prediction of combustion chamber flows.

7.1. Three-dimensional Jet

The method chosen to predict the three-dimensional jet was successful in showing that the kidney-shaped deformation could be achieved with a potential flow model. Whilst the basic model could be improved in certain aspects, it can be used for generating deformed jet patterns. Possible applications include the prediction of chimney plumes, by environmentalists, and the prediction of interference effects between the jet exhaust and flow over the wing of a V.T.O.L. aircraft.

As far as the author is aware, current practice for computing the effects of the plume from the jet on the wing, entail representing the jet by two or three line singularities to incorporate the blockage and entrainment effects. These singularities are placed along an experimentally determined jet path and not allowed to deform. The singularities can be incorporated into programs solving a second kind Fredholm Integral equation for the wing pressure distribution (Panel method programs), where the effects of the jet on the wing can be calculated. The results obtained from the programs compare favourably with experimental data.

As computers increase in speed, it will be possible to increase the complexity of the jet model, using the method discussed in this thesis. The jet deformation, together with its subsequent effect on the wing pressure distribution, can then be calculated iteratively.

By this means, the interaction between the jet and the wing will then be modelled more accurately. Thompson(1971) noted that the computed pressure distribution behind the irrotational jet did not compare favourably with experimental results. Even allowing for this, the method described here could be used to improve the modelling of the jet within a panel method program.

It was the lack of agreement between experimental and computed values of surface pressure which led Thompson to predict the three-dimensional jet by solving the Navier-Stokes equations. Similarly for the combustion chamber designer, it would probably be the omission of viscous effects from potential models of the jets which would lead him to the same result. Solving the Navier-Stokes equations by finite-difference methods allows the program to compute not merely a single ideal jet, but any number of jets with viscous effects already incorporated. Solution of the Navier-Stokes equations by finite-differences is a complex problem, but conceptually tidier than predicting irrotational jets with viscous effects added almost as an afterthought.

Hubble's original intention was to calculate the vorticity distribution around a jet in crossflow. One reason for wanting the vorticity is if the forces on the jet are required: Joukowski's theorem can be used to estimate them, provided the vorticity is transformed to circulation. Also, by concentrating on the vorticity alone, an advantage is gained over streamfunction- vorticity methods in that the program is confined only to the region of interaction between the crossflow and the jet. As a result the mesh should be smaller, leading to a reduction in computing time.

The logical development, therefore, is to solve the three-dimensional vorticity transport equation by finite-difference methods. However this entails an added complication in that the direction of the vorticity vector is unknown in three-dimensions, whereas in two-dimensions it is known. The knowledge of the direction is important since the induced velocity direction cannot be found without it. The author believes that the solution of the three-dimensional vorticity transport equation by finite - differences is the best method for calculating the viscous jet in crosswind, even though the unknown vorticity direction adds further difficulty to an already complex problem. However, work on the jet had to be curtailed before a solution could be found to the problem of the direction of the vorticity vector.

At this point work on the two-dimensional viscous flow investigation was started.

7.2. The Solution of Two-Dimensional Viscous Flows by Vorticity/Integral Methods.

Hubble's (1967) proposal of an approximate method for solving the vorticity transport equation was shown to be in error. Consequent upon this, a finite difference solution of the full vorticity transport equation was adopted, and this was linked to an Integral equation solution of the poisson equation for satisfying the boundary conditions. The author believes that this is a theoretically sound method with the results obtained so far in general agreement with those of other investigators.

One obvious disadvantage with the method is the computer time taken to calculate any particular flow situation. It is believed that the majority of this time was used to set up the data for the solution of the Integral equation, and the subsequent calculation of the velocity field. Three aspects are immediately apparent:-

(i) in calculating the effect of the vorticity field at the surface collocation points, every mesh point carrying vorticity was taken into account.
Similarly (ii) in calculating the mesh point velocity, all the surface sheets together with all the mesh points having vorticity were used.
Finally (iii) the mesh point data was not stored and retrieved efficiently.

Regarding the first point, a simple analysis on an N X M mesh shows that for each iteration the total number of mesh movements required to set up the Integral equation data, is of the order of $2N^2M + 2NM^2$ i.e. 20,020 for a 22 X 13 mesh. This assumes that all mesh points carry vorticity, which appears a valid assumption since the results show that only a few iterations are required before the vorticity spreads throughout the duct. Some numerical experimentation is required to determine whether the effect of mesh points "far away" from a surface collocation point was small in relation to mesh points close by. If this were the case, and results showed that, for example, only the 8 mesh points closest to the collocation point need be used, the total number of mesh movements is reduced to 560. This represents a considerable saving in computer time.

Considering the second point, the calculation of mesh point velocity, an analysis shows that the total number of mesh movements per iteration is $2N^2M + 2NM^2 + N^2M^2 - NM$ i.e. 101, 530 for the mesh above. If numerical experimentation showed, for example, that only the 10 closest mesh points need be considered, or the 10 closest points plus all surface sheets, then the number of mesh movements is reduced to 2860 and 22,880 respectively. This again represents a considerable saving in computer time.

Regarding the third point, the ring package used, Dennison (1973), is inefficient in storing ring information, and consequently, retrievel is also inefficient. The difficulty appears to be that the ring pointers, which enable the computer to locate the data within the rings, are not stored effectively. These ring pointers give the locations

of adjacent mesh points and are contained within each mesh point data area. Thus to locate data two mesh points away from the current position, necessitates finding the intermediate mesh point. If the data for this point is not present in the computer core, one page of data would be placed onto disc, and the page containing the required point substituted into the core. With large structures such as those used in this investigation, there could be a large amount of page swopping in order to move around the mesh.

Taking all three points together, it can be appreciated why the method took a significant amount of computer time. Any future development work on this method should be aimed at reducing the number of mesh operations highlighted above.

The ring package has already been rewritten into Fortran IV at Rolls-Royce (1971) Ltd., Bristol, such that the pointers to all the mesh points are kept in the core, and the data on disc. This indicates that the movement around the mesh points should be faster, but tests are required to establish if this is the case, or if any further savings in time could be achieved.

When this particular investigation was started, the author could find no other reference to similar Vorticity/ Integral methods of solving viscous flows. Even now, to the authors knowledge, there is only one other investigator, Coulmy (1976), who is using this approach. Coulmy is at present evaluating the technique, and has not yet compared it with experiment.

This present investigation has shown that the Vorticity/ Integral method is capable of predicting low Reynolds Number flows, but the requirements for solutions at high Reynolds numbers should now be examined. Two aspects must be considered: (i) Fromm's (1969a) finite-difference equations

were used by him to Re = 4000 only,and hence a different formulation of the Vorticity transport equation is required. (ii) A suitable turbulence model is needed which can be easily incorporated into the Vorticity/Integral method. The second requirement is considered by the author to be the most important step to be taken in the future.

The major advantage of the Vorticity/Integral approach is that the flow field development is calculated in terms of vorticity. This mirrors the actual flow exactly since only the boundary layer and wake regions have non-zero vorticity. Calculating the flow development in this manner gives insights which would be hard to explain from consideration of pressure-velocity interaction. Lighthill(1963) quotes the case of a candle being blown out as an example of this. The airflow during the puff consists of an irrotational 'source' flow, which falls off rapidly with distance, and a vorticity-induced flow. The candle does not respond until the lip-generated vortex ring, each portion of which inducesa forward motion in the others, has reached the candle.

At the present time, the flow around or within any two-dimensional geometry can be calculated by the method set out here. The solution of the Integral equation is performed by specifying singularities around the surface, so that the surface geometry must be known. This method is much more general than the calculation of image positions, Payne (1956, 1958), which may be complex in the general case.

The author believes that the Vorticity/Integral method as described here is a useful technique for calculating two-dimensional viscous flows. However, in extending the technique to three-dimensional viscous flows, once more the difficulty of orienting the vorticity vector (previously mention for the 3-D jet) is encountered. The author was unable to investigate this problem further as the time limit for the investigation had expired.

7.3 Relevance to Prediction of Combustion Chamber Flows

Much work remains to be done before even a two-dimensional combustion chamber can be successfully modelled. It is the authors belief, however, that the Vorticity/Integral method will form the aerodynamic core of a combustion chamber optimising program.

Only incompressible flows have been discussed here. Stricker (1976) has solved compressible flows by placing source singularities in the flow field. The strengths of the sources are calculated so that the continuity and energy equations are satisfied at each mesh point. This is accomplished using the Integral equation approach already outlined. The work necessary to extend the Vorticity/Integral method to compressible flows would be small; the requirement is merely to add a source at each mesh point, and calculate their strengths iteratively.

8. CONCLUSIONS

These are best set out under three separate headings:-

8.1 Three-dimensional Jet

1. The type of irrotational flow model described here could be incorporated in a wing pressure distribution program. It is believed that this would allow the interference between the engine exhaust plume and the wing flow to be more accurately calculated.

2. It is believed that viscous effects in jet flows can be most readily dealt with by solving the full vorticity transport equation by finite-difference methods.

3. To extend the method to three-dimensions it will be necessary to consider the orientation of the vorticity vector.

8.2 Two-Dimensional Viscous Flow

1. The Vorticity/Integral method provides a foundation for the calculation of two-dimensional viscous flows.

2. The reason for the long computer times was the time required to set up the data necessary for the solution of the Fredholm Integral equation. Further numerical experimentation should lead to a radical reduction in computer time. The improvements to the ring package structure have already been carried out.

3. The numerical solution of the Fredholm Integral equation can be accommodated to any surface geometry. This has obvious advantages within a general design program, especially when used with the automatic mesh fitting routine at Rolls-Royce (1971) Ltd.,Bristol, to give the finite-difference mesh for the vorticity calculation.

4. To predict higher Reynolds number flows, both a turbulence model and a different finite-difference form of the Vorticity transport equation would be necessary. The incorporation of a suitable turbulence model into the computational method is the next most-important step to be taken in the future.

5. The Vorticity/Integral method mirrors the physical flow field, and has the further advantage over stream-function-vorticity methods of having the mesh only in the non zero vorticity regions i.e. boundary layer, wake etc.

8.3 Relevance to Combustion Chamber Flows

1. It was felt that the Vorticity/Integral method would form the aerodynamic core of a combustion chamber optimising program at some stage in the future.

REFERENCES

ABRAMOWITZ, M, STEGUN, 1965 Handbook of Mathematical Functions
Dover Publications, Inc., New York.

APELT, C.J. 1961 The Steady Flow of a Viscous Fluid Past a
Circular Cylinder at Reynold's Numbers 40 and 44.
A.R.C. R & M No. 3175.

BATCHELOR, G.K. 1967 An introduction to Fluid Dynamics.
Cambridge University Press.

BLACKMORE, K. 1976 Private Communication.
School of Mathematics Bath University.

CHANG, H.C. 1942 Aufrollung Eines Zylindrischen Strahles
Durch Querwind.
Phd. Thesis Göttingen.

CHORIN,A.J. 1973 Numerical Study of Slightly Viscous Flow
J. Fluid.Mech. Vol.57. Pt.4.

CLOSE, D. 1970 AHO9P - A Computer Program for the Analysis
of Airflow Distribution and Pressure Drop in an Annular
Combustor.
Rolls-Royce Derby CRR 00029.

COULMY, G. 1976 An Extension of the Discrete Distribution
Singularities Method for the Computation of the Velocity
Field with non-zero Divergence or Curl.
Presented at Euromech Colloquium 75 on the Calculation
of Flow Fields by Means of Panel Methods.

COURANT, R., HILBERT D. 1953 Methods of Mathematical Physics
Vol. 1.

CROWLEY, W.P. 1968 Numerical Advection Experiments.
Monthly Weather Review, 96,1.

DAILY, J.W. & HARLEMAN,D.R.S. 1966 Fluid Dynamics.
Addison & Westley.

DENNISON, C. 1973 Scheme D. Compiler System
Rolls-Royce (1971) Ltd., B.E.D.

DUFF, G.F.D., NAYLOR, D. 1966 Differential Equations of Applied
Mathematics.
John Wiley & Sons Inc.

DUNCAN, W.J., THOM, A.S.,YOUNG, A.D. 1960 Mechanics of Fluids
Edward Arnold.

FANNING, A.E., MUELLER, T.J. 1973 Numerical and Experimental
Investigation of the Oscillating Wake of a Blunt-Based Body.
AIAA Journal Vol.11 No. 11.

REFERENCES (Contd)

FROMM, J.E. 1964 The Time Dependent Flow of an Incompressible Viscous Fluid.
In Fundamental Methods in Hydrodynamics Eds.B.Alder & S. Fembach.

FROMM, J.E. 1969a Numerical Solutions of Two-Dimensional Stall in Fluid Diffusers.
High Speed Computing in Fluid Dynamics Physics of Fluids Supplement II.

FROMM, J.E. 1969b Practical Investigation of Convective Difference Approximations of Reduced Dispersion.
High Speed Computing in Fluid Dynamics Physics of Fluids Supplement II.

GOLDSTEIN, R.J.et al 1969 Laminar Separation, Reattachment, and Transition of the Flow Over a Downstream - Facing Step.
Transactions of the ASME ASME No. 69 - WA/FE-5.

GOSMAN, A.D., et al 1969 Heat and Mass Transfer in Recirculating Flows. Academic Press.

HACKETT, J.E., MILLER, H.R. 1969 The Aerodynamics of the Lifting Jet in a Cross Flowing Stream.
NASA SP-218.

HESS, J.L., SMITH, A.M.O. 1966 Calculation of Potential flow about Arbitrary Bodies.
Progress in Aeronautical Sciences Pergammon Press Series.

HUBBLE, P.E. - 1964 The Distortion and Mixing of a Jet in a Cross wind.
Bristol Siddeley Engines Limited GN.7227 May 1964.

HUBBLE, P.E. 1967 A Numerical Approach to the Estimation of Gas Turbine Combustion Chamber Performance.
Combustion in Advanced Gas Turbine Systems Ed I.E. Smith. Cranfield International Symposium Series Vol 10.

HUBBLE, P.E., PAUL, R.K. 1968 Diffusion and Convection of Vorticity in Fluid Flow.
Rolls-Royce (1971) Ltd., B.E.D. Note No. 166.

KAWAGUTI, M. 1965 Numerical Solutions of the Navier-Stokes Equations for the Flow in a Channel with a Step.
Mathematics Research Centre University of Wisconsin
MRC TECH Summary Report #574

KAWAGUTI, M. 1953 Numerical Solution of the Navier-Stokes Equations for the flow around a Circular Cylinder at Reynolds Number 40.
Jour. Phy. Soc. Japan Vol. 8. No. 6.

KUCHEMANN, D., WEBER, J. 1953 Aerodynamics of Propulsion
McGraw Hill.

REFERENCES (Contd)

LAMB, H. 1932 Hydrodynamics 6th Edition.
Cambridge University Press.

LIGHTHILL, M.J. 1963 Introduction. Boundary Layer Theory
Theory. in Laminar Boundary Layers
Fluid Motion Memoirs Ed.L. Rosenhead.

MARGASON,R.J. 1969 Analysis of a Jet in a Subsonic Crosswind
NASA SP-218

MARGASON, R.J. 1969 Analytic Description of Jet-Wake Cross
Sections for a Jet Normal to Subsonic Free Stream.
NASA - SP-218

MASON J.G. 1968 Flow Synthesis by Singularities, Two-
Dimensional and Axisymmetric Problems.
Rolls-Royce Derby IAM 99801

MILLS, R.D. 1968 Numerical Solutions of Viscous Flow Through
a Pipe Orifice at Low Reynolds Numbers.
J. Mech.Eng.Sci. Vol. 10 No.2.

MILNE-THOMSON, L.M. 1966
Theoretical Aerodynamics.

MUELLER, T.J., O'LEARY , R.A. 1970
Physical and Numerical Experiments in Laminar
Incompressible Separating and Re-attaching Flows.
AIAA 3rd Fluids,Plasma Dynamics Conference.

MUELLER, T.J. 1974 Private Communication.

PAYNE, R.B. 1956 A Numerical Method for Calculating the
Starting and Perturbation of a Two-Dimensional Jet at
Low Reynolds Number.
Aero.Res.Counc(Lond) Rep. and Mem. No. 3047

PAYNE, R.B. 1958 Calculations of Unsteady Viscous Flow past
a Circular Cylinder.
J. Fluid Mech. Vol.4. Pt. 1.

PEACEMAN, D.W., RACHFORD, H.H. 1955 The Numerical Solution
of Parabolic and Elliptic Differential Equations.
J.SOC. Indust.Appl. Math. Vol.3. No. 1.

PEARSON, C.E. 1965 A Computational Method for Viscous
Flow Problems.
J. Fluid. Mech. Vol.21. Pt.4.

RILEY K.P. 1973 A Useful Curve Fitting Procedure.
Rolls-Royce(1971) Ltd., B.E.D. Rept.No. AP:5757

REFERENCES (Contd)

ROBERTSON J.M. 1965 Hydrodynamics in Theory and Application
Prentice-Hall.

ROSENHEAD, L. 1966 Laminar Boundary Layers.
Oxford University Press.

RUBBERT, P.E. 1969 Calculation of Jet Interference Effects on V/STOL Aircraft by a Non-Planar Potential Flow Method.
NASA SP-218

SCHLICHTING 1968 Boundary Layer Theory.
McGraw-Hill.

SKIFSTAD, J.G. 1969 Numerical Treatment of Line Singularities for Modelling a Jet in a Low-Speed Cross Flow.
NASA SP-218

SMITH, G.D. 1969 Numerical Solution of Partial Differential Equations.
Oxford University Press.

SON, J.S., HANRATTY, T.J. 1969 Numerical Solution for the Flow around a Cylinder at Reynolds Numbers of 40,200 and 500
J. Fluid. Mech. Vol.35 pt.2.

STRICKER, R. 1976 On An Integral Equation Method for Calculation of the Fully Nonlinear Potential flow about Arbitrary Section Shapes.
Presented at Euromech Colloquium 75 on the Calculation of Flow Fields by Means of Panel Methods.

THOM, A. 1933 The Flow Past Circular Cylinders at low speeds.
Proc.Roy.Soc.,A.Vol. 141. Pl 10.

THOMPSON, J.F. 1971 Two Approaches to the 3-D Jet-In-Crosswind Problem: A Vortex Lattice Model and a Numerical Solution of the Navier-Stokes Equations.
Ph.d Thesis Georgia Institute of Technology.

VON MISES, R. 1953 Theory of Flight
McGraw-Hill.

WANG, Y.L. LONGWELL, P.A. 1964 Laminar Flow in the Inlet Section of Parallel Plates.
A.I.Ch.E.Jour. Vol.10. No.3.

WHITTAKER, M. 1965 Some Aerodynamic Aspects of Gas Turbine Combustion Chambers.
Bristol Siddeley Engines Limited, GN 8080

REFERENCES (Contd)

WOOLER, P.T. 1969 Development of an Analytical Model for the Flow of a Jet into a Subsonic Crosswind. Analysis of a Jet in a Subsonic Crosswind. NASA SP-218

WU, J.C., THOMPSON, J.F. 1973 Numerical Solutions of Time-Dependent Incompressible Navier-Stokes Equations Using an Integro-Differential Formulation. Computers & Fluids Vol.1. pp 197 - 215

WYLIE, C.R. 1966 Advanced Engineering Mathematics 3rd Edition McGraw-Hill.

APPENDIX 1.

Verification that the potential for a source satisfies Laplaces equation

Consider the potential of a 2-D source. From Robertson (1965), it is

$$\phi = \frac{\sigma}{2\pi} \log_e r \qquad \text{A1.1}$$

Where σ = source strength and $r = \sqrt{x^2+y^2}$

Substituting A1.1 into the Laplace equation

$$\nabla^2\phi = 0 = \nabla.\nabla\phi = \nabla.\nabla\left(\frac{\sigma}{2\pi}\log_e r\right)$$

Now $\nabla\left(\frac{\sigma}{2\pi}\log_e r\right) = \frac{\sigma}{2\pi r}\cdot\hat{\underline{r}} = \frac{\sigma}{2\pi r^2}\underline{r}$

Where $\hat{\underline{r}}$ is a unit vector $(= \underline{r}/r)$

So $\nabla.\nabla\phi = \nabla.\left(\frac{\sigma}{2\pi r^2}\underline{r}\right) = \frac{\sigma}{2\pi}\left\{\frac{1}{r^2}\nabla.\underline{r} + \underline{r}.\nabla\left(\frac{1}{r^2}\right)\right\}$

$$= \frac{\sigma}{2\pi}\left\{\frac{2}{r^2} + \underline{r}.\left(-\frac{2}{r^3}\hat{\underline{r}}\right)\right\}$$

$$= \frac{\sigma}{2\pi}\left\{\frac{2}{r^2} + \underline{r}.\left(-\frac{2}{r^4}\underline{r}\right)\right\}$$

$$= \frac{\sigma}{2\pi}\left\{\frac{2}{r^2} + \left(-\frac{2}{r^2}\right)\right\} = 0$$

hence the potential for a source satisfies Laplace's equation. Exactly the same procedure would be used to prove that the potential for a uniform stream also satisfies Laplace's equation, where ϕ in A1.1 would be set equal to U_x

APPENDIX 2.

Derivation and Method of Solution of Second kind Fredholm Integral Equations.

The Neumann problem involves the determination of the potential in a space for which the normal derivative has been specified on the boundary.

Consider a distribution of sources over the surface of a non-porous body, fig A2. F1.

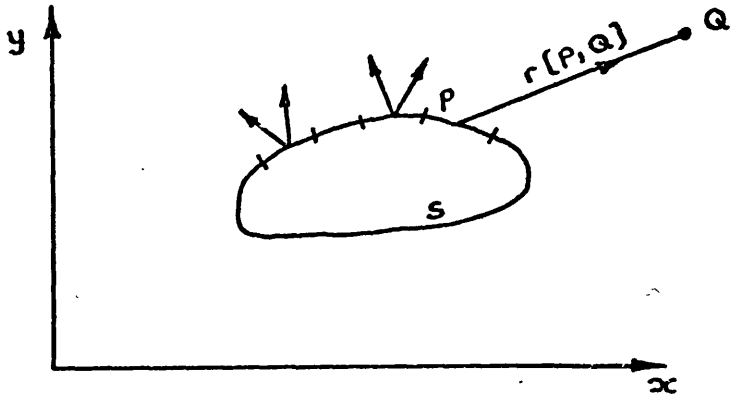

Where [ ] denotes functional dependance

FIG A2.F1. SOURCE DISTRIBUTION OVER SURFACE S

Let the intensity per unit area of the sources be $\sigma/4\pi$ varying over the surface S of the body. The potential at a point Q in the fluid space outside the body due to this source intensity is,

$$-\frac{\sigma}{4\pi r}\,dS \qquad \text{A2.1}$$

Where r = radial distance of Q from surface element being considered.

The potential at a point Q due to the whole body is

$$\phi_Q = -\frac{1}{4\pi}\int_S \frac{\sigma[p]}{r[p,Q]}\,dS \qquad \text{A2.2}$$

Where p = the location on the body surface of the element considered, and

$r[p,Q] = \overline{pQ}$, the radius from p to Q

The normal derivative to the body surface is taken, and the limiting value is considered as Q approaches a general point, say b, on the boundary surface

$$\left.\frac{\partial \phi}{\partial n}\right|_b = q_b - \frac{1}{4\pi}\int_S \frac{\partial}{\partial n}\left(\frac{\sigma[P]}{r[P,Q]}\right) dS \qquad \text{A2.3}$$

Where q_b = the direct contribution to the velocity from the source strength on the surface at point b. This is

$$q_b = -2\pi\frac{\sigma}{4\pi} = -\frac{\sigma}{2} \qquad \text{A2.4}$$

Thus the Integral equation to be solved for the unknown source-intensity distribution appears in the form of a Fredholm Integral equation of the second kind.

$$\sigma[b] = -2\left.\frac{\partial \phi}{\partial n}\right|_b - \frac{1}{2\pi}\int_S \sigma[P]\frac{\partial}{\partial n}\left(\frac{1}{r[b,P]}\right) dS \qquad \text{A2.5}$$

For a more detailed description of this derivation, see Hess et al(1966) and others.

The Neumann problem can be redefined if vortex singularities are used in place of sources. In this case, the Neumann problem would involve the determination of the streamfunction in a space for which the normal derivative has been specified on the boundary.

The derivation of the Integral equation would be exactly the same as above, the final form being

$$\sigma[b] = -2\left.\frac{\partial \psi}{\partial n}\right|_b - \frac{1}{2\pi}\int_S \sigma[P]\frac{\partial}{\partial n}\left(\frac{1}{r[b,P]}\right) dS \qquad \text{A2.6}$$

Solution of the Integral Equation for Irrotational Flow Through a Duct.

The sheet singularities comprising the duct surfaces are: Vortex sheets along the solid boundaries, source sheets along the duct inlet and exit boundaries. The reason for this choice in singularities is explained in Section 6.21.

Following Hess the surface singularities are divided into an arbitrary number of discrete sheet singularities. The orientation of some of the individual sheet axes and the direction of the local vorticity vector are shown in fig. A2.F2

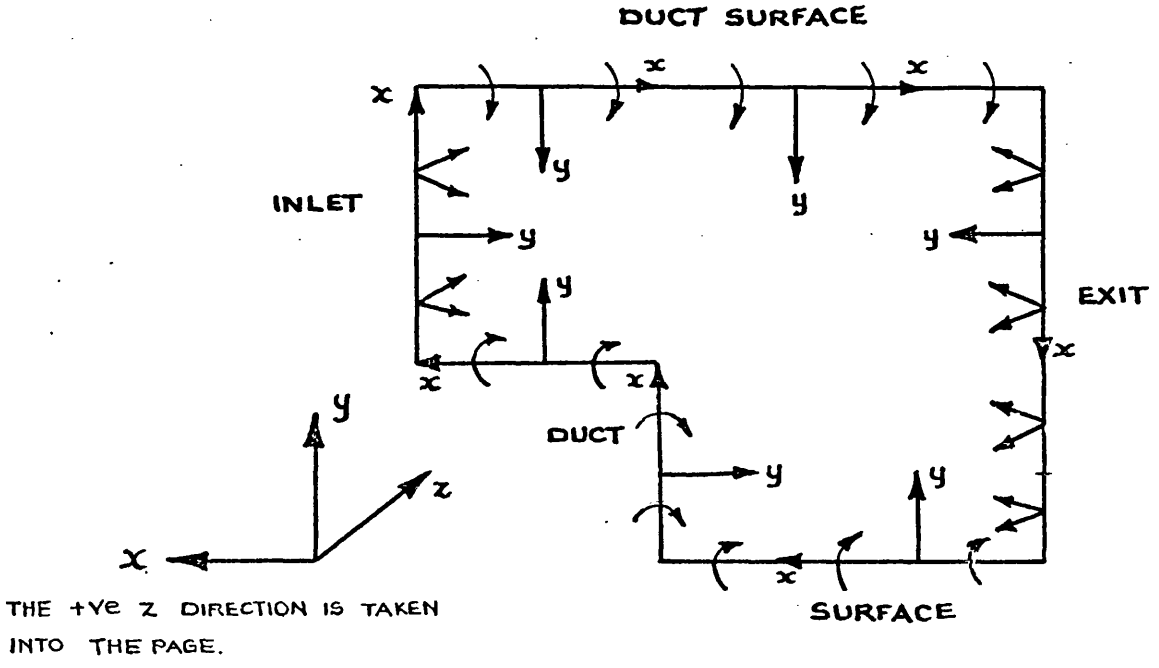

FIG A2.F2. BOUNDARY VORTEX SHEETS

It is worth emphasising the following points:-

(1) A right-hand axis system is assumed, with +ve vorticity in +z direction.

(2) The local normal vector to the vortex sheet points into the flow domain.

(3) The correct sign for the local vorticity and sheet strengths is obtained by solving the Integral equation. Those orientations shown in fig. A2.F2 are initial guesses.

The approximate solution to the Integral equation is obtained as follows:

(1) Each sheet is selected in turn, with the collocation point chosen to be the sheet mid-point. For each sheet an equation is set up equating the velocity induced at the collocation point, to the sheet boundary condition. The velocity is composed of contributions from every sheet.

The significance of the collocation point is that the solution to the Integral equation is exact at this location.

(2) Select each sheet in turn as a field sheet. Calculate the velocity induced by the sheet at the collocation point, in terms of the sheet strength (section 6.23).

Thus an equation of the form is established for each collocation sheet

$$a_{11}\sigma_1 + a_{12}\sigma_2 + a_{13}\sigma_3 + \text{---} + a_{1n}\sigma_n = [B.C] \qquad \text{A2.7}$$

where a_{11} to a_{1n} are the known coefficients of the source strengths and σ_1 to σ_n are the unknown source strengths and $[B.C]$ is the boundary condition for collocation sheet

The boundary conditions are:

1) for a vortex sheet, $[B.C] = 0$ (tangential velocity)
2) for a source sheet at the duct inlet, $[B.C]$ = V INLET (Normal Velocity
3) for a source sheet at the duct exit, $[B.C]$ = - V OUTLET "

The explanation of the boundary conditions is given in Section 6.21.

The N equations for the N unknown source/vortex sheet strengths can be summarised in the matrix equation.

$$A\sigma = B \qquad \text{A2.8}$$

Where A = $[N \times N]$ matrix of coefficients.
σ = $[N]$ column matrix of source/vortex sheet strengths.
B = $[N]$ column matrix of sheet boundary condition.

Equation A2.8 is solved using a Gauss-Seidal technique for the unknown source strengths.

From these, the velocity distribution throughout the interior of the duct can now be calculated (Section 6.23).

APPENDIX 3

To calculate the velocity induced by a vortex sheet strip

The velocity induced at an interrogation point by a vortex sheet strip is given by the surface integral

$$\underline{V}_p = \frac{1}{4\pi} \int \underline{\gamma} \wedge \frac{\underline{r}}{|\underline{r}|^3} \, ds \qquad \text{A3.1}$$

Where $\underline{\gamma}$ is the vortex sheet strength vector having the same direction as the vorticity vector $\underline{\omega}$.

A3.1 can be rewritten as

$$\underline{V}_p = \frac{1}{4\pi} \int_{x_1}^{x_2} dx \int_{z_1}^{z_2} \underline{\gamma} \wedge \frac{\underline{r}}{|\underline{r}|^3} \, dz \qquad \text{A3.2}$$

for the strip QMNT, fig. A3.F1.[178] Evaluating the cross product gives

$$V_p = \frac{1}{4\pi} \int_{x_1}^{x_2} dx \int_{z_1}^{z_2} \frac{\gamma \, r(x,z) \sin\alpha(x,z)}{r(x,z)^3} \, dz \qquad \text{A3.3}$$

in a direction perpendicular to plane APD. This may be written as

$$V_p = \frac{\gamma}{4\pi} \int_{x_1}^{x_2} I_1 \, dx \qquad \text{A3.4}$$

Where

$$I_1 = \int_{z_1}^{z_2} \frac{\sin\alpha(x,z)}{r(x,z)^2} \, dz$$

From fig A3.F1[178]

$$r^2 = h^2 / \sin^2\alpha$$

hence

$$I_1 = \int_{z_1}^{z_2} \frac{\sin^3\alpha}{h^2} \, dz \qquad \text{A3.5}$$

Following Milne-Thomson (1966), from fig. A3.F1,[178]

$Z = AB = AD - BD = AD - h \cot\alpha$. Since AD is constant $dZ = h \operatorname{cosec}^2\alpha \, d\alpha$

Substituting in A3.5

$$I_1 = \int_{\alpha_1}^{\alpha_2} \frac{\sin\alpha}{h} \, d\alpha = \frac{1}{h}\left[\cos\alpha_1 - \cos\alpha_2\right] \qquad \text{A3.6}$$

Substituting A3.6 into A3.4 gives

$$V_p = \frac{\sigma}{4\pi} \int_{x_1}^{x_2} \frac{1}{h} \left[\cos \alpha_1 - \cos \alpha_2 \right] dx \qquad \text{A3.7}$$

Where Vp is in a direction perpendicular to plane APD.

APD is at an angle β to the sheet QMNT. The velocity given by A3.7 can be resolved into components parallel and perpendicular to the sheet, as follows:

$$V_{p_x} = -V_p \sin \beta \quad \text{and} \quad V_{p_y} = V_p \cos \beta \qquad \text{A3.8}$$

Substituting in A3.7 .

$$V_{p_x} = \frac{\sigma}{4\pi} \int_{x_1}^{x_2} \frac{1}{h} \left[\cos \alpha_2 - \cos \alpha_1 \right] \sin \beta \, dx$$

$$V_{p_y} = \frac{\sigma}{4\pi} \int_{x_1}^{x_2} \frac{1}{h} \left[\cos \alpha_1 - \cos \alpha_2 \right] \cos \beta \, dx \qquad \text{A3.9}$$

Again, following Milne-Thomson, from fig. A3.F1,[178]

$X = EB = EK - BK = EK - J \cot \beta$. Since EK is constant $dx = J \operatorname{cosec}^2 \beta \, d\beta$

Substituting this into A3.9 gives.

$$V_{p_x} = \frac{\sigma}{4\pi} \int_{\beta_1}^{\beta_2} \frac{1}{h} \left[\cos \alpha_2 - \cos \alpha_1 \right] \frac{J}{\sin \beta} \, d\beta \qquad \text{A3.10}$$

$$V_{p_y} = \frac{\sigma}{4\pi} \int_{\beta_1}^{\beta_2} \frac{1}{h} \left[\cos \alpha_1 - \cos \alpha_2 \right] \frac{J \cos \beta}{\sin^2 \beta} \, d\beta \qquad \text{A3.11}$$

Evaluating first A3.10. From fig. A3.F1.[176]

$$J = h \sin \beta$$

hence

$$V_{P_x} = \frac{\sigma}{4\pi} \int_{\beta_1}^{\beta_2} \left[\cos \alpha_2 - \cos \alpha_1\right] d\beta \qquad \text{A3.12}$$

Now $\cos \alpha_1 = \frac{AD}{AP} = \frac{AD}{\sqrt{AD^2 + h^2}} = \frac{\sin \beta}{\sqrt{\sin^2 \beta + a_1^2}}$

Where $a_1 = \frac{J}{AD}$

Similarily $\cos \alpha_2 = \frac{\sin \beta}{\sqrt{\sin^2 \beta + a_2^2}}$

Where $a_2 = \frac{J}{CD}$

Substituting into A3.12

$$V_{P_x} = \frac{\sigma}{4\pi} \int_{\beta_1}^{\beta_2} \left[\frac{\sin \beta}{\sqrt{\sin^2 \beta + a_2^2}} - \frac{\sin \beta}{\sqrt{\sin^2 \beta + a_1^2}}\right] d\beta \qquad \text{A3.13}$$

Let $d\gamma = -\sin \beta \, d\beta \quad \therefore \gamma = \cos \beta \quad$ AND $\sin^2 \beta = 1 - \gamma^2$

Hence

$$V_{P_x} = \frac{\sigma}{4\pi} \int_{\cos\beta_1}^{\cos\beta_2} \left\{\left[\frac{1}{\sqrt{1 - \gamma^2 + a_1^2}}\right] - \left[\frac{1}{\sqrt{1 - \gamma^2 + a_2^2}}\right]\right\} d\gamma \qquad \text{A3.14}$$

Let $a_{22} = \sqrt{1 + a_2^2}$ and $a_{11} = \sqrt{1 + a_1^2}$

Also $a_{22} = \sqrt{1 + J^2/CD^2} = \frac{SP}{CD} = \frac{1}{\cos \delta_2}$

and similarly $a_{11} = \frac{1}{\cos \delta_1}$

Substituting into A3.14

$$V_{P_x} = \frac{\sigma}{4\pi} \int_{\cos\beta_1}^{\cos\beta_2} \left[\frac{1}{\sqrt{a_{11}^2 - \gamma^2}} - \frac{1}{\sqrt{a_{22}^2 - \gamma^2}}\right] d\gamma$$

Which gives on integrating

$$V\rho_x = \frac{\sigma}{4\pi}\left[\text{SIN}^{-1}\left(\frac{\gamma}{a_{11}}\right) - \text{SIN}^{-1}\left(\frac{\gamma}{a_{22}}\right)\right]_{\cos\beta_1}^{\cos\beta_2}$$

which is

$$V\rho_x = \frac{\sigma}{4\pi}\left\{\left[\text{SIN}^{-1}(\cos\beta_2\cos\delta_1) - \text{SIN}^{-1}(\cos\beta_2\cos\delta_2)\right] - \left[\text{SIN}^{-1}(\cos\beta_1\cos\delta_1) - \text{SIN}^{-1}(\cos\beta_1\cos\delta_2)\right]\right\} \quad \text{A3.15}$$

Evaluating the component $V\rho_y$

$$V\rho_y = \frac{\sigma}{4\pi}\int_{\beta_1}^{\beta_2}\frac{1}{h}\left[\cos\alpha_1 - \cos\alpha_2\right]\frac{J\cos\beta}{\text{SIN}^2\beta}\,d\beta \quad \text{A3.11}$$

Using the same substitutions for $\cos\alpha_1$ and $\cos\alpha_2$, and $J = h\,\text{SIN}\,\beta$

$$V\rho_y = \frac{\sigma}{4\pi}\int_{\beta_1}^{\beta_2}\left[\frac{\cos\beta}{\sqrt{\text{SIN}^2\beta + a_1^2}} - \frac{\cos\beta}{\sqrt{\text{SIN}^2\beta + a_2^2}}\right]d\beta \quad \text{A3.16}$$

Let $d\gamma = \cos\beta\,d\beta \quad \therefore \gamma = \text{SIN}\,\beta$

Hence

$$V\rho_y = \frac{\sigma}{4\pi}\int_{\text{SIN}\beta_1}^{\text{SIN}\beta_2}\left[\frac{1}{\sqrt{a_1^2 + \gamma^2}} - \frac{1}{\sqrt{a_2^2 + \gamma^2}}\right]d\gamma \quad \text{A3.17}$$

which gives on integrating

$$V\rho_y = \frac{\sigma}{4\pi}\left[\text{SINH}^{-1}\left(\frac{\gamma}{a_1}\right) - \text{SINH}^{-1}\left(\frac{\gamma}{a_2}\right)\right]_{\text{SIN}\beta_1}^{\text{SIN}\beta_2}$$

$$V_{Py} = \frac{\nabla}{4\pi}\left\{\left[\text{SINH}^{-1}\left(\frac{\text{SIN}\,\beta_2}{\text{TAN}\,\delta_1}\right) - \text{SINH}^{-1}\left(\frac{\text{SIN}\,\beta_2}{\text{TAN}\,\delta_2}\right)\right]\right.$$

$$\left. - \left[\text{SINH}^{-1}\left(\frac{\text{SIN}\,\beta_1}{\text{TAN}\,\delta_1}\right) - \text{SINH}^{-1}\left(\frac{\text{SIN}\,\beta_1}{\text{TAN}\,\delta_2}\right)\right]\right\} \quad \text{A3.18}$$

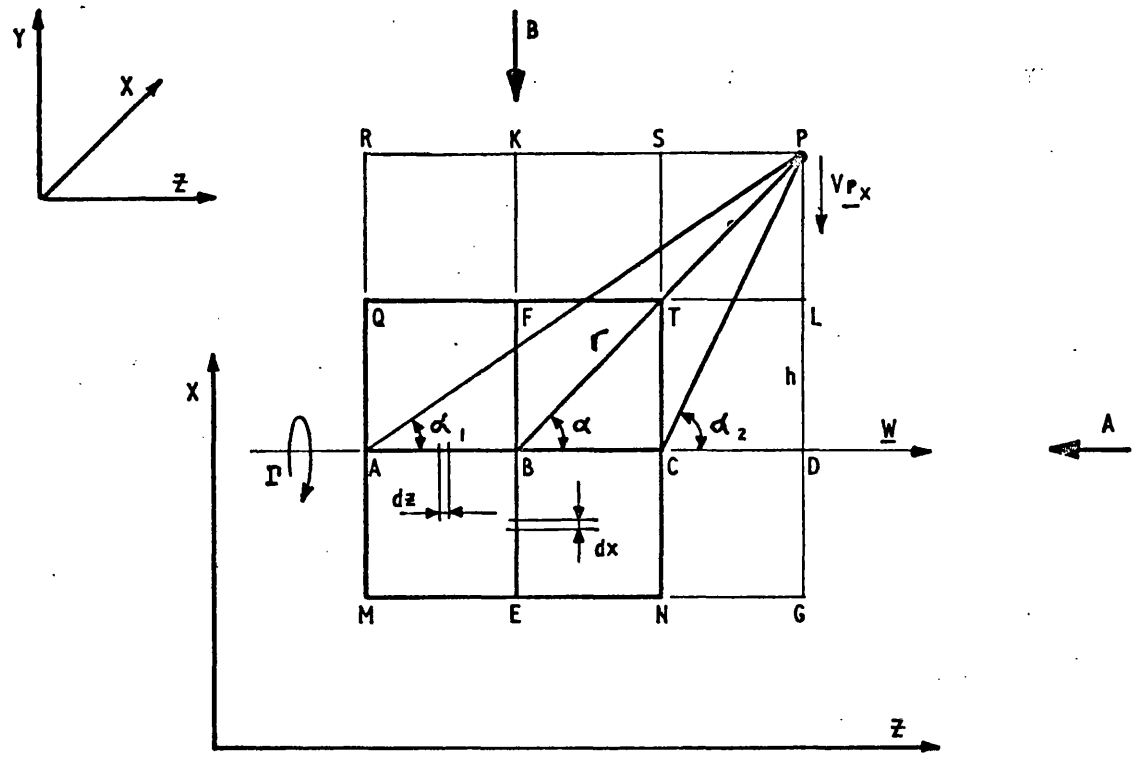

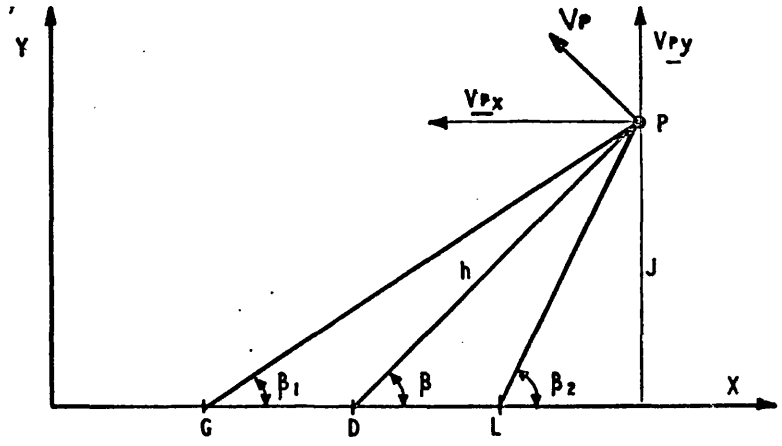

VIEW ON ARROW A

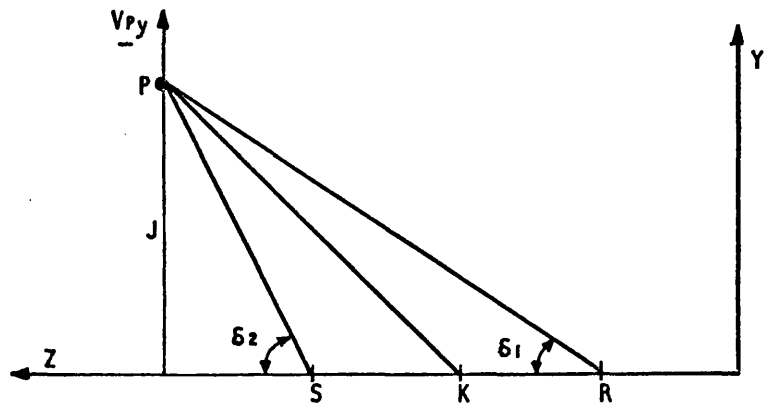

VIEW ON ARROW B

FIG.A3.F1. VELOCITY FIELD OF A 3-D VORTEX SHEET STRIP

APPENDIX 4.

DESCRIPTION OF 3D JET COMPUTER PROGRAM

A4.1 SELECTION OF INTERROGATION POINTS.

The coding of the program (written in Fortran IV) is contained in Appendix 5. The program predicts the behaviour of the 3-D jet by calculating the effect of each singularity on every other singularity. This entailed calculating the velocity induced at specific points, known as interrogation points, by the singularities.

Fig. A4.F1[190] shows the way the AVS and CVS may be approximated by means of singularities. Upon superimposing these two sheets it is apparent that the vortex filament and vortex rings intersect. The interrogation points in the working section are taken to be those intersection points (where V_1, V_2, V_3 intersect R_1 and R_2, fig. A4.F1[190]).

The working section has been enlarged in fig. A4.F2[191]. For demonstration purposes, the following singularities have been shown:-

1) 5 vortex filaments, V_1 to V_5.
2) 2 vortex rings, R_1 and R_2, representing the cylindrical sections between A1 and A_2, A_2 and A_3 respectively.
3) 2 semi-infinite cylindrical vortex sheets from $+\infty$ to A_1 and A_3 to $-\infty$. A ring of interrogation points is arranged on each of these sheets. For the top sheet, they are shown at position T, where distances TA_1 = A1 R_1. For the bottom sheet they are at B, where distances R_2 A_3 = A_3B.

The singularities are treated as follows:

1) The vortex filaments shown in fig. A4.F2[191], are divided into 5 segments.
   a) $+\infty$ to T
   b) T to R_1
   c) R_1 to R2
   d) R_2 to B
   e) B to $-\infty$

2) The vortex rings are divided into straight line segments joining the interrogation points.

3) The semi-infinite vortex sheets are divided into plane strips, shaded in fig. A4.F3 which are formed as follows:

a) Upper sheet

i) from $+\infty$ to A_1 halfway between the vortex filaments.

ii) straight lines between the intersection points on A_1.

b) Lower sheet.

i) from A_3 to $-\infty$, again halfway between the vortex filaments.

ii) straight lines between the intersection points on A_3.

4) The part of the CVS in the working section may be represented by a vortex ring or a cylindrical section, depending on the relative position of the section and the interrogation point, section 4.26. The vortex ring approximation has been described in (2). The planestrips representing the cylindrical section are shown shaded in fig A4. F3, and are formed as follows

a) Section between A_1 and A_2

i) straight lines halfway between the vortex filaments

ii) straight lines joining the intersection points, both on A_1 and A_2

b) Section between A_2 and A_3

as for (a), except that the intersection points are on both A_2 and A_3

Before the jet is deformed, the intersection points on A_2 will be the same for both cylindrical sections.

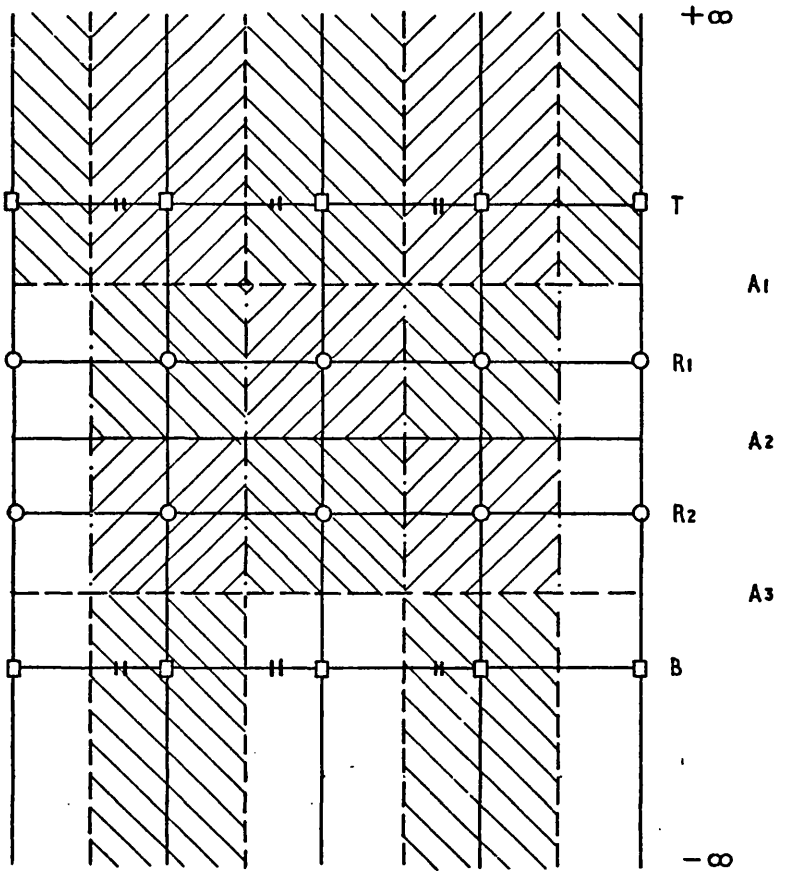

FIG A4.F3
DEVELOPED VIEW
OF WORKING SECTION.

A4.2 PROGRAM LOGIC

The flow diagram for the program [195] is shown in fig. A5.F1. Each block has been labelled and will be described separately. The coding corresponding to the blocks has been labelled accordingly.

a) BLOCK A.

On the first iteration, all the interrogation point coordinates are calculated and stored. There is only one vortex ring in the working section at this stage; more are added as the calculation progresses. If the calculation is to be restarted, then all coordinates are read from the results file of the previous run.

As the vortex ring circulation is most conveniently calculated separately, this is read into the program as data. The vortex filament circulation is more easily calculated within the program using equation 4.4

At Rolls-Royce Bristol is a program for drawing views of engineering components. The output from the 3-D jet program was arranged in such a way that it could be used as input to this drawing program. Thus the working section became a component, and isometric views for example , drawn of it. Certain constants required by this program are set within this block, and printed as required.

b) BLOCK B.

Each iteration consists of the following:

1) Calculating the velocity at every interrogation point from the effects of all the singularities present.

2) Calculating the new position of the interrogation points from the velocity and time step.

3) Introducing a new vortex ring into the working section.

At the beginning of each iteration the coordinates of the vortex strip edges, where they intersect the points rings (T and B, fig. A4.F4[192]) and the vortex rings (R_1 R_2, R_3, fig.A4.F4[192]), are calculated using subroutine CRVFIT. These are then stored with the strip local x-axis direction cosines, fig. A4.F4[192], so that the corner coordinates of all cylindrical sectionstrips, e.g. D, can be easily calculated during the iteration.

The end coordinates of the top semi-infinite strip e.g. A, are also calculated and stored. On the first iteration only, those for the bottom semi-infinite strips are calculated.

c) BLOCK C.

Each interrogation point is chosen by:

1) Selecting each ring in turn (T, R_1, R_2, B fig. A4.F3)[181]

2) Selecting each point on that ring in turn.

Incorporating the conclusions of section 4.26, the following singularities were used to calculate the velocity at the interrogation points on rings as follows:

1) Interrogation points on Ring T.

   a) All vortex singularities, except the one from $+\infty$ to $-\infty$ through the interrogation point, for the AVS.

   b) All top and bottom semi-infinite sheets strips, for the CVS.

   c) Cylindrical section strips on R_1, for the CVS.

   d) Vortex ring R_2, again for the CVS.

2) Interrogation points on Ring R_1.

   a) as 1(a), 1(b), 1(c).

   b) Cylindrical section strips on R_2, for the CVS.

3) Interrogation points on Ring R_2.

   as 1(a), 1(b), 1(c), 2(b).

4) Interrogation points on Ring B.

   a) as 1(a), 1(b), 2(b)

   b) Vortex ring R_1

The procedure for choosing field points i.e. points having singularities associated with them, is also as above. These singularities are used to calculate part of the induced velocity at the interrogation point. The singularities associated with each field point is as follows:

1) Field point on ring T.
   a) semi-infinite vortex filament between $+\infty$ and T
   b semi-infinite vortex sheet strip between $+\infty$ and A_1

2) Field point on ring R_1.
   a) segment of vortex filament between T and R_1
   b) either the segment of vortex ring PQ.fig A 4.F5 193 in the direction of the local vorticity vector, or the cylindrical section strip between A_1 and A_2. The choice depends on whether the interrogation point is on an adjacent ring or not, see section 4.26.

3) Field point on ring R_2.
   a) segment of vortex filament between R_1 and R_2
   b) See 2b, except the cylindrical section sheet strip is between A_2 and A_3.

4) Field point on ring B.
   a) segment of vortex filament between R_2 and B, B and $-\infty$
   b) semi-infinite vortex sheet strip between A_3 and $-\infty$

Having decided upon an interrogation point and selected those singularities which are to be used for the particular field point, the velocity induced by one of the following may be calculated:

1) Segments of filament and vortex ring.

2) Segment of filament and cylindrical section sheet strip

3) Segment of filament and semi-infinite sheet strip.

1) Filament and Vortex ring

The subroutine FILRIN is used to calculate the velocity induced by a segment of a vortex filament and ring. Coordinate markers are set in the main program, so that the filament and ring segments are located from the subroutine.

If any filament segment is part of the filament passing through the interrogation point, it is ignored in the subroutine.

2) Filament and Cylindrical section sheet strips.

The velocity induced by the filament segment is calculated using subroutine FILRIN.

The end coordinates of the sheet strip are calculated from the coordinates and direction cosines previously stored (Block B). Subroutine SHEET calculates the contribution to the interrogation point velocity induced by the sheet strip.

3) Filament and Semi-Infinite sheet strip.

The routine is the same as 2) with the numerical infinity being set at $1X10^6$ or $-1X10^6$.

d) BLOCK D

Having calculated all the interrogation point velocities, the coordinates of the points are printed with the plotting constants. At the same time, the new interrogation point coordinates are found from the velocity at the point, and the timestep. The results are arranged so that with a minimum of editing, they can be used as input to the plotting program, whose output is a plan, end elevation & isometric view of the working section.

The working section is lengthened by replacing a part of the bottom semi-infinite vortex sheet by a vortex ring. The height of the new cylindrical section equals distance A_2 to A_3 (fig.A4.F3[181]). Hence the ring of interrogations points at B, now become interrogation points on vortex ring R_3 (not shown).

The interrogation point coordinates at the new position B (not shown) are then stored. These points are at a distance equal to A_2 to A_3 below the position B shown in fig. A4.F3.[181]

The flow diagrams for the subroutines FILRIN, SHEET and CRVFIT are shown in fig. A5.F2.[196] The coding for each subroutine is shown in Appendix 5.

Each subroutine will be described separately:

1) Subroutine FILRIN

The velocities induced by a segment of vortex filament and/or ring are calculated using this subroutine. The position of the segments and the interrogation point are shown in relation to the field point in fig. A4.F6.

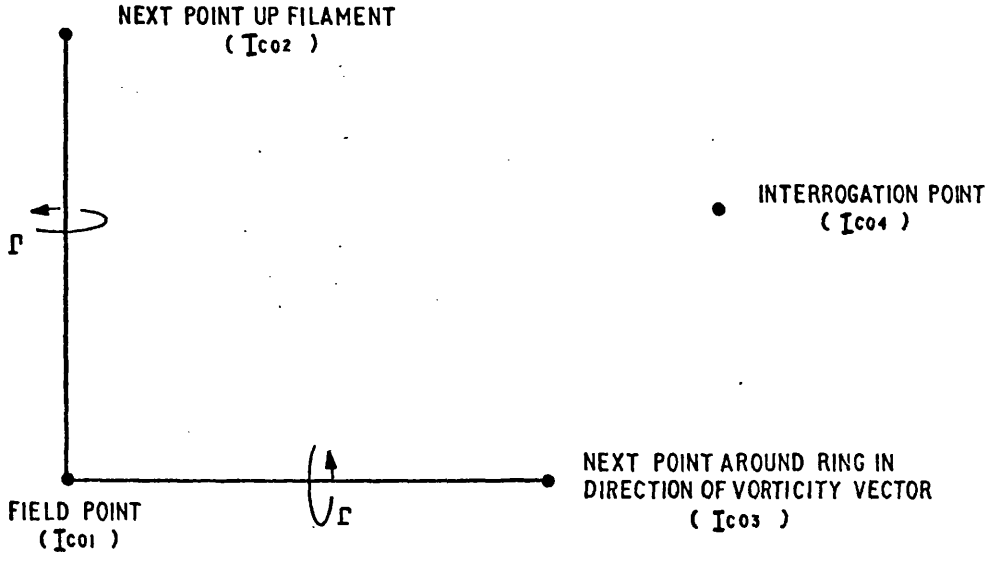

FIG.A4.F6 VORTEX SEGMENTS USED IN FILRIN

The coordinate markers for use in the subroutine, are also shown in brackets. Equation 4.10 was used to calculate the velocity at the interrogation point.

2) Subroutine SHEET

The position of the coordinate markers used to locate the ends of the sheet and the interrogation point, are shown in fig. A4.F7

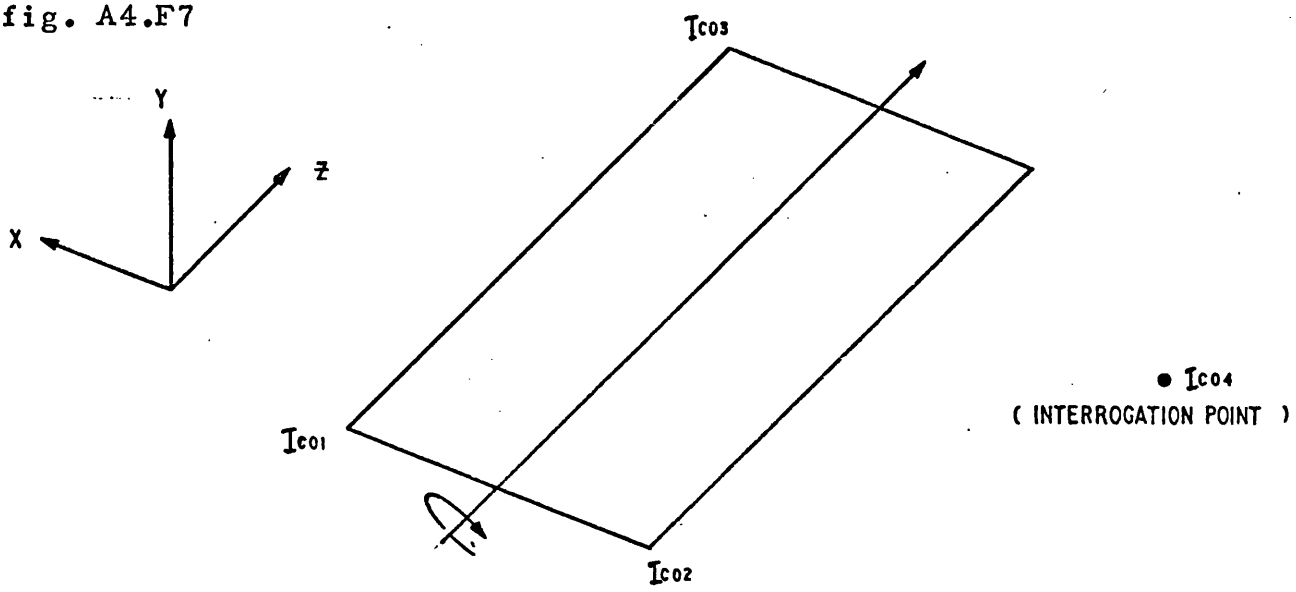

FIG. A4.F7 VORTEX STRIP SECTION FOR USE IN SHEET

The position of the field point in relation to the strip, is dependent upon whether or not a cylindrical section strip or a semi-infinite strip is being considered:-

1) Cylindrical Section Strip:

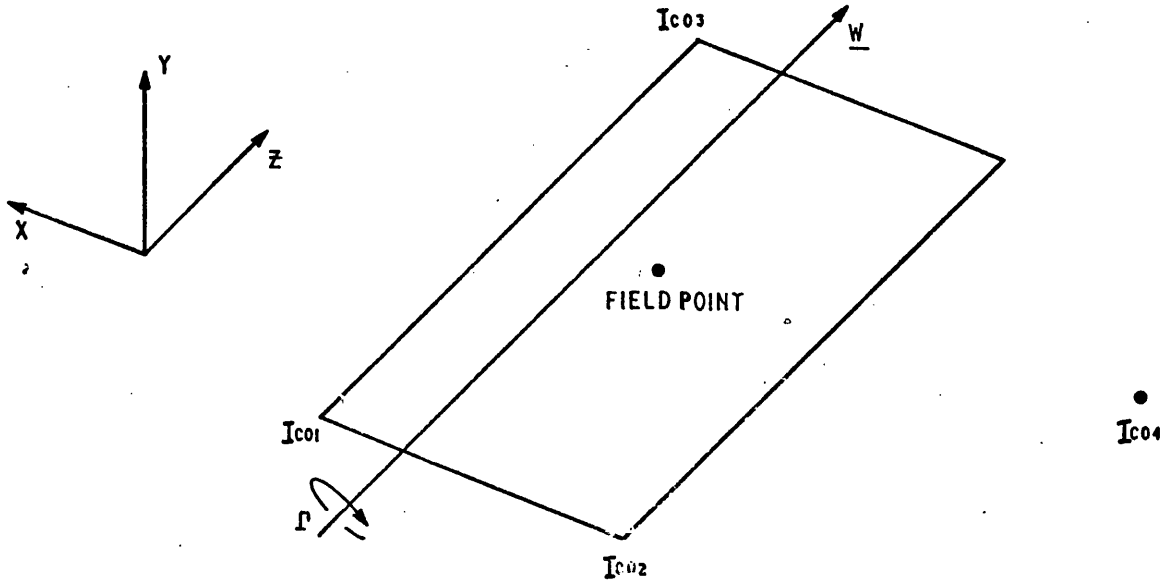

FIG. A4.F8(a) FIELD POINT ON CYLINDRICAL STRIP.

2) Semi-infinite strip:

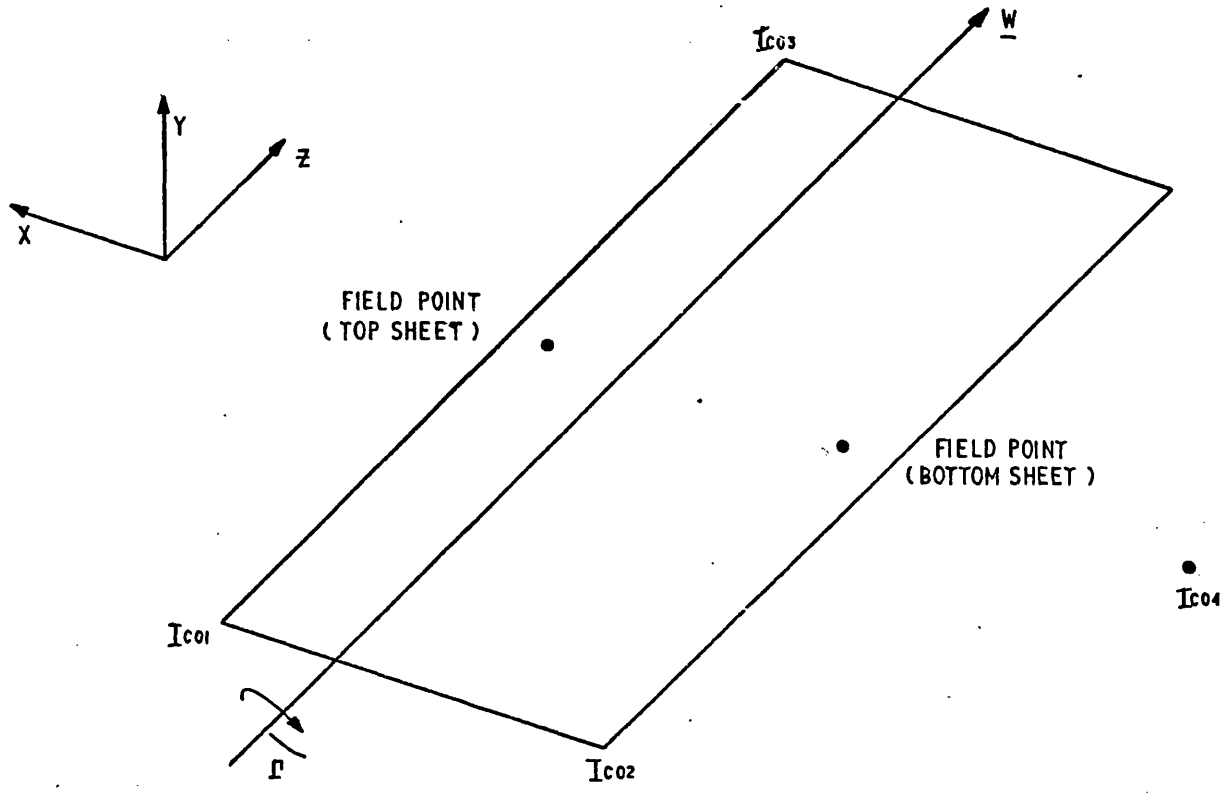

FIG.A4.F8(b) FIELD POINT ON SEMI-INFINITE STRIP

In fig. A4.F8(a), the field point is in the centre of the cylindrical section strip.

In fig. A4.F8(b), the local normal always points into the jet. For the bottom sheet, therefore, ICO1 and ICO3 will be at $-\infty$, and for the top sheet IC02 will be at $+\infty$. The distances between the field point and the nearest edge of the sheet equals TA_1 and A_3B for the top and bottom sheets respectively.

The equation for the velocity components is 4.11. The method used in the subroutine, is to transform the interrogation point coordinates into the strip axis system. Once the velocity has been calculated, it is then transformed back into the jet axis system.

3) Subroutine CRVFIT.

This subroutine is used to calculate the intersection coordinates between the edges of the cylindrical section strips and the vortex rings, and between the semi-infinite strip edges and the points rings. The method is based on Riley (1973), except that a Newton-Raphson routine was incorporated to determine accurately the intersection points. The subroutine is called each time the points are to be calculated on a ring.

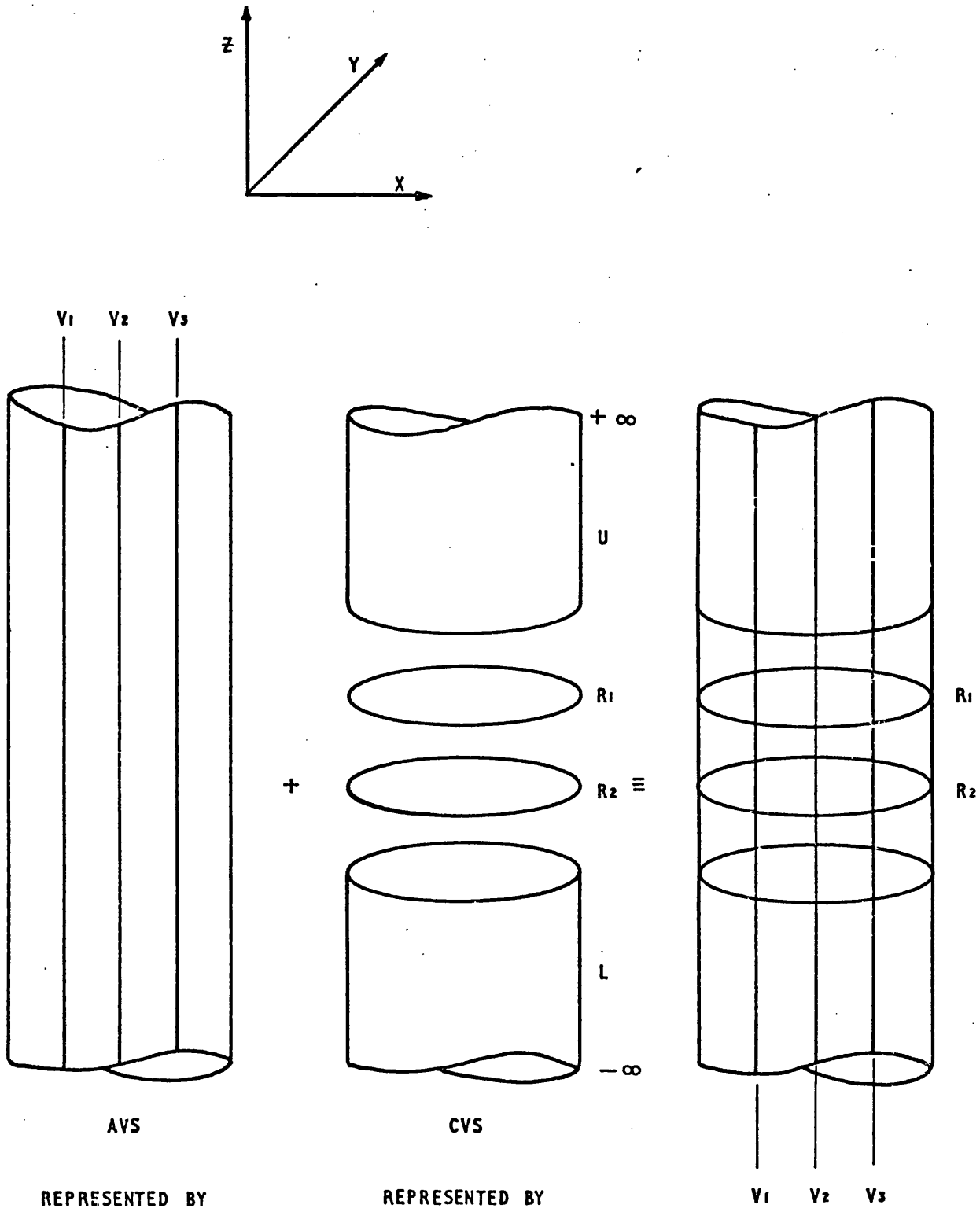

FIG.A4.F1. SUPERPOSITION OF INFINITE CYLINDRICAL VORTEX SHEETS
+ APPROXIMATIONS

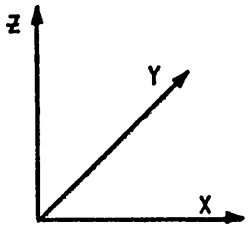

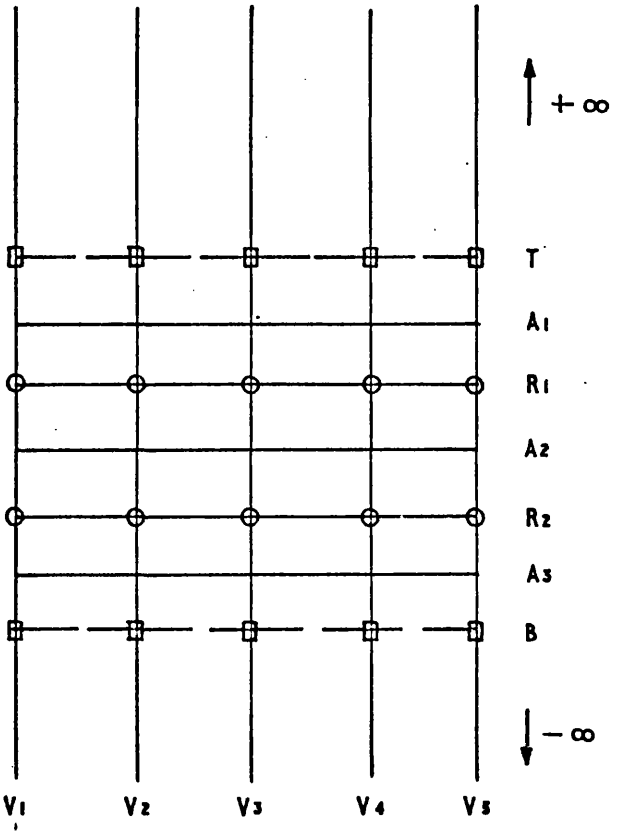

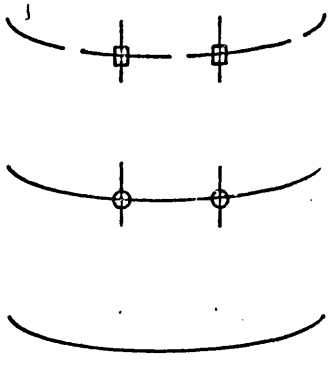

POINTS SELECTED ON SEMI-INFINITE CYLINDRICAL VORTEX SHEETS AS INTERROGATION POINTS

INTERSECTION POINTS BETWEEN VORTICES AND VORTEX RINGS CLASSED AS INTERROGATION POINTS

SINGULARITY BOUNDARIES

FIG.A4.F2. POSITION OF INTERROGATION POINTS AND CYLINDRICAL VORTEX SHEET BOUNDARIES ON DEVELOPED CYLINDER

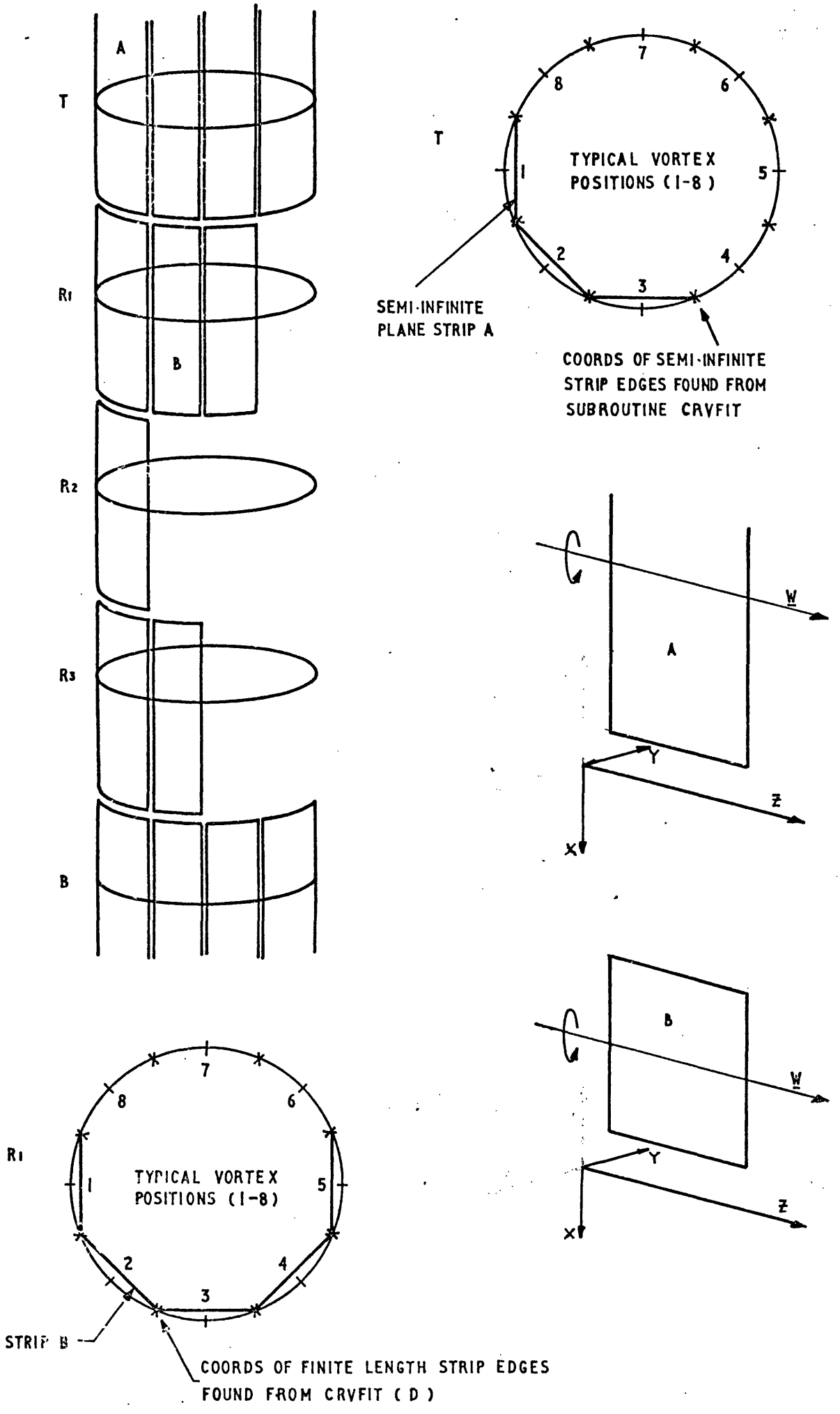

FIG.A4.F4. POSITION OF VORTEX STRIP EDGES ON POINTS AND VORTEX RINGS

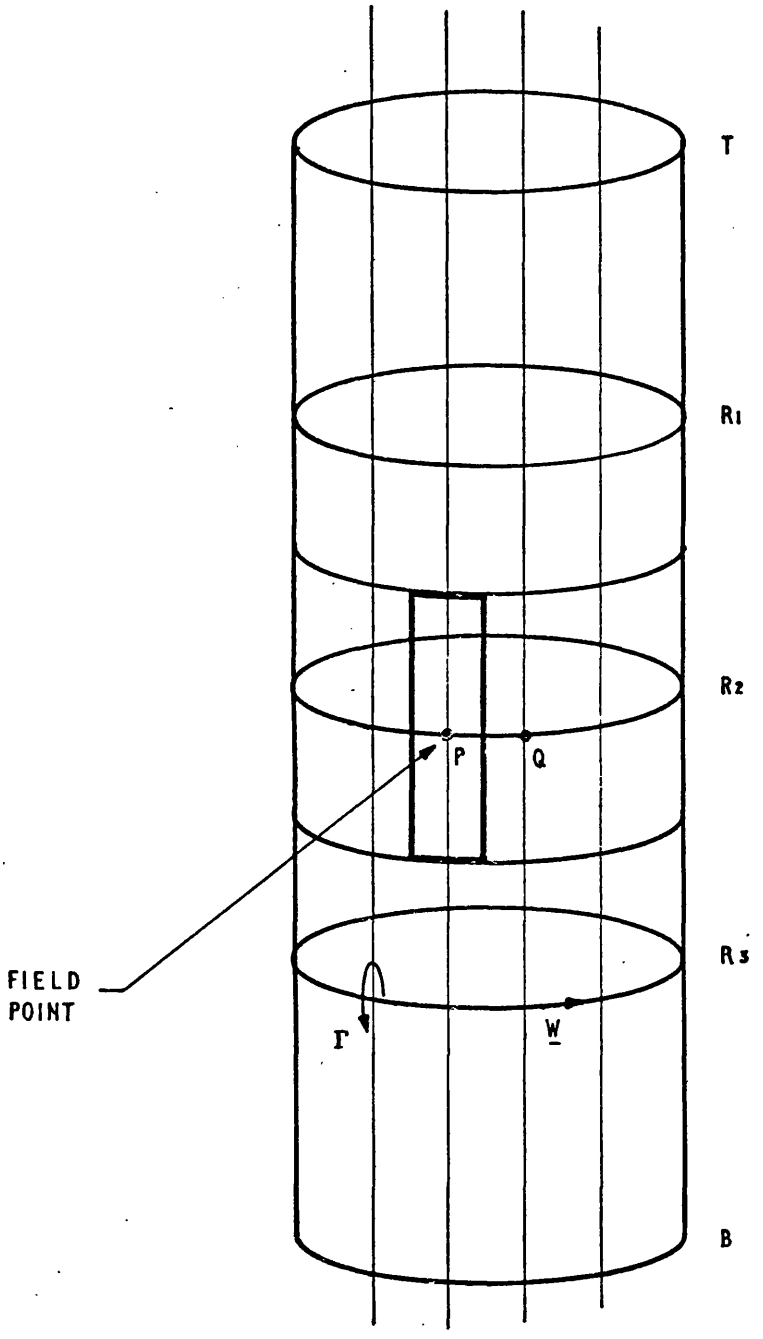

FIG.A4.F5. POSITION OF VORTEX RING SEGMENT AND CYLINDRICAL SECTION STRIP IN RELATION TO FIELD POINT

APPENDIX 5.

This contains the following:-

1) Flow diagram of the program.

2) Details of the data input.

3) Program coding for the 3D jet.

4) Typical output from the program

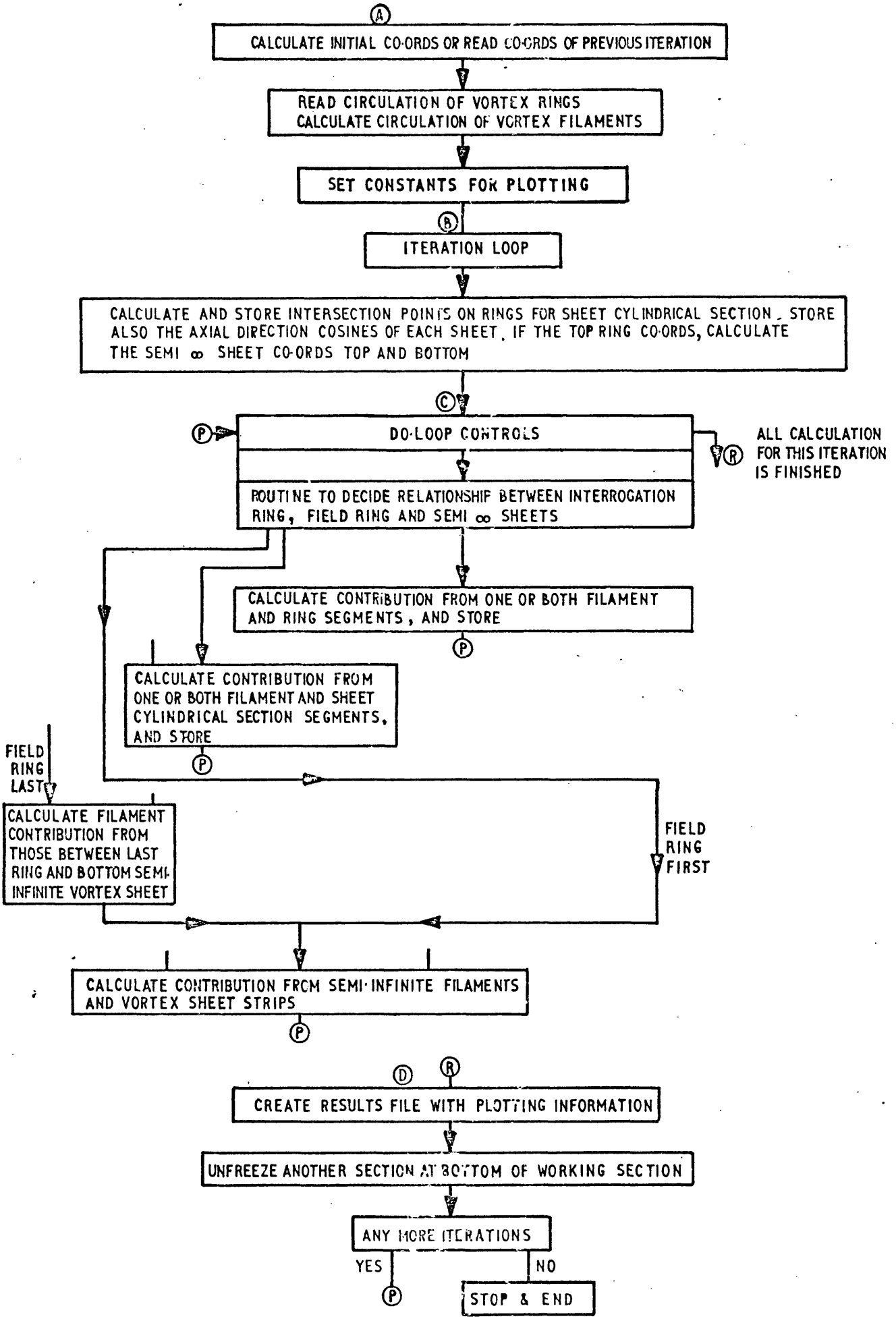

FIG. A5.F1. FLOW DIAGRAM FOR 3D JET IN CROSSWIND

SUBROUTINE 'FILRIN'

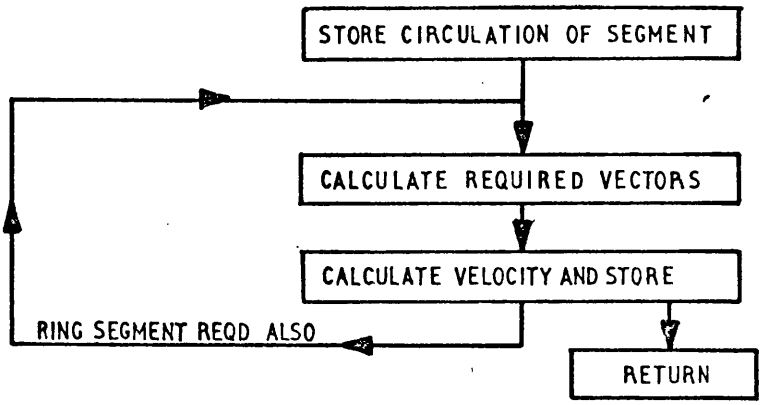

SUBROUTINE 'SHEET'

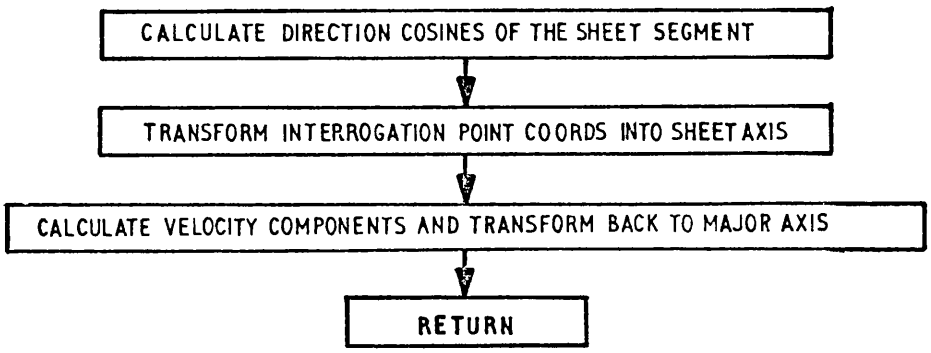

SUBROUTINE 'CRVFIT'

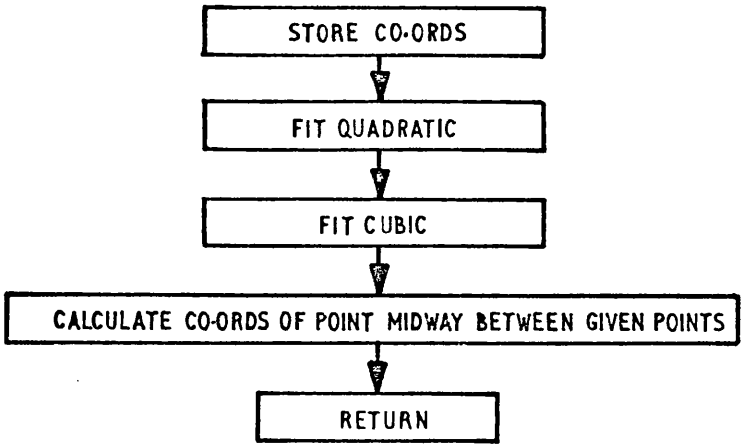

FIG.A5.F2. SUBROUTINE FLOW DIAGRAMS

NUMBER OF RINGS	NR	USUALLY 1 IF FIRST ITERATION
NUMBER OF VORTEX FILAMENTS	NF	
NUMBER OF ITERATIONS	II	(ALL FORMAT = I4)
MARKER		IF POSITIVE, CO-ORDINATES TO BE READ IF NEGATIVE, CO-ORDINATES TO BE CALCULATED
TIME STEP	STEP	
Z CO-ORDINATE OF TOP POINTS RING	Z TOP	(ALL FORMAT = 7.0)
SPACE BETWEEN RINGS	SPACE	

NEW CARD — MARKER POSITIVE ONLY

N = 0

N = N + 1

X, Y, Z CO-ORDINATES OF N^{th} INTERROGATION POINT	REPEAT UNTIL N EQUALS THE NUMBER OF INTERROGATION POINTS. PUT 3 NUMBERS/CARD AND START A NEW CARD IF NECESSARY (FORMAT = Ø.Ø)

NEW CARD

CIRCULATION OF VORTEX RINGS FROM TOP TO BOTTOM	NUMBER IS (NR-2). CIRCULATION CALCULATED FROM EQN 4.5 EACH CIRCULATION ON A NEW CARD

NEW CARD

CROSSFLOW AND JET VELOCITIES	(FORMAT = F5.0)

INPUT FOR GENERAL PROGRAM

The coding for the program to calculate the three-dimensional jet in a crosswind is given.

```
      COMMON X(500),Y(500),Z(500),DX(30),DY(30),DZ(30),
     1SX(100),SY(100),SZ(100),GAMMAR(30),GAMMAF(30),
     2ICO1,ICO2,ICO3,ICO4,I4,PI,IDUM,MARKER,VX,VY,VZ,XVELY,VELJET,
     3SVX(500),SVY(500),SVZ(500),WO(100),NF,IC2D,IC1D,
     4CX(500),CY(500),CZ(500),DL(500),DM(500),DN(500)
C
C  READ NO RINGS NO FILAMENTS NO ITERATIONS RESPECTFULLY
C
      READ(1,1000)NR,NF,II,MARKER,STEP,ZTOP,SPACE
 1000 FORMAT(4I4,3F7.0)
      WRITE(2,2030)NR,NF,II,MARKER,STEP,ZTOP,SPACE
 2030 FORMAT(1H ,4I6,3F10.5)
      IDUM = NF
      IBLOK = 1
C
C  READ OR CALC ALL CONTROL POINT COORDINATES
C
      PI=4.0*ATAN(1.0)
      DO 1 I=1,NR
      IF(MARKER) 12,999,9
    9 READ(1,1001)(X(I1),Y(I1),Z(I1),I1=IBLOK,IDUM)
 1001 FORMAT(3E13.5)
      WRITE(2,2000)(X(I1),Y(I1),Z(I1),I1=IBLOK,IDUM)
      GO TO 13
   12 JA=0
      DO 10 I1=IBLOK,IDUM
      X(I1) = -COS(FLOAT(JA)*PI/FLOAT(NF))
      Y(I1) = -SIN(FLOAT(JA)*PI/FLOAT(NF))
      Z(I1) = ZTOP-FLOAT(I-1)*SPACE
      WRITE(2,2000) X(I1),Y(I1),Z(I1)
 2000 FORMAT(1H0,3E16.6)
   10 JA = JA+2
   13 X(IDUM+1) = X(IBLOK)
      Y(IDUM+1) = Y(IBLOK)
      Z(IDUM+1) = Z(IBLOK)
      WRITE(2,2031)X(IDUM+1),Y(IDUM+1),Z(IDUM+1)
      IBLOK = IDUM+2
    1 IDUM = ((I+1)*NF)+I
C
C  RETAIN COPY OF LAST RING COORDS IN DUMMY ARRAY
C
      IBLOK = ((NR-1)*NF)+NR
      DX(NF+1) = X(IBLOK)
      DY(NF+1) = Y(IBLOK)
      DZ(NF+1) = Z(IBLOK)
      WRITE(2,2031)DX(NF+1),DY(NF+1),DZ(NF+1)
      DO 2 I=1,NF
      DX(I) = X(IBLOK)
      DY(I) = Y(IBLOK)
      DZ(I) = Z(IBLOK)
      WRITE(2,2031)DX(I),DY(I),DZ(I)
 2031 FORMAT(1H0,3F24.6)
    2 IBLOK = IBLOK+1
C
C  READ RING CIRCULATION
C
      IDUM = NR-2
      READ(1,1003)(GAMMAR(I1),I1=1,IDUM)
 1003 FORMAT(F5.0)
      WRITE(2,2002)(GAMMAR(I1),I1=1,IDUM)
```

BLOCK A

```
 2002 FORMAT(1H0,3F24.6)
C
C  CALCULATE FILAMENT CIRCULATION
C
      RADJET = SQRT(DX(1)**2+DY(1)**2)
      READ(1,1004)XVELY,VELJET
 1004 FORMAT(2F5.0)
      WRITE(2,2032)XVELY,PI,RADJET,VELJET
 2032 FORMAT(1H0,4F24.6)
      DO 3 I=1,NF
      GAMMAF(I) = 4.0*XVELY*RADJET*SIN(PI/FLOAT(NF))*SIN(2.0*FLOAT(I-1
     1)*PI/FLOAT(NF))
      WRITE(2,2003)GAMMAF(I)
 2003 FORMAT(1H0,F24.6)
    3 CONTINUE
C
C  SET CONSTANTS FOR DATA INPUT TO PLOTTING PROGRAM
C
      IFMNK = 1
      ISFNK = 2
      IBDNK = 3
      IENDNK = 11
      XMOVE = 0.0
      YMOVE = 0.0
      ZMOVE = 0.0
      ROTLX = 1.0
      ROTNX = 0.0
      ROTNX = 0.0
      ROTLY = 0.0
      ROTNY = 1.0
      ROTNY = 0.0
      ITRRT = 1
C
C  ITERATION DO LOOP CONTROL
C
      DO 50 I1=1,II
      TIME = FLOAT(I1-1)*STEP
C
C  CALCULATE AND STORE RING INTERSECTION POINTS AND LOCAL SHEET
C  X-AXIS DIRECTION COSINES
C
      NRD = NR - 1
      DO 200 ID1=1,NRD
      IC1D = ((ID1-1)*NF)+ID1
      IC2D = IC1D - 1
      CALL CRVFIT
      DO 201 ID2=1,NF
      IF(ID2.NE.1) GO TO 203
C
C  FIRST TIME THRO-CALC COORD MARKERS
C
      IF(ID1.NE.1) GO TO 202
      IC1D = IC2D
      GO TO 203
  202 IC1D = IC2D-ID1+1
  203 IC1 = IC1D+ID2
      IC2 = IC2D+ID2
      RIUS = SQRT((X(IC2+1)-X(IC2))**2+(Y(IC2+1)-Y(IC
     12))**2+(Z(IC2+1)-Z(IC2))**2)
      DLR = (X(IC2+1)-X(IC2))/RIUS
```

END OF BLOCK A

```
      DMR = (Y(IC2+1)-Y(IC2))/RIUS
      DNR = (Z(IC2+1)-Z(IC2))/RIUS
      RIUS2 = SQRT((CX(IC2+1)-CX(IC2))**2+(CY(IC2
     1+1)-CY(IC2))**2+(CZ(IC2+1)-CZ(IC2))**2)
      DLS = (CX(IC2+1)-CX(IC2))/RIUS2
      DMS = (CY(IC2+1)-CY(IC2))/RIUS2
      DNS = (CZ(IC2+1)-CZ(IC2))/RIUS2
      DLN = DMS*DNR-DMR*DNS
      DMN = DLR*DNS-DLS*DNR
      DNN = DLS*DMR-DLR*DMS
      ROOT=SQRT(DLN**2+DMN**2+DNN**2)
      DL(IC1) = DLN/ROOT
      DM(IC1) = DMN/ROOT
      DN(IC1) = DNN/ROOT
  201 CONTINUE
C
C   IF TOP RING CALCULATE AND STORE SHEET COORDS
C
      IF(ID1.NE.1) GO TO 200
      DO 204 ID2=1,NF
      IC1 = IC1D + ID2
      SX(IC1) = CX(IC1)
      SY(IC1) = CY(IC1)
      SZ(IC1) = CZ(IC1) - SPACE/2.0
      ERROR = SZ(IC1) - (CZ(IC1D+1)-SPACE/2.0)
      IF(ABS(ERROR).GE.1.0E-06) SZ(IC1) = CZ(IC1D+1)-SPACE/2.0
      IF(I1.NE.1) GO TO 204
      IC2 = IC1 + NF + 1
      SX(IC2) = SX(IC1)
      SY(IC2) = SY(IC1)
      SZ(IC2) = SZ(IC1) - FLOAT(NR-2)*SPACE
  204 CONTINUE
      SX(IC1+1) = SX(IC1D+1)
      SY(IC1+1) = SY(IC1D+1)
      SZ(IC1+1) = SZ(IC1D+1)
      IF(I1.NE.1) GO TO 200
      SX(IC2+1) = SX(IC1D+1)
      SY(IC2+1) = SY(IC1D+1)
      SZ(IC2+1) = SZ(IC1D+1) - FLOAT(NR-2)*SPACE
  200 CONTINUE
C
C   CONTROL RING DO LOOP CONTROL
C
      DO 42 I2=1,NRD
C
C   CONTROL POINT DO LOOP CONTROL
C
      DO 41 I3=1,NF
      SUMVX = 0.0
      SUMVY = 0.0
      SUMVZ = 0.0
C
C   FIELD RING DO LOOP CONTROL--BRICK DECISION ROUTINE
C
      DO 40 I4=1,NR
      IF(I4.EQ.1.OR.I4.EQ.NR)GO TO 20
      IF(I2-2)15,16,17
   15 IF(I4.EQ.2)GO TO 6
      GO TO 7
   16 IF(I4.EQ.2.OR.I4.EQ.3)GO TO 6
```

BLOCK B

END OF BLOCK B

```
      GO TO 7
   17 IF(I2.EQ.(NR-1))GO TO 18
      IF(I4.EQ.(I2-1).OR.I4.EQ.I2.OR.I4.EQ.(I2+1))GO TO 6
      GO TO 7
   18 IF(I4.EQ.(I2-1).OR.I4.EQ.I2)GO TO 6
      GO TO 7
C
C  CALCULATE FILAMENT AND RING CONTRIBUTION
C
    7 DO 5 IDUM=1,NF
      IF(IDUM.NE.1)GO TO 58
C
C  FIRST TIME THRU-SET COORD MARKERS
C
      ICO1D = ((I4-1)*NF)+(I4-1)
      ICO2D = ((I4-2)*NF)+(I4-2)
      ICO4 = ((I2-1)*NF)+I3+(I2-1)
   58 IF(IDUM.EQ.I3)GO TO 4
C
C  CONTROL AND FIELD POINT DIFFERENT-CALC FIL AND RING
C
      MARKER = 0
      ICO1 = ICO1D + IDUM
      ICO2 = ICO2D + IDUM
      GO TO 59
C
C  CONTROL AND FIELD POINT SAME-CALC ONLY RING
C
    4 MARKER = 1
      ICO1 = ICO1D + IDUM
      ICO2 = ICO1 + 1
   59 CALL FILRIN
      SUMVX = SUMVX + VX
      SUMVY = SUMVY + VY
      SUMVZ = SUMVZ + VZ
    5 CONTINUE
      GO TO 40
C
C  CALCULATE FILAMENT AND SHEET (FINITE LENGTH SECTION) CONTRIBUTION
C  CALCULATE FILAMENT CONTB FIRST
C
    6 DO 8 IDUM=1,NF
      IF(IDUM.NE.1)GO TO 60
C
C  FIRST TIME THRU-SET MARKERS
C
      ICO1D = ((I4-1)*NF)+(I4-1)
      ICO2D = ((I4-2)*NF)+(I4-2)
      ICO4 = ((I2-1)*NF)+I3+(I2-1)
   60 IF(IDUM.EQ.I3)GO TO 8
C
C  FIELD POINT NOT CONTROL POINT
C
      ICO1 = ICO1D + IDUM
      ICO2 = ICO2D + IDUM
      MARKER = -1
      CALL FILRIN
      SUMVX = SUMVX + VX
      SUMVY = SUMVY + VY
      SUMVZ = SUMVZ + VZ
```

BLOCK C

```
      8 CONTINUE
C
C   CALC SHEET(FINITE LENGTH SECTION) CONTRIBUTION
C
        DO 11 IDUM=1,NF
        IF(IDUM.NE.1)GO TO 62
C
C   FIRST TIME THRU-CALC COORD MARKERS
C
        IC2D = ((I4-1)*NF)+(I4-1)
        IC1D = IC2D - I4 + 1
        ICO1 = (2*(NF+1))+1
        ICO2 = ICO1+1
        ICO3 = ICO2+1
     62 IC1 = IC1D+IDUM
        IC2 = IC2D+IDUM
        SX(ICO1) = CX(IC2) - (SPACE*DL(IC1)/2.0)
        SY(ICO1) = CY(IC2) - (SPACE*DN(IC1)/2.0)
        SZ(ICO1) = CZ(IC2) - (SPACE*DN(IC1)/2.0)
        SX(ICO2) = CX(IC2) + (SPACE*DL(IC1)/2.0)
        SY(ICO2) = CY(IC2) + (SPACE*DN(IC1)/2.0)
        SZ(ICO2) = CZ(IC2) + (SPACE*DN(IC1)/2.0)
        SX(ICO3) = CX(IC2+1) - (SPACE*DL(IC1)/2.0)
        SY(ICO3) = CY(IC2+1) - (SPACE*DN(IC1)/2.0)
        SZ(ICO3) = CZ(IC2+1) - (SPACE*DN(IC1)/2.0)
        CALL SHEET
        SUMVX = SUMVX + VX
        SUMVY = SUMVY + VY
        SUMVZ = SUMVZ + VZ
     11 CONTINUE
        GO TO 40
C
C   FIELD RING EITHER FIRST OR LAST
C
     20 IF(I4.EQ.1)GO TO 22
C
C   SELECTED FIELD RING IS LAST ON JET
C   CALC PENULTIMATE  FILS
C
        DO 21 IDUM=1,NF
        IF(IDUM.NE.1)GO TO 55
C
C   FIRST TIME THRU-CALC COORD MARKERS
C
        ICO1D = ((NR-1)*NF)+(NR-1)
        ICO2D = ((NR-2)*NF)+(NR-2)
        ICO4 = ((I2-1)*NF)+I3+(I2-1)
        MARKER = -1
     55 IF(IDUM.EQ.I3)GO TO 21
C
C   CONTROL AND FIELD POINT DIFFERENT
C
        ICO1 = ICO1D + IDUM
        ICO2 = ICO2D + IDUM
        CALL FILRIN
        SUMVX = SUMVX + VX
        SUMVY = SUMVY + VY
        SUMVZ = SUMVZ + VZ
     21 CONTINUE
C
```

BLOCK C

```
C   CALC SEMI-INFINITE FILS
C
   22 DO 25 IDUM=1,NF
      IF(IDUM.NE.1)GO TO 52
C
C   FIRST TIME THRU-CALC COORD MARKERS
C
      ICO4 = ((I2-1)*NF)+I3+(I2-1)
      MARKER = -1
      IF(I4.EQ.NR)GO TO 51
C
C   FIELD RING IS FIRST ON JET
C
      ICO2 = (NR*NF)+NR+1
      Z(ICO2) = 1.0E6
      GO TO 52
   51 ICO1 = (NR*NF)+NR+1
      ICO2D = ((NR-1)*NF)+(NR-1)
      Z(ICO1) = -1.0E6
   52 IF(IDUM.EQ.I3)GO TO 25
C
C   CONTROL AND FIELD POINT DIFFERENT
C
      IF(I4.EQ.NR)GO TO 23
      ICO1 = IDUM
      X(ICO2) = X(ICO1)
      Y(ICO2) = Y(ICO1)
      GO TO 24
   23 ICO2 = ICO2D + IDUM
      X(ICO1) = X(ICO2)
      Y(ICO1) = Y(ICO2)
   24 CALL FILRIN
      SUMVX = SUMVX + VX
      SUMVY = SUMVY + VY
      SUMVZ = SUMVZ + VZ
   25 CONTINUE
C
C   CALC SEMI-INFINITE SHEET CONTRIBUTION
C
      DO 30 IDUM=1,NF
      IF(IDUM.NE.1)GO TO 27
      ICO4 = ((I2-1)*NF)+I3+(I2-1)
      IF(I4.EQ.NR)GO TO 26
C
C   FIELD RING IS FIRST ON JET
C
      ICO2 = (2*NF)+NR
      SZ(ICO2) = 1.0E6
      GO TO 27
C
C   FIELD RING IS LAST ON JET
C
   26 ICO2D = NF + 1
      ICO1 = (2*NF)+NR
      ICO3 = (2*NF)+NR+1
      SZ(ICO1) = -1.0E6
      SZ(ICO3) = -1.0E6
   27 IF(I4.EQ.NR)GO TO 28
C
C   FIELD RING FIRST ON JET
```

BLOCK C

```
C
      ICO1 = IDUM
      ICO3 = IDUM+1
      SX(ICO2) = SX(ICO1)
      SY(ICO2) = SY(ICO1)
      GO TO 29
C
C  FIELD RING LAST ON JET
C
   28 ICO2 = ICO2D+IDUM
      SX(ICO1) = SX(ICO2)
      SY(ICO1) = SY(ICO2)
      SX(ICO3) = SX(ICO2+1)
      SY(ICO3) = SY(ICO2+1)
   29 CALL SHEET
      SUMVX = SUMVX + VX
      SUMVY = SUMVY + VY
      SUMVZ = SUMVZ + VZ
   30 CONTINUE
C
C     FIELD RING D-L END
C
   40 CONTINUE
C
C     ALL FIELD RINGS INTERROGATED-STORE VELY IN ARRAY
C
      ICO4 = ((I2-1)*NF)+I3+(I2-1)
      SVX(ICO4) = SUMVX
      SVY(ICO4) = SUMVY
      SVZ(ICO4) = SUMVZ
C
C     CONTROL PT D-L END
C
   41 CONTINUE
C
C     CONTROL RING D-L END
C
   42 CONTINUE
C
C     ALL CONTROL RINGS INTERROGATED--CALC NEW RING COORDS
C
C  CONSTRUCT FORMERS IN OUTPUT FILE
C
      DO 34 IDUM=1,NR
      WRITE(2,3000)IFORMK
 3000 FORMAT(1H1,I3,1H;)
      WRITE(2,3001)IDUM
 3001 FORMAT(1H ,I2,1H;)
      ICO4D = ((IDUM-1)*NF)+(IDUM-1)
      IBLOK1 = NF + 1
      DO 33 IBLOK=1,IBLOK1
      ICO4 = ICO4D+IBLOK
      WRITE(2,3002)X(ICO4),Y(ICO4),Z(ICO4)
 3002 FORMAT(1H ,3(E13.5,1H;))
      IF(IDUM.EQ.NR.OR.IBLOK.EQ.IBLOK1) GO TO 33
      X(ICO4) = X(ICO4)+(STEP*SVX(ICO4))+(STEP*XVELY)
      Y(ICO4) = Y(ICO4)+(STEP*SVY(ICO4))
      Z(ICO4) = Z(ICO4)+(STEP*SVZ(ICO4))
   33 CONTINUE
      IUM = ICO4D+1
```

END OF BLOCK C

```
      X(IC04) = X(IUM)
      Y(IC04) = Y(IUM)
      Z(IC04) = Z(IUM)
      WRITE(2,3003)
 3003 FORMAT(1H+,42X,3H*;*)
   34 CONTINUE
C
C  CONSTRUCT SURFACE IN OUTPUT FILE
C
      WRITE(2,3004)ISFMK                                    BLOCK
 3004 FORMAT(1H ,I3,1H;)                                      D
      DO 300 IDUM=1,4
  300 WRITE(2,3004)ITRRT
      DO 301 IDUM=1,NR
      IPRINT = NR+1-IDUM
  301 WRITE(2,3006)IPRINT,XMOVE,YMOVE,ZMOVE,ROTLX,ROTMX,ROTNX,
     1ROTLY,ROTMY,ROTNY,ITRRT
 3006 FORMAT(1H ,I3,1H;,9(F4.0,1H;),I3,1H;)
      IBLOK = 2+NRD
      DO 302 IDUM=1,IBLOK
  302 WRITE(2,3007)
 3007 FORMAT(1H ,4H  *;)
C
C  CONSTRUCT BODY IN OUTPUT FILE
C
      WRITE(2,3008)IBDMK,ITRRT,ITRRT,ITRRT
 3008 FORMAT(1H ,4(I3,1H;))
      WRITE(2,3009)XMOVE,YMOVE,ZMOVE,ROTLX,ROTMX,ROTNX,
     1ROTLY,ROTMY,ROTNY
 3009 FORMAT(1H ,9(F4.0,1H;))
      DO 303 IDUM=1,4
  303 WRITE(2,3010)ITRRT
 3010 FORMAT(1H ,I3,1H;)
      WRITE(2,3011)IENDMK
 3011 FORMAT(1H ,3H*;*/1H ,I2,2H;*/1H ,2H**)
C
C  CREATE NEW RING AT PIPE EXIT
C
      IC1D = (NR*NF)+NR
      IC3D = NF+1
      NFD = NF-1
      DO 39 IDUM=1,NFD
      IC1 = IC1D+IDUM
      IC3 = IC3D+IDUM
      X(IC1) = DX(IDUM)
      Y(IC1) = DY(IDUM)
      Z(IC1) = DZ(IDUM)-(FLOAT(I1)*SPACE)
   39 SZ(IC3) = SZ(IC3)-SPACE
      NR = NR+1
      GAMMAR(NR-2) = GAMMAR(NR-3)
C
C     ITERATION D-L END                                      END OF
C
   50 CONTINUE                                              BLOCK  D
  999 STOP
      END
C
C
C
```

```
C
C
      SUBROUTINE FILRIN
C
C  SUBR CALCS VELY INDUCED AT POINT IN SPACE BY SEGMENTS OF INFINITE
C  VORTEX FILAMENTS AND VORTEX RINGS TAKEN TOGETHER OR SEPARATELY
C
      COMMON X(500),Y(500),Z(500),DX(30),DY(30),DZ(30),
     1SX(100),SY(100),SZ(100),GAMMAR(30),GAMMAF(30),
     2IC01,IC02,IC03,IC04,I4,PI,IDUM,MARKER,VX,VY,VZ,XVELY,VELJET,
     3SVX(500),SVY(500),SVZ(500),W0(100),NF,IC2D,IC1D,
     4CX(500),CY(500),CZ(500),DL(500),DM(500),DN(500)
      IF(MARKER)500,500,501
  500 CIRCUL = GAMMAF(IDUM)
      IDENT = -1
      GO TO 502
  501 CIRCUL = GAMMAR(I4-1)
C
C  CALC FILAMENT UNIT VECTOR
C
  502 ELENTH = SQRT((X(IC02)-X(IC01))**2+(Y(IC02)-Y(IC01
     1))**2+(Z(IC02)-Z(IC01))**2)
      EDL = (X(IC02)-X(IC01))/ELENTH
      EDM = (Y(IC02)-Y(IC01))/ELENTH
      EDN = (Z(IC02)-Z(IC01))/ELENTH
C
C  CALC RADIUS VECTOR
C
      RVX = X(IC04)-((X(IC02)+X(IC01))/2.0)
      RVY = Y(IC04)-((Y(IC02)+Y(IC01))/2.0)
      RVZ = Z(IC04)-((Z(IC02)+Z(IC01))/2.0)
C
C  CALC COMPONENTS AND MODULUS OF T VECTOR R
C
      VDX = (EDM*RVZ)-(EDN*RVY)
      VDY = (EDN*RVX)-(EDL*RVZ)
      VDZ = (EDL*RVY)-(EDM*RVX)
      VM  = SQRT(VDX**2+VDY**2+VDZ**2)
C
C  CALC MAGNITUDE OF VELOCITY
C
      TDOTR = (EDL*RVX)+(EDM*RVY)+(EDN*RVZ)
      VMAG = (((TDOTR+(ELENTH/2.0))/SQRT(VM**2+(TDOTR+(ELENTH/2.0))**2)
     1)-((TDOTR-(ELENTH/2.0))/SQRT(VM**2+(TDOTR-(ELENTH/2.0))**2)))*
     2CIRCUL/(VM*4.0*PI)
C
C  CALC VELY VECTOR
C
      VX = VDX*VMAG/VM
      VY = VDY*VMAG/VM
      VZ = VDZ*VMAG/VM
      IF(MARKER)506,503,506
  503 IF(IDENT)504,507,505
C
C  STORE VELYS IN DUMMY AREA
C
  504 DVX = VX
      DVY = VY
      DVZ = VZ
      IDENT = 1
```

```
      ICO2 = ICO1 + 1
      GO TO 501
C
C   CALC VELOCITY VECTOR DUE TO BOTH FIL AND RING
C
  505 VX = VX + DVX
      VY = VY + DVY
      VZ = VZ + DVZ
  506 RETURN
  507 WRITE(2,7005)
 7005 FORMAT(1H ,33HSUBR FILRIN FAILS IN IDENT MARKER)
      STOP
      END
C
C
C
      SUBROUTINE SHEET
C
C   SUBR CALCULATES VELOCITY INDUCED AT POINT IN SPACE BY SEGMENT OF A
C   VORTEX SHEET ITSELF SKEWED IN SPACE
C
      COMMON X(500),Y(500),Z(500),DX(30),DY(30),DZ(30),
     1SX(100),SY(100),SZ(100),GAMMAR(30),GAMMAF(30),
     2ICO1,ICO2,ICO3,ICO4,I4,PI,IDUM,MARKER,VX,VY,VZ,XVELY,VELJET,
     3SVX(500),SVY(500),SVZ(500),W0(100),NF,IC2D,IC1D,
     4CX(500),CY(500),CZ(500),DL(500),DM(500),DN(500)
C
C   SUBROUTINE STATEMENT FUNCTION
C
      ARG(A,B) = (A/B)/SQRT(1.0-(A/B)**2)
C
C   CALC X-AXIS DIRECTION COSINES
C
      UMOD = SQRT((SX(ICO1)-SX(ICO2))**2+(SY(ICO1)-SY(IC
     102))**2+(SZ(ICO1)-SZ(ICO2))**2)
      UDL = (SX(ICO1)-SX(ICO2))/UMOD
      UDM = (SY(ICO1)-SY(ICO2))/UMOD
      UDN = (SZ(ICO1)-SZ(ICO2))/UMOD
C
C   CALC Z-AXIS DIRECTION COSINES
C
      DMODD = SQRT((SX(ICO3)-SX(ICO1))**2+(SY(ICO3)-SY(I
     1CO1))**2+(SZ(ICO3)-SZ(ICO1))**2)
      DDL = (SX(ICO3)-SX(ICO1))/DMODD
      DDM = (SY(ICO3)-SY(ICO1))/DMODD
      DDN = (SZ(ICO3)-SZ(ICO1))/DMODD
C
C   CALC Y-AXIS DIRECTION COSINES
C
      EWDL = (UDN*DDM)-(UDM*DDN)
      EWDM = (UDL*DDN)-(UDN*DDL)
      EWDN = (UDM*DDL)-(UDL*DDM)
C
C   CALC TRANSFORMED FIELD POINT COORDS
C
      SPTNU = ((UDL*X(ICO4))+(UDM*Y(ICO4))+(UDN*Z(ICO4)))-((
     1UDL*SX(ICO2))+(UDN*SY(ICO2))+(UDN*SZ(ICO2)))
      SPTD  = ((DDL*X(ICO4))+(DDM*Y(ICO4))+(DDN*Z(ICO4)))-((
     1DDL*SX(ICO2))+(DDN*SY(ICO2))+(DDN*SZ(ICO2)))
      SPTNU = ((EWDL*X(ICO4))+(EWDM*Y(ICO4))+(EWDN*Z(ICO4)))
```

```
     1=((EWDL*SX(ICU2))+(EWDM*SY(ICU2))+(EWDN*SZ(ICU2)))
C
C   CALC CONSTANTS IN VELY TERMS
C
      CON1 = (SQRT(SPTNU**2+SPTD**2))/SPTD
      CON2 = (SQRT((SPTD-DMODD)**2+SPTNU**2))/(SPTD-DMODD)
C
C   CALC ANGLES
C
      SINB1 = SPTNU/SQRT(SPTNU**2+SPTNU**2)
      SINB2 = SPTNU/SQRT(SPTNU**2+(SPTNU-UMOD)**2)
      COSB1 = SPTNU/SQRT(SPTNU**2+SPTNU**2)
      COSB2 = (SPTNU-UMOD)/SQRT(SPTNU**2+(SPTNU-UMOD)**2)
C
C   CALC VELY TERMS
C
      VLX = ((ATAN(ARG(COSB2,CON1))-ATAN(ARG(COSB2,CON2)))-(
     1ATAN(ARG(COSB1,CON1))-ATAN(ARG(COSB1,CON2))))*VELJET/(4.0*PI)
      VLY = ((-ASINH(SINB2*(SPTD-DMODD)/SPTNU)+ASINH(SINB2*SPTD/SPTNU))
     1-(-ASINH(SINB1*(SPTD-DMODD)/SPTNU)+ASINH(SINB1*SPTD/SPTNU)))*VEL
     2JET/(4.0*PI)
C
C   CALC TRANSFORMED VELYS
C
      VX = (UDL*VLX)+(EWDL*VLY)
      VY = (UDM*VLX)+(EWDM*VLY)
      VZ = (UDN*VLX)+(EWDN*VLY)
      RETURN
      END
C
C   FUNCTION SUBROUTINE FOR SHEET
C
      FUNCTION ASINH(A)
      IF ( ABS(A).GT.1.0 ) GO TO 539
      ASINH=ALOG(A+SQRT(A*A+1.0))
      RETURN
  539 ASINH=ALOG( ABS(A) * ( 1.0+SQRT( 1.0+1.0/(A*A) ) ) )
      IF (A.LT.0.0) ASINH=-ASINH
      RETURN
      END
C
C
C
      SUBROUTINE CRVFIT
C
C   SUBROUTINE INTERPOLATES FOR SHEET POINTS USING PARAMETRIC CUBICS
C
      COMMON X(500),Y(500),Z(500),DX(30),DY(30),DZ(30),
     1SX(100),SY(100),SZ(100),GAMMAR(30),GAMMAF(30),
     2IC01,IC02,IC03,IC04,I4,PI,IDUM,MARKER,VX,VY,VZ,XVELY,VELJET,
     3SVX(500),SVY(500),SVZ(500),W0(100),NF,IC2D,IC1D,
     4CX(500),CY(500),CZ(500),DL(500),DM(500),DN(500)
      INTEGER A,D,E
C
C   SET UP ROUTINE
C
      DO 118 IDUM=1,NF
      IC1 = IC1D + IDUM
      IC2 = IC2D + IDUM
      IF(IDUM.NE.1)GO TO 117
```

```
      W0(81) = X(IC2)
      W0(82) = Y(IC2)
      W0(83) = Z(IC2)
      W0(84) = 2.0
      D = 0
      W0(86) = X(IC2+1)
      W0(87) = Y(IC2+1)
      W0(88) = Z(IC2+1)
      W0(89) = 2.0
  117 IF(IDUM.EQ.NF)IC2 = IC2D
      W0(91) = X(IC2+2)
      W0(92) = Y(IC2+2)
      W0(93) = Z(IC2+2)
      W0(94) = 2.0
C
C   START OF INTERPOLATION ROUTINE
C
      W0(2)=SQRT((W0(81)-W0(86))**2+(W0(82)-W0(87))**2+(W0(83)-W0(88))*
     1*2)
      W0(3)=SQRT((W0(86)-W0(91))**2+(W0(87)-W0(92))**2+(W0(88)-W0(93))*
     1*2)+W0(2)
      J=3
      A=0
  103 W0(21)=W0(2)/(W0(3)-W0(2))
      W0(22)=(W0(A+81)-W0(A+86)-W0(21)*(W0(A+86)-W0(A+91)))/(-W0(2)**2-
     1W0(21)*(W0(2)**2-W0(3)**2))
      W0(23)=(W0(A+81)-W0(A+86)+W0(22)*W0(2)**2)/(-W0(2))
  101 W0(A+52)=W0(23)
  102 W0(A+56)=W0(23)+2.0*W0(22)*W0(2)
      A=A+1
      J=J-1
      IF ( J ) 104,104,103
  104 J=2
      A=4
  105 W0(21)=1.0/SQRT(W0(A+52)**2+W0(A+53)**2+W0(A+54)**2)
      W0(A+42)=W0(A+52)*W0(21)
      W0(A+43)=W0(A+53)*W0(21)
      W0(A+44)=W0(A+54)*W0(21)
      A=A-4
      IF ( D ) 106,115,106
  115 J=J-1
      IF ( J ) 106,106,105
  106 J=3
      A=0
      E=0
  107 W0(E+53)=W0(A+81)
      W0(E+54)=W0(A+42)
      W0(E+55)=(3.0*(W0(A+86)-W0(A+81))-W0(2)*(W0(A+46)+2.0*W0(A+42)))/
     1(W0(2)**2)
      W0(E+56)=(W0(2)*(W0(A+46)+W0(A+42))+2.0*(W0(A+81)-W0(A+86)))/(W0(
     12)**3)
      E=E+4
      A=A+1
      J=J-1
      IF ( J ) 108,108,107
  108 D=IRINT(W0(84))
      W0(14)=W0(2)/FLOAT(D)
  109 J=3
      E=0
  110 W0(21)=W0(E+53)+W0(14)*(W0(E+54)+W0(14)*(W0(E+55)+W0(14)*W0(E+56)
```

```
     1))
      IF(J.EQ.3) CX(IC1) = W0(21)
      IF(J.EQ.2) CY(IC1) = W0(21)
      IF(J.EQ.1) CZ(IC1) = W0(21)
      E=E+4
      J=J-1
      IF ( J ) 112,112,110
  112 J=10
      A=0
  113 W0(A+81)=W0(A+86)
      W0(A+42)=W0(A+46)
      A=A+1
      J=J-1
      IF ( J ) 118,118,113
  118 CONTINUE
      CX(IC1D) = CX(IC1)
      CY(IC1D) = CY(IC1)
      CZ(IC1D) = CZ(IC1)
      RETURN
      END
C
C  FUNCTION SUBROUTINES FOR CRVFIT
C
      FUNCTION IRINT(X)
      Y=ABS ( X-FLOAT(INT(X)) )
      IRINT=IINT(X)
      IF (X.LT.0.0) GO TO 116
      IF (Y.GE.0.5) IRINT=IRINT+1
      RETURN
  116 IF (Y.LT.0.5 .AND. Y.NE.0.0) IRINT=IRINT+1
      RETURN
      END
C
C
C
      FUNCTION IINT(X)
      IINT=INT(X)
      IF (X.GE.0.0) RETURN
      Y=X-FLOAT(IINT)
      IF (Y.NE.0.0) IINT=IINT-1
      RETURN
      END
++
```


FILE DELETED

A sample of the output obtained from the three-dimensional jet in a crosswind program is included. The asterisks are used to edit the output file in order to use it as input to the plotting program.

CARD NR. SEVERITY DETAILS DIAGNOSIS OF PROBLEM

17 I CONTROL VARIABLE IN COMMON OR EQUIVALENCED, OPTIMIZATION MAY BE INHIBITED.

3 16 12 -1 .00010 .40000 .20000

X	Y	Z	
-.100000E+01	-0.	.400000E+00	
-.923880E+00	-.382683E+00	.400000E+00	
-.707107E+00	-.707107E+00	.400000E+00	
-.382683E+00	-.923880E+00	.400000E+00	
.171512E-14	-.100000E+01	.400000E+00	
.382683E+00	-.923880E+00	.400000E+00	
.707107E+00	-.707107E+00	.400000E+00	
.923880E+00	-.382683E+00	.400000E+00	
.100000E+01	.343025E-14	.400000E+00	
.923880E+00	.382683E+00	.400000E+00	
.707107E+00	.707107E+00	.400000E+00	
.382683E+00	.923880E+00	.400000E+00	
.161709E-13	.100000E+01	.400000E+00	
-.382683E+00	.923880E+00	.400000E+00	
-.707107E+00	.707107E+00	.400000E+00	
-.923880E+00	.382683E+00	.400000E+00	
-1.000000		-0.000000	.400000
-.100000E+01	-0.	.200000E+00	
-.923880E+00	-.382683E+00	.200000E+00	
-.707107E+00	-.707107E+00	.200000E+00	
-.382683E+00	-.923880E+00	.200000E+00	
.171512E-14	-.100000E+01	.200000E+00	
.382683E+00	-.923880E+00	.200000E+00	
.707107E+00	-.707107E+00	.200000E+00	
.923880E+00	-.382683E+00	.200000E+00	
.100000E+01	.343025E-14	.200000E+00	
.923880E+00	.382683E+00	.200000E+00	

X	Y	Z
.707107E+00	.707107E+00	.200000E+00
.382683E+00	.923880E+00	.200000E+00
.161709E-13	.100000E+01	.200000E+00
-.382683E+00	.923880E+00	.200000E+00
-.707107E+00	.707107E+00	.200000E+00
-.923880E+00	.382683E+00	.200000E+00

-1.000000 -0.000000 .200000

-.100000E+01	-0.	0.
-.923880E+00	-.382683E+00	0.
-.707107E+00	-.707107E+00	0.
-.382683E+00	-.923880E+00	0.
.171512E-14	-.100000E+01	0.
.382683E+00	-.923880E+00	0.
.707107E+00	-.707107E+00	0.
.923880E+00	-.382683E+00	0.
.100000E+01	.343025E-14	0.
.923880E+00	.382683E+00	0.
.707107E+00	.707107E+00	0.
.382683E+00	.923880E+00	0.
.161709E-13	.100000E+01	0.
-.382683E+00	.923880E+00	0.
-.707107E+00	.707107E+00	0.
-.923880E+00	.382683E+00	0.

-1.000000	-0.000000	0.000000
-1.000000	-0.000000	0.000000
-1.000000	-0.000000	0.000000
-.923880	-.382683	0.000000
-.707107	-.707107	0.000000
-.382683	-.923880	0.000000
.000000	-1.000000	0.000000

X	Y	Z	
.382683	-.923880	0.000000	
.707107	-.707107	0.000000	
.923880	-.382683	0.000000	
1.000000	.000000	0.000000	
.923880	.382683	0.000000	
.707107	.707107	0.000000	
.382683	.923880	0.000000	
.000000	1.000000	0.000000	
-.382683	.923880	0.000000	
-.707107	.707107	0.000000	
-.923880	.382683	0.000000	
20.000000			
3000.000000	3.141593	1.000000	100.000000
0.000000			
895.894009			
1655.396276			
2162.879466			
2341.083864			
2162.879466			
1655.396276			
895.894009			
-.000000			
-895.894009			
-1655.396276			
-2162.879466			
-2341.083864			
-2162.879466			
-1655.396276			
-895.894009			

```
      X             Y             Z
 1;
1;
 -.10000E+01; -0.           ;    .40000E+00;
 -.92388E+00;  -.38268E+00;    .40000E+00;
 -.70711E+00;  -.70711E+00;    .40000E+00;
 -.38268E+00;  -.92388E+00;    .40000E+00;
  .17151E-14;  -.10000E+01;    .40000E+00;
  .38268E+00;  -.92388E+00;    .40000E+00;
  .70711E+00;  -.70711E+00;    .40000E+00;
  .92388E+00;  -.38268E+00;    .40000E+00;
  .10000E+01;   .34302E-14;    .40000E+00;
  .92388E+00;   .38268E+00;    .40000E+00;
  .70711E+00;   .70711E+00;    .40000E+00;
  .38268E+00;   .92388E+00;    .40000E+00;
  .16171E-13;   .10000E+01;    .40000E+00;
 -.38268E+00;   .92388E+00;    .40000E+00;
 -.70711E+00;   .70711E+00;    .40000E+00;
 -.92388E+00;   .38268E+00;    .40000E+00;
 -.10000E+01; -0.           ;    .40000E+00;*;*
```

```
      X              Y              Z
  1;
 2;
  -.10000E+01; -0.            ;    .20000E+00;
  -.92388E+00;  -.38268E+00;    .20000E+00;
  -.70711E+00;  -.70711E+00;    .20000E+00;
  -.38268E+00;  -.92388E+00;    .20000E+00;
   .17151E-14;  -.10000E+01;    .20000E+00;
   .38268E+00;  -.92388E+00;    .20000E+00;
   .70711E+00;  -.70711E+00;    .20000E+00;
   .92388E+00;  -.38268E+00;    .20000E+00;
   .10000E+01;   .34302E-14;    .20000E+00;
   .92388E+00;   .38268E+00;    .20000E+00;
   .70711E+00;   .70711E+00;    .20000E+00;
   .38268E+00;   .92388E+00;    .20000E+00;
   .16171E-13;   .10000E+01;    .20000E+00;
  -.38268E+00;   .92388E+00;    .20000E+00;
  -.70711E+00;   .70711E+00;    .20000E+00;
  -.92388E+00;   .38268E+00;    .20000E+00;
  -.10000E+01; -0.            ;    .20000E+00;*;*
```

```
        X              Y              Z

    1;
   3;
    -.10000E+01; -0.          ;   0.          ;
    -.92388E+00;  -.38268E+00;   0.          ;
    -.70711E+00;  -.70711E+00;   0.          ;
    -.38268E+00;  -.92388E+00;   0.          ;
     .17151E-14;  -.10000E+01;   0.          ;
     .38268E+00;  -.92388E+00;   0.          ;
     .70711E+00;  -.70711E+00;   0.          ;
     .92388E+00;  -.38268E+00;   0.          ;
     .10000E+01;   .34302E-14;   0.          ;
     .92388E+00;   .38268E+00;   0.          ;
     .70711E+00;   .70711E+00;   0.          ;
     .38268E+00;   .92388E+00;   0.          ;
     .16171E-13;   .10000E+01;   0.          ;
    -.38268E+00;   .92388E+00;   0.          ;
    -.70711E+00;   .70711E+00;   0.          ;
    -.92388E+00;   .38268E+00;   0.          ;
    -.10000E+01; -0.          ;   0.          ;*;*
    2;
    1;
    1;
    1;
    1;
    3;  0.;  0.;  0.;  1.;  0.;  0.;  0.;  1.;  0.;  1;
    2;  0.;  0.;  0.;  1.;  0.;  0.;  0.;  1.;  0.;  1;
    1;  0.;  0.;  0.;  1.;  0.;  0.;  0.;  1.;  0.;  1;
    *;
    *;
    *;
    *;
    3;  1;  1;  1;
    0.;  0.;  0.;  1.;  0.;  0.;  0.;  1.;  0.;
    1;
    1;
    1;
    1;
*;*
11;*
**
```

```
      X              Y              Z
 1;
1;
 -.96082E+00;   -.31429E-13;    .40936E+00;
 -.84923E+00;   -.46831E+00;    .40936E+00;
 -.54683E+00;   -.82820E+00;    .40937E+00;
 -.13678E+00;   -.10095E+01;    .40937E+00;
  .28137E+00;   -.10000E+01;    .40937E+00;
  .62859E+00;   -.83825E+00;    .40937E+00;
  .86738E+00;   -.58601E+00;    .40937E+00;
  .99853E+00;   -.29706E+00;    .40937E+00;
  .10392E+01;    .96218E-15;    .40937E+00;
  .99853E+00;    .29706E+00;    .40937E+00;
  .86738E+00;    .58601E+00;    .40937E+00;
  .62859E+00;    .83825E+00;    .40937E+00;
  .28137E+00;    .10000E+01;    .40937E+00;
 -.13678E+00;    .10095E+01;    .40937E+00;
 -.54683E+00;    .82820E+00;    .40937E+00;
 -.84923E+00;    .46831E+00;    .40937E+00;
 -.96082E+00;   -.31429E-13;    .40936E+00;*;*
```

```
          X              Y              Z
    1;
   2;
    -.96082E+00;    .51608E-13;    .20936E+00;
    -.84923E+00;   -.40831E+00;    .20936E+00;
    -.54683E+00;   -.82820E+00;    .20937E+00;
    -.13678E+00;   -.10095E+01;    .20937E+00;
     .28137E+00;   -.10000E+01;    .20937E+00;
     .62859E+00;   -.83825E+00;    .20937E+00;
     .86738E+00;   -.58601E+00;    .20937E+00;
     .99853E+00;   -.29706E+00;    .20937E+00;
     .10392E+01;    .14240E-14;    .20937E+00;
     .99853E+00;    .29706E+00;    .20937E+00;
     .86738E+00;    .58601E+00;    .20937E+00;
     .62859E+00;    .83825E+00;    .20937E+00;
     .28137E+00;    .10000E+01;    .20937E+00;
    -.13678E+00;    .10095E+01;    .20937E+00;
    -.54683E+00;    .82820E+00;    .20937E+00;
    -.84923E+00;    .40831E+00;    .20937E+00;
    -.96082E+00;    .51608E-13;    .20936E+00;*;*
```

```
      X              Y              Z
  1;
3;
 -.10000E+01; -0.           ;  0.          ;
 -.92388E+00;  -.38268E+00;  0.          ;
 -.70711E+00;  -.70711E+00;  0.          ;
 -.38268E+00;  -.92388E+00;  0.          ;
  .17151E-14;  -.10000E+01;  0.          ;
  .38268E+00;  -.92388E+00;  0.          ;
  .70711E+00;  -.70711E+00;  0.          ;
  .92388E+00;  -.38268E+00;  0.          ;
  .10000E+01;   .34302E-14;  0.          ;
  .92388E+00;   .38268E+00;  0.          ;
  .70711E+00;   .70711E+00;  0.          ;
  .38268E+00;   .92388E+00;  0.          ;
  .16171E-13;   .10000E+01;  0.          ;
 -.38268E+00;   .92388E+00;  0.          ;
 -.70711E+00;   .70711E+00;  0.          ;
 -.92388E+00;   .38268E+00;  0.          ;
 -.10000E+01; -0.           ;  0.          ;*;*
```

```
        X               Y               Z

  1;
 4;
  -.10000E+01; -0.          ;   -.20000E+00;
  -.92388E+00;  -.38268E+00;   -.20000E+00;
  -.70711E+00;  -.70711E+00;   -.20000E+00;
  -.38268E+00;  -.92388E+00;   -.20000E+00;
   .17151E-14;  -.10000E+01;   -.20000E+00;
   .38268E+00;  -.92388E+00;   -.20000E+00;
   .70711E+00;  -.70711E+00;   -.20000E+00;
   .92388E+00;  -.38268E+00;   -.20000E+00;
   .10000E+01;   .34302E-14;   -.20000E+00;
   .92388E+00;   .38268E+00;   -.20000E+00;
   .70711E+00;   .70711E+00;   -.20000E+00;
   .38268E+00;   .92388E+00;   -.20000E+00;
   .16171E-13;   .10000E+01;   -.20000E+00;
  -.38268E+00;   .92388E+00;   -.20000E+00;
  -.70711E+00;   .70711E+00;   -.20000E+00;
  -.92388E+00;   .38268E+00;   -.20000E+00;
  -.10000E+01; -0.          ;   -.20000E+00;*;*
  2;
  1;
  1;
  1;
  1;
  4;  0.;  0.;  0.;  1.;  0.;  0.;  0.;  1.;  0.;  1;
  3;  0.;  0.;  0.;  1.;  0.;  0.;  0.;  1.;  0.;  1;
  2;  0.;  0.;  0.;  1.;  0.;  0.;  0.;  1.;  0.;  1;
  1;  0.;  0.;  0.;  1.;  0.;  0.;  0.;  1.;  0.;  1;
  *;
  *;
  *;
  *;
  *;
  3;  1;  1;  1;
  0.;  0.;  0.;  1.;  0.;  0.;  0.;  1.;  0.;
  1;
  1;
  1;
  1;
*;*
11;*
**
```

```
      X              Y              Z
  1;
1;
 -.88667E+00;    .80525E-04;    .43463E+00;
 -.74311E+00;   -.56240E+00;    .43169E+00;
 -.35914E+00;   -.96999E+00;    .42854E+00;
  .13175E+00;   -.11238E+01;    .42680E+00;
  .57560E+00;   -.10305E+01;    .42606E+00;
  .86916E+00;   -.78100E+00;    .42991E+00;
  .99997E+00;   -.48922E+00;    .43513E+00;
  .10272E+01;   -.22671E+00;    .43854E+00;
  .10254E+01;   -.22579E-04;    .43956E+00;
  .10272E+01;    .22667E+00;    .43853E+00;
  .99997E+00;    .48917E+00;    .43511E+00;
  .86914E+00;    .78094E+00;    .42985E+00;
  .57556E+00;    .10304E+01;    .42593E+00;
  .13167E+00;    .11236E+01;    .42632E+00;
 -.35922E+00;    .96911E+00;    .42992E+00;
 -.74230E+00;    .56255E+00;    .43321E+00;
 -.88667E+00;    .80525E-04;    .43463E+00;*;*
```

```
        X               Y               Z

    1;
   2;
    -.89443E+00;    .81582E-04;    .23730E+00;
    -.75421E+00;   -.50646E+00;    .23683E+00;
    -.37150E+00;   -.98832E+00;    .23363E+00;
     .13270E+00;   -.11563E+01;    .22639E+00;
     .59357E+00;   -.10592E+01;    .22222E+00;
     .89097E+00;   -.79551E+00;    .22802E+00;
     .10166E+01;   -.49372E+00;    .23737E+00;
     .10404E+01;   -.22760E+00;    .24312E+00;
     .10379E+01;   -.22579E-04;    .24478E+00;
     .10404E+01;    .22756E+00;    .24311E+00;
     .10166E+01;    .49367E+00;    .23735E+00;
     .89095E+00;    .79545E+00;    .22797E+00;
     .59353E+00;    .10592E+01;    .22212E+00;
     .13262E+00;    .11561E+01;    .22609E+00;
    -.37158E+00;    .98744E+00;    .23337E+00;
    -.75339E+00;    .50661E+00;    .23672E+00;
    -.89443E+00;    .81582E-04;    .23730E+00;*;*
```

```
      X              Y              Z

 1;
3;
 -.93478E+00;    .77819E-04;    .26554E-01;
 -.82398E+00;   -.45657E+00;    .24919E-01;
 -.52243E+00;   -.80320E+00;    .21923E-01;
 -.11674E+00;   -.96401E+00;    .22452E-01;
  .28227E+00;   -.93352E+00;    .30385E-01;
  .60005E+00;   -.77268E+00;    .40756E-01;
  .82271E+00;   -.54591E+00;    .43844E-01;
  .95823E+00;   -.28323E+00;    .40082E-01;
  .10047E+01;   -.22548E-04;    .37514E-01;
  .95823E+00;    .28319E+00;    .40071E-01;
  .82270E+00;    .54585E+00;    .43817E-01;
  .60003E+00;    .77260E+00;    .40701E-01;
  .28222E+00;    .93340E+00;    .30271E-01;
 -.11684E+00;    .96377E+00;    .22283E-01;
 -.52236E+00;    .80304E+00;    .21945E-01;
 -.82384E+00;    .45673E+00;    .24946E-01;
 -.93478E+00;    .77819E-04;    .26554E-01;*;*
```

```
      X              Y              Z
 1;
4;
 -.10000E+01; -0.           ;   -.20000E+00;
 -.92388E+00;  -.38268E+00;   -.20000E+00;
 -.70711E+00;  -.70711E+00;   -.20000E+00;
 -.38268E+00;  -.92388E+00;   -.20000E+00;
  .17151E-14;  -.10000E+01;   -.20000E+00;
  .38268E+00;  -.92388E+00;   -.20000E+00;
  .70711E+00;  -.70711E+00;   -.20000E+00;
  .92388E+00;  -.38268E+00;   -.20000E+00;
  .10000E+01;   .34302E-14;   -.20000E+00;
  .92388E+00;   .38268E+00;   -.20000E+00;
  .70711E+00;   .70711E+00;   -.20000E+00;
  .38268E+00;   .92388E+00;   -.20000E+00;
  .16171E-13;   .10000E+01;   -.20000E+00;
 -.38268E+00;   .92388E+00;   -.20000E+00;
 -.70711E+00;   .70711E+00;   -.20000E+00;
 -.92388E+00;   .38268E+00;   -.20000E+00;
 -.10000E+01; -0.           ;   -.20000E+00;*;*
```

```
          X               Y               Z
   1;
  5;
   -.10000E+01; -0.          ;   -.40000E+00;
   -.92388E+00;   -.38268E+00;   -.40000E+00;
   -.70711E+00;   -.70711E+00;   -.40000E+00;
   -.38268E+00;   -.92388E+00;   -.40000E+00;
    .17151E-14;   -.10000E+01;   -.40000E+00;
    .38268E+00;   -.92388E+00;   -.40000E+00;
    .70711E+00;   -.70711E+00;   -.40000E+00;
    .92388E+00;   -.38268E+00;   -.40000E+00;
    .10000E+01;    .34302E-14;   -.40000E+00;
    .92388E+00;    .38268E+00;   -.40000E+00;
    .70711E+00;    .70711E+00;   -.40000E+00;
    .38268E+00;    .92388E+00;   -.40000E+00;
    .16171E-13;    .10000E+01;   -.40000E+00;
   -.38268E+00;    .92388E+00;   -.40000E+00;
   -.70711E+00;    .70711E+00;   -.40000E+00;
   -.92388E+00;    .38268E+00;   -.40000E+00;
   -.10000E+01; -0.          ;   -.40000E+00;*;*
   2;
   1;
   1;
   1;
   1;
   5;  0.;  0.;  0.;  1.;  0.;  0.;  0.;  1.;  0.;  1;
   4;  0.;  0.;  0.;  1.;  0.;  0.;  0.;  1.;  0.;  1;
   3;  0.;  0.;  0.;  1.;  0.;  0.;  0.;  1.;  0.;  1;
   2;  0.;  0.;  0.;  1.;  0.;  0.;  0.;  1.;  0.;  1;
   1;  0.;  0.;  0.;  1.;  0.;  0.;  0.;  1.;  0.;  1;
   *;
   *;
   *;
   *;
   *;
   *;
   3;  1;  1;  1;
   0.;  0.;  0.;  1.;  0.;  0.;  0.;  1.;  0.;
   1;
   1;
   1;
   1;
*;*
11;*
**
```

APPENDIX 6

SOLUTION OF THE DIFFUSION EQUATION FOR 2 CHARACTERISTIC CASES.

For this investigation, the diffusion equation is written as

$$\frac{\partial w}{\partial t} = \nu \frac{\partial^2 w}{\partial y^2} \qquad \text{A6.1}$$

Where w is the vorticity and

ν is the kinematic viscosity.

The characteristic cases are:-

1) diffusion of vorticity from a solid boundary

2) diffusion of vorticity already present in the flowfield.

A6.1 DIFFUSION OF VORTICITY FROM A SOLID BOUNDARY

The following boundary conditions apply:-

a) $w(y,0) = 0$

At all points in the flowfield, at time $t=0$, the flow is irrotational

b) $w \rightarrow 0$ as $y \rightarrow \infty$

At infinity the flow is irrotational for all t

c) $\partial w/\partial y \rightarrow 0$ as $y \rightarrow \infty$

d) $\partial w/\partial y = 0$ at $y=0$

At $y=0$, $u=v=0$.

Thus, Prandtls two-dimensional boundary layer equation

$$u \frac{\partial u}{\partial x} + v \frac{\partial u}{\partial y} = -\frac{1}{\rho} \frac{\partial p}{\partial x} + \nu \frac{\partial^2 u}{\partial y^2}$$

reduces to

$$\frac{1}{\rho} \frac{\partial p}{\partial x} = \nu \left(\frac{\partial^2 u}{\partial y^2} \right)_{y=0}$$

Using Bernoulli's equation to obtain $\partial p / \partial x$ in terms of u

$$p + \frac{1}{2}\rho u^2 = \text{CONSTANT}$$

gives

$$\frac{1}{\rho}\frac{\partial p}{\partial x} + u\frac{\partial u}{\partial x} = 0$$

hence

$$\frac{1}{\rho}\frac{\partial p}{\partial x} = 0$$

This means that

$$\left(\frac{\partial^2 u}{\partial y^2}\right)_{y=0} = 0$$

The two-dimensional definition of vorticity is

$$\omega = \frac{\partial v}{\partial x} - \frac{\partial u}{\partial y}$$

At $y = 0$, $v = 0$, $\frac{\partial v}{\partial x} = 0$, hence

$$\omega = -\left(\frac{\partial u}{\partial y}\right)_{y=0} \quad \text{AND} \quad \frac{\partial \omega}{\partial y} = -\left(\frac{\partial^2 u}{\partial y^2}\right)_{y=0}.$$

hence $\frac{\partial \omega}{\partial y} = 0$ AT $y = 0$

e) $$\int_0^\infty \omega \, dy = U_{SURFACE} \quad , t > 0$$

To justify this, consider a vortex sheet separating two flows, one at speed U, and the other at speed zero

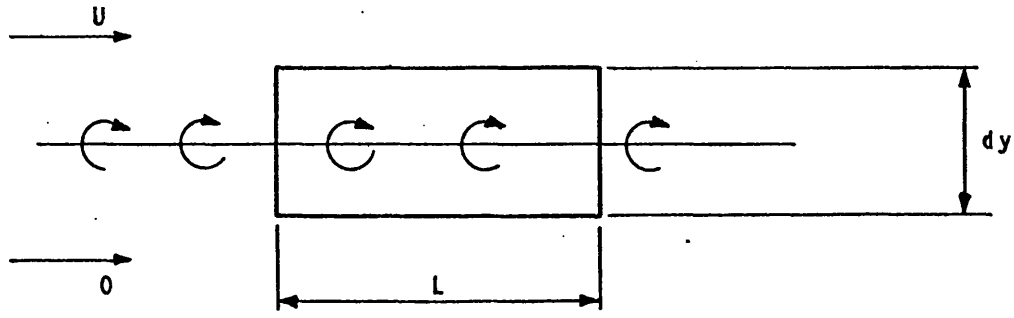

Fig A6.F1 VORTEX SHEET.

From Duncan et al (1960).

$$\sigma = d\Gamma/ds = U \qquad \text{A6.2}$$

and $$\Gamma = \oint U \, ds \qquad \text{A6.3}$$

Where σ = Vortex strength, and

Γ = circulation.

Applying A6.3 to the box in the diagram above, gives

$$\Gamma = UL \qquad \text{A6.4}$$

Using Stokes Theorem eqn A6.3 becomes

$$\Gamma = \oint \underline{U} . \underline{ds} = \int_{SURF} (CURL \, \underline{U}) . \underline{dA} = \int_{SURF} \underline{\omega} . \underline{dA} \qquad \text{A6.5}$$

Where $\underline{\omega} = CURL \, \underline{U}$ by definition.

Applying A6.5 to the box above gives

$$\Gamma = \int \omega L \, dy = L \int \omega \, dy \qquad \text{A6.6}$$

Equating A6.6 and A6.4 gives boundary condition e

See also Fromm (1964)

Boundary Conditions (b) and (c) allow Fourier cosine transforms of A6.1 to be taken, giving.

$$\frac{\partial w_c(s,t)}{\partial t} = \nu\left[-\sqrt{\frac{2}{\pi}}\, w'(0) - s^2 w_c(s,t)\right] \qquad \text{A6.7}$$

Duff et al (1966)

Where $w_c(s,t)$ is the Fourier cosine transform of $w(y,t)$

Boundary condition (d) reduces A6.7 to

$$\frac{\partial w_c(s,t)}{\partial t} = -\nu s^2 w_c(s,t) \qquad \text{A6.8}$$

from which a solution can be obtained

$$w_c(s,t) = A e^{-\nu s^2 t} \qquad \text{A6.9}$$

When t = 0, $A = w_c(S,0)$, hence

$$w_c(s,t) = w_c(s,0)\, e^{-\nu s^2 t} \qquad \text{A6.10}$$

Boundary condition (a) can be transformed giving

$$w_c(s,0) = \sqrt{\frac{2}{\pi}} \int_0^\infty 0.\cos sy\, dy = G\sqrt{\frac{2}{\pi}} \qquad \text{A6.11}$$

Where G is a constant

A6.10 becomes

$$w_c(s,t) = G\sqrt{\frac{2}{\pi}}\, e^{-\nu s^2 t} \qquad \text{A6.12}$$

The full solution can be obtained by taking Fourier inverse transforms.

Following Duff et al

$$\omega(y,t) = \sqrt{\frac{2}{\pi}} \int_0^\infty \omega_c(s,t) \cos sy \, ds$$

hence $$\omega(y,t) = \frac{2G}{\pi} \int_0^\infty e^{-\nu s^2 t} \cos sy \, ds$$

or $$\omega(y,t) = \mathrm{Re} \frac{2G}{\pi} \int_0^\infty e^{isy - \nu s^2 t} \, ds \qquad \text{A6.13}$$

Where Re = real part of.

Consider the integral

$$I = \int_0^\infty e^{-\nu s^2 t} \cos sy \, ds \qquad \text{A6.14}$$

Integrating by parts gives

$$I = \left| e^{-\nu s^2 t} \frac{\sin sy}{y} \right|_0^\infty + \int_0^\infty \frac{\sin sy}{y} (2\nu s t) e^{-\nu s^2 t} \, ds$$

which on substitution of the limits gives

$$I = \frac{2\nu t}{y} \int_0^\infty s e^{-\nu s^2 t} \sin sy \, ds \qquad \text{A6.15}$$

From A6.14

$$\frac{dI}{dy} = -\int_0^\infty s e^{-\nu s^2 t} \sin sy \, ds$$

which can be substituted into A6.15, giving

$$I = -\frac{2\nu t}{y} \frac{dI}{dy}$$

Separating the variables and integrating gives

$$\log_e I = -\frac{1}{2\nu t} \frac{y^2}{2} + A$$

hence $I = e^{A - y^2/4\mathcal{D}t} = Be^{-y^2/4\mathcal{D}t}$

When $y = 0$, $B = I$ and from A6.14 $B = \int_0^\infty e^{-\mathcal{D}s^2 t}\, ds$

Let $\eta = s\sqrt{\mathcal{D}t}$ then $ds = \frac{1}{\sqrt{\mathcal{D}t}}\, d\eta$

hence $$B = \int_0^\infty e^{-\eta^2} \frac{1}{\sqrt{\mathcal{D}t}}\, d\eta = \frac{1}{2}\sqrt{\frac{\pi}{\mathcal{D}t}}$$

hence $$I = \frac{1}{2}\sqrt{\frac{\pi}{\mathcal{D}t}}\, e^{-y^2/4\mathcal{D}t} \qquad \text{A6.16}$$

Substituting into A6.13 gives

$$\omega(y,t) = \frac{G}{\sqrt{\pi \mathcal{D} t}}\, e^{-y^2/4\mathcal{D}t} \qquad \text{A6.17}$$

Using boundary condition e gives

$$\int_0^\infty \frac{G}{\sqrt{\pi \mathcal{D} t}}\, e^{-y^2/4\mathcal{D}t}\, dy = u_{SURFACE} \qquad \text{A6.18}$$

Let $\eta = \frac{y}{2\sqrt{\mathcal{D}t}}$ therefore $dy = 2\sqrt{\mathcal{D}t}\, d\eta$

A6.18 becomes

$$\frac{2G}{\sqrt{\pi}} \int_0^\infty e^{-\eta^2}\, d\eta = \frac{2G}{\sqrt{\pi}} \cdot \frac{\sqrt{\pi}}{2} = u_{SURFACE}$$

hence $G = u_{SURFACE}$

Equation A6.17 becomes

$$\omega(y,t) = \frac{U_{SURFACE}}{\sqrt{\pi \nu t}} e^{-y^2/4\nu t} \qquad \text{A6.19}$$

Rosenhead (1966)

A6.2 DIFFUSION OF VORTICITY ALREADY PRESENT IN THE FLOWFIELD.

The following boundary conditions apply:-

a) $\omega(y,0) = \varphi(y)$

Where $\varphi(y)$ is the vorticity distribution in the free stream

b) $\omega \to 0$ As $y \to \infty$

c) $\partial\omega/\partial y \to 0$ AS $y \to \infty$

d) $\partial\omega/\partial y = 0$ AT $y = 0$

As for case 1, Fourier cosine transforms are taken, giving the solution

$$\omega_c(s,t) = \omega_c(s,0)\, e^{-\nu s^2 t} \qquad \text{A6.10}$$

Boundary condition (a) can be transformed to

$$\omega_c(s,0) = \sqrt{\frac{2}{\pi}} \int_0^\infty \varphi(y) \cos sy \, dy$$

hence for case 2, A6.10 becomes.

$$\omega_c(s,t) = \sqrt{\frac{2}{\pi}} \int_0^\infty \varphi(y)\, e^{-\nu s^2 t} \cos sy \, dy \qquad \text{A6.20}$$

As the integral is a function of its limits, A6.20 can be written

$$\omega_c(s,t) = \sqrt{\frac{2}{\pi}} \int_0^\infty \varphi(\xi)\, e^{-\nu s^2 t} \cos s\xi \, d\xi$$

Taking Fourier inverse transforms, as before, this becomes

$$w(y,t) = \frac{2}{\pi}\int_0^\infty e^{-\nu s^2 t}\cos sy\,ds\int_0^\infty \varphi(\tau)\cos s\tau\,d\tau$$

which can be written as

$$w(y,t) = \frac{2}{\pi}\int_0^\infty \varphi(\tau)\int_0^\infty e^{-\nu s^2 t}\cos sy\cos s\tau\,ds\,d\tau \qquad \text{A6.21}$$

Duff et al (1966)

Consider first the inner integral over S, i.e.

$$\int_0^\infty e^{-\nu s^2 t}\cos sy\cos s\tau\,ds$$

This is equivalent to

$$\frac{1}{2}\int_0^\infty e^{-\nu s^2 t}\left[\cos(\tau+y)s + \cos(\tau-y)s\right]ds \qquad \text{A6.22}$$

Now $$\int_0^\infty e^{-\nu s^2 t}\cos(\tau+y)s\,ds = \frac{1}{2}\sqrt{\frac{\pi}{\nu t}}\,e^{-(\tau+y)^2/4\nu t}$$

and $$\int_0^\infty e^{-\nu s^2 t}\cos(\tau-y)s\,ds = \frac{1}{2}\sqrt{\frac{\pi}{\nu t}}\,e^{-(\tau-y)^2/4\nu t}$$

from equation A6.14, and the result of the integration, A6.16.

hence A6.22 becomes

$$\frac{1}{4}\sqrt{\frac{\pi}{\nu t}}\left[e^{-(\tau+y)^2/4\nu t} + e^{-(\tau-y)^2/4\nu t}\right]$$

Substituting this into A6.21 gives

$$w(y,t) = \frac{1}{2\sqrt{\pi D t}} \int_0^\infty q(\tau) \left[e^{-(\tau+y)^2/4Dt} + e^{-(\tau-y)^2/4Dt} \right] d\tau$$

APPENDIX 7.

ORDER OF MAGNITUDES ARGUMENT ON VORTICITY TRANSPORT EQUATION.

The vorticity transport equation is

$$\frac{\partial w}{\partial t} + u\frac{\partial w}{\partial x} + v\frac{\partial w}{\partial y} = \nu\left[\frac{\partial^2 w}{\partial x^2} + \frac{\partial^2 w}{\partial y^2}\right] \qquad \text{A7.1}$$

This can be transformed into non-dimensional form by using the following non-dimensional variables.

$$u_o = \frac{u}{V_\infty}\ ,\quad v_o = \frac{v}{V_\infty}\ ,\quad x_o = \frac{x}{L}\ ,\quad y_o = \frac{y}{L}\ ,\quad t_o = \frac{t V_\infty}{L}\ ,\quad w_o = \frac{wL}{V_\infty}$$

Now $$\frac{\partial w}{\partial t} = \frac{\partial}{\partial t_o}\left(\frac{w_o V_\infty}{L}\right)\frac{\partial t_o}{\partial t} = \frac{V_\infty^2}{L^2}\frac{\partial w_o}{\partial t_o}$$

Similarly $$\frac{\partial w}{\partial x} = \frac{V_\infty}{L^2}\frac{\partial w_o}{\partial x_o}$$ and

$$\frac{\partial^2 w}{\partial x^2} = \frac{\partial}{\partial x_o}\left(\frac{\partial w}{\partial x}\right)\frac{\partial x_o}{\partial x} = \frac{V_\infty}{L^3}\frac{\partial^2 w_o}{\partial x_o^2}$$

etc

Substituting into A7.1 and rearranging.

$$\frac{\partial w_o}{\partial t_o} + u_o\frac{\partial w_o}{\partial x_o} + v_o\frac{\partial w_o}{\partial y_o} = \frac{1}{Re_L}\left[\frac{\partial^2 w_o}{\partial x_o^2} + \frac{\partial^2 w_o}{\partial y_o^2}\right] \qquad \text{A7.2}$$

Where $Re_L = \dfrac{V_\infty L}{\nu}$

The boundary conditions for the boundary layer region are

$u_o = v_o = 0$ FOR $y = 0$

$u_o \to 1$ FOR $y \to \infty$

From Schlichting (1968), the dimensionless boundary layer thickness $\delta/L \left(\equiv \delta\right)$ is very small compared with unity $(\delta << 1)$.

Thus an order of magnitude can now be estimated for each of the terms.

With reference to Daily & Harleman (1966), with $\delta << 1$, a scale for decreasing orders of magnitudes is as follows

$$\frac{1}{\delta^2} \; , \; \frac{1}{\delta} \; , \; 1, \; \delta, \; \delta^2$$

Using the notation $\sim o(\;)$ expressing "is the order of" the boundary layer relations,

$$u >> v \quad , \quad x >> y \; , \; \frac{\partial u}{\partial y} >> \frac{\partial u}{\partial x}$$

can be used to set down the relative magnitudes of distances, velocities and vorticity as follows

$$x_o \sim o(1) \qquad y_o \sim o(\delta)$$

$$u_o \sim o(1)$$

$$v_o \sim o(\delta)$$

$$\omega_o \left(= \frac{\partial v_o}{\partial x_o} - \frac{\partial u_o}{\partial y_o}\right) \sim o\left(\delta - \frac{1}{\delta}\right)$$

$$\left[\frac{\partial \omega_o}{\partial x_o} \sim o\left(\delta - \frac{1}{\delta}\right) \quad \text{AND} \quad \frac{\partial \omega_o}{\partial y_o} \sim o\left(1 - \frac{1}{\delta^2}\right) \right]$$

From Daily, the term $\dfrac{\partial \omega_o}{\partial t_o}$ is the same order as $u_o \dfrac{\partial \omega_o}{\partial x_o}$

Hence from A7.2

$$\frac{\partial \omega_o}{\partial t_o} + u_o \frac{\partial \omega_o}{\partial x_o} + v_o \frac{\partial \omega_o}{\partial y_o} = \frac{1}{Re_L}\left[\frac{\partial^2 \omega_o}{\partial x_o^2} + \frac{\partial^2 \omega_o}{\partial y_o^2}\right]$$

$$\left(\delta - \frac{1}{\delta}\right) \quad 1\left(\delta - \frac{1}{\delta}\right) \quad \delta\left(1 - \frac{1}{\delta^2}\right) = \frac{1}{Re_L}\left[\left(\delta - \frac{1}{\delta}\right) \quad \left(\frac{1}{\delta} - \frac{1}{\delta^3}\right)\right]$$

Consider the terms on the right hand side.. The term $\frac{\partial^2 \omega_o}{\partial x_o^2}$ can be eliminated since it is smaller than $\partial^2 \omega_o / \partial y_o^2$.

Also, the order of Re_L must be $\frac{1}{\delta^2}$ to satisfy the Boundary Layer concept that the viscous term is to be comparable to the inertia term. This leads to A7.3

$$\frac{\partial \omega_o}{\partial t_o} + u_o \frac{\partial \omega_o}{\partial x_o} + v_o \frac{\partial \omega_o}{\partial y_o} = \frac{1}{Re_L}\left[\frac{\partial^2 \omega_o}{\partial y_o^2}\right]$$

$$\left(\delta - \frac{1}{\delta}\right) \quad \left(\delta - \frac{1}{\delta}\right) \quad \left(\delta - \frac{1}{\delta}\right) = \delta^2\left[\frac{1}{\delta} - \frac{1}{\delta^3}\right] \qquad \text{A7.3}$$

Thus incorporating the boundary layer conditions it can be seen that only one of the viscous terms can be eliminated from the vorticity transport equation on an 'order of magnitudes' argument.

APPENDIX 8

Stability Criteria

The stability criteria used in the investigation were taken from Fromm (1964, 1969b), where details of the analysis are given. They apply to the vorticity transport equation only

$$\frac{\partial \omega}{\partial t} + u\frac{\partial \omega}{\partial x} + v\frac{\partial \omega}{\partial y} = \nu\left[\frac{\partial^2 \omega}{\partial x^2} + \frac{\partial^2 \omega}{\partial y^2}\right] \qquad \text{A8.1}$$

The stability of the diffusion process is assured if the following criterion is obeyed

$$\frac{\nu \delta t}{a^2} \leq \frac{1}{4} \qquad \text{A8.2}$$

Where a = $\delta_x = \delta_y$ (mesh interval)

For the second order representation of A8.1 for mesh points near the wall, the low wave-number modes ($O(2\delta x)$) are stable if

$$(\alpha^2 + \beta^2) \leq 1 \qquad \text{A8.3}$$

Where $\alpha = u\delta t/\delta_x$ AND $\beta = v\delta t/\delta_y$

The next mode $(O(3\delta x))$ is stable if

$$\alpha + \beta \leq 1 \qquad \text{A8.4}$$

In practice, only these two criteria were satisfied, and no stability problems were encountered.

For mesh points away from the boundaries, the vorticity was calculated using the fourth-order convection approximation. For this scheme, in order for the most troublesome mode to be damped.

$$\alpha \leq 0.5 \qquad \text{A8.5}$$

All these criteria were used to establish the correct relationship between $Re, \omega, \delta t, a, u$ and v.

For meshes where $\delta x \neq \delta y$ then a was set to the smallest mesh interval, in order to cater for the worst case.

APPENDIX 9

DERIVATION OF FINITE - DIFFERENCE EQUATIONS

The equations used by Fromm (1969a) were not formally derived either in that paper or in Fromm (1969b). It was not immediately clear how the various forms were derived, but it was considered worthwhile to derive them from first principles, to gain an insight into these rather complex second and fourth-order finite-difference formulations.

This derivation is given here.

Both analytic and numerical solutions of the Vorticity transport equation are limited by the non-linear convection terms. Although numerical solutions can be obtained, they are liable to be inaccurate because the finite-difference approximations of the convection terms may introduce errors. Crowley (1968) developed equations for these terms in both the advective and conservative forms i.e. where the dependant variable in the finite-difference equation was not necessarily conserved and where it was identically conserved respectively.

Fromm used the advective form, expressed conservatively*, for the second and fourth-order approximations to the convective terms.

A9.1 Second Order Advective Scheme

Stirlings interpolation formula is (Wylie (1966))

$$f(x_0+rh) = f_0 + \frac{r}{1!}\frac{(\delta f_{1/2} + \delta f_{-1/2})}{2} + \frac{r^2}{2!}\delta^2 f_0 + \frac{r(r^2-1)}{3!}\frac{(\delta^3 f_{1/2} + \delta^3 f_{-1/2})}{2} + \frac{r^2(r^2-1)}{4!}\delta^4 f_0 + \cdots$$

A9.1

Where

$$\delta f_{1/2} + \delta f_{-1/2} = f_1 - f_0 + f_0 - f_{-1} = f_1 - f_{-1}$$

$$\delta^2 f_0 = \delta f_{1/2} - \delta f_{-1/2} = f_1 - 2f_0 + f_{-1}$$

$$\delta^3 f_{1/2} + \delta^3 f_{-1/2} = \delta^2 f_1 - \delta^2 f_0 + \delta^2 f_0 - \delta^2 f_{-1} = f_2 - 2f_1 + 2f_{-1} - f_{-2}$$

and $\delta^4 f_0$ can be shown to be

$$f_2 - 4f_1 + 6f_0 - 4f_{-1} + f_{-2}$$

* written to resemble the conservative form

For the second order form, only the first three terms are used from the right hand side of A9.1, for the later approximation of $\partial\omega/\partial x$.

The new value of ω can be obtained from the vorticity values at the mesh points $i-1,j$; i,j ; $i+1,j$ as follows:

$$\omega^* = \omega^n_{i,j} + \frac{r}{2}\left(\omega^n_{i+1,j} - \omega^n_{i-1,j}\right) + \frac{r^2}{2}\left(\omega^n_{i+1,j} - 2\omega^n_{i,j} + \omega^n_{i-1,j}\right)$$

Substituting $\omega^{n+1}_{i,j} = \omega^*$ and $-\alpha = r$ (CROWLEY(1968))gives

$$\omega^{n+1}_{i,j} = \omega^n_{i,j} - \frac{\alpha}{2}\left(\omega^n_{i+1,j} - \omega^n_{i-1,j}\right) + \frac{\alpha^2}{2}\left(\omega^n_{i+1,j} - 2\omega^n_{i,j} + \omega^n_{i-1,j}\right)$$

A9.2

The terms $\omega^{n+1}_{i,j}$ and $\omega^n_{i,j}$ are associated with the time derivative in the Vorticity transport equation, with the remaining terms associated with the derivative $\partial(u\omega)/\partial x$.

Equation A9.2 can be written

$$\omega^{n+1}_{i,j} = \omega^n_{i,j} + B \qquad \text{A9.3}$$

Where $$B = -\frac{\alpha}{2}\left(\omega^n_{i+1,j} - \omega^n_{i-1,j}\right) + \frac{\alpha^2}{2}\left(\omega^n_{i+1,j} - 2\omega^n_{i,j} + \omega^n_{i-1,j}\right)$$

Neglecting the diffusion terms and the corresponding variation in j, A9.3 can be seen to be equivalent to equation 6 in Fromm (1969a) if the following transformation is made to B, to enable the conservative form to be obtained.

$$B = C_{i-1/2,j} - C_{i+1/2,j}$$

Where $$C_{i-1/2,j} = A_{11}\alpha\left(\omega^n_{i-1,j} + \omega^n_{i,j}\right) + A_{12}\alpha^2\left(\omega^n_{i-1,j} - \omega^n_{i,j}\right) \qquad \text{A9.4}$$

and $$C_{i+1/2,j} = A_{11}\alpha\left(\omega^n_{i,j} + \omega^n_{i+1,j}\right) + A_{12}\alpha^2\left(\omega^n_{i,j} - \omega^n_{i+1,j}\right)$$

Using the method of undetermined coefficients, as follows, the values of A_{11} and A_{12} can be found

$$B = A_{11}\alpha\left(\omega^{n}_{i-1,j} - \omega^{n}_{i+1,j}\right) + A_{12}\alpha^{2}\left(\omega^{n}_{i-1,j} - 2\omega^{n}_{i,j} + \omega^{n}_{i+1,j}\right) \qquad \text{A9.5}$$

Equating A9.3 and A9.5

$$A_{11} = \tfrac{1}{2} \qquad \text{and} \qquad A_{12} = \tfrac{1}{2}$$

which when substituted into A9.4 gives

$$C_{i-\frac{1}{2},j} = \tfrac{1}{2}\alpha\left(\omega^{n}_{i-1,j} + \omega^{n}_{i,j}\right) + \tfrac{1}{2}\alpha^{2}\left(\omega^{n}_{i-1,j} - \omega^{n}_{i,j}\right)$$

$$C_{i+\frac{1}{2},j} = \tfrac{1}{2}\alpha\left(\omega^{n}_{i,j} + \omega^{n}_{i+1,j}\right) + \tfrac{1}{2}\alpha^{2}\left(\omega^{n}_{i,j} - \omega^{n}_{i+1,j}\right) \qquad \text{A9.6}$$

NB $\alpha = \alpha_{i-\frac{1}{2},j}$ in $C_{i-\frac{1}{2},j}$ and $\alpha = \alpha_{i+\frac{1}{2},j}$ in $C_{i+\frac{1}{2},j}$, Fromm(1969b)

A9.2 Fourth Order Advective Scheme

The five terms on the right hand side of A9.1 are used for the Fourth-order form. The new value of w can be obtained from the vorticity values at the mesh points $i-2,j$; $i-1,j$; i,j; $i+1,j$; $i+2,j$ as follows

$$\omega^{*} = \omega^{n}_{i,j} + \frac{r}{2}\left(\omega^{n}_{i+1,j} - \omega^{n}_{i-1,j}\right) + \frac{r^{2}}{2}\left(\omega^{n}_{i+1,j} - 2\omega^{n}_{i,j} + \omega^{n}_{i-1,j}\right) +$$

$$+ \frac{1}{12}\left(r^{3} - r\right)\left(\omega^{n}_{i+2,j} - 2\omega^{n}_{i+1,j} + 2\omega^{n}_{i-1,j} - \omega^{n}_{i-2,j}\right) +$$

$$+ \frac{1}{24}\left(r^{4} - r^{2}\right)\left(\omega^{n}_{i+2,j} - 4\omega^{n}_{i+1,j} + 6\omega^{n}_{i,j} - 4\omega^{n}_{i-1,j} + \omega^{n}_{i-2,j}\right)$$

A9.7

Substituting $w^{n+1}_{i,j} = w^*$ and $r = -\alpha$ and with some algebraic manipulation, A9.7 becomes

$$w^{n+1}_{i,j} = w^n_{i,j} + B$$

Where

$$B = -\frac{\alpha}{12}\left[8\left(w^n_{i+1,j} - w^n_{i-1,j}\right) - \left(w^n_{i+2,j} - w^n_{i-2,j}\right)\right] -$$

$$- \frac{\alpha^2}{24}\left[30 w^n_{i,j} - 16\left(w^n_{i+1,j} + w^n_{i-1,j}\right) + \left(w^n_{i+2,j} + w^n_{i-2,j}\right)\right] -$$

$$- \frac{\alpha^3}{12}\left[-2\left(w^n_{i+1,j} - w^n_{i-1,j}\right) + \left(w^n_{i+2,j} - w^n_{i-2,j}\right)\right] +$$

$$+ \frac{\alpha^4}{24}\left[6 w^n_{i,j} - 4\left(w^n_{i+1,j} + w^n_{i-1,j}\right) + \left(w^n_{i+2,j} + w^n_{i-2,j}\right)\right]$$

A9.8

Crowley (1968)

By ignoring the diffusion terms and any variation in j, A9.8 can be shown to be equivalent to equation 5 in Fromm (1969a) if the same transformation is made to B, again to enable the conservative form to be obtained.

$$B = C_{i-1/2,j} - C_{i+1/2,j}$$

Where $C_{i-1/2,j} = A_{11}\alpha\left(w^n_{i-1,j} + w^n_{i,j}\right) + A_{12}\alpha\left(w^n_{i-2,j} + w^n_{i+1,j}\right) +$

$$+ A_{21}\alpha^2\left(w^n_{i-1,j} - w^n_{i,j}\right) + A_{22}\alpha^2\left(w^n_{i-2,j} - w^n_{i+1,j}\right) +$$

$$+ A_{31}\alpha^3\left(w^n_{i-1,j} + w^n_{i,j}\right) + A_{32}\alpha^3\left(w^n_{i-2,j} + w^n_{i+1,j}\right) +$$

$$+ A_{41}\alpha^4\left(w^n_{i-1,j} - w^n_{i,j}\right) + A_{42}\alpha^4\left(w^n_{i-2,j} - w^n_{i+1,j}\right) \qquad \text{A9.9}$$

$C_{i+1/2,j}$ can be obtained from A9.9 by permutation of the suffices. Using the method of undetermined coefficients as above, the coefficients in A9.9 can be evaluated.

Consider the first two terms in $C_{i-1/2,j}$ and $C_{i+1/2,j}$

$$A_{11}\alpha\left(w^n_{i-1,j} + w^n_{i,j}\right) + A_{12}\alpha\left(w^n_{i-2,j} + w^n_{i+1,j}\right) \qquad C_{i-1/2,j}$$

$$A_{11}\alpha\left(w^n_{i,j} + w^n_{i+1,j}\right) + A_{12}\alpha\left(w^n_{i-1,j} + w^n_{i+2,j}\right) \qquad C_{i+1/2,j}$$

$$B = C_{i-1/2,j} - C_{i+1/2,j}$$

hence for the first two terms

$$B = A_{11}\alpha\left(w^n_{i-1,j} - w^n_{i+1,j}\right) + A_{12}\alpha\left(w^n_{i-2,j} + w^n_{i+1,j} - w^n_{i-1,j} - w^n_{i+2,j}\right)$$

$$B = \alpha\left(A_{11} - A_{12}\right)\left(w^n_{i-1,j} - w^n_{i+1,j}\right) + A_{12}\alpha\left(w^n_{i-2,j} - w^n_{i+2,j}\right) \qquad \text{A9.10}$$

By comparing equations A9.8 and A9.10

$$A_{11} = \frac{7}{12} \qquad \text{and} \qquad A_{12} = -\frac{1}{12}$$

which on substituting in A9.9 gives for the first two terms

$$C_{i-\frac{1}{2},j} = \frac{7}{12}\alpha\left(w^n_{i-1,j} + w^n_{i,j}\right) - \frac{1}{12}\alpha\left(w^n_{i-2,j} + w^n_{i+1,j}\right)$$

Continuing with the above method the remaining coefficients were determined, giving finally

$$C_{i-\frac{1}{2},j} = \frac{7}{12}\alpha\left(w^n_{i-1,j} + w^n_{i,j}\right) - \frac{1}{12}\alpha\left(w^n_{i-2,j} + w^n_{i+1,j}\right) +$$

$$+ \frac{15}{24}\alpha^2\left(w^n_{i-1,j} - w^n_{i,j}\right) - \frac{1}{24}\alpha^2\left(w^n_{i-2,j} - w^n_{i+1,j}\right) -$$

$$- \frac{1}{12}\alpha^3\left(w^n_{i-1,j} + w^n_{i,j}\right) + \frac{1}{12}\alpha^3\left(w^n_{i-2,j} + w^n_{i+1,j}\right) -$$

$$- \frac{3}{24}\alpha^4\left(w^n_{i-1,j} - w^n_{i,j}\right) + \frac{1}{24}\alpha^4\left(w^n_{i-2,j} - w^n_{i+1,j}\right)$$

A9.11

A9.11 should be compared with equation 7 of Fromm(1969a). The following remarks are relevant:

1) Both equations are analogous.

2) Corresponding coefficients are identical.

3) The assumption is made that $\alpha = \alpha_{i-\frac{1}{2},j}$, Fromm(1969b)

4) The suffices of some terms differ. To be more definite, Fromm's equation contains no terms with the suffix $i+1,j$. Itwould appear that this discrepancy has arisen from a misprint in Fromm's paper. This is confirmed by the appearance of the correct form of the equation (i.e. containing terms with the $i+1,j$ suffix) in Fromm(1969b).

Crowley (1968) also details a second and fourth order conservative formulation which can be used for the convective terms in the vorticity transport equation. Although this formulation was not used in this investigation, the equations will be derived here for completeness.

The term $\partial(uw)/\partial x$ accounts for the transport of the vorticity by the fluid. If this term is regarded as the divergence of a flux, Green's theorem can be applied; consequently, in any zone, the decrease of vorticity with time is proportional to the net flux out of the zone. The flux across a zone boundary at $i+1/2, j$ is

$$(uw)_{i+1/2,j} = F_{i+1/2,j} = \frac{1}{\Delta t}\int_{x_{i+1/2,j}-u\Delta t}^{x_{i+1/2,j}} w(s)\,ds \qquad \text{A9.12}$$

A9.3 Second Order Conservative Scheme

If w is assumed to vary linearly between i,j and $i+1,j$, and the following transformation is used

$$s = x_{i,j} + \theta h$$

Where $h = \Delta x$, substituting into A9.12 will give

$$F_{i+1/2,j} = \frac{\Delta x}{\Delta t}\int_{1/2-\alpha}^{1/2}\left[w_{i,j} + \theta\left(w_{i+1,j} - w_{i,j}\right) + \cdots\right]d\theta \qquad \text{A9.13}$$

Neglecting second and higher order differences, and integrating A9.13 gives

$$\frac{\Delta t}{\Delta x}F_{i+1/2,j} = \left[\theta\Big|_{1/2-\alpha}^{1/2} w_{i,j} + \frac{\theta^2}{2}\Big|_{1/2-\alpha}^{1/2}\left(w_{i+1,j} - w_{i,j}\right)\right]$$

which on substituting of the limits and rearranging gives

$$\frac{\Delta t}{\Delta x}F_{i+1/2,j} = \frac{\alpha}{2}\left(w_{i+1,j} + w_{i,j}\right) - \frac{\alpha^2}{2}\left(w_{i+1,j} - w_{i,j}\right) \qquad \text{A9.14}$$

If α is evaluated at $i+\frac{1}{2},j$ from $u_{i+\frac{1}{2},j}\,\Delta t/\Delta x$, then equation A9.14 corresponds with equation 15 of Cowley (1968)

A9.4 Fourth Order Conservative Scheme

A cubic is fitted through w at the mesh points $i-1,j$; i,j ; $i+1,j$; $i+2,j$ and the following transformation used

$$s = x_{i-1,j} + \theta h \cdot \qquad \text{A9.15}$$

Where $h = \Delta x$

The vorticity can be expressed as

$$w(i-1,j+\theta h) = w_{i-1,j} + \theta\,\Delta w_{i-1,j} + \frac{\theta(\theta-1)}{2!}\Delta^2 w_{i-1,j} + \frac{\theta(\theta-1)(\theta-2)}{3!}\Delta^3 w_{i-1,j} + \cdots$$

A9.16

Substituting A9.15 and A9.16 into A9.12 gives

$$F_{i+\frac{1}{2},j} = \frac{\Delta x}{\Delta t}\int_{3/2-\alpha}^{3/2}\Big[w_{i-1,j} + \theta(w_{i,j} - w_{i-1,j}) + \frac{\theta^2-\theta}{2}(w_{i+1,j} - 2w_{i,j} + w_{i-1,j}) +$$
$$+ \frac{(\theta^3-3\theta^2+2\theta)}{6}(w_{i+2,j} - 3w_{i+1,j} + 3w_{i,j} - w_{i-1,j}) + \cdots\Big]d$$

A9.17

Neglecting fourth and higher order differences, A9.17 can be rearranged as follows

$$\frac{\Delta t}{\Delta x} F_{i+1/2,j} = \int_{3/2-\alpha}^{3/2} \left[w_{i-1,j} + \theta \left(\frac{1}{3} w_{i+2,j} - \frac{3}{2} w_{i+1,j} + 3 w_{i,j} - \frac{11}{6} w_{i-1,j} \right) + \right.$$

$$+ \frac{\theta^2}{2} \left(-w_{i+2,j} + 4 w_{i+1,j} - 5 w_{i,j} + 2 w_{i-1,j} \right) +$$

$$\left. + \frac{\theta^3}{6} \left(w_{i+2,j} - 3 w_{i+1,j} + 3 w_{i,j} - w_{i-1,j} \right) \right] d\theta$$

A9.18

On Integrating, substitution of the limits and rearranging, A9.18 becomes

$$\frac{\Delta t}{\Delta x} F_{i+1/2,j} = \frac{\alpha}{16} \left[9 \left(w_{i+1,j} + w_{i,j} \right) - \left(w_{i+2,j} + w_{i-1,j} \right) \right] -$$

$$- \frac{\alpha^2}{48} \left[27 \left(w_{i+1,j} - w_{i,j} \right) - \left(w_{i+2,j} - w_{i-1,j} \right) \right] -$$

$$- \frac{\alpha^3}{12} \left[\left(w_{i+1,j} + w_{i,j} \right) - \left(w_{i+2,j} + w_{i-1,j} \right) \right] +$$

$$+ \frac{\alpha^4}{24} \left[3 \left(w_{i+1,j} - w_{i,j} \right) - \left(w_{i+2,j} - w_{i-1,j} \right) \right]$$

which corresponds with equation 16 Crowley (1968) if α is evaluated at $i+1/2, j$ from $u_{i+1/2,j} \Delta t / \Delta x$.

Crowley in his paper carried out tests for one and two dimensional problems, using both advective and conservative formulations for each case. For the one dimensional problem, greater accuracy was achieved by using the conservative form rather than the advective form, and the most accurate result came from the fourth order scheme in conservative form.

For the two-dimensional problem, the results were not qualitatively different when using either the advective or conservative schmes. Crowley noted that since his test problem involved non-divergent flow, this result was not too surprising, although he still felt that the more accurate solution would come from equations in conservative form.

Fromm (1969b) contended that whilst there was fairly general agreement that the conservative form was more accurate, there was little precise information to explain this. In his companion paper, Fromm (1969a), he used the advective form expressed conservatively for the fourth order equations; This is the form used in the present investigation.

APPENDIX 10

DESCRIPTION OF THE COMPUTER PROGRAM TO PREDICT VISCOUS FLOWS.

A10.1 Introduction

The program flow diagram is shown in Fig. A11.F1.[272] If this is compared with the program text, Appendix 11, it can be seen that each block in the flow diagram denotes one of the programs comprising the program suite. The similarity between the flow diagram and the general description of viscous flow development, Lighthill (1963), can also be seen.

All programs were written in Scheme D, an extension of an autocode developed at Rolls-Royce (1971) Ltd., Bristol Engine Division. This enables the data to be stored in a ring structure, Dennison (1973), making it easily accessible from any Scheme D program.

The data is stored in entities whose size depends on the particular users requirements. These entities are placed in rings, and may be accessed using standard instruction.

Each program will now be described separately.

A10.2. DATA INPUT & MESH CREATION

The data input is divided into the following sections:

1. (a) Definition of the body boundaries

   (b) Definition of the flow region using 1(a)

2. Definition of the mesh.

3. Flow data.

An example of the data input can be seen in Appendix 11. This particular format was chosen so that the programs could be incorporated into the COMET data management system. This is currently under development at the Bristol Engine Division.

The first two sections of data are required for the mesh generation program, which fits a mesh between any 2-D boundaries and is available to any user of COMET. The mesh is created using the ring structure, which makes interrogation of the mesh by any other program straightforward.

Each mesh point has an entity assocated with it, to store the 19 data items for each point. The data is shown in fig A10.F 1

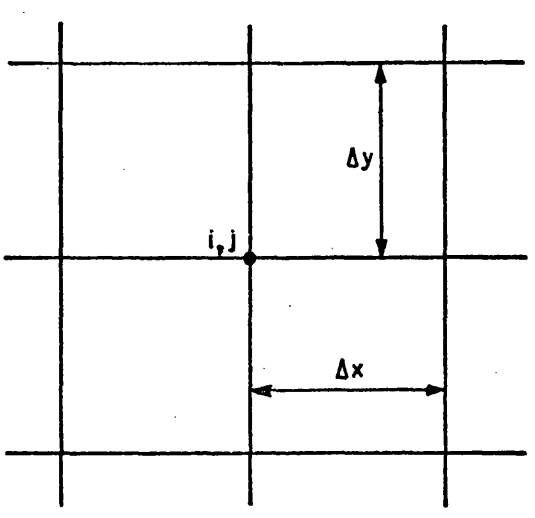

DATA STORED AT Pt i,j

DATA WORD	
1	x
2	y
3	Δx
4	$U_{i,j+1/2}$
5	$V_{i+1/2,j}$
6	W^{n-1}
7	W^{n}
8	W^{n+1}
9	σ
10	MESH POINT MARKER
11	x COLLOCATION POINT
12	y COLLOCATION POINT
13	x SHEET END POINT
14	y SHEET END POINT
15	VELOCITY MARKER
16	SOURCE OR VORTEX SHEET MARKER
17	Δy
18	USED FOR TEMP. STORAGE
19	ADDRESS MARKER

Fig. A10.F1 Storage of Data in Entities.

A control block at the start of program 55 calls the programs to read the data, section 1 & 2, and run the required mesh fitting program. When the mesh has been fitted, program 55 is itself run, to process the flow data. Some of this data is stored for use by other programs in the suite. A flow diagram for 55 is shown in fig. A11.F2.[273]

If the run has been restarted, assuming convergence has not been reached, then the previously stored information is updated i.e. total number of iterations to be performed, which iterations are to be plotted and printed, or only printed etc. Also, any plotting vectors from previous iterations are removed from the ring structure. This means that the vectors from the next set of iterations only will be stored. Control is then passed to 10003 for solving the matrix equation, whose coefficients have been stored by the previous run.

If this is the very first iteration, then the first part of 10008, the plotting vector program, is run. This calculates the coordinates of the duct outline and the end coordinates of the mesh columns, and stores them all on the ring structure in preparation for any plotting of results

If the run has not been restarted, control is then switched to program 10002, to set up the mesh markers which will be used by every program throughout all the subsequent iterations.

A10.3 MESH MARKERS & MATRIX OF COEFFICIENTS

The flow diagram for this program is shown in fig A11.F3[274]. The program is called once only, at the beginning of the computational cycle. Its purpose is to:

1. Allocate mesh point markers denoting:

   a) their position in the flow field relative to the boundaries

   b) the number and type of velocity components stored at the mesh point.

2. Calculate the coefficients of the matrix equation A 2.8 for the initial irrotational flow.

1a. Mesh point markers.

A table of these markers is shown in 10.1, with a illustrative diagram in fig. A10.F2. Any program may interrogate this marker and deduce the position of the mesh point. This is easier and quicker than calculating the mesh point position every time it is needed. The marker is stored in the tenth position of each mesh point data area, fig A10.F1[254].

MARKER	POSITION OF MESH POINT
0	ON SOLID BOUNDARY.
1	ON INLET FLUID BDRY, ADJACENT TO SOLID BDRY.
-1	ADJACENT TO SOLID BOUNDARY
2	ON EXIT FLUID BOUNDARY.
-2	ON INLET FLUID BOUNDARY.
3	ADJACENT TO INLET FLUID BOUNDARY.
-3	REMAINING FIELD POINTS.

TABLE 10.1 MESH POINT MARKERS.

1b Velocity component markers.

This marker is calculated from both the position of the mesh point and the mesh point marker. A table of these markers is shown in 10.2, and the marker is stored in the fifteenth data position fig A10.F1.[254] These markers are illustrated in fig. A10.F3.

They are used when calculating the velocity components and for calculating the streaklines in the plotting program.

MARKER	VELOCITY COMPONENTS CALCULATED AT A MESH POINT
0	BOTH $u_{i,j+1/2}$ and $v_{i+1/2,j}$
1	ONLY $v_{i+1/2,j}$
-1	NO COMPONENTS
2	ONLY $u_{i,j+1/2}$

VELOCITY COMPONENT MARKER

TABLE 10.2

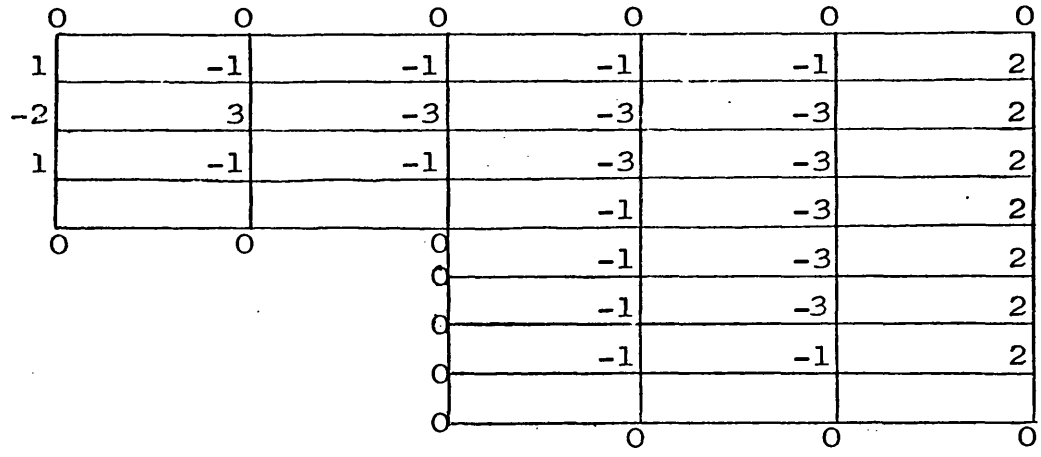

FIG A10.F2 MESH POINT MARKERS.

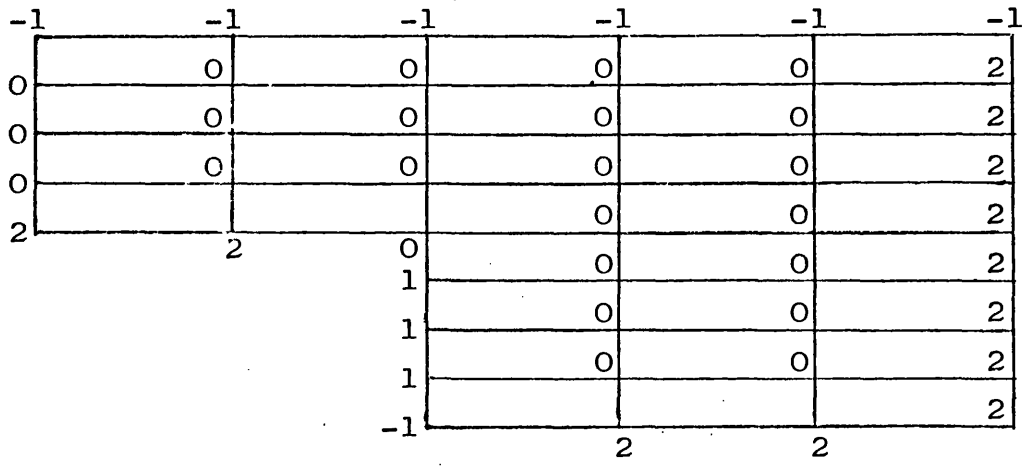

FIG A10. F3 VELOCITY COMPONENT MARKERS.

2. Matrix coefficients

The coefficients A and B of the matrix equation A2.8 are calculated for the irrotational flow at the start of the computations. For details see Appendix 2.

The coefficients are stored in entities for future access. The coefficients of A represent the weighting factors of one surface singularity on another. As such they remain constant throughout the cycle of computations. The coefficients of B are dependent on the vorticity present in the flow field, and will change at every iteration until convergence.

A10.4. SOLUTION OF SINGULARITY STRENGTHS

The program flow diagram is shown in fig A11.F4.[275] As the coding for the Gauss-Seidal solution routine already existed in the COMET system, it was adpated for use in this program suite. The theory is given in Smith (1969).

Once the strengths have been calculated, they are stored in the ninth data word of the surface mesh point data area, fig. A10.F1.[254] The correct mesh point is the one at the origin of the sheet local axis system, fig. A10.F4.

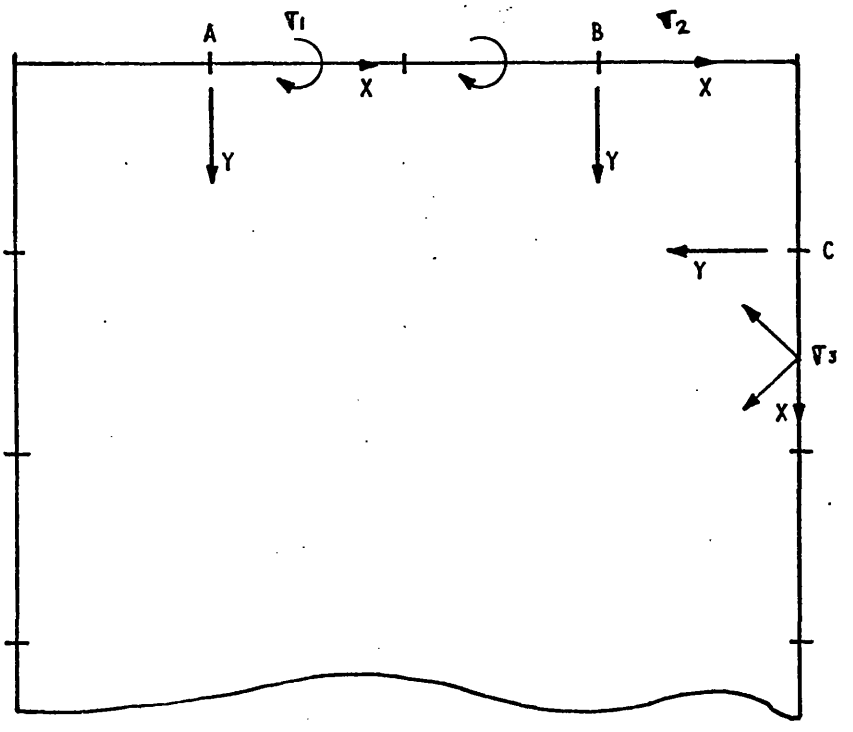

FIG A10.F4. MESH POINT LOCATION FOR STORING SURFACE SHEET STRENGTH

τ_1 is stored in the data area of mesh point A and σ_2, σ_3 in the data areas of points B and C respectively.

A10.5 CALCULATION OF THE VELOCITY

The program flow diagram is shown in fig A11.F5.[276] Each mesh point is selected in turn, and its data interrogated to establish one of the following:-

1) If it is the first iteration

2) Whether it is a general mesh point

3) Whether it is on the duct inlet or exit.

1. First Iteration

The only singularities present during the initial irrotational flow are the surface sheet singularities. The velocity components $U_{i,j+1/2}$ AND $V_{i+1/2,j}$ are calculated directly and stored in the fourth and fifth data words of each mesh point, fig A10.F1.[254]

The velocity components induced by the duct inlet and exit source sheets, are calculated from equation 6.15. Those from the solid surface vortex sheets are calculated from equation 6.16.

For any other iteration, the procedure depends on the mesh point position. The vorticity in the duct is represented by discrete vortex filaments at the mesh points, as mentioned in 6.23. Incorrect results were formed when the velocity was calculated directly, due to the $(1/r)$ term in equation 4.7. The halfway mesh points were too close to the inducing vortex.

The method eventually used was to calculate the velocity components at the mesh intersection points, and use linear interpolation to calculate the components at the halfway mesh points, (Section 6.23).

2. General Mesh Point

The velocity components induced by a vortex filament are given by equation 4.7. The required components $U_{i,j+1/2}$, $V_{i+1/2,j}$ are calculated and stored as above.

3. Inlet or Exit Point

For this investigation, a uniform velocity profile was specified across the duct inlet, which means that the vorticity is zero there, (Section 6.22). The velocity components, $u_{i,j+1/2}$, $v_{i+1/2,j}$ induced by the surface and field singularities, were calculated directly. Had the vorticity not been zero there, then the technique adopted for the duct exit would have had to be used.

The method adopted for the exit section entailed dealing separately with its own vorticity. The U velocity components induced by both the surface singularities and the field vorticity NOT on the duct exit, are stored at the EXIT, J + ½ mesh points.

The U velocity components induced by the duct exit vorticity are calculated at the EXIT, J Mesh points, and linear interpolation used to calculate the velocity at the EXIT, J + ½ points. These components are added to those previously stored to give the exit velocity profile. This routine ensures that any errors associated with the linear interpolation at the duct exit, are kept to a minimum. The significance of this will be seen in section A10.7, where it is shown how continuity is enforced between the duct inlet and exit.

The surface vorticity is calculated from the velocity components adjacent to the surface. The equations are given in section 6.22

A10.6 CALCULATION OF VORTICITY

The flow field vorticity is calculated in program 10005, whose flow diagram is shown in fig A11.F6.[277] Each mesh point is selected in turn and certain data e.g. velocity and vorticity values, mesh marker, is stored in dummy data stores.

If the point is on the duct inlet then the vorticity is calculated directly from the prescribed inlet velocity distribution. If it is not, then a number of other mesh points are selected, fig A10.F5, and their equivalent data transfered to other dummy stores.

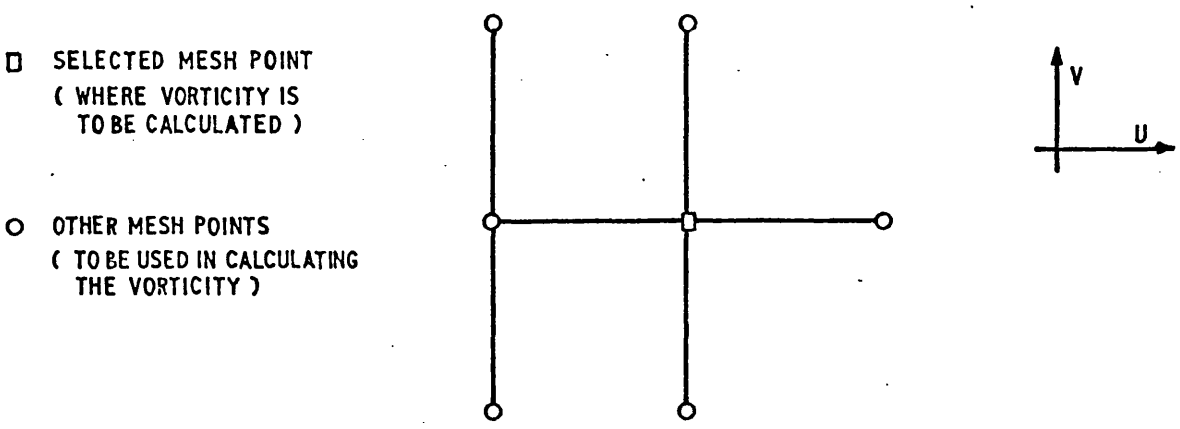

Fig A10.F5 MESH POINT SELECTION

If the selected point is on the duct exit, then enough information has been stored for the vorticity to be calculated there. Should the point be in the flow field, then the contribution to the new vorticity value from diffusion of the vorticity can be calculated and stored.

The finite-difference version of the vorticity transport equation used, was taken from Fromm(1969a) section 6.22. It is an upwind differencing type of formulation, where more information is used from the local upstream direction. FigA10.F6 shows the variation of mesh position for $\pm U$.

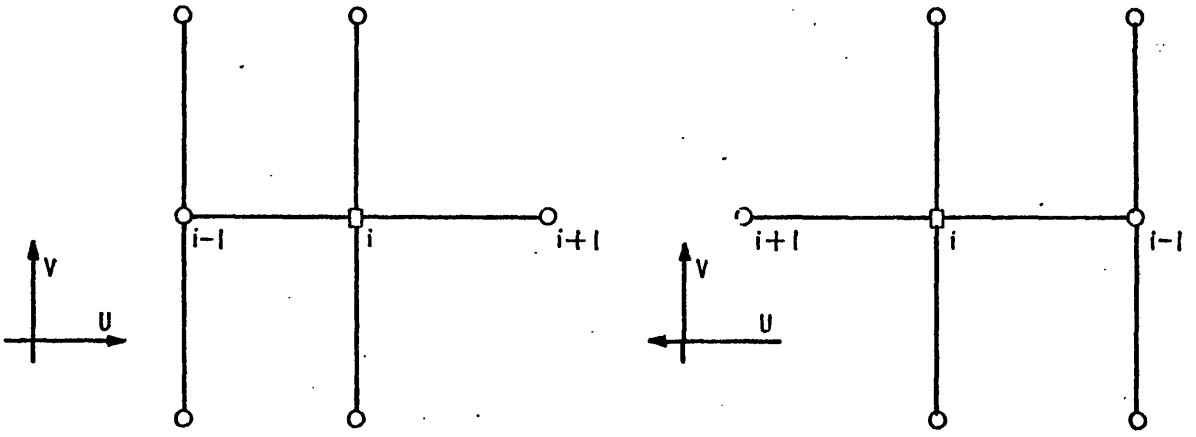

Fig A10.F6 MESH POINT ORIENTATION

For any mesh point, i,j, the components $u_{i,j}$, $v_{i,j}$ are calculated from the surrounding components, fig. A10.F7, as follows

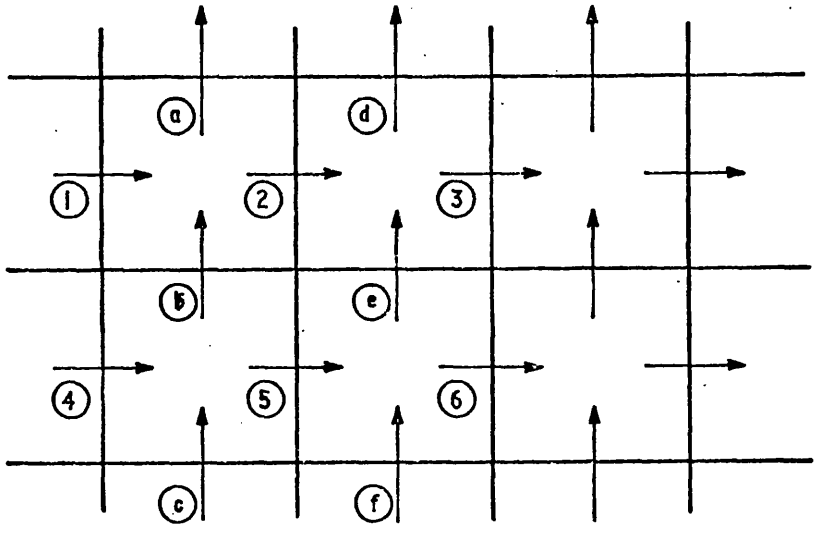

FIG A10.F7 CALCULATION OF AVERAGE VELOCITIES

$$u_{i,j} = (u_1 + 2u_2 + u_3 + u_4 + 2u_5 + u_6)/8 \qquad \text{A10.1}$$

$$v_{i,j} = (v_a + 2v_b + v_c + v_d + 2v_e + v_f)/8$$

For mesh points in the flow field, Fromm uses the fourth order approximation to the vorticity transport equation. This entails using information from the i-2 and j-2 mesh position fig. A10.F8

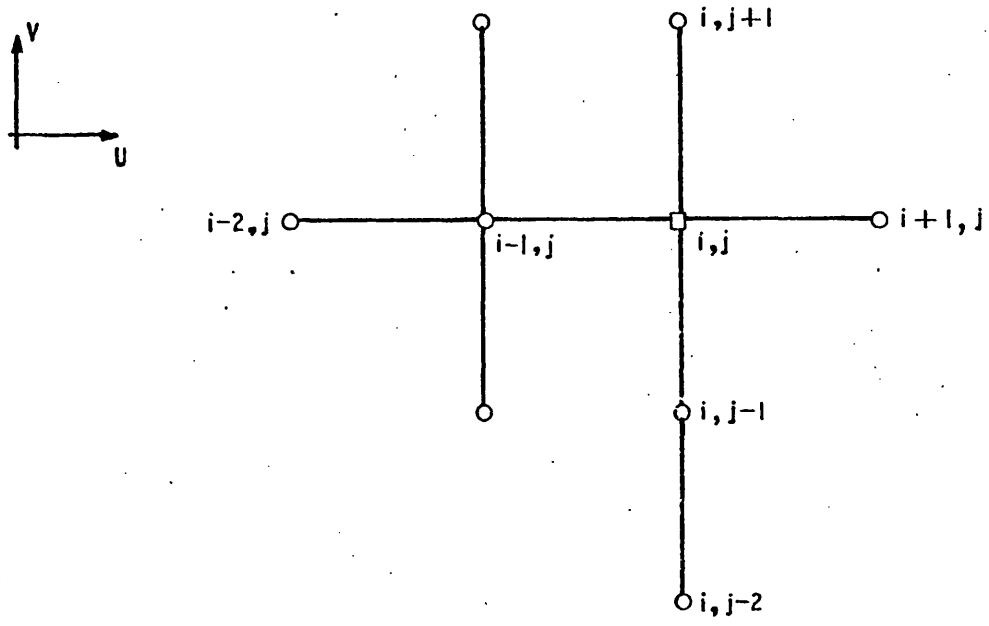

FIG A 10.F8 FOURTH - ORDER MESH POSITIONS

For mesh points adjacent to the solid surfaces, inlet, and possibly the exit, fluid boundaries, difficulties arise prescribing the values at the i-2 and j-2 positions. Since they are not in the flow field, Fromm uses a second-order approximation to the vorticity transport equation. The mesh point positions are shown in fig. A10.F9, and are dependant on the velocity direction as for the fourth order mesh

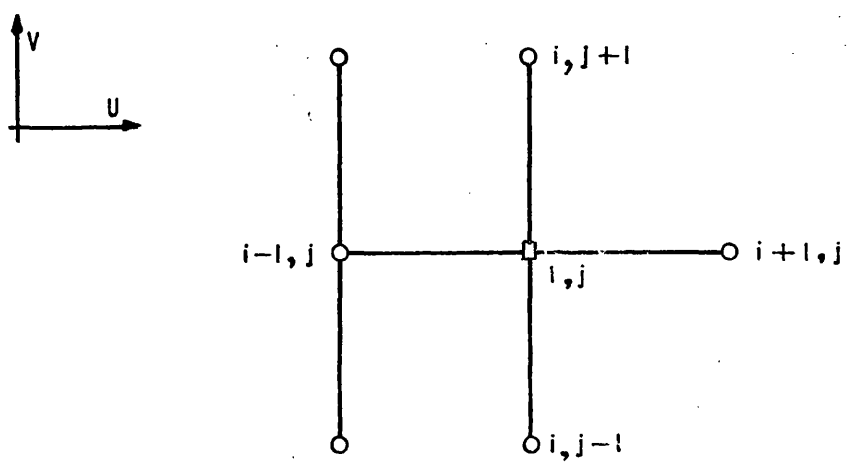

FIG A10.F9 SECOND-ORDER MESH POSITIONS.

When the new vorticity value has been calculated, it is stored in the eighth data position, fig A10.F1.[254] Once the vorticity values at all the mesh points have been found, the values are overwritten into the seventh data position ready for the next iteration.

A10.7 EFFECT OF VORTICITY AT SURFACE.

The program flow diagram is shown in fig A11.F7.[278] The reasons for calculating this effect at every iteration are given in Section 6.24.

The store addresses of the surface sheets and those field mesh points having vorticity, are stored in a dummy array for access by the program. This saves the time consuming process of scanning the mesh at each iteration to find those addresses. The area under the inlet velocity profile is calculated and stored ready for comparison with the area under the exit profile.

For each surface sheet not on the exit boundary, the procedure is as follows:-

1) Calculate the velocity component induced by all the field vorticity at the sheet collocation points:-

   a) tangential component at the duct vortex sheets

   b) normal component at the duct source sheets.

2) Temporarily store each component.

For each of the exit surface sheets, the procedure is different:-

A) Calculate the normal velocity component at the sheet collocation point induced by all the field vorticity NOT on the exit boundary.

B) Calculate the normal velocity component at the duct exit mesh points induced by the exit vorticity.

C) Linearly interpolate the velocity components (B) to calculate the components at the sheet collocation points. These are then added to (A)

The area under the exit velocity profile is calculated using the trapezium rule, and compared with the area under the inlet velocity profile, see above. The difference in the areas is converted into a linear increment in velocity, section 6.24, to be added to each of the velocity components comprising the exit velocity profile. This linear increment is temporarily stored for each of the exit sheets.

Using the information for each sheet, it is possible to recalculate the vector B, equation A2.8, to take account of the field vorticity. The procedure is:-

1) For each solid surface collocation point, the velocity induced by all the surface sheets must be equal and opposite to that induced by the field vorticity. This ensures that the boundary condition of zero velocity on the outside of the sheets is maintained. The correct velocity is extracted from the information temporarily stored, and restored in vector B.

2) For the duct inlet collocation points, the velocity induced by the surface sheets should again be equal and opposite to that induced by the field vorticity, so that the prescribed velocity distribution is maintained. The surface sheets velocity is stored in vector B.

3) For the duct exit collocation points, the velocity induced by the surface sheets should be the linear velocity increments previously calculated. This ensures that the velocity induced at the duct exit, by the surface and field singularities, satisfies continuity.

These increments are also stored in Vector B.

Having obtained the new vector B for all the surface sheets, it is possible to recalculate the strengths of those sheets, by using the Gauss-Seidal program, 10003.

A10.8 CONTROL PROGRAM

The program flow diagram is shown in A11.F8 (279). Based upon the data input, the current iteration is either printed, plotted and printed or ignored. If it is to be plotted, program 10008 is run to assemble the velocity vector coordinates, for the streakline plot, and the coordinates of the velocity and vorticity profiles.

If this iteration is not the last in the current run, control is switched to 10003, to re-solve the matrix equation A2.8 for the new surface sheet strengths.

If the iteration is the last, and some of the previous iterations involved plots, then program 10009 is run to assemble a magnetic tape of plotting information. If none of the iterations involved plots,all available mesh information is stored ready for the next series of runs, and the computation stopped.

A10.9 PLOTTING COORDINATES AND INSTRUCTIONS.

The last two programs in the suite are concerned with plotting. They are

1) 10008, to assembling all the plotting coordinates.
2) 10009, for preparing a magnetic tape of plotting information.

1. Program 10008

The flow diagram for this program is shown in A11.F9.280
The program is run as a subroutine from two different programs. The first section of 10008 is run from program 55, to assemble the basic plot data. This consists of:-

a) duct outline coordinates.

b) mesh column end coordinates.

This information is stored for easy access by the rest of the program each time a plot is called for.

The second section is run from program 10007, the control program. Each time a plot is requested, three pictures are produced by 10008:-

a) Streakline plot, where streaklines are defined as instantaneous velocity vectors.
b) U-velocity component plot across the duct.
c) Vorticity profile across the duct.

All these plots are contained within the duct outline.

On entry to the program the duct outline and column coordinates are retrieved from their storage locations, and stored within the ring structure ready for plotting. A reference velocity and vorticity are chosen as follows:- the reference velocity is the maximum velocity across the inlet section, and the reference vorticity is the absolute value of surface vorticity at the inlet. These values are stored so that the plots may be sealed.

Each mesh point is selected in turn, and the coordinates of the points on the velocity and vorticity profiles for this mesh location are calculated and stored. The mesh point velocity marker is examined and either X or Y streaklines, or both, are calculated. The X streakline is the velocity vector at $i+1/2, j$, the Y streakline at $i, j+1/2$.

Considering the X streakline, the v component is stored for the $i+1/2, j$ position but the u component is not known. It is calculated from the average of the surrounding components as follows, fig. A10.F10

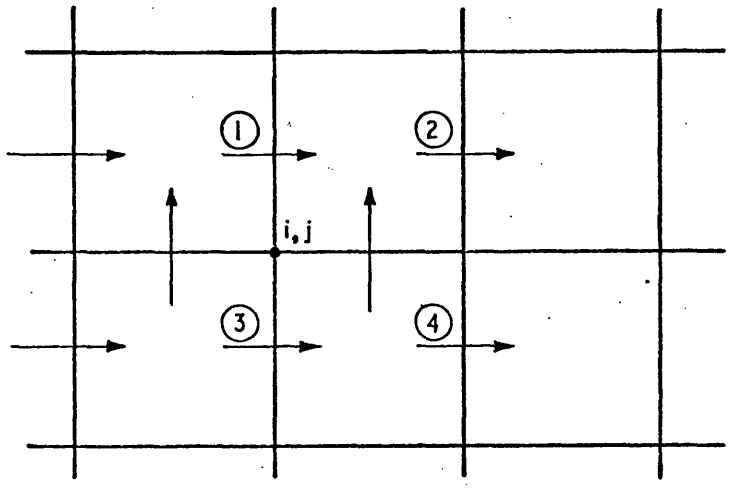

FIG A10.F10 CALCULATION OF STREAKLINE COMPONENTS.

$V_{i+1/2,j}$ is known

$$u_{i+1/2,j} = (u_1 + u_2 + u_3 + u_4)/4 \qquad \text{A10.2}$$

A similar procedure is performed for $V_{i,j+1/2}$

Knowing all the components at both $i+1/2, j$ and $i, j+1/2$ enables the velocity vector to be calculated, and scaled. The coordinates, angle of inclination and the magnitude of the streakline are stored ready for plotting.

Once all the plotting information has been assembled, control is switched back to 10007, for the mesh information to be printed.

2. Program 10009

When all the iterations in the present run have been computed, program 10007 calls program 10009 if one or more of those iterations involves a plot. The program flow diagram is shown in A10.F10.[281] This program is one of the COMET programs and although it wasn't written by the author, was adapted by him to cater for streaklines.

The program takes all the coordinates, angles etc. stored by program 10008, and converts these to a series of plotting instructions. These are then stored on a magnetic tape ready for

processing by another system program.

This program is run from 10009 and converts the information on the magnetic tape to instructions which will operate the plotter.

APPENDIX 11

This appendix contains the following -

1) Flow diagrams of the computer programs.

2) Details of the data input.

3) Program coding.

4) Typical output from the program

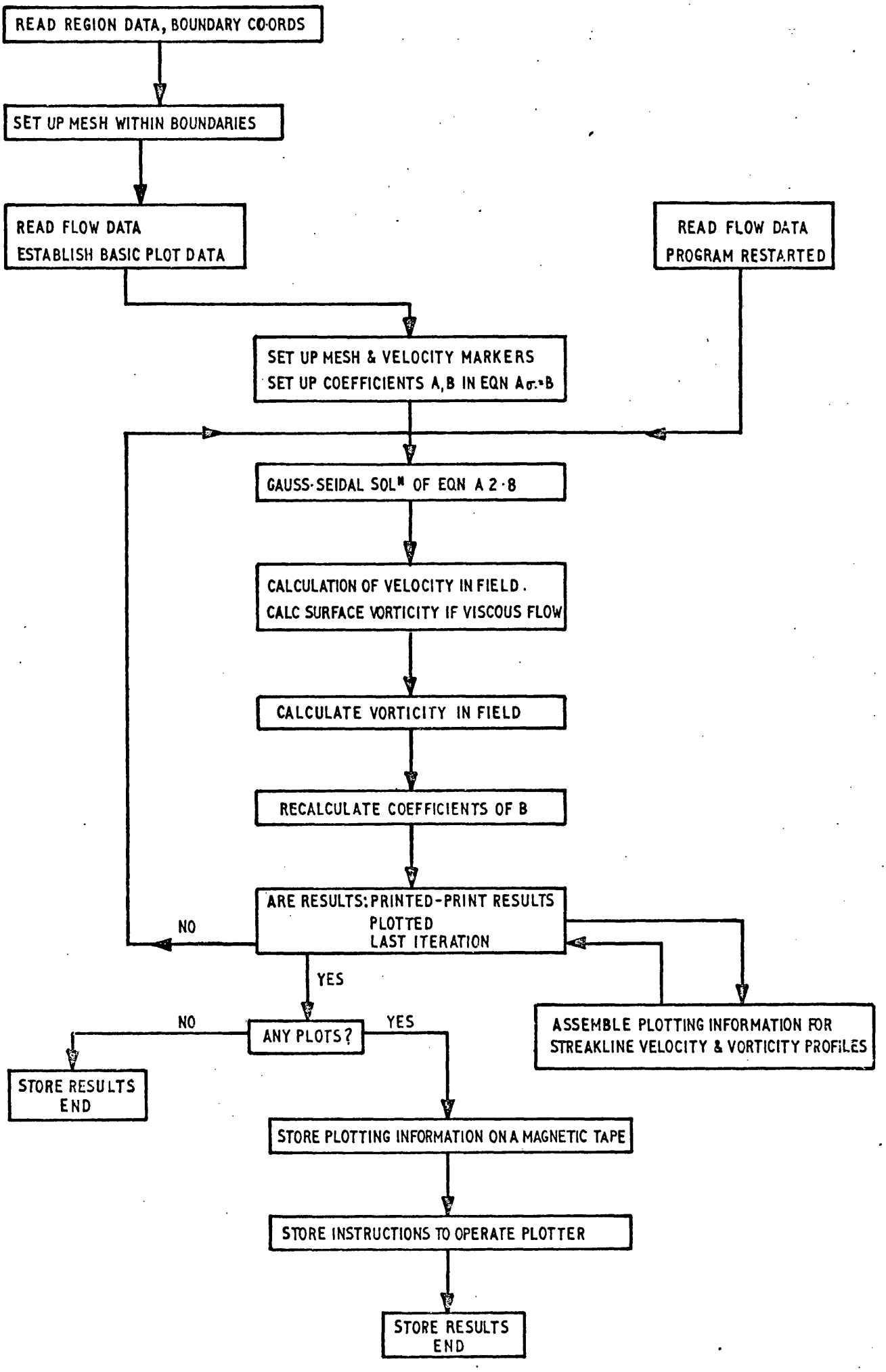

FIG. AII. F1. PROGRAM SUITE FLOW DIAGRAM

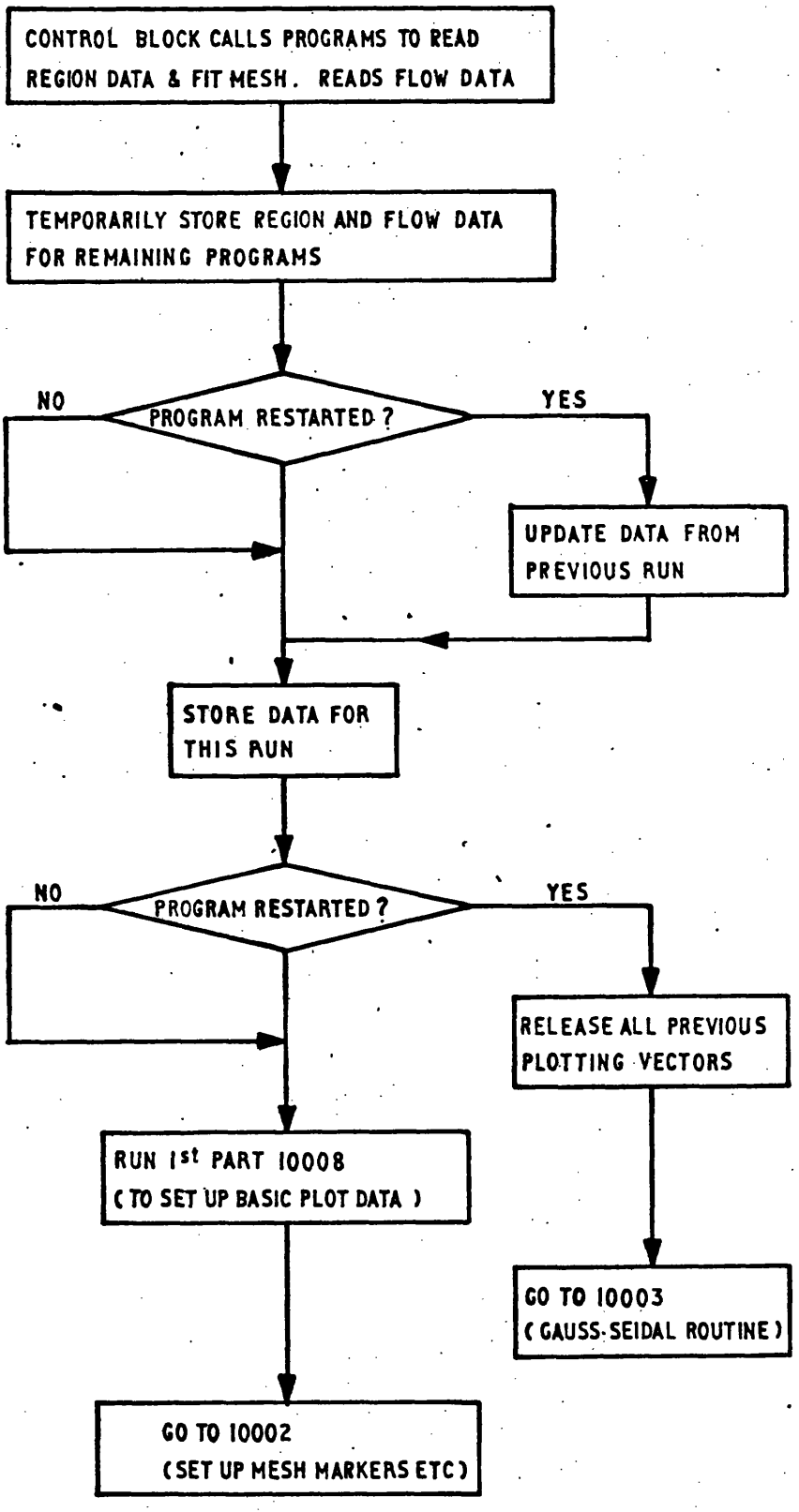

FIG. A11. F2. FLOW DIAGRAM FOR PROGRAM 55

DATA INPUT & MESH CREATION

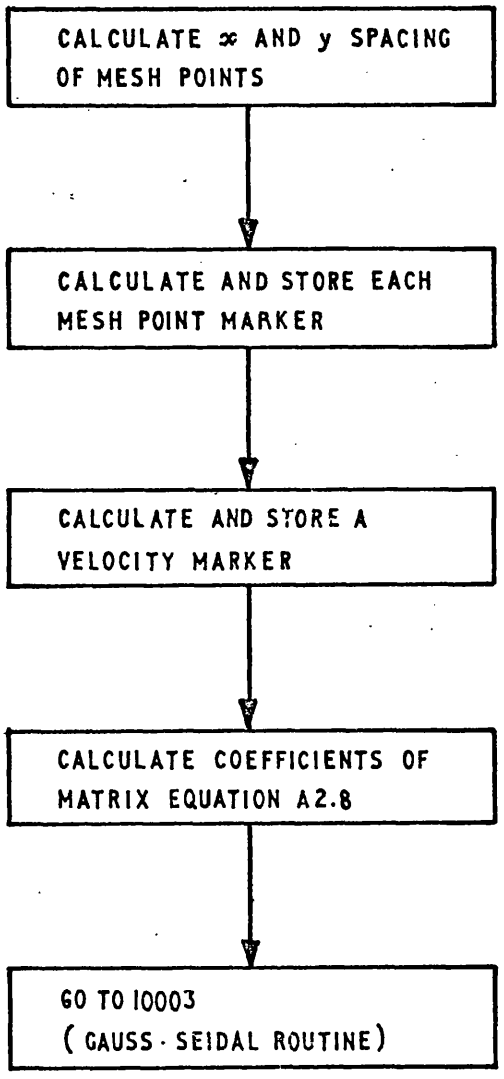

FIG.AII.F3. FLOW DIAGRAM OF 10002
MESH MARKERS & MATRIX OF COEFFICIENTS

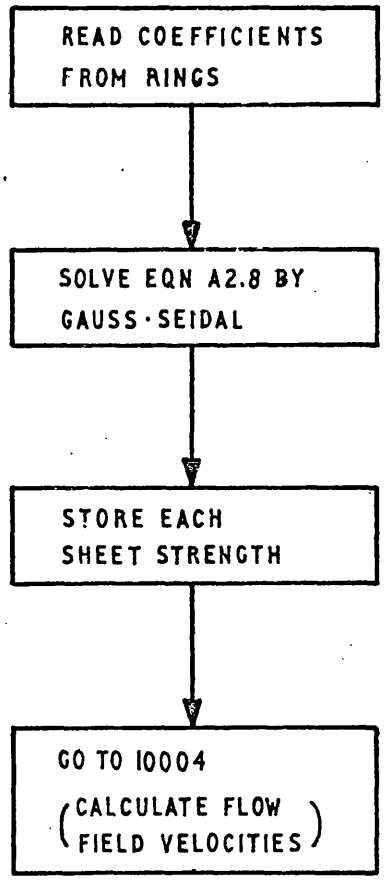

FIG.AII.F4. FLOW DIAGRAM FOR 10003
GAUSS·SEIDAL ROUTINE

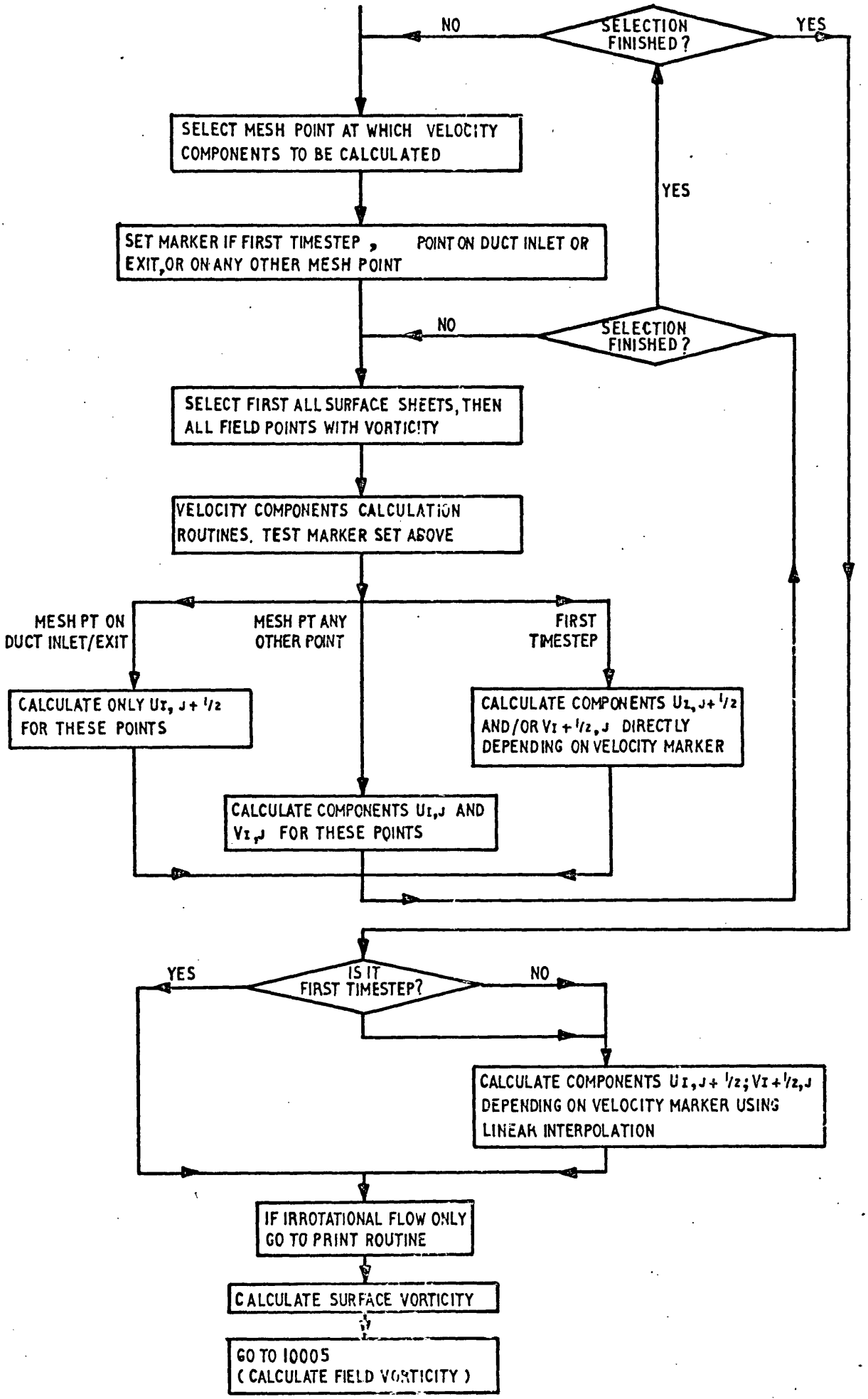

FIG.AII.F5. FLOW DIAGRAM OF 10004

CALCULATION OF VELOCITY COMPONENTS

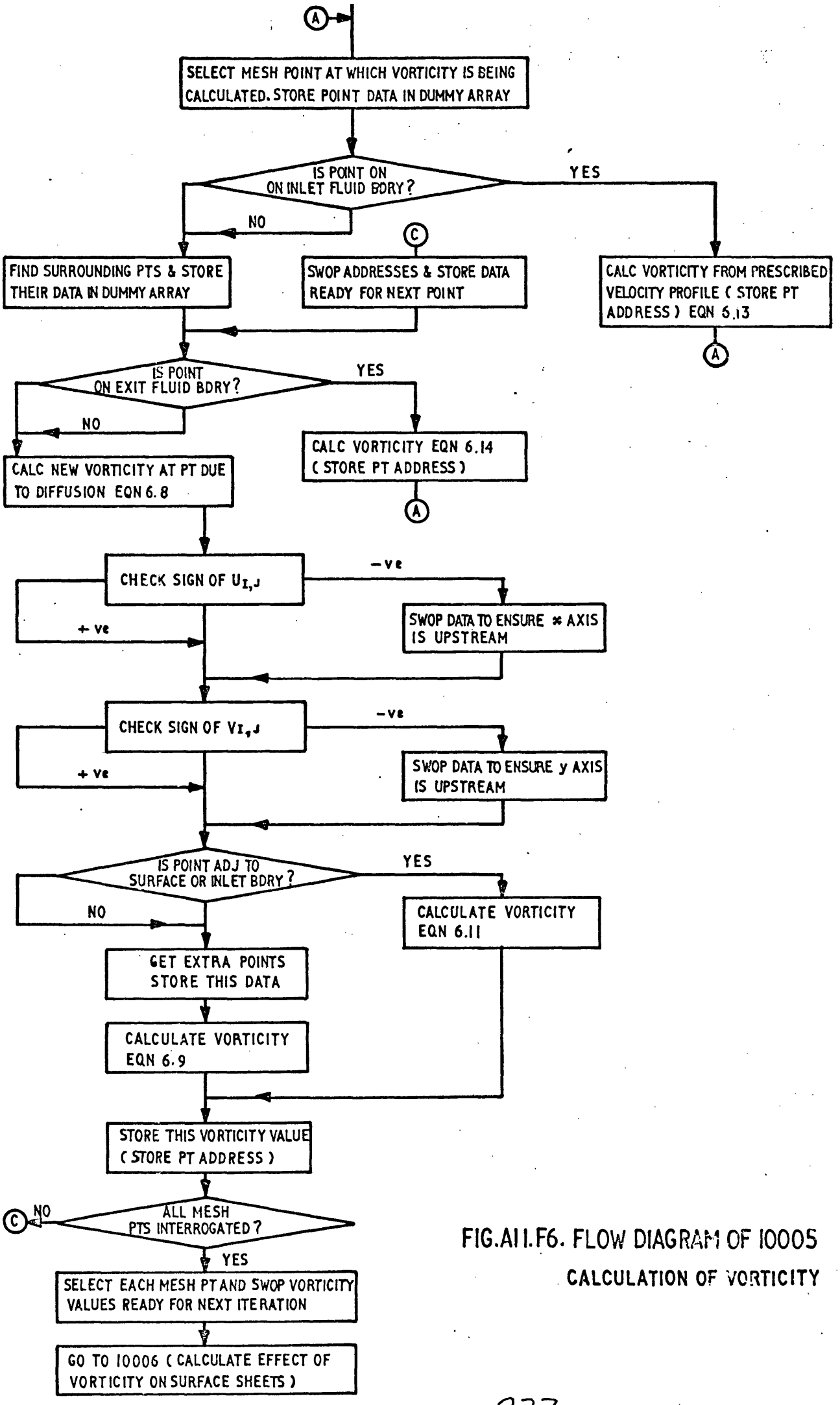

FIG.AII.F6. FLOW DIAGRAM OF 10005
CALCULATION OF VORTICITY

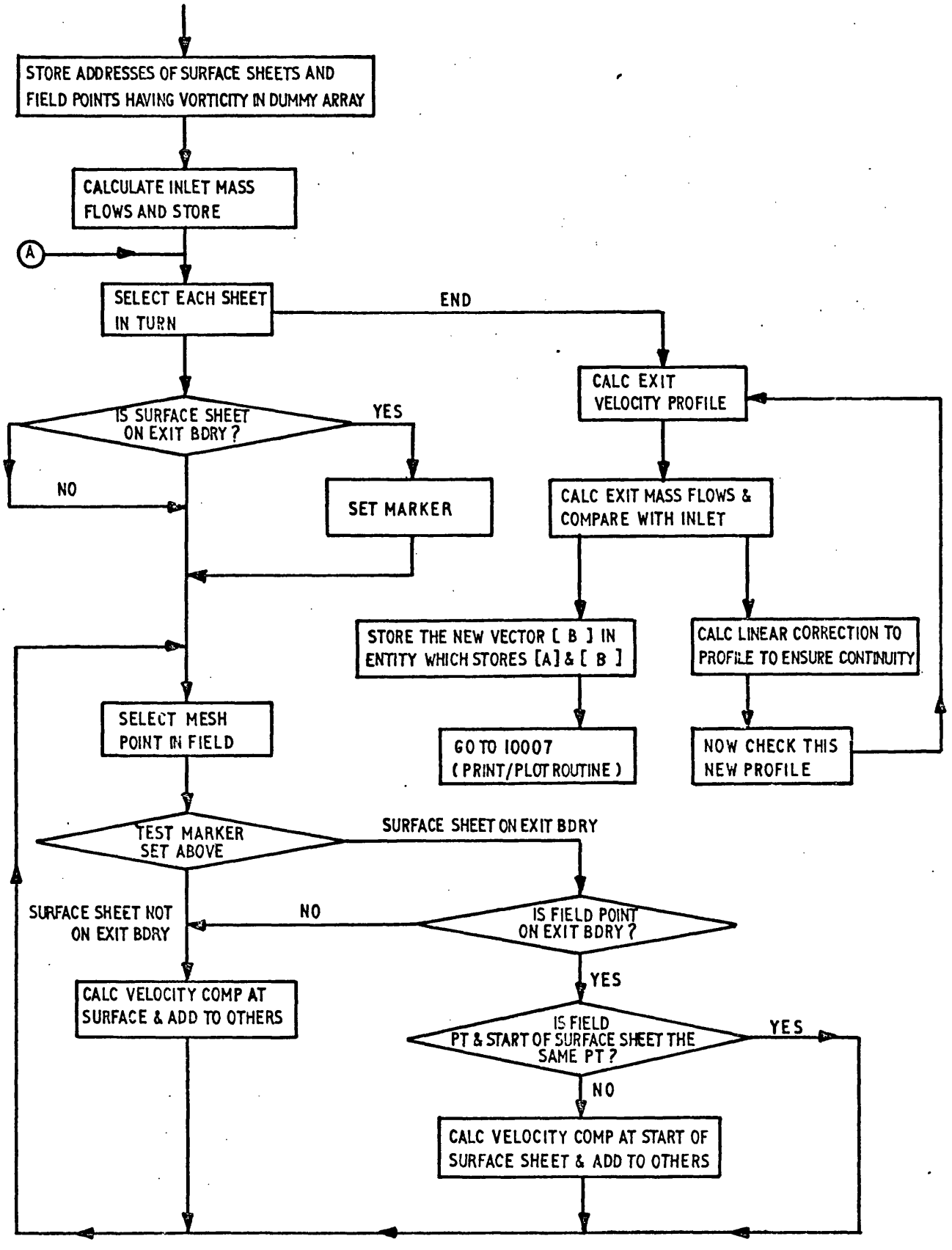

FIG. AII.F7. FLOW DIAGRAM OF 10006

CALCULATION OF EFFECT OF FIELD VORTICITY AROUND SURFACE

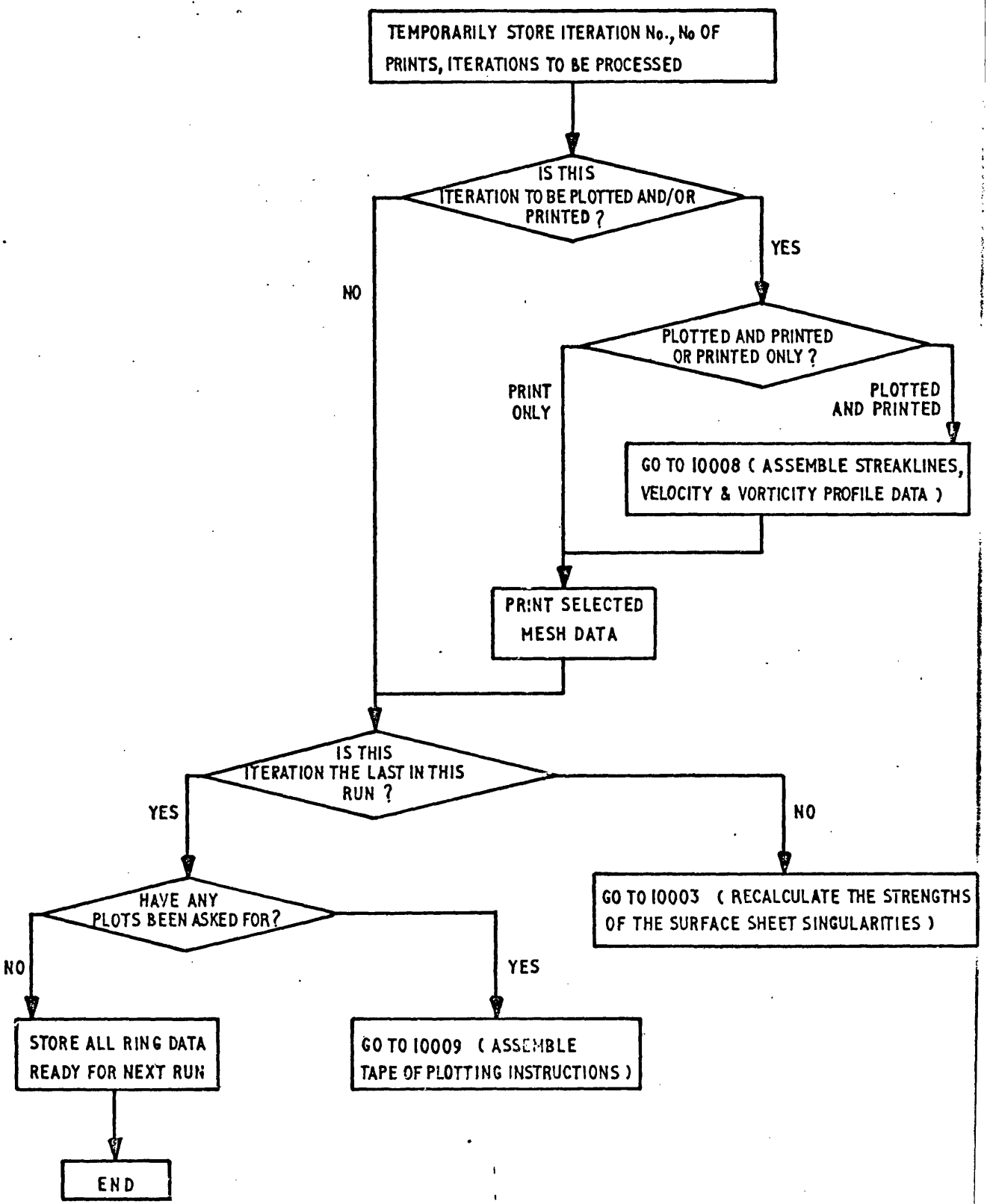

FIG.AII.F8. FLOW DIAGRAM OF 10007 CONTROL PROGRAM

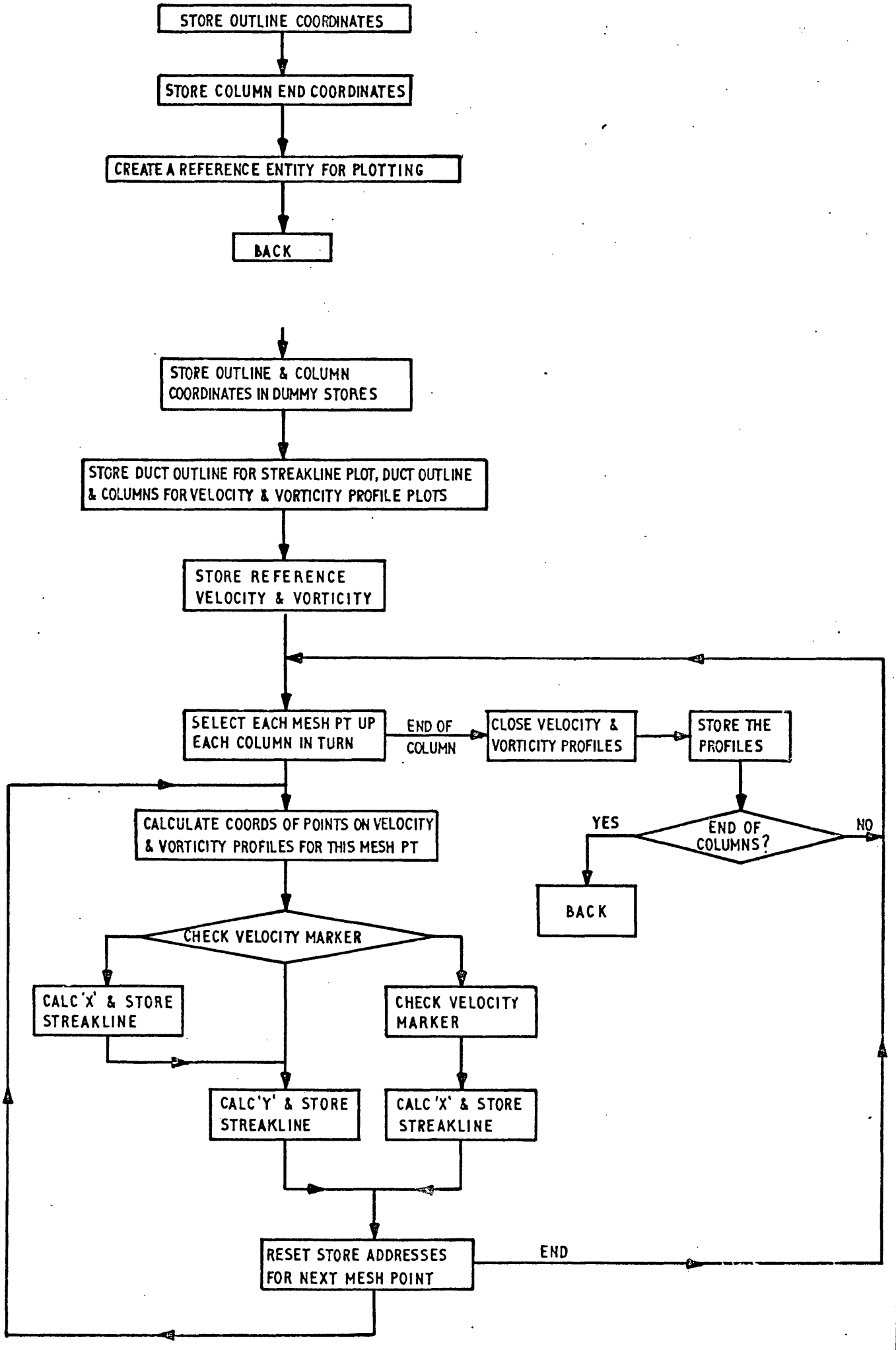

FIG.AII.F9. FLOW DIAGRAM OF 10008
ASSEMBLE PLOTTING CO-ORDINATES

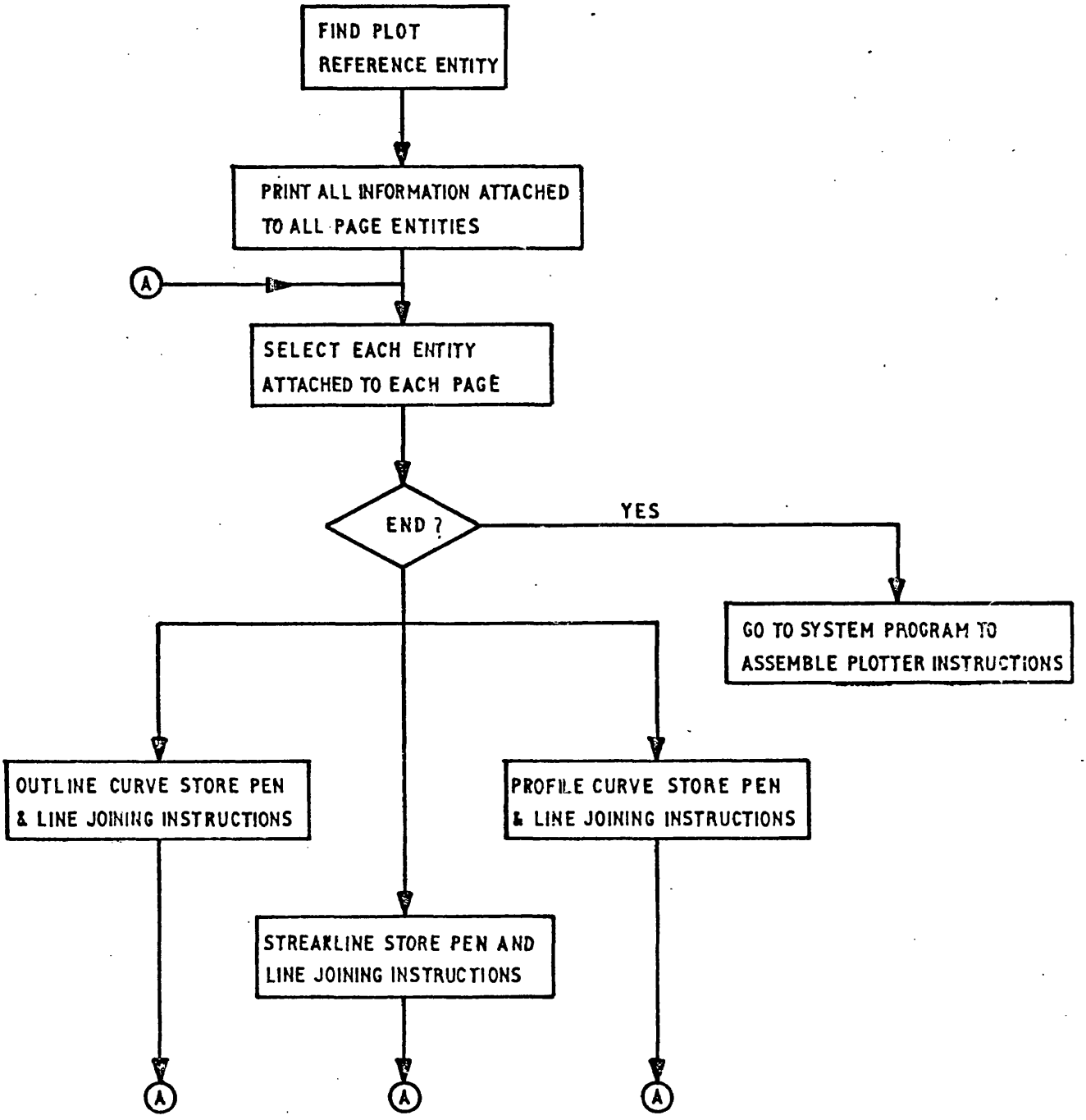

FIG.AII.FIO. FLOW DIAGRAM OF 10009
ASSEMBLE PLOTTING INSTRUCTIONS

DATA INPUT

All the programs written for predicting viscous flows are written in Scheme D Autocode, and use the ring structuring facilities, Dennison (1973), available within the COMET data management system. By structuring the data in rings, any other Scheme D program can easily interrogate the structure, and alter the data accordingly.

The data is fed into the COMET systems by filling out questionaires known as Data Types. These are given a unique number which corresponds with the program which analysises the data. Thus program 50 interrogates the data from Data Type 50, and carries out the users requests indicated by the data he has supplied in using that Data Type.

The input data is stored in a structured form known as a COMET Record, for which a hard copy can be obtained. For this investigation, only the curve definitions describing the boundaries of the flow region were stored on the Record, although other information concerning the flow region could be stored there if necessary.

The ring structure for the mesh, however, is completely distinct from the ring structure for the Record. Program 50 calls the programms to fit the mesh, if required, and these use the Record ring structure to establish the mesh ring structure. All the viscous flow programs use the mesh ring structure.

Three Data Types are used to define a rotational flow problem:-

1) Data Type 50, to define the boundary curves, the flow region and the mesh, fig. All.F11.[286]

2) Data Type 55, to specify the type of flow, flow data and plotting-printing requirements, All. F12.[288]

3) Data Type 52, to recover the flow region from the mesh ring structure, when the computation is restarted, All.F13.[289]

Every Data Type is divided into options, known as rows, which require the user to supply certain specific data. Thus Row 3, Data Type 50, can be used to define any two-dimensional section through an engineering component, by giving the coordinates of points along the curves comprising the section. These points can be joined by either straight lines, circular arcs or parametric cubic spline curves, Fig. A11. F11.[286]

The data chosen to illustrate the use of the three Data Types is for the viscous flow of Reynolds Number = 16 through the duct with a backward facing step, fig. 6.12.[114] The data specifies the duct and region boundaries, information to start the prediction, and has explanatory notes written alongside.

101;50	Control Number 101 indicates a Data Type number is to follow
102;1	Control number 102 indicates an item of data, the first, is to follow.
3;1;1;1	Row 3; Design1; Curve 1; straight lines and circular arcs to define boundary curve.
1.5; 2.7	x;y of 1st point on boundary.
1; 1.5; 3	Joined by a straight line to x; y of 2nd point.
1; 3.6; 3	Joined by a straight line to x; y of 3rd point.
1; 3.6; 2.4 1; 1.9; 2.4 1; 1.9; 2.7	and so on
1; 1.5; 2.7; 3;←	3 to end definition of curve 1. ← signifies end of this Row definition.
5; 1; 1; 1	Row 5; Major Region; Region Number; 1 outer boundary no inner boundaries.

2; 1; 1; 3;←	Design 1, curve 1 form an outer boundary to the region. 3 ends region definition.
6; 1; 16; 1; ∅	Row 6; Region 1; 16 extra data words required (3 already supplied) see fig A10.F1; 1, m, of normal required stored at boundary; tolerance on mesh fitting zero
1; N; M; 2	Cartesian Mesh; N columns; M rows; specified limits of mesh to be given.
1.5; 2.4; 3.6; 3; 1;←	Lower left hand mesh coordinates; upper right hand mesh coordinates; mesh to be automatically spaced.
112;←	Control number 112 signifies end of this Data Type.
101; 55 102;2	Second item of data.
3; 1; 1; 2; 1;←	Row 3; Region 1; Internal flow; Rotational flow; start computation.
4; 1; .09375; .006666667;4	Row 4; Region 1; kinematic viscosity; timestep; 4 iterations in this run
1; 1; 2; 2; 2; 3; 1; 4; 4;←	Plot and print iteration1; Print iterations 2 and 3; Plot and print iteration 4; 4 ends this Row.
112;← 110;←	Control number 110 indicates that specification of data from Data Types has finished.
V_{IN};- V_{OUT}	Specified inlet velocity (uniform distribution only); - exit velocity (negative since it is leaving the region).

This data is typed into a computer disc file using a remote access terminal, and can be used with the programs described in Appendix 10 to have the first four iterations performed. Many iterations will be necessary before convergence has been achieved, with the number of iterations per computer run depending on the run time for each iteration. The data which restarts the prediction is given below, again with explanatory notes alongside.

```
101; 52
102; 1                          First Item of data.
3;1; ←                          Row 3; Region 1 - finds the correct
                                region from the mesh ring structure.

112;←
101;55
102;2
3; 1; 1; 2; 2;                  Row 3; Region 1; Internal flow ;
                                Rotational flow; Restart computations

4; 1; .09375; .006666667;3      Only 3 iterations in this run
1; 3; 4;←                       Plot and print the 3rd iteration only.

112;←
110;←
                                Velocities at inlet and exit are
                                not specified with this data.
```

This data file is used each time a new run is required. When the convergence criteria, given below, is satisfied at each mesh point, a message is printed in the output to the effect that convergence has been achieved, and no more runs are required. The convergence criteria used for the flow predictions was:-

$$\lambda \leq \frac{\omega^n - \omega^{n-1}}{\omega^n}$$

Where λ = .005, Gosman et al (1969).

ROW 3. CREATE NEW CURVES ON COMET RECORD

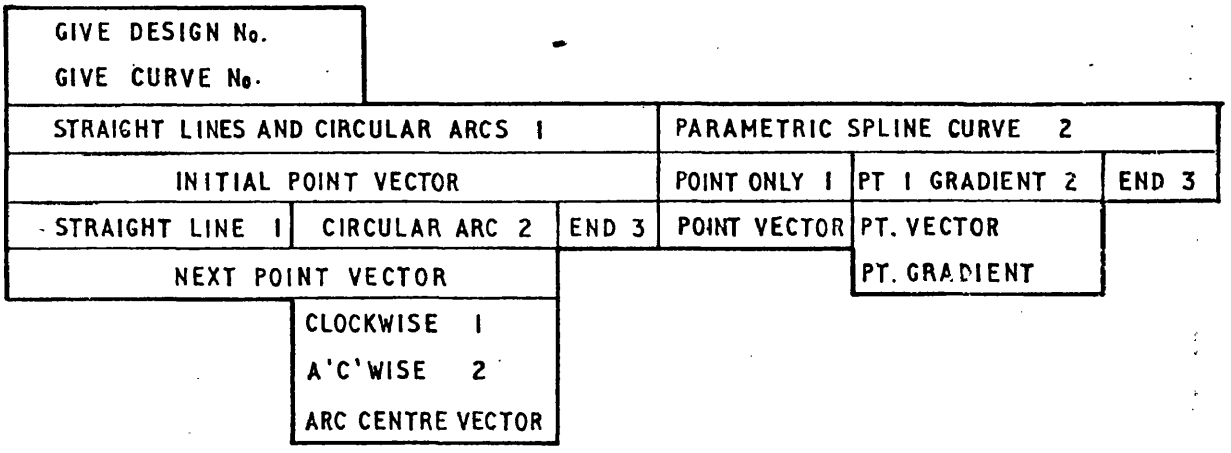

ROW 4. OTHER OPTIONS FOR CURVES ON COMET RECORD

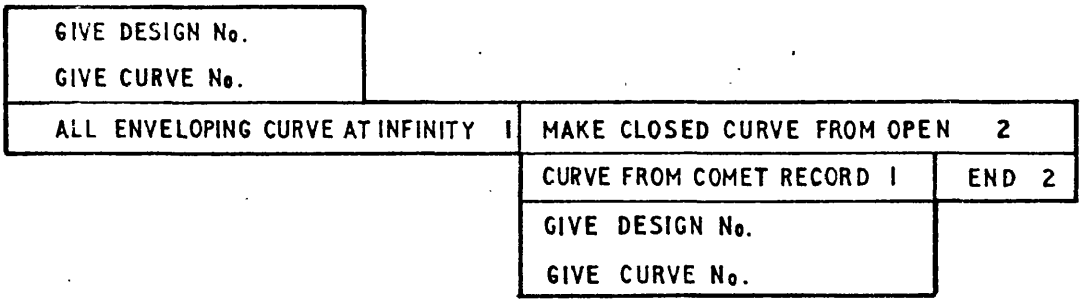

FIG.A11.F11. DATA TYPE 50

(CONTINUED OVERLEAF)

ROW 5. REGION DEFINITIONS REGION Nos. MUST BE UNIQUE

MAJOR REGION 1	SUB-REGION 2
GIVE REGION No. GIVE No. OF INNER & OUTER BDS	GIVE MAJOR REGION No. GIVE OWN REGION No. GIVE No. OF INNER & OUTER BDS.

REGION DEFINED BY FOLLOWING		
INNER BD. 1	OUTER BD. 2	END 3
GIVE DESIGN No. GIVE CURVE No.		

ROW 6. ORTHOGONAL MESH DEFINITION

GIVE REGION No.
GIVE No. OF EXTRA DATA WORDS REQUIRED (DEFAULT VALUE IS Ø)
GIVE 1 IF NORMAL REQUIRED / 2 IF TANGENT (DEFAULT VALUE IS 1)
GIVE TOLERANCE AS PERCENTAGE OF COL/ROW WIDTH (DEFAULT VALUE IS Ø)

2D CARTESIAN MESH 1	2D PLANE POLAR MESH 2
No. OF COLUMNS No. OF ROWS	No. OF RADII No. OF RINGS
AUTOMATIC LIMITS 1	SPECIFIED LIMITS 2 GIVE x_L (2) GIVE x_H (2)
AUTOMATIC SPACING 1	AUTOMATIC & SELECTED SPACING 2

COLUMNS 1	ROWS 2	END 3
COLUMN No GIVE VALUE	ROW No. GIVE VALUE	

FIG.AII. FII. DATA TYPE 50 cont.

ROW 3. SPECIFY PROBLEM
GIVE REGION No.

INTERNAL FLOW	1		EXTERNAL FLOW	2
IRROTATIONAL FLOW ONLY	1	/	ROTATIONAL FLOW ONLY	2
START COMPUTATIONS	1	/	RESTART COMPUTATION	2
			GIVE FREESTREAM VELOCITY	

ROW 4. CONDITIONS APPLIED TO REGION
GIVE REGION No.

GIVE KINEMATIC VISCOSITY			
GIVE TIMESTEP			
GIVE Nº OF ITERATIONS IN THIS RUN			
PLOT & PRINT 1	PRINT ONLY 2	NONE 3	END 4
GIVE ITERATION NUMBER			

FIG. A11.F12. DATA TYPE 55

ROW 3. MUST BE USED BEFORE ANY OTHER ROW .

GIVE REGION N_0.

ROW 4. MESH POINT LABELLING - GIVE LABEL

GIVE CURVE NUMBER 1				END 2
ALONG ROW L TO R 1	ALONG ROW R TO L 2	UP COL 3	DOWN COL 4	END 5
GIVE DISTANCE FROM CURVE IN TERMS OF MESH POINTS (1st MESH PT. IN FROM CURVE IS 1 ETC.)				

ROW 5. FINITE DIFFERENCE EQUATION

GIVE LABEL N_0. OF POINTS AT WHICH EQN IS APPLICABLE & SCAN N_0
EQN SPECIFIED IN SUBRNS 1
GIVE SUBR LABEL
GIVE N_0. PTS REQUIRED IN ADDITION TO WORKING PT X 2
GIVE RELATIVE ADDRESS OF EACH PT TO WORKING PT

ROW 6. BOUNDARY CONDITIONS

GIVE CURVE N_0		
WHOLE CURVE 1	PART CURVE 2 GIVE $P_1(z)$ $P_2(z)$	POINT 3 GIVE $P(z)$
BOUNDARY CONDITIONS SPECIFIED IN SUBROUTINE 1		
GIVE LABEL OF SUBR		
GIVE N_0 PTS REQUIRED IN ADDITION TO WORKING PT		

FIG.A11. F13. PART OF DATA TYPE 52

The Scheme D coding for the following programs is included:

Program 1, loads all subsequent programs onto a magnetic tape,

Program 55,

Programs 10002 to 10009.

```
        ␣␣/Z/␣␣
        ␣␣TSG␣␣
        PROG0381
        00001
        OUTU(FOCDW98)
        END
        ␣␣

        1000;␣␣

        ␣␣FTS␣␣
        ␣␣G/R␣␣
        00055
        OBJTpROG(2500)
        L/LINDEX(1134)
        TEXSTORE(430)
        CONSTORE(100)
        D-STORES(350)
        A-STORES(12200)
        W-STORES(3500)
        N-STORES(350)
        COMMENT=THIS CONTROL BLOCK USES LABELS 1-31
        DATA IS GIVEN IN D0A(6)
        C IS USED TO JUMP TO USERS LABEL
        ALL OTHER INTERGERS ARE RESTORED TO USERS VALUES
        THE FIRST 52 N-STORES ARE USED TO STORE INTEGERS␣
        3.L=INT'A10
        'W0=0
        TEXT=
        JOB NUMBER␣
        PRINT(90)='A3(1)
        'D101=L
        24.L='D101
        'D51=INT'A2L
        0=RINT(&4*FRAC('A2L*10))
        'D47(2)='A3L(2)
        'D64='D51-55
        J'D64.12.25.12
        25.0=INT'A1Q
        'D52=INT'A20
        J'D52.36.12.0
        26.TEXT=
        DATA TYPE␣
        PRINT(30)='D51(1)
        TEXT=
        ITEM NUMBER␣
        PRINT(30)='D52(1)
        'D78(2)='D51(2)
        R=INT(D47+&-10)
        JR.1.2.0
        9.N126(26)=A(26)
        C=R
        A=195+V
        B=P
        D(23)=N103(23)
        JSC
        N100(26)=A(26)
        A(26)=N120(26)
        EXIT
```

```
        1.JS9
        2.Q=RINT(&4*FRAC('A2Q*10))
        10.Q=INT'A1Q
        N=0
        'D40=INT'A2Q
        'D53='D40
        J'D40.11.15.11
        11.R=INT(D48+&-10)
        JR.4.5.0
        4.JS9
        5.N=RINT(&4*FRAC('A2Q*10))
        U(2)=0
        16.M=INT'A1M
        'D54=INT'A2M
        J'D54.17.14.16
        17.S=RINT(&4*FRAC('A1M*10))
        T=S
        27.'D150U=10*FRAC'A0S
        P=INT(10*FRAC'D150U)
        'D64=INT'D150U(.5-P)
        J'D64.22.23.21.
        21.P=S+P
        P='A0P
        22.P=P+INT'D150U
        'D195V(P)='A1S(P)
        COMMENT='MISSING DATA
        23.'D106U=P
        R=INT(&3*FRAC((D150U+&-8)*10))
        JR.29.18.0
        29.JS9
        18.S=S+P+1
        U=U+1
        V=V+P
        'D64=INT'A3M-S+T
        J'D64.27.13.0
        13.U=U-1
        V=V-RINT'D106U
        R=RINT(&3*FRAC((D150U+&-8)*&4))
        JR.30.28.0
        30.JS9
        28.JU.13.16.0
        14.R=RINT(&3*FRAC(D48+&-10))
        JR.6.10.0
        6.JS9
        J10
        15.R=RINT(&3*FRAC(D47+&-10))
        JR.7.8.0
        7.JS9
        8.D64=INT'A2Q
        J'D64.20.19.20
        20.Q=RINT(&4*FRAC('A0Q*10))
        19.Q=RINT(&4*FRAC('A0Q*10))
        J25
        12.L='D101
        L=INT'A1L
        'D101=L
        'D64=INT'A2L
        J'D64.24.31.0.
        31.TODISC
        BACK
```

```
.18     COMMENT=END OF CONTROL BLOCK↵

.19     398.TEXT=BEGIN ITEM
.20     ↵
.21     START
;22     FURTHR(RINGS001/'A5000)
;23     EXIT
;24     99.EXIT
;25     101.TEXT=VISCOUS INCOMPRESSIBLE FLUID FLOW SOLUTION
;26     ↵
127     GET(95/1/1/Z)
128     D(2)=0
129     SEARCH(Z/1/Y/0/'D0A)            #FIND REGION KEA
130     JY.99.201.0
131     201.TEXT=
132     REGION NOT FOUND↵
133     J0
134     102.'W0;='D0A-1          #INTERNAL FLOW
135     J'W0.202.207.0
136     202.'W0;='D1A-1          #ROTATIONAL
137     J'W0.203.204.0
138     203.TEXT=
139     INTERNAL--ROTATIONAL--RESTART↵
140     'W101D(B)='D0A(B)
141     WRITE='W101D(B)
142     D;=D+B
143     EXIT
144     204.TEXT=
145     INTERNAL--ROTATIONAL--START↵
146     'W101D(B)='D0A(B)
147     WRITE='W101D(B)
148     D;=D+B
149     EXIT
150     207.'W0;='D1A-1          #IRROTATIONAL ONLY
151     J'W0.208.209.0
152     208.TEXT=
153     INPUT DATA INCORRECT CANNOT RESTART AN 'IRROTATIONAL ONLY'(
154     )OPTION↵
155     J0
156     209.TEXT=
157     INTERNAL--IRROTATIONAL ONLY--START↵
158     'W101D(B)='D0A(B)
159     WRITE='W101D(B)
160     D;=D+B
161     EXIT
162     103.TEXT=
163     EXTERNAL FLOW OPTIONS NOT AVAILABLE AT PRESENT↵
164     J0
165                     #USE LABELS 212-219 INCLUSIVELY

166     110.'W101D(3)='D1A(3)           #STORE REGION INFORMATION
167     'W98;='D0A
168     WRITE='W101D(3)
169     D;=D+3
170     'W100;=D  #STORE NO OF DATA ITEMS BEFORE OUTPUT INFORMATION
171     EXIT
172     111.'W102D;='D0A                #PLOT/PRINT REQUEST
173     D;=D+1
174     E;=E+1
```

```
175     EXIT
176     112.'W102D;=-'D0A                    #PRINT ONLY REQUEST
177     D;=D+1
178     E;=E+1
179     EXIT
180     113.E;=0                    #NO PRINT REQUESTS
181     EXIT

182     #INSERT HERE OPTIONS FOR CURVE + POINT BOUNDARY CONDITIONS


183     399.TEXT=END ITEM
184
185     D;='W100
186     'W101D;=E
187     'W0;='W102-1
188     J'W0.301.305.0
189     301.E(2)=0                   #PROGRAM RESTARTED
190     ENTSTP(Y/4/F/G/4/D)
191     ENDATA(F/0/U)
192     H;=U+INT('A5001U)+1
193     'W100D;='W100D+'A5000H
194     H;=H+1
195     J;=D
196     302.'W102J;=SIGN('W102J)('A5000H+ABS('W102J))
197     J;=J+1
198     J302(E)
199     'W99;='A5000H+1              #STORE CURRENT ITERATION NO
200     TAKE(Y/4/F/G)
201     FREE(F)
202     J306
203     305.'W99;=1
204     306.H;=D+E+4
205     CHAD(90/H)
206     0;=INT('W98)
207     MAKE(90/0/G/F)
208     PUTEND(Y/4/F/1) #RECREATE ENTITY TO HOLD REGION INFORMATION
209     ENDATA(F/0/U)
210     'A50000;='W98                #REGION NUMBER
211     D;=D+1
212     E;=E+1
213     'A5001U(D)='W100(D)                  #STORE BASIC REGION DATA
214     WRITE='A5001U(D)
215     0;=0+D
216     'A50010;='W99
217     'A50020(E)='W100D(E)
218     WRITE='A50020(E)                     #STORE PLOT/PRINT REQUESTS
219     'W0;='W102-1
220     J'W0.307.320.0               #IF RESTART--FREE PLOT ENTITIES
221     307.I(4)=0
222     ENTSTP(Y/3/I/J/1/0)
223     ENTSTP(I/2/K/L/1/0)                  #GET PLOTTING REFERENCE ENTITY
224     ENTR(K/1/N)                  #NUMBER OF PAGE ENTITIES
225     JN.310.316.0
226     310.P(8)=0 #FREE ALL PREVIOUS PAGE/VECTOR PLOTTING ENTITIES
227     X;=-1
228     311.ENTSTP(K/1/P/0/1/0)
229     J311(N)
230     312.ENTR(P/1/N)              #NUMBER OF VECTOR ENTITIES
231     T(2)=0
```

```
232     313.ENTSTR(P/1/T/U/1/U)
233     J313(H)
234     314.V(2)=T(2)
235     ENTSTP(P/1/T/U/X/U)
236     TAKE(P/1/V/1)
237     FREE(V)
238     J314(H)
239     R(2)=P(2)
240     ENTSTP(K/1/P/U/X/U)
241     TAKE(K/1/R/1)
242     FREE(R)
243     J312(H)
244     316.TODISC
245     START
246     FURTHR(RINGS001/'A0)
247     FSP(1)
248     MPC(15)
249     OUT(10003000)

250     320.TODISC
251     START
252     FURTHR(RINGS001/'A0)
253     FSP(1)
254     MPC(15)
255     RUN(10008000)           #RUN 10008 TO ESTABLISH PLOT BASIC DATA
256     OUT(10002199)
257
258     1000;
259
```

```
1       ␣␣FT/␣␣
2       ␣␣GSR␣␣
3       10002
4       OBJTPROG(2500)
5       L/LINDEX(1134)
6       TEXSTORE(430)
7       CONSTORE(100)
8       D-STORES(350)
9       A-STORES(7200)
10      W-STORES(6100)
11      N-STORES(350)
12      199,A(24)=0
13      W/O TEST
14      RESTART(0)
15      #TEXT=
16      #FROMN MARKER ROUTINE
17      202,ENTSTP(Y/1/W/X/1/0) #COLUMN ENTITY KEA/AE IN W/X
18      W;=W
19      JW,203,310,0
20      203,U(2)=0
21      204,ENTSTP(W/1/U/V/1/0) #COLUMN INTERSECTION KEA/AE IN U/V
22      U;=U
23      JU,205,202,0
24      205,A(2)=0
25      206,ENTSTP(U/1/A/B/1/0) #MESH POINT KEA/AE IN A/B
26      A;=A
27      ENDATA(A/0/0)
28      A00(2)=A10(2)
29      A20(17)=0

30      215,ENTR(U/1/F) #IS NUMBER OF MESH POINTS JOINED TO U GT 1
31      G;=F-1
32      JG,207,204,0
33      207,F;=0
34      Q(4)=0
35      RNGSTP(A/2/Q/R/1/0) #A ROW INTERSECTION POINT KEA/AE IN Q/R
36      208,ENTSTP(Y/2/S/T/1/0)          #ROW ENTITY KEA/AE IN S/T
37      JS,209,212,0
38      209,C(2)=0
39      210,ENTSTP(S/1/C/D/1/0) #ROW INTERSECT POINT KEA/AE IN C/D
40      JC,211,208,0
41      211,0;=Q-C #DOES THIS R,I,P, CORRESPOND TO ROW CONTAINING A
42      J0,210,220,210
43      212,TEXT=CANNOT FIND ROW INTERSECTION POINT CORRESPONDING TO
44      ROW CONTAINING THE MESH POINT KEA/AE A/B␣
45      J0

46      220,C(2)=U(2) #FIND + STORE NEXT COLUMN INTERSECTION POINT
47      E(2)=0
48      ENTSTP(W/1/C/D/1/0)
49      ENTSTP(C/1/E/F/1/0) # KEA/AE OF MESH PT ATTACHED TO NEXT I.P
50      221,ENTSTP(U/1/A/B/1/0) #FIND NEXT VERTICAL MESH POINT
51      G(2)=0
52      RNGSTP(A/2/G/H/1/0) # ROW I.P FOR THIS NEW MESH POINT
53      222,ENTSTP(Y/2/S/T/1/0)          #FIND NEXT ROW ENTITY
54      JS,223,212,0
55      223,I(2)=0
56      224,ENTSTP(S/1/I/J/1/0)          #ROW I.POINT
57      JI,225,222,0
```

```
58      225.0;=I-G
59      J0.224.226.224
60      226.0;=E-A #IS MESH POINT ALSO ATTACHED TO NEXT C.I.P
61      J0.230.275.230

62      230.Q(2)=0                  #NO--
63      231.ENTSTP(S/1/Q/R/1/0)             #SELECT R.I.P
64      JQ.232.255.0
65      232.I(2)=0
66      ENTSTP(Q/2/I/J/1/0) #SELECT MESH POINT ATTACHED TO R.I.P
67      0;=I-A              #IS MESH POINT ALSO ATTACHED TO A R.I.P
68      J0.231.235.231
69      235.G(2)=W(2)               #YES--
70      ENTSTP(Y/1/G/H/1/0) #IS COL ENT LAST IN COL ENTITY RING
71      JG.240.250.0
72      240.G(2)=0                  #NO--
73      ENTSTP(Y/1/G/H/1/0) #IS COL ENT FIRST IN COL ENTITY RING
74      0;=G-W
75      J0.245.241.245
76      241.G;=-1                   #YES--DUCT INLET SECTION
77      H(2)=A(2)
78      ENTSTP(U/1/H/I/G/0) #FIND PREVIOUS VERTICAL MESH POINT
79      ENDATA(H/0/I)
80      JA9I.243.242.243
81      242.ENDATA(A/0/I)
82      A0I(2)=A1I(2)
83      A2I(17)=0
84      A9I;=1
85      #WRITE=A0I(19)
86      J221
87      243.ENDATA(A/0/I)
88      A0I(2)=A1I(2)
89      A2I(17)=0
90      A9I;=-2
91      #WRITE=A0I(19)
92      J221

93      245.ENDATA(A/0/I) #NO--COL ENT NOT FIRST, STEP MET
94      A0I(2)=A1I(2)
95      A2I(17)=0
96      ENDATA(Q/0/0)
97      #WRITE=A00(6)
98      W0;=3-A10 #CHECK CONTINUATION MARKER FOR LEFT-HAND ENT
99      JW0.221.246.0
100     246.G;=-1                   #RESET L.H ENTITY FN MARKER TO -1
101     ENTSTP(S/1/Q/R/G/0)
102     H;=A
103     I;=2
104     ENTSTP(Q/2/H/I/G/0)
105     ENDATA(H/0/I)
106     A9I;=-1
107     #WRITE=A0I(19)
108     J221

109     250.ENDATA(A/0/I) #YES--COL ENT IS LAST -DUCT EXIT
110     A0I(2)=A1I(2)
111     A2I(17)=0
112     A9I;=2
113     A15I;=1
114     #WRITE=A0I(19)
```

```
115     Q(2)=0
116     602,ENTSTP(S/1/Q/R/1/0)
117     J0,603,212,0
118     603,I(2)=0
119     604,ENTSTP(Q/2/I/J/1/0)
120     PRINT(1060)=I(1)
121     JI,605,602,0
122     605,0;=I-A
123     J0,604,606,604
124     606,G;=-1
125     ENTSTP(Q/2/I/J/G/0)
126     ENDATA(I/0/0)
127     W0;=A90+1
128     JW0,0,221,600
129     600,A90=3
130     J221

131     255,G;=-1 #NO--MESH PT NOT ATTACHED TO R.I.P
132     H(2)=A(2)
133     ENTSTP(0/1/H/I/G/0) #CHECK PREVIOUS VERT MESH PT FM
134     ENDATA(H/0/0)
135     JA90,257,256,257
136     256,ENDATA(A/0/I)
137     A0I(2)=A1I(2)
138     A2I(17)=0
139     A9I;=-1
140     #WRITE=A0I(19)
141     J221
142     257,Q(2)=0
143     258,ENTSTP(S/1/Q/R/1/0)
144     G(2)=0
145     259,ENTSTP(Q/2/G/H/1/0) #FIND R.I.P WITH THIS MESH PT
146     JG,263,258,0
147     263,0;=G-A
148     J0,259,264,259
149     264,G;=-1
150     H;=A
151     I;=2
152     ENTSTP(Q/2/H/I/G/0)
153     ENDATA(H/0/0)
154     W0;=3-ABS(A90)
155     JW0,265,267,0
156     265,W0;=1+A90
157     JW0,266,267,266
158     266,W0;=2+A90
159     JW0,269,268,0
160     267,ENDATA(A/0/I)
161     A0I(2)=A1I(2)
162     A2I(17)=0
163     A9I;=-3
164     #WRITE=A0I(19)
165     J221
166     268,ENDATA(A/0/I)
167     A0I(2)=A1I(2)
168     A2I(17)=0
169     A9I;=3
170     #WRITE=A0I(19)
171     J221
172     269,ENDATA(A/0/I)
173     A0I(2)=A1I(2)
```

```
174     A2I(17)=0
175     A9I;=-1
176     #WRITE=A0I(19)
177     J221

178     275,ENDATA(A/0/I) #YES--MESH PT ATTACHED TO NEXT C.I.P.
179     A0I(2)=A1I(2)
180     A2I(17)=0
181     Q(2)=0
182     276,ENTSTP(S/1/Q/R/1/U)          #SELECT R.I.P
183     JQ,277,286,0
184     277,G(2)=0
185     ENTSTP(Q/2/G/H/1/0)
186     0;=G-A            #IS MESH POINT ALSO ATTACHED TO A R.I.P
187     JO,276,278,276
188     278,G;=-1                  #YES--
189     H(2)=A(2)
190     ENTSTP(U/1/H/I/G/U)
191     ENDATA(H/0/U)
192     W0;=A90+2 #IF DUCT INLET,RESET FM MARKER OF ENT BELOW
193     JW0,280,279,280
194     279,A90;=1
195     #WRITE=A00(19)
196     J298
197     280,G(2)=W(2)
198     ENTSTP(Y/1/G/H/1/U) #IS THIS MESH PT ON DUCT EXIT
199     JG,286,285,0
200     285,ENDATA(A/0/I) #YES--SET SOURCE SHEET MARKER
201     A15I;=1
202     #WRITE=A0I(19)
203     J288
204     286,G;=-1 #NO--MESH POINT NOT ATTACHED TO R.I.P
205     H(2)=A(2)
206     ENTSTP(U/1/H/I/G/U)
207     ENDATA(H/0/U)
208     JA90,287,288,287
209     287,A90;=-1
210     #WRITE=A00(19)
211     288,ENDATA(C/0/U)                #CHECK FOR L.H. ENTITY
212     #WRITE=A00(6)
213     JA10,289,298,0
214     289,W0;=A10-1
215     JW0,290,298,0
216     290,Q(2)=0 #L.H MESH PT PRESENT-FIND R.S OF R.I.P FOR A
217     291,ENTSTP(S/1/Q/R/1/U)
218     G(2)=0
219     292,ENTSTP(Q/2/G/H/1/U)
220     JG,293,291,0
221     293,0;=G-A
222     JO,292,296,292
223     296,G;=-1                  #CHECK FM OF LH MESH POINT
224     H;=A
225     I;=2
226     ENTSTP(Q/2/H/I/G/U)
227     ENDATA(H/0/U)
228     JA90,297,298,297
229     297,A90;=-1
230     #WRITE=A00(19)
231     298,U(2)=C(2)              #RESET C.I.P MARKERS
232     J215
```

```
233     310,A(24)=0 #ALLOCATE VELOCITY MARKERS TO EACH MESH PT
234     W/O TEST
235     #TEXT=
236     #VELOCITY MARKER ROUTINE
237     320,ENTSTP(Y/1/N/X/1/0)          #COLUMN ENTITY
238     JW.321.520.0
239     321,U(2)=0
240     322,ENTSTP(W/1/U/V/1/0)          #FIND C.I.P.
241     JU.323.320.0
242     323,A(2)=0
243     ENTSTP(U/1/A/B/1/0)              #FIND FIRST MESH POINT
244     Q(4)=0
245     RNGSTP(A/2/Q/R/1/0)              #R.I.P ADDRESS IN Q
246     325,ENTSTP(Y/2/S/T/1/0)          #ROW ENTITY
247     JS.326.329.0
248     326,C(2)=0
249     327,ENTSTP(S/1/C/D/1/0)
250     JC.328.325.0
251     328,0;=Q-C #CHECK FOR CORRECT ROW ENTITY USING R.I.P.'S
252     J0.327.332.327
253     329,TEXT=CANNOT FIND R.I.P. CORRESPONDING TO MESH POINT A/B_
254     J0

255     332,ENTR(U/1/0)
256     0;=0-1          #CHECK NO MESH POINTS GT 1
257     J0.350.333.0
258     333,ENDATA(U/0/0)
259     W0;=A00-2                #CHECK IF RH ENTITY
260     JW0.334.334.342
261     334,Q(2)=0               #YES--
262     335,ENTSTP(S/1/Q/R/1/0)
263     C(2)=0
264     336,ENTSTP(Q/2/C/D/1/0)          #FIND CORRECT R.I.P.
265     JC.337.335.0
266     337,0;=C-A
267     J0.336.340.336
268     340,ENTSTP(Q/2/C/D/1/0)
269     JC.150.335.0
270     150,ENDATA(C/0/0)                #CHECK FM OF R.H. ENTITY
271     JA90.341.342.341
272     341,ENDATA(A/0/0)
273     A140;=1
274     #WRITE=A00(19)
275     J322
276     342,ENDATA(A/0/0)
277     A140;=-1
278     #WRITE=A00(19)
279     J322

280     350,C(2)=A(2)            #NUMBER OF MESH PTS GT 1
281     351,ENTSTP(U/1/C/D/1/0)
282     JC.352.322.0
283     352,Q(2)=0
284     353,ENTSTP(S/1/Q/R/1/0) #CHECK IF THIS IS ALSO A R.I.P.
285     J0.354.390.0
286     354,E(2)=0
287     ENTSTP(Q/2/E/F/1/0)
288     0;=E-A
```

```
289     JO.353.358.353
290     358.E(2)=0                  #YES--IT IS AN R.I.P.
291     ENTSTP(Y/1/E/F/1/O)
292     O;=W-E
293     JO.368.361.368
294     361.ENDATA(Q/0/O) #COL ENT IS FIRST--DUCT INLET
295     W0;=A00-2
296     JW0.362.362.364
297     362.E;=A
298     F;=2
299     ENTSTP(Q/2/E/F/1/O)
300     ENDATA(E/0/O)               #CHECK RH MESH POINT FM
301     JA90.363.364.363
302     363.ENDATA(A/0/O)
303     A140;=0
304     A150;=1
305     #WRITE=A00(19)
306     J395
307     364.ENDATA(A/0/O)
308     A140;=2
309     A150;=1
310     #WRITE=A00(19)
311     J395

312     368.ENDATA(Q/0/O)                   #COL ENTITY NOT FIRST
313     W0;=A00-2
314     JW0.369.369.385
315     369.E;=A
316     F;=2
317     ENTSTP(Q/2/E/F/1/O)
318     ENDATA(E/0/O)               #CHECK RH MESH POINT FM
319     JA90.370.378.370
320     370.G(2)=S(2)
321     ENTSTP(Y/2/G/H/1/O)
322     I(2)=0
323     371.ENTSTP(G/1/I/J/1/O)
324     JI.372.374.0
325     372.K(2)=0
326     ENTSTP(I/2/K/L/1/O)
327     O;=K-C
328     JO.371.373.371
329     373.ENDATA(A/0/O) #MESH PT ABOVE IS ALSO A R.I.P.
330     A140;=1
331     #WRITE=A00(19)
332     J395
333     374.ENDATA(A/0/O) #MESH PT ABOVE IS NOT A R.I.P.
334     A140;=0
335     #WRITE=A00(19)
336     J395

337     378.G(2)=S(2)
338     ENTSTP(Y/2/G/H/1/O)
339     I(2)=0
340     379.ENTSTP(G/1/I/J/1/O)
341     JI.380.382.0
342     380.K(2)=0
343     ENTSTP(I/2/K/L/1/O)
344     O;=K-C
345     JO.379.381.379
346     381.ENDATA(A/0/O) #MESH PT ABOVE IS A R.I.P.
```

```
347     A140;=-1
348     #WRITE=A00(19)
349     J395
350     382,ENDATA(A/0/U)                    #MESH PT ABOVE IS NOT A R.I.P.
351     A140;=2
352     #WRITE=A00(19)
353     J395

354     385,E(2)=W(2)                #NO RH MESH POINT
355     ENTSTP(Y/1/E/F/1/0)
356     JE,378,386,0
357     386,ENDATA(A/0/0)
358     A140;=2
359     #WRITE=A00(19)
360     J395

361     390,ENDATA(A/0/U) #NO--MESH POINT A IS NOT A R.I.P.
362     JA90,391,392,391
363     391,A140;=0
364     #WRITE=A00(19)
365     J395
366     392,A140;=2
367     #WRITE=A00(19)

368     395,A(2)=C(2)
369     ENTSTP(Y/2/S/T/1/0)
370     J351



371     520,B(23)=0                  #SET MESH SPACINGS
372     A;=1
373     J522
374     521,A;=A+1
375     B(2)=0
376     522,ENTSTP(Y/A/B/C/1/0)
377     JB,523,531,0
378     523,D(2)=0
379     524,ENTSTP(B/1/D/E/1/0)
380     JD,525,522,0
381     525,ENTR(D/A/F)
382     F;=F-1
383     JF,526,524,0
384     526,G(2)=0
385     ENTSTP(D/A/G/H/1/0)
386     I(2)=G(2)
387     527,ENTSTP(D/A/I/J/1/U)
388     ENDATA(G/0/U)
389     ENDATA(I/0/P)
390     Q;=A-1
391     JQ,529,528,0
392     528,A160;=A1P-A10                    #Y--MESH SPACING
393     #WRITE=A00(19)
394     J530
395     529,A20;=A0P-A00                     #X--MESH SPACING
396     WRITE=A00(19)
397     JA0P,539,540,539
398     539,W0;=A9P-2
399     JW0,530,540,530
400     540,A2P;=A20
```

```
401     WRITE=A0P(19)
402     530.G(2)=I(2)
403     J527(F)
404     J524
405     531.J521(2)


406     400.A(24)=0 #CALCULATE KERNAL OF INTEGRAL EQUATION
407     W43(2)=READ                 #INLET & EXIT VELOCITIES
408     WRITE=W43(2)
409     #TEXT=
410     #KERNAL CALCULATION ROUTINE
411     PAGE
412     401.ENTSTP(Y/3/A/B/1/0)          #THE MATRIX OF COEFFICIENTS
413     JA.402.407.0
414     402.C(2)=0
415     403.ENTSTP(A/1/C/D/1/0)
416     JC.404.401.0
417     404.ENTR(C/1/0)
418     J0.405.406.0
419     405.G;=G+0 #NUMBER OF INTERSECTION POINTS I.E.
420     J403 #NUMBER OF SURFACE SINGULARITY SHEETS
421     406.ENTR(C/2/0)
422     J0.405.403.0
423     407.ENTR(Y/1/A)
424     ENTR(Y/2/B)
425     H;=A*B          #MAX NO OF MESH POINTS IN REGION
426     A(2)=0
427     ENTSTP(Y/4/A/B/2/0)              #REGION NUMBER
428     ENDATA(A/0/B)
429     0;=A0B
430     A(6)=0
431     H;=H+G          #ENSURE KEA ADDRESS ENTITY IS LARGE ENOUGH
432     CHAD(90/H)
433     MAKE(90/0/B/A)
434     PUT(Y/4/A/1)
435     ENDATA(A/0/B)
436     A0B(H)=0
437     A(2)=0
438     G;=G+1              #NO OF COEFFICIENTS + 1
439     CHAD(90/G)
440     MAKE(90/0/B/A)
441     PUT(Y/4/A/1)
442     ENDATA(A/0/B)
443     A0B;=0              #NUMBER OF ENTITIES IN RING
444     A1B;=0              #REGION NUMBER
445     A2B;=G              #NUMBER OF SURFACE SHEETS + 1
446     W49;=0


447     412.ENTSTP(Y/3/C/D/1/0)          #COLLOCATION CURVE
448     JC.413.490.0
449     413.E(2)=0
450     W46;=0          #COLLOCATION POINT MARKER
451     414.ENTSTP(C/1/E/F/1/0)          #COLLOCATION SPEC POINT
452     JE.415.412.0
453     415.G;=1
454     416.ENTR(E/G/0)
455     J0.409.417.0
456     417.0;=G-1 #SET G AS RS FOR OUTER/INNER BOUNDARY
```

```
457     JO.408.418.0
458     418.G;=2
459     J416
460     408.W(2)=0 #TO GET LAST SHEET END POINT ON THIS CURVE
461     J(2)=0
462     W46;=-1
463     ENTSTP(C/1/W/X/1/O)
464     G;=1
465     ENTR(W/G/O)
466     JO.510.509.0
467     509.G;=2
468     510.ENTSTP(W/G/J/K/1/O)
469     J423
470     409.JW46.410.420.0
471     410.J(2)=0
472     J422
473     420.H(2)=0
474     W46;=1
475     ENTSTP(E/G/H/I/1/O)                #COLLOCATION I.P.
476     J(2)=H(2)
477     422.ENTSTP(E/G/J/K/1/O)
478     JJ.423.414.0
479     423.N;=1
480     ENTR(H/N/O)
481     JO.425.424.0
482     424.N;=2
483     425.W(2)=0
484     ENTSTP(H/N/W/X/1/O)
485     ENDATA(W/0/O)
486     W0(2)=A00(2)
487     W6;=A90            #FROMM MARKER
488     W35;=A150           #SOURCE/VORTEX SHEET MARKER
489     #WRITE=A00(2)
490     A(2)=0
491     ENTSTP(Y/4/A/B/2/O)
492     ENDATA(A/0/O)
493     A00;=A00+1
494     O;=O+INT(A00)
495     A00;=W             #STORE KEA OF COLLOCATION POINT
496     N;=1
497     ENTR(J/N/O)
498     JO.427.426.0
499     426.N;=2
500     427.A(2)=0
501     ENTSTP(J/N/A/B/1/O)
502     ENDATA(A/0/O)
503     #WRITE=A00(2)
504     W2(2)=A00(2)
505     W4;=(W0+W2)/2 #X,Y COORDS OF COLLOCATION POINT W4,5
506     W5;=(W1+W3)/2
507     #PRINT(116)=W4(2)
508     ENDATA(W/0/O)
509     A100(2)=W4(2)
510     A120(2)=W2(2)
511     #WRITE=A00(2)
512     #WRITE=A100(2)
513     #WRITE=A120(2)
514     A(2)=0
515     ENTSTP(Y/4/A/B/1/O)
516     ENDATA(A/0/B)
```

```
517     A0B;=A0B+1
518     0;=INT(A1B)
519     B;=INT(A2B)
520     W41(2)=C(2)
521     C(2)=0
522     CHAD(90/B)
523     MAKE(90/0/D/C)
524     PUTEND(A/1/C/1)
525     ENDATA(C/0/D)
526     A0D;=0
527     C(2)=W41(2)

528     JW6.482.470.482          #PRESTORAGE OF R.H.S. VECTOR
529     470.JW35.472.471.0
530     471.0;=INT(W49)
531     W500;=0 #COLLOCATION POINT ON A SOLID BDRY/VORTEX SHEET
532     PRINT(116)=W500(1)
533     W49;=W49+1
534     J487
535     472.W(2)=0
536     473.ENTSTP(Y/2/W/X/1/0)
537     JW.474.478.0
538     474.A(2)=0
539     ENTSTP(W/1/A/B/1/0)
540     0;=A-H          #CHECK IF COLLOCATION POINT ON DUCT INLET
541     J0.473.477.473
542     477.0;=INT(W49)
543     W500;=W43 #COLLOCATION PT ON DUCT INLET--SET VELOCITY
544     PRINT(116)=W500(1)
545     W49;=W49+1
546     J487
547     478.0;=INT(W49)
548     W500;=W44 #COLLOCATION POINT ON DUCT EXIT--SET EXIT VELOCITY
549     PRINT(116)=W500(1)
550     W49;=W49+1
551     J487
552     482.W48;=2-W6
553     JW48.477.478.0

554     487.L(2)=0
555     430.ENTSTP(Y/3/L/M/1/0).          #FIELD CURVE
556     JL.431.465.0
557     431.P(2)=0
558     W47;=0          #FIELD POINT MARKER
559     432.ENTSTP(L/1/P/Q/1/0)          #FIELD SPEC POINT
560     JP.433.430.0
561     433.R;=1
562     434.ENTR(P/R/0)
563     J0.438.435.0
564     435.0;=R-1  #SET R AS RS FOR OUTER/INNER BOUNDARY
565     J0.437.436.0
566     436.R;=2
567     J434
568     437.U(4)=0      #TO GET LAST SHEET END POINT ON THIS CURVE
569     W47;=-1
570     ENTSTP(L/1/W/X/1/0)
571     R;=1
572     ENTR(W/R/0)
573     J0.515.514.0
574     514.R;=2
```

```
515.ENTSTP(W/R/U/V/1/0)
J443
438.JW47.439.440.0
439.U(2)=0
J442
440.S(2)=0
W47;=1
ENTSTP(P/R/S/T/1/0)
U(2)=S(2)
442.ENTSTP(P/R/U/V/1/0)
JU.443.432.0
443.N;=1
ENTR(S/N/0)
J0.501.500.0
500.N;=2
501.W(2)=0
ENTSTP(S/N/W/X/1/0)
ENDATA(W/0/U)
W7(2)=A00(2)
#PRINT(115)=A00(2)
W11;=A150        #SOURCE/VORTEX SHEET MARKER
N;=1
ENTR(U/N/0)
J0.506.505.0
505.N;=2
506.W(2)=0
ENTSTP(U/N/W/X/1/0)
ENDATA(W/0/U)
#PRINT(115)=A00(2)
W9(2)=A00(2)

W20;=SQRT((W4-W7)^2+(W5-W8)^2)          #R1
W21;=SQRT((W4-W9)^2+(W5-W10)^2)         #R2
JW11.446.445.0

445.W22;=((W4-W7)(W4-W9)+(W5-W8)(W5-W10))/(W20*W21)
W29;=W22-1
JW29.160.161.161
160.W22;=1.0
161.W22;=-2*SIGN(((W4-W9)(W5-W8)-(W4-W7)(W5-W10))-1&-15)(
)*ARCCOS(W22) #VORTEX SHEET---VX LOCAL
W23;=2*LOG(W20/W21)                #VY LOCAL
J447

446.W22;=2*LOG(W20/W21) #SOURCE SHEET VX LOCAL AXIS
W23;=((W4-W7)(W4-W9)+(W5-W8)(W5-W10))/(W20*W21)
W29;=W23-1
JW29.162.163.163
162.W23;=1.0
163.W23;=-2*SIGN(((W4-W7)(W5-W10)-(W4-W9)(W5-W8))-1&-15)(
)*ARCCOS(W23) #VY LOCAL AXIS

447.W24;=(W9-W7)/SQRT((W9-W7)^2+(W10-W8)^2) #FIELD
W29;=W24-1 #SHEET ORIENTATION
JW29.164.165.165
164.W24;=ARCCOS(1.0)
J166
165.W24;=ARCCOS(W24)
166.W25;=W10-W8
JW25.451.451.450
```

```
631     450.W24;=8*ARCTAN(1)-W24
632     451.W26;=W22*COS(W24)+W23*SIN(W24) #VX MAIN AXIS
633     W27;=W22*SIN(W24)-W23*COS(W24)          #VY MAIN AXIS

634     W28;=(W2-W0)/SQRT((W2-W0)^2+(W3-W1)^2)  #COLLOCATION
635     W29;=W28-1 #SHEET ORIENTATION
636     JW29.167.168.168
637     167.W28;=ARCCOS(1.0)
638     J169
639     168.W28;=ARCCOS(W28)
640     169.W29;=W3-W1
641     JW29.453.453.452
642     452.W28;=8*ARCTAN(1)-W28
643     453.A(2)=0
644     ENTSTP(Y/4/A/B/1/0)
645     ENDATA(A/0/B)
646     B;=INT(A0B)
647     W41(2)=C(2)
648     C(2)=0
649     ENTSTP(A/1/C/D/B/0)
650     ENDATA(C/0/D)
651     A0D;=A0D+1
652     D;=D+INT(A0D)
653     JW35.455.454.0
654     454.A0D;=W26*COS(W28)+W27*SIN(W28) #VTANG--SOLID BDRY
655     J460
656     455.A0D;=W26*SIN(W28)-W27*COS(W28) #VNORM--FLUID BDRY

657     460.C(2)=W41(2)
658     S(2)=U(2)                  #RESET FIELD SHEET ADDRESSES
659     JW47.442.0.432

660     465.H(2)=J(2) #RESET COLLOCATION SHEET ADDRESSES
661     JW46.422.0.414

662     490.A(2)=0
663     ENTSTP(Y/4/A/B/1/0)
664     ENDATA(A/0/B)
665     W48;=RINT(A0B)-INT(W49)
666     JW48.0.491.0          #CHECK ON NO OF R.H.S'S
667     491.A0B;=A0B+1
668     0;=INT(A1B)
669     B;=INT(A2B)
670     C(2)=0
671     CHAD(90/B)
672     MAKE(90/0/D/C)
673     PUTEND(A/1/C/1)
674     ENDATA(C/0/D)
675     A0D;=W49
676     W;=0
677     492.X;=W49-100
678     JX.494.493.493
679     493.X;=W49
680     A1D(X)=W50W(X)        #STORE R.H.S VECTOR IN ENTITY
681     #WRITE=A1D(X)
682     J495
683     494.A1D(100)=W50W(100)
684     #WRITE=A1D(100)
685     W49;=W49-100
686     D;=D+100
```

```
687     W;=W+100.
688     J492

689     495.OUT(10003000)
690     ..

691     1000;..

692     ../FT..
693     ..GSR..
694     1003
695     OBJTPROG(2500)
696     L/LINDEX(1154)
697     TEXSTORE(430)
698     CONSTORE(100)
699     D-STORES(350)
700     A-STORES(7200)
701     W-STORES(6100)
702     N-STORES(350)

703     COMMENT=SOLUTION OF DIAGONALLY DOMINANT MATRICES
704             ORDER OF MATRIX IS IN U
705             W1 ETC. CONTAINS THE COEFFICIENTS OF ROWS FOLLOWED
706             BY R.H.S. AS COLUMN
707             RESULTS ARE IN W1R WHERE R=U(U+1)..

708     A(24)=0
709     W/O TEST
710     ENTSTP(Y/4/A/B/1/0)
711     ENDATA(A/0/U)
712     U;=RINT(A00)-1
713     R;=U(U+1)
714     S;=U*U                  #MARKER FOR R.H.S.
715     U;=U+1
716     10.ENTSTP(A/1/C/D/1/0)
717     ENDATA(C/0/U)
718     N;=RINT(A00)
719     11.X;=N-100
720     JX.12.13.13
721     12.W1P(100)=A10(100)
722     #WRITE=W1P(100)
723     N;=N-100
724     O;=O+100
725     P;=P+100
726     J11
727     13.W1P(N)=A10(N)
728     #WRITE=W1P(N)
729     P;=P+N
730     J10(U)
731     U;=U-1

732     #GET FIRST EST BY ASSUMING OFF-DIAGONAL TERMS ARE ZERO


733     92.W1R;=W1S/W1T
734     R;=R+1
735     S;=S+1
736     T;=T+U+1
737     J92(U)
```

```
738     COMMENT=PUT ROW NUMBER IN Q AND COLUMN NUMBER IN P␣
739     93.Q;=1
740     N;=0
741     R;=U(U+1)
742     94.P;=1
743     W0;=0
744     T;=U(Q-1)-1
745     95.T;=T+1
746     M;=Q-P
747     JM.96,97.96
748     96.W0;=W0+W1T*W1R
749     97.P;=P+1
750     R;=R+1
751     J95(U)
752     R;=U(U+1)+Q-1
753     T;=(U+1)(Q-1)
754     S;=U*U+Q-1
755     W0;=(W1S-W0)/W1T
756     J98(W0/W1R/&-5)
757     N;=N+1
758     M;=U-N
759     JM.98,99.0
760     98.W1R;=W0
761     Q;=Q+1
762     T;=(U+1)(Q-1)
763     M;=U-Q
764     R;=U(U+1)
765     JM.94,94.93
766     99.R;=U(U+1)
767     A(2)=0
768     ENTSTP(Y/4/A/B/2/0)
769     ENDATA(A/0/U)
770     W;=INT(A0U)
771     V;=1
772     110.ENDATA(A/V/X)
773     X;=INT(A0X)
774     ENDATA(X/0/U)
775     A80;=W1R
776     R;=R+1
777     #PRINT(118)=A10U(2)
778     #PRINT(118)=A80(1)
779     V;=V+1
780     J110(W)
781     OUT(10004000)
782     ␣␣
783     1000;␣␣
784     ␣␣F/T␣␣
785     ␣␣GSR␣␣
786     10004
787     OBJTPROG(2500)
788     L/LINDEX(1134)
789     TEXSTORE(430)
790     CONSTORE(100)
791     D-STORES(350)
792     A-STORES(7200)
793     W-STORES(6100)
```

```
794     N=STORES(350)
795     W/O TEST
796     A(24)=0
797     ENTSTP(Y/4/C/D/4/O)
798     ENDATA(C/0/O)
799     O;=O+2+INT(A10)
800     W99;=A00                    #ITERATION
801     10.ENTSTP(Y/1/A/B/1/O)              #COLUMN ENTITY
802     JA.11.120.0
803     11.C(2)=0
804     12.ENTSTP(A/1/C/D/1/O)              #COLUMN INTERSECTION POINT
805     JC.13.10.0
806     13.ENTR(C/1/X)
807     X;=X-1
808     JX.18.17.0
809     17.X;=1
810     18.E(2)=0
811     19.ENTSTP(C/1/E/F/1/O)              #COLLOCATION POINT
812     ENDATA(E/0/O)
813     W0(18)=A00(18)
814     #WRITE=W0(2)
815     W3(2)=0
816     W17;=0

817     W100;=RINT(1+W14)                   #WHICH VELOCITY COMPONENTS
818     JW100.20.116.0
819     20.W100;=RINT(W99-1)                #WHICH TIMESTEP
820     JW100.21.32.0
821     21.JW9.22.24.22             #CHECK COLLOCATION POINT F.M.
822     22.W100;=1-W9
823     JW100.23.30.23
824     23.W100;=ABS(W9)-2
825     JW100.31.30.31
826     24.G(2)=0
827     ENTSTP(Y/1/G/H/1/O) #IS COLLOCATION PT ON DUCT INLET
828     O;=A-G
829     JO.25.30.25
830     25.I(2)=A(2)
831     ENTSTP(Y/1/I/J/1/O) #IS COLLOCATION PT ON DUCT EXIT
832     JI.116.30.116

833     30.U;=40 #COLLOCATION PT IS AN INLET/EXIT MESH PT
834     J35

835     31.U;=50 #COLLOCATION POINT IS A FIELD MESH POINT
836     J35

837     32.U;=60 #FIRST TIMESTEP--CALC VELY FIELD DIRECT

838     35.G(4)=0
839     ENTSTP(Y/4/G/H/2/O) #FIELD POINT ADDRESS ENTITY
840     ENDATA(G/0/O)
841     W;=INT(A00)
842     V;=1
843     36.ENDATA(G/V/I)
844     I;=INT(A0I)                 #FIELD POINT ADDRESS
845     ENDATA(I/0/O)
846     W18(18)=A00
847     #WRITE=W18(2)
848     38.JU
```

```
849     COMMENT=VELOCITY CALCULATION ROUTINES_

850     40.JW33.43.41.0 #INLET/EXIT MESH PT--CALC U I.J+1/2
851     41.JW27.62.43.62

852     43.W100;=(W30-W18)/SQRT((W30-W18)^2+(W31-W19)^2)
853     W101;=W100-1
854     JW101.500.501.501
855     500.W100;=ARCCOS(1.0)
856     J502
857     501.W100;=ARCCOS(W100)
858     502.W101;=W31-W19
859     JW101.45.45.44
860     44.W100;=8*ARCTAN(1)-W100
861     45.JW33.97.92.0


862     50.JW33.54.51.0 #FIELD MESH PT--CALC U AND V
863     51.JW27.52.54.52 #COMPONENTS AT MESH POINT

864     52.0;=E-I #ARE COLLOCATION & FIELD PTS THE SAME
865     JU.53.110.53
866     53.W100;=W20*W34 #VORTEX REPRESENTATION OF VORTICITY
867     W3;=W3+(2*W24*W100(W19-W1)/((W18-W0)^2+(
868     )(W19-W1)^2)) #U COLLATION PT
869     W4;=W4+(2*W24*W100(W0-W18)/((W1-W19)^2+(
870     )(W0-W18)^2)) #V COLLATION PT
871     J110

872     54.W100;=(W30-W18)/SQRT((W30-W18)^2+(W31-W19)^2)
873     W101;=W100-1
874     JW101.503.504.504
875     503.W100;=ARCCOS(1.0)
876     J505
877     504.W100;=ARCCOS(W100)
878     505.W101;=W31-W19
879     JW101.56.56.55
880     55.W100;=8*ARCTAN(1)-W100
881     56.JW33.58.57.0

882     57.W102;=SQRT((W0-W18)^2+(W1-W19)(
883     )^2) #FIELD PT ON VORTEX SHEET
884     W103;=SQRT((W0-W30)^2+(W1-W31)^2)
885     W104;=((W0-W18)(W0-W30)+(W1-W19)(W1-W31))/(W102*W103)
886     W101;=W104-1
887     JW101.506.507.507
888     506.W104;=1.0
889     507.W104;=-2*W26*SIGN(((W0-W30)(W1-W19)-(W0-W18)(
890     )(W1-W31))-1&-15)*ARCCOS(W104)
891     W105;=2*W26*LOG(W102/W103)
892     W3;=W3+(W104*COS(W100)+W105*SIN(W100)) #U COLL PT
893     W4;=W4+(W104*SIN(W100)-W105*COS(W100)) #V COL PT
894     J110

895     58.W102;=SQRT((W0-W18)^2+(
896     )(W1-W19)^2) #FIELD PT ON SOURCE SHEET
897     W103;=SQRT((W0-W30)^2+(W1-W31)^2)
```

```
898     W104;=2*W26*LOG(W102/W103)
899     W105;=((W0-W18)(W0-W30)+(W1-W19)(W1-W31))/(W102*W103)
900     W101;=W105-1
901     JW101.508.509.509
902     508.W105;=1.0
903     509.W105;=-2*W26*SIGN((W0-W18)(W1-W31)-(W0-W30)(
904     )(W1-W19))-1&-15)*ARCCOS(W105)
905     W3;=W3+(W104*COS(W100)+W105*SIN(W100)) #U COL PT
906     W4;=W4+(W104*SIN(W100)-W105*COS(W100)) #V COL PT
907     J110


908     60.JW33.85.61.0 #CALCULATE U I.J+1/2 & V I+1/2.J DIRECTLY
909     61.JW27.62.85.62

910     62.W100;=W20*W34 #VORTEX REP OF FIELD VORTICITY
911     0;=U-60
912     J0.0.75.63              #IS THIS THE FIRST TIMESTEP

913     63.W101;=W9-2 #NO--CHECK IF COLL PT IS ON EXIT BDRY
914     JW101.0.64.69
915     64.W101;=W27-2 #YES--IS FIELD POINT ON EXIT BDRY
916     JW101.77.65.77
917     65.0;=E-I #YES--ARE THEY THE SAME MESH POINT
918     J0.80.110.80
919     69.JW9.77.70.77         #CHECK IF SURFACE POINT
920     70.JW15.77.71.0         #INLET OR EXIT BOUNDARY POINT
921     71.W101;=W27-2 #EXIT--IS FIELD POINT ON EXIT BOUNDARY
922     JW101.77.110.77

923     75.W101;=RINT(1-ABS(W14))
924     JW101.76.78.77
925     76.W4;=W4+(2*W24*W100(W0+W2/2-W18)/((W1-W19)^2+(
926     )(W0+W2/2-W18)^2)) #V COLL PT
927     77.W3;=W3+(2*W24*W100(W19-(W1+W16/2))/((W18-W0)^2+(
928     )(W19-(W1+W16/2))^2)) #U COLL PT
929     J110
930     78.JW14.79.0.116
931     79.W4;=W4+(2*W24*W100(W0+W2/2-W18)/((W1-W19)^2+(
932     )(W0+W2/2-W18)^2)) #V COLL PT
933     J110
934     80.W17;=W17+(2*W24*W100(W19-W1)/((W18-W0)^2+(
935     )(W19-W1)^2)) #SAME MESH PT
936     J110

937     85.W100;=ARCCOS((W30-W18)/SQRT((W30-W18)^2+(W31-W19)^2))
938     W101;=W31-W19
939     JW101.87.87.86
940     86.W100;=8*ARCTAN(1)-W100
941     87.JW33.95.90.0

942     90.W101;=RINT(1-ABS(W14)) #SOLID BDRY--VORTEX SHEETS
943     JW101.91.93.92
944     91.W102;=SQRT((W0+W2/2-W18)^2+(W1-W19)^2)
945     W103;=SQRT((W0+W2/2-W30)^2+(W1-W31)^2)
946     W104;=-2*W26*SIGN(((W0+W2/2-W30)(W1-W19)-(W0+W2/2-W18)(
947     )(W1-W31))-1&-15)*ARCCOS(((W0+W2/2-W18)(W0+W2/2-W30)+(
948     )(W1-W19)(W1-W31))/(W102*W103))
949     W105;=2*W26*LOG(W102/W103)
950     W4;=W4+(W104*SIN(W100)-W105*COS(W100))   #V COLL PT
```

```
951     92.W102;=SQRT((W0-W18)^2+(W1+W16/2-W19)^2)
952     W103;=SQRT((W0-W30)^2+(W1+W16/2-W31)^2)
953     W104;=-2*W26*SIGN(((W0-W30)(W1+W16/2-W19)-(W0-W18)(
954     )(W1+W16/2-W31))-1&-15)*ARCCOS(((W0-W18)(W0-W30)+(
955     )(W1+W16/2-W19)(W1+W16/2-W31))/(W102*W103))
956     W105;=2*W26*LOG(W102/W103)
957     W3;=W3+(W104*COS(W100)+W105*SIN(W100)) #U COLL PT
958     J110
959     93.JW14,94.0.116
960     94.W102;=SQRT((W0+W2/2-W18)^2+(W1-W19)^2)
961     W103;=SQRT((W0+W2/2-W30)^2+(W1-W31)^2)
962     W104;=-2*W26*SIGN(((W0+W2/2-W30)(W1-W19)-(W0+W2/2-W18)(
963     )(W1-W31))-1&-15)*ARCCOS(((W0+W2/2-W18)(W0+W2/2-W30)+(
964     )(W1-W19)(W1-W31))/(W102*W103))
965     W105;=2*W26*LOG(W102/W103)
966     W4;=W4+(W104*SIN(W100)-W105*COS(W100)) #V COLL PT
967     J110

968     95.W101;=RINT(1-ABS(W14)) #IN/EXIT BDRY--USE SOURCE SHEETS
969     JW101.96.98.97
970     96.W102;=SQRT((W0+W2/2-W18)^2+(W1-W19)^2)
971     W103;=SQRT((W0+W2/2-W30)^2+(W1-W31)^2)
972     W104;=2*W26*LOG(W102/W103)
973     W105;=-2*W26*SIGN(((W0+W2/2-W18)(W1-W31)-(W0+W2/2-W30)(
974     )(W1-W19))-1&-15)*ARCCOS(((W0+W2/2-W18)(W0+W2/2-W30)+(
975     )(W1-W19)(W1-W31))/(W102*W103))
976     W4;=W4+(W104*SIN(W100)-W105*COS(W100)) #V COLL PT
977     97.W102;=SQRT((W0-W18)^2+(W1+W16/2-W19)^2)
978     W103;=SQRT((W0-W30)^2+(W1+W16/2-W31)^2)
979     W104;=2*W26*LOG(W102/W103)
980     W105;=-2*W26*SIGN(((W0-W18)(W1+W16/2-W31)-(W0-W30)(
981     )(W1+W16/2-W19))-1&-15)*ARCCOS(((W0-W18)(W0-W30)+(
982     )(W1+W16/2-W19)(W1+W16/2-W31))/(W102*W103))
983     W3;=W3+(W104*COS(W100)+W105*SIN(W100)) #U COLL PT
984     J110
985     98.JW14.99.0.116
986     99.W102;=SQRT((W0+W2/2-W18)^2+(W1-W19)^2)
987     W103;=SQRT((W0+W2/2-W30)^2+(W1-W31)^2)
988     W104;=2*W26*LOG(W102/W103)
989     W105;=-2*W26*SIGN(((W0+W2/2-W18)(W1-W31)-(W0+W2/2-W30)(
990     )(W1-W19))-1&-15)*ARCCOS(((W0+W2/2-W18)(W0+W2/2-W30)+(
991     )(W1-W19)(W1-W31))/(W102*W103))
992     W4;=W4+(W104*SIN(W100)-W105*COS(W100)) #V COLL PT


993     110.V;=V+1              #SELECT NEXT FIELD POINT
994     J36(W)
995     J113
996     111.ENDATA(G/V/I) #GET FIELD PTS WITH VORTICITY
997     W;=INT(A0I)
998     JW.112.113.0
999     112.V;=V+1
1000    U;=U+1
1001    J36
1002    113.J111(2)

1003    116.ENDATA(E/0/U)
1004    W101;=ABS(W4)-.000001
1005    JW101.118.117.117
1006    117.W4;=0
```

```
1007    118.A00(18)=W0(18)              #STORE NEW VELOCITY COMPONENTS
1008    #LINE
1009    #WRITE=A00(19)
1010    J19(X)          #SELECT NEXT COLLOCATION POINT
1011    J12

1012    120.W100;=W99-1          #WHICH TIMESTEP
1013    JW100.125.170.0

1014    125.A(24)=0 #CALC VELY COMPS BY LINEAR INTERPOLATION
1015    140.ENTSTP(Y/2/A/B/1/0)          #ROW ENTITY
1016    JA.141.170.0
1017    141.C(2)=0
1018    142.ENTSTP(A/1/C/D/1/0)          #ROW INTERSECTION POINT
1019    JC.143.140.0
1020    143.ENTR(C/2/X)
1021    X;=X-1
1022    JX.145.144.0
1023    144.X;=1
1024    145.E(2)=0
1025    146.ENTSTP(C/2/E/F/1/0)          #MESH POINT
1026    ENDATA(E/0/0)
1027    W0(18)=A00(18)
1028    #WRITE=W0(19)
1029    W100;=RINT(1-ABS(W14))
1030    JW100.150.160.153
1031    150.G(2)=E(2)
1032    ENTSTP(C/2/G/H/1/0)
1033    ENDATA(G/0/0)
1034    #WRITE=A00(19)
1035    W101;=2-A90     #IS NEXT HORIZONTAL POINT ON EXIT BOUNDARY
1036    JW101.151.153.151
1037    151.W4;=(W4+A40)/2
1038    153.I(6)=0
1039    RNGSTP(E/1/I/J/1/0)          #C.I.P.
1040    ENDATA(I/0/0)
1041    #WRITE=A00(6)
1042    RNGSTP(I/2/K/L/1/0)          #COLUMN ENTITY
1043    ENTSTP(Y/1/M/N/1/0)
1044    0;=M-K
1045    J0.154.165.154
1046    154.M(2)=K(2)
1047    K;=E
1048    L;=1
1049    ENTSTP(I/1/K/L/1/0)          #NEXT VERTICAL MESH POINT
1050    ENDATA(K/0/0)
1051    #WRITE=A00(19)
1052    ENTSTP(Y/1/M/N/1/0)
1053    JM.155.156.0
1054    155.ENDATA(K/0/0)
1055    W3;=(W3+A30)/2
1056    J165
1057    156.ENDATA(K/0/0)
1058    W3;=W3+((W17+A170)/2)          #CALC EXIT VELOCITY PROFILE
1059    J165
1060    160.JW14.161.0.167
1061    161.G(2)=E(2)
1062    ENTSTP(C/2/G/H/1/0)
1063    ENDATA(G/0/0)
```

```
1064    #WRITE=A00(19)
1065    W101;=2-A90
1066    JW101.162.165.162
1067    162.W4;=(W4+A40)/2

1068    165.ENDATA(E/0/0)
1069    A00(18)=W0(18)
1070    #WRITE=A00(19)

1071    167.J146(X)
1072    J142


1073    170.A(24)=0          #SURFACE VORTICITY CALCULATION
1074    171.ENTSTP(Y/3/A/B/1/0)          #CURVE ENTITY
1075    JA.172.235.0
1076    172.C(2)=0
1077    173.ENTSTP(A/1/C/D/1/0)      #CURVE SPECIFIED POINTS
1078    JC.176.171.0
1079    176.E;=1
1080    177.ENTR(C/E/0) #SET E AS RS FOR OUTER/INNER BOUNDARY
1081    J0.182.178.0
1082    178.0;=E-1
1083    J0.173.179.0
1084    179.E;=2
1085    J177
1086    182.F(2)=0
1087    183.ENTSTP(C/E/F/G/1/0)          #INTERSECTION POINT
1088    JF.184.173.0
1089    184.H;=1
1090    ENTR(F/H/0) #SET H AS RS FOR COL/ROW I.P. MESH POINTS
1091    J0.186.185.0
1092    185.H;=2
1093    186.I(2)=0
1094    ENTSTP(F/H/I/J/1/0)          #MESH POINT
1095    ENDATA(I/0/0)
1096    #WRITE=A00(2)
1097    JA90.183.190.183
1098    190.W0(18)=A00(18)
1099    W5;=W6
1100    W6;=0
1101    W18(4)=0                  #SET DUMMY VELOCITY STORES
1102    ENDATA(F/0/0)
1103    #WRITE=A00(6)
1104    JA10.192.225.0          #CHECK CONTINUATION MARKER
1105    192.W100;=A10-2
1106    JW100.195.215.205

1107    195.K(9)=0          #STORE V I-1/2,J--FIND CORRECT R.I.P
1108    RNGSTP(I/2/K/L/1/0)
1109    RNGSTP(K/3/M/N/1/0)          #ROW ENTITY
1110    196.ENTSTP(M/1/P/Q/1/0)          #R.I.P
1111    197.ENTSTP(P/2/R/S/1/0)          #ROW MESH POINT
1112    JR.198.196.0
1113    198.0;=I-R
1114    J0.197.200.197
1115    200.K;=-1
1116    ENTSTP(P/2/R/S/K/0)          #GET PREVIOUS ROW MESH POINT
1117    ENDATA(R/0/0)
1118    #WRITE=A00(2)
```

```
1119    W18;=A40          #STORE V I-1/2,J
1120    W19;=A20          #STORE X-SPACING

1121    205,K(9)=0      #STORE U I,J-1/2--FIND CORRECT C.I.P
1122    RNGSTP(I/1/K/L/1/0)
1123    RNGSTP(K/2/M/N/1/0)       #COLUMN ENTITY
1124    206,ENTSTP(N/1/P/Q/1/0)     #C.I.P
1125    207,ENTSTP(P/1/R/S/1/0)      #COLUMN MESH POINT
1126    JR,208,206,0
1127    208,0;=I-R
1128    J0,207,210,207
1129    210,K;=-1
1130    ENTSTP(P/1/R/S/K/0)      #GET PREVIOUS COLUMN MESH POINT
1131    ENDATA(R/0/0)
1132    #WRITE=A00(2)
1133    W20;=A30          #STORE U I,J-1/2
1134    W21;=A160          #STORE Y-SPACING
1135    J225

1136    215,K(9)=0      #STORE V I-1/2,J--FIND CORRECT R.I.P
1137    RNGSTP(I/2/K/L/1/0)
1138    RNGSTP(K/3/M/N/1/0)        #ROW ENTITY
1139    216,ENTSTP(N/1/P/Q/1/0)     #R.I.P
1140    217,ENTSTP(P/2/R/S/1/0)       #ROW MESH POINT
1141    JR,218,216,0
1142    218,0;=I-R
1143    J0,217,220,217
1144    220,K;=-1
1145    ENTSTP(P/2/R/S/K/0)      #GET PREVIOUS ROW MESH POINT
1146    ENDATA(R/0/0)
1147    #WRITE=A00(2)
1148    W18;=A40          #STORE V I-1/2,J
1149    W19;=A20          #STORE X-SPACING

1150    225,ENDATA(F/0/0)
1151    JA00,240,240,0
1152    240,W100;=A00-2
1153    JW100,241,242,243
1154    241,W6;=(W4/W2)-(W3/W16)
1155    J246
1156    242,W6;=W4/W2
1157    J246
1158    243,W6;=-W3/W16

1159    246,ENDATA(F/0/0)
1160    JA10,247,230,0
1161    247,W100;=A10-2
1162    JW100,250,251,252
1163    250,W6;=W6+((W20/W21)-(W18/W19))
1164    J230
1165    251,W6;=W6-(W18/W19)
1166    J230
1167    252,W6;=W6+(W20/W21)

1168    230,ENDATA(I/0/0)
1169    A00(18)=W0(18)
1170    #WRITE=W0(19)
1171    J183

1172    235,A(2)=0
```

```
1173    ENTSTP(Y/4/A/B/4/U)
1174    ENDATA(A/0/U)
1175    W101;=A20-1
1176    JW101.237.236.0
1177    236.OUT(10007000)                    #IRROTATIONAL FLOW ONLY
1178    237.OUT(10005000)
1179    ..
1180    1000;..
1181    ..F/T..
1182    ..GSR..
1183    10005
1184    OBJTPROG(2500)
1185    L/LINDEX(1134)
1186    TEXSTORE(430)
1187    CONSTORE(100)
1188    D-STORES(350)
1189    A-STORES(7200)
1190    W-STORES(6100)
1191    N-STORES(350)
1192    W/O TEST
1193    #A;=-10187
1194    #D0A=1
1195    A(2)=0
1196    ENTSTP(Y/4/A/B/4/U)
1197    ENDATA(A/0/U)
1198    0;=0+RINT(A10)
1199    W199;=A00                            #TIMESTEP
1200    0;=0-1
1201    W198;=A00                            #KINEMATIC VISCOSITY
1202    #0;=0+3
1203    #W200;=A00-1
1204    #JW200.12.13.0
1205    #12.A;=-10187
1206    #D0A=0
1207    13.W180(4)=4          #NO OF POINTS FOR F(U) & F(V) CALC
1208    A(24)=0
1209    1.ENTSTP(Y/1/A/B/1/U)                #COLUMN ENTITY
1210    JA.2.112.0
1211    2.C(2)=0
1212    3.ENTSTP(A/1/C/D/1/0) #COLUMN INTERSECTION POINT
1213    JC.4.1.0
1214    4.ENTR(C/1/X)
1215    X;=X-1
1216    JX.6.5.0
1217    5.X;=1
1218    6.E(2)=0
1219    7.ENTSTP(C/1/E/F/1/0)                #COLLOCATION POINT
1220    ENDATA(E/0/U)
1221    JA90.10.111.10
1222    10.W;=24
1223    JS300
1224    W160;=A20
1225    W161;=A160
1226    G(2)=E(2)
1227    I;=-1
1228    ENTSTP(C/1/G/H/I/0)
1229    ENDATA(G/0/U)
```

```
1230    W;=12
1231    JS300
1232    W163;=A160
1233    W200;=1-W34
1234    JW200.11.14.11          #INLET BOUNDARY OR FIELD
1235    11.W200;=2+W34
1236    JW200.18.14.18

1237    14.W120;=0 #INLET FLUID BDRY--DIFFUSION CONTRIBUTION
1238    W121;=W12-W24 #INLET BDRY VORTICITY FROM U-GRADIENT
1239    ENDATA(E/0/0)
1240    A70;=W121(1)
1241    W200;=ABS(W121)-1&-5
1242    JW200.15.17.17
1243    15.W200;=1-A180
1244    JW200.16.17.0 #NOT STORED,STORED
1245    16.T(2)=0
1246    ENTSTP(Y/4/T/U/2/0)
1247    ENDATA(T/0/0)
1248    0;=0+RINT(A00)+1
1249    A00;=A00+1
1250    0;=0+RINT(A00)
1251    A00;=E                          #STORE KEA
1252    ENDATA(E/0/0)
1253    A180;=1                         #UPDATE MARKER
1254    17.X;=X-1
1255    JX.7.3.0

1256    18.H(2)=E(2) #FIELD MESH PT--CALC BASIC STORES MODULE
1257    ENTSTP(C/1/H/I/1/0)
1258    ENDATA(H/0/0)
1259    W;=36
1260    JS300
1261    I(4)=0
1262    RNGSTP(E/2/I/J/1/0)
1263    RNGSTP(I/3/K/L/1/0)             #ROW ENTITY
1264    I;=K
1265    J(2)=0
1266    19.ENTSTP(I/1/J/K/1/0) #ROW INTERSECTION POINT
1267    L(2)=0
1268    20.ENTSTP(J/2/L/M/1/0)          #MESH POINT
1269    JL.21.19.0
1270    21.U;=E-L
1271    JU.20.25.20
1272    25.I;=J         #SET I AS R.I.P. KEA
1273    J;=E
1274    K;=2
1275    L;=-1
1276    ENTSTP(I/2/J/K/L/0)
1277    ENDATA(J/0/0)
1278    W;=60
1279    JS300
1280    W162;=A20
1281    K(2)=A(2)
1282    M;=-1
1283    ENTSTP(Y/1/K/L/M/0)             #PREVIOUS COLUMN ENTITY
1284    L(2)=0
1285    26.ENTSTP(K/1/L/M/1/0) #GET C.I.P WITH MESH POINT J
1286    N(2)=0
1287    27.ENTSTP(L/1/N/0/1/P)          #MESH POINT
```

```
1288    JN.28.26.0
1289    28.P;=J-N
1290    JP.27.33.27
1291    33.K;=L          #SET K AS C.I.P. KEA
1292    L;=J
1293    M;=1
1294    N;=-1
1295    ENTSTP(K/1/L/M/N/0)
1296    JL.151.150.0
1297    150.W180;=W180-1
1298    W183;=W183-1
1299    W48(12)=0
1300    J152
1301    151.ENDATA(L/0/0)
1302    W;=48
1303    JS300
1304    152.M;=J
1305    N;=1
1306    ENTSTP(K/1/M/N/1/0)
1307    JN.158.155.0
1308    155.T(2)=A(2)
1309    V;=-1
1310    ENTSTP(Y/1/T/U/V/0)
1311    ENTSTP(T/1/K/0/1/0)
1312    ENDATA(K/0/0)
1313    W0;=A00-1
1314    JW0.156.157.159
1315    156.W0;=A00-2
1316    JW0.157.159.0
1317    157.M;=0
1318    ENTSTP(K/1/M/N/2/0)
1319    158.ENDATA(M/0/0)
1320    W;=72
1321    JS300
1322    J160
1323    159.W180;=W180-1
1324    W181;=W181-1
1325    W72(12)=0
1326    160.N;=E
1327    0;=2
1328    ENTSTP(I/2/N/0/1/P)
1329    JN.34.65.0 #NOT EXIT. EXIT FLUID BOUNDARY. FAIL
1330    34.ENDATA(N/0/0)
1331    W;=108
1332    JS300
1333    P(2)=A(2)
1334    ENTSTP(Y/1/P/Q/1/0)          #NEXT COLUMN ENTITY
1335    Q(2)=0
1336    35.ENTSTP(P/1/Q/R/1/0) #GET C.I.P. WITH MESH POINT N
1337    S(2)=0
1338    36.ENTSTP(Q/1/S/T/1/0)          #MESH POINT
1339    JS.37.35.0
1340    37.0;=N-S
1341    JU.36.40.36
1342    40.P;=Q          #SET P AS C.I.P. KEA
1343    Q;=N
1344    R;=1
1345    S;=-1
1346    ENTSTP(P/1/Q/R/S/0)
1347    JQ.166.165.0
```

```
1348    165,W182;=W182-1
1349    W183;=W183-1
1350    W96(12)=0
1351    J70
1352    166,ENDATA(Q/0/0)
1353    W;=96
1354    JS300
1355    J70


1356    50,ENDATA(E/0/0) #SWOP ADDRESSES TO FORM NEW MODULE
1357    JA90,51,7,51
1358    51,L;=J
1359    ENDATA(L/0/0)
1360    W;=48
1361    JS300
1362    J;=M
1363    ENDATA(J/0/0)
1364    W;=60
1365    JS300
1366    W162;=A20
1367    T;=1
1368    ENTSTP(K/1/M/T/1/0)
1369    JM,133,130,0
1370    130,T(2)=A(2)
1371    V;=-1
1372    ENTSTP(Y/1/T/U/V/0)
1373    ENTSTP(T/1/K/D/1/0)
1374    ENDATA(K/0/0)
1375    W0;=A00-1
1376    JW0,131,132,134
1377    131,W0;=A00-2
1378    JW0,132,134,0
1379    132,M;=0
1380    T;=1
1381    ENTSTP(K/1/M/T/2/0)
1382    133,ENDATA(M/0/0)
1383    W;=72
1384    JS300
1385    J135
1386    134,W180;=W180-1
1387    W181;=W181-1
1388    W72(12)=0
1389    T;=1
1390    135,G;=E
1391    ENDATA(G/0/0)
1392    W;=12
1393    JS300
1394    W163;=A160
1395    E;=H
1396    ENDATA(E/0/0)
1397    W;=24
1398    JS300
1399    W160;=A20
1400    W161;=A160
1401    ENTSTP(C/1/H/T/1/0)
1402    ENDATA(H/0/0)
1403    W;=36
1404    JS300
1405    W200;=2-W34
```

```
1406    JW200.55.65.55 #NOT EXIT. EXIT FLUID BOUNDARY. NOT EXIT
1407    55.Q;=N
1408    ENDATA(Q/0/U)
1409    W;=96
1410    JS300
1411    ENTSTP(P/1/N/T/1/U)
1412    JN.143.140.0
1413    140.T(2)=A(2)
1414    ENTSTP(Y/1/T/U/1/U)
1415    ENTSTP(T/1/P/D/1/U)
1416    ENDATA(P/0/U)
1417    W0;=A00-1
1418    JW0.141.142.144
1419    141.W0;=A00-2
1420    JW0.142.144.0
1421    142.N;=0
1422    T;=1
1423    ENTSTP(P/1/N/T/2/U)
1424    143.ENDATA(N/0/U)
1425    W;=108
1426    JS300
1427    J145
1428    144.W181;=W181-1
1429    W182;=W182-1
1430    W108(12)=0
1431    145.R(4)=0
1432    RNGSTP(J/2/R/S/1/U)
1433    RNGSTP(R/3/T/U/1/U)                    #ROW ENTITY
1434    R;=T
1435    S(2)=0
1436    56.ENTSTP(R/1/S/T/1/U)                 #ROW INTERSECTION POINT
1437    U(2)=0
1438    57.ENTSTP(S/2/U/V/1/U)                 #MESH POINT
1439    JU.58.56.0
1440    58.U;=J-U
1441    JU.57.60.57
1442    60.I;=S          #SET I AS R.I.P. KEA
1443    J70


1444      #EXIT FLUID BDRY
1445    65.W20*U;=(1/W180)(W60+W24+W48+W12)*W199/W162 #F(U)
1446    W201;=W63*W199/(0.5(W161+W163))          #F(V)
1447    W121;=0.5(W40+W16)+W200(W64-0.5(W40+W16))+W201(W17-W41)
1448    W122;=W121
1449    J108


1450    70.W120;=(W198*W199)(((W64-2*W28+W112)/((0.5(W160+W162))(
1451    )^2))+((W16-2*W28+W40)/((0.5(W161+W163))^2)))

1452    W200;=0.125(W60+2*W24+W108+W48+2*W12+W96) #CHECK U I,J
1453    JW200.71.71.72
1454    71.U;=1          #VELOCITY IS POSITIVE--SET MARKER
1455    J79
1456    72.U;=-1 #VELY IS NEGATIVE--SET MARKER AND SWOP STORES
1457    T;=0
1458    73.W130T;=W60T          #PUT IN DUMMY STORES
1459    T;=T+2
1460    J73(6)
```

```
1461    T;=0
1462    74.W60T;=W108T          #TRANSFER DIRECT
1463    T;=T+2
1464    J74(6)
1465    W60;=-W60
1466    T;=0
1467    75.W108T;=W130T         #TRANSFER FROM DUMMY
1468    T;=T+2
1469    J75(6)
1470    W108;=-W108
1471    W130;=W160
1472    W160;=W162
1473    W162;=W130
1474    T;=0
1475    76.W130T;=W48T
1476    T;=T+2
1477    J76(6)
1478    T;=0
1479    77.W48T;=W96T
1480    T;=T+2
1481    J77(6)
1482    W48;=-W48
1483    T;=0
1484    78.W96T;=W130T
1485    T;=T+2
1486    J78(6)
1487    W96;=-W96
1488    W24;=-W24
1489    W12;=-W12

1490    79.W200;=0.125(W75+2*W63+W51+W39+2*W27+W15) #CHECK V I,J
1491    JW200.81.81.82
1492    81.V;=1             #VELOCITY IS POSITIVE--SET MARKER
1493    J90
1494    82.V;=-1                    #NEGATIVE VELOCITY--SWOP STORES
1495    T;=0
1496    83.W130T;=W13T
1497    T;=T+2
1498    J83(6)
1499    T;=0
1500    84.W13T;=W37T
1501    T;=T+2
1502    J84(6)
1503    W15;=-W15
1504    T;=0
1505    85.W37T;=W130T
1506    T;=T+2
1507    J85(6)
1508    W39;=-W39
1509    W130;=W161
1510    W161;=W163
1511    W163;=W130
1512    T;=0
1513    86.W130T;=W49T
1514    T;=T+2
1515    J86(6)
1516    T;=0
1517    87.W49T;=W73T
1518    T;=T+2
```

```
1519    J87(6)
1520    W51;=-W51
1521    T;=0
1522    88.W73T;=W130T
1523    T;=T+2
1524    J88(6)
1525    W75;=-W75
1526    W27;=-W27
1527    W63;=-W63


1528    90.W200;=ABS(W34)-1
1529    JW200.91.92.0              #FIELD. ADJACENT TO SURFACE. FAIL
1530    91.W200;=3-W34
1531    JW200.93.92.0 #FIELD. NEXT TO INLET + EXIT FLUID BDRY. FAIL

1532    92.T;=250 #SECOND ORDER CONVECTION APPROXIMATION
1533    W;=255
1534    JS200
1535    J107


1536    93.JU.94.0.97 #FOURTH ORDER CONVECTION APPROXIMATION
1537    94.R;=J          #GET EXTRA POINTS TO COMPLETE MODULE
1538    S;=2
1539    T;=-1
1540    ENTSTP(I/2/R/S/T/0)
1541    ENDATA(R/0/U)
1542    W;=84
1543    JS300
1544    R;=N
1545    S;=2
1546    ENTSTP(I/2/R/S/1/0)
1547    ENDATA(R/0/U)
1548    W;=300
1549    JS300
1550    T;=270
1551    J102
1552    97.W200;=2-W70
1553    JW200.99.98.0 #FIELD. ADJACENT TO EXIT BOUNDARY. FAIL
1554    98.T;=250
1555    J102
1556    99.R;=N
1557    S;=2
1558    ENTSTP(I/2/R/S/1/0)
1559    ENDATA(R/0/U)
1560    W;=84
1561    JS300
1562    W84;=-W84
1563    R;=J
1564    S;=2
1565    T;=-1
1566    ENTSTP(I/2/R/S/T/0)
1567    ENDATA(R/0/U)
1568    W;=300
1569    JS300
1570    W300;=-W300
1571    T;=270

1572    102.JV.103.0.104 #GET EXTRA PTS TO COMPLETE MODULE
```

```
1573    103.S;=G
1574    W;=-1
1575    ENTSTP(C/1/S/F/W/0)
1576    ENDATA(S/0/0)
1577    W;=0
1578    JS300
1579    S;=H
1580    ENTSTP(C/1/S/F/1/0)
1581    ENDATA(S/0/0)
1582    W;=312
1583    JS300
1584    W;=275
1585    J105
1586    104.S;=H
1587    ENTSTP(C/1/S/F/1/0)
1588    ENDATA(S/0/0)
1589    W;=0
1590    JS300
1591    W3;=-W3
1592    S;=G
1593    W;=-1
1594    ENTSTP(C/1/S/F/W/0)
1595    ENDATA(S/0/0)
1596    W;=312
1597    JS300
1598    W315=-W315
1599    W;=275

1600    105.JS200


1601    107.W121;=W28+(W204-W205)+(W206-W207) #CONVECTION CONTBN
1602    W122;=W121+W120          #W I,J AT TIME N+1
1603    108.ENDATA(E/0/0)
1604    A70;=W122
1605    W200;=ABS(W122)-1&-5
1606    JW200.109.111.111
1607    109.W200;=1-A180
1608    JW200.110.111.0                              #NOT STORED,STORED
1609    110.T(2)=0
1610    ENTSTP(Y/4/T/0/2/0)
1611    ENDATA(T/0/0)
1612    0;=0+RINT(A00)+1
1613    A00;=A00+1
1614    0;=0+RINT(A00)
1615    A00;=E
1616    ENDATA(E/0/0)
1617    A180;=1
1618    111.X;=X-1
1619    JX.50.3.0


1620    112.A(24)=0 #SWOP VORTICITY VALUES FOR NEXT ITERATION
1621    W200;=0
1622    113.ENTSTP(Y/1/A/B/1/0)          #COLUMN ENTITY
1623    JA.114.125.0
1624    114.C(2)=0
1625    115.ENTSTP(A/1/C/D/1/0)          #C.I.P.
1626    JC.116.113.0
1627    116.ENTR(C/1/X)
```

```
1628    X;=X-1
1629    JX.119.118.0
1630    118.X;=1
1631    119;E(2)=0
1632    120.ENTSTP(C/1/E/F/1/U)          #COLLOCATION POINT
1633    ENDATA(E/0/U)
1634    #WRITE=A00(2)
1635    JA90.121.122.121
1636    121.A50(2)=A60(2)
1637    JA180.307.122.122
1638    307.W121;=ABS((A60-A50)/A60)              # CONVERGENCE ?
1639    W122;=W121-W200
1640    JW122.308.122.122
1641    308.W200;=W121          #STORE MAX VALUE
1642    122.J120(X)
1643    J115


1644    125.W122;=W200-.005              # CHECK CONVERGENCE
1645    TEXT=
1646    MAXIMUM ERROR OVER MESH␣
1647    PRINT(115)=W200(1)
1648    JW122.310.309.309
1649    309.ENTSTP(Y/4/P/U/4/U)
1650    ENDATA(P/0/U)
1651    U;=U+RINT(A10)+2
1652    P;=RINT(A00)
1653    TEXT=
1654    CONVERGED SOLUTION AT ITERATION␣
1655    PRINT(40)=P
1656    310.OUT(10006000)


1657    COMMENT=SUBROUTINE TO CALCULATE VALUES OF ALPHAS␣

1658    200.W200;=(1/W180)(W60+W24+W48+W12)*W199/W162 #ALPHA I-1/2,J
1659    W201;=(1/W182)(W24+W108+W12+W96)*W199/W160 #ALPHA I+1/2,J
1660    W202;=(1/W183)(W63+W27+W51+W15)*W199/W163 #ALPHA I,J-1/2
1661    W203;=(1/W181)(W75+W39+W63+W27)*W199/W161 #ALPHA I,J+1/2
1662    W180(4)=4
1663    JST
1664    EXIT

1665    #SUBROUTINE CALCULATES VORTICITY FUNCTIONS FOR SECOND ORDER
1666    #CONVECTIVE APPROXIMATION

1667    250.W204;=0.5(W200)(W64+W28)+0.5(W200^2)(W64-W28) #F I-1/2,J
1668    W205;=0.5(W201)(W28+W112)+0.5(W201^2)(W28-W112) #F I+1/2,J
1669    JSW
1670    EXIT
1671    255.W206;=0.5(W202)(W17+W29)+0.5(W202^2)(W17-W29) #F I,J-1/2
1672    W207;=0.5(W203)(W29+W41)+0.5(W203^2)(W29-W41) #F I,J+1/2
1673    EXIT

1674    COMMENT=SUBR CALCS VORTICITY FUNCTIONS FOR FOURTH ORDER
1675    CONVECTIVE APPROXIMATION␣

1676    270.W204;=(7*W200/12)(W64+W28)-(W200/12)(W88+W112)+(
1677    )(15*W200^2/24)(W64-W28)-(W200^2/24)(W88-W112)-(
1678    )(W200^3/12)(W64+W28)+(W200^3/12)(W88+W112)-(
```

```
1679    )(3*W200^4/24)(W64-W28)+(W200^4/24)(W88-W112) #F I-1/2,J
1680    W205;=(7*W201/12)(W28+W112)-(W201/12)(W64+W304)+(
1681    )(15*W201^2/24)(W28-W112)-(W201^2/24)(W64-W304)-(
1682    )(W201^3/12)(W28+W112)+(W201^3/12)(W64+W304)-(
1683    )(3*W201^4/24)(W28-W112)+(W201^4/24)(W64-W304) #F I+1/2,J
1684    JSW
1685    EXIT
1686    275,W206;=(7*W202/12)(W17+W29)-(W202/12)(W5+W41)+(
1687    )(15*W202^2/24)(W17-W29)-(W202^2/24)(W5-W41)-(
1688    )(W202^3/12)(W17+W29)+(W202^3/12)(W5+W41)-(
1689    )(3*W202^4/24)(W17-W29)+(W202^4/24)(W5-W41) #F I,J-1/2
1690    W207;=(7*W203/12)(W29+W41)-(W203/12)(W17+W317)+(
1691    )(15*W203^2/24)(W29-W41)-(W203^2/24)(W17-W317)-(
1692    )(W203^3/12)(W29+W41)+(W203^3/12)(W17+W317)-(
1693    )(3*W203^4/24)(W29-W41)+(W203^4/24)(W17-W317) #F I,J+1/2
1694    EXIT

1695    COMMENT=SUBROUTINE TO STORE DATA

1696    300,W0W(2)=A30(1)
1697    W2W(2)=A40(1)
1698    W4W(2)=A60(1)
1699    W6W(2)=A20(1)
1700    W8W(2)=A160(1)
1701    W10W(2)=A90(1)
1702    #WRITE=A00(2)
1703    #WRITE=W0W(12)
1704    EXIT
1705

1706    1000;

1707    F/T
1708    GSR
1709    10006
1710    OBJTPROG(2500)
1711    L/LINDEX(1134)
1712    TEXSTORE(430)
1713    CONSTORE(100)
1714    D-STORES(350)
1715    A-STORES(7200)
1716    W-STORES(6100)
1717    N-STORES(350)
1718    A(24)=0
1719    W/O TEST
1720    ENTSTP(Y/4/A/B/1/0)
1721    ENDATA(A/0/0)
1722    W42;=RINT(A00)-1                    #NO OF R.H.S'S
1723    ENTSTP(Y/4/A/B/1/0)                 #KEA ADDRESS ENTITY
1724    ENDATA(A/0/0)
1725    X;=RINT(A00)+1
1726    1,W100V;=A00                #STORE ALL THE ADDRESSES
1727    V;=V+1
1728    0;=0+1
1729    J1(X)
1730    W;=RINT(A00)+1
1731    2,W100V;=A00
1732    V;=V+1
1733    0;=0+1
1734    J2(W)
```

```
1735    A(2)=0
1736    W40;=0
1737    ENTSTP(Y/1/A/B/1/U)                    #COLUMN ENTITY
1738    5.ENTSTP(A/1/C/D/1/U)                  #C.I.P.
1739    JC.6.12.0
1740    6.ENTR(C/1/E)
1741    E;=E-1
1742    JE.7.5.0
1743    7.F(2)=0
1744    8.ENTSTP(C/1/F/G/1/U)                  #MESH POINT
1745    ENDATA(F/0/U)
1746    W40;=W40+A30*A160  #CALCULATE INLET MASS FLOW
1747    J8(E)
1748    J5

1749    12.A(7)=0
1750    X;=RINT(W100)
1751    W;=0
1752    T;=RINT(W100)+1
1753    T;=RINT(W100+W100T)+2                  #TO STORE R.H.S. VECTOR
1754    S;=T              #MARKER
1755    R;=T+RINT(W42) #STORE EXIT W CONTB ON EXIT POINTS
1756    W100R;=0 #FIRST VALUE IN VELY PROFILE
1757    W100S;=0
1758    13.A;=RINT(W101W)  #SELECT COLLOCATION POINT ADDRESS
1759    ENDATA(A/0/U)
1760    W0(18)=A00(18)
1761    #TEXT=
1762    #COLLOCATION POINT
1763    #WRITE=W0(2)
1764    W50;=2-W9                  #IS COLLOCATION POINT ON EXIT
1765    JW50.15.21.0
1766    15.JW15.17.23.0
1767    17.JW9.23.19.23
1768    19.C;=RINT(W102W)
1769    ENDATA(C/0/U)
1770    W50;=2-A90
1771    JW50.23.21.0
1772    21.E;=-1                   #COLLOCATION POINT ON EXIT
1773    W101W;=-W101W
1774    J25
1775    23.E;=1  #COLLOCATION POINT ON OTHER SURFACE
1776    25.W41;=ARCCOS((W12-W0)/SQRT((W12-W0)^2+(W13-W1)^2))
1777    W90;=W13-W1
1778    JW90.28.28.27
1779    27.W41;=8*ARCTAN(1)-W41
1780    28.U;=RINT(W100)+1
1781    V;=RINT(W100U)
1782    32.B;=RINT(W101U)  #SELECT FIELD POINT ADDRESS
1783    ENDATA(B/0/U)
1784    W18(18)=A00(18)
1785    #TEXT=
1786    #FIELD POINT
1787    #WRITE=W18(18)

1788    52.JE.45.0.33  #OTHER SURFACE.COLL PT ON EXIT BDRY
1789    33.W50;=2-W27
1790    JW50.45.34.45  #FIELD POINT NOT ON EXIT.ON EXIT BDRY
1791    34.F;=A-B
1792    JF.35.55.35  #NOT SAME PT.SAME PT.NOT SAME PT
```

```
35.F;=R-(T+RINT(W42)) #STORE SET FOR FIRST PT ON EXIT
JF.36.55.0
36.W51;=(W0-W18)^2+(W1-W19)^2
W52;=2*W24*W20*W34(W19-W1)/W51          #VX
W53;=2*W24*W20*W34(W0-W18)/W51          #VY
JW15.39.38.0
38.W100R;=W100R+(W52*COS(W41)+W53*SIN(W41))  #STORE PROFILE
J55      # FROM
39.W100R;=W100R+(W52*SIN(W41)-W53*COS(W41))  #EXIT VORTICITY
J55

45.W51;=(W10-W18)^2+(W11-W19)^2
W52;=2*W24*W20*W34(W19-W11)/W51                #VX
W53;=2*W24*W20*W34(W10-W18)/W51                #VY
JW15.47.46.0
46.W100S;=W100S+(W52*COS(W41)+W53*SIN(W41))  #STORE NEW R.H.S
J55
47.W100S;=W100S+(W52*SIN(W41)-W53*COS(W41))  #VECTOR

55.U;=U+1
J32(V)
JE.61.0.60
60.R;=R+1
W100R;=0
61.S;=S+1
W100S;=0
W;=W+1
J13(X)

Q;=T+2*RINT(W42)  #EXIT VELOCITY PROFILE MARKER
R;=T+RINT(W42)          #EXIT VORTICITY MARKER
S;=T              #(FIELD-EXIT)VORTICITY MARKER
W;=0
65.A;=RINT(W101W)
JA.67.0.66
66.W100Q;=W100S+((W100R+W101R)/2)  #CALC EXIT VELY PROFILE
Q;=Q+1
R;=R+1
67.S;=S+1
W;=W+1
J65(X)
P;=Q-(T+2*RINT(W42))  #NO OF VELY VECTORS ON DUCT EXIT
W60(2)=0
73.W52(4)=0
M;=1
N;=P-2
Q;=T+2*RINT(W42)
W;=0
75.A;=RINT(W101W)
JA.77.0.78
77.W;=W+1
J75
78.JM.79.83.0
79.B;=RINT(ABS(W102W))
ENDATA(B/0/U)
#WRITE=A00(2)
W53;=A160
W60;=A160
B;=RINT(ABS(W103W))
ENDATA(B/0/U)
```

```
1850    #WRITE=A0U(2)
1851    W54;=A160
1852    W52;=W100Q((W53/2)+(W54/4))  #FIRST TERM IN TRAPEZIUM
1853    N;=0          # + EXTRA AREA
1854    Q;=Q+1
1855    J77
1856    83.B;=RINT(ABS(W103W))
1857    ENDATA(B/0/U)
1858    #WRITE=A0U(2)
1859    W55;=A160
1860    W61;=W61+W54
1861    W52;=W52+W100Q((W53/4)+(W54/2)+(W55/4))  #SUM OTHER TERMS
1862    W53(2)=W54(2)       #   EXCEPT END
1863    Q;=Q+1
1864    W;=W+1
1865    J83(N)
1866    W60;=W60+W54
1867    W52;=W52+W100Q((W53/4)+(W54/2))  #AREA OF EXIT VELY PROFILE

1868    W51;=ABS(ABS(W40)-ABS(W52))-1&-2  #AREA CONVERG CHECK
1869    JW51.85.90.90
1870    85.W56;=-(W40+W52)/(0.75*W60+W61)  #CHANGE IN VELY COMPS
1871    N;=T+3*RINT(W42)
1872    Q;=T+2*RINT(W42)
1873    87.W100Q;=W100Q+W56
1874    W100N;=W100Q
1875    N;=N+1
1876    Q;=Q+1
1877    J87(P)
1878    J73

1879    90.N;=T+3*RINT(W42)              #STORE NEW R.H.S. VECTOR
1880    R;=T+RINT(W42)  #N,NEW PROFILE MARKER;R,EXIT VORT CONT MARKER
1881    S;=T            #(FIELD-EXIT) VORTICITY MARKER
1882    W;=0
1883    E;=0
1884    A(4)=0
1885    ENTSTP(Y/4/A/B/1/0)
1886    ENDATA(A/0/U)
1887    B;=INT(A0U)
1888    ENTSTP(A/1/C/D/B/0)
1889    91.G;=RINT(W101W)
1890    JG.94.V.102
1891    94.ENDATA(G/0/0)
1892    JA90.99.95.99
1893    95.JA150.99.98.0
1894    98.ENDATA(C/0/D)          #DUCT SURFACE POINT
1895    D;=D+E
1896    A1D;=-W100S
1897    J103
1898    99.W15;=A30          #DUCT INLET POINT
1899    ENDATA(C/0/D)
1900    D;=D+E
1901    A1D;=W15-W100S
1902    J103
1903    102.ENDATA(C/0/D)      #DUCT EXIT POINT
1904    D;=D+E
1905    A1D;=W100N-(W100S+((W100R+W101R)/2))
1906    N;=N+1
1907    R;=R+1
```

```
1908    103.S;=S+1
1909    W;=W+1
1910    E;=E+1
1911    J91(X)

1912    OUT(10007000)
1913    ▲▲

1914    1000;▲▲

1915    ▲▲F/T▲▲
1916    ▲▲GSR▲▲
1917    10007
1918    OBJTPROG(2500)
1919    L/LINDEX(1134)
1920    TEXSTORE(430)
1921    CONSTORE(100)
1922    D-STORES(350)
1923    A-STORES(7200)
1924    W-STORES(6100)
1925    N-STORES(350)
1926    W/O TEST
1927    A(24)=0
1928    ENTSTP(Y/4/A/B/4/O)
1929    ENDATA(A/0/U)
1930    O;=O+RINT(A10)+2
1931    W200;=A00                  #CURRENT ITERATION NUMBER
1932    C;=A10            #NUMBER OF PRINTS
1933    W0(C)=A20(C)               #STORE ITERATIONS TO BE PROCESSED
1934    #WRITE=W0(C)
1935    10.W101;=ABS(W0D)-W200  #ITERATION TO BE PLOTTED OR PRINTED
1936    JW101.11.14.11
1937    11.D;=D+1
1938    C;=C-1
1939    JC.10.40.0                 #NOT THIS ITERATION
1940    14.JW0D.15.0.20
1941    15.RUN(10008050)  #PLOTTED FIRST---STORE
1942                 # STREAKLINES + VORTICITY PROFILES

1943    20.PAGE                    #PRINT MESH DATA
1944    A(24)=0
1945    ENTSTP(Y/4/A/B/4/O)
1946    ENDATA(A/0/U)
1947    W101;=A20-1
1948    JW101.22.21.0
1949    21.TEXT=(41)IRROTATIONAL▲
1950    J23
1951    22.TEXT=(41)ROTATIONAL ▲
1952    23.TEXT= FLOW(5)ITERATION ▲
1953    O;=O+RINT(A10)+2
1954    PRINT(30)=A00(1)
1955    O;=O-3
1956    TEXT=
1957    (9)KINEMATIC VISCOSITY▲
1958    PRINT(26)=A00(1)
1959    TEXT=   TIMESTEP▲
1960    PRINT(26)=A10(1)
1961    W101;=A10(A30-1)
1962    TEXT=   FLOW ELAPSED TIME▲
1963    PRINT(26)=W101(1)
```

```
1964    LINE
1965    TEXT=
1966    (3)X MESH PT(4)Y MESH PT(5)U I J+1/2(5)V I+1/2 J(6)W N-1(
1967    )(9)W N(9)F.M.(9)V.M.␣
1968    LINES(2)

1969    30.ENTSTP(Y/1/E/F/1/0)              #COLUMN ENTITY
1970    JE.31.40.0
1971    31.G(2)=0
1972    32.ENTSTP(E/1/G/H/1/0)              #COLUMN INTERSECTION POINT
1973    JG.33.30.0
1974    33.ENTR(G/1/I)
1975    I;=I-1
1976    JI.35.34.0
1977    34.I;=1
1978    35.J(2)=0
1979    36.ENTSTP(G/1/J/K/1/0)              #MESH POINT
1980    ENDATA(J/0/0)
1981    PRINT(115)=A00(2)
1982    PRINT(115)=A30(4)
1983    PRINT(115)=A90(1)
1984    PRINT(115)=A140(1)
1985    LINE
1986    J36(I)
1987    J32

1988    40.ENDATA(A/0/0)
1989    0;=0+RINT(A10)+1
1990    W101;=A00-A10
1991    JW101.41.42.0  #NOT LAST ITERATION, LAST ITERATION
1992    41.A10;=A10+1
1993    OUT(10003000)

1994    42.ENTSTP(Y/3/L/M/1/0)              #CURVE ENTITY
1995    ENTSTP(L/2/P/Q/1/0)  #PLOTTING REFERENCE ENTITY
1996    ENTR(P/1/R)
1997    JR.46.45.0
1998    45.TEXT=
1999    PLOT PROGRAM HAS NOT BEEN CALLED␣
2000    TODISC
2001    END

2002    46.TEXT=
2003    ASSEMBLE PLOTTING VECTORS␣
2004    OUT(10009000)  #RUN PROG TO ASSEMBLE PLOT INSTRUCTIONS
2005    ␣␣

2006    1000;␣␣

2007    ␣␣F/T␣␣
2008    ␣␣GSR␣.
2009    10008
2010    OBJTPROG(2500)
2011    L/LINDEX(1134)
2012    TEXSTORE(430)
2013    CONSTORE(100)
2014    D-STORES(350)
2015    A-STORES(7200)
2016    W-STORES(6100)
2017    N-STORES(350)
```

```
2018    W/O TEST
2019    A(24)=0                    #COLLECT OUTLINE COORDINATES
2020    1.ENTSTP(Y/3/A/B/1/O)              #CURVE ENTITY
2021    JA.2.21.0
2022    2.C(3)=0
2023    3.ENTSTP(A/1/C/D/1/O)              #SPECIFIED POINT ENTITY
2024    JC.4.20.0
2025    4.F;=1
2026    5.ENTR(C/F/O)
2027    JO.10.6.0
2028    6.O;=F-1  #SET E AS R.S. FOR OUTER/INNER BOUNDARY.
2029    JO.3.7.0
2030    7.F;=2
2031    J5
2032    10.G(2)=0
2033    11.ENTSTP(C/F/G/H/1/O)             #INTERSECTION POINT
2034    JG.12.2.0
2035    12.JE.14.13.0
2036    13.E;=G  #STORE FIRST INTERSECT PT ADDRESS TO CLOSE CURVE
2037    14.ENDATA(G/O/O)
2038    W101I(2)=A30(2)                    #STORE COORDINATES
2039    #WRITE=W101I(2)
2040    I;=I+2
2041    J11
2042    20.ENDATA(E/O/O)
2043    W101I(2)=A30(2)                    #CLOSE FIRST CURVE
2044    #WRITE=W101I(2)
2045    I;=I+2
2046    J1
2047    21.W100;=I  #STORE NO OF COORDS COMPRISING THE OUTLINE

2048    A(8)=0           #COLLECT COLUMN COORDINATES
2049    22.ENTSTP(Y/1/A/B/1/O)             #COLUMN ENTITY
2050    JA.23.18.0
2051    23.C(2)=0
2052    24.ENTSTP(A/1/C/D/1/O)             #C.I.P.
2053    JC.25.22.0
2054    25.ENDATA(C/O/O)
2055    W0;=1-A00
2056    JW0.24.29.28
2057    28.W0;=3-A00
2058    JW0.24.29.0
2059    29.W102I(2)=A30(2)                 #STORE COORDINATES
2060    #WRITE=W102I(2)
2061    I;=I+2
2062    J;=J+2
2063    31.ENTSTP(A/1/C/D/1/O)  #FIND WHERE COL LEAVES REGION
2064    ENDATA(C/O/O)
2065    W0;=1-A00
2066    JW0.34.31.32
2067    32.W0;=3-A00
2068    JW0.34.31.0
2069    34.W102I(2)=A30(2)  #STORE COORDS WHERE THIS HAPPENS
2070    #WRITE=W102I(2)
2071    I;=I+2
2072    J;=J+2
2073    J24
2074    38.K;=I-J
2075    W101K;=J  #STORE NO OF COORDS OF ALL COLUMNS
```

```
2076    I;=I+2
2077    ENTSTP(Y/4/E/F/1/0)                    #REGION DATA ENTITY
2078    ENDATA(E/0/0)
2079    0;=RINT(A00)
2080    CHAD(90/I)
2081    MAKE(90/0/H/G)  #MAKE ENTITY TO HOLD BASIC PLOT DATA
2082    PUT(Y/4/G/1)
2083    ENDATA(G/0/0)
2084    41.W0;=I-100
2085    JW0,43,42,42
2086    42.A00(I)=W100L(I)  #STORE BASIC PLOT DATA
2087    #WRITE=A00(I)
2088    J44
2089    43.A00(100)=W100L(100)
2090    #WRITE=A00(100)
2091    I;=I-100
2092    L;=L+100
2093    0;=0+100
2094    J41

2095    44.A(8)=0
2096    ENTSTP(Y/4/A/B/2/0)
2097    ENDATA(A/0/0)
2098    B;=RINT(A00)
2099    ENTSTP(Y/3/C/D/1/0)                    #CURVE ENTITY
2100    CHAD(90/0)
2101    MAKE(90/B/F/E)
2102    PUT(C/2/E/1)                #CREATE PLOTTING REFERENCE ENTITY
2103    BACK



2104    50.A(24)=0
2105    W/0 TEST
2106    ENTSTP(Y/3/C/D/1/0)
2107    ENTSTP(C/2/A/B/1/0)  #A--PLOTTING REFERENCE ENTITY
2108    C(2)=0
2109    ENTSTP(Y/4/C/D/4/0)
2110    ENDATA(C/0/0)
2111    B;=A00              #REGION NUMBER
2112    E;=-1
2113    ENTSTP(Y/4/C/D/E/0)
2114    ENDATA(C/0/0)
2115    E;=A00
2116    0;=0+E+1
2117    W99;=E+RINT(A00)+2  #TOTAL NO OF WORDS IN BASIC PLOT DATA
2118    0;=0-E-1
2119    E;=W99
2120    52.W100F;=A00  #STORE BASIC PLOT DATA IN DUMMY STORES
2121    F;=F+1
2122    0;=0+1
2123    J52(E)

2124    D(3)=0              #STORE DUCT OUTLINE FOR STREAKLINE PLOT
2125    CHAD(90/1)
2126    MAKE(90/B/E/D)              #CREATE PAGE ENTITY
2127    PUTEND(A/1/D/1)
2128    ENDATA(D/0/0)
2129    A00;=10                     #STORE SCALE
2130    I;=RINT(W100)+1
```

```
2131    CHAD(90/I)
2132    I;=I-1
2133    MAKE(90/B/H/G)
2134    PUTEND(D/1/G/1)
2135    ENDATA(G/0/0)
2136    A00;=1              #LINE STYLE
2137    54.A10;=W101K       #STORE OUTLINE COORDS
2138    K;=K+1
2139    0;=0+1
2140    J54(I)

2141    K;=0  #STORE DUCT OUTLINE FOR VELOCITY PROFILE PLOT
2142    CHAD(90/1)
2143    MAKE(90/B/H/E)          #PAGE ENTITY
2144    PUTEND(A/1/E/1)
2145    ENDATA(E/0/0)
2146    A00;=10
2147    I;=I+1
2148    CHAD(90/I)
2149    I;=I-1
2150    MAKE(90/B/H/G)
2151    PUTEND(E/1/G/1)             #OUTLINE VECTOR
2152    ENDATA(G/0/0)
2153    A00;=1
2154    56.A10;=W101K
2155    K;=K+1
2156    0;=0+1
2157    J56(I)
2158    J;=RINT(W101K)/4            #NO OF COLUMNS
2159    CHAD(90/5)
2160    58.G(2)=0
2161    MAKE(90/B/H/G)
2162    PUTEND(E/1/G/1)             #COLUMN VECTOR
2163    ENDATA(G/0/0)
2164    A00;=1
2165    A10(4)=W102K(4)
2166    #WRITE=A10(4)
2167    K;=K+4
2168    J58(J)

2169    K;=0  #STORE DUCT OUTLINE FOR VORTICITY PROFILE PLOT
2170    CHAD(90/1)
2171    MAKE(90/B/H/F)          #PAGE ENTITY
2172    PUTEND(A/1/F/1)
2173    ENDATA(F/0/0)
2174    A00;=10
2175    I;=I+1
2176    CHAD(90/I)
2177    I;=I-1
2178    MAKE(90/B/H/G)
2179    PUTEND(F/1/G/1)             #OUTLINE VECTOR
2180    ENDATA(G/0/0)
2181    A00;=1
2182    60.A10;=W101K
2183    K;=K+1
2184    0;=0+1
2185    J60(I)
2186    CHAD(90/5)
2187    62.G(2)=0
2188    MAKE(90/B/H/G)
```

```
2189    PUTEND(F/1/G/1)                    #COLUMN VECTOR
2190    ENDATA(G/0/U)
2191    A00;=1
2192    A10(4)=W102K(4)
2193    #WRITE=A10(4)
2194    K;=K+4
2195    J62(J)


2196    G(7)=0
2197    W8(2)=0
2198    ENTSTP(Y/1/H/I/1/0)
2199    200.ENTSTP(H/1/J/K/1/U)
2200    JJ.201.209.0
2201    201.ENTR(J/1/X)
2202    X;=X-1
2203    JX.203.202.0
2204    202.X;=1
2205    203.L(2)=0
2206    204.ENTSTP(J/1/L/M/1/U)
2207    ENDATA(L/0/U)
2208    JW8.206.205.0
2209    205.W8;=ABS(A60)  #STORE VORTICITY AS REFERENCE
2210    206.W0;=ABS(A30)-W9
2211    JW0.207.208.208
2212    207.W9;=ABS(A30)  #STORE VELOCITY AS REFERENCE
2213    208.X;=X-1
2214    JX.204.200.0

2215    209.G(7)=0
2216    64.ENTSTP(Y/1/H/I/1/0)             #COLUMN ENTITY
2217    JH.65.190.0
2218    65.C;=0
2219    J(2)=0
2220    66.ENTSTP(H/1/J/K/1/0)             #C.I.P.
2221    JJ.67.64.0
2222    67.ENTR(J/1/X)
2223    X;=X-1
2224    JX.72.70.0

2225    70.L(2)=0
2226    X;=1
2227    ENTSTP(J/1/L/M/1/0)                #MESH POINT
2228    ENDATA(L/0/0)
2229    W200C;=A00+(A30*A20/W9)  #VELOCITY PROFILE POINT
2230    W0;=A140+1
2231    JW0.110.111.0
2232    110.W201C;=A10+A160/2
2233    J112
2234    111.W201C;=A10
2235    112.W202C;=A00+(A60*A20/W8)  #VORTICITY PROFILE POINT
2236    W203C;=A10
2237    C;=C+4
2238    C;=(C-2)/4              #NO OF POINTS IN BASIC PROFILE
2239    0;=2(C+1)+1
2240    CHAD(90/0)
2241    MAKE(90/8/0/G)          #MAKE VELOCITY PROFILE ENTITY
2242    PUTEND(E/1/G/1)
2243    ENDATA(G/0/0)
2244    A00;=3
```

```
2245    G;=0
2246    A10(2)=W200G(2)                    #STORE BASE POINT
2247    #WRITE=A10(2)
2248    220.A30(2)=W202G(2)                #STORE REMAINING POINTS
2249    #WRITE=A30(2)
2250    G;=G+4
2251    O;=O+2
2252    J220(C)
2253    O;=2*C+1
2254    CHAD(90/O)
2255    MAKE(90/B/O/G)              #MAKE VORTICITY PROFILE ENTITY
2256    PUTEND(F/1/G/1)
2257    ENDATA(G/0/U)
2258    A00;=3
2259    G;=0
2260    221.A10(2)=W204G(2)                #STORE POINTS ON PROFILE
2261    #WRITE=A10(2)
2262    G;=G+4
2263    O;=O+2
2264    J221(C)
2265    C;=0
2266    ENDATA(L/0/U)
2267    W0;=A140+1
2268    JW0.77.66.0  #CALC COMP.NU COMP-SELECT NEW C.I.P.

2269    72.L(2)=0
2270    73.ENTSTP(J/1/L/M/1/O)             #MESH POINT
2271    ENDATA(L/0/U)
2272    JC.75.74.0
2273    74.W200C(2)=A00(2)  #VELOCITY PROFILE BASE POINTS
2274    #WRITE=W200C(2)
2275    C;=C+2
2276    W100(14)=0
2277    75.W200C;=A00+(A30*A20/W9) #VELOCITY PROFILE POINT
2278    W201C;=A10+A160/2
2279    W202C;=A00+(A60*A20/W8)  #VORTICITY PROFILE POINT
2280    W203C;=A10
2281    C;=C+4
2282    77.W100(2)=A30(2)
2283    #WRITE=A00(2)
2284    #WRITE=W100(2)
2285    Q(4)=0
2286    RNGSTP(L/2/Q/R/1/O)
2287    RNGSTP(Q/3/S/T/1/O)                #ROW ENTITY
2288    Q;=S
2289    R(2)=0
2290    78.ENTSTP(Q/1/R/S/1/O)             #R.I.P.
2291    T(2)=0
2292    80.ENTSTP(R/2/T/U/1/O)
2293    JT.81.78.0
2294    81.O;=T-L
2295    JO.80.82.80
2296    82.Q;=R                    #RESET Q TO BE THE R.I.P.
2297    ENDATA(J/0/U)
2298    W0;=A00-1
2299    JW0.83.86.85               #IS CONTINUATION MARKER 1 OR 3
2300    83.W0;=3-A00
2301    JW0.85.86.0
2302    85.P;=0                    #NO-CONT' MARKER IS EITHER 0 OR 1
2303    ENDATA(L/0/U)
```

```
2304    J87
2305    86.P;=L
2306    ENTSTP(J/1/P/M/1/O)
2307    ENDATA(P/0/U)
2308    #WRITE=A00(2)
2309    W102(2)=A30(2)
2310    #WRITE=W102(2)
2311    87.W0;=1-A90
2312    JW0.88.90.88
2313    88.W0;=2+A90
2314    JW0.92.90.92
2315    90.R(2)=-1                  #POINTS P AND/OR L ON INLET
2316    J100
2317    92.R;=L                     #POINTS P AND/OR L NOT ON INLET
2318    S;=2
2319    T;=-1
2320    ENTSTP(Q/2/R/S/T/O)
2321    JR.231.230.0
2322    230.S;=H
2323    ENTSTP(Y/1/S/I/T/U)
2324    J100
2325    231.ENDATA(R/0/O)
2326    W108(2)=A30(2)
2327    #WRITE=A00(2)
2328    #WRITE=W108(2)
2329    S;=H
2330    ENTSTP(Y/1/S/I/T/O)  #SELECT PREVIOUS COL ENTITY
2331    T;=0
2332    94.ENTSTP(S/1/T/K/1/O)          #PREVIOUS C.I.P.
2333    V;=0
2334    96.ENTSTP(T/1/V/M/1/O)
2335    JV.97.94.0
2336    97.O;=V-R
2337    JO.96.99.96
2338    99.S;=T                     #RESET S AS PREVIOUS C.I.P.
2339    100.V;=H
2340    ENTSTP(Y/1/V/I/1/O)
2341    JV.102.101.0
2342    101.U(2)=-1                 #POINTS U & V  ON EXIT
2343    I;=1
2344    J130
2345    102.U;=L
2346    T;=2
2347    ENTSTP(Q/2/U/T/1/O)
2348    JU.235.130.0
2349    235.ENDATA(U/0/O)
2350    W104(2)=A30(2)
2351    #WRITE=A00(2)
2352    #WRITE=W104(2)
2353    U;=0
2354    J130


2355    120.JR.121.121.122              #RESET MODULE
2356    121.R;=T
2357    122.W108(2)=W106(2)
2358    #WRITE=W108(2)
2359    N;=L
2360    W110(2)=W100(2)
2361    #WRITE=W110(2)
```

```
2362    L;=P
2363    W100(2)=W102(2)
2364    #WRITE=W100(2)
2365    JU.125.125.126
2366    125.W;=U
2367    126.W112(2)=W104(2)
2368    #WRITE=W112(2)
2369    X;=X-1
2370    JX.183.66.0


2371    183.ENDATA(L/0/0)
2372    W200C;=A00+(A30*A20/W9)  #VELOCITY PROFILE POINT
2373    W201C;=A10+A160/2
2374    W202C;=A00+(A60*A20/W8)  #VORTICITY PROFILE POINT
2375    W203C;=A10
2376    C;=C+4
2377    130.ENDATA(L/0/0)                #CHECK VELOCITY MARKER
2378    W0;=1-ABS(A140)
2379    JW0.132.170.142
2380    132.JU.258.240.0
2381    240.W0(4)=A(4)
2382    A(4)=0
2383    RNGSTP(L/2/A/B/1/0)
2384    RNGSTP(A/3/C/D/1/0)              #ROW ENTITY
2385    Q;=C
2386    A(2)=0
2387    241.ENTSTP(Q/1/A/B/1/0)          #R.I.P.
2388    C(2)=0
2389    242.ENTSTP(A/2/C/D/1/0)
2390    JC.243.241.0
2391    243.Q;=C-L
2392    JU.242.245.242
2393    245.U;=L
2394    ENTSTP(A/2/U/D/1/0)
2395    JU.248.247.0
2396    247.ENTSTP(Q/1/A/B/1/0)
2397    ENTSTP(A/2/U/D/2/0)
2398    248.Q;=A                    #RESET Q TO BE R.I.P.
2399    A(2)=0
2400    250.ENTSTP(V/1/A/B/1/0)          #NEXT C.I.P.
2401    C(2)=0
2402    251.ENTSTP(A/1/C/D/1/0)
2403    JC.252.250.0
2404    252.Q;=C-U
2405    JU.251.253.251
2406    253.V;=A                    #RESET V TO BE NEXT C.I.P.
2407    A(4)=W0(4)
2408    J262

2409    258.ENTSTP(V/1/U/M/1/0)  #CALC 'X' STREAKLINE
2410    JU.262.261.0
2411    261.W0;=A
2412    A;=H
2413    ENTSTP(Y/1/A/I/1/0)
2414    ENTSTP(A/1/V/K/1/0)
2415    ENTSTP(V/1/U/M/2/0)
2416    A;=W0
2417    262.ENDATA(U/0/0)
2418    #WRITE=A00(2)
```

```
2419    W104(2)=A30(2)
2420    #WRITE=W104(2)
2421    W10;=(W100+W104+W110+W112)/4  #AVERAGE U-COMPONENT
2422    W11;=SQRT(W10^2+W101^2)
2423    ENDATA(L/0/U)
2424    W3(3)=A00(3)
2425    #WRITE=W3(3)
2426    W6;=A160
2427    W12;=W11*W5/W9          #SCALED VELOCITY VECTOR
2428    CHAD(90/5)
2429    MAKE(90/B/0/G)
2430    PUTEND(D/1/G/1)
2431    ENDATA(G/0/U)
2432    A00;=2
2433    JW10.133.133.136
2434    133.JW101.134.134.135
2435    134.A10;=ARCSIND(ABS(W101)/W11)
2436    J139
2437    135.A10;=-ARCSIND(ABS(W101)/W11)
2438    J139
2439    136.JW101.137.137.138
2440    137.A10;=90+ARCSIND(ABS(W10)/W11)
2441    J139
2442    138.A10;=-90-ARCSIND(ABS(W10)/W11)
2443    139.A20;=W3+(W5/2)-((W12/2)(W10/W11))
2444    A30;=W4-(W12/2)(W101/W11)
2445    A40;=A20+W12

2446    142.JP.143.144.0  #CALCULATE 'Y' STREAKLINE
2447    143.P;=L
2448    ENTSTP(J/1/P/M/1/0)
2449    ENDATA(P/0/U)
2450    #WRITE=A00(2)
2451    W102(2)=A30(2)
2452    #WRITE=W102(2)
2453    144.JR.147.270.155  #NOT ON INLET.NOT THERE.ON INLET
2454    147.T;=R
2455    ENTSTP(S/1/T/M/1/0)
2456    JT.150.320.0
2457    320.W0(2)=A(2)
2458    A;=H
2459    B;=-1
2460    ENTSTP(Y/1/A/I/B/0)
2461    ENTSTP(A/1/S/K/1/0)
2462    ENTSTP(S/1/T/M/2/0)
2463    A(2)=W0(2)
2464    JT.150.148.0
2465    148.W10;=(W103+W109+W101)/3  #AVERAGE V-COMPONENT
2466    J158
2467    150.ENDATA(T/0/U)
2468    #WRITE=A00(2)
2469    W106(2)=A30(2)
2470    #WRITE=W106(2)
2471    JV.157.0.152            #NOT ON EXIT.NOT THERE.ON EXIT
2472    152.W103;=W107
2473    W101;=W109
2474    J157
2475    155.T;=0
2476    W107;=W103
2477    W109;=W101
```

```
2478    J157
2479    156,W10;=(W107+W103+W109)/3 #AVERAGE V-COMPONENT
2480    J158

2481    270,W0(5)=A(5)
2482    A(5)=0
2483    RNGSTP(P/2/A/B/1/0)
2484    RNGSTP(A/3/C/D/1/0)                  #ROW ENTITY
2485    A;=C
2486    B(2)=0
2487    271,ENTSTP(A/1/B/C/1/0)
2488    D(2)=0
2489    272,ENTSTP(B/2/D/E/1/0)
2490    JD,273,271,0
2491    273,0;=D-P
2492    J0,272,274,272
2493    274,T;=P
2494    D;=-1
2495    ENTSTP(B/2/T/E/D/0)
2496    JT,276,285,0
2497    276,A(2)=0
2498    278,ENTSTP(S/1/A/B/1/0)              #PREVIOUS C.I.P.
2499    C(2)=0
2500    279,ENTSTP(A/1/C/D/1/0)
2501    JC,280,278,0
2502    280,0;=C-T
2503    J0,279,281,279
2504    281,S;=A                    #RESET S AS PREVIOUS C.I.P
2505    A(5)=W0(5)
2506    ENDATA(T/0/0)
2507    #WRITE=A00(2)
2508    W106(2)=A30(2)
2509    #WRITE=W106(2)
2510    W10;=(W107+W103+W101)/3
2511    J158
2512    285,W10;=(W103+W101)/2
2513    A(5)=W0(5)
2514    J158

2515    157,W10;=(W107+W103+W109+W101)/4  #AVERAGE V-COMPONENT
2516    158,W11;=SQRT(W10^2+W100^2)
2517    ENDATA(L/0/0)
2518    W3(3)=A00(3)
2519    #WRITE=W3(3)
2520    W6;=A160
2521    W12;=W11*W5/W9
2522    CHAD(90/5)
2523    MAKE(90/B/0/G)
2524    PUTEND(D/1/G/1)
2525    ENDATA(G/0/0)
2526    A00;=2
2527    JW100,160,160,163
2528    160,JW10,161,161,162
2529    161,A10;=ARCSIND(ABS(W10)/W11)
2530    J166
2531    162,A10;=-ARCSIND(ABS(W10)/W11)
2532    J166
2533    163,JW10,164,164,165
2534    164,A10;=90+ARCSIND(ABS(W100)/W11)
2535    J166
```

```
2536    165,A10;=-90-ARCSIND(ABS(W100)/W11)
2537    166,A20;=W3-(W12/2)(W100/W11)
2538    A30;=W4+(W6/2)-((W12/2)(W10/W11))
2539    A40;=A20+W12
2540    J120

2541    170,JA140,171,0,120
2542    171,JU,310,290,0
2543    290,W0(4)=A(4)
2544    A(4)=0
2545    RNGSTP(L/2/A/B/1/U)
2546    RNGSTP(A/3/C/D/1/U)                    #ROW ENTITY
2547    Q;=C
2548    A(2)=0
2549    291,ENTSTP(Q/1/A/B/1/U)                #R.I.P.
2550    C(2)=0
2551    292,ENTSTP(A/2/C/D/1/U)
2552    JC,293,291,0
2553    293,U;=C-L
2554    JU,292,295,292
2555    295,U;=L
2556    ENTSTP(A/2/U/D/1/U)
2557    JU,298,297,0
2558    297,ENTSTP(Q/1/A/B/1/U)
2559    ENTSTP(A/2/U/D/2/U)
2560    298,Q;=A                  #RESET Q TO BE R.I.P.
2561    A(2)=0
2562    300,ENTSTP(V/1/A/B/1/U)                #NEXT C.I.P.
2563    C(2)=0
2564    301,ENTSTP(A/1/C/D/1/U)
2565    JC,302,300,0
2566    302,U;=C-U
2567    JU,301,303,301
2568    303,V;=A                  #RESET V TO BE NEXT  C.I.P.
2569    A(4)=W0(4)
2570    J312

2571    310,ENTSTP(V/1/U/M/1/U)  #CALCULATE 'X' STREAKLINE
2572    JU,312,311,0
2573    311,W0;=A
2574    A;=H
2575    ENTSTP(Y/1/A/I/1/U)
2576    ENTSTP(A/1/V/K/1/U)
2577    ENTSTP(V/1/U/M/2/U)
2578    A;=W0
2579    312,ENDATA(U/0/U)
2580    #WRITE=A00(2)
2581    W104(2)=A30(2)
2582    #WRITE=W104(2)
2583    JP,315,316,0
2584    315,P;=L
2585    ENTSTP(J/1/P/M/1/U)
2586    ENDATA(P/0/U)
2587    #WRITE=A00(2)
2588    W102(2)=A30(2)
2589    #WRITE=W102(2)
2590    316,W10;=(W100+W104+W110+W112)/4
2591    W11;=SQRT(W10^2+W101^2)
2592    ENDATA(L/0/U)
2593    W3(3)=A00(3)
```

```
2594    #WRITE=W3(3)
2595    W6;=A160
2596    W12;=W11*W5/W9
2597    CHAD(90/5)
2598    MAKE(90/B/0/G)
2599    PUTEND(D/1/G/1)
2600    ENDATA(G/0/U)
2601    A00;=2
2602    JW10.173.173.176
2603    173.JW101.174.174.175
2604    174.A10;=ARCSIND(ABS(W101)/W11)
2605    J179
2606    175.A10;=-ARCSIND(ABS(W101)/W11)
2607    J179
2608    176.JW101.177.177.178
2609    177.A10;=90+ARCSIND(ABS(W10)/W11)
2610    J179
2611    178.A10;=-90-ARCSIND(ABS(W10)/W11)
2612    179.A20;=W3+(W5/2)-((W12/2)(W10/W11))
2613    A30;=W4-(W12/2)(W101/W11)
2614    A40;=A20+W12
2615    J120


2616    190.BACK
2617    
2618    1000;
2619    F/T
2620    GSR
2621    10009
2622    OBJTPROG(2500)
2623    L/LINDEX(1134)
2624    TEXSTORE(430)
2625    CONSTORE(100)
2626    D-STORES(350)
2627    A-STORES(7200)
2628    W-STORES(6100)
2629    N-STORES(350)
2630    PAGE
2631    TEXT=BEGIN
2632    TEXT=END
2633    TEXT=L
2634    TEXT=S
2635    TEXT=TC
2636    TEXT=500A
2637    TEXT=       /
2638    TEXT=PAGE
2639    TEXT=C
2640    TEXT=R
2641    TEXT=TP
2642    COMMENT=THIS PROGRAM PREPARES A MAGNETIC TAPE OF DRAWING
2643    INSTRUCTIONS FROM DATA ON RS Z.HUNG ON THIS RS IS A RING
2644    OF PAGE ENTITIES AND ON EACH OF THESE IS HUNG A RING OF
2645    VECTORS.EACH VECTOR CONSISTS OF A LIST OF XY VALUES TO
2646    BE PLOTTED AS A CONTINUOUS LINE.EACH PAGE ENTITY HAS A
2647    SCALE AS DATA.THE PROGRAM CHECKS THAT THE COORDINATES
2648    GIVEN WILL FIT ON TO THE 30 INCH DRUM PLOTTER AT THE
2649    GIVEN SCALE AND IF NOT THE MAXIMUM POSSIBLE SCALE IS USED
```

```
2650    MO/P(1)
2651    A(24)=0
2652    ENTSTP(Y/3/A/B/1/O)          #CURVE ENTITY
2653    ENTSTP(A/2/X/C/1/O)          #PLOTTING REFERENCE ENTITY
2654    A(3)=0
2655    34.O=1
2656    ENTSTP(X/1/W/O/1/A)
2657    JW.31.32.0
2658    31.ENDATA(W/O/E)
2659    TEXT=
2660    NEXT PAGE
2661    TEXT=
2662    SCALE
2663    PRINT(0024)=A0E
2664    V=0
2665    36.O=1
2666    ENTSTP(W/1/V/O/1/A)
2667    JV.33.34.0
2668    33.TEXT=
2669    NEXT LINE
2670
2671    INFO(V/A/B/C/D)
2672    D=(D-1)/2
2673    ENDATA(V/O/E)
2674    PRINT(1024)=A0E
2675    35.PRINT(1024)=A1E
2676    PRINT(0024)=A2E
2677    E=E+2
2678    J35(D)
2679    J36
2680    32.A=0
2681    W=0
2682    29.O=1
2683    ENTSTP(X/1/W/O/1/D)
2684    JW.7.2.0
2685    1.W300=-&+10
2686    W301=&+10
2687    W302=-&+10
2688    W303=&+10
2689    V=0
2690    28.O=1
2691    ENTSTP(W/1/V/O/1/D)
2692    JV.6.7.0
2693    6.INFO(V/D/E/F/G)
2694    G=(G-1)/2
2695    ENDATA(V/1/E)
2696    D=0
2697    12.W304=W300D-A0E
2698    JW304.8.9.9
2699    9.W300D=A0E
2700    8.W304=W301D-A0E
2701    JW304.10.11.11
2702    10.W301D=A0E
2703    11.E=E+2
2704    J12(G)
2705    D=2
2706    E=E-2*G+1
2707    J12(2)
2708    J28
2709    7.ENDATA(W/O/E)
```

```
2710    W304=A0E
2711    J19
2712    W305=W304*(W300-W301)-150
2713    JW305.13.14.14
2714    13.W305=150-W300+W301
2715    JW305.15.16.16
2716    15.W304=INT(150/(W300-W301))
2717    J17
2718    16.W304=1/(1+INT((W300-W301)/150))
2719    17.TEXT=
2720    SCALE GIVEN TOO LARGE IN X DIRECTION␣
2721    14.W305=W304*(W302-W303)-68
2722    JW305.18.19.19
2723    18.W305=70-W302+W303
2724    JW305.20.21.21
2725    20.W304=INT(68/(W302-W303))
2726    J22
2727    21.W304=1/(1+INT((W302-W303)/150))
2728    22.TEXT=
2729    SCALE GIVEN TOO LARGE IN Y DIRECTION␣
2730    19.TEXT=
2731    SCALE USED␣
2732    PRINT(0024)=W304
2733    D=-530
2734    W0A=D1D
2735    JS3
2736    W0A=0
2737    JS3
2738    W0A=150
2739    JS3
2740    W0A=W304
2741    JS3
2742    W0A=0
2743    JS3
2744    W0A=68
2745    JS3
2746    W0A=W304
2747    JS3
2748    23.V=0
2749    27.W0A=D7D
2750    JS3
2751    W0A=0
2752    JS3
2753    D=1
2754    ENTSTP(W/1/V/D/1/C)
2755    JV.30.25.0
2756    30.INFO(V/E/F/G/H)
2757    ENDATA(V/0/E)
2758    E=RINT(A0E+100
2759    JE
2760    101.H=(H-1)/2-1          #STRAIGHT LINES WITH NO SYMBOLS
2761    ENDATA(V/1/E)
2762    W0A=D5D
2763    JS3
2764    W0A=0
2765    JS3
2766    W0A=A0E
2767    JS3
2768    W0A=A1E
2769    JS3
```

```
2770    W0A=D7D
2771    JS3
2772    W0A=1
2773    JS3
2774    JH.26.27.0
2775    26.W0A=D5D
2776    JS3
2777    W0A=0
2778    JS3
2779    W0A=A2E
2780    JS3
2781    W0A=A3E
2782    JS3
2783    E=E+2
2784    J26(H)
2785    J27
2786    102,ENDATA(V/0/E)        #STRAIGHT LINES WITH ARROWHEADS
2787    W0A=D21D
2788    JS3
2789    W0A=2
2790    JS3
2791    W0A=D19D
2792    JS3
2793    W0A=A1E
2794    JS3
2795    W0A=A2E
2796    JS3
2797    W0A=A3E
2798    JS3
2799    W0A=D5D
2800    JS3
2801    W0A=0
2802    JS3
2803    W0A=A2E
2804    JS3
2805    W0A=A3E
2806    JS3
2807    W0A=D7D
2808    JS3
2809    W0A=1
2810    JS3
2811    W0A=D5D
2812    JS3
2813    W0A=44
2814    JS3
2815    W0A=A4E
2816    JS3
2817    W0A=A3E
2818    JS3
2819    W0A=D19D
2820    JS3
2821    W0A=0
2822    JS3
2823    W0A=A2E
2824    JS3
2825    W0A=A3E
2826    JS3
2827    W0A=D21D
2828    JS3
2829    W0A=5
```

```
2830    JS3
2831    J27
2832    103,H=(H-1)/2          #CURVES WITH X'S PLOTTED
2833    ENDATA(V/1/E)
2834    W0A=D21D
2835    JS3
2836    W0A=2
2837    JS3
2838    W0A=D7D
2839    JS3
2840    W0A=1
2841    JS3
2842    W0A=D17D
2843    JS3
2844    W0A=3
2845    JS3
2846    JH,40,27,0
2847    40,W0A=A0E
2848    JS3
2849    W0A=A1E
2850    JS3
2851    E=E+2
2852    J40(H)
2853    M=61
2854    W0A:=M
2855    JS3
2856    W0A=D21D
2857    JS3
2858    W0A=5
2859    JS3
2860    J27
2861    25,W0A=D15D
2862    JS3
2863    J29
2864    2,C=61465
2865    D=-530
2866    W0A=D3D
2867    JS3
2868    W0A:=C
2869    JS3
2870    W0A(256)=0
2871    MWRITE=W0(256)
2872    W0=0
2873    MLBWRITE=W0
2874    TODISC
2875    OUTU(FQJSW49)
2876    END
2877    3,A=A+1
2878    I=256-A
2879    JI,4,5,0
2880    5,MWRITE=W0(256)
2881    A=0
2882    4,EXIT
2883
2884    1000:
2885
```

The output included in this appendix is only a small sample of what is normally obtained. When the data is being created, the user decides on the amount and type of output which he requires.

For the computer runs described in this thesis, a complete print out of the contents of the mesh stores was usually obtained every three iterations. This was sufficient for calculating the variation of reattachment point position with time in the stepped duct studies.

OUTPUT FROM PROGRAM 50

```
SCHEME D PROGRAM   00050   DATE 09/03/76   TIME 39H 20M 09S   (TWO)

JOB NUMBER       1002
DATA TYPE   50
ITEM NUMBER      1USED AT BEGINNING OF AN ITEM
CURVE & REGION GEOMETRY DEFN.

SET UP STRUCTURE FROM THE BEGINNING

DATA TYPE 50  NEW CURVE

TEST RESULTS
D                    0


STRAIGHT LINES & CIRCULAR ARCS

TEST RESULTS
E                    9   A5538  0.000000000&+ 0   A5533  1.000000000&+ 0   E                    9   A5562  0.000000000&+ 0
A5557  2.000000000&+ 0   E                    9   A5586  0.000000000&+ 0   A5581  3.000000000&+ 0   E                    9
A5610  0.000000000&+ 0   A5605  4.000000000&+ 0   E                    9   A5634  0.000000000&+ 0   A5629  5.000000000&+ 0
E                    9   A5658  0.000000000&+ 0   A5653  6.000000000&+ 0   E                    9   A5682  0.000000000&+ 0
A5677  1.000000000&+ 0


REGION DEFN.
NOTE  ALL REGION NOS. MUST BE UNIQUE

TEST RESULTS
G                    0


MAJOR REGION

TEST RESULTS
D                   14   A5701  1.000000000&+ 0


DT50 CURVE GIVEN

TEST RESULTS
G                    1   H                   11   A5712  1.000000000&+ 0

USED AT THE END OF AN ITEM

MI/J TSNJ00371    POSITION-BEFORE BLOCK 1

SCHEME D PROGRAM   00050.  ENDS 21  RUN/ELAPSE/PRINT   00H 00M 01S/00H 00M 10S/00H 00M 44S   LOG TIME 00H 00M 22S          7900
```

```
SCHEME D PROGRAM   00052   DATE 09/03/76   TIME 39H 20M 21S   (TWU)

JOB NUMBER       1002                          COMET SYSTEM STARTS TO PROCESS DATA FROM DATA TYPE 52
DATA TYPE   52
ITEM NUMBER     2

TEST RESULTS
C                  39   C                  40   C                  41   C                  42   C                  80

M1/O TSNJ00971    POSITION-BEFORE BLOCK 1

SCHEME D PROGRAM   00052   ENDS 20  RUN/ELAPSE/PRINT   00H 00M 00S/00H 00M 09S/00H 00M 45S   LOG TIME 00H 00M 22S          7905
```

SCHEME D PROGRAM 00221 DATE 09/03/76 TIME 39H 20M 33S (TWO)

RING STRUCTURE OF TWO DIM MESH FIT
FINISHED

OUTPUT FROM MESH FITTING PROGRAM

NEXT CURVE

CHANGE POINT
1.50000 2.70000
INT PTS
3.00000 0.00000 0.00000 1.50000 2.70000 0.00000 -1.00000 0.00000 0.00000
3.00000 1.00000 0.00000 1.50000 2.75000 0.00000 -1.00000 0.00000 0.00000
3.00000 1.00000 0.00000 1.50000 2.80000 0.00000 -1.00000 0.00000 0.00000
3.00000 1.00000 0.00000 1.50000 2.85000 0.00000 -1.00000 0.00000 0.00000
3.00000 1.00000 0.00000 1.50000 2.90000 0.00000 -1.00000 0.00000 0.00000
3.00000 1.00000 0.00000 1.50000 2.95000 0.00000 -1.00000 0.00000 0.00000

CHANGE POINT
1.50000 3.00000
INT PTS
2.00000 1.00000 0.00000 1.50000 3.00000 0.00000 -1.00000 0.00000 0.00000
2.00000 3.00000 0.00000 1.60000 3.00000 0.00000 0.00000 1.00000 0.00000
2.00000 3.00000 0.00000 1.70000 3.00000 0.00000 0.00000 1.00000 0.00000
2.00000 3.00000 0.00000 1.80000 3.00000 0.00000 0.00000 1.00000 0.00000
2.00000 3.00000 0.00000 1.90000 3.00000 0.00000 0.00000 1.00000 0.00000
2.00000 3.00000 0.00000 2.00000 3.00000 0.00000 0.00000 1.00000 0.00000
2.00000 3.00000 0.00000 2.10000 3.00000 0.00000 0.00000 1.00000 0.00000
2.00000 3.00000 0.00000 2.20000 3.00000 0.00000 0.00000 1.00000 0.00000
2.00000 3.00000 0.00000 2.30000 3.00000 0.00000 0.00000 1.00000 0.00000
2.00000 3.00000 0.00000 2.40000 3.00000 0.00000 0.00000 1.00000 0.00000
2.00000 3.00000 0.00000 2.50000 3.00000 0.00000 0.00000 1.00000 0.00000
2.00000 3.00000 0.00000 2.60000 3.00000 0.00000 0.00000 1.00000 0.00000
2.00000 3.00000 0.00000 2.70000 3.00000 0.00000 0.00000 1.00000 0.00000
2.00000 3.00000 0.00000 2.80000 3.00000 0.00000 0.00000 1.00000 0.00000
2.00000 3.00000 0.00000 2.90000 3.00000 0.00000 0.00000 1.00000 0.00000
2.00000 3.00000 0.00000 3.00000 3.00000 0.00000 0.00000 1.00000 0.00000
2.00000 3.00000 0.00000 3.10000 3.00000 0.00000 0.00000 1.00000 0.00000
2.00000 3.00000 0.00000 3.20000 3.00000 0.00000 0.00000 1.00000 0.00000
2.00000 3.00000 0.00000 3.30000 3.00000 0.00000 0.00000 1.00000 0.00000
2.00000 3.00000 0.00000 3.40000 3.00000 0.00000 0.00000 1.00000 0.00000
2.00000 3.00000 0.00000 3.50000 3.00000 0.00000 0.00000 1.00000 0.00000

CHANGE POINT
3.60000 3.00000
INT PTS
0.00000 3.00000 0.00000 3.60000 3.00000 0.00000 0.00000 1.00000 0.00000
1.00000 3.00000 0.00000 3.60000 2.95000 0.00000 1.00000 0.00000 0.00000
1.00000 3.00000 0.00000 3.60000 2.90000 0.00000 1.00000 0.00000 0.00000
1.00000 3.00000 0.00000 3.60000 2.85000 0.00000 1.00000 0.00000 0.00000
1.00000 3.00000 0.00000 3.60000 2.80000 0.00000 1.00000 0.00000 0.00000
1.00000 3.00000 0.00000 3.60000 2.75000 0.00000 1.00000 0.00000 0.00000
1.00000 3.00000 0.00000 3.60000 2.70000 0.00000 1.00000 0.00000 0.00000
1.00000 3.00000 0.00000 3.60000 2.65000 0.00000 1.00000 0.00000 0.00000
1.00000 3.00000 0.00000 3.60000 2.60000 0.00000 1.00000 0.00000 0.00000
1.00000 3.00000 0.00000 3.60000 2.55000 0.00000 1.00000 0.00000 0.00000
1.00000 3.00000 0.00000 3.60000 2.50000 0.00000 1.00000 0.00000 0.00000
1.00000 3.00000 0.00000 3.60000 2.45000 0.00000 1.00000 0.00000 0.00000

CHANGE POINT
3.60000 2.40000

```
INT PTS
      1.00000     2.00000     0.00000     3.60000     2.40000     0.00000     1.00000     0.00000     0.00000
      3.00000     2.00000     0.00000     3.50000     2.40000     0.00000     0.00000    -1.00000     0.00000
      3.00000     2.00000     0.00000     3.40000     2.40000     0.00000     0.00000    -1.00000     0.00000
      3.00000     2.00000     0.00000     3.30000     2.40000     0.00000     0.00000    -1.00000     0.00000
      3.00000     2.00000     0.00000     3.20000     2.40000     0.00000     0.00000    -1.00000     0.00000
      3.00000     2.00000     0.00000     3.10000     2.40000     0.00000     0.00000    -1.00000     0.00000
      3.00000     2.00000     0.00000     3.00000     2.40000     0.00000     0.00000    -1.00000     0.00000
      3.00000     2.00000     0.00000     2.90000     2.40000     0.00000     0.00000    -1.00000     0.00000
      3.00000     2.00000     0.00000     2.80000     2.40000     0.00000     0.00000    -1.00000     0.00000
      3.00000     2.00000     0.00000     2.70000     2.40000     0.00000     0.00000    -1.00000     0.00000
      3.00000     2.00000     0.00000     2.60000     2.40000     0.00000     0.00000    -1.00000     0.00000
      3.00000     2.00000     0.00000     2.50000     2.40000     0.00000     0.00000    -1.00000     0.00000
      3.00000     2.00000     0.00000     2.40000     2.40000     0.00000     0.00000    -1.00000     0.00000
      3.00000     2.00000     0.00000     2.30000     2.40000     0.00000     0.00000    -1.00000     0.00000
      3.00000     2.00000     0.00000     2.20000     2.40000     0.00000     0.00000    -1.00000     0.00000
      3.00000     2.00000     0.00000     2.10000     2.40000     0.00000     0.00000    -1.00000     0.00000
      3.00000     2.00000     0.00000     2.00000     2.40000     0.00000     0.00000    -1.00000     0.00000

CHANGE POINT
      1.90000     2.40000
INT PTS
      3.00000     0.00000     0.00000     1.90000     2.40000     0.00000     0.00000    -1.00000     0.00000
      3.00000     1.00000     0.00000     1.90000     2.45000     0.00000    -1.00000     0.00000     0.00000
      3.00000     1.00000     0.00000     1.90000     2.50000     0.00000    -1.00000     0.00000     0.00000
      3.00000     1.00000     0.00000     1.90000     2.55000     0.00000    -1.00000     0.00000     0.00000
      3.00000     1.00000     0.00000     1.90000     2.60000     0.00000    -1.00000     0.00000     0.00000
      3.00000     1.00000     0.00000     1.90000     2.65000     0.00000    -1.00000     0.00000     0.00000

CHANGE POINT
      1.90000     2.70000
INT PTS
      3.00000     3.00000     0.00000     1.90000     2.70000     0.00000    -1.00000     0.00000     0.00000
      3.00000     2.00000     0.00000     1.80000     2.70000     0.00000     0.00000    -1.00000     0.00000
      3.00000     2.00000     0.00000     1.70000     2.70000     0.00000     0.00000    -1.00000     0.00000
      3.00000     2.00000     0.00000     1.60000     2.70000     0.00000     0.00000    -1.00000     0.00000

CHANGE POINT
      1.50000     2.70000
INT PTS

CHANGE POINT

SCHEME D PROGRAM  00221   ENDS 21  RUN/ELAPSE/PRINT   00H 00M 18S/00H 00M 26S/00H 00M 52S   LOG TIME 00H 00M 41S          14505
```

```
SCHEME D PROGRAM   00052   DATE 09/03/76   TIME 39H 21M 04S   (TWO)

SCHEME D PROGRAM   00052   ENDS 20  RUN/ELAPSE/PRINT   00H 00M 00S/00H 00M 00S/00H 00M 52S   LOG TIME 00H 00M 41S          14505



SCHEME D PROGRAM   00226   DATE 09/03/76   TIME 39H 21M 07S   (TWO)

SCHEME D PROGRAM   00226   ENDS 21  RUN/ELAPSE/PRINT   00H 00M 15S/01H 51M 24S/00H 00M 52S   LOG TIME 00H 00M 56S          17583
```

```
SCHEME D PROGRAM   00052   DATE 09/03/76   TIME 41H 12M 36S   (TWO)

                                                                    OUTPUT FROM DATA TYPE 55
MI/O TSNJ00971   POSITION-BEFORE BLOCK 1

SCHEME D PROGRAM   00052   ENDS 21  RUN/ELAPSE/PRINT   00H 00M 00S/00H 00M 18S/00H 00M 53S   LOG TIME 00H 00M 56S          17603

JOB NUMBER       1002
DATA TYPE   55
ITEM NUMBER     3BEGIN ITEM
VISCOUS INCOMPRESSIBLE FLUID FLOW SOLUTION

TEST RESULTS
W0     1.000000000&+ 0   W0     0.000000000&+ 0


INTERNAL--RUTATIONAL--START
  2.000000000&+ 0  1.000000000&+ 0

TEST RESULTS
D                   2   W98    1.000000000&+ 0

  1.875000000&- 1  3.333333000&- 3  4.000000000&+ 0

TEST RESULTS
D                   5   W100   5.000000000&+ 0   W107   1.000000000&+ 0   D                   6   E                   1
W108   4.000000000&+ 0   D                   7   E                   2

END ITEM

TEST RESULTS
D                   5   W106   2.000000000&+ 0   W0     0.000000000&+ 0   W99    1.000000000&+ 0   H                  11
D                   1   A6204  1.000000000&+ 0   D                   6   E                   3

  5.000000000&+ 0  2.000000000&+ 0  1.000000000&+ 0  1.875000000&- 1  3.333333000&- 3
  4.000000000&+ 0

TEST RESULTS
D                1210   A6211  1.000000000&+ 0

  2.000000000&+ 0  1.000000000&+ 0  4.000000000&+ 0

TEST RESULTS
W0     0.000000000&+ 0
    7224
    7251
    7278
    7305
    7332
    7359
    7386
    7413
    7440
    7467
    7494
    7521
    7548
    7575
    7602
    7682
```

353

KINEMATIC VISCOSITY 0.187500 ROTATIONAL TIMESTEP 0.003333 FLOW ITERATION 1 FLOW ELAPSED TIME 0.000000

RESULTS FROM ITERATION 1

X MESH PT	Y MESH PT	U I,J+1/2	V I+1/2,J	W N-1	W N	F.M.	V.M.
1.50000&+ 0	2.70000&+ 0	5.00000&+ 0	0.00000&+ 0	0.00000&+ 0	-1.00000&+ 2	0.00000&+ 0	2.00000&+ 0
1.50000&+ 0	2.75000&+ 0	5.00000&+ 0	-8.77092&- 2	0.00000&+ 0	-7.27596&-11	1.00000&+ 0	0.00000&+ 0
1.50000&+ 0	2.80000&+ 0	5.00000&+ 0	-8.78495&- 2	0.00000&+ 0	2.91038&-11	-2.00000&+ 0	0.00000&+ 0
1.50000&+ 0	2.85000&+ 0	5.00000&+ 0	-7.39188&- 2	0.00000&+ 0	-2.91038&-11	-2.00000&+ 0	0.00000&+ 0
1.50000&+ 0	2.90000&+ 0	5.00000&+ 0	-4.59223&- 2	0.00000&+ 0	8.73115&-11	-2.00000&+ 0	0.00000&+ 0
1.50000&+ 0	2.95000&+ 0	5.00000&+ 0	-6.93173&- 3	0.00000&+ 0	-4.36557&-11	1.00000&+ 0	0.00000&+ 0
1.50000&+ 0	3.00000&+ 0	0.00000&+ 0	0.00000&+ 0	0.00000&+ 0	1.00000&+ 2	0.00000&+ 0	-1.00000&+ 0
1.60000&+ 0	2.70000&+ 0	5.02650&+ 0	0.00000&+ 0	0.00000&+ 0	-1.00530&+ 2	0.00000&+ 0	2.00000&+ 0
1.60000&+ 0	2.75000&+ 0	5.00184&+ 0	-1.38358&- 1	0.00000&+ 0	-2.49438&+ 1	-1.00000&+ 0	0.00000&+ 0
1.60000&+ 0	2.80000&+ 0	4.97200&+ 0	-1.50279&- 1	0.00000&+ 0	0.00000&+ 0	3.00000&+ 0	0.00000&+ 0
1.60000&+ 0	2.85000&+ 0	4.94272&+ 0	-1.34451&- 1	0.00000&+ 0	0.00000&+ 0	3.00000&+ 0	0.00000&+ 0
1.60000&+ 0	2.90000&+ 0	4.91863&+ 0	-9.49171&- 2	0.00000&+ 0	0.00000&+ 0	3.00000&+ 0	0.00000&+ 0
1.60000&+ 0	2.95000&+ 0	4.90172&+ 0	-4.05102&- 2	0.00000&+ 0	2.45474&+ 1	-1.00000&+ 0	0.00000&+ 0
1.60000&+ 0	3.00000&+ 0	0.00000&+ 0	0.00000&+ 0	0.00000&+ 0	9.80345&+ 1	0.00000&+ 0	-1.00000&+ 0
1.70000&+ 0	2.70000&+ 0	5.10802&+ 0	0.00000&+ 0	0.00000&+ 0	-1.02160&+ 2	0.00000&+ 0	2.00000&+ 0
1.70000&+ 0	2.75000&+ 0	5.02814&+ 0	-3.08181&- 1	0.00000&+ 0	-2.51628&+ 1	-1.00000&+ 0	0.00000&+ 0
1.70000&+ 0	2.80000&+ 0	4.93813&+ 0	-3.40384&- 1	0.00000&+ 0	-1.31908&- 1	-3.00000&+ 0	0.00000&+ 0
1.70000&+ 0	2.85000&+ 0	4.86000&+ 0	-2.94750&- 1	0.00000&+ 0	0.00000&+ 0	-3.00000&+ 0	0.00000&+ 0
1.70000&+ 0	2.90000&+ 0	4.80452&+ 0	-2.06550&- 1	0.00000&+ 0	-5.88591&- 2	-3.00000&+ 0	0.00000&+ 0
1.70000&+ 0	2.95000&+ 0	4.77361&+ 0	-1.00301&- 1	0.00000&+ 0	2.39803&+ 1	-1.00000&+ 0	0.00000&+ 0
1.70000&+ 0	3.00000&+ 0	0.00000&+ 0	0.00000&+ 0	0.00000&+ 0	9.54721&+ 1	0.00000&+ 0	-1.00000&+ 0
1.80000&+ 0	2.70000&+ 0	5.41765&+ 0	0.00000&+ 0	0.00000&+ 0	-1.08353&+ 2	0.00000&+ 0	2.00000&+ 0
1.80000&+ 0	2.75000&+ 0	5.08006&+ 0	-1.04418&+ 0	0.00000&+ 0	-2.58947&+ 1	-1.00000&+ 0	0.00000&+ 0
1.80000&+ 0	2.80000&+ 0	4.83044&+ 0	-8.31831&- 1	0.00000&+ 0	-3.71273&- 1	-3.00000&+ 0	0.00000&+ 0
1.80000&+ 0	2.85000&+ 0	4.67425&+ 0	-5.94320&- 1	0.00000&+ 0	0.00000&+ 0	-3.00000&+ 0	0.00000&+ 0
1.80000&+ 0	2.90000&+ 0	4.58441&+ 0	-3.78198&- 1	0.00000&+ 0	-1.10105&- 1	-3.00000&+ 0	0.00000&+ 0
1.80000&+ 0	2.95000&+ 0	4.54047&+ 0	-1.81861&- 1	0.00000&+ 0	2.29169&+ 1	-1.00000&+ 0	0.00000&+ 0

X	Y	$U_{i,j+1/2}$	$V_{i+1/2,j}$	WN-1	WN	F.M.	V.M.
1.80000&+ 0	3.00000&+ 0	0.00000&+ 0	0.00000&+ 0	0.00000&+ 0	9.08094&+ 1	0.00000&+ 0	-1.00000&+ 0
1.90000&+ 0	2.40000&+ 0	0.00000&+ 0	0.00000&+ 0	0.00000&+ 0	0.00000&+ 0	0.00000&+ 0	-1.00000&+ 0
1.90000&+ 0	2.45000&+ 0	0.00000&+ 0	-3.62212&- 1	0.00000&+ 0	-3.62212&+ 0	0.00000&+ 0	1.00000&+ 0
1.90000&+ 0	2.50000&+ 0	0.00000&+ 0	-8.04253&- 1	0.00000&+ 0	-8.04253&+ 0	0.00000&+ 0	1.00000&+ 0
1.90000&+ 0	2.55000&+ 0	0.00000&+ 0	-1.30826&+ 0	0.00000&+ 0	-1.30826&+ 1	0.00000&+ 0	1.00000&+ 0
1.90000&+ 0	2.60000&+ 0	0.00000&+ 0	-1.89861&+ 0	0.00000&+ 0	-1.89861&+ 1	0.00000&+ 0	1.00000&+ 0
1.90000&+ 0	2.65000&+ 0	0.00000&+ 0	-2.53442&+ 0	0.00000&+ 0	-2.53442&+ 1	0.00000&+ 0	1.00000&+ 0
1.90000&+ 0	2.70000&+ 0	5.16408&+ 0	-2.60385&+ 0	0.00000&+ 0	-1.29320&+ 2	0.00000&+ 0	0.00000&+ 0
1.90000&+ 0	2.75000&+ 0	4.55928&+ 0	-1.80902&+ 0	0.00000&+ 0	-2.69840&+ 1	-1.00000&+ 0	0.00000&+ 0
1.90000&+ 0	2.80000&+ 0	4.34859&+ 0	-1.18995&+ 0	0.00000&+ 0	-8.34487&- 1	-3.00000&+ 0	0.00000&+ 0
1.90000&+ 0	2.85000&+ 0	4.24487&+ 0	-7.83082&- 1	0.00000&+ 0	0.00000&+ 0	-3.00000&+ 0	0.00000&+ 0
1.90000&+ 0	2.90000&+ 0	4.19052&+ 0	-4.79642&- 1	0.00000&+ 0	-1.48247&- 1	-3.00000&+ 0	0.00000&+ 0
1.90000&+ 0	2.95000&+ 0	4.16488&+ 0	-2.28864&- 1	0.00000&+ 0	2.11114&+ 1	-1.00000&+ 0	0.00000&+ 0
1.90000&+ 0	3.00000&+ 0	0.00000&+ 0	0.00000&+ 0	0.00000&+ 0	8.32976&+ 1	0.00000&+ 0	-1.00000&+ 0
2.00000&+ 0	2.40000&+ 0	9.92575&- 1	0.00000&+ 0	0.00000&+ 0	-1.98515&+ 1	0.00000&+ 0	2.00000&+ 0
2.00000&+ 0	2.45000&+ 0	1.04300&+ 0	-2.75386&- 1	0.00000&+ 0	-5.11615&+ 0	-1.00000&+ 0	0.00000&+ 0
2.00000&+ 0	2.50000&+ 0	1.16916&+ 0	-5.66666&- 1	0.00000&+ 0	-5.78155&- 1	-1.00000&+ 0	0.00000&+ 0
2.00000&+ 0	2.55000&+ 0	1.41030&+ 0	-8.51301&- 1	0.00000&+ 0	-9.61294&- 1	-1.00000&+ 0	0.00000&+ 0
2.00000&+ 0	2.60000&+ 0	1.82278&+ 0	-1.09719&+ 0	0.00000&+ 0	-1.44929&+ 0	-1.00000&+ 0	0.00000&+ 0
2.00000&+ 0	2.65000&+ 0	2.42419&+ 0	-1.25048&+ 0	0.00000&+ 0	-2.04837&+ 0	-1.00000&+ 0	0.00000&+ 0
2.00000&+ 0	2.70000&+ 0	3.02777&+ 0	-1.25326&+ 0	0.00000&+ 0	-1.43089&+ 1	-1.00000&+ 0	0.00000&+ 0
2.00000&+ 0	2.75000&+ 0	3.40168&+ 0	-1.10737&+ 0	0.00000&+ 0	0.00000&+ 0	-3.00000&+ 0	0.00000&+ 0
2.00000&+ 0	2.80000&+ 0	3.57804&+ 0	-8.82838&- 1	0.00000&+ 0	0.00000&+ 0	-3.00000&+ 0	0.00000&+ 0
2.00000&+ 0	2.85000&+ 0	3.65775&+ 0	-6.43575&- 1	0.00000&+ 0	0.00000&+ 0	-3.00000&+ 0	0.00000&+ 0
2.00000&+ 0	2.90000&+ 0	3.69395&+ 0	-4.15244&- 1	0.00000&+ 0	-1.38116&- 1	-3.00000&+ 0	0.00000&+ 0
2.00000&+ 0	2.95000&+ 0	3.70885&+ 0	-2.02864&- 1	0.00000&+ 0	1.88131&+ 1	-1.00000&+ 0	0.00000&+ 0
2.00000&+ 0	3.00000&+ 0	0.00000&+ 0	0.00000&+ 0	0.00000&+ 0	7.41771&+ 1	0.00000&+ 0	-1.00000&+ 0
2.10000&+ 0	2.40000&+ 0	1.58110&+ 0	0.00000&+ 0	0.00000&+ 0	-3.16219&+ 1	0.00000&+ 0	2.00000&+ 0
2.10000&+ 0	2.45000&+ 0	1.63721&+ 0	-1.69424&- 1	0.00000&+ 0	-7.78913&+ 0	-1.00000&+ 0	0.00000&+ 0
2.10000&+ 0	2.50000&+ 0	1.74987&+ 0	-3.43884&- 1	0.00000&+ 0	-2.68920&- 2	-3.00000&+ 0	0.00000&+ 0

X	Y	$U_{i,j+1/2}$	$V_{i+1/2,j}$	WN-1	WN	F.M.	V.M.
2.10000E+ 0	2.55000E+ 0	1.92524E+ 0	-4.99684E- 1	0.00000E+ 0	5.81461E- 2	-3.00000E+ 0	0.00000E+ 0
2.10000E+ 0	2.60000E+ 0	2.15942E+ 0	-6.20041E- 1	0.00000E+ 0	9.90549E- 2	-3.00000E+ 0	0.00000E+ 0
2.10000E+ 0	2.65000E+ 0	2.43066E+ 0	-6.89672E- 1	0.00000E+ 0	1.60386E- 1	-3.00000E+ 0	0.00000E+ 0
2.10000E+ 0	2.70000E+ 0	2.69877E+ 0	-6.98806E- 1	0.00000E+ 0	9.84452E- 1	-3.00000E+ 0	0.00000E+ 0
2.10000E+ 0	2.75000E+ 0	2.92448E+ 0	-6.49113E- 1	0.00000E+ 0	0.00000E+ 0	-3.00000E+ 0	0.00000E+ 0
2.10000E+ 0	2.80000E+ 0	3.09056E+ 0	-5.53383E- 1	0.00000E+ 0	0.00000E+ 0	-3.00000E+ 0	0.00000E+ 0
2.10000E+ 0	2.85000E+ 0	3.20077E+ 0	-4.28444E- 1	0.00000E+ 0	0.00000E+ 0	-3.00000E+ 0	0.00000E+ 0
2.10000E+ 0	2.90000E+ 0	3.26646E+ 0	-2.88264E- 1	0.00000E+ 0	-9.69777E- 2	-3.00000E+ 0	0.00000E+ 0
2.10000E+ 0	2.95000E+ 0	3.29849E+ 0	-1.43195E- 1	0.00000E+ 0	1.66838E+ 1	-1.00000E+ 0	0.00000E+ 0
2.10000E+ 0	3.00000E+ 0	0.00000E+ 0	0.00000E+ 0	0.00000E+ 0	6.59698E+ 1	0.00000E+ 0	-1.00000E+ 0
2.20000E+ 0	2.40000E+ 0	1.95782E+ 0	0.00000E+ 0	0.00000E+ 0	-3.91564E+ 1	0.00000E+ 0	2.00000E+ 0
2.20000E+ 0	2.45000E+ 0	1.99569E+ 0	-9.63323E- 2	0.00000E+ 0	-9.70276E+ 0	-1.00000E+ 0	0.00000E+ 0
2.20000E+ 0	2.50000E+ 0	2.06791E+ 0	-1.98456E- 1	0.00000E+ 0	-4.36436E- 2	-3.00000E+ 0	0.00000E+ 0
2.20000E+ 0	2.55000E+ 0	2.17273E+ 0	-2.87176E- 1	0.00000E+ 0	0.00000E+ 0	-3.00000E+ 0	0.00000E+ 0
2.20000E+ 0	2.60000E+ 0	2.30327E+ 0	-3.54157E- 1	0.00000E+ 0	0.00000E+ 0	-3.00000E+ 0	0.00000E+ 0
2.20000E+ 0	2.65000E+ 0	2.44822E+ 0	-3.93618E- 1	0.00000E+ 0	0.00000E+ 0	-3.00000E+ 0	0.00000E+ 0
2.20000E+ 0	2.70000E+ 0	2.59346E+ 0	-4.02447E- 1	0.00000E+ 0	0.00000E+ 0	-3.00000E+ 0	0.00000E+ 0
2.20000E+ 0	2.75000E+ 0	2.72548E+ 0	-3.81033E- 1	0.00000E+ 0	0.00000E+ 0	-3.00000E+ 0	0.00000E+ 0
2.20000E+ 0	2.80000E+ 0	2.83475E+ 0	-3.33063E- 1	0.00000E+ 0	0.00000E+ 0	-3.00000E+ 0	0.00000E+ 0
2.20000E+ 0	2.85000E+ 0	2.91677E+ 0	-2.64254E- 1	0.00000E+ 0	0.00000E+ 0	-3.00000E+ 0	0.00000E+ 0
2.20000E+ 0	2.90000E+ 0	2.97081E+ 0	-1.80851E- 1	0.00000E+ 0	-5.88035E- 2	-3.00000E+ 0	0.00000E+ 0
2.20000E+ 0	2.95000E+ 0	2.99887E+ 0	-8.95898E- 2	0.00000E+ 0	1.51111E+ 1	-1.00000E+ 0	0.00000E+ 0
2.20000E+ 0	3.00000E+ 0	0.00000E+ 0	0.00000E+ 0	0.00000E+ 0	5.99773E+ 1	0.00000E+ 0	-1.00000E+ 0
2.30000E+ 0	2.40000E+ 0	2.18332E+ 0	0.00000E+ 0	0.00000E+ 0	-4.36665E+ 1	0.00000E+ 0	2.00000E+ 0
2.30000E+ 0	2.45000E+ 0	2.20588E+ 0	-5.25221E- 2	0.00000E+ 0	-1.08626E+ 1	-1.00000E+ 0	0.00000E+ 0
2.30000E+ 0	2.50000E+ 0	2.24847E+ 0	-1.12230E- 1	0.00000E+ 0	-2.77618E- 2	-3.00000E+ 0	0.00000E+ 0
2.30000E+ 0	2.55000E+ 0	2.30918E+ 0	-1.63864E- 1	0.00000E+ 0	0.00000E+ 0	-3.00000E+ 0	0.00000E+ 0
2.30000E+ 0	2.60000E+ 0	2.38356E+ 0	-2.02907E- 1	0.00000E+ 0	0.00000E+ 0	-3.00000E+ 0	0.00000E+ 0
2.30000E+ 0	2.65000E+ 0	2.46570E+ 0	-2.26501E- 1	0.00000E+ 0	0.00000E+ 0	-3.00000E+ 0	0.00000E+ 0
2.30000E+ 0	2.70000E+ 0	2.54930E+ 0	-2.33114E- 1	0.00000E+ 0	0.00000E+ 0	-3.00000E+ 0	0.00000E+ 0

KINEMATIC VISCOSITY 0.187500 ROTATIONAL TIMESTEP 0.003333 FLOW ITERATION 4 FLOW ELAPSED TIME 0.010000

X MESH PT	Y MESH PT	U I,J+1/2	V I+1/2,J	W N-1	W N	F.M.	V.M.
1.50000&+ 0	2.70000&+ 0	5.00000&+ 0	0.00000&+ 0	-1.00000&+ 2	-1.00000&+ 2	0.00000&+ 0	2.00000&+ 0
1.50000&+ 0	2.75000&+ 0	5.00000&+ 0	8.42906&- 1	-1.45519&-10	-3.05590&-10	1.00000&+ 0	0.00000&+ 0
1.50000&+ 0	2.80000&+ 0	5.00000&+ 0	7.31345&- 1	5.82077&-11	2.91038&-11	-2.00000&+ 0	0.00000&+ 0
1.50000&+ 0	2.85000&+ 0	5.00000&+ 0	6.70592&- 3	5.82077&-11	1.30967&-10	-2.00000&+ 0	0.00000&+ 0
1.50000&+ 0	2.90000&+ 0	5.00000&+ 0	-7.20833&- 1	2.18279&-10	4.94765&-10	-2.00000&+ 0	0.00000&+ 0
1.50000&+ 0	2.95000&+ 0	5.00000&+ 0	-8.35558&- 1	1.30967&-10	7.71252&-10	1.00000&+ 0	0.00000&+ 0
1.50000&+ 0	3.00000&+ 0	0.00000&+ 0	0.00000&+ 0	1.00000&+ 2	1.00000&+ 2	0.00000&+ 0	-1.00000&+ 0
1.60000&+ 0	2.70000&+ 0	1.39088&+ 0	0.00000&+ 0	-2.88492&+ 1	-2.78176&+ 1	0.00000&+ 0	2.00000&+ 0
1.60000&+ 0	2.75000&+ 0	6.07650&+ 0	1.11467&+ 0	-1.57498&+ 1	-1.46519&+ 1	-1.00000&+ 0	0.00000&+ 0
1.60000&+ 0	2.80000&+ 0	1.02098&+ 1	9.56016&- 1	-6.89318&+ 0	-6.06555&+ 0	3.00000&+ 0	0.00000&+ 0
1.60000&+ 0	2.85000&+ 0	1.02300&+ 1	2.08576&- 2	-4.00156&- 2	-3.11543&- 3	3.00000&+ 0	0.00000&+ 0
1.60000&+ 0	2.90000&+ 0	6.09394&+ 0	-9.10871&- 1	6.92949&+ 0	6.07866&+ 0	3.00000&+ 0	0.00000&+ 0
1.60000&+ 0	2.95000&+ 0	1.38811&+ 0	-1.06652&+ 0	1.59009&+ 1	1.46959&+ 1	-1.00000&+ 0	0.00000&+ 0
1.60000&+ 0	3.00000&+ 0	0.00000&+ 0	0.00000&+ 0	2.93791&+ 1	2.77623&+ 1	0.00000&+ 0	-1.00000&+ 0
1.70000&+ 0	2.70000&+ 0	9.25036&- 1	0.00000&+ 0	-2.47419&+ 1	-1.85007&+ 1	0.00000&+ 0	2.00000&+ 0
1.70000&+ 0	2.75000&+ 0	6.28918&+ 0	4.78356&- 1	-1.78092&+ 1	-1.54033&+ 1	-1.00000&+ 0	0.00000&+ 0
1.70000&+ 0	2.80000&+ 0	1.21151&+ 1	3.31020&- 1	-9.29659&+ 0	-9.05185&+ 0	-3.00000&+ 0	0.00000&+ 0
1.70000&+ 0	2.85000&+ 0	1.21476&+ 1	1.71319&- 2	-6.74371&- 2	-5.52410&- 2	-3.00000&+ 0	0.00000&+ 0
1.70000&+ 0	2.90000&+ 0	6.32519&+ 0	-2.14037&- 1	9.28955&+ 0	9.01622&+ 0	-3.00000&+ 0	0.00000&+ 0
1.70000&+ 0	2.95000&+ 0	9.28531&- 1	-2.57955&- 1	1.81237&+ 1	1.55866&+ 1	-1.00000&+ 0	0.00000&+ 0
1.70000&+ 0	3.00000&+ 0	0.00000&+ 0	0.00000&+ 0	2.56627&+ 1	1.85706&+ 1	0.00000&+ 0	-1.00000&+ 0
1.80000&+ 0	2.70000&+ 0	9.49824&- 1	0.00000&+ 0	-2.72052&+ 1	-1.89965&+ 1	0.00000&+ 0	2.00000&+ 0
1.80000&+ 0	2.75000&+ 0	6.58083&+ 0	-2.31799&- 3	-1.86198&+ 1	-1.58118&+ 1	-1.00000&+ 0	0.00000&+ 0
1.80000&+ 0	2.80000&+ 0	1.25177&+ 1	-4.64780&- 1	-8.23790&+ 0	-8.96040&+ 0	-3.00000&+ 0	0.00000&+ 0
1.80000&+ 0	2.85000&+ 0	1.24217&+ 1	-4.58766&- 1	6.90827&- 2	1.55797&- 1	-3.00000&+ 0	0.00000&+ 0
1.80000&+ 0	2.90000&+ 0	6.47588&+ 0	-2.16003&- 1	8.45896&+ 0	9.32877&+ 0	-3.00000&+ 0	0.00000&+ 0
1.80000&+ 0	2.95000&+ 0	9.40852&- 1	-2.81801&- 2	1.85494&+ 1	1.59844&+ 1	-1.00000&+ 0	0.00000&+ 0

X	Y	$U_{i,j+1/2}$	$V_{i+1/2,j}$	WN-1	WN	F.M.	V.M
1.80000&+ 0	3.00000&+ 0	0.00000&+ 0	0.00000&+ 0	2.66623&+ 1	1.88170&+ 1	0.00000&+ 0	-1.00000&+ 0
1.90000&+ 0	2.40000&+ 0	0.00000&+ 0	0.00000&+ 0	0.00000&+ 0	0.00000&+ 0	0.00000&+ 0	-1.00000&+ 0
1.90000&+ 0	2.45000&+ 0	0.00000&+ 0	-6.24621&- 2	6.93990&- 1	-6.24621&- 1	0.00000&+ 0	1.00000&+ 0
1.90000&+ 0	2.50000&+ 0	0.00000&+ 0	-7.89410&- 2	-5.87425&- 2	-7.89410&- 1	0.00000&+ 0	1.00000&+ 0
1.90000&+ 0	2.55000&+ 0	0.00000&+ 0	-1.72490&- 1	-2.06902&+ 0	-1.72490&+ 0	0.00000&+ 0	1.00000&+ 0
1.90000&+ 0	2.60000&+ 0	0.00000&+ 0	-3.62666&- 1	-5.03218&+ 0	-3.62666&+ 0	0.00000&+ 0	1.00000&+ 0
1.90000&+ 0	2.65000&+ 0	0.00000&+ 0	-7.00028&- 1	-9.15882&+ 0	-7.00028&+ 0	0.00000&+ 0	1.00000&+ 0
1.90000&+ 0	2.70000&+ 0	1.41671&+ 0	-1.26117&+ 0	-5.33011&+ 1	-4.09459&+ 1	0.00000&+ 0	0.00000&+ 0
1.90000&+ 0	2.75000&+ 0	7.66850&+ 0	-1.97336&+ 0	-2.48361&+ 1	-2.24205&+ 1	-1.00000&+ 0	0.00000&+ 0
1.90000&+ 0	2.80000&+ 0	1.31035&+ 1	-2.19710&+ 0	-8.69541&+ 0	-9.64425&+ 0	-3.00000&+ 0	0.00000&+ 0
1.90000&+ 0	2.85000&+ 0	1.21491&+ 1	-1.47790&+ 0	6.63990&- 2	2.31097&- 1	-3.00000&+ 0	0.00000&+ 0
1.90000&+ 0	2.90000&+ 0	6.18227&+ 0	-5.74435&- 1	7.96064&+ 0	8.81585&+ 0	-3.00000&+ 0	0.00000&+ 0
1.90000&+ 0	2.95000&+ 0	8.84816&- 1	-7.28016&- 4	1.75363&+ 1	1.53940&+ 1	-1.00000&+ 0	0.00000&+ 0
1.90000&+ 0	3.00000&+ 0	0.00000&+ 0	0.00000&+ 0	2.48914&+ 1	1.76964&+ 1	0.00000&+ 0	-1.00000&+ 0
2.00000&+ 0	2.40000&+ 0	-5.49000&- 1	0.00000&+ 0	8.08310&+ 0	1.09800&+ 1	0.00000&+ 0	2.00000&+ 0
2.00000&+ 0	2.45000&+ 0	-1.27611&+ 0	-1.26514&- 1	1.57825&+ 0	3.01667&+ 0	-1.00000&+ 0	0.00000&+ 0
2.00000&+ 0	2.50000&+ 0	-1.42997&+ 0	-3.62502&- 1	-1.01516&+ 0	-5.25655&- 1	-1.00000&+ 0	0.00000&+ 0
2.00000&+ 0	2.55000&+ 0	-1.54414&+ 0	-8.48070&- 1	-1.43483&+ 0	-1.77070&+ 0	-1.00000&+ 0	0.00000&+ 0
2.00000&+ 0	2.60000&+ 0	-1.46869&+ 0	-1.54148&+ 0	-3.10400&+ 0	-3.74687&+ 0	-1.00000&+ 0	0.00000&+ 0
2.00000&+ 0	2.65000&+ 0	4.02123&- 1	-2.39687&+ 0	-6.97784&+ 0	-7.88666&+ 0	-1.00000&+ 0	0.00000&+ 0
2.00000&+ 0	2.70000&+ 0	4.65204&+ 0	-3.28515&+ 0	-1.30597&+ 1	-1.28917&+ 1	-1.00000&+ 0	0.00000&+ 0
2.00000&+ 0	2.75000&+ 0	8.87060&+ 0	-3.70494&+ 0	-9.49512&+ 0	-1.10422&+ 1	-3.00000&+ 0	0.00000&+ 0
2.00000&+ 0	2.80000&+ 0	1.07285&+ 1	-3.10071&+ 0	-3.30294&+ 0	-4.88959&+ 0	-3.00000&+ 0	0.00000&+ 0
2.00000&+ 0	2.85000&+ 0	9.67725&+ 0	-1.86781&+ 0	1.11210&+ 0	1.64682&+ 0	-3.00000&+ 0	0.00000&+ 0
2.00000&+ 0	2.90000&+ 0	4.78006&+ 0	-6.70047&- 1	7.09826&+ 0	8.02946&+ 0	-3.00000&+ 0	0.00000&+ 0
2.00000&+ 0	2.95000&+ 0	5.83236&- 1	4.18512&- 2	1.41881&+ 1	1.22786&+ 1	-1.00000&+ 0	0.00000&+ 0
2.00000&+ 0	3.00000&+ 0	0.00000&+ 0	0.00000&+ 0	1.78508&+ 1	1.16547&+ 1	0.00000&+ 0	-1.00000&+ 0
2.10000&+ 0	2.40000&+ 0	-4.00046&- 1	0.00000&+ 0	4.50408&+ 0	8.12092&+ 0	0.00000&+ 0	2.00000&+ 0
2.10000&+ 0	2.45000&+ 0	-5.16051&- 1	-9.41531&- 2	-2.77263&- 1	1.47857&+ 0	-1.00000&+ 0	0.00000&+ 0
2.10000&+ 0	2.50000&+ 0	1.47705&- 1	-4.68287&- 1	-1.40709&+ 0	-8.95082&- 1	-3.00000&+ 0	0.00000&+ 0

```
SCHEME D PROGRAM   00050   DATE 17/05/76   TIME 09H 27M 36S   (TWO)

JOB NUMBER       1002
DATA TYPE   50
ITEM NUMBER      1USED AT BEGINNING OF AN ITEM
CURVE & REGION GEOMETRY DEFN.

ADD TO EXISTING STRUCTURE
USED AT THE END OF AN ITEM

MI/O TSN000221    POSITION-BEFORE BLOCK 1

SCHEME D PROGRAM   00050   ENDS 21  RUN/ELAPSE/PRINT   00H 00M 00S/00H 00M 08S/00H 00M 37S   LOG TIME 00H 00M 20S          7035

JOB NUMBER       1002
DATA TYPE   55
ITEM NUMBER      2BEGIN ITEM
VISCOUS INCOMPRESSIBLE FLUID FLOW SOLUTION

TEST RESULTS
W0     1.00000000&+ 0   W0     1.00000000&+ 0


INTERNAL--ROTATIONAL--RESTART
  2.00000000&+ 0  2.00000000&+ 0

TEST RESULTS
D                    2   W98    1.00000000&+ 0

  1.87500000&- 1  3.33333300&- 3  3.00000000&+ 0

TEST RESULTS
D                    5   W100   5.00000000&+ 0   W107  -3.00000000&+ 0   D                  6   E                  1

END ITEM

TEST RESULTS
D                    5   W106   1.00000000&+ 0   W0     1.00000000&+ 0   H                730   W105   9.70000000&+ 1
H                  731   J                    5   W107  -9.70000000&+ 1   J                  6   W99    9.50000000&+ 1
H                   10   0                    1   A5724  1.00000000&+ 0   D                  6   E                  2

  5.00000000&+ 0  2.00000000&+ 0  2.00000000&+ 0  1.87500000&- 1  3.33333300&- 3
  9.70000000&+ 1

TEST RESULTS
0                  730   A5731  9.50000000&+ 1

  1.00000000&+ 0 -9.70000000&+ 1

TEST RESULTS
W0     1.00000000&+ 0
MAXIMUM ERROR OVER MESH  6.01872&- 3  FROM ITERATION  95
MAXIMUM ERROR OVER MESH  5.53071&- 3                  96
MAXIMUM ERROR OVER MESH  5.06703&- 3                  97
```

DATA TYPE 50 IS USED TO PICK UP THE RING STRUCTURE FROM THE PREVIOUS RUN

DATA TYPE 55

359

KINEMATIC VISCOSITY 0.187500 ROTATIONAL TIMESTEP 0.003333 ITERATION 97 FLOW ELAPSED TIME 0.320000

PRINT-OUT OF MESH AFTER ITERATION 97

X MESH PT	Y MESH PT	U I,J+1/2	V I+1/2,J	W N-1	W N	F.M.	V.M.
1.50000&+ 0	2.70000&+ 0	5.00000&+ 0	0.00000&+ 0	-1.00000&+ 2	-1.00000&+ 2	0.00000&+ 0	2.00000&+ 0
1.50000&+ 0	2.75000&+ 0	5.00000&+ 0	7.14363&- 1	-1.50176&- 8	-1.50467&- 8	1.00000&+ 0	0.00000&+ 0
1.50000&+ 0	2.80000&+ 0	5.00000&+ 0	6.17348&- 1	-3.84171&- 9	-3.88536&- 9	-2.00000&+ 0	0.00000&+ 0
1.50000&+ 0	2.85000&+ 0	5.00000&+ 0	6.60174&- 3	5.58794&- 9	5.57338&- 9	-2.00000&+ 0	0.00000&+ 0
1.50000&+ 0	2.90000&+ 0	5.00000&+ 0	-6.06318&- 1	1.73313&- 8	1.75351&- 8	-2.00000&+ 0	0.00000&+ 0
1.50000&+ 0	2.95000&+ 0	5.00000&+ 0	-7.07526&- 1	2.66737&- 8	2.70957&- 8	1.00000&+ 0	0.00000&+ 0
1.50000&+ 0	3.00000&+ 0	0.00000&+ 0	0.00000&+ 0	1.00000&+ 2	1.00000&+ 2	0.00000&+ 0	-1.00000&+ 0
1.60000&+ 0	2.70000&+ 0	1.56698&+ 0	0.00000&+ 0	-3.13396&+ 1	-3.13397&+ 1	0.00000&+ 0	2.00000&+ 0
1.60000&+ 0	2.75000&+ 0	6.05531&+ 0	9.02018&- 1	-1.49145&+ 1	-1.49145&+ 1	-1.00000&+ 0	0.00000&+ 0
1.60000&+ 0	2.80000&+ 0	9.57080&+ 0	7.85077&- 1	-5.47550&+ 0	-5.47550&+ 0	3.00000&+ 0	0.00000&+ 0
1.60000&+ 0	2.85000&+ 0	9.58009&+ 0	1.57436&- 2	-2.46454&- 3	-2.46450&- 3	3.00000&+ 0	0.00000&+ 0
1.60000&+ 0	2.90000&+ 0	6.07201&+ 0	-7.53811&- 1	5.47649&+ 0	5.47649&+ 0	3.00000&+ 0	0.00000&+ 0
1.60000&+ 0	2.95000&+ 0	1.57439&+ 0	-8.72399&- 1	1.49631&+ 1	1.49631&+ 1	-1.00000&+ 0	0.00000&+ 0
1.60000&+ 0	3.00000&+ 0	0.00000&+ 0	0.00000&+ 0	3.14878&+ 1	3.14878&+ 1	0.00000&+ 0	-1.00000&+ 0
1.70000&+ 0	2.70000&+ 0	1.18195&+ 0	0.00000&+ 0	-2.36389&+ 1	-2.36389&+ 1	0.00000&+ 0	2.00000&+ 0
1.70000&+ 0	2.75000&+ 0	6.13417&+ 0	3.44599&- 1	-1.53976&+ 1	-1.53976&+ 1	-1.00000&+ 0	0.00000&+ 0
1.70000&+ 0	2.80000&+ 0	1.10090&+ 1	2.71765&- 1	-7.43838&+ 0	-7.43838&+ 0	-3.00000&+ 0	0.00000&+ 0
1.70000&+ 0	2.85000&+ 0	1.10305&+ 1	2.66316&- 2	-4.11725&- 2	-4.11724&- 2	-3.00000&+ 0	0.00000&+ 0
1.70000&+ 0	2.90000&+ 0	6.17119&+ 0	-1.77461&- 1	7.38002&+ 0	7.38002&+ 0	-3.00000&+ 0	0.00000&+ 0
1.70000&+ 0	2.95000&+ 0	1.19741&+ 0	-1.97615&- 1	1.55252&+ 1	1.55252&+ 1	-1.00000&+ 0	0.00000&+ 0
1.70000&+ 0	3.00000&+ 0	0.00000&+ 0	0.00000&+ 0	2.39482&+ 1	2.39482&+ 1	0.00000&+ 0	-1.00000&+ 0
1.80000&+ 0	2.70000&+ 0	1.13794&+ 0	0.00000&+ 0	-2.27587&+ 1	-2.27587&+ 1	0.00000&+ 0	2.00000&+ 0
1.80000&+ 0	2.75000&+ 0	6.22554&+ 0	4.12131&- 1	-1.50746&+ 1	-1.50746&+ 1	-1.00000&+ 0	0.00000&+ 0
1.80000&+ 0	2.80000&+ 0	1.13733&+ 1	-8.18159&- 3	-7.54483&+ 0	-7.54483&+ 0	-3.00000&+ 0	0.00000&+ 0
1.80000&+ 0	2.85000&+ 0	1.13417&+ 1	-1.64754&- 1	7.11130&- 2	7.11131&- 2	-3.00000&+ 0	0.00000&+ 0
1.80000&+ 0	2.90000&+ 0	6.19402&+ 0	-1.33133&- 1	7.70502&+ 0	7.70503&+ 0	-3.00000&+ 0	0.00000&+ 0
1.80000&+ 0	2.95000&+ 0	1.13500&+ 0	-4.37824&- 2	1.52809&+ 1	1.52809&+ 1	-1.00000&+ 0	0.00000&+ 0

X	Y	$U_{i,j+1/2}$	$V_{i+1/2,j}$	WN+1	WN	F.M.	V.M.
1.80000&+ 0	3.00000&+ 0	0.00000&+ 0	0.00000&+ 0	2.27720&+ 1	2.27720&+ 1	0.00000&+ 0	-1.00000&+ 0
1.90000&+ 0	2.40000&+ 0	0.00000&+ 0	0.00000&+ 0	0.00000&+ 0	0.00000&+ 0	0.00000&+ 0	-1.00000&+ 0
1.90000&+ 0	2.45000&+ 0	0.00000&+ 0	-1.51749&- 1	-1.51749&+ 0	-1.51749&+ 0	0.00000&+ 0	1.00000&+ 0
1.90000&+ 0	2.50000&+ 0	0.00000&+ 0	-3.25595&- 2	-3.25594&- 1	-3.25595&- 1	0.00000&+ 0	1.00000&+ 0
1.90000&+ 0	2.55000&+ 0	0.00000&+ 0	1.83605&- 1	1.83605&+ 0	1.83605&+ 0	0.00000&+ 0	1.00000&+ 0
1.90000&+ 0	2.60000&+ 0	0.00000&+ 0	3.44378&- 1	3.44378&+ 0	3.44378&+ 0	0.00000&+ 0	1.00000&+ 0
1.90000&+ 0	2.65000&+ 0	0.00000&+ 0	2.90798&- 1	2.90799&+ 0	2.90798&+ 0	0.00000&+ 0	1.00000&+ 0
1.90000&+ 0	2.70000&+ 0	1.46080&+ 0	-9.78469&- 2	-3.01945&+ 1	-3.01945&+ 1	0.00000&+ 0	0.00000&+ 0
1.90000&+ 0	2.75000&+ 0	6.95915&+ 0	-3.68990&- 1	-1.72901&+ 1	-1.72901&+ 1	-1.00000&+ 0	0.00000&+ 0
1.90000&+ 0	2.80000&+ 0	1.19112&+ 1	-9.08410&- 1	-7.99490&+ 0	-7.99490&+ 0	-3.00000&+ 0	0.00000&+ 0
1.90000&+ 0	2.85000&+ 0	1.13999&+ 1	-7.72533&- 1	1.61349&- 1	1.61349&- 1	-3.00000&+ 0	0.00000&+ 0
1.90000&+ 0	2.90000&+ 0	6.07045&+ 0	-3.52142&- 1	7.75620&+ 0	7.75620&+ 0	-3.00000&+ 0	0.00000&+ 0
1.90000&+ 0	2.95000&+ 0	1.08338&+ 0	-1.10101&- 2	1.48941&+ 1	1.48941&+ 1	-1.00000&+ 0	0.00000&+ 0
1.90000&+ 0	3.00000&+ 0	0.00000&+ 0	0.00000&+ 0	2.16677&+ 1	2.16677&+ 1	0.00000&+ 0	-1.00000&+ 0
2.00000&+ 0	2.40000&+ 0	-3.62106&- 1	0.00000&+ 0	7.24211&+ 0	7.24212&+ 0	0.00000&+ 0	2.00000&+ 0
2.00000&+ 0	2.45000&+ 0	-1.53376&+ 0	-2.18975&- 1	3.78350&+ 0	3.78350&+ 0	-1.00000&+ 0	0.00000&+ 0
2.00000&+ 0	2.50000&+ 0	-2.58413&+ 0	-1.94888&- 1	1.29015&+ 0	1.29015&+ 0	-1.00000&+ 0	0.00000&+ 0
2.00000&+ 0	2.55000&+ 0	-2.73109&+ 0	-1.69850&- 1	-8.93014&- 1	-8.93014&- 1	-1.00000&+ 0	0.00000&+ 0
2.00000&+ 0	2.60000&+ 0	-2.10226&+ 0	-3.04935&- 1	-3.29296&+ 0	-3.29296&+ 0	-1.00000&+ 0	0.00000&+ 0
2.00000&+ 0	2.65000&+ 0	6.88135&- 2	-7.32807&- 1	-6.48102&+ 0	-6.48102&+ 0	-1.00000&+ 0	0.00000&+ 0
2.00000&+ 0	2.70000&+ 0	4.27902&+ 0	-1.45174&+ 0	-1.12945&+ 1	-1.12945&+ 1	-1.00000&+ 0	0.00000&+ 0
2.00000&+ 0	2.75000&+ 0	8.90988&+ 0	-2.07338&+ 0	-1.03158&+ 1	-1.03158&+ 1	-3.00000&+ 0	0.00000&+ 0
2.00000&+ 0	2.80000&+ 0	1.14014&+ 1	-2.02393&+ 0	-5.42359&+ 0	-5.42359&+ 0	-3.00000&+ 0	0.00000&+ 0
2.00000&+ 0	2.85000&+ 0	1.03176&+ 1	-1.36281&+ 0	1.18753&+ 0	1.18753&+ 0	-3.00000&+ 0	0.00000&+ 0
2.00000&+ 0	2.90000&+ 0	5.26414&+ 0	-5.24649&- 1	7.69136&+ 0	7.69136&+ 0	-3.00000&+ 0	0.00000&+ 0
2.00000&+ 0	2.95000&+ 0	8.65198&- 1	3.67054&- 2	1.30741&+ 1	1.30741&+ 1	-1.00000&+ 0	0.00000&+ 0
2.00000&+ 0	3.00000&+ 0	0.00000&+ 0	0.00000&+ 0	1.73040&+ 1	1.73040&+ 1	0.00000&+ 0	-1.00000&+ 0
2.10000&+ 0	2.40000&+ 0	-3.48260&- 1	0.00000&+ 0	6.96521&+ 0	6.96521&+ 0	0.00000&+ 0	2.00000&+ 0
2.10000&+ 0	2.45000&+ 0	-1.53452&+ 0	-1.10349&- 1	3.76127&+ 0	3.76127&+ 0	-1.00000&+ 0	0.00000&+ 0
[illegible]	[illegible]	[illegible]	[illegible]	[illegible]	1.06876&+ 0	-3.00000&+ 0	0.00000&+ 0

```
SCHEME D PROGRAM   00050   DATE 18/05/76   TIME 15H 06M 13S   (TWO)

JOB NUMBER       1002
DATA TYPE   50
ITEM NUMBER      1USED AT BEGINNING OF AN ITEM
CURVE & REGION GEOMETRY DEFN.

ADD TO EXISTING STRUCTURE
USED AT THE END OF AN ITEM

MI/O TSNR01141    POSITION-BEFORE BLOCK 1

SCHEME D PROGRAM   00050   ENDS 21  RUN/ELAPSE/PRINT   00H 00M 00S/00H 00M 14S/00H 00M 37S   LOG TIME 00H 00M 20S          7034

JOB NUMBER       1002
DATA TYPE   55
ITEM NUMBER      2BEGIN ITEM
VISCOUS INCOMPRESSIBLE FLUID FLOW SOLUTION

TEST RESULTS
W0      1.00000000&+ 0   W0      1.00000000&+ 0


INTERNAL--ROTATIONAL--RESTART
  2.00000000&+ 0  2.00000000&+ 0

TEST RESULTS
D                  2   W98    1.00000000&+ 0

 1.87500000&- 1  3.33333300&- 3  3.00000000&+ 0

TEST RESULTS
D                  5   W100   5.00000000&+ 0   W107   3.00000000&+ 0   D                  6   E                  1

END ITEM

TEST RESULTS
D                  5   W106   1.00000000&+ 0   W0     1.00000000&+ 0   H                730   W105   1.00000000&+ 2
H                731   J                  5   W107   1.00000000&+ 2   J                  6   W99    9.80000000&+ 1
H                 10   D                  1   A5724  1.00000000&+ 0   D                  6   E                  2

  5.00000000&+ 0  2.00000000&+ 0  2.00000000&+ 0  1.87500000&- 1  3.33333300&- 3
  1.00000000&+ 2

TEST RESULTS
D                730   A5731  9.80000000&+ 1

  1.00000000&+ 0  1.00000000&+ 2

TEST RESULTS
W0      1.00000000&+ 0
MAXIMUM ERROR OVER MESH  4.62919&- 3
CONVERGED SOLUTION AT ITERATION    98
MAXIMUM ERROR OVER MESH  4.21805&- 3
CONVERGED SOLUTION AT ITERATION    99
MAXIMUM ERROR OVER MESH  3.83395&- 3
CONVERGED SOLUTION AT ITERATION   100
```

CONVERGENCE IS ASSUMED WHEN
MAX ERROR ≤ 0.005

ROTATIONAL FLOW ITERATION 100

KINEMATIC VISCOSITY 0.187500 TIMESTEP 0.003333 FLOW ELAPSED TIME 0.330000

X MESH PT	Y MESH PT	U I,J+1/2	V I+1/2,J	W N-1	W N	F.M.	V.M.
1.50000&+ 0	2.70000&+ 0	5.00000&+ 0	0.00000&+ 0	-1.00000&+ 2	-1.00000&+ 2	0.00000&+ 0	2.00000&+ 0
1.50000&+ 0	2.75000&+ 0	5.00000&+ 0	7.14363&- 1	-1.53377&- 8	-1.56870&- 8	1.00000&+ 0	0.00000&+ 0
1.50000&+ 0	2.80000&+ 0	5.00000&+ 0	6.17348&- 1	-4.26371&- 9	-4.19095&- 9	-2.00000&+ 0	0.00000&+ 0
1.50000&+ 0	2.85000&+ 0	5.00000&+ 0	6.60165&- 3	6.11180&- 9	6.14091&- 9	-2.00000&+ 0	0.00000&+ 0
1.50000&+ 0	2.90000&+ 0	5.00000&+ 0	-6.06318&- 1	1.74914&- 8	1.78115&- 8	-2.00000&+ 0	0.00000&+ 0
1.50000&+ 0	2.95000&+ 0	5.00000&+ 0	-7.07526&- 1	2.81434&- 8	2.82744&- 8	1.00000&+ 0	0.00000&+ 0
1.50000&+ 0	3.00000&+ 0	0.00000&+ 0	0.00000&+ 0	1.00000&+ 2	1.00000&+ 2	0.00000&+ 0	-1.00000&+ 0
1.60000&+ 0	2.70000&+ 0	1.56698&+ 0	0.00000&+ 0	-3.13397&+ 1	-3.13397&+ 1	0.00000&+ 0	2.00000&+ 0
1.60000&+ 0	2.75000&+ 0	6.05531&+ 0	9.02018&- 1	-1.49145&+ 1	-1.49145&+ 1	-1.00000&+ 0	0.00000&+ 0
1.60000&+ 0	2.80000&+ 0	9.57080&+ 0	7.85077&- 1	-5.47550&+ 0	-5.47550&+ 0	3.00000&+ 0	0.00000&+ 0
1.60000&+ 0	2.85000&+ 0	9.58009&+ 0	1.57434&- 2	-2.46441&- 3	-2.46437&- 3	3.00000&+ 0	0.00000&+ 0
1.60000&+ 0	2.90000&+ 0	6.07201&+ 0	-7.53811&- 1	5.47649&+ 0	5.47649&+ 0	3.00000&+ 0	0.00000&+ 0
1.60000&+ 0	2.95000&+ 0	1.57439&+ 0	-8.72399&- 1	1.49631&+ 1	1.49631&+ 1	-1.00000&+ 0	0.00000&+ 0
1.60000&+ 0	3.00000&+ 0	0.00000&+ 0	0.00000&+ 0	3.14878&+ 1	3.14878&+ 1	0.00000&+ 0	-1.00000&+ 0
1.70000&+ 0	2.70000&+ 0	1.18195&+ 0	0.00000&+ 0	-2.36389&+ 1	-2.36389&+ 1	0.00000&+ 0	2.00000&+ 0
1.70000&+ 0	2.75000&+ 0	6.13417&+ 0	3.44599&- 1	-1.53976&+ 1	-1.53976&+ 1	-1.00000&+ 0	0.00000&+ 0
1.70000&+ 0	2.80000&+ 0	1.10090&+ 1	2.71765&- 1	-7.43838&+ 0	-7.43838&+ 0	-3.00000&+ 0	0.00000&+ 0
1.70000&+ 0	2.85000&+ 0	1.10305&+ 1	2.66314&- 2	-4.11722&- 2	-4.11722&- 2	-3.00000&+ 0	0.00000&+ 0
1.70000&+ 0	2.90000&+ 0	6.17119&+ 0	-1.77461&- 1	7.38002&+ 0	7.38002&+ 0	-3.00000&+ 0	0.00000&+ 0
1.70000&+ 0	2.95000&+ 0	1.19741&+ 0	-1.97615&- 1	1.55252&+ 1	1.55252&+ 1	-1.00000&+ 0	0.00000&+ 0
1.70000&+ 0	3.00000&+ 0	0.00000&+ 0	0.00000&+ 0	2.39482&+ 1	2.39482&+ 1	0.00000&+ 0	-1.00000&+ 0
1.80000&+ 0	2.70000&+ 0	1.13794&+ 0	0.00000&+ 0	-2.27587&+ 1	-2.27587&+ 1	0.00000&+ 0	2.00000&+ 0
1.80000&+ 0	2.75000&+ 0	6.22554&+ 0	4.12131&- 1	-1.50746&+ 1	-1.50746&+ 1	-1.00000&+ 0	0.00000&+ 0
1.80000&+ 0	2.80000&+ 0	1.13733&+ 1	-8.18167&- 3	-7.54483&+ 0	-7.54483&+ 0	-3.00000&+ 0	0.00000&+ 0
1.80000&+ 0	2.85000&+ 0	1.13417&+ 1	-1.64754&- 1	7.11133&- 2	7.11133&- 2	-3.00000&+ 0	0.00000&+ 0
1.80000&+ 0	2.90000&+ 0	6.19462&+ 0	-1.33133&- 1	7.70503&+ 0	7.70503&+ 0	-3.00000&+ 0	0.00000&+ 0
1.80000&+ 0	2.95000&+ 0	1.13800&+ 0	-4.37827&- 2	1.52889&+ 1	1.52889&+ 1	-1.00000&+ 0	0.00000&+ 0

X	Y	$U_{i,j+1/2}$	$V_{i+1/2,j}$	WN-1	WN	F.M.	V.M.
1.80000&+ 0	3.00000&+ 0	0.00000&+ 0	0.00000&+ 0	2.27720&+ 1	2.27720&+ 1	0.00000&+ 0	-1.00000&+ 0
1.90000&+ 0	2.40000&+ 0	0.00000&+ 0	0.00000&+ 0	0.00000&+ 0	0.00000&+ 0	0.00000&+ 0	-1.00000&+ 0
1.90000&+ 0	2.45000&+ 0	0.00000&+ 0	-1.51749&- 1	-1.51749&+ 0	-1.51749&+ 0	0.00000&+ 0	1.00000&+ 0
1.90000&+ 0	2.50000&+ 0	0.00000&+ 0	-3.25597&- 2	-3.25597&- 1	-3.25597&- 1	0.00000&+ 0	1.00000&+ 0
1.90000&+ 0	2.55000&+ 0	0.00000&+ 0	1.83605&- 1	1.83605&+ 0	1.83605&+ 0	0.00000&+ 0	1.00000&+ 0
1.90000&+ 0	2.60000&+ 0	0.00000&+ 0	3.44377&- 1	3.44377&+ 0	3.44377&+ 0	0.00000&+ 0	1.00000&+ 0
1.90000&+ 0	2.65000&+ 0	0.00000&+ 0	2.90798&- 1	2.90798&+ 0	2.90798&+ 0	0.00000&+ 0	1.00000&+ 0
1.90000&+ 0	2.70000&+ 0	1.46080&+ 0	-9.78471&- 2	-3.01945&+ 1	-3.01945&+ 1	0.00000&+ 0	0.00000&+ 0
1.90000&+ 0	2.75000&+ 0	6.95915&+ 0	-3.68990&- 1	-1.72901&+ 1	-1.72901&+ 1	-1.00000&+ 0	0.00000&+ 0
1.90000&+ 0	2.80000&+ 0	1.19112&+ 1	-9.08410&- 1	-7.99490&+ 0	-7.99490&+ 0	-3.00000&+ 0	0.00000&+ 0
1.90000&+ 0	2.85000&+ 0	1.13999&+ 1	-7.72533&- 1	1.61349&- 1	1.61349&- 1	-3.00000&+ 0	0.00000&+ 0
1.90000&+ 0	2.90000&+ 0	6.07045&+ 0	-3.52143&- 1	7.75620&+ 0	7.75620&+ 0	-3.00000&+ 0	0.00000&+ 0
1.90000&+ 0	2.95000&+ 0	1.08338&+ 0	-1.10104&- 2	1.48941&+ 1	1.48941&+ 1	-1.00000&+ 0	0.00000&+ 0
1.90000&+ 0	3.00000&+ 0	0.00000&+ 0	0.00000&+ 0	2.16677&+ 1	2.16677&+ 1	0.00000&+ 0	-1.00000&+ 0
2.00000&+ 0	2.40000&+ 0	-3.62106&- 1	0.00000&+ 0	7.24212&+ 0	7.24212&+ 0	0.00000&+ 0	2.00000&+ 0
2.00000&+ 0	2.45000&+ 0	-1.53376&+ 0	-2.18976&- 1	3.78350&+ 0	3.78350&+ 0	-1.00000&+ 0	0.00000&+ 0
2.00000&+ 0	2.50000&+ 0	-2.58413&+ 0	-1.94888&- 1	1.29015&+ 0	1.29015&+ 0	-1.00000&+ 0	0.00000&+ 0
2.00000&+ 0	2.55000&+ 0	-2.73169&+ 0	-1.69851&- 1	-8.93015&- 1	-8.93015&- 1	-1.00000&+ 0	0.00000&+ 0
2.00000&+ 0	2.60000&+ 0	-2.10227&+ 0	-3.04936&- 1	-3.29296&+ 0	-3.29296&+ 0	-1.00000&+ 0	0.00000&+ 0
2.00000&+ 0	2.65000&+ 0	6.88133&- 2	-7.32807&- 1	-6.48102&+ 0	-6.48102&+ 0	-1.00000&+ 0	0.00000&+ 0
2.00000&+ 0	2.70000&+ 0	4.27903&+ 0	-1.45174&+ 0	-1.12945&+ 1	-1.12945&+ 1	-1.00000&+ 0	0.00000&+ 0
2.00000&+ 0	2.75000&+ 0	8.90988&+ 0	-2.07338&+ 0	-1.03158&+ 1	-1.03158&+ 1	-3.00000&+ 0	0.00000&+ 0
2.00000&+ 0	2.80000&+ 0	1.14014&+ 1	-2.02393&+ 0	-5.42359&+ 0	-5.42359&+ 0	-3.00000&+ 0	0.00000&+ 0
2.00000&+ 0	2.85000&+ 0	1.03176&+ 1	-1.36281&+ 0	1.18753&+ 0	1.18753&+ 0	-3.00000&+ 0	0.00000&+ 0
2.00000&+ 0	2.90000&+ 0	5.26414&+ 0	-5.24649&- 1	7.69136&+ 0	7.69136&+ 0	-3.00000&+ 0	0.00000&+ 0
2.00000&+ 0	2.95000&+ 0	8.65198&- 1	3.67050&- 2	1.30741&+ 1	1.30741&+ 1	-1.00000&+ 0	0.00000&+ 0
2.00000&+ 0	3.00000&+ 0	0.00000&+ 0	0.00000&+ 0	1.73040&+ 1	1.73040&+ 1	0.00000&+ 0	-1.00000&+ 0
2.10000&+ 0	2.40000&+ 0	-3.48260&- 1	0.00000&+ 0	6.96521&+ 0	6.96521&+ 0	0.00000&+ 0	2.00000&+ 0
2.10000&+ 0	2.45000&+ 0	-1.53452&+ 0	-1.10349&- 1	3.76127&+ 0	3.76127&+ 0	-1.00000&+ 0	0.00000&+ 0
2.10000&+ 0	2.50000&+ 0	-2.46211&+ 0	-3.84471&- 1	1.06876&+ 0	1.06876&+ 0	-3.00000&+ 0	0.00000&+ 0

X	Y	$U_{i,j+1/2}$	$V_{i+1/2,j}$	WN-1	WN	F.M.	V.M.
2.10000&+ 0	2.55000&+ 0	-2.11113&+ 0	-8.88161&- 1	-1.13326&+ 0	-1.13326&+ 0	-3.00000&+ 0	0.00000&+ 0
2.10000&+ 0	2.60000&+ 0	-6.77518&- 1	-1.65330&+ 0	-3.11179&+ 0	-3.11179&+ 0	-3.00000&+ 0	0.00000&+ 0
2.10000&+ 0	2.65000&+ 0	1.88906&+ 0	-2.26534&+ 0	-5.00831&+ 0	-5.00831&+ 0	-3.00000&+ 0	0.00000&+ 0
2.10000&+ 0	2.70000&+ 0	5.27851&+ 0	-2.79596&+ 0	-6.34345&+ 0	-6.34345&+ 0	-3.00000&+ 0	0.00000&+ 0
2.10000&+ 0	2.75000&+ 0	8.37278&+ 0	-2.85654&+ 0	-5.72162&+ 0	-5.72162&+ 0	-3.00000&+ 0	0.00000&+ 0
2.10000&+ 0	2.80000&+ 0	9.66986&+ 0	-2.34045&+ 0	-2.43240&+ 0	-2.43240&+ 0	-3.00000&+ 0	0.00000&+ 0
2.10000&+ 0	2.85000&+ 0	8.22029&+ 0	-1.41985&+ 0	2.39731&+ 0	2.39731&+ 0	-3.00000&+ 0	0.00000&+ 0
2.10000&+ 0	2.90000&+ 0	3.94307&+ 0	-4.65513&- 1	6.92077&+ 0	6.92077&+ 0	-3.00000&+ 0	0.00000&+ 0
2.10000&+ 0	2.95000&+ 0	5.67071&- 1	1.07133&- 1	9.85447&+ 0	9.85447&+ 0	-1.00000&+ 0	0.00000&+ 0
2.10000&+ 0	3.00000&+ 0	0.00000&+ 0	0.00000&+ 0	1.13414&+ 1	1.13414&+ 1	0.00000&+ 0	-1.00000&+ 0
2.20000&+ 0	2.40000&+ 0	-2.23590&- 1	0.00000&+ 0	4.47181&+ 0	4.47181&+ 0	0.00000&+ 0	2.00000&+ 0
2.20000&+ 0	2.45000&+ 0	-9.12390&- 1	-6.80725&- 2	2.27621&+ 0	2.27621&+ 0	-1.00000&+ 0	0.00000&+ 0
2.20000&+ 0	2.50000&+ 0	-1.25266&+ 0	-4.17501&- 1	3.63153&- 1	3.63153&- 1	-3.00000&+ 0	0.00000&+ 0
2.20000&+ 0	2.55000&+ 0	-5.57449&- 1	-1.01550&+ 0	-1.21504&+ 0	-1.21504&+ 0	-3.00000&+ 0	0.00000&+ 0
2.20000&+ 0	2.60000&+ 0	9.50624&- 1	-1.69150&+ 0	-2.48480&+ 0	-2.48480&+ 0	-3.00000&+ 0	0.00000&+ 0
2.20000&+ 0	2.65000&+ 0	3.08309&+ 0	-2.26881&+ 0	-3.35425&+ 0	-3.35425&+ 0	-3.00000&+ 0	0.00000&+ 0
2.20000&+ 0	2.70000&+ 0	5.39864&+ 0	-2.56732&+ 0	-3.52030&+ 0	-3.52030&+ 0	-3.00000&+ 0	0.00000&+ 0
2.20000&+ 0	2.75000&+ 0	7.15654&+ 0	-2.44380&+ 0	-2.53943&+ 0	-2.53943&+ 0	-3.00000&+ 0	0.00000&+ 0
2.20000&+ 0	2.80000&+ 0	7.49590&+ 0	-1.88352&+ 0	-1.59028&- 1	-1.59028&- 1	-3.00000&+ 0	0.00000&+ 0
2.20000&+ 0	2.85000&+ 0	5.94570&+ 0	-1.05795&+ 0	2.94963&+ 0	2.94963&+ 0	-3.00000&+ 0	0.00000&+ 0
2.20000&+ 0	2.90000&+ 0	2.67576&+ 0	-2.77131&- 1	5.45616&+ 0	5.45616&+ 0	-3.00000&+ 0	0.00000&+ 0
2.20000&+ 0	2.95000&+ 0	3.34586&- 1	1.51376&- 1	6.62320&+ 0	6.62320&+ 0	-1.00000&+ 0	0.00000&+ 0
2.20000&+ 0	3.00000&+ 0	0.00000&+ 0	0.00000&+ 0	6.69171&+ 0	6.69171&+ 0	0.00000&+ 0	-1.00000&+ 0
2.30000&+ 0	2.40000&+ 0	-6.20660&- 2	0.00000&+ 0	1.24132&+ 0	1.24132&+ 0	0.00000&+ 0	2.00000&+ 0
2.30000&+ 0	2.45000&+ 0	-1.40070&- 1	-3.45079&- 2	4.46844&- 1	4.46844&- 1	-1.00000&+ 0	0.00000&+ 0
2.30000&+ 0	2.50000&+ 0	1.25579&- 1	-3.22891&- 1	-3.70813&- 1	-3.70813&- 1	-3.00000&+ 0	0.00000&+ 0
2.30000&+ 0	2.55000&+ 0	9.46955&- 1	-8.06856&- 1	-1.11626&+ 0	-1.11626&+ 0	-3.00000&+ 0	0.00000&+ 0
2.30000&+ 0	2.60000&+ 0	2.21506&+ 0	-1.31950&+ 0	-1.69049&+ 0	-1.69049&+ 0	-3.00000&+ 0	0.00000&+ 0
2.30000&+ 0	2.65000&+ 0	3.72095&+ 0	-1.70483&+ 0	-1.92879&+ 0	-1.92879&+ 0	-3.00000&+ 0	0.00000&+ 0
2.30000&+ 0	2.70000&+ 0	5.10595&+ 0	-1.84092&+ 0	-1.62906&+ 0	-1.62906&+ 0	-3.00000&+ 0	0.00000&+ 0

X	Y	$U_{i,j+1/2}$	$V_{i+1/2,j}$	WN-1	WN	F.M.	V.M.
2.30000&+ 0	2.75000&+ 0	5.88895&+ 0	-1.66455&+ 0	-6.34884&- 1	-6.34885&- 1	-3.00000&+ 0	0.00000&+ 0
2.30000&+ 0	2.80000&+ 0	5.62842&+ 0	-1.20858&+ 0	9.99392&- 1	9.99392&- 1	-3.00000&+ 0	0.00000&+ 0
2.30000&+ 0	2.85000&+ 0	4.18802&+ 0	-6.17891&- 1	2.77305&+ 0	2.77306&+ 0	-3.00000&+ 0	0.00000&+ 0
2.30000&+ 0	2.90000&+ 0	1.79874&+ 0	-1.03715&- 1	3.96723&+ 0	3.96723&+ 0	-3.00000&+ 0	0.00000&+ 0
2.30000&+ 0	2.95000&+ 0	2.06885&- 1	1.56507&- 1	4.37012&+ 0	4.37012&+ 0	-1.00000&+ 0	0.00000&+ 0
2.30000&+ 0	3.00000&+ 0	0.00000&+ 0	0.00000&+ 0	4.13769&+ 0	4.13770&+ 0	0.00000&+ 0	-1.00000&+ 0
2.40000&+ 0	2.40000&+ 0	6.27437&- 2	0.00000&+ 0	-1.25487&+ 0	-1.25487&+ 0	0.00000&+ 0	2.00000&+ 0
2.40000&+ 0	2.45000&+ 0	4.74564&- 1	-1.21331&- 2	-1.04618&+ 0	-1.04618&+ 0	-1.00000&+ 0	0.00000&+ 0
2.40000&+ 0	2.50000&+ 0	1.21037&+ 0	-1.93177&- 1	-1.01706&+ 0	-1.01706&+ 0	-3.00000&+ 0	0.00000&+ 0
2.40000&+ 0	2.55000&+ 0	2.06232&+ 0	-5.02559&- 1	-1.08827&+ 0	-1.08827&+ 0	-3.00000&+ 0	0.00000&+ 0
2.40000&+ 0	2.60000&+ 0	3.03516&+ 0	-8.23006&- 1	-1.13679&+ 0	-1.13679&+ 0	-3.00000&+ 0	0.00000&+ 0
2.40000&+ 0	2.65000&+ 0	3.99466&+ 0	-1.04466&+ 0	-9.99866&- 1	-9.99867&- 1	-3.00000&+ 0	0.00000&+ 0
2.40000&+ 0	2.70000&+ 0	4.70224&+ 0	-1.09210&+ 0	-5.39376&- 1	-5.39377&- 1	-3.00000&+ 0	0.00000&+ 0
2.40000&+ 0	2.75000&+ 0	4.86245&+ 0	-9.42433&- 1	2.85309&- 1	2.85309&- 1	-3.00000&+ 0	0.00000&+ 0
2.40000&+ 0	2.80000&+ 0	4.34288&+ 0	-6.38484&- 1	1.34302&+ 0	1.34302&+ 0	-3.00000&+ 0	0.00000&+ 0
2.40000&+ 0	2.85000&+ 0	3.09164&+ 0	-2.81835&- 1	2.31835&+ 0	2.31835&+ 0	-3.00000&+ 0	0.00000&+ 0
2.40000&+ 0	2.90000&+ 0	1.30161&+ 0	6.31366&- 3	2.91251&+ 0	2.91252&+ 0	-3.00000&+ 0	0.00000&+ 0
2.40000&+ 0	2.95000&+ 0	1.49370&- 1	1.41938&- 1	3.11409&+ 0	3.11409&+ 0	-1.00000&+ 0	0.00000&+ 0
2.40000&+ 0	3.00000&+ 0	0.00000&+ 0	0.00000&+ 0	2.98739&+ 0	2.98740&+ 0	0.00000&+ 0	-1.00000&+ 0
2.50000&+ 0	2.40000&+ 0	1.30676&- 1	0.00000&+ 0	-2.61352&+ 0	-2.61352&+ 0	0.00000&+ 0	2.00000&+ 0
2.50000&+ 0	2.45000&+ 0	8.43543&- 1	-5.58935&- 3	-1.96986&+ 0	-1.96985&+ 0	-1.00000&+ 0	0.00000&+ 0
2.50000&+ 0	2.50000&+ 0	1.88297&+ 0	-9.34501&- 2	-1.49667&+ 0	-1.49667&+ 0	-3.00000&+ 0	0.00000&+ 0
2.50000&+ 0	2.55000&+ 0	2.74577&+ 0	-2.51360&- 1	-1.15695&+ 0	-1.15695&+ 0	-3.00000&+ 0	0.00000&+ 0
2.50000&+ 0	2.60000&+ 0	3.49854&+ 0	-4.15679&- 1	-8.70831&- 1	-8.70832&- 1	-3.00000&+ 0	0.00000&+ 0
2.50000&+ 0	2.65000&+ 0	4.08249&+ 0	-5.22457&- 1	-5.23350&- 1	-5.23352&- 1	-3.00000&+ 0	0.00000&+ 0
2.50000&+ 0	2.70000&+ 0	4.37120&+ 0	-5.29809&- 1	-2.69315&- 2	-2.69330&- 2	-3.00000&+ 0	0.00000&+ 0
2.50000&+ 0	2.75000&+ 0	4.23111&+ 0	-4.31456&- 1	6.22895&- 1	6.22893&- 1	-3.00000&+ 0	0.00000&+ 0
2.50000&+ 0	2.80000&+ 0	3.59500&+ 0	-2.60036&- 1	1.32531&+ 0	1.32531&+ 0	-3.00000&+ 0	0.00000&+ 0
2.50000&+ 0	2.85000&+ 0	2.50504&+ 0	-7.49008&- 2	1.92072&+ 0	1.92072&+ 0	-3.00000&+ 0	0.00000&+ 0
2.50000&+ 0	2.90000&+ 0	1.05689&+ 0	6.42104&- 2	2.30656&+ 0	2.30656&+ 0	-3.00000&+ 0	0.00000&+ 0

X	Y	$U_{i,j+1/2}$	$V_{i+1/2,j}$	W_{N-1}	W_N	F.M.	V.M.
2.50000&+ 0	2.95000&+ 0	1.27330&- 1	1.24510&- 1	2.50981&+ 0	2.50981&+ 0	-1.00000&+ 0	0.00000&+ 0
2.50000&+ 0	3.00000&+ 0	0.00000&+ 0	0.00000&+ 0	2.54660&+ 0	2.54660&+ 0	0.00000&+ 0	-1.00000&+ 0
2.60000&+ 0	2.40000&+ 0	1.55882&- 1	0.00000&+ 0	-3.11765&+ 0	-3.11765&+ 0	0.00000&+ 0	2.00000&+ 0
2.60000&+ 0	2.45000&+ 0	1.01132&+ 0	-9.85284&- 3	-2.40215&+ 0	-2.40215&+ 0	-1.00000&+ 0	0.00000&+ 0
2.60000&+ 0	2.50000&+ 0	2.21169&+ 0	-3.84699&- 2	-1.78552&+ 0	-1.78552&+ 0	-3.00000&+ 0	0.00000&+ 0
2.60000&+ 0	2.55000&+ 0	3.08706&+ 0	-9.61112&- 2	-1.26206&+ 0	-1.26206&+ 0	-3.00000&+ 0	0.00000&+ 0
2.60000&+ 0	2.60000&+ 0	3.71774&+ 0	-1.57694&- 1	-8.01749&- 1	-8.01750&- 1	-3.00000&+ 0	0.00000&+ 0
2.60000&+ 0	2.65000&+ 0	4.09247&+ 0	-1.93713&- 1	-3.46250&- 1	-3.46252&- 1	-3.00000&+ 0	0.00000&+ 0
2.60000&+ 0	2.70000&+ 0	4.16174&+ 0	-1.84396&- 1	1.51166&- 1	1.51163&- 1	-3.00000&+ 0	0.00000&+ 0
2.60000&+ 0	2.75000&+ 0	3.87542&+ 0	-1.28939&- 1	6.89349&- 1	6.89347&- 1	-3.00000&+ 0	0.00000&+ 0
2.60000&+ 0	2.80000&+ 0	3.22064&+ 0	-4.60895&- 2	1.21514&+ 0	1.21514&+ 0	-3.00000&+ 0	0.00000&+ 0
2.60000&+ 0	2.85000&+ 0	2.23483&+ 0	3.50737&- 2	1.66202&+ 0	1.66202&+ 0	-3.00000&+ 0	0.00000&+ 0
2.60000&+ 0	2.90000&+ 0	9.55482&- 1	8.99244&- 2	2.00312&+ 0	2.00312&+ 0	-3.00000&+ 0	0.00000&+ 0
2.60000&+ 0	2.95000&+ 0	1.22085&- 1	1.10040&- 1	2.26501&+ 0	2.26501&+ 0	-1.00000&+ 0	0.00000&+ 0
2.60000&+ 0	3.00000&+ 0	0.00000&+ 0	0.00000&+ 0	2.44171&+ 0	2.44171&+ 0	0.00000&+ 0	-1.00000&+ 0
2.70000&+ 0	2.40000&+ 0	1.58837&- 1	0.00000&+ 0	-3.17675&+ 0	-3.17674&+ 0	0.00000&+ 0	2.00000&+ 0
2.70000&+ 0	2.45000&+ 0	1.05822&+ 0	-1.78008&- 2	-2.52833&+ 0	-2.52833&+ 0	-1.00000&+ 0	0.00000&+ 0
2.70000&+ 0	2.50000&+ 0	2.32123&+ 0	-1.69994&- 2	-1.91648&+ 0	-1.91647&+ 0	-3.00000&+ 0	0.00000&+ 0
2.70000&+ 0	2.55000&+ 0	3.20786&+ 0	-2.13107&- 2	-1.34901&+ 0	-1.34901&+ 0	-3.00000&+ 0	0.00000&+ 0
2.70000&+ 0	2.60000&+ 0	3.78839&+ 0	-2.66287&- 2	-8.24278&- 1	-8.24279&- 1	-3.00000&+ 0	0.00000&+ 0
2.70000&+ 0	2.65000&+ 0	4.07143&+ 0	-2.42813&- 2	-3.24429&- 1	-3.24433&- 1	-3.00000&+ 0	0.00000&+ 0
2.70000&+ 0	2.70000&+ 0	4.04817&+ 0	-7.73213&- 3	1.68422&- 1	1.68417&- 1	-3.00000&+ 0	0.00000&+ 0
2.70000&+ 0	2.75000&+ 0	3.70997&+ 0	2.20662&- 2	6.53090&- 1	6.53087&- 1	-3.00000&+ 0	0.00000&+ 0
2.70000&+ 0	2.80000&+ 0	3.06435&+ 0	5.64084&- 2	1.10853&+ 0	1.10853&+ 0	-3.00000&+ 0	0.00000&+ 0
2.70000&+ 0	2.85000&+ 0	2.13677&+ 0	8.38758&- 2	1.51422&+ 0	1.51422&+ 0	-3.00000&+ 0	0.00000&+ 0
2.70000&+ 0	2.90000&+ 0	9.27572&- 1	9.75045&- 2	1.87112&+ 0	1.87112&+ 0	-3.00000&+ 0	0.00000&+ 0
2.70000&+ 0	2.95000&+ 0	1.24313&- 1	9.91161&- 2	2.20051&+ 0	2.20052&+ 0	-1.00000&+ 0	0.00000&+ 0
2.70000&+ 0	3.00000&+ 0	0.00000&+ 0	0.00000&+ 0	2.48625&+ 0	2.48625&+ 0	0.00000&+ 0	-1.00000&+ 0
2.80000&+ 0	2.40000&+ 0	1.53651&- 1	0.00000&+ 0	-3.07303&+ 0	-3.07302&+ 0	0.00000&+ 0	2.00000&+ 0
2.80000&+ 0	2.45000&+ 0	1.04913&+ 0	-2.50380&- 2	-2.50944&+ 0	-2.50944&+ 0	-1.00000&+ 0	0.00000&+ 0

X	Y	$U_{i,j+1/2}$	$V_{i+1/2,j}$	W_{N-1}	W_N	F.M.	V.M.
2.80000&+ 0	2.50000&+ 0	2.31952&+ 0	-1.35150&- 2	-1.94744&+ 0	-1.94743&+ 0	-3.00000&+ 0	0.00000&+ 0
2.80000&+ 0	2.55000&+ 0	3.21108&+ 0	4.03431&- 3	-1.39810&+ 0	-1.39810&+ 0	-3.00000&+ 0	0.00000&+ 0
2.80000&+ 0	2.60000&+ 0	3.77942&+ 0	2.32813&- 2	-8.68671&- 1	-8.68674&- 1	-3.00000&+ 0	0.00000&+ 0
2.80000&+ 0	2.65000&+ 0	4.03653&+ 0	4.28531&- 2	-3.61245&- 1	-3.61251&- 1	-3.00000&+ 0	0.00000&+ 0
2.80000&+ 0	2.70000&+ 0	3.98927&+ 0	6.24160&- 2	1.25705&- 1	1.25697&- 1	-3.00000&+ 0	0.00000&+ 0
2.80000&+ 0	2.75000&+ 0	3.64527&+ 0	8.02531&- 2	5.90338&- 1	5.90332&- 1	-3.00000&+ 0	0.00000&+ 0
2.80000&+ 0	2.80000&+ 0	3.01711&+ 0	9.30325&- 2	1.02726&+ 0	1.02726&+ 0	-3.00000&+ 0	0.00000&+ 0
2.80000&+ 0	2.85000&+ 0	2.11983&+ 0	9.79596&- 2	1.43569&+ 0	1.43569&+ 0	-3.00000&+ 0	0.00000&+ 0
2.80000&+ 0	2.90000&+ 0	9.31799&- 1	9.56418&- 2	1.82576&+ 0	1.82577&+ 0	-3.00000&+ 0	0.00000&+ 0
2.80000&+ 0	2.95000&+ 0	1.28946&- 1	9.10484&- 2	2.21380&+ 0	2.21381&+ 0	-1.00000&+ 0	0.00000&+ 0
2.80000&+ 0	3.00000&+ 0	0.00000&+ 0	0.00000&+ 0	2.57891&+ 0	2.57891&+ 0	0.00000&+ 0	-1.00000&+ 0
2.90000&+ 0	2.40000&+ 0	1.47186&- 1	0.00000&+ 0	-2.94374&+ 0	-2.94373&+ 0	0.00000&+ 0	2.00000&+ 0
2.90000&+ 0	2.45000&+ 0	1.02207&+ 0	-2.99604&- 2	-2.44300&+ 0	-2.44299&+ 0	-1.00000&+ 0	0.00000&+ 0
2.90000&+ 0	2.50000&+ 0	2.27560&+ 0	-1.69089&- 2	-1.92958&+ 0	-1.92957&+ 0	-3.00000&+ 0	0.00000&+ 0
2.90000&+ 0	2.55000&+ 0	3.16530&+ 0	5.65909&- 3	-1.41425&+ 0	-1.41425&+ 0	-3.00000&+ 0	0.00000&+ 0
2.90000&+ 0	2.60000&+ 0	3.73565&+ 0	3.16126&- 2	-9.03791&- 1	-9.03796&- 1	-3.00000&+ 0	0.00000&+ 0
2.90000&+ 0	2.65000&+ 0	3.99562&+ 0	5.61478&- 2	-4.06172&- 1	-4.06182&- 1	-3.00000&+ 0	0.00000&+ 0
2.90000&+ 0	2.70000&+ 0	3.95464&+ 0	7.61878&- 2	7.34561&- 2	7.34439&- 2	-3.00000&+ 0	0.00000&+ 0
2.90000&+ 0	2.75000&+ 0	3.62354&+ 0	8.97322&- 2	5.32498&- 1	5.32488&- 1	-3.00000&+ 0	0.00000&+ 0
2.90000&+ 0	2.80000&+ 0	3.01348&+ 0	9.57401&- 2	9.71429&- 1	9.71424&- 1	-3.00000&+ 0	0.00000&+ 0
2.90000&+ 0	2.85000&+ 0	2.13192&+ 0	9.47503&- 2	1.39609&+ 0	1.39609&+ 0	-3.00000&+ 0	0.00000&+ 0
2.90000&+ 0	2.90000&+ 0	9.45151&- 1	8.95797&- 2	1.81787&+ 0	1.81788&+ 0	-3.00000&+ 0	0.00000&+ 0
2.90000&+ 0	2.95000&+ 0	1.33276&- 1	8.49392&- 2	2.24867&+ 0	2.24868&+ 0	-1.00000&+ 0	0.00000&+ 0
2.90000&+ 0	3.00000&+ 0	0.00000&+ 0	0.00000&+ 0	2.66550&+ 0	2.66551&+ 0	0.00000&+ 0	-1.00000&+ 0
3.00000&+ 0	2.40000&+ 0	1.41854&- 1	0.00000&+ 0	-2.83709&+ 0	-2.83707&+ 0	0.00000&+ 0	2.00000&+ 0
3.00000&+ 0	2.45000&+ 0	9.94448&- 1	-3.22404&- 2	-2.37408&+ 0	-2.37406&+ 0	-1.00000&+ 0	0.00000&+ 0
3.00000&+ 0	2.50000&+ 0	2.22459&+ 0	-2.09563&- 2	-1.89513&+ 0	-1.89512&+ 0	-3.00000&+ 0	0.00000&+ 0
3.00000&+ 0	2.55000&+ 0	3.10801&+ 0	-2.72230&- 4	-1.41005&+ 0	-1.41005&+ 0	-3.00000&+ 0	0.00000&+ 0
3.00000&+ 0	2.60000&+ 0	3.68279&+ 0	2.42909&- 2	-9.22511&- 1	-9.22519&- 1	-3.00000&+ 0	0.00000&+ 0
[illegible]	[illegible]	[illegible]	[illegible]	[illegible]	[illegible]	[illegible]	[illegible]

X	Y	$U_{i,j+1/2}$	$V_{i+1/2,j}$	W_{N-1}	W_N	F.M.	V.M.
3.00000&+ 0	2.70000&+ 0	3.92805&+ 0	6.62438&- 2	3.18985&- 2	3.18811&- 2	-3.00000&+ 0	0.00000&+ 0
3.00000&+ 0	2.75000&+ 0	3.61402&+ 0	7.84258&- 2	4.89848&- 1	4.89833&- 1	-3.00000&+ 0	0.00000&+ 0
3.00000&+ 0	2.80000&+ 0	3.01943&+ 0	8.40451&- 2	9.35879&- 1	9.35871&- 1	-3.00000&+ 0	0.00000&+ 0
3.00000&+ 0	2.85000&+ 0	2.14673&+ 0	8.44202&- 2	1.37651&+ 0	1.37651&+ 0	-3.00000&+ 0	0.00000&+ 0
3.00000&+ 0	2.90000&+ 0	9.56503&- 1	8.20121&- 2	1.82111&+ 0	1.82112&+ 0	-3.00000&+ 0	0.00000&+ 0
3.00000&+ 0	2.95000&+ 0	1.36169&- 1	7.97747&- 2	2.27793&+ 0	2.27794&+ 0	-1.00000&+ 0	0.00000&+ 0
3.00000&+ 0	3.00000&+ 0	0.00000&+ 0	0.00000&+ 0	2.72337&+ 0	2.72339&+ 0	0.00000&+ 0	-1.00000&+ 0
3.10000&+ 0	2.40000&+ 0	1.38031&- 1	0.00000&+ 0	-2.76065&+ 0	-2.76063&+ 0	0.00000&+ 0	2.00000&+ 0
3.10000&+ 0	2.45000&+ 0	9.71812&- 1	-3.16475&- 2	-2.31695&+ 0	-2.31693&+ 0	-1.00000&+ 0	0.00000&+ 0
3.10000&+ 0	2.50000&+ 0	2.17989&+ 0	-2.20241&- 2	-1.85931&+ 0	-1.85930&+ 0	-3.00000&+ 0	0.00000&+ 0
3.10000&+ 0	2.55000&+ 0	3.05547&+ 0	-4.15328&- 3	-1.39606&+ 0	-1.39605&+ 0	-3.00000&+ 0	0.00000&+ 0
3.10000&+ 0	2.60000&+ 0	3.63336&+ 0	1.66068&- 2	-9.27695&- 1	-9.27704&- 1	-3.00000&+ 0	0.00000&+ 0
3.10000&+ 0	2.65000&+ 0	3.91495&+ 0	3.56858&- 2	-4.58903&- 1	-4.58920&- 1	-3.00000&+ 0	0.00000&+ 0
3.10000&+ 0	2.70000&+ 0	3.90344&+ 0	5.05688&- 2	5.35609&-3	5.33564&- 3	-3.00000&+ 0	0.00000&+ 0
3.10000&+ 0	2.75000&+ 0	3.60385&+ 0	6.07084&- 2	4.62669&- 1	4.62651&- 1	-3.00000&+ 0	0.00000&+ 0
3.10000&+ 0	2.80000&+ 0	3.02062&+ 0	6.69754&- 2	9.14476&- 1	9.14466&- 1	-3.00000&+ 0	0.00000&+ 0
3.10000&+ 0	2.85000&+ 0	2.15370&+ 0	7.08126&- 2	1.36568&+ 0	1.36568&+ 0	-3.00000&+ 0	0.00000&+ 0
3.10000&+ 0	2.90000&+ 0	9.61916&- 1	7.32380&- 2	1.82280&+ 0	1.82282&+ 0	-3.00000&+ 0	0.00000&+ 0
3.10000&+ 0	2.95000&+ 0	1.37479&- 1	7.43326&- 2	2.29166&+ 0	2.29168&+ 0	-1.00000&+ 0	0.00000&+ 0
3.10000&+ 0	3.00000&+ 0	0.00000&+ 0	0.00000&+ 0	2.74956&+ 0	2.74958&+ 0	0.00000&+ 0	-1.00000&+ 0
3.20000&+ 0	2.40000&+ 0	1.35321&- 1	0.00000&+ 0	-2.70644&+ 0	-2.70642&+ 0	0.00000&+ 0	2.00000&+ 0
3.20000&+ 0	2.45000&+ 0	9.53504&- 1	-2.56768&- 2	-2.26877&+ 0	-2.26875&+ 0	-1.00000&+ 0	0.00000&+ 0
3.20000&+ 0	2.50000&+ 0	2.14262&+ 0	-1.34975&- 2	-1.82534&+ 0	-1.82533&+ 0	-3.00000&+ 0	0.00000&+ 0
3.20000&+ 0	2.55000&+ 0	3.01180&+ 0	5.09095&- 3	-1.37862&+ 0	-1.37862&+ 0	-3.00000&+ 0	0.00000&+ 0
3.20000&+ 0	2.60000&+ 0	3.59292&+ 0	2.15637&- 2	-9.25201&- 1	-9.25209&- 1	-3.00000&+ 0	0.00000&+ 0
3.20000&+ 0	2.65000&+ 0	3.88328&+ 0	3.22051&- 2	-4.67288&- 1	-4.67304&- 1	-3.00000&+ 0	0.00000&+ 0
3.20000&+ 0	2.70000&+ 0	3.88199&+ 0	3.73432&- 2	-8.72957&- 3	-8.74817&- 3	-3.00000&+ 0	0.00000&+ 0
3.20000&+ 0	2.75000&+ 0	3.59098&+ 0	3.95158&- 2	4.47877&- 1	4.47861&- 1	-3.00000&+ 0	0.00000&+ 0
3.20000&+ 0	2.80000&+ 0	3.01332&+ 0	4.22287&- 2	9.02495&- 1	9.02487&- 1	-3.00000&+ 0	0.00000&+ 0
[illegible]	[illegible]	2.14960&+ 0	4.84376&- 2	1.35746&+ 0	1.35747&+ 0	-3.00000&+ 0	0.00000&+ 0

X	Y	$U_{i,j+1/2}$	$V_{i+1/2,j}$	WN-1	WN	F.M.	V.M.
3.20000&+ 0	2.90000&+ 0	9.60460&- 1	5.79371&- 2	1.81673&+ 0	1.81674&+ 0	-3.00000&+ 0	0.00000&+ 0
3.20000&+ 0	2.95000&+ 0	1.37461&- 1	6.53316&- 2	2.28625&+ 0	2.28626&+ 0	-1.00000&+ 0	0.00000&+ 0
3.20000&+ 0	3.00000&+ 0	0.00000&+ 0	0.00000&+ 0	2.74920&+ 0	2.74922&+ 0	0.00000&+ 0	-1.00000&+ 0
3.30000&+ 0	2.40000&+ 0	1.31962&- 1	0.00000&+ 0	-2.63925&+ 0	-2.63924&+ 0	0.00000&+ 0	2.00000&+ 0
3.30000&+ 0	2.45000&+ 0	9.32110&- 1	7.97673&- 3	-2.20009&+ 0	-2.20008&+ 0	-1.00000&+ 0	0.00000&+ 0
3.30000&+ 0	2.50000&+ 0	2.10440&+ 0	3.41080&- 2	-1.78268&+ 0	-1.78267&+ 0	-3.00000&+ 0	0.00000&+ 0
3.30000&+ 0	2.55000&+ 0	2.97598&+ 0	5.30712&- 2	-1.35783&+ 0	-1.35783&+ 0	-3.00000&+ 0	0.00000&+ 0
3.30000&+ 0	2.60000&+ 0	3.56784&+ 0	5.58804&- 2	-9.18381&- 1	-9.18385&- 1	-3.00000&+ 0	0.00000&+ 0
3.30000&+ 0	2.65000&+ 0	3.86908&+ 0	4.58208&- 2	-4.68838&- 1	-4.68847&- 1	-3.00000&+ 0	0.00000&+ 0
3.30000&+ 0	2.70000&+ 0	3.87404&+ 0	2.89019&- 2	-1.45435&- 2	-1.45544&- 2	-3.00000&+ 0	0.00000&+ 0
3.30000&+ 0	2.75000&+ 0	3.58256&+ 0	1.04642&- 2	4.40845&- 1	4.40835&- 1	-3.00000&+ 0	0.00000&+ 0
3.30000&+ 0	2.80000&+ 0	2.99891&+ 0	-3.60068&- 3	8.95129&- 1	8.95125&- 1	-3.00000&+ 0	0.00000&+ 0
3.30000&+ 0	2.85000&+ 0	2.13010&+ 0	-6.31594&- 3	1.34628&+ 0	1.34628&+ 0	-3.00000&+ 0	0.00000&+ 0
3.30000&+ 0	2.90000&+ 0	9.47954&- 1	7.55814&- 3	1.79245&+ 0	1.79246&+ 0	-3.00000&+ 0	0.00000&+ 0
3.30000&+ 0	2.95000&+ 0	1.35277&- 1	3.06663&- 2	2.24067&+ 0	2.24068&+ 0	-1.00000&+ 0	0.00000&+ 0
3.30000&+ 0	3.00000&+ 0	0.00000&+ 0	0.00000&+ 0	2.70553&+ 0	2.70554&+ 0	0.00000&+ 0	-1.00000&+ 0
3.40000&+ 0	2.40000&+ 0	1.15235&- 1	0.00000&+ 0	-2.30470&+ 0	-2.30470&+ 0	0.00000&+ 0	2.00000&+ 0
3.40000&+ 0	2.45000&+ 0	8.79498&- 1	1.89453&- 1	-1.99153&+ 0	-1.99153&+ 0	-1.00000&+ 0	0.00000&+ 0
3.40000&+ 0	2.50000&+ 0	2.04925&+ 0	2.22951&- 1	-1.71334&+ 0	-1.71334&+ 0	-3.00000&+ 0	0.00000&+ 0
3.40000&+ 0	2.55000&+ 0	2.95730&+ 0	1.83204&- 1	-1.35574&+ 0	-1.35574&+ 0	-3.00000&+ 0	0.00000&+ 0
3.40000&+ 0	2.60000&+ 0	3.58196&+ 0	1.23583&- 1	-9.35916&- 1	-9.35915&- 1	-3.00000&+ 0	0.00000&+ 0
3.40000&+ 0	2.65000&+ 0	3.90151&+ 0	6.95902&- 2	-4.83319&- 1	-4.83319&- 1	-3.00000&+ 0	0.00000&+ 0
3.40000&+ 0	2.70000&+ 0	3.90978&+ 0	2.39950&- 2	-1.69143&- 2	-1.69151&- 2	-3.00000&+ 0	0.00000&+ 0
3.40000&+ 0	2.75000&+ 0	3.60557&+ 0	-2.16156&- 2	4.52352&- 1	4.52351&- 1	-3.00000&+ 0	0.00000&+ 0
3.40000&+ 0	2.80000&+ 0	2.99192&+ 0	-7.57002&- 2	9.14374&- 1	9.14375&- 1	-3.00000&+ 0	0.00000&+ 0
3.40000&+ 0	2.85000&+ 0	2.08560&+ 0	-1.35712&- 1	1.35195&+ 0	1.35195&+ 0	-3.00000&+ 0	0.00000&+ 0
3.40000&+ 0	2.90000&+ 0	9.00663&- 1	-1.76671&- 1	1.73644&+ 0	1.73644&+ 0	-3.00000&+ 0	0.00000&+ 0
3.40000&+ 0	2.95000&+ 0	1.19338&- 1	-1.45944&- 1	2.04858&+ 0	2.04858&+ 0	-1.00000&+ 0	0.00000&+ 0
3.40000&+ 0	3.00000&+ 0	0.00000&+ 0	0.00000&+ 0	2.38675&+ 0	2.38675&+ 0	0.00000&+ 0	-1.00000&+ 0
3.50000&+ 0	2.40000&+ 0	3.19242&- 2	0.00000&+ 0	-6.38477&- 1	-6.38484&- 1	0.00000&+ 0	2.00000&+ 0

X	Y	$U_{i,j+1/2}$	$V_{i+1/2,j}$	W_{N-1}	W_N	F.M.	V.M.
3.50000&+ 0	2.45000&+ 0	7.67779&- 1	3.42183&- 1	-1.61031&+ 0	-1.61032&+ 0	-1.00000&+ 0	0.00000&+ 0
3.50000&+ 0	2.50000&+ 0	2.05654&+ 0	3.72126&- 1	-1.68962&+ 0	-1.68962&+ 0	3.00000&+ 0	0.00000&+ 0
3.50000&+ 0	2.55000&+ 0	3.04712&+ 0	2.75087&- 1	-1.39013&+ 0	-1.39013&+ 0	3.00000&+ 0	0.00000&+ 0
3.50000&+ 0	2.60000&+ 0	3.68801&+ 0	1.64430&- 1	-9.65335&- 1	-9.65329&- 1	3.00000&+ 0	0.00000&+ 0
3.50000&+ 0	2.65000&+ 0	4.00253&+ 0	8.14551&- 2	-4.98340&- 1	-4.98332&- 1	3.00000&+ 0	0.00000&+ 0
3.50000&+ 0	2.70000&+ 0	4.01104&+ 0	2.20945&- 2	-1.71529&- 2	-1.71448&- 2	3.00000&+ 0	0.00000&+ 0
3.50000&+ 0	2.75000&+ 0	3.71249&+ 0	-3.64299&- 2	4.67361&- 1	4.67368&- 1	3.00000&+ 0	0.00000&+ 0
3.50000&+ 0	2.80000&+ 0	3.08392&+ 0	-1.17185&- 1	9.44848&- 1	9.44854&- 1	3.00000&+ 0	0.00000&+ 0
3.50000&+ 0	2.85000&+ 0	2.09771&+ 0	-2.25203&- 1	1.38886&+ 0	1.38887&+ 0	3.00000&+ 0	0.00000&+ 0
3.50000&+ 0	2.90000&+ 0	7.95378&- 1	-3.21017&- 1	1.71936&+ 0	1.71936&+ 0	3.00000&+ 0	0.00000&+ 0
3.50000&+ 0	2.95000&+ 0	3.91854&- 2	-2.93930&- 1	1.68857&+ 0	1.68857&+ 0	-1.00000&+ 0	0.00000&+ 0
3.50000&+ 0	3.00000&+ 0	0.00000&+ 0	0.00000&+ 0	7.83715&- 1	7.83708&- 1	0.00000&+ 0	-1.00000&+ 0
3.60000&+ 0	2.40000&+ 0	3.62017&- 1	0.00000&+ 0	-7.24032&+ 0	-7.24033&+ 0	0.00000&+ 0	2.00000&+ 0
3.60000&+ 0	2.45000&+ 0	9.95094&- 1	0.00000&+ 0	-5.75236&+ 0	-5.75236&+ 0	2.00000&+ 0	2.00000&+ 0
3.60000&+ 0	2.50000&+ 0	2.52189&+ 0	0.00000&+ 0	-4.27841&+ 0	-4.27841&+ 0	2.00000&+ 0	2.00000&+ 0
3.60000&+ 0	2.55000&+ 0	3.34598&+ 0	0.00000&+ 0	-2.94634&+ 0	-2.94634&+ 0	2.00000&+ 0	2.00000&+ 0
3.60000&+ 0	2.60000&+ 0	3.80411&+ 0	0.00000&+ 0	-1.82858&+ 0	-1.82858&+ 0	2.00000&+ 0	2.00000&+ 0
3.60000&+ 0	2.65000&+ 0	4.01275&+ 0	0.00000&+ 0	-8.85637&- 1	-8.85631&- 1	2.00000&+ 0	2.00000&+ 0
3.60000&+ 0	2.70000&+ 0	4.01768&+ 0	0.00000&+ 0	-3.52656&- 2	-3.52586&- 2	2.00000&+ 0	2.00000&+ 0
3.60000&+ 0	2.75000&+ 0	3.81859&+ 0	0.00000&+ 0	8.15315&- 1	8.15321&- 1	2.00000&+ 0	2.00000&+ 0
3.60000&+ 0	2.80000&+ 0	3.36876&+ 0	0.00000&+ 0	1.75957&+ 0	1.75958&+ 0	2.00000&+ 0	2.00000&+ 0
3.60000&+ 0	2.85000&+ 0	2.54990&+ 0	0.00000&+ 0	2.88221&+ 0	2.88221&+ 0	2.00000&+ 0	2.00000&+ 0
3.60000&+ 0	2.90000&+ 0	1.02136&+ 0	0.00000&+ 0	4.22762&+ 0	4.22762&+ 0	2.00000&+ 0	2.00000&+ 0
3.60000&+ 0	2.95000&+ 0	3.63155&- 1	0.00000&+ 0	5.72983&+ 0	5.72982&+ 0	2.00000&+ 0	2.00000&+ 0
3.60000&+ 0	3.00000&+ 0	0.00000&+ 0	0.00000&+ 0	7.26310&+ 0	7.26310&+ 0	0.00000&+ 0	-1.00000&+ 0

ASSEMBLE PLOTTING VECTORS

ASSEMBLY OF PLOTTING COORDINATES

```
BEGINENDLSTC506A        /PAGECRTP
NEXT PAGE
SCALE  10.0000
NEXT LINE
    1.0000
    1.5000    2.7000
    1.5000    2.7500
    1.5000    2.8000
    1.5000    2.8500
    1.5000    2.9000
    1.5000    2.9500
    1.5000    3.0000
    1.6000    3.0000
    1.7000    3.0000
    1.8000    3.0000
    1.9000    3.0000
    2.0000    3.0000
    2.1000    3.0000
    2.2000    3.0000
    2.3000    3.0000
    2.4000    3.0000
    2.5000    3.0000
    2.6000    3.0000
    2.7000    3.0000
    2.8000    3.0000
    2.9000    3.0000
    3.0000    3.0000
    3.1000    3.0000
    3.2000    3.0000
    3.3000    3.0000
    3.4000    3.0000
    3.5000    3.0000
    3.6000    3.0000
    3.6000    2.9500
    3.6000    2.9000
    3.6000    2.8500
    3.6000    2.8000
    3.6000    2.7500
    3.6000    2.7000
    3.6000    2.6500
    3.6000    2.6000
    3.6000    2.5500
    3.6000    2.5000
    3.6000    2.4500
    3.6000    2.4000
    3.5000    2.4000
    3.4000    2.4000
    3.3000    2.4000
    3.2000    2.4000
    3.1000    2.4000
    3.0000    2.4000
    2.9000    2.4000
    2.8000    2.4000
    2.7000    2.4000
    2.6000    2.4000
    2.5000    2.4000
    2.4000    2.4000
    2.3000    2.4000
    2.2000    2.4000
    2.1000    2.4000
```

```
    2.0000    2.4000
    1.9000    2.4000
    1.9000    2.4500
    1.9000    2.5000
    1.9000    2.5500
    1.9000    2.6000
    1.9000    2.6500
    1.9000    2.7000
    1.8000    2.7000
    1.7000    2.7000
    1.6000    2.7000
    1.5000    2.7000
NEXT LINE
    2.0000
    4.0861    1.4500
    2.7214    1.5503
NEXT LINE
    2.0000
    9.2103    1.5059
    2.7429    1.5952
NEXT LINE
    2.0000
    7.5855    1.4500
    2.7683    1.5509
NEXT LINE
    2.0000
    5.5042    1.4859
    2.7938    1.6147
NEXT LINE
    2.0000
    3.5703    1.4500
    2.8219    1.5502
NEXT LINE
    2.0000
    0.0519    1.4771
    2.8499    1.6229
NEXT LINE
    2.0000
   -3.4320    1.4500
    2.8780    1.5502
NEXT LINE
    2.0000
   -5.4010    1.4859
    2.9061    1.6147
NEXT LINE
    2.0000
   -7.4849    1.4500
    2.9316    1.5509
NEXT LINE
    2.0000
   -9.1114    1.5059
    2.9571    1.5952
NEXT LINE
    2.0000
   -4.0471    1.4500
    2.9785    1.5502
NEXT LINE
    2.0000
   14.4604    1.5843
    2.7210    1.6167
```

```
NEXT LINE
   2.0000
  13.5786    1.6127
   2.7410    1.6895
NEXT LINE
   2.0000
   7.1044    1.5394
   2.7675    1.6615
NEXT LINE
   2.0000
   5.4740    1.5681
   2.7921    1.7327
NEXT LINE
   2.0000
   2.1314    1.5043
   2.8214    1.6958
NEXT LINE
   2.0000
   0.0876    1.5470
   2.8498    1.7530
NEXT LINE
   2.0000
  -1.9994    1.5042
   2.8783    1.6959
NEXT LINE
   2.0000
  -5.2438    1.5679
   2.9075    1.7328
NEXT LINE
   2.0000
  -6.9020    1.5393
   2.9324    1.6616
NEXT LINE
   2.0000
 -13.0837    1.6125
   2.9587    1.6895
NEXT LINE
   2.0000
 -14.0836    1.5843
   2.9789    1.6167
NEXT LINE
   2.0000
  14.7715    1.6882
   2.7219    1.7126
NEXT LINE
   2.0000
   5.3643    1.7133
   2.7466    1.7870
NEXT LINE
   2.0000
   5.3631    1.6387
   2.7692    1.7619
NEXT LINE
   2.0000
   1.7922    1.6631
   2.7973    1.8369
NEXT LINE
   2.0000
   1.4299    1.5899
```

```
NEXT LINE
   2.0000
   0.1364   1.6381
   2.8497   1.8619
NEXT LINE
   2.0000
  -1.1541   1.5897
   2.8772   1.8103
NEXT LINE
   2.0000
  -1.1706   1.6632
   2.9018   1.8369
NEXT LINE
   2.0000
  -4.6350   1.6383
   2.9300   1.7621
NEXT LINE
   2.0000
  -3.0776   1.7132
   2.9520   1.7869
NEXT LINE
   2.0000
 -12.5932   1.6880
   2.9777   1.7126
NEXT LINE
   2.0000
   9.4391   1.7886
   2.7231   1.8117
NEXT LINE
   2.0000
   5.9627   1.8105
   2.7459   1.8899
NEXT LINE
   2.0000
   2.3463   1.7377
   2.7724   1.8624
NEXT LINE
   2.0000
  -0.0514   1.7588
   2.8001   1.9412
NEXT LINE
   2.0000
   0.1580   1.6863
   2.8247   1.9137
NEXT LINE
   2.0000
  -0.6203   1.7349
   2.8516   1.9651
NEXT LINE
   2.0000
  -0.5667   1.6866
   2.8761   1.9134
NEXT LINE
   2.0000
  -0.8715   1.7625
   2.9013   1.9375
NEXT LINE
   2.0000
  -1.2762   1.7381
```